

Non-First Order Degradation and Time-Dependent Sorption of Organic Chemicals in Soil

ACS SYMPOSIUM SERIES **1174**

Non-First Order Degradation and Time-Dependent Sorption of Organic Chemicals in Soil

Wenlin Chen, Editor

Syngenta Crop Protection, LLC, Greensboro, North Carolina

Aleksandar Sabljic, Editor

Institute Rudjer Boskovic, Zagreb, Croatia

Steven A. Cryer, Editor

Dow AgroSciences, LLC, Indianapolis, Indiana

Rai S. Kookana, Editor

CSIRO Land and Water, Glen Osmond, Australia

**Sponsored by the
ACS Division of Agricultural and Food Chemistry, Inc.**



American Chemical Society, Washington, DC

Distributed in print by Oxford University Press



Library of Congress Cataloging-in-Publication Data

Non-first order degradation and time-dependent sorption of organic chemicals in soil / Wenlin Chen, editor, Syngenta Crop Protection, LLC, Greensboro, North Carolina, Aleksandar Sabljic, editor, Institute Rudjer Boskovic, Zagreb, Croatia, Steven A. Cryer, editor, Dow AgroSciences, LLC, Indianapolis, Indiana, Rai S. Kookana, editor, CSIRO, Land and Water Flagship, Glen Osmond, Australia ; sponsored by the ACS Division of Agricultural and Food Chemistry, Inc.

pages cm. -- (ACS symposium series ; 1174)

Includes bibliographical references.

ISBN 978-0-8412-2978-5

1. Soil absorption and adsorption. 2. Soils--Organic compound content. 3. Agricultural chemicals--Biodegradation. 4. Organic compounds--Biodegradation. 5. Soil chemistry. I. Chen, Wenlin, 1962- editor. II. Sabljic, Aleksandar, editor. III. Cryer, Steven A., editor. IV. Kookana, Rai S., editor. V. American Chemical Society. Division of Agricultural and Food Chemistry. VI. Title: Sorption of organic chemicals in soil.

S592.5.N66 2014

631.4'32--dc23

2014038715

The paper used in this publication meets the minimum requirements of American National Standard for Information Sciences—Permanence of Paper for Printed Library Materials, ANSI Z39.48n1984.

Copyright © 2014 American Chemical Society

Distributed in print by Oxford University Press

All Rights Reserved. Reprographic copying beyond that permitted by Sections 107 or 108 of the U.S. Copyright Act is allowed for internal use only, provided that a per-chapter fee of \$40.25 plus \$0.75 per page is paid to the Copyright Clearance Center, Inc., 222 Rosewood Drive, Danvers, MA 01923, USA. Republication or reproduction for sale of pages in this book is permitted only under license from ACS. Direct these and other permission requests to ACS Copyright Office, Publications Division, 1155 16th Street, N.W., Washington, DC 20036.

The citation of trade names and/or names of manufacturers in this publication is not to be construed as an endorsement or as approval by ACS of the commercial products or services referenced herein; nor should the mere reference herein to any drawing, specification, chemical process, or other data be regarded as a license or as a conveyance of any right or permission to the holder, reader, or any other person or corporation, to manufacture, reproduce, use, or sell any patented invention or copyrighted work that may in any way be related thereto. Registered names, trademarks, etc., used in this publication, even without specific indication thereof, are not to be considered unprotected by law.

PRINTED IN THE UNITED STATES OF AMERICA

Foreword

The ACS Symposium Series was first published in 1974 to provide a mechanism for publishing symposia quickly in book form. The purpose of the series is to publish timely, comprehensive books developed from the ACS sponsored symposia based on current scientific research. Occasionally, books are developed from symposia sponsored by other organizations when the topic is of keen interest to the chemistry audience.

Before agreeing to publish a book, the proposed table of contents is reviewed for appropriate and comprehensive coverage and for interest to the audience. Some papers may be excluded to better focus the book; others may be added to provide comprehensiveness. When appropriate, overview or introductory chapters are added. Drafts of chapters are peer-reviewed prior to final acceptance or rejection, and manuscripts are prepared in camera-ready format.

As a rule, only original research papers and original review papers are included in the volumes. Verbatim reproductions of previous published papers are not accepted.

ACS Books Department

Editors' Biographies

Wenlin Chen

Wenlin Chen is a senior scientist at Syngenta Crop Protection, LLC, Greensboro, North Carolina, U.S.A. His area of work focuses on mathematical descriptions of pesticide environmental fate and transport and applications to water quality and ecological risk assessments. He holds a Ph.D. in soil science from Cornell University and has authored/co-authored more than 60 peer-reviewed papers, book chapters, and invited lectures/presentations. He has contributed to the development of pesticide exposure models, scenarios, and risk assessment methods in the U.S. and internationally through several scientific work groups including the FIFRA Environmental Model Validation Task Force, FQPA Drinking Water Exposure Work Group, Environmental Exposure Work Group, and IUPAC Advisory Committee on Crop Protection Chemistry. His current interests include kinetics of rate-limited metabolism, sampling design, and statistical modeling of environmental monitoring data.

Aleksandar Sabljic

Aleksandar Sabljic is Head of Department of Physical Chemistry at Institute Rudjer Boskovic in Zagreb, Croatia since 2002. His research interests and expertise span a wide range of subjects but his recent research is focused on modeling sorption of organic chemicals in soil, their biodegradation in aquatic and soil environments and tropospheric degradation of volatile/semi-volatile chemicals.

After receiving Ph.D. in chemistry from the University of Zagreb (Croatia), he was the Fogarty International Fellow at National Institutes of Health, Bethesda, Maryland (1981-1985). For an extended period (1988-1998), he was Visiting Scientist at Forschungszentrum Karlsruhe and University of Karlsruhe in Germany.

Steven A. Cryer

Cryer received a B.S. in chemical engineering from Texas A&M University, and master's and doctorate degrees in chemical engineering from Cornell University, with emphasis in applied math and hydrodynamic stability. Steve is a strong industrial leader advocating new approaches and scientific advancement to address issues relevant for the agrochemical community, authoring or coauthoring over 80 peer-reviewed papers and conference abstracts, 6 book chapters, multiple

invited presentations and guest lectures, and expert panel participation in areas of wet granulation, pesticide runoff, and volatility of organic chemicals from soil. Steve has been on the adjunct faculty at several Indiana University Departments and has 25 years of experience with Dow AgroSciences.

Rai S. Kookana

Dr. Rai Kookana is a Chief Research Scientist with CSIRO and is also affiliated as a Professor in the School of Agriculture, Food and Wine (University of Adelaide). With a Ph.D. from the University of Western Australia (1989), he has been involved in pesticide research for last 25 years. Dr. Kookana's current research interests include fate of nanoparticles, pesticides and micropollutants (e.g. pharmaceuticals and personal care products) in the environment. He has published 175 journal papers, 15 book chapters, with an H-Index (ISI) of 33 and a total citation > 4500. Dr Kookana has edited three books on environmental contaminants. He is on the editorial boards of 4 international journals. In 2012, Dr. Kookana was elected Fellow of the Soil Science Society of America.

Chapter 1

Introduction

**Wenlin Chen,^{*}1 Aleksandar Sabljic,² Steven A. Cryer,³
and Rai S. Kookana⁴**

¹Syngenta Crop Protection, LLC, P.O. Box 27419-8300,
Greensboro, North Carolina 27419-8300, U.S.A.

²Department of Physical Chemistry, Institute Rudjer Boskovic,
POB 180, HR-10002 Zagreb, Croatia

³Dow AgroSciences, LLC, 9330 Zionsville Road,
Indianapolis, Indiana 46268, U.S.A.

⁴CSIRO, Land and Water Flagship, PMB 2, Glen Osmond 5064, Australia

^{*}E-mail: Wenlin.chen@syngenta.com.

Pesticides are essential tools for crop protection and disease prevention. These agricultural chemicals (and their associated uses) continue to be subject to increased regulatory scrutiny, even though modern pesticides have become safer, more effective, and target specific. Pesticide persistence, off-target movement to ground and surface water systems, and potential for impacting non-target organisms are the major focus for regulatory assessments. Sorption and degradation are among the dominant processes that determine the fate and ecological risk of pesticides in the environment. This book addresses pesticide sorption and degradation processes in the context of regulatory evaluation, yet with a special focus on the chemistry-soil-environment interactions to better quantify the increasingly observed non-first-order and time-dependent behavior in the environmental fate studies.

Degradation of agricultural chemicals is commonly described by pseudo first-order (PFO) kinetics, with the underlying assumption that the rate of degradation is only proportional to the concentration of the degrading compound. The other “reactant” (or reactants) involved in the degradation process is

assumed to be invariant or can be effectively incorporated into the PFO rate constant. For enzyme-catalyzed degradation or biodegradation, the process may become rate-limited when the substrate (i.e. the chemical of interest) is not freely available to microbial metabolism (I), resulting in poor fit of the PFO kinetics to experimental observations. This is particularly true when sorption and diffusion are prominent in controlling mass transfer between the cell surfaces and microbial-absent regions in soil where chemicals are adsorbed, bound or physically entrapped (e.g., in inter-/intra-particle micropores). In such cases, non-first-order degradation and time-dependent sorption may occur simultaneously. Non-first-order degradation may also be induced by microbial dynamics when bioactivity fluctuates over the course of a laboratory study or due to temperature/moisture and/or other agronomic and environmental changes under field conditions.

A common practice to describe pesticide sorption (physical and/or chemical process by which the pesticide becomes bound to a solid substrate) is to assume equilibrium (steady state) during partitioning between the solution and solid phases. In contrast, time-dependent sorption typically describes the process of increasing sorption (or decreasing in a desorption mode) of an organic compound with time in soil. Various physical/chemical mechanisms responsible for time-dependent sorption may include inter-/intra-particle micropore diffusion, surface site adsorption, partitioning, and hydrogen or chemical bonding (2–4).

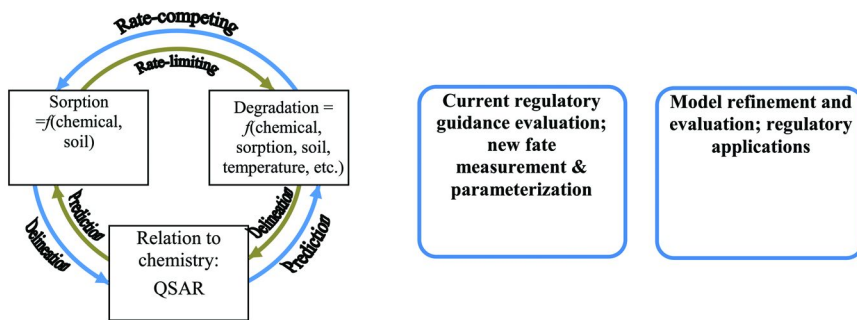
When non-first-order degradation and time-dependent sorption exist, the conventional PFO and equilibrium sorption approaches may not be adequate predictors of the fate and transport behavior of agriculturally important chemicals. The recent publications (5, 6) of regulatory guidance for calculating non-first-order kinetics for pesticide environmental risk and exposure assessments, both in the European Union (EU) and North America Free Trade Agreement (NAFTA), have renewed the interest in refining the measurements, interpretation and use of kinetic data. This ACS book summarizes the combined work recently presented at the 246th ACS National Meeting symposium of Non-First-Order Dissipation and Time-Dependent Sorption of Organic Chemicals in Soil: Measurement, Modeling, and Impact on Environmental Exposure Predictions, September 8 - 12, 2013, Indianapolis, Indiana, USA; and the findings from the International Union of Pure and Applied Chemistry (IUPAC) research project (2010-018-2-600): Review of Pesticide Environmental Fate Parameters and Their Quantitative Relationship with Soil and Climate Conditions (7). Conventional and novel approaches for time-dependent sorption and degradation presented in this book will benefit a large audience of readers, including the regulatory community, academia, government, and industry scientists.

The chapters are arranged according to the three general topics as illustrated in the diagram below. The book starts (Chapter 2) with the interactions of the fate processes (sorption and degradation) and their relationship with chemistry (quantitative structure-activity relationship, or QSAR) and the soil and environmental conditions (Chapters 3, 4, and 5). Evaluation of current NAFTA regulatory kinetics guidance and an overview of using time-dependent sorption studies in EU regulatory exposure assessment are provided in Chapters 6 and 7, respectively. Approaches for data delineation of degradation kinetics and

parameterization are presented in Chapters 8, 9, and 10. New experimental design and methods to measure and quantify time-dependent sorption and irreversibility are described in Chapters 11, 12, 13, and 14. The last section of the book is dedicated to the development of the coupled sorption and degradation kinetics on the EU FOCUS-PRZM model (Chapter 15) and followed by several model evaluation and validation case studies to demonstrate the impact of non-first-order degradation and time- and soil-dependent sorption on the overall environmental fate and transport processes in field conditions (Chapters 16, 17, and 18).

Interaction of fate processes, chemistry and the environment

Regulatory application, measurement, parameterization, and modeling



It is anticipated the state of knowledge and information presented in this book will provide the foundation for stimulating discussion and development of new approaches, leading to more accurate pesticide environmental fate and exposure predictions through improved study measurements, model parameterization, and use of sound kinetics of degradation and sorption algorithms. We realize that the conventional use of the PFO kinetics and instantaneous sorption assumptions has its advantages and may be valid in many cases. However, the text presented here, including discussion of new experimental methods, analysis of kinetics, structure-activity relationships, and refined modeling tools will provide valuable insights to the reader on this topic. We hope that this book will be useful to the broad agrochemical research community including environmental scientists, risk assessors/regulators, students, and general practitioners in environmental exposure, risk assessment, and risk management.

Acknowledgments

The editors extend their sincere thanks to all contributing authors for their hard work to make this book possible, and to all the peer-reviewers who dedicated time to the quality of the book publication. Special thanks are due to Scott Yates and Dirk Young for coordinating the ACS symposium. We acknowledge the financial support from the American Chemical Society Agro-Chemical Division, IUPAC, and Syngenta Crop Protection, LLC, for sponsorship of the symposium and the IUPAC research project (2010-018-2-600). Guidance/assistance received

from the ACS Editorial staff, namely, Julia Johnson, Tim Marney, Arlene Furman, Bob Hauserman, and Ashlie Carlson are greatly appreciated. A special thanks to Julia Johnson for her day-to-day assistance, patience, and always timely response during the book preparation. Cover art photograph is “Barley harvest in Washington’s Palouse Hills”, image number K3937-14, downloaded from <http://www.ars.usda.gov/News/docs.htm?docid=23559>.

References

1. Bosma, T. N. P.; Middeldorp, P. J. M.; Schraa, G.; Zehnder, A. J. B. *Environ. Sci. Technol.* **1997**, *31*, 248–252.
2. Brusseau, M. L.; Rao, P. S. C.; Gillham, R. W. *Crit. Rev. Environ. Control* **1989**, *19*, 33–99.
3. Chen, W.; Wagenet, R. *J. Environ. Sci. Technol.* **1995**, *29*, 2725–2734.
4. Pignatello, J. J. *Adv. Agron.* **2000**, *69*, 1–73.
5. NAFTA Technical Working Group on Pesticides. *NAFTA Guidance for Evaluating and Calculating Degradation Kinetics in Environmental Media*; 2012; http://www.epa.gov/oppefed1/ecorisk_ders/degradation_kinetics/NAFTA_Degradation_Kinetics.htm.
6. FOCUS Work Group on Degradation Kinetics. *Guidance Document on Estimating Persistence and Degradation Kinetics from Environmental Fate Studies on Pesticides in EU Registration*, Report of the FOCUS Work Group on Degradation Kinetics, EC Document Reference Sanco/10058/2005 version 2.0; 2006; <http://focus.jrc.ec.europa.eu/dk/docs/finalreportFOCDegKin04June06linked.pdf>.
7. Chen, W. *Chem. Int.* **2011**, *33*, 23.

Chapter 2

Coupled Sorption and Degradation Kinetics and Non-First Order Behavior

Wenlin Chen,^{*1} Volker Laabs,² Rai S. Kookana,³
and William C. Koskinen⁴

¹Syngenta Crop Protection, LLC, P.O. Box 18300,
Greensboro, North Carolina 27419-8300, U.S.A.

²BASF SE, Crop Protection, Speyerer Straße 2,
D-67117 Limburgerhof, Germany

³CSIRO Land and Water, PMB 2, Glen Osmond,
Adelaide, South Australia 5064, Australia

⁴University of Minnesota, Soil, Water, and Climate, 6028A,
1991 Upper Buford Circle, St. Paul, Minnesota, 55108, U.S.A.

*E-mail: wenlin.chen@syngenta.com.

The spatial distribution of organic compounds in the microscopic soil/pore-water system due to sorption has fundamental implications on determining first-order or non-first order behaviour and assessing bioavailability/biodegradability. If only the fraction of the organic compounds in the microbe-accessible region (e.g., soil pore water) is directly subject to intracellular transformation, sorption into microbe-absent regions (e.g., intra-particle/intra-aggregate micro-pores/interstitial spaces) may become rate-limiting to biodegradation, thus a non-first order decline may be expected in the soil-water system. In this paper, several data sets with direct measurements of soil pore water concentrations are used to elucidate the effect of sorption/desorption on biodegradation. Macro rate constants equivalent to the Double First-Order in Parallel (DFOP) model are derived for gauging the non-first order behavior and for calculating the micro kinetic rate constants of sorption and biodegradability from standard laboratory soil metabolism and batch sorption studies. Two new bioavailability factors (short-term and long-term) are developed to delineate the confounding effect of sorption

and a compound's specific biodegradability on the overall degradation rate in the bulk soil system. The bioavailability factors are shown to be useful in the development of predictive regressions for degradation using soil and environmental factors. Discussions on data interpretation and implications for coordinated study designs of different fate studies are provided.

Introduction

Many published and regulatory required soil metabolism studies have shown that microbial degradation of pesticides can be a non-first order process. Various non-first order degradation models have been proposed to best fit data and to derive representative or worst-case half-life values in order to satisfy the input requirement of the regulatory models for environmental exposure and risk assessments (1, 2). None of these models, however, are mechanistically based, i.e., they are difficult to use for interpreting the observed data and lack of insight into the underlying processes which require cross-examination of other environmental fate studies such as sorption. The aim of this chapter is to offer an approach that couples the two most important fate processes, sorption and degradation, and delineates the effects of soil and other environmental conditions on non-first order behavior.

Interaction between sorption and degradation of organic chemicals in soil is not a new phenomenon. The root cause of the interdependent relationship is the microscopic heterogeneity in distributions of chemical substrates and microbial degraders in the soil pore that prevents metabolism from occurring at the right place and right time. On a microscopic soil pore scale, sorption separates substrate (pesticide) from its degrader (microorganisms) by mass transfer (primarily via diffusion) of the substrate molecules to the soil intra-aggregate/intra-particle pores/interstitial space or organic matrix where microbial access is limited. Soil micro pores with diameters $<0.1 \mu\text{m}$ are abundant while typical size of indigenous bacteria is larger than $0.5 \mu\text{m}$ in diameter³. Bacteria (single or in colonies) typically inhabit in soil pores $\geq 2 \mu\text{m}$ in diameter and the majority of soil pores are smaller than this size with soil moisture content at field capacity levels (3, 4). As a result, physical exclusion of microbes from the micro pores/interstice of soil particles/micro-aggregates may imply that only the fraction of organic compounds in the microbe-accessible region (e.g., in the bulk soil solution or aqueous phase) may be directly subject to intracellular transformation (3–6). This may also include substances sorbed (reversible or irreversible) into the organic matrix in the microbe-accessible regions such as larger pores or micro surfaces in desolate areas. Mass transfer of organic compounds from the microbe-absent regions (or sorbed phase as a general term) thus may become a rate-limiting step to microbial degradation in the soil pore system.

Conceptually, sorption and degradation are initially two competing processes for available molecules in soil pore water when a compound is freshly applied (Figure 1). As more molecules become adsorbed and transferred via diffusion in to the micro pores or intra-particle structure inaccessible to microbes, degradation

rate in the aqueous phase may become limited/controlled by the release speed from the microbial absent zones depending on the intrinsic biodegradability of the compound.

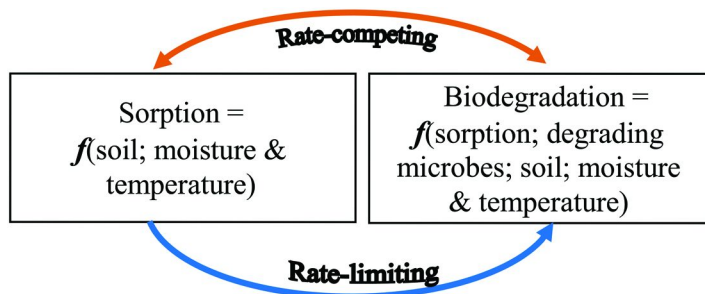


Figure 1. Sorption and biodegradation as a function of environmental factors and their mutual relationship in the soil-pore water system.

Soil variables influencing both pesticide sorption and degradation processes may operate in two ways: (i) variables that predominantly influence the sorption of substances and thereby change the availability of substances for degradation (7); and (ii) variables that indeed influence sorption and degradation processes independently from each other. Sometimes these two mechanisms may not be differentiated easily, as soil parameters are often interrelated and may thereby influence degradation predominantly via their correlation with soil sorption. The independent and/or interrelated soil and environmental variables can influence the interactions between degradation and sorption differently under different macroscopic conditions. Therefore, delineating the exact impacts by various variables requires a detailed description of the two interacting processes in the micro soil-water environment.

In this chapter, we first present a set of mathematical solutions for the coupled sorption and degradation kinetics. Several published literature data sets with direct measurements of soil pore water concentrations are used to elucidate the effect of sorption on degradation. Two macro rate constants equivalent to the Double First-Order in Parallel (DFOP, FOCUS Guidance) are defined and used to measure system deviation from first-order and to estimate micro rate parameters from standard laboratory soil metabolism and batch sorption studies. Two new bioavailability factors are proposed to help delineate the coupled influence of sorption and biodegradability on the overall degradation of the bulk soil system. Attempt is also made to investigate predictive relationships of degradation rates with the new bioavailability factors and soil/environmental variables available from published literature data.

For the sake of simplicity, we use degradation interchangeably with biodegradation on the understanding that degradation through abiotic processes such as hydrolysis is not considered in the context of the discussion herein and that the final breakdown product is not necessarily CO_2 .

Theory

The interactions between sorption and degradation on the pore scale can be conceptualized as a two-step process (Figure 2): 1) mass transfer between the sorbed phase and microbial cell surface in the bulk solution; and 2) biological uptake and transformation (8). For chemicals in the sorbed phase, mass transfer primarily involves desorption (i.e., from the sorbing surfaces inside the nano/micro pores or interstice) and diffusion to the bulk soil solution where microbial colonies reside. For chemicals in the bulk soil solution, the mass transfer process plays a competing role for the dissolved molecules by diffusion into the microbial-absent regions and/or adsorption onto the micro surfaces of soil particles.

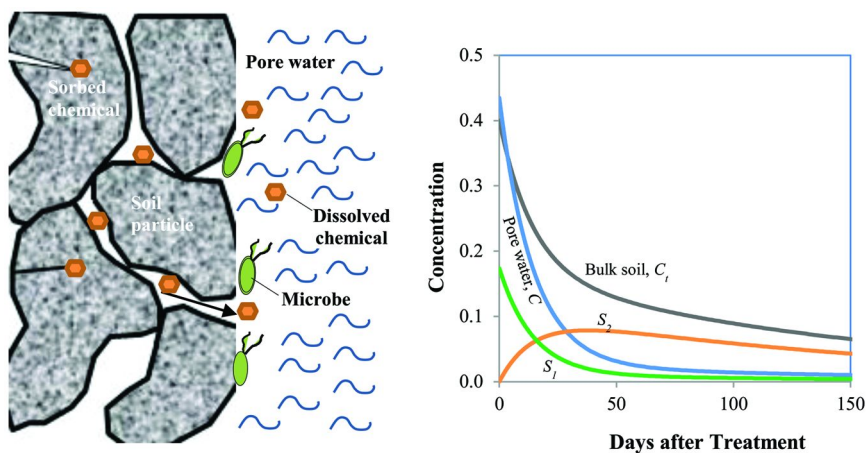


Figure 2. Schematic representation of the soil pore scale distributions of pesticide molecules and microorganisms in the soil-water system (left). The concentration-time course on the right was simulated by Eqs. 5-8 (with parameters: $f=0.2$, $\mu_w=0.1 \text{ d}^{-1}$, $\alpha=0.01 \text{ d}^{-1}$, $K_d=2 \text{ ml/g}$, and $\rho/\theta=3.25 \text{ g/cm}^3$). Concentrations in the aqueous phase (C) and on the instantaneous sorption sites (S_i) decrease faster than the total bulk soil concentration (C_t) which exhibits a clear non-first order decline due to the formation (adsorption) and decline (desorption) on the time-dependent sorbed phase (S_2). (see color insert)

A pseudo first order (PFO) reaction can be used to simplify the lumped microbial uptake and subsequent intra-cellular transformation process given that concentrations of organic chemicals are generally low in the bulk soil solution (8). Since degradation on the sorbed phase is expected to be minimal, the mass balance of an organic chemical in a bulk soil unit can be written:

$$\frac{d}{dt} [\theta C + \rho S] = -\mu_w \theta C \quad (1)$$

Where C is concentration in the dissolved phase; $\mu\text{g/L}$; S is concentration in the adsorbed phase, $\mu\text{g/g}$; θ is volumetric soil moisture content, cm^3/cm^3 ; ρ is soil bulk density, g/cm^3 ; μ_w is degradation rate constant in the soil pore water or aqueous phase, day^{-1} ; t is time, day.

The sorption term (S) in Eq. 1 is described by a two-site kinetics model, which takes into account the bi-phasic behaviour commonly observed in the adsorption-time curve where the initial portion of adsorption takes place quickly and is then followed by a gradual time-dependent phase (9–14). The first type of sorption site(s) (denoted as S_1) is presumably related to the sorbing regions/micro surfaces directly exposed to the soil bulk solution so that sorption in these areas may reach local equilibrium almost instantaneously. The second type of sorption sites (S_2) may represent the sorbing regions inside the micro pores/interstice where diffusion through the micro tortuous space/channels is a slow time-dependent process (15). Assuming Freundlich equilibrium sorption for S_1 , the two-site sorption model can be expressed as the equations below:

$$S = S_1 + S_2 \quad (2)$$

$$S_1 = fK_f C^{1/n} \quad (3)$$

$$\frac{dS_2}{dt} = \alpha[(1-f)K_f C^{1/n} - S_2] \quad (4)$$

Where S_1 is the amount sorbed at the equilibrium sorption sites, $\mu\text{g/g}$; S_2 is the amount sorbed at the time-dependent sorption sites, $\mu\text{g/g}$; f is soil fraction of the equilibrium sorption sites, dimensionless; K_f is Freundlich sorption coefficient when ultimate sorption equilibrium is reached, unit dependent on S_1 and C ; n is Freundlich constant; α is desorption rate constant (or mass transfer coefficient), day^{-1} . Other variables are defined in Eq. 1. For linear sorption isotherms (i.e., $n=1$), the Freundlich coefficient K_f is traditionally termed as sorption partition coefficient and denoted by K_d (unit: ml/g). When K_d is normalized by soil organic carbon, the resulting parameter is denoted as K_{oc} (unit: ml/g).

For linear equilibrium sorption, Eqs. 1-4 can be solved analytically with initial conditions (i.e., at $t=0$, $C=C_0$; $S_1=fK_dC_0$; and $S_2=0$) (16–18). For consistency and complete expressions of defined parameters and variables, several closed-form solutions of key variables are provided below:

$$C = \frac{C_0}{(\lambda_1 - \lambda_2)} [(\alpha + \lambda_1) \exp(\lambda_1 t) - (\alpha + \lambda_2) \exp(\lambda_2 t)] \quad (5)$$

$$S_1 = fK_d C \quad (6)$$

$$S_2 = \frac{\alpha(1-f)K_d C_0}{(\lambda_1 - \lambda_2)} [\exp(\lambda_1 t) - \exp(\lambda_2 t)] \quad (7)$$

$$C_t = C_{t0} [A \exp(\lambda_1 t) + (1-A) \exp(\lambda_2 t)] \quad (8)$$

Where C_t is total bulk soil concentration, $\mu\text{g/g}$; C_{t0} is initial concentration in bulk soil, $\mu\text{g/g}$; A , λ_1 and λ_2 are three “lumped” macro constants which are determined by the micro kinetic parameters α and μ_w and associated equilibrium sorption properties below:

$$\lambda_1 = \frac{1}{2} \left(-(\mu_w + \alpha R)/R_1 + \sqrt{(\mu_w + \alpha R)^2/R_1^2 - 4\alpha\mu_w/R_1} \right) \quad (9)$$

$$\lambda_2 = \frac{1}{2} \left(-(\mu_w + \alpha R)/R_1 - \sqrt{(\mu_w + \alpha R)^2/R_1^2 - 4\alpha\mu_w/R_1} \right) \quad (10)$$

$$R_1 = 1 + fK_d \rho/\theta \quad (11)$$

$$R = 1 + K_d \rho/\theta \quad (12)$$

And
$$A = \frac{1}{\lambda_1 - \lambda_2} \left[\alpha + \lambda_1 + \frac{\alpha(R - R_1)}{R_1} \right] \quad (13)$$

By definition, $f = S_1/(S_1 + S_2)$ when the overall sorption equilibrium is reached at both S_1 and S_2 . It is easy to show that

$$f = K_{d1}/K_d \quad (14)$$

where K_{d1} is the sorption partition coefficient at the instantaneous sorption sites. K_{d1} may be estimated as the measured S/C ratios in a short time period such as 24-hr in the commonly adopted batch equilibration studies.

The coupled kinetics (Eqs. 5-8) reduces to a first order process when the sorption rate constant α is 0 (and $f=1$) or when it is significantly small comparing to the aqueous phase degradation rate constant μ_w . In this case, λ_1 becomes 0 (or approximates to 0) and the equations reduce to a single term of exponential decay. When time-dependent sorption exists, the model is able to predict separate concentrations in the aqueous phase (C) and on the instantaneous and time-dependent sorption sites (S_1 , and S_2) (Figure 2, right panel). Concentration declines in the aqueous phase (C) and on the instantaneous sorption sites (S_1) are typically faster than the total bulk soil system (C_t) due to degradation in the aqueous phase and continuing sorption at the time-dependent sorption sites (S_2). Formation (adsorption) and decline (desorption) can simultaneously take place on S_2 , which contributes to the total system non-first order behavior.

Data Sets

Experimental data obtained from seven published laboratory incubation studies (16, 17, 19–23) (Table1) are used to evaluate the coupled kinetics and the related bioavailability and biodegradability concepts in later sections. Published data of soil column leaching studies are not included given their relatively short

experimental time period (typically in hours) and saturated conditions. Four of the seven studies (16, 17, 19, 20) have used the coupled kinetics model for their data analysis, so their results of model parameters are directly cited here. Three other studies, one by Shelton and Parkin²¹ and two by Krieger et al. (22, 23) (Table 1), did not use the coupled kinetics model but reported the complete measurement data of time-dependent sorption and degradation. Therefore, these published data are used in the current work to fit the coupled kinetics. A brief description of the model-fitting process and the resulting parameters for each of the three studies are provided below.

Table 1. Summary of Published Studies with Complete Measurements of Sorption and Degradation Kinetics Used in Current Analysis

<i>Study</i>	<i>Chemical</i>	<i>No. of soils</i>	<i>Treatment conditions</i>
Beulke et al. (16)	Ethofumesate and Metazachlor	2	Incubation temperature 20 °C; soil moisture at 60% field holding capacity (FHC).
Guo et al. (17)	2,4-D	1	Soil amended with 4 different levels of activated carbon (AC); only data for treatment without AC were used. incubation temperature at 24 °C; soil moisture at field capacity.
Krieger et al. (22)	Oryzalin and metabolites (only parent data used)	4	Incubation temperature 25 °C; soil moisture at 100 kPa.
Krieger et al. (23)	Florasulam and a metabolite (only parent data used)	3*	Incubation temperature ranged from 5 to 35°C; four different soil moisture levels at 40% FHC, 0, 0.05 and 15 bar.
Heiermann et al. (19)	Chlorotoluron	1	Four incubation temperature treatments at 1, 10, 20, and 30 °C; and 3 soil moisture treatments (40%, 60%, and 80% FHC).
Shaner et al. (20)	Mesotrione	4	Incubation temperature 25 °C; soil moisture at 105% FHC.
Shelton and Parkin (21)	Carbofuran	1	Incubation temperature 26 °C; and 5 soil moisture treatments (10-20%, Table 1).

* Only data for two soils (Marcham sandy clay loam and Naicam-Hoodoo clay loam) with apparent K_d measurements are used.

Shelton and Parkin Study (21)

The study was conducted on a Hatsboro silt loam (1.5% OM, and pH 6.05) at five different soil moisture levels (20%, 17.5%, 15%, 12.5, and 10%). All samples were incubated under constant temperature 26 °C. Concentrations of carbofuran both in soil pore water (C) and on the sorbed phase (S) were measured with soil solution samples extracted by a mechanical pressing technique. Detailed descriptions of the experiments, analytical method, and resulting data are available in Shelton and Parkin²¹.

Table 2. Measured and Newly Fitted Parameters from the Shelton and Parkin Carbofuran Soil Degradation Study (21). The Coupled Kinetics Was Simultaneously Fitted to the Measurement Data of Both Apparent K_d (Denoted as K_d^A) and the Soil Solution Concentration C (Two R^2 Values Were Provided).

Gravimetric Soil Water Content (%)	Measured Bulk Soil DT50 (d) *	μ_w (d ⁻¹)	α (d ⁻¹)	$K_d^{\text{§}}$ (ml/g)	$f^{\text{¶}}$	R^2
20.0	4.1	0.25	0.049	0.17	0.35	K_d^A : 0.94 C : 0.85
17.5	4.0	0.30	0.025	0.17	0.41	K_d^A : 0.94 C : 0.83
15.0	4.6	0.31	0.016	0.17	0.59	K_d^A : 0.95 C : 0.85
12.5	7.4	0.15	0.026	0.17	0.35	K_d^A : 0.95 C : 0.96
10.0	13.9	0.08	0.102	0.10	0.39	K_d^A : 0.96 C : 0.98

* Based on the measured % C¹⁴ applied (total of sorbed and aqueous phases). § Sorption equilibrium K_d (0.17 ml/g) was measured in the air-dry soil 21-day incubation treatment except the lowest moisture 10% treatment for which the K_d was fitted from the data. ¶ The fraction of instantaneous sorption (f) was taken as the ratio of the Day 0 measured S/C to K_d (Eq. 14).

The coupled kinetics was fitted simultaneously to the measured concentrations of carbofuran in soil solution and the corresponding ratios of S/C at each sampling point. Results of the best-fit parameters are provided in Table 2. In the optimization process, except the lowest moisture treatment (10%), the equilibrium sorption partition coefficient (K_d) was fixed to the observed value (0.17 ml/g) from the air-dry soil treatment after 21-day incubation where microbial degradation was found minimal (21). The K_d value for the lowest moisture treatment had to be optimized from the data in order to have a best model fit. The fraction of instantaneous sorption sites (f) were taken as the ratio of the apparent K_d measured on Day 0 to the ultimate equilibrium K_d based on Eq. 14.

Krieger et al. Studies (22, 23)

The first Krieger et al. study (22) was conducted for oryzalin and its degradates on four soils in batch incubation at 25 °C (Table 3). Only parent oryzalin data are used in this work. Total soil concentration declines were measured at eight time points from Day 0 to Day 183 after oryzalin treatment. Beginning on Day 15, apparent K_d was measured at six sampling time points by 24-hr desorption with 0.01 N CaCl₂ as the ratio of the total organic solvent-extracted amount (i.e. S) to the CaCl₂-water extract. Ratios of the 24-hr desorption to 5-minute desorption were also reported but are not used for the model fitting exercise. To obtain the parameters of the underlying degradation and sorption kinetics, the measured total soil concentrations and apparent K_d values at each sampling point were simultaneously fitted to the model. Results are reported in Table 3.

The second Krieger et al. study (23) dealt with degradation and sorption of florasulam and its degradate under different temperature and soil moisture conditions. Again, only parent florasulam data are interested in this work. Three soils (Cuckney, Marcham, and Naicam-Hoodoo) were involved in the study. Only Marcham and Naicam-Hoodoo had apparent K_d measurements in addition to total soil concentration declines. As a result, the Cuckney data are not used in our analysis. The Marcham soil had five different temperature treatments and the Naicam-Hoodoo had four, all at the 40% field holding capacity (FHC) moisture level (Table 3). At 20 °C, the Marcham soil had additional three soil moisture treatments at 0, 0.05 and 15 bar. The apparent K_d measurements were only available for the treatments of 40% FHC at 10 °C and 20 °C for Marcham, and 40% FHC at 20 °C for Naicam-Hoodoo. Study details and results are available in Krieger et al. (23).

Given the multi-treatments and limited apparent K_d measurements, a stepwise model fitting procedure is adopted. A full 4-parameter fit (μ_w , α , K_d , and f , Table 3) of the coupled kinetics are first applied to the three treatments of Marcham and Naicam-Hoodoo having apparent K_d data. The fitted sorption-related parameter values (α , K_d , and f) are then fixed and 1-parameter fit (μ_w) is subsequently performed for different temperature treatments of corresponding soils. This step assumes negligible sorption change under different temperature conditions. For the three different moisture treatments on the Marcham soil at 20 °C, no parameter fitting is made. Instead, these data are used to directly compare to the model calibrated at 40% FHC at 20 °C. Results of the best-fit parameters are reported in Table 3. Discussions are provided in the later sections.

Results and Discussion

Data-Model Comparison

Many plots of the data-model comparisons were made available from the cited publications (16, 17, 19, 20), thus they are not duplicated here. An example of the newly model fitted data set of Krieger et al. (23) is displayed in Figure 3. The

model describes the observed data sufficiently well. An interesting trend in the apparent K_d is that it has not shown a plateau after 60 days, indicating that the rate of degradation in the aqueous phase was fast and had not been completely limited by the slower desorption during the time period. The continuing increasing apparent K_d is attributed to the rapid decline of concentrations in the soil pore water due to degradation.

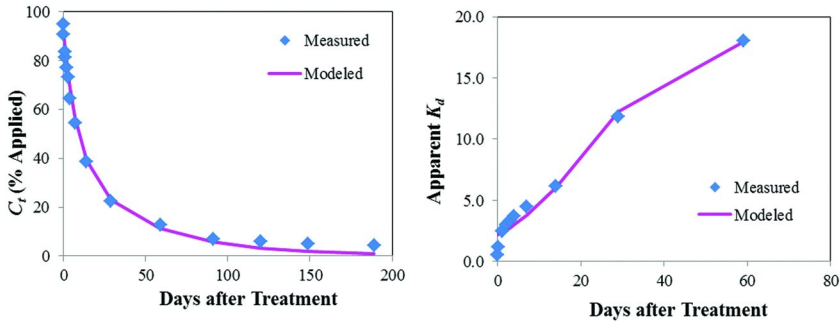


Figure 3. Measured and model-predicted total soil concentrations (left) and apparent K_d (right) of florasulam in a Naicam-Hoodoo clay loam at 20°C and 40% field holding capacity moisture content. Model parameters are provided in Table 3. Study data: Krieger et al. (23).

To illustrate a model comparison with more elaborated measurements of soil pore water and the sorbed mass using centrifugation technique at near field capacity levels, the recent batch incubation study by Shaner et al. (20) is used. In this study, mesotrione degradation was investigated for four different soils. Results of the study showed that the coupled kinetics were able to predict the measured individual declines in the pore water and on the sorbed phase generally well (Figure 4; only one soil is shown). Since the measured sorbed phase concentrations included both instantaneous and time-dependent sorption, the total sorbed amount ($S_1 + S_2$) was plotted in the figure. Although the total amount of sorption (black dash line and circles) was initially overestimated and later underestimated by the model, there was no direct data to show this was related to the quantity of S_1 or S_2 , or both. Mathematical constraints of the optimization process were quite strong since individual declines had to be fitted simultaneously to avoid over-fitting of one process over another. Consistent with the simulation in Figure 2, the measured dissipation in pore water was fast due to degradation and sorption. The total bulk soil system demonstrated a clear non-first order decline. Detailed results for other soils are available in Shaner et al. (20).

Table 3. Measured and Newly Model-Fitted Parameters for Oryzalin and Florasulam from the Studies by Krieger et al. (1998 and 2000) (22, 23). Full Model Fits (with 4 Parameters) Were Applied to Soils with Available Measurements of Both Apparent K_d (denoted as K_d^A) and the Total Soil Concentration C_t (Two R^2 Values below). When only C_t Data Available, One Parameter (μ_w) Was Fitted and Other Sorption Parameters Were Held Constant to the Values from the Corresponding Full Model Fits.

<i>Soil</i>	<i>T</i> (°C)	<i>Gravimetric Soil Water Content (%)</i>	<i>Measured Bulk Soil DT50 (d)</i>	μ_w (d^{-1})	α (d^{-1})	K_d (ml/g)	f	R^2
Oryzalin Study ²²								
Fox Sandy Loam [§]	25	7.9*	42	1.086	0.00807	5.75	0.85	K_d^A : 0.95 C_t : 0.99
Traver Loam [§]	25	17.8*	25	1.005	0.01425	6.87	0.96	K_d^A : 0.96 C_t : 0.97
Hanford Sandy Loam [§]	25	8.5*	24	2.643	0.00091	8.05	0.95	K_d^A : 0.96 C_t : 1.00
Millhopper sand [§]	25	2.2*	176	1.416	0.00061	12.89	0.59	K_d^A : 0.86 C_t : 0.84
Florasulam Study ²³								
Marcham sandy clay loam [§]	10	21.4	23	0.196	0.0169	2.09	0.30	K_d^A : 0.93 C_t : 1.00
Marcham sandy clay loam [¶]	5	21.4	18	0.196	0.0169	2.09	0.30	C_t : 0.85
Marcham sandy clay loam [§]	20	21.4	4.1	0.715	0.0071	2.09	0.30	K_d^A : 0.98 C_t : 0.95

Continued on next page.

Table 3. (Continued). Measured and Newly Model-Fitted Parameters for Oryzalin and Florasulam from the Studies by Krieger et al. (1998 and 2000) (22, 23). Full Model Fits (with 4 Parameters) Were Applied to Soils with Available Measurements of Both Apparent K_d (denoted as K_d^A) and the Total Soil Concentration C_t (Two R^2 Values below). When only C_t Data Available, One Parameter (μ_w) Was Fitted and Other Sorption Parameters Were Held Constant to the Values from the Corresponding Full Model Fits.

Soil	T ($^{\circ}\text{C}$)	Gravimetric Soil Water Content (%)	Measured Bulk Soil DT50 (d)	μ_w (d^{-1})	α (d^{-1})	K_d (ml/g)	f	R^2
Marcham sandy clay loam	15	21.4	7.4	0.403	0.0071	2.09	0.30	C_t : 0.88
Marcham sandy clay loam	25	21.4	1.3	2.118	0.0071	2.09	0.30	C_t : 0.97
Naicam-Hoodoo clay loam [§]	20	31.1	8.5	0.601	0.0316	4.43	0.49	K_d^A : 0.97 C_t : 1.00
Naicam-Hoodoo clay loam	35	31.1	1.7	3.203	0.0316	4.43	0.49	C_t : 0.99
Naicam-Hoodoo clay loam	10	31.1	46	0.165	0.0316	4.43	0.49	C_t : 0.98
Naicam-Hoodoo clay loam	5	31.1	85	0.079	0.0316	4.43	0.49	C_t : 0.98

* 75% of the field holding capacity. § Full 4-parameter fit. * The 5 $^{\circ}\text{C}$ treatment of Marcham used the sorption parameters from the 4-parameter fit to the 10 $^{\circ}\text{C}$ treatment.

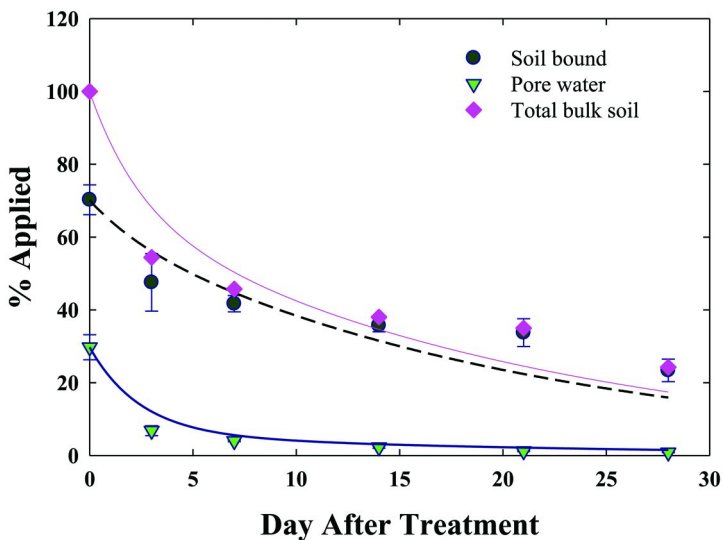


Figure 4. Measured and model-predicted mesotrione concentrations in soil pore water and on the sorbed phase of a Spinks loamy sand soil. Concentrations are expressed as percent of total applied mass. Total concentrations in bulk soil are the sum of the amount in the aqueous and sorbed pools in % applied. Measured and modeled data are re-plotted based on results from Shaner et al. (20).

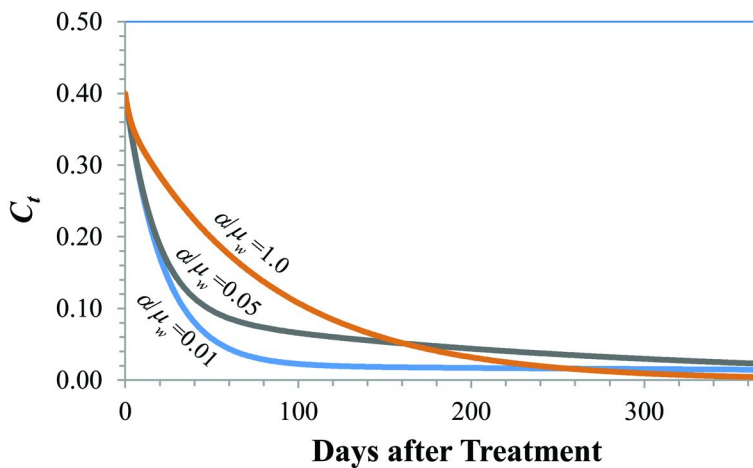


Figure 5. Simulated bulk soil concentration with three different rate constant ratios (α/μ_w) of sorption to degradation in the soil aqueous phase. Other parameters were the same as used in Figure 2: $f=0.2$, $K_d=2$ ml/g, and $\rho/\theta=3.25$ g/cm³. (see color insert)

Effect of Time-Dependent Sorption

One of the benefits with the coupled kinetics model is its ability to readily delineate the effect of sorption on degradation. To do this, we can use the ratio α/μ_w to measure the relative easiness (or bioavailability) of sorbed compound to be released to the soil pore water and subsequently metabolized by microorganisms. Larger ratios indicate relatively faster desorption than degradation so that mass supply is sufficient for degradation in the soil pore water. To illustrate, simulated concentrations in the total bulk soil system with three different rate constant ratios of desorption to aqueous phase degradation (α/μ_w) are plotted in Figure 5. It is seen that the total system concentration becomes less bi-phasic and follows first-order more closely as the α/μ_w ratio increases to 1 (i.e., yellow line in Figure 5). Strong bi-phasic decline (i.e., fast early decline followed by a slowed phase) is associated with the two smaller α/μ_w ratios (blue and black lines), indicating rate-limiting effect of desorption when sorption becomes relatively slower than degradation.

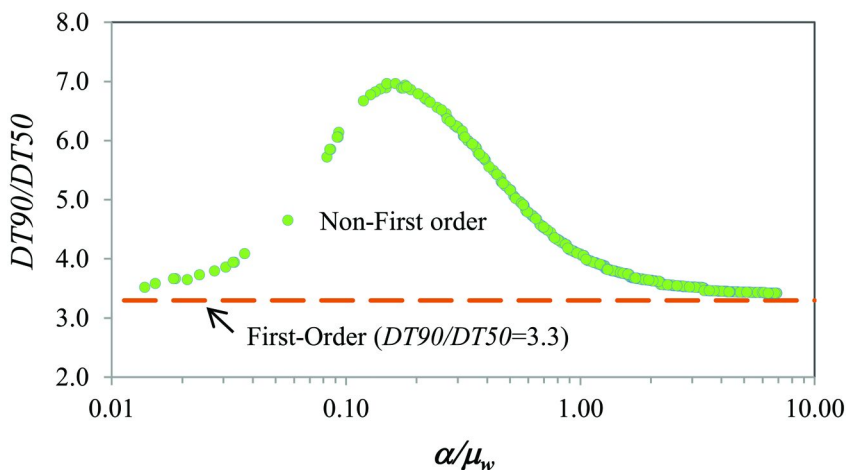


Figure 6. Effect of rate constant ratio (α/μ_w) on system non-first order behavior. Other parameters used in the simulations are held constant at $f=0.3$, $K_d=1$ ml/g, and $\rho/\theta=2.5$ g/cm³.

It should be pointed out that the effect of sorption rate constant on the kinetic behavior of degradation is not monotonic, i.e., the system can be approximately first-order when the ratio α/μ_w becomes either significantly small or large (≥ 1). Significantly small α/μ_w means that sorption is extremely slower than degradation, resulting in the majority of the applied chemical in the soil aqueous phase (recall adsorption rate is proportional to desorption by a factor of K_d) being available for quick first-order microbial degradation. As illustrated in Figure 6, for a true first-order process, the $DT90/DT50$ ratio is approximately 3.3 (dashed line), where $DT50$ and $DT90$ are two degradation time points corresponding to 50% and 90%

of total applied mass degraded, respectively. With everything else held constant, large deviations from the 3.3 line occurred when α/μ_w is valued between 0.05 and 1.0 (Figure 6), indicating strong system non-first order behavior in this range. However, this range may vary as it will be shown later that other system parameters (such as θ , f and K_d) can alter the system non-first order behavior as well.

To examine the effect of α/μ_w with measured data, results of the Shaner et al. study (20) with measured and model-predicted total system decline curves of four soils are plotted in Figure 7. The data-fitted ratios (α/μ_w) are indicated on each of the fitted curves by the coupled kinetics (black dash lines). As shown in the figure, the coupled kinetics approach predicted the full time scale noticeably better than the first-order model (solid pink lines) which underestimated the earlier and overestimated the later measured concentrations (except the Haxton soil). For the Haxton soil, the α/μ_w ratio was the smallest (0.013). The better fit with a first-order model on this soil is consistent with the simulation study which shows that first-order generally holds when the α/μ_w ratio falls outside of the range 0.05 to 1.0.

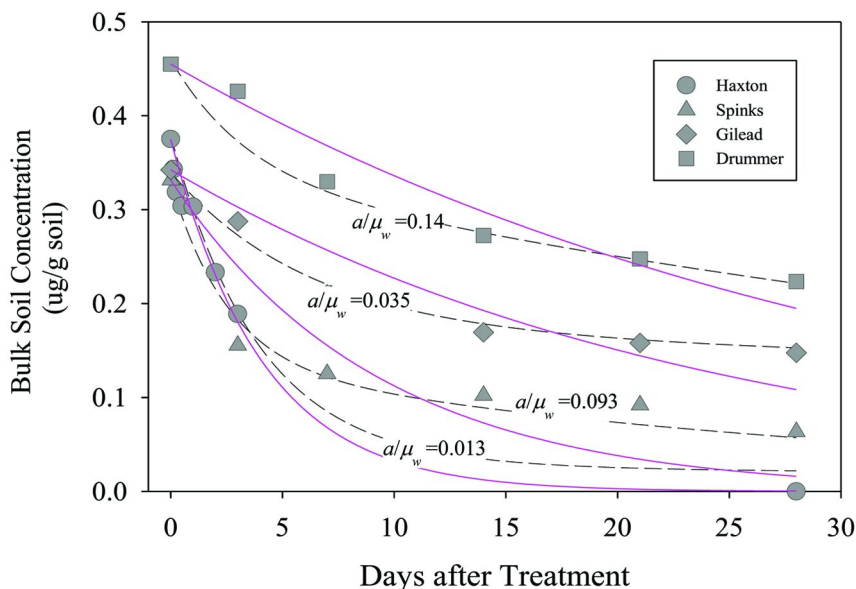


Figure 7. Measured (dots) and predicted (lines) total bulk soil concentrations in the Shaner et al. study (20). Pink lines are fitted by first-order and the black lines are by the coupled kinetics. Indicated in the figure are the ratios (α/μ_w) of sorption rate constant to aqueous phase degradation rate constant. (see color insert)

Effect of Soil Moisture

Soil moisture plays a critical role in microbial survival by maintaining cell hydration and serving as a medium for nutrient supply (24). Many studies have found that pesticide degradation decreases as soil becomes drier (21, 25–27). The decrease in degradation (represented by $DT50$) was found to follow a power

function relationship with soil water content (25). In the coupled kinetics (Eqs. 5-8), soil water (θ) determines the micro space where microbial degradation takes place. It is thus expected that a similar impact of soil water on the $DT50$ value may be accounted for by the model and the overall non-first order behavior may vary correspondingly.

To evaluate the effect, the coupled kinetics was simulated over a range of soil moisture contents from 0.07 to 0.4 cm^3/cm^3 soil, with other parameters held constant (Figure 8). Values of $DT50$ and the ratio of $DT90/DT50$ were calculated for each simulation and plotted against the soil water content (θ) (all other parameters were held constant). Results of the simulations show that $DT50$ decreases rapidly as θ increases, indicating faster degradation when soil is wetter (Figure 8). Interestingly, the decline trend follows a power function, consistent with the experimental observations by Walker (25) and others (27). Response of the $DT90/DT50$ ratio to θ changes is not monotonic, thus moisture may increase or reduce the deviation of the underlying kinetics from first-order in the presence of time-dependent sorption.

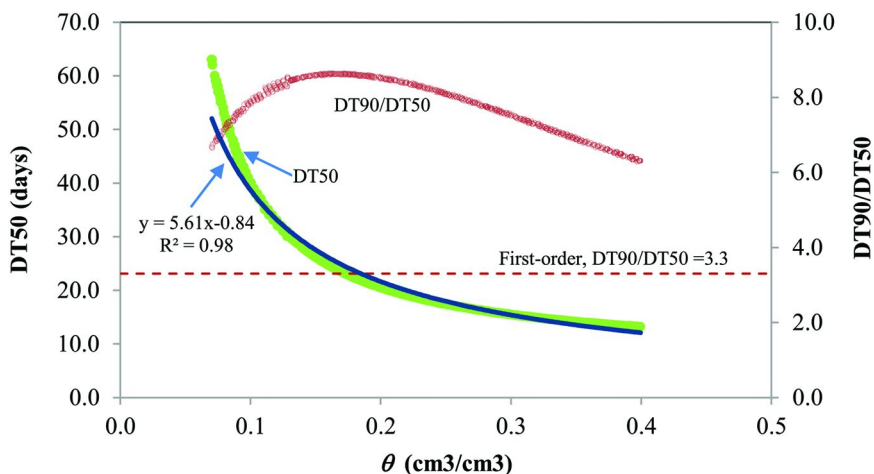


Figure 8. Effect of soil moisture on microbial degradation. The green circles are $DT50$ values obtained from simulations of the coupled sorption and degradation kinetics (Eqs. 5-8) with variable soil moisture content (θ) ranging from 0.07 to 0.40 cm^3/cm^3 . Other parameters were $f=0.3$, $\mu_w=0.1 \text{ d}^{-1}$, $\alpha=0.01 \text{ d}^{-1}$, $K_d=1 \text{ ml/g}$, and $\rho=1.0 \text{ g/cm}^3$. Red dots are $DT90/DT50$ values. The blue line was fitted by the Walker power function between $DT50$ and soil water content.

The soil moisture effect observed from the model simulations is examined with the published experimental data for carbofuran degradation by the Shelton and Parkin study (21). Measured and modeled ratios of S/C (or apparent K_d) at each sampling point are plotted in Figure 9 for the five different soil moisture treatments (Table 2). The model-measurement comparison suggests that the coupled kinetics describes the measured data reasonably well under the various soil moisture conditions. The optimized aqueous phase degradation rate constants

(μ_w , Table 2) are comparable among the first three high moisture treatments (15% - 20%), ranging from 0.25 to 0.31 d⁻¹. However, as soil moisture decreased to below 15%, carbofuran metabolism in the soil aqueous phase becomes noticeably prohibited, with the smallest degradation rate constant (0.08 d⁻¹) corresponding to the lowest moisture treatment at 10%. Similar results are reflected in the measured total bulk soil DT50 values (Table 2). Interestingly, the response of sorption kinetics to the five different soil moisture levels is not monotonic, with the desorption rate constant (α) decreasing from 0.049 to 0.016 d⁻¹ then increasing to 0.102 d⁻¹ as soil moisture content progressively decreases from 20% to 10%. Sorption equilibrium parameters (K_d and f) also vary across different treatments, indicating potential effect of sorption sites under different soil hydration conditions.

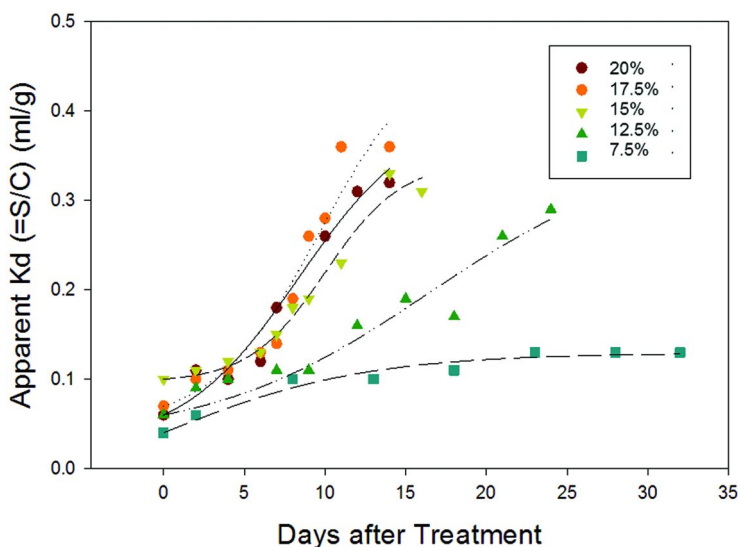


Figure 9. Measured and modeled apparent K_d ($K_d^A = S/C$) values of carbofuran at various time points after treatment in a Hatsboro silt loam in Shelton and Parkin (21). Indicated in the figure are five different soil moisture levels in the degradation study. Lines are predicted by the coupled kinetics model with parameters reported in Table 2. (see color insert)

System equilibrium between degradation and sorption kinetics is not observed in the measured and modeled apparent K_d values with the exception of the lowest soil moisture treatment (10%) where there appears a plateau is reached at around 23 days after carbofuran application (Figure 9). As pointed out by Shelton and Parkin (21), microbial degradation in the soil pore water was relatively faster than desorption so that sorption was the “rate-limiting” factor at higher moisture levels. With decreasing soil moisture, metabolism became progressively inhibited due to desiccation of the carbofuran-hydrolyzing microorganisms, resulting in the control of the overall process by the degradation kinetics. Consistent with

these observations, comparison of the optimized kinetic rate constants in Table 2 provides a quantitative confirmation that the aqueous metabolism rates were much faster than sorption when soil moisture content was higher. Metabolism became much slower when soil moisture was below 15%, thus limiting the overall kinetics in the total system.

The decrease of microbial metabolism in the soil pore water appeared to follow the Walker power function relationship with moisture contents (Figure 10). The same relationship also holds for the bulk soil *DT50*, which suggests that the overall effect of soil moisture on degradation is twofold: 1) the amount of water that directly influences the resulting amount of substance in solution available for degradation; 2) at certain soil moisture limits (such as desiccation or anaerobic conditions) where the microbial ability for substance degradation is impacted. The first effect is taken into account by the coupled kinetics model directly as shown in Figure 8. The second effect, however, requires the corresponding change in the metabolism rate constant (μ_w) of the model to reflect the changes of microbial activity under different soil water conditions.

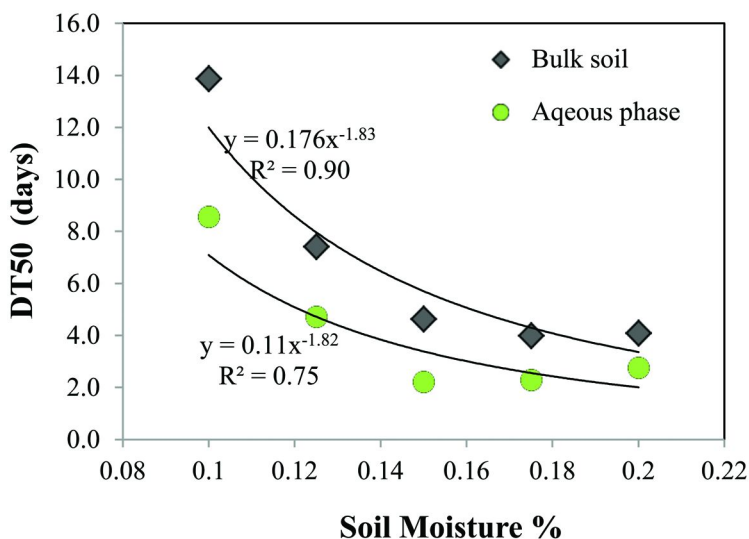


Figure 10. Relationship of carbofuran degradation in soil pore water and total bulk system with variable soil moisture contents. Data source: Shelton and Parkin (21).

The moisture effect on the degradation of florasulam, however, was not found as significant in the Krieger et al. study (22). As mentioned previously, four different soil moisture treatments corresponding to 40% FHC, 0, 0.05 and 15 bar on a Marcham sandy clay loam soil were designed in the study. Temperature for these treatments was fixed at 20 °C. Using the calibrated parameters from the 40% FHC treatment (corresponding to 20°C and 21.4% moisture in Table 3), the model predicted very well the measured total soil concentration declines for the other three moisture treatments at 40.6% (0 bar), 25.4% (0.05 bar) and 15.5% (15 bar) on

the same soil (Figure 11, only the 15 bar treatment is shown). The minimal impact of soil moisture on degradation in this study may be attributed to the relatively high moisture levels at which the soil was able to maintain even at the 15 bar pressure (i.e. 15.5%). Recall that in the Shelton and Parkin study (21), significant decrease in carbofuran degradation rate was observed only when soil moisture decreased to below 15%.

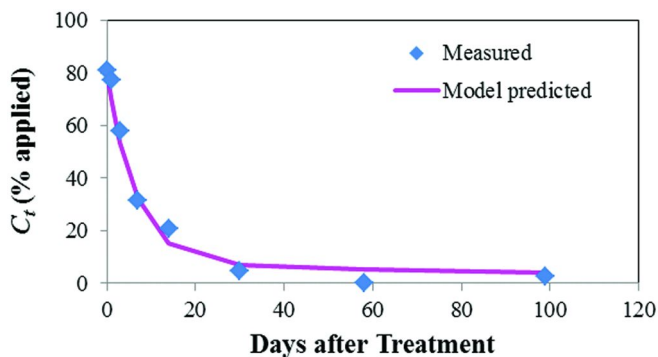


Figure 11. Model independent predictions of florasulam degradation on a Marcham sandy clay loam at 15.5% soil moisture content (15 bar) and 20 °C. Model parameters were calibrated from a different treatment at 40% FHC (21.4%). Data source: Krieger et al. study (22).

Relation to Double First-Order in Parallel.

It is interesting to observe that the analytical solutions for the concentration in soil water (Eq. 5) and the total bulk soil system (Eq. 8) are both double exponential decay, a decline pattern well observed in many soil metabolism and field dissipation studies (28, 29). The model is also termed as Double First-Order in Parallel (DFOP) by the EU FOCUS kinetics guidance document (2) and used by the NAFTA technical guidance (1) for evaluating and calculating pesticide kinetics parameters. DFOP is identical to Eq. 8 with different symbols to denote the macro parameters:

$$M = M_0 [g \exp(-k_1 t) + (1 - g) \exp(-k_2 t)] \quad (15)$$

where M is mass per unit volume of bulk soil; M_0 is the initial value of M at time 0; k_1 and k_2 are two macro rate constants, day⁻¹; g is the fraction of degradation associated with rate constant k_1 .

Assuming k_1 is the smaller rate constant in Eq. 15 (i.e., $k_1 < k_2$), Eqs. 8 and 15 becomes identical by setting $A=g$; $\lambda_1 = -k_1$; and $\lambda_2 = -k_2$. From the definition of the proxy variable A (Eq.), it is easy to show

$$\alpha = [k_1 + g(k_2 - k_1)] \frac{R_1}{R} \quad (16)$$

$$\mu_w = \frac{k_1 k_2 R_1}{\alpha} \quad (17)$$

Eqs. 16 and 17 establish a method to estimate the two important parameters in the coupled kinetics: sorption rate constant (α) and microbial metabolism rate constant in the soil pore water (μ_w) using the fitted DFOP coefficients (g , k_1 and k_2) and the sorption equilibrium parameters (f and K_d) measured for the same soil. It is expected that this method is desirable since it does not require direct measurement of the soil aqueous phase degradation, given that sorption equilibrium parameters are relatively easy to measure. For example, the fraction of the instantaneous sorption sites (f) can be taken as the ratio (i.e. Eq. 14) of the Day 0 measured S/C to the ultimate equilibrium K_d which can be achieved under long term incubation studies when degradation is minimized. Robustness of the method may be achieved by coordinating soil metabolism and sorption equilibrium studies on the same soil type and laboratory conditions.

It is intuitively expected that the two lumped macro rate constants (λ_1 and λ_2 , or, k_1 and k_2 in DFOP) may be used to measure the system non-first order behavior (analogous to α/μ_w in previous section). Perfect first order is attained when the two macro constants are equal or the ratio between them is 1. The closer the ratio is to 1, the better approximation of the kinetic system is to first order. The specific ratio of λ_2/λ_1 is expected to be greater than 1 because the absolute value of the second macro constant (λ_2) is always larger than that of the first (i.e., λ_1) based on Eqs. 9 and 10. In other words, for a clear non-first order decline, the second exponential has to decay significantly faster than the first, exhibiting a pronounced biphasic degradation pattern.

To investigate the system behavior under a wide range of possible combinations of different equilibrium and kinetic parameters, a total of 5000 Monte Carlo simulations were conducted with the coupled kinetics model (Eqs. 5-8) assuming four independent and uniform probability distributions of K_d (0-10 ml/g), f (0-1), α (0-0.69 d⁻¹), and μ_w (0-0.69 d⁻¹). The ranges in parentheses are the minimum and maximum values in each uniform distribution. Values of $DT50$ and $DT90$ and the corresponding macro rate constants (λ_1 and λ_2) were calculated from each simulated decline curve of the bulk soil concentration.

Results of the $DT90/DT50$ ratios were plotted against the corresponding ratios of λ_2/λ_1 in Figure 12. Similar to the previous findings, there is no 1-to-1 monotonic relationship between the two sets of ratios. Generally, as the λ_2/λ_1 ratio increases, initial increasing deviation from first-order is observed despite noticeable variability. However, continued increase in the λ_2/λ_1 ratio after near 50 reduces the deviation from the first order line and the system falls back to approximately first-order. The $DT90/DT50$ ratios are at around 10 or smaller when the λ_2/λ_1 ratio is near or less than 10 or greater than 50. We will show in the next section that the system can be effectively approximated as a first order process when the λ_2/λ_1 ratio falls within the two regions (i.e., $\lambda_2/\lambda_1 \leq 10$, or ≥ 50).

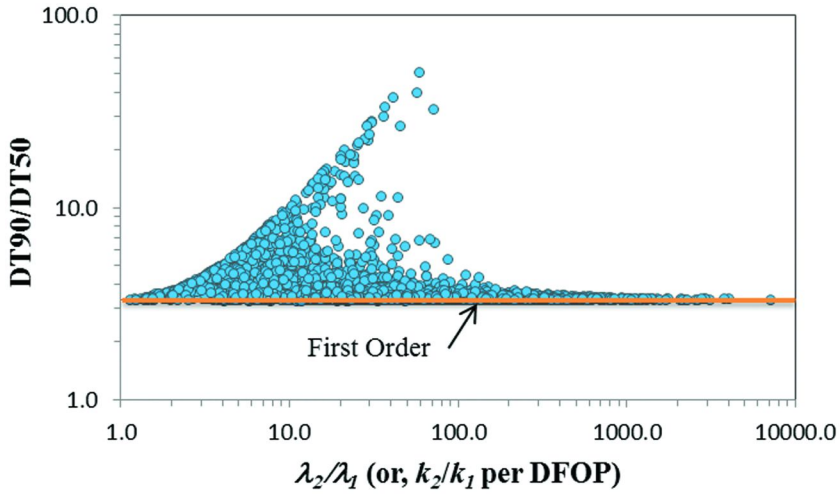


Figure 12. Effect of the macro rate constants in DFOP on system non-first order behavior. Results were from 5000 Monte Carlo simulations with the coupled kinetics assuming four uniform probability distributions of K_d (0-10 ml/g), f (0-1), α (0-0.69 d^{-1}), and μ_w (0-0.69 d^{-1}). The ratio of soil bulk density to moisture content (i.e., ρ/θ) was fixed at 2.5. Degradation times of DT50 and DT90 were determined from the decline of total bulk soil concentration for each Monte Carlo simulation.

Bioavailability Factor

The non-first order behavior is shown to be dependent not only on the relative comparison of the macro or micro kinetic rate constants (i.e., λ_2/λ_1 and α/μ_w) but also on the equilibrium parameters (f and K_d) and water content in the soil water system. It would be useful if the effects of these influential factors can be integrated into a single quantitative measure to gauge degradation under different conditions. To this end, we rearrange Eq. 1 to give:

$$\frac{dC}{dt} = - \frac{\mu_w}{1 + \frac{\rho}{\theta} \frac{d(S_1 + S_2)}{dC}} C \quad (18)$$

The expression in the denominator on the right side of Eq. 18 is a correction factor for the aqueous phase metabolism rate constant (μ_w). That is, Eq. 18 becomes simple first order if we define a bioavailability factor (B_f) as:

$$B_f = \frac{1}{1 + \frac{\rho}{\theta} \left(fK_d + \frac{dS_2}{dC} \right)} \quad (19)$$

Eq. 18 is then simplified to a form of the first order model:

$$\frac{dC}{dt} = -B_f \mu_w C \quad (20)$$

Equation 20 suggests that the overall effective degradation rate is determined by the aqueous phase metabolism rate constant (μ_w) discounted by the bioavailability of the compound at the time when microbial breakdown takes place. The product $B_f^* \mu_w$ is an effective rate constant of degradation while the aqueous metabolism rate constant (μ_w) essentially represents the microbial activity or optimal breakdown in the soil pore water (i.e. no rate-limiting by sorption). The optimal rate constant (μ_w) is, therefore, a measure of potential degradation or biodegradability inherent to a specific compound under given temperature/moisture and microbial conditions.

It should be pointed out that Eq. 20 is a true first order only if B_f is constant, such is the case when sorption is instantaneous and in equilibrium linearly with local solution. In this case, $dS_2/dC=(1-f)K_d$, and

$$B_f = \frac{1}{1 + \frac{\rho}{\theta} K_d} \quad (21)$$

In Eq. 21, B_f is a function of equilibrium sorption and the relative proportions of soil and water in the system. It approaches unity when K_d is small, meaning that for non-sorbing (or weakly sorbing) compounds, they are completely (or approximately 100%) available to microbial transformation in the soil water system. Correspondingly, for strong sorbing molecules, very large K_d diminishes bioavailability, resulting in retarded microbial transformation in the liquid phase. Interestingly, higher bioavailability may also be achieved in systems where the proportion of the soil mass is relatively small to water (i.e., small ρ/θ such as in an aerobic aquatic system). Experimental implications of this may lie with the applicability of measuring biodegradability (μ_w) using an aquatic system such as approaches often adapted in remediation studies where chemical biodegradability is evaluated by inoculating specific microbial strains into aquatic test assays in absence of environmental sediments (30, 31). Validity of similar study designs to simulate the soil pore water environment, however, deserves more research, especially in the aspects of dilution of the indigenous microorganisms and achieving true aerobic conditions in laboratory aquatic setups.

Clearly, B_f is not a constant when time-dependent sorption exists. In this case, the ratio dS_2/dC in Eq. 19 is a function of time. However, constant B_f may be derived for two asymptotic time points: short-term at time near 0, and long-term when t approaches ∞ . We denote the first as short-term bioavailability B_{fS} , and the second as a long-term one B_{fL} .

Short-Term Bioavailability Factor B_{fs} .

In the early stage after a compound is applied to soil, majority of the chemical (except strong and instantaneous sorbing molecules) is expected to be bioavailable to microbial transformation as sorption continues with time relatively slowly. This is often shown in the observed bi-phasic concentration decline of soil metabolism studies where initial degradation is much faster than the later stage. The initial bioavailability may be quantified from Eq. 19, assuming S_2 is approximately 0 or relatively small comparing to S_1 in the early stage:

$$B_{fs} = \frac{1}{1 + \frac{\rho}{\theta} f K_d} \quad (22)$$

Long-Term Bioavailability Factor B_{fl} .

For aged soil residues, desorption from the microbial-inaccessible sites becomes more important in determining the bioavailability to microbial breakdown in the soil pore water. Using the analytical solutions Eqs. 5 and 7, it can be shown that

$$\frac{dS_2}{dC} = \frac{(1-f)\alpha K_d}{\alpha + \lambda_1} \quad \text{when } t \rightarrow \infty \quad (23)$$

Substituting the ratio dS_2/dC into Eq. 19 gives

$$B_{fl} = \frac{1}{1 + K_d \frac{\rho}{\theta} \left(f + \frac{(1-f)\alpha}{\alpha + \lambda_1} \right)} \quad (24)$$

Eq. 24 shows that B_{fl} is a function of both equilibrium and kinetic sorption parameters as well as the associated environmental conditions implicitly reflected in the biodegradability (μ_w) and soil:water ratio (ρ/θ). The calculation is exact when degradation in the soil pore water is completely limited by desorption. This is equivalent to the case where μ_w is approximately equal to α . Using this condition and assuming no instantaneous sorption (i.e., $f=0$), Zhang et al. provided an approximation for B_f . As shown in Figure 13, the two approaches converge as the ratio α/μ_w decreases. However, when sorption rate increases relative to degradation (i.e., α/μ_w becomes larger), the Zhang et al. approximation tends to under-estimate B_f .

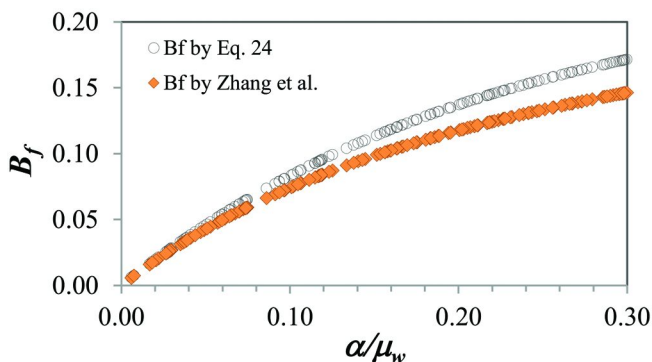


Figure 13. Comparison of bioavailability factors calculated by Eq. 24 (black circles) and the Zhang et al. approximation (orange diamonds),

$$B_f = 1 / \left[1 + K_d \frac{\rho}{\theta} (1 + \mu_w / (\alpha K_d \rho / \theta)) \right] \text{ after using consistent symbols for Eq. 16 in Zhang et al. (32).}$$

Relationship of B_f with Degradation Time

The parameter B_f is essentially a correcting factor for the metabolism rate in the soil pore water to account for the effect of sorption and the associated micro environmental conditions. For first order, degradation time (e.g., DT_{50} and DT_{90}) is inversely related to the effective rate constant (i.e., $B_f * \mu_w$). For non-first order, the inverse relationship may vary as B_f is time-dependent due to continuous sorption. It would be desirable to identify conditions under which the underlying kinetics may be approximated by first-order and the inverse relationship holds so that degradation parameters can be estimated by either the short-term or long-term bioavailability factors defined above. Such relationships would benefit regression studies aimed at predicting degradation with soil and other environmental variables.

To investigate the B_f effect, results of the DT_{50} values obtained from each of the 5000 Monte Carlo simulations as described in the previous section were plotted as a function of the aqueous phase rate constant (μ_w , black circles) and its two products with the short-term ($\mu_w * B_{fS}$) (orange circles on the left) and the long-term bioavailability factors ($\mu_w * B_{fL}$) (orange circles on the right) in Figure 14. Two observations can be made from these simulations. First, DT_{50} is not perfectly and inversely correlated with μ_w as it should hold for perfect first-order kinetics. Significant variability exists in the relationship despite an overall inverse trend over the 5000 simulations made with assumed distributions of equilibrium and kinetic parameters. Second, the vast scatter suggests that neither the short-term nor the long-term bioavailability factors can be used as a universal correcting quantity to accurately reduce the underlying kinetics to a first-order equivalent.

However, under certain conditions using the two macro rate constants, λ_1 and λ_2 , the two bioavailability factors can be quite effective to simplify a coupled sorption-degradation system into a first order reaction as shown in Figures 15 and 16 below.

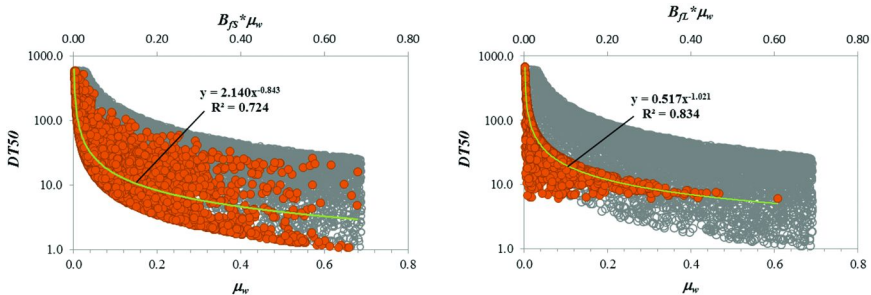


Figure 14. Degradation time (DT_{50}) as function of biodegradability (μ_w) and the short-term (B_{JS}) and long-term (B_{FL}) bioavailability factors. Open black circles are plotted with μ_w on the bottom x-axis. Orange circles are plotted with the effective rate constants as the products of ($\mu_w * B_{JS}$) or ($\mu_w * B_{FL}$) using the top x-axis. Results were from 5000 Monte Carlo simulations described in Figure 11. (see color insert)

When the macro rate constant ratio (λ_2/λ_1) is equal to or less than 10, it is quite significant to observe from Figure 15 that the scatter in data points coalesce into a much better correlation of DT_{50} and DT_{90} associated with the short-term bioavailability factor (i.e., $\mu_w * B_{JS}$) (orange circles). It can be shown that the closer the (λ_2/λ_1) ratio is to 1, the more accurate the inverse relationship becomes, indicating increasing robustness of the short-term bioavailability for reducing degradation to first-order. The long-term bioavailability factor is relatively less effective (results not shown). Kinetic sorption becomes less influential (or rate-limiting) on degradation as the (λ_2/λ_1) ratio approaches to unity. In these cases, degradation kinetics is expected to be more related to the instantaneous sorption properties. That is, the short-term bioavailability plays a more effective role in determining the overall speed of degradation.

For kinetics systems of larger (λ_2/λ_1) ratios, the long-term bioavailability factor becomes more important in determining degradation time. As illustrated in Figure 16, when the two macro rate constants differ further apart (i.e., $\lambda_2/\lambda_1 \geq 50$), almost a perfect inverse relationship of DT_{50} and DT_{90} with the long-term bioavailability B_{JS} is established for the most part (except in the area of μ_w near 0). Comparatively, the short-term bioavailability factor is less influential under these conditions (not shown). Larger differences between λ_1 and λ_2 suggest more prominent effects of sorption kinetics on degradation. Slow sorption becomes the rate-controlling step for metabolism in the soil pore water. As a result, the overall degradation can be approximated as a first order process with the effective rate constant best determined by the long-term bioavailability factor (B_{FL}). This makes sense as the quantity B_{FL} (Eq. 24) incorporates the combined effect of

sorption (equilibrium and kinetic), biodegradability (μ_w), and the associated micro environmental conditions.

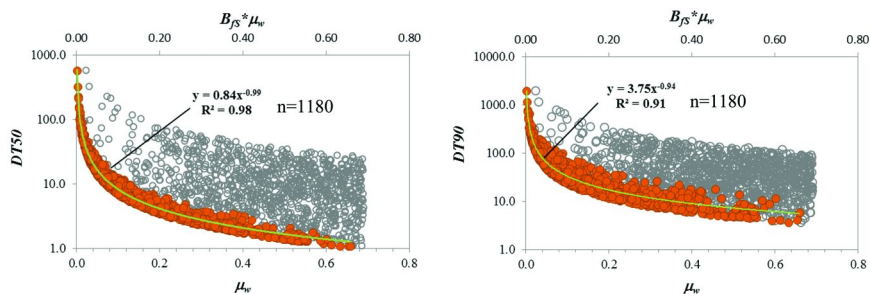


Figure 15. Relationship of short-term bioavailability factor (B_{JS}) and biodegradability (μ_w) with degradation time (DT_{50} , left; and DT_{90} , right) when $\lambda_2/\lambda_1 \leq 10$. Open black circles are plotted with μ_w (i.e., bottom x-axis). Orange circles are plotted with B_{JS} correction (i.e., $\mu_w * B_{JS}$ on top x-axis). Results were from 5000 Monte Carlo simulations as described in Figure 12. (see color insert)

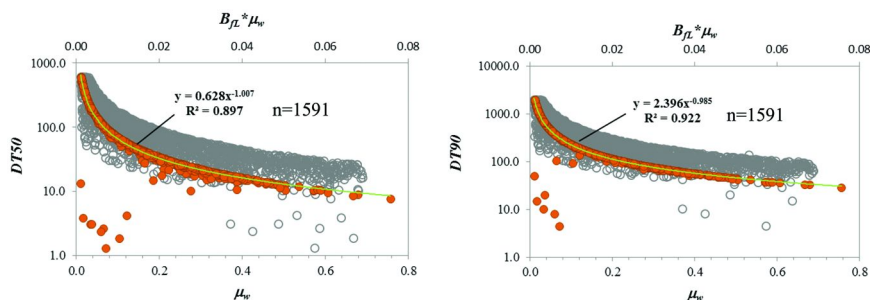


Figure 16. Inverse relationship of degradation time (DT_{50} , left; and DT_{90} , right) with biodegradability (μ_w) and long-term bioavailability (B_{FL}) when $\lambda_2/\lambda_1 \geq 50$. Open black circles are plotted with μ_w (bottom x-axis). Orange circles are plotted with B_{FL} correction (i.e., $\mu_w * B_{FL}$ on top x-axis). Results were from 5000 Monte Carlo simulations as in Figure 10. (see color insert)

The effectiveness of the two bioavailability factors is demonstrated in the experimental results of eight pesticides and 35 data points obtained from the seven literature studies as summarized in Table 1 (Figure 17). Only DT_{50} data are used here since most DT_{90} values were not provided in these published studies. Results in Figure 17 show that μ_w alone could not provide a good correlation with DT_{50} . However, applying the bioavailability factors effectively reduces the scatter (orange circles), resulting in a reasonable inverse relationship with the measured DT_{50} data. The short-term bioavailability factor appears to outperform its long-term counterpart to form a tighter relationship. The median λ_2/λ_1 ratio for the 35 experiments is 8.9 with the majority smaller than 15. This is consistent with

the Monte Carlo simulation results in that relatively small λ_2/λ_1 ratios support the short-term bioavailability as a better factor to estimate the effective first-order rate constant.

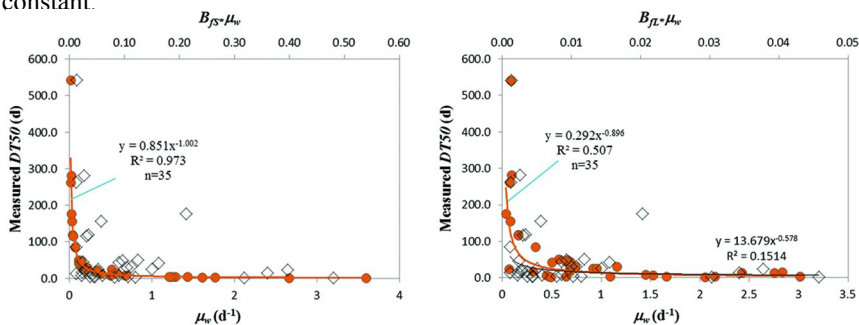


Figure 17. Inverse relationship of measured DT50 with the short-term (B_{fs}) (orange circles on left) and long-term bioavailability factors (B_{fl}) (orange circles on right) and biodegradability (μ_w) (black circles) from published literature data (Table 1). (see color insert)

Correlation of Degradation with Soil and Environmental Factors

The analysis of the two bioavailability factors may shed light on the search for predictive regressions between degradation and soil and environmental factors. On a macroscopic level, degradation time under a set of specific environmental conditions is expected to be an inverse function of a compound's biodegradability corrected by the in situ bioavailability. Since biodegradability is compound-specific and dependent on temperature, moisture and microbial conditions, it may be logical to use a surrogate variable (or variables) to represent the breakdown conditions in a regression analysis.

To illustrate, we take the data from the seven published studies described previously and assume that the biodegradability (μ_w) of a compound in a specific experiment is a function of temperature, soil moisture and organic matter. Although soil organic matter (SOM) may correlate with both microbial activity and substance sorption, the latter is already accounted for by the definition of the two bioavailability factors. Specifically, a multiplicative power function is hypothesized for biodegradability:

$$\mu_w = T^{a1} OC^{a2} \theta^{a3} \quad 25$$

where T is temperature, °C; OC is soil organic carbon, %; and $a1$, $a2$, and $a3$ are regression constants, and other variables are defined previously.

Using the inverse relationship of $DT50$ with μ_w and B_{fs} , we then have

$$DT50 = \frac{a_4}{B_{JS} T^{a_1} OC^{a_2} \theta^{a_3}} \quad 26$$

where a_4 is an additional regression constant.

Applying Eq. 26 to a regression with the experimental data suggests that only B_{JS} and T are two significant variables and the other two soil factors OC and θ have minimal contribution (Figure 18). Presumably, the effects of OC and θ may be implicitly accounted for by the regression considering B_{JS} being a function of K_d and θ by definition (Eq. 22). Results of the regression-predicted and measured $DT50$ are plotted in Figure 18.

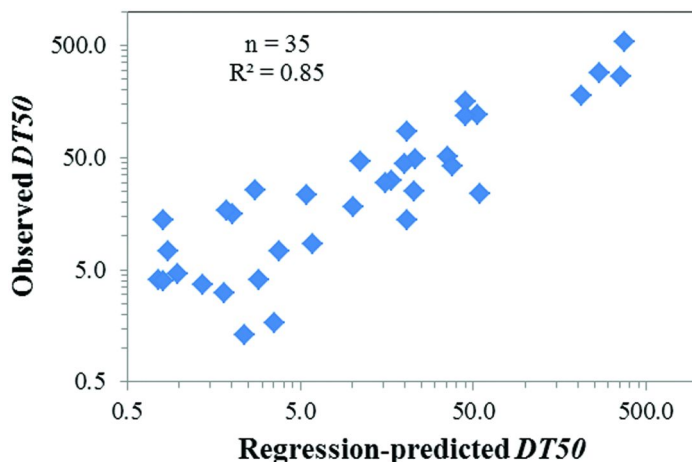


Figure 18. Measured and regression model-predicted $DT50$ for eight pesticides in six published studies (Table 1). Regression of Eq 26 was used to fit the data. Best fit parameters were: $a_1=0.91$, $a_2=0$, $a_3=0$, and $a_4=11.1$.

Although much scatter exists (which may reflect the unaccounted chemical-specificity in μ_w), the above example demonstrates the potential usefulness of the proposed bioavailability factors to associate degradation time with other environmental factors. More experimental data are needed to further evaluate and validate the proposed concept. The vast majority of current environmental fate studies in the published literature have largely focused on sorption and degradation as two separate topics. Relatively few studies have provided measured data of the required sorption and degradation parameters to calculate the proposed bioavailability factors. In a recent study, Ghafoor et al. (33) was able to develop regressions to predict degradation rate constants based on the equilibrium sorption coefficient (via a bioavailability factor similar to Eq. 21), organic carbon content and other soil properties for a broad range of tested soils and pesticides. In contrast to the simple regression given here,

their regressions were developed on a compound/study-specific basis so that the inherent biodegradability factor did not need to be accounted for separately.

Assuming biodegradability is directly proportional to microbial population, Struijs and Van Den Berg (30) showed that specific biotransformation rates in different environmental media could be estimated from a compound's biodegradability adjusted by a bioavailability factor of the underlying medium. The authors emphasized that standardized biodegradability measurements are necessary for inter-media extrapolation in the assessment of environmental biodegradation rates. The adjustment approach of biodegradability by bioavailability for chemicals other than pesticides was also demonstrated in a soil/water slurry batch study by Zhang et al. (32). In this study, naphthalene biodegradation was predicted well only after a bioavailability factor determined by time-dependent sorption was applied to adjust the first-order rate constant measured in water without presence of the soil/sediment.

It is noteworthy that the concept of biodegradability which is defined as the soil pore water metabolic transformation rate constant may benefit the effort to delineate the confounding effects of soil properties such as the soil organic matter (SOM) on both sorption and degradation. SOM is often the prime sorbent for pesticides in soils, but is also often correlated with the biodegradation of organic chemicals in soil (34). In a Canadian study by Gaultier et al. (35), 2,4-D sorption was found to be positively and mineralization negatively correlated with SOM in topsoil samples. The authors concluded that although the microbial activity also increases with SOM, this influence on mineralization is overcompensated by the decreased availability of 2,4-D for degradation, due to increased sorption to SOM. Similar findings were obtained by Aletto et al. (36) in an S-metolachlor study where a better correlation of the mineralization rate was achieved by the quotient of microbial biomass (also correlated with SOM) over the soil sorption coefficient (K_d), in comparison with its individual correlations with K_d and microbial biomass. The better correlation by the biomass/ K_d quotient is consistent with the relationships expected from the concepts of biodegradability (which would be a direct function of biomass) and bioavailability (which is an inverse function of K_d , i.e. Eq. 21).

Likewise, bioavailability distinguishes from biodegradability in relationships with soil properties and it is more a function of sorption (equilibrium and time-dependent). Assuming complete linear equilibrium sorption, Ghafoor et al. (33) was able to delineate and quantify the competing effect of SOM on biodegradability (microbial biomass) and bioavailability (sorption) and showed that the correlation of pesticide degradation with SOM differs for high- and low-sorbing substances. The analysis suggested that degradation of higher K_{oc} pesticides is likely to have a negative correlation with SOM due to bioavailability constraints, while low-sorbing compounds tend to show a positive correlation with SOM, presumably due to a positive influence of SOM on microbial biomass (or biodegradability). This hypothesis led to a set of successful regressions between degradation rate constants and SOM as well as other soil properties for more than 19 pesticide-study combinations.

Similar results were obtained by Villaverde et al. (37), who observed that for acidic herbicides (dicamba, 2-4-D, and flupyr-sulfuron-methyl), there was a

positive correlation of SOM with both K_d and degradation rate (exception: no correlation with either parameter for mesulfuron-methyl). The authors proposed, similarly as later Aletto et al. (36), to consider for the prediction of the microbial degradation of pesticides in soil, besides the SOM content, an availability factor, exhibiting K_d in the denominator of a quotient. In contradiction to this, however, a study from Bolan and Baskaran (38) indicated that while 2,4-D sorption continuously increased with increasing SOM, the degradation of 2,4-D decreased from low-OC soils to a minimum at ca. 10% OC, and then increased again with further increasing OC content of soils. This ambivalence of findings indicates that the effects of SOM on pesticide degradation may involve other factors unaccounted for in their contributions to the estimates of bioavailability and biodegradability.

Summary and Conclusions

The coupled kinetics of sorption and degradation is a robust and flexible model with mechanistic specificity to interpreting various first and non-first order data. It is equivalent to the DFOP model but with macro parameters elaborating the equilibrium and micro kinetic rate constants of both sorption and degradation. Specifically, the rate constants of sorption (α) and metabolism in soil water (m_w) can be derived from the DFOP parameters measured on bulk soils (λ_1, λ_2). The macro parameters thus can be used as a tool to estimate biodegradability and sorption rate constants through combined standard laboratory soil metabolism and batch sorption studies. This highlights the importance of collaborative experimental designs between different environmental fate studies. For example, in addition to sorption and soil metabolism studies, new research may be conducted to evaluate assays to measure biodegradability relevant to the soil pore water environment.

Biodegradability is defined as the microbial transformation rate constant in the soil pore water. This is a parameter after removing the effect of sorption. By this definition, biodegradability is chemical-specific (i.e., related to compound's molecular structure) and should also be a function of the in situ degrading microbial biomass and activity as well as other environmental variables (such as temperature). In order to compare the inherent degradability of different chemicals, standardized tests of biodegradability in soil should be established so that the effects of the indigenous microbes and other environmental factors can be normalized. Such data should benefit the development of quantitative structure–activity relationship (QSAR models) models (39).

Two new bioavailability factors are proposed, one for short-term when pesticide is freshly applied, the other applies to long-term or when pesticide is sufficiently aged after application. The newly proposed bioavailability factors are shown to be useful in delineating potential relationships between degradation and soil properties. System non-first order behavior can be measured by the α/μ_w ratio given other physical-chemical parameters being constant (i.e., K_d, f , and ρ/θ), or by the ratio of the two macro parameters (λ_2/λ_1) for a broader range of conditions. Analysis of a large number (5000) of Monte Carlo simulations suggests that when

the λ_2/λ_1 ratio in DFOP is ≤ 10 (or ≥ 50), system degradation can be approximated as a first order process and the rate constant equals the product of bioavailability and biodegradation. In terms of degradation time such as DT50, an inverse relationship with bioavailability and biodegradation exists.

Predicting degradation of pesticides by soil and environmental factors remains far from satisfactory. The complicated interactions among soil properties and their interrelated effects on degradation and sorption may easily confound the analysis of limited data. In order to develop more reliable and accurate predictive models, there is a need to collect robust experimental data from systematically coordinated measurements of both sorption and degradation for a broad range of chemistry in a variety of representative soils and conditions. The present work provides a modeling framework for future development of potential multivariate regressions for predicting pesticide biodegradation and sorption kinetics with soil properties (e.g. SOM, pH, and mineral constituents such as volcanic ash versus oxidic/ferralitic soils) and climate conditions. Such effort will undoubtedly benefit the elucidation of the underlying mechanisms in observed data, sound assessment based on the totality of studies, and ultimately better product designs to meet the increasing demand for agricultural sustainability and environmental protection.

References

1. NAFTA Technical Working Group on Pesticides. *NAFTA Guidance for Evaluating and Calculating Degradation Kinetics in Environmental Media*; 2012; http://www.epa.gov/oppefed1/ecorisk_ders/degradation_kinetics/NAFTA_Degradation_Kinetics.htm.
2. FOCUS Work Group on Degradation Kinetics. *Guidance Document on Estimating Persistence and Degradation Kinetics from Environmental Fate Studies on Pesticides in EU Registration, Report of the FOCUS Work Group on Degradation Kinetics, EC Document Reference Sanco/10058/2005 version 2.0*; 2006; <http://focus.jrc.ec.europa.eu/dk/docs/finalreportFOCDegKin04June06linked.pdf>.
3. Alexander, M. *Environ. Sci. Technol.* **2000**, *34*, 4259–4265.
4. Scow, K. M. In *Sorption and Degradation of Pesticides and Organic Chemicals in Soil*; Linn, D. M., Carski, T. H., Brusseau, M. L., Chang, F. H., Eds.; SSSA Spec. Publ. 32; SSSA: Madison, WI, 1993; pp 73–114.
5. Ogram, A. V.; Jessup, R. E.; Ou, L. T.; Rao, P. S. C. *Appl. Environ. Microbiol.* **1985**, *49*, 582–587.
6. Speitel, G. E.; Lu, C. J.; Turakhia, M.; Sho, X.-J. *Environ. Sci. Technol.* **1988**, *22*, 68–74.
7. Harper, S. *Rev. Weed Sci.* **1994**, *6*, 207–255.
8. Bosma, T. N. P.; Middeldorp, P. J. M.; Schraa, G.; Zehnder, A. J. B. *Environ. Sci. Technol.* **1996**, *31*, 248–252.
9. Selim, H. M.; Davidson, J. M.; Rao, P. S. C. *Soil Sci. Soc. Am. J.* **1977**, *41*, 3–10.
10. Cameron, D. A.; Klute, A. *Water Resour. Res.* **1977**, *13*, 183–188.

11. van Genuchten, M. T.; Wagenet, R. J. *Soil Sci. Soc. Am. J.* **1989**, *53*, 1303–1310.
12. Streck, T.; Poletika, N. N.; Jury, W. A.; Farmer, W. J. *Water Resour. Res.* **1995**, *31*, 811–822.
13. Chen, W.; Wagenet, R. J. *Environ. Sci. Technol.* **1995**, *29*, 2725–2734.
14. Chen, W.; Wagenet, R. J. *Soil Sci. Soc. Am. J.* **1997**, *61*, 360–371.
15. Pignatello, J. J. *Adv. Agron.* **2000**, *69*, 1–73.
16. Beulke, S.; Heiermann, M.; Malkomes, H.-P.; Nordmeyer, H.; Pestemer, W.; Richter, O. In *proceedings of the X Symposium Pesticide Chemistry: Environmental Fate of Xenobiotics*; September 30–October 2, 1996, Castelnuovo Fogliani, Piacenza, Italy, 1996; La Goliardica Pavese: Pavia, Italy, 1996; pp 337–344.
17. Guo, L.; Jury, W. A.; Wagenet, R. J.; Flury, M. *J. Contam. Hydrol.* **2000**, *43*, 45–62.
18. Chen, W.; Cheplick, M.; Reinken, G.; Jones, R. In *Non-First Order Degradation and Time-Dependent Sorption of Organic Chemicals in Soil*; Chen, W., Sabljic, A. Steven, A. C., Kookana, R., Eds.; ACS Symposium Series 1174; American Chemical Society: Washington, DC, 2014; pp 277–299.
19. Heiermann, M.; Beulke, S.; Malkomes, H.-P.; Nordmeyer, H.; Pestemer, W.; Richter, O. In *Proceedings of the X Symposium Pesticide Chemistry: Environmental Fate of Xenobiotics*; September 30–October 2, 1996, Castelnuovo Fogliani, Piacenza, Italy, 1996; La Goliardica Pavese: Pavia, Italy, 1996; pp 363–370.
20. Shaner, D.; Brunk, G.; Nissen, S.; Westra, P.; Chen, W. *J. Environ. Qual.* **2012**, *41*, 170–178.
21. Shelton, D. R.; Parkin, T. B. *J. Agric. Food Chem.* **1991**, *39*, 2063–2068.
22. Krieger, M. S.; Merritt, D. A.; Wolt, J. D.; Patterson, V. L. *J. Agric. Food Chem.* **1998**, *46*, 3292–3299.
23. Krieger, M. S.; Pillar, F.; Ostrander, J. A. *J. Agric. Food Chem.* **2000**, *48*, 4757–4766.
24. Wang, G.; Or, D. *Environ. Microbiology.* **2010**, *12*, 1363–1373.
25. Walker, A. *J. Environ. Qual.* **1974**, *3*, 396–401.
26. Walker, A. *Weed Res.* **1978**, *18*, 305–313.
27. Hardy, I. A. J.; Jones, R. L.; Allen, R.; Gatzweiler, E. W. *Proc. of the XII Symposium Pesticide Chemistry*; Piacenza, Italy, 2003.
28. Scow, K. M.; Simkins, S.; Alexander, M. *Appl. Environ. Microbiol.* **1986**, *51*, 1028–1035.
29. Gustafson, D. I.; Holden, L. R. *Environ. Sci. Technol.* **1990**, *24*, 1032–1030.
30. Struijs, J.; Van Den Berg, R. *Water Res.* **1995**, *29*, 255–262.
31. Gamerdinger, A. P.; Achin, R. S.; Traxler, R. W. *Soil Sci. Soc. Am. J.* **1997**, *61*, 1618–1626.
32. Zhang, W. X.; Bouwer, E. J.; Ball, W. P. *Groundwater Monit. Rem.* **1998**, *18*, 126–138.
33. Ghafoor, A.; Moeys, J.; Stenström, J.; Tranter, G.; Jarvis, N. J. *Environ. Sci. Technol.* **2011**, *45*, 6411–6419.
34. Calvet, R. *Environ. Health Perspec.* **1989**, *83*, 145–177.

35. Gaultier, J.; Farenhorst, A.; Cathcart, J.; Goddard, T. *Soil Biol. Biochem.* **2008**, *40*, 217–227.
36. Alletto, L.; Benoit, P.; Bolognesi, B.; Couffignal, M.; Bergheaud, V.; Dumény, V.; Longueval, C.; Barriuso, E. *Soil Tillage Res.* **2013**, *128*, 97–103.
37. Villaverde, J.; Kah, M.; Brown, C. D. *Pest Manage. Sci.* **2008**, *64*, 703–710.
38. Bolan, N.; Baskaran, S. *Aust. J. Soil Res.* **1996**, *34*, 1041–1053.
39. Sabljic, A.; Y. Nakagawa. In *Non-First Order Degradation and Time-Dependent Sorption of Organic Chemicals in Soil*; Chen, W., Sabljic, A., Steven, A. C., Kookana, R., Eds.; ACS Symposium Series 1174; American Chemical Society: Washington, DC, 2014; pp 57–84.

Chapter 3

Terrestrial Field Degradation Based on Soil, Climatic, and Geographic Factors

Robin Sur*

Bayer CropScience LP, 2 TW Alexander Drive,
Research Triangle Park, North Carolina 27709, United States
*E-mail: robin.sur@bayer.com.

Field degradation data of pesticides and their metabolites from North America, Europe, and the Tropics have been reviewed, assessed, and compared. The study focused on field residue trial data with degradation as the only or predominant dissipation process and included kinetic evaluations with and without normalization to reference conditions for soil temperature and moisture to study the effect of climate and soil separately. The Köppen-Trewartha classification has been used to group North American and European trial data into similar climate groups before comparison. Generally, non-normalized field degradation followed a temperature gradient and was slower in temperate regions compared to the subtropics and tropics. Within North America degradation in Canada was slower compared to the U.S. and within the U.S. pesticide degradation on temperate sites was slower than on subtropical ones. Between Northern and Southern Europe and between Europe and North America non-normalized and normalized degradation was generally not different. Upon normalization the latitudinal trend across North America disappeared and soil properties became evident as drivers for degradation. Only normalized field degradation on cold and dry sites low in organic matter in the Pacific Northwest as well as on intensely weathered sites with acidic soils in the Southeast was slower compared to other regions in the U.S..

Introduction

Soil degradation studies with pesticides and their metabolites under laboratory conditions in the dark usually provide data on degradation as the only relevant dissipation process (1). Here, microbial degradation is often the major pathway driving overall degradation of most organic chemicals in soil, although abiotic reactions including hydrolysis and oxidation-reduction can also take place. Under field conditions the suite of degradation reactions might be supplemented by photochemical reactions, while additional environmental fate processes may significantly contribute to the overall dissipation of a compound, i.e. leaching, plant uptake, volatilization, and run-off/erosion (2). The vast majority of terrestrial field dissipation (TFD) studies with pesticides and their metabolites have been conducted across North America and Europe to fulfill regulatory requirements for product registrations. Depending on the rationale for carrying out a TFD study the design and the endpoints obtained may differ. In principle, TFD studies are designed to answer two questions. The first one deals with the overall environmental fate of a compound under realistic outdoor conditions including all possible routes to identify the main drivers and reaction products of dissipation. In this case lumped dissipation endpoints would be obtained from a TFD study (3, 4). If a TFD study is intended to provide endpoints to be used in numerical leaching models, however, all dissipation processes other than microbial degradation (and abiotic processes related to soil which cannot be separated from biodegradation, i.e. hydrolysis and redox reactions) need to be excluded by the experimental design or post-processing of the test results (5, 6).

The main focus of the present article is on *microbial degradation* in the field only and its quantitative evaluation and comparison between geographical regions. TFD studies on the overall fate of a compound under realistic outdoor conditions served as suitable data basis, when these data showed (e.g., at least one residues free soil layer that was sampled per time interval; no sloped trial site) and it could be concluded from the general environmental fate characteristics (low volatilization potential due to low vapor pressure and Henry constant, photolytically stable, low mobility based on adsorption coefficient) that other dissipation processes than microbial degradation were negligible or when these processes had been excluded after field data post-processing, e.g. according to the procedures described in (6). In the absence of appropriate field *degradation* data for tropical regions also field *dissipation* data with major dissipation pathways other than microbial degradation and laboratory degradation data have been discussed. In addition, laboratory soil degradation data also provided important weight of evidence to support findings from the field.

Effect of Soil Temperature and Moisture on Degradation

Soil moisture content and temperature fluctuations in a typical environmental range are generally acknowledged to effect reaction rates. The effect of both environmental parameters on soil degradation can be quantitatively described by the Walker and the Arrhenius equations, respectively (7–9). In general, wet and warm weather conditions favor quick biodegradation, whereas cold and

dry conditions result in slower reactivity. Multi-year terrestrial field dissipation (TFD) studies of slowly degrading compounds usually show typical multi-phase degradation curves with a relatively quick degradation in summer followed by a slowdown in autumn and even a winter pause in reactivity, followed by a continuation of degradation in the following spring (10). Similarly, cold and/or dry geographical regions lead to overall longer degradation half-lives compared to warm and/or wet regions (11). The season of the application might also have an impact with spring applications in the northern hemisphere normally leading to quicker degradation compared to applications in the autumn (10).

The normalization of field degradation half-lives to reference conditions for soil moisture and temperature is an established methodology to compensate for the effects of weather conditions on degradation (12). Commonly and in this article, soil moisture at field capacity (pF 2.0) and a soil temperature of 20°C are used as reference conditions. This approach is usually applied to derive half-lives that can be used in numerical leaching models. The conceptual model for the governing factors of pesticide degradation in soil is depicted in Figure 1. In principle, the soil degradation half-life is a function of weather, soil, and study conditions like application rate, type of formulation, and mode of application. Normalization only compensates for the short-term effect of weather on soil temperature and moisture. The long-term effect of climate on soil formation cannot be compensated for by normalization. Geography has a direct influence on soil formation based on the available parent material and the topography; it also impacts the locally existing weeds, diseases, or pests and in turn determines the selection of the study design to best control the infestation.

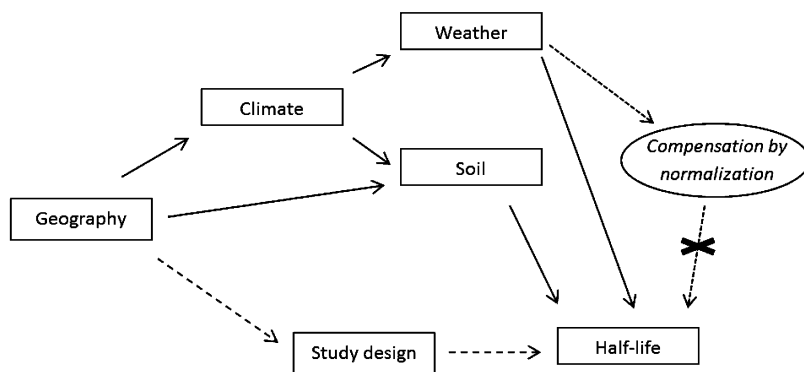


Figure 1. Conceptual model for soil degradation. Normalization of half-lives to reference conditions for soil temperature and moisture eliminates the short-term effect of weather on soil degradation.

In principle, the temperature dependency of soil degradation rates can either be described using the Arrhenius equation or the similar ‘Q₁₀ rule’ stating that a change in temperature of 10 K results in a Q₁₀-fold change of the degradation rate (Figure 2). It is assumed that soil temperatures at or below 0°C halt any

kind of microbial degradation. The effect of soil moisture on degradation as described by the Walker equation (7, 8) is illustrated in Figure 3; the degradation rate increases with soil moisture up to field capacity, beyond which no further increase is assumed. Both equations have been combined in the formula below to calculate the normalized half-life from the actual half-life using correction factors for soil moisture and temperature (12):

$$DT_{50}(FC, 20^{\circ}\text{C}) = DT_{50}(T, \theta) Q_{10}^{\frac{T-T_{ref}}{10K}} \left(\frac{\theta}{\theta_{FC}} \right)^B$$

$$\text{with: } Q_{10} = e^{\frac{10E_a}{RTT_{ref}}} = 2.58 \quad (9)$$

E_a :	Arrhenius activation energy (65.4 kJ mol ⁻¹)
R:	Gas constant (8.314 J K ⁻¹ mol ⁻¹)
FC:	field capacity (pF 2 = 0.1 bar)
T:	Temperature (K)
T_{ref} :	Reference temperature (293.15 K)
θ :	gravimetric soil moisture
B:	Walker exponent (0.7 based on reference (9, 13))
DT_{50} :	half-life

These fundamental relationships of environmental conditions on degradation can be applied in a ‘time-step normalization’ approach to consider daily soil moisture and temperature data for normalization rather than long-term averages to increase the accuracy of this procedure. Here, reported-time to concentration curves are replaced by transformed-time to concentration curves (12). This leads to a compressed time axis for days with lower temperatures than 20°C, e.g. a day at 10°C is converted to 0.4 time-step days (based on a Q_{10} of 2.58; reference (9)) reflecting its degradation potential compared to a day with on average 20°C. Long-term winter periods with temperatures below 0°C are compressed to a 0-day long period. By this procedure normalized degradation curves are obtained that would be observed if temperature and moisture were kept constant at reference conditions throughout the study.

Through this approach compound degradation rates from different climate regions can be compared without being biased by short-term weather factors to study solely the effects of soil properties and soil microbiology on degradation. However, long-term climate can still have an indirect effect on degradation by influencing the formation of ‘zonal soils’ defined as being unique to certain climate regions (14).

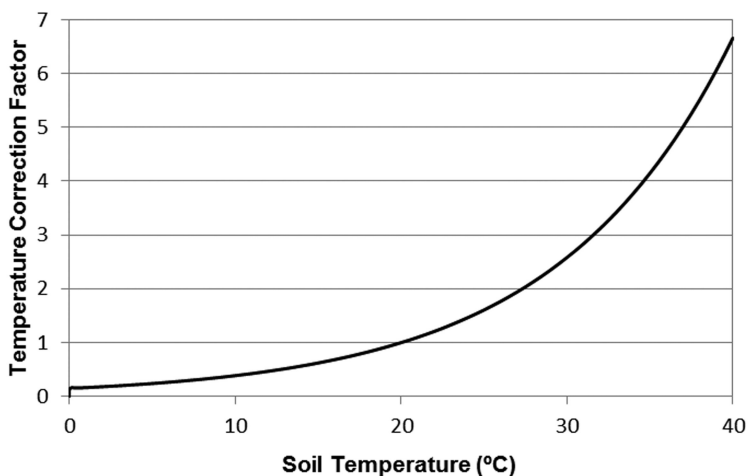


Figure 2. Temperature correction factor as a function of soil temperature based on a Q_{10} of 2.58 (9). The reference temperature is set to 20°C. The degradation rate at 30°C is 2.58-fold greater than at 20°C and at 10°C it is 2.58-fold smaller. No degradation is assumed at or below 0°C.

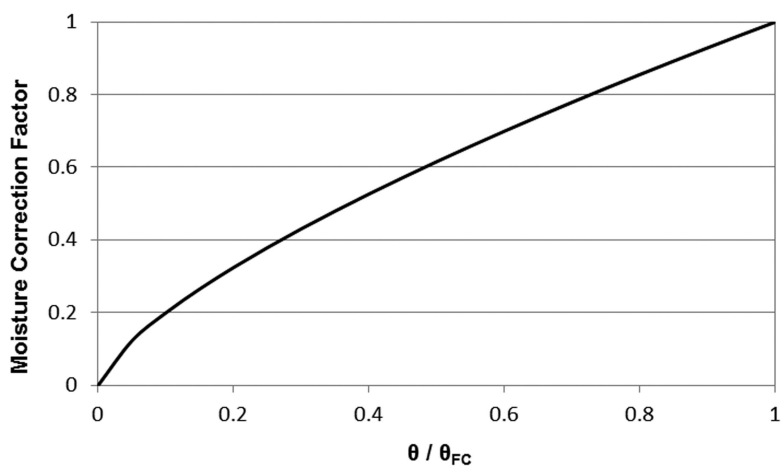


Figure 3. Effect of gravimetric soil moisture on degradation based on the Walker equation (7, 8) using an exponent B of 0.7 (9, 13). θ_{FC} is the gravimetric soil moisture at field capacity (pF 2). Degradation at 37% field capacity is only half as fast compared to 100% field capacity. The degradation rate does not increase beyond field capacity.

Kinetic Evaluations

The kinetic evaluation of degradation data after normalization usually follows the guidance provided in (10) to derive modeling endpoints that can be used as input in numerical leaching models. Either the half-life is directly derived from a single first-order (SFO) fit to all data points or, if the fit is visually and statistically not acceptable, a conservative half-life of a bi-phasic fit is chosen. In case the DT90 has not been reached in the study this can be either the SFO half-life of the slow compartment of the double-first order in parallel (DFOP) model or the SFO half-life of the slow phase of the hockey-stick (HS) model. If the DT90 has been reached during the study a conservative SFO is back-calculated from the DT90 of the first-order multiple compartment (FOMC) model ($DT50_{SFO} = DT90_{FOMC}/3.32$). The objective is to derive in any case an SFO half-life, which is compliant with degradation routines used in numerical leaching models and that conservatively describes at least 90% of the degradation of the compound. In this article only the DT50 for kinetic evaluations of normalized data is provided because the corresponding DT90 is always 3.32-fold larger.

Kinetic endpoints for non-normalized field data were derived according to the procedure also described in (10) for non-normalized degradation curves ('trigger evaluation'). Among three different kinetic models, i.e. the SFO, DFOP, or the FOMC model, the DT50 and DT90 of the model that best described the degradation were selected.

A comparison of half-lives between normalized and non-normalized data sets is difficult to interpret, because the non-normalized half-life is always a true DT50, i.e. the time between application and when 50% of the initially applied amount has degraded. For normalized data, however, this is only the case if an SFO fit was chosen to represent the degradation of the entire curve reasonably well. In case the half-life of the slower compartment or phase of the DFOP or HS model, respectively, have been chosen as kinetic endpoint this half-life is longer than the true DT50 and comparisons should not be made. In this study the half-lives reported for the normalized data sets are a mixture of DT50 values and half-lives of the slower compartments/phases of DFOP and HS models and therefore comparisons between normalized and non-normalized data were not undertaken.

Terrestrial Field Dissipation in North America

Sur (15) investigated the standard, non-normalized field degradation behavior of 26 pesticides including metabolites across the contiguous United States and Canada in 19 states and 4 provinces, respectively, totaling 44 TFD sites to examine the effect of pedoclimatic conditions on degradation (Figure 4). In order to compare sites a 'site classification index' was calculated by dividing the half-life (and the DT90) of a given compound at a specific site by the geometric mean half-life (and DT90) of this compound on all sites. An index of greater than 1 indicated a relatively slow degrading site whereas a value less than 1 showed a relatively quick degrading site. This index approach to compare sites was deemed

necessary, because the degradation of the compounds was not studied at all sites. Hence, any potential bias caused by a not even distribution of slowly and quickly degrading compounds across the sites could be eliminated by this methodology.

The analysis showed that the half-lives and the DT90s generally followed the temperature gradient between Canada and the United States. Degradation in the U.S. was significantly faster than in Canada (Table 1, t-test, significance level 5%). In a second step, the Köppen-Trewartha classification (16, 17) was used to further refine the analysis and to categorize all sites according to common climate characteristics into five different regions covering the range from boreal to subtropical climate (Figure 4), i.e. ‘subtropical dry-summer’ (California), ‘subtropical humid’ (e.g., North Carolina and Georgia), ‘temperate continental’ (e.g., New York State), ‘temperate-boreal steppe’ (e.g., Saskatchewan, North Dakota, Nebraska), and ‘temperate-boreal cold desert’ (Washington State). Again it became evident that the temperate zones resulted in slower degradation compared to the warmer subtropical regions in the Southeast and the Southwest (Table 1, t-test, significance level 5%). Sites within the temperate and subtropical regions did not differ in degradation rates (Table 1, t-test, significance level 5%).

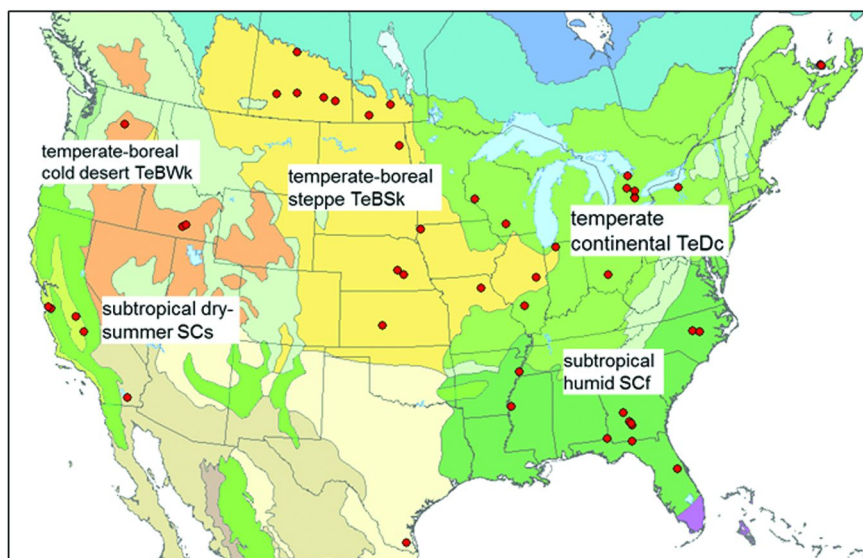


Figure 4. Experimental field trial sites (red dots) and Köppen-Trewartha climate regions in the U.S. and in Canada. The sites in Texas (SBSH) and in southern California (SBWh) were omitted as they do not fit into the selected classes. Ecozones based on (16). (see color insert)

Table 1. Mean Site Classification Indices for Five Köppen-Trewartha Climate Regions within the U.S. and Canada and Separately for U.S. and Canada Based on Non-Normalized Degradation Kinetics of 26 Compounds

		<i>Index Geometric Mean</i>		
<i>Climate Class</i>		<i>DT50 (90% CI)</i>	<i>DT90 (90% CI)</i>	<i>n (trials)</i>
SCf	Subtropical humid	0.58 (0.41-0.82) ¹	0.70 (0.53-0.92) ¹	20
SCs	Subtropical dry	0.73 (0.52-1.03) ²	0.70 (0.53-0.92) ¹	18
TeDc	Temperate continental	1.08 (0.89-1.32)	1.19 (0.98-1.45)	27
TeBWk	Temperate cold desert	1.31 (0.94-1.83)	1.08 (0.89-1.32)	15
TeBSk	Temperate boreal steppe	1.32 (1.09-1.59)	1.24 (1.05-1.46)	39
U.S. total		0.89 (0.78-1.02) ³	0.90 (0.80-1.00) ³	95
Canada total		1.51 (1.19-1.92)	1.48 (1.24-1.75)	26

DT50 and DT90 clearly follow a temperature gradient, i.e. degradation at sites in Canada is significantly slower than in the U.S.. The same holds true for degradation at sites in temperate climate zones, which is slower compared to subtropical zones (CI: confidence interval, n: number). Sites within the subtropical and temperate climate class do not show differences; ¹ DT50/DT90 on a subtropical site (SCf, SCs) is faster than on any of the temperate sites (TeDc, TeBWk, TeBSk); ² DT50 is faster than on two of the temperate sites (TeBWk, TeBSk) but equal to temperate site TeDc; ³ DT50/DT90 in Canada are slower compared to the U.S. sites, all comparisons based on t-test, 5% significance level.

Whereas non-normalized TFD data from North America clearly showed a quicker degradation from north to south in accordance with increasing average temperature, this trend disappeared upon normalization to a reference temperature of 20°C and soil moisture at field capacity. Sur and Schäfer (18) investigated the normalized field degradation of 21 compounds across North America. The evaluation included 30 TFD study locations extending over 16 states and four provinces in the contiguous United States and in Canada, respectively. Generally, the degradation rates among the majority of the sites did not differ. No statistically significant differences in degradation between Canada and the U.S. were observed (Table 2, t-test, 5% significance level) in contrast to the non-normalized data that without such normalization would have suggested different soil reactivity. Also degradation in the temperate climate region in its entirety was not anymore slower than in the subtropical region as it appeared based on the non-normalized dataset. However, it was found that degradation at the sites in Washington State in the Pacific Northwest (‘temperate-boreal cold desert’) and in the Southeast (‘subtropical humid’) was significantly slower when compared to the two quickest degrading regions, i.e. ‘subtropical dry-summer’ (California) and ‘temperate continental’. The general conditions for microbial degradation at the site in Washington were unfavorable due to the cold and exceptionally dry climatic

conditions; in addition, the soil was coarse-textured and exhibited only 0.3% organic carbon in the top 30 cm. The slowly degrading ‘subtropical-humid’ regions of the Southeast were associated with intensely weathered, acidic soils exhibiting pH values usually below 6. It seems possible that these soils would have different microbial populations than soils of more neutral pH. Low pH values as observed in the southeastern region of the United States have been found to negatively impact soil microbial communities (19). Conceptually, it appears that the short-term effect of weather on degradation had been compensated for by normalization, but environmental differences that impact soil morphology and microbiology are not resolved by the current methodology. However, further work is needed to confirm these findings, because in some cases there were only a limited number of trial sites available to represent a climatic region.

Table 2. Mean Site Classification Indices for Five Köppen-Trewartha Climate Regions within the U.S. and Canada and Separately for U.S. and Canada Based on Normalized Degradation Kinetics of 21 Compounds

	<i>Climate Class</i>	<i>Index Geometric Mean DT50 (90% CI)</i>	<i>n (trials)</i>
SCs	Subtropical dry	0.83 (0.68-1.02) ¹	12
TeDc	Temperate continental	0.88 (0.72-1.07) ¹	12
TeBSk	Temperate boreal steppe	1.00 (0.83-1.21)	18
SCf	Subtropical humid	1.21 (1.03-1.43)	14
TeBWk	Temperate cold desert	1.27 (0.96-1.68)	11
Canada total		0.84 (0.54-1.29)	6
U.S. total		1.03 (0.95-1.13)	63

Degradation rates do not follow a clear climate pattern upon normalization. ¹ Degradation at sites in subtropical dry and temperate continental regions is significantly faster than on subtropical humid and temperate cold desert sites but not different compared to temperate boreal steppe (t-test, 5% significance level). Differences indicate different soil reactivity of the sites/regions. CI: confidence interval, n: number of trials.

Terrestrial Field Dissipation in Europe

The North American continent covers a more diverse range of climate types with more extreme temperature differences and drier conditions compared to Europe. European and North American trial sites have only the SCs climate class (subtropical dry-summer) in common. The only other climate class in Europe is the TeDo class (oceanic climate with coldest month over 0°C). The North American sites however even cover arid (cold desert, TeBWk) and semi-arid (boreal steppe, TeBSk) climate as well as colder continental climate (coldest month below 0°C). In order to evaluate whether the more uniform climate in Europe also becomes manifest in the behavior of pesticides in the field, Sur (20)

investigated the non-normalized field degradation of 27 active ingredients and metabolites throughout eight European countries. Whereas the U.S. and Canadian trial sites extended across five different Köppen-Trewartha climate classes, the European sites were described by only two classes (Figure 5). Only compounds were considered that had degradation data from both climatic regions available to facilitate a better comparison; therefore there was no need to calculate a site classification index as for the North American sites, instead half-lives were directly compared. The 174 trials were conducted in the temperate-marine (TeDo) ecoregion of Northern and Central Europe (Northern and Central France, United Kingdom, Sweden, Germany, The Netherlands, Northern Italy) and 36 in the subtropical dry summer Ecoregion (SCs) of Southern Europe (Portugal, Southern France, and Spain). Significant differences of DT50 and DT90 values and of variances between both datasets were not observed (t-test, F-test, 5% significance level, Table 3). After normalization of the same dataset to reference conditions for soil temperature and moisture the results provided in Table 4 were obtained showing again no significant differences of half-lives and variances between Northern and Southern Europe (t-test, F-test, 5% significance level) suggesting that soil reactivity across Europe does not differ significantly. Obviously lower temperatures and higher soil moisture in Northern Europe have a similar net effect on degradation as higher temperatures and less soil moisture in Southern Europe, which is why also the non-normalized half-lives between both regions do not differ.

Table 3. Endpoints of Non-Normalized Field Degradation Fits According to (10) from Northern/Central (TeDo) and Southern Europe (SCs)

	<i>Trigger Endpoints (non-normalized)</i>			
	<i>DT50 (d) (90% CI)</i>		<i>DT90 (d) (90% CI)</i>	
	<i>TeDo</i>	<i>SCs</i>	<i>TeDo</i>	<i>SCs</i>
Geometric Mean	41 (34-49)	35 (26-48)	227 (193-266)	217 (156-301)
Median	49	39	243	229
90 th Percentile	240	102	1000	986
n (trials)	174	36	174	36
n (compounds)	27	27	27	27

Geometric mean DT50 and DT90 and respective variances from both regions are statistically not different (t-test, F-test, 5% significance level). Classification according to Köppen-Trewartha (16). (CI: confidence interval, n: number.)

It is justified, therefore, to combine results from all locations to derive a robust field degradation rate constant for a given compound. Further, these results suggest it may be possible to define a representative field rate constant across Europe using fewer test locations.

Table 4. Endpoints of normalized field degradation fits according to (10) from Northern/Central (TeDo) and Southern Europe (SCs)

	<i>Modeling Endpoints (normalized)</i>	
	<i>DT50 (d) (90% CI)</i>	
	<i>TeDo</i>	<i>SCs</i>
Geometric Mean	41 (35-48)	50 (35-73)
Median	47	64
90 th Percentile	165	158
n (trials)	174	36
n (compounds)	27	27

Geometric mean DT50 values and variances from both regions are statistically not different (t-test, F-test, 5% significance level). Classification according to Köppen-Trewartha (16). (CI: confidence interval, n: number.)

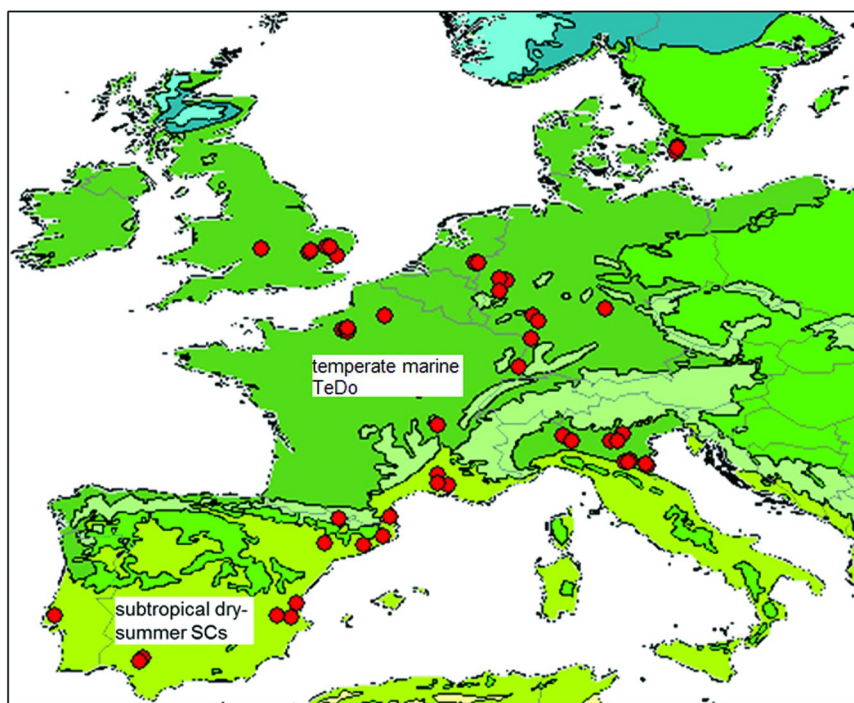


Figure 5. Experimental field trial sites (red dots) and Köppen-Trewartha climate regions in Europe. All sites except for one fit into the TeDo (53 sites) and SCs (12 sites) climate classes; the site in Northern Spain (TeM) was omitted from the analysis. Ecozones based on (16).

Comparison of Terrestrial Field Dissipation between North America and Europe

Sur (15) extended the aforementioned studies to an intercontinental scale and compared non-normalized field degradation data from the U.S. and Canada on the one hand side to European results on the other. The dataset consisted of 19 compounds including seven insecticides, five fungicides, four herbicides, and three metabolites, all of which had dissipation data from both continents available. Geometric mean DT50 and DT90 values did not differ between the continents and neither did the variance of the DT90 values (t-test, F-test, 5% significance level). However, the variances of the half-lives showed a significant difference (F-test, 5% significance level) with the confidence range being larger in North America compared to Europe presumably reflecting the greater heterogeneity in soil and climatic conditions (Table 5).

Table 5. Endpoints of Non-Normalized Field Degradation Fits According to (10) from North America (U.S. and Canada) and Europe (EU)

	<i>Trigger Endpoints (non-normalized)</i>			
	<i>DT50 (d) (90% CI)</i>		<i>DT90 (d) (90% CI)</i>	
	<i>U.S./CAN</i>	<i>EU</i>	<i>U.S./CAN</i>	<i>EU</i>
Geometric Mean	42 (29-59)	33 (25-42)	189 (134-267)	178 (138-230)
Median	57	44	385	256
90 th Percentile	355	187	1000	1000
n (trials)	85	113	85	113
n (compounds)	19	19	19	19

Geometric mean DT50 and DT90 from both regions are statistically not different (t-test, 5% significance level). DT50 variances are statistically different, DT90 variances are not (F-test, 5% significance level) (CI: confidence interval, n: number.)

Furthermore, Sur and Schaefer (18) investigated TFD half-lives between North America and Europe after normalization. The comparison of half-lives of 21 compounds comprising four fungicides, four herbicides, five insecticides and eight soil metabolites with TFD data available from 96 trials across the contiguous United States and Canada and 126 trials from Europe showed no significant (Table 6, t-test, 5% significance level) overall difference between both continents after normalization to reference conditions for soil moisture and temperature. Geometric mean half-lives calculated over all compounds amounted to 39 days in North America compared to 31 days in Europe. The 90% confidence intervals ranged from 29 days to 53 days and 24 to 39 days, respectively. On the level of the individual compounds three of the 21 agrochemicals revealed 4- to 5-fold longer half-lives in North America compared to Europe. These differences were for fungicides with half-lives greater than 100 days in North

America. The differences may be explained by 2- to 20-fold higher application rates in the United States and in Canada according to regional labels. In addition, degradation of one of the three fungicides was retarded by lag-phases, which were only observed in U.S.-American field trials indicating temporary inhibition of pesticide degrading microbes. Higher application rates have been found to slow down or temporarily inhibit degradation processes in the field for some compounds (21). The normalized half-lives of the remaining 18 compounds, however, did not show any significant differences between the continents. Table 7 compiles a comparison of the kinetic endpoints for these 18 compounds between North America and Europe, which are practically identical.

Table 6. Endpoints of Normalized Field Degradation Fits According to (10) from North America (U.S. and Canada) and Europe (EU)

	<i>Modeling Endpoints (normalized)</i>	
	<i>DT50 (d) (90% CI)</i>	
	<i>U.S. and Canada</i>	<i>EU</i>
Geometric Mean	39 (29-53)	31 (24-39)
Median	64	42
90 th Percentile	249	168
n (trial sites)	96	126
n (compounds)	21	21

Geometric means and variances from both regions are statistically not different (t-test, F-test, 5% significance level), CI: confidence interval, n: number.

Terrestrial Field Dissipation in Tropical Regions

Outside North America and Europe, there have been relatively few studies conducted under controlled conditions on soils from tropical regions. Available laboratory studies under standardized conditions on the pathway and degradation kinetics of pesticides however reveal no systematic difference between tropical and temperate regions (22). The proportion of degradation on overall dissipation determined in relatively scarce TFD studies from tropical regions is difficult to assess, as many results have been obtained without following harmonized experimental protocols allowing addressing the extent of the different routes of dissipation. Often lumped dissipation half-lives have been reported including not only degradation but also other dissipation processes (23, 24). The purpose here was more to identify the principal dissipation pathways, i.e. leaching and run-off under typical heavy rainfall events or volatilization potential at high temperatures rather than deriving microbial degradation rates. Generally, microbial degradation is expected to occur faster in tropical compared to temperate regions due to

higher year round temperatures and wetter soil conditions. Also the conditions for enhanced degradation due to faster enzymatic adaptation are more favorable (25). Leaching and run-off as well as volatilization are often significant additional dissipation processes due to higher rainfall intensities and elevated temperatures throughout the seasons further reducing observed dissipation times in tropical field trials (23). When comparing data from the tropics with temperate regions care must be taken that in the former regions the application rates might be higher due to higher pest and disease pressure and year round crop cultivation and also the agronomic practices might differ from other regions affecting the overall degradation additionally (21).

Table 7. Endpoints of Normalized Field Degradation Fits According to (10) from North America (U.S. and Canada) and Europe (EU) without Three Outlier Fungicides

	<i>Modeling Endpoints (normalized)</i>	
	<i>DT50 (d) (90% CI)</i>	
	<i>U.S. and Canada</i>	<i>EU</i>
Geometric Mean	27 (19-37)	28 (22-37)
Median	35	36
90 th Percentile	180	171
n (trial sites)	78	104
n (compounds)	18	18

Three fungicides showing significantly different half-lives between North America and the EU were removed from the original dataset compiled in Table 6. Geometric means and variances from both regions are statistically not different (t-test, F-test, 5% significance level), CI: confidence interval, n: number.

Sanchez-Bayo and Hyne (24) performed a literature review and compared non-normalized dissipation half-lives of 24 herbicides and 22 insecticides between tropical and non-tropical soils mainly based on field data. Volatility losses at higher temperatures in the tropics were found to be a major pathway for 38% of the compounds. Dissipation in the tropics was at least twice as fast for half of the insecticides and 55% of the herbicides. At least five herbicides (21%) and two insecticides (9%) showed also *significantly* faster dissipation from tropical compared to temperate soils. For the other compounds statistical significance tests were not performed due to the limited number of data points available. Longer half-lives in the tropics were found for 3 herbicides and 3 insecticides, which accounted for 13% of the 46 compounds investigated.

Although normalized field degradation rates from tropical regions excluding other dissipation processes than microbial and soil related abiotic degradation are not found in the scientific literature these are expected not to be different

from temperate regions based on the above mentioned comparison of laboratory degradation rates. However, the findings on acidic subtropical humid soils as reported in Table 2 suggest that lower soil pH values, which are typical for tropical regions, give rise to longer half-lives. A systematic approach to compare temperate with tropical soils should therefore include the assessment of pH related effects on degradation.

Discussion

Several other studies support the concept of similar pesticide degradation behavior on field trial sites and laboratory soils across different continents. Hardy et al. (12) did not find differences between North America and Europe when studying the field dissipation of isoxaflutole and two of its soil metabolites. Walker et al. (26) compared the laboratory degradation of simazine in 16 soils from Europe, Canada, and Asia with field dissipation data on the same soils. Using the laboratory derived half-lives and the site specific weather data for predicting the residue decline on the TFD sites using the routines described by Walker and Barnes (27), field residues were generally over predicted, however for six sites a close agreement between observed and predicted residues was achieved. No obvious trend of laboratory and field half-lives with geographic region was found. But there were significantly positive correlations of half-lives with the soil properties organic carbon and clay content as well as pH. The relative unimportance of geography on degradation is supported by work from Fierer and Jackson (19). They investigated the biogeography of soil bacterial communities across North and South America in 98 soil samples. Similarity between soil bacterial communities did not depend on geographical latitude. More important predictors were soil properties, the most important of which was soil pH for microbial diversity and richness. Generally, diversity and richness decreased with pH.

The variability in soil degradation rates on smaller regional and field scales is already large and underpins the significance of soil properties on pesticide degradation compared to geography. The median standard deviation of the laboratory degradation half-lives of five different pesticides (propryzamide, linuron, simazine, metamitron, metazachlor) in 18 soils from the UK was as high as 40% (6). Soil properties and microbial composition driving pesticide degradation vary already considerably on a much smaller spatial scale and even within a single agricultural field similarly high variability has been observed. Walker et al. (28) found that the degradation of isoproturon within small subsets of an agricultural field treated at the same nominal rate ranged considerably from 6.5 to 30 days. Faster subsets were found to have generally higher pH, larger microbial biomass and greater microbial diversity. Price et al. (29) and Price (30) also found a high spatial variability of degradation rates on agricultural fields for isoproturon, chlorpyrifos, and chlorothalonil with degradation strongly correlated with pH and microbial activity. Proper sampling strategies as recommended by regulatory guidance documents on conducting TFD studies are aimed at balancing this variability (3–6).

Kah et al. (31) did not find any general correlation of degradation half-lives with any major soil property (e.g., pH, clay, organic carbon, cation exchange capacity, and biological activity) for six acidic and four basic pesticides on nine soils from temperate regions. The main reason was that the dominant soil parameters driving degradation varied among different pesticides. Whereas for some pesticides clear correlations with some soil parameters existed, this could not be generalized nor extrapolated to other classes of agrochemicals. Biological activity and organic carbon content e.g. were the best predictors for variability among the degradation rates for only two of the ten compounds investigated. However, Ghafoor et al. (32, 33) successfully developed a general multiplicative model to explain variability among soil degradation rates of pesticides using the predictors soil sorption constant as surrogate for bioavailability, as well as organic carbon and clay contents as surrogates for microbial biomass and activity. In addition, soil depth was used to increase model performance. The model was applied to 19 pesticide-study combinations on contrasting soils taken from the scientific literature and including the data from Kah et. al. (31). The model was able to explain 73% of the variability in degradation rates between soils and after removal of four outlier datasets even 80% could be explained.

Conclusions

The following conclusions with regard to field degradation of pesticides and their metabolites can be drawn based on the present review of the scientific literature:

1. Weather and climate are important drivers of field degradation rates of pesticides and their metabolites as expressed by ranges in soil temperature and moisture. Degradation speeds up under warm and wet conditions and slows down under cold and dry conditions. Field degradation is expected to be quicker in the tropics compared to temperate regions. Field degradation in Canada is generally slower compared to the United States. Within the United States sites in subtropical regions degrade quicker than in temperate regions. Within Europe no significant differences are observed between Northern and Southern Europe. At a cross-continental scale field dissipation between North America and Europe is generally not different.
2. Normalization of field degradation rates to reference conditions for soil temperature and moisture eliminates the short-term effect of weather and unveils the effect of abiotic and biotic soil properties on degradation. Following normalization in general no significant differences in degradation were observed neither within Europe and North America nor cross-continentially between both continents suggesting that soil properties and microbial composition responsible for degradation are quite similar within and across these continents. Normalization of field degradation rates makes it possible and allows rate constants to be

- compared from field studies conducted globally, but also allows a rate constant defined at limited geography to be extended to other regions in many cases.
3. Within North America slower normalized degradation rates were only observed under extreme climate and soil conditions (low pH and low organic carbon content in soil). However, further data is needed for final confirmation of the findings. General extrapolation of these data to other continents should be avoided; however, they may be useful to extrapolate to other regions with similarly extreme conditions.
 4. The design of TFD studies may also have an impact on degradation (use rate, formulation, application method - surface application or incorporation). Higher application rates e.g. may slow down pesticide degradation. This must be considered when comparing half-lives from different regions where product label rates may differ due to different weeds, diseases and pests.
 5. Generally the factors contributing to similarities and differences of degradation across regions and sites within a region are still not fully understood and need to be studied further.

References

1. *OECD Guideline No. 307 for the testing of chemicals* (2002); Aerobic and Anaerobic Transformation in Soil.
2. Fenner, K.; Canonica, S.; Wackett, L. P.; Elsner, M. *Science* **2013**, *341*, 752–758.
3. *Fate, Transport and Transformation Test Guidelines*; OPPTS 835.6100 Terrestrial Field Dissipation, United States Environmental Protection Agency, 2008.
4. *Harmonization of Guidance for Terrestrial Field Studies of Pesticide Dissipation under the North American Free Trade Agreement*; Regulatory Directive DIR2006-01, Pest Management Regulatory Agency, Ottawa, Canada, 2006.
5. *Dutch CTB Authorization Manual - Plant Protection Products. Risk for the environment: 4 I B Leaching to groundwater*, ver. 0.2; 2003.
6. Anon. *EFSA J.* **2010**, *8*, 1936.
7. Walker, A. *J. Environ. Qual.* **1974**, *3*, 396–401.
8. Walker, A. *Weed Res.* **1978**, *18*, 305–313.
9. Anon. *EFSA J.* **2007**, *622*, 1–32.
10. *Guidance Document on Estimating Persistence and Degradation Kinetics from Environmental Fate Studies on Pesticides in EU Registration*; Report of the FOCUS Work Group on Degradation Kinetics, EC Document Reference Sanco/10058/2005 version 2.0.
11. *FOCUS groundwater scenarios in the EU review of active substances*; Report of the FOCUS Groundwater Scenarios Workgroup, EC, Document Reference Sanco/321/2000 rev.2.

12. Hardy I. A. J.; Jones R. L.; Allen, R.; Gatzweiler, E. W. XII Symposium Pesticide Chemistry, Piacenza, Italy, 2003.
13. Gottesbüren, B. Ph.D. Thesis, University of Hannover, Germany, 1991.
14. Jenny, H. *Factors of soil formation. A System of Quantitative Pedology*; McGraw-Hill: New York, 1941.
15. Sur, R. *13th IUPAC International Congress of Pesticide Chemistry*, San Francisco, CA, 2014.
16. Global Ecological Zones for FAO Forest Reporting: 2010 update; Forest Resources Assessment Working Paper 179. FAO, Rome.
17. Kottek, M.; Grieser, J.; Beck, C.; Rudolf, B.; Rubel, F. *Meteorol. Z.* **2006**, *15*, 259–263.
18. Sur, R.; Schäfer, D. 246th National Meeting of the American Chemical Society, Division of Agrochemicals, Indianapolis, IN, 2013.
19. Fierer, N.; Jackson, R. B. *Proc. Natl. Acad. Sci. U.S.A.* **2006**, *103*, 626–631.
20. Sur, R. SETAC Europe 24th annual meeting, Basel, Switzerland, May 11–15, 2014.
21. Skidmore, M. W.; Kirkpatrick, D.; Shaw, D. *Pestic. Sci.* **1994**, *42*, 101–107.
22. Racke, K. D.; Skidmore, M. W.; Hamilton, D. J.; Unsworth, J. B.; Miyamoto, J.; Cohen, S. Z. *Pure Appl. Chem.* **1997**, *69*, 1349–1371.
23. Arbeli, Z.; Fuentes, C. L. *Soil Biology and Agriculture in the Tropics*; Soil Biology; Springer: Berlin, 2010; Vol. 21, pp 251–274.
24. Sanchez-Bayo, F.; Hyne, R. V. *Integr. Environ. Assess. Manage.* **2011**, *7*, 577–586.
25. Arbeli, Z.; Fuentes, C. L. *Crop. Prot.* **2007**, *26*, 1733–1746.
26. Walker, A.; Hance, R. J.; Allen, J. G.; Briggs, G. G.; Chen, Y.-L.; Gaynor, J. D.; Hogue, E. J.; Malquori, A.; Moody, K.; Moyer, J. R.; Pestemer, W.; Rahman, I. A.; Smith, A. E.; Streibig, J. C.; Torstensson, N. T. L.; Widyanto, L. S.; Zandvoort, R. *Weed Res.* **1983**, *23*, 373–383.
27. Walker, A.; Barnes, A. *Pestic. Sci.* **1978**, *12*, 123–132.
28. Walker, A.; Jurado-Exposito, M.; Bending, G. D.; Smith, V. J. R. *Environ. Pollut.* **2001**, *111*, 407–415.
29. Price, O. R.; Walker, A.; Wood, M.; Oliver, M. A. In *Pesticide behavior in soils and water*; Symposium Proceedings No. 78; British Crop Protection Council, Brighton, U.K., November 13–15, 2001; pp. 233–238.
30. Price, O. R. Ph.D. thesis. Department of Soil Science, School of Life Sciences, University of Reading, U.K., 2002.
31. Kah, M.; Beulke, S.; Brown, C. *J. Agric. Food. Chem.* **2007**, *55*, 4487–4492.
32. Ghafoor, A.; Moeys, J.; Stenström, J.; Tranter, G.; Jarvis, N. J. *Sci. Technol.* **2011**, *45*, 6411–6419.
33. Ghafoor, A.; Jarvis, N. J.; Thierfelder, T.; Stenström, J. *Sci. Total Environ.* **2011**, *409*, 1900–1908.

Chapter 4

Biodegradation and Quantitative Structure-Activity Relationship (QSAR)

Aleksandar Sabljic*,¹ and Yoshiaki Nakagawa²

¹Department of Physical Chemistry, Institute Rudjer Boskovic, P.O.B. 180,
HR-10002, Zagreb, Croatia

²Division of Applied Life Sciences, Graduate School of Agriculture, Kyoto
University, Oiwake-cho, Kitashirakawa, Sakyo-ku, Kyoto 606-8502, Japan

*E-mail: sabljic@irb.hr.

The biodegradability of organic compounds in terrestrial and aquatic systems is one of the most important factors related to their environmental fate, their adverse effects to humans and the environment and, consequently, their chemical risk assessment. Today there is an array of models for classifying the biodegradability of organic chemicals. Those models range from the simple group contribution models, models based on chemometric methods up to the expert systems based on various artificial intelligence techniques. The objectives of this report are (i) to review and evaluate the published biodegradability classification models and (ii) to recommend the reliable procedures for estimating biodegradability of organic chemicals in the environment. The evaluation procedure has shown that the majority of biodegradability models evaluated in this review have classification rates in the 85-90% range and thus all have a solid classification power. The recommended procedure is to use all evaluated and available models for classifying biodegradability of organic chemicals, i.e. the appropriate BIOWIN model, the set of structural rules, the MultiCASE system, the appropriate CATABOL model and the multivariate PLS model. If there is a consensus between applied models, classification of biodegradation may be considered as very reliable. However, if there is agreement between only four or three of those models, such classification should be considered as reliable or only reasonable, respectively.

Introduction

The persistence of pesticides in terrestrial and aquatic environments (1–4) is one of the most important factors in evaluating their fate as well as their possible adverse effects (5). Biodegradation (mineralization) is the most important process for the removal of pesticides from terrestrial and aquatic environments, once applied to crops. It was assumed that pesticides in terrestrial and aquatic environments are completely bioavailable to microorganisms. While this is generally true for aquatic environments, the studies in the last two decades have revealed that the chemical residues in terrestrial environments are only partially bioavailable to microorganisms and that the biodegradation process is in competition with processes related to transport and mobility and, primarily, with the sorption of pesticides to soils (6). Thus, the ability to measure or reliably estimate the potential microbial biodegradability of pesticides under realistic environmental conditions is of critical importance for the accurate environmental and human risk assessment.

Today, there is no unique or standardized test or parameter that can be used as a universal quantitative or qualitative measure for evaluating the biodegradability potential of chemicals under realistic environmental conditions. Consequently, the general or class-specific qualitative and quantitative models for estimating the biodegradability potential of chemicals have been developed for different environmental endpoints (7–10). The biodegradation studies with mixed microbiological culture that mimic realistic environmental conditions can be loosely classified as screening tests, grab sample tests, biological treatment simulations or field studies. The screening tests normally employ an inoculum and defined mineral salts medium, and the extent of degradation is determined either directly by measuring the disappearance of the parent chemical or indirectly as the biochemical oxygen demand (BOD), CO₂ evolution, chemical oxygen demand (COD) or dissolved organic carbon disappearance. The reproducibility of individual tests is often poor, especially between laboratories, and in some cases even within the same laboratory. This is especially true for the screening tests (11). The variability may be also large for the grab sample tests and field studies as was demonstrated by two extensive reports (12, 13).

Results are often highly dependent upon the test protocol. Thus, during the last two decades the Organization for Economic Cooperation and Development (OECD) has developed standard test guidelines for a series of biodegradability tests (14) like the ready biodegradability test (OECD 301C) also known as the MITI-I test, the inherent biodegradability – modified MITI test (II) (OECD 302C), the aerobic mineralization in surface water – simulation biodegradation test (OECD 309), the ready biodegradability – CO₂ in sealed vessels (headspace test) (OECD 310), the anaerobic biodegradability of organic compounds in digested sludge – measurement of gas production (OECD 311) and similar (http://www.oecd-ilibrary.org/environment/oecd-guidelines-for-the-testing-of-chemicals-section-3-degradation-and-accumulation_2074577x).

The test guidelines developed by the OECD and the US EPA's Office of Pollution Prevention and Toxics and Office of Pesticide Programs

(<http://www.epa.gov/opptsfrs/home/guidelin.htm>) contain the detailed description of specific analytical protocol as well as the criteria for evaluating tested chemicals as biodegradable or non-biodegradable.

One of the most important screening tests for biodegradability is the MITI-I test (OECD 301C). In this screening test the initial concentration of the test substance is quite high (100 mg/L). The test measures BOD, normally lasts for 28 days and, if the oxygen consumption due to degradation of test chemical reaches or exceeds 60% of the theoretical value, the test chemical is classified as easily biodegradable. The largest available screening data set (nearly 1500 chemicals) is the collection of MITI-I test data (15). Another large database of biodegradation information is the BIODEG database, developed by the US EPA and the Syracuse Research Corporation (SRC) (10), includes over 6600 records with biodegradation information on 815 chemicals. The BIOLOG database, also developed by US EPA and SRC, is the index of published literature on the biodegradation and microbial toxicity of chemical substances and contains over 62,600 records covering close to 8000 different chemicals (10). The International Uniform Chemical Information Database (IUCLID), originally developed by the European Chemical Bureau for existing chemicals in collaboration with European Union Member States and Industry, is another source of information on biodegradation. The current version of IUCLID database is 5.5.1 and it is available from <http://iuclid.eu/>. There is also a useful website (<http://umbbd.ethz.ch/>) that includes also the biocatalytic mechanisms, i.e. The University of Minnesota Biocatalysis/Biodegradation Database.

Another source of critically reviewed data for BOD has been prepared by the American Institute of Chemical Engineers, Design Institute for Physical Properties (DIPPR)[®] and is commercially available at <http://software.epcon.com/aiche-dippr-database>. The DIPPR database includes 34 chemical properties for nearly 700 pure chemicals selected from U.S. Environmental Protection Agency regulatory lists (16). Each BOD data point in the DIPPR database has been critically evaluated using a 10-point criteria system which utilizes five rating parameters (rating parameter, experimental protocol, temperature, seed acclimation, chemical concentrations, internal consistency) (17). Data sources received a score between 0 and 2 for each parameter which were then summed for all parameters. For each chemical that had multiple data points from multiple sources, only the highest rated data point was chosen for the database.

Besides the screening tests for biodegradability, there is also a significant database of semi-quantitative biodegradability estimates based on experts' surveys conducted by the US EPA (18, 19). This database can be useful for developing the qualitative and quantitative models for estimating biodegradability and for testing the models developed for screening tests data. In an early survey performed in 1988 the semi-quantitative biodegradability estimates were collected from 22 experts for 50 chemicals (18). The survey chemicals were selected to be representative of chemicals from the pre-manufacture notices received previously by the US EPA Office of Toxic Substances. Each expert rated the primary and ultimate biodegradability of each chemical on a semi-quantitative scale using hours, days, weeks, months, and longer as the approximate time that will be required for a specific process to be completed. The arithmetic mean

was calculated for each chemical after assigning the numerical values (longer = 1; months = 2; weeks = 3; days = 4; hours = 5) to the individual responses as a measure of its biodegradability potential. One of the first general QSAR models (7) was developed using those biodegradability data based on a survey of expert knowledge. Later on in 1994, an extended survey was performed (19) in which 17 experts evaluated the potential biodegradability of 200 organic chemicals, with 50 chemicals originating from the first survey. The 200 survey chemicals covered a very wide range of structures and molecular weights, the majority of which were multifunctional.

There are far fewer biodegradability data that are both quantitative and environmentally relevant like the measured half-lives or rate constants in aquatic and terrestrial systems. Furthermore, such quantitative data usually exist for a specific set of conditions, a single class of chemicals, e.g. polychlorinated biphenyls, and a limited number of data points. Thus, the measured half-lives or rate constants are not suitable for developing general quantitative or qualitative biodegradability models with a wide applicability domain. A similar situation exists for pesticide field dissipation studies and bioremediation research.

In this chapter an extensive evaluation of general models for estimating the complete biodegradation (mineralization) of organic chemicals will be given. First, the structure and main characteristics of such biodegradability models will be described. The focus will be on more recent modeling efforts in this research area since several review articles have already been published on this subject (8–10, 20, 21) as well as on the “standard” models like the BIOWIN™ package, the MultiCASE system, and similar approaches. The most significant part of this chapter will be on the results and discussion of the evaluation of general models for estimating biodegradability. Models will be evaluated in terms of their accuracy and range of applicability. A particular emphasis will be given to the results of external validation. All potential limitations of individual models will be clearly described. Finally, the specific recommendations will be given on the reliable procedure for estimating biodegradability of organic chemicals in the environment.

BIOWIN Models from EPI Suite Package

The Biodegradation Probability Program (BIOWIN™), developed by the SRC on behalf of the US EPA (19, 22, 23), is the most widely used software for evaluating the biodegradability potential of organic chemicals. It can be freely downloaded and used but only as part of the Estimation Programs Interface suite (EPI Suite, version 4.11) at <http://www.epa.gov/opptintr/exposure/pubs/episuite.htm>). Like all models in EPI Suite, BIOWIN is intended for the screening-level application. The current version 4.10 of the BIOWIN software has been developed and improved at several stages (19, 22, 23). The first two modules (Biowin1 and Biowin2) have been developed and improved already in early 90's (19, 24, 25) and are still in regular use to estimate the probability for the rapid aerobic biodegradation of an organic chemical in the presence of mixed

populations of environmental microorganisms. The enhanced version of Biowin1 (linear model) and Biowin2 (nonlinear model) modules (19) were developed using a database of weight-of-evidence (qualitative) biodegradability evaluations for 295 chemicals in the BODEG database (<http://syrrres.com/esc/efdb.htm>) and consequently those modules classify organic chemicals as being easily or poorly biodegradable. Biodegradability estimates are based upon 36 chemical fragments plus a molecular weight fragment which are developed using the multiple linear and nonlinear regression analyses and the dataset consisting of 186 easily biodegradable chemicals and 109 poorly biodegradable chemicals. Both, the linear and nonlinear models classified the easily biodegradable chemicals quite accurately, i.e. 97.3% of correct classification. However, the results are significantly poorer in classifying the slowly biodegradable chemicals, 76.1% for Biowin1 module and 86.2% for Biowin2 module. Thus, both modules seem to be suitable for evaluating only the easily biodegradable chemicals. However, their classification of poorly biodegradable chemicals should be taken with caution particularly since those classification results are for the training set.

The other two models using Biowin3 and Biowin4 modules allow for the semi-quantitative prediction of primary and ultimate biodegradation rates using the multiple linear regressions (19). The training set for those two models consisted of estimates of primary and ultimate biodegradation rates for 200 chemicals, gathered in a survey of 17 biodegradation experts (18, 19). Each expert rated the primary and ultimate biodegradability of each chemical on a semi-quantitative scale, i.e. hours, days, weeks, months, and longer than months. The arithmetic mean was calculated for each chemical after assigning numerical values to the individual scores as follows: 5 = hours; 4 = days; 3 = weeks; 2 = months; 1 = longer and used as the primary or ultimate biodegradation rate, i.e. the input for multiple linear regression. The independent variables were the same as those used in the Biowin1 and Biowin2 modules; i.e. 36 structural fragments plus molecular weight. For the Biowin3 and Biowin4 models, the correlation coefficients (R^2) between experts' estimates and calculated biodegradation rates for the survey chemicals were very similar, slightly above 0.7. On a qualitative level Biowin3 and Biowin4 modules classified the easily biodegradable chemicals more accurately, i.e. 84.9% and 93.5% of correct classification. Results were much poorer for classifying poorly biodegradable chemicals, 79.0% for primary biodegradation and 71.7% for ultimate biodegradation. Again, both modules seem to be more suitable for evaluating the easily biodegradable chemicals.

Shortly after their development, the enhanced version of Biowin1 and Biowin2 modules for estimating the aerobic biodegradability potential have been externally evaluated on a large set of MITI-I data (8, 26). Unfortunately, both modules performed poorly in estimating the biodegradability of organic chemicals based on MITI-I test. Namely, the Biowin1 and Biowin2 modules were able to correctly classify only about 60% of organic chemicals from the MITI-I data set. Consequently, the Biowin1 and Biowin2 modules were re-parameterized by using the MITI-I dataset, resulting in Biowin5 and Biowin6 modules, respectively (27). The training set for Biowin5 and Biowin6 modules consisted of biodegradability results from the MITI-I test (pass/no pass) for 884 organic chemicals. This data set was divided into randomly selected training and validation set. The new

coefficients were derived for the training set using the same fragment library and molecular weight as independent variables. From these results, the fragment library was modified by deleting some fragments and adding or refining others and the new set of independent variables (42 chemical fragments and molecular weight) was fit to the training set data. The resulting linear and nonlinear regression models (Biowin5 and Biowin6) accurately classified 81% of chemical in the validation set. Both models were more accurate in classifying the easily biodegradable chemicals.

The most recent module in BIOWIN program (Biowin7) is quite different from all previous models since this is a screening-level model for predicting the anaerobic ultimate degradation in sludge (23). Biowin7 module was developed from a data set of 169 chemicals tested for methanogenic anaerobic biodegradation using the serum bottle method OECD 311 (28). The new module uses 37 fragments to classify a chemical as being degraded fast or slow under anaerobic conditions. This module does not use the molecular weight as a variable. The Biowin7 module correctly classified 90% of chemicals in the training set and 77% or 91% in the two independent validation sets (n=35 or 23), respectively. The accuracy of predictions of fast and slow degradation was equal for the training-set chemicals. However, the fast-degradation predictions were less accurate than slow-degradation predictions for the validation sets. The comparison of signs of the fragment coefficients for all seven Biowin modules shows that the majority of positive and negative contributions are the same for both aerobic and anaerobic ultimate biodegradation. However, this generalization should not be used to infer common degradation pathways for aerobic and anaerobic biodegradation processes.

In 2004, a battery use of Biowin modules was recommended in order to improve the qualitative prediction for fast biodegradability under aerobic conditions (29). Bayesian analysis suggested that a battery consisting of Biowin3 and Biowin5 modules has the enhanced predictive power in comparison to individual modules. For example, if the Biowin3 results are “weeks”, “days to weeks” or “days” and if Biowin5 predictions is 0.5 or more, then the chemical is evaluated to be easily biodegradable. In all other cases, the chemical is evaluated to be poorly biodegradable. Application of the battery to 374 pre-manufacture notice (PMN) substances showed that this approach significantly reduced both the false positives for easily biodegradable chemicals and the overall misclassification rate. Similar results were obtained for a set of 63 pharmaceuticals using a battery consisting of Biowin3 and Biowin6 modules. The additional guidance on the regulatory interpretation of the Biowin modules results is given in the EU Technical Guidance Document (TGD) for the assessment of new and existing chemicals (30) as well as in the more recent guidance for REACH implementation (31). More specifically, the combined use of Biowin1 and Biowin2 modules are recommended in those documents.

The comparison of coefficient signs of all seven Biowin modules gives interesting results that are, in general, consistent with the common knowledge about the relationships between chemical structure and biodegradability of organic chemicals. All seven coefficients for the tertiary amine, aromatic NH/NH₂, and aromatic nitro fragments are negative while all seven coefficients

are positive for ester, phosphate ester, aldehyde, aliphatic and aromatic acid, aliphatic and aromatic alcohol, and unsubstituted phenyl groups. The molecular weight term was uniformly negative in all six aerobic models while it was not used as variable in Biowin7 module. For five additional fragments—aliphatic ether, pyridine, aromatic chlorine, aliphatic chlorine, and quaternary carbon—six out of seven coefficients were negative. Finally, for three fragments—aromatic ether, aliphatic amine, and C₄ terminal alkyl—the coefficients were positive in six of seven models. Pyridine and linear C₄ terminal alkyl are the only fragments for which all aerobic modules are in disagreement with the anaerobic module. Thus, it seems, contrary to the previous assumptions (32), that the majority of structure-biodegradability relationships applicable to aerobic environments are also applicable to anaerobic environments. Namely, the major positive and negative contributions are the same for aerobic and anaerobic ultimate degradation. A new rule for anaerobic conditions might be that the unsaturated (olefinic) hydrocarbons degrade much faster than the saturated hydrocarbons.

The seven models (Biowin 1-7) were developed from four quite different training sets. Consequently, their applicability domains defined by the range of fragments and molecular weights (MW) in the training sets will be also very different. In addition, for the semi-quantitative Biowin 3 and 4 modules, the maximum and minimum values of ultimate or primary degradation rates also define their applicability domain. However, there are several general features of Biowin 1-7 modules related to their applicability domains. Namely, it is generally accepted that the biodegradability estimates will be more accurate for compounds that are within the corresponding applicability domain. Thus, the biodegradability estimates will be less accurate for (i) chemicals that are outside the MW range of the training set, (ii) chemicals having more instances of a given fragment than the maximum for the training set compounds, (iii) chemicals having a functional group(s) or other structural features not represented in the model's fragment library, and (iv) chemicals that have no fragments in the model's fragment library, i.e. the estimate is based only on their molecular weight. For example, for Biowin3 module the largest percentage of misclassified chemicals was obtained for chemicals for which prediction was based on the molecular weight alone (33). All these points should be taken into account when evaluating the quality of biodegradability estimates by the Biodegradation Probability Program (BIOWIN™).

The fragment (group) contribution models like all Biowin modules lack the ability to incorporate the effects of substituent positions, i.e. structural isomers, on biodegradability of organic chemicals. A classic example is biodegradability of naphthoic acid isomers in the MITI-I test. Biowin5 and 6 modules predict that 1-naphthoic acid and 2-naphthoic acid pass the MITI-I test, i.e. that both isomers are easily biodegradable. However, while 1-naphthoic acid has failed the MITI test, the 2-naphthoic acid has passed the test as predicted by Biowin5 and 6 modules. There are a number of similar examples in the relevant literature since it is well known that isomers or chemicals with minor differences in chemical structure can be degraded at very different rates or even by different pathways (32). The basic assumption of fragment contribution models like Biowin modules is the linear additivity of fragment contributions irrespectively of their type

or number. While this assumption works reasonably well for small molecules contain only commonly found fragments in small numbers, the wrong prediction becomes more likely even if fragments with positive contribution are present in larger numbers. A typical example is *cis*-cyclopentane tetracarboxylic acid with the multiple carboxylic acid groups that are favorable for easy biodegradability. BIOWIN's prediction is that this chemical should be easily degraded but in reality it is not easily degraded (25). Finally, it is very likely that some fragments significant for biodegradation are not included into the fragments library of respective Biowin module. Examples are phosphonate, imidazole ring, ethoxylate ether and cycloaliphatics. Adding more and/or better defined fragments into the model's fragment library can improve its predictive performance but this is not always the case. The users of Biodegradation Probability Program (BIOWIN™) should be aware of all potential models' shortcomings which are clearly described in its online manual.

Logical Structural Rules for Biodegradability Classification

Classification models based on the set of logical structural rules have been also developed and improved in several stages (8, 17, 26, 34, 35) by the application of appropriate artificial intelligence techniques. These techniques are easily applied to the large sets of molecular descriptors, and do not require any *a priori* assumptions regarding the model structure. Specifically, two decades ago Gamberger et al. (34) applied the inductive machine-learning methods (36) to derive the first strict rules, i.e. the structural requirements, for fast or slow biodegradation. The training set consisting of 160 chemicals, a combination of experts' judgments for 48 chemicals (18) and 112 substances from the BIODEG database (10), was used to develop three simple structure-based rules by means of an example based learning system. This set of rules combines the structural requirements necessary for fast (easy) biodegradation as follow:

- Chemicals with at least one acyclic C–O bond and the molecular weight below 180
- Chemicals built of C, H, N, and O atoms, without a nitro group and having more C–O bonds than rings
- Chemicals built of C, H, N, and O atoms, without a nitro group and the molecular weight in the range from 95 to 135.

The low molecular weight; the presence of only C, H, N, and O atoms; the presence of acyclic CO bonds as well as acid, ester, and anhydride groups were found to stimulate biodegradation while the presence of rings, quaternary carbons, and tertiary and aromatic amines results in slow biodegradation. This set of rules was evaluated on the two small test sets, i.e. 23 and 17 chemicals. The prediction results were excellent, 96% and 100% respectively (34, 35).

This simple set of structural rules was also very successful in classifying easily biodegradable chemicals from the BIODEG and MITI-I data bases, i.e. 85.4% and 88.7%, respectively (26). Unfortunately, it was not equally successful in evaluating poorly degradable chemicals since only 70.4% or 62.3% of chemicals was correctly classified.

Consequently, several efforts have been made (8, 17, 26) to develop an extended set of structural rules that will more correctly estimate the biodegradability potential of chemicals from the BIODEG and MITI-I data bases. The most recent effort in this area was performed using the inductive machine learning method and biodegradation data for 762 substances measured according to the MITI-I test protocol in order to develop structural rules for fast ultimate biodegradation (8). The following seven rules have been derived for the easy biodegradation (i.e., the chemical will biodegrade fast if any of the following seven rules applies):

- esters, amides, or anhydrides with a larger number of ester groups than rings
- all chemicals with at least one acyclic C–O bond and the molecular weight below 129
- chemicals built of C, H, N, and O atoms and with larger number of esters groups than rings but without a nitro group
- organic acids with molecular weight below 173 and with more acid groups than halogen atoms
- chemicals built of C, H, N, and O atoms with the molecular weight below 129 having equal number of aromatic amino groups and acid groups but without a nitro group
- esters, amides, or anhydrides with the molecular weight below 173 and at least one acyclic C–O bond
- chemicals built of C, H, N, and O atoms with the molecular weight below 173 and at least one acyclic C–O bond, equal number of aromatic amino groups and acid groups, but without a nitro group

This set of 7 rules is based only on 11 structural descriptors, selected from a pool of 17 (Table I). It was possible to correctly classify 84.3% of chemicals from the MITI-I database with a well-balanced classification of easily (84.9%) and poorly (83.7%) biodegradable chemicals. An analysis of structural descriptors present in the biodegradation rules was performed to extract information on the requirements for either easy or poor biodegradation. The low molecular weight (below 173); presence of only C, H, N, and O atoms in a chemical; presence of C–O bonds; acyclic structures; as well as acid, ester, amide, and anhydride functional groups all seem to be stimulating features for biodegradation. On the other hand, the presence of rings, aromatic amines, halogen atoms, or a nitro group seems to retard the biodegradation process. These findings are also consistent with the general experience (32) and earlier findings (34).

Table I. The Complete Set of Structural Descriptors Used to Develop Seven Structural Rules for Fast Ultimate Biodegradation (MITI-I data) by the Inductive Machine Learning Method (8, 26)

Structural descriptors

Presence of heterocyclic nitrogen atom

Presence of ester, amide, or anhydride groups

Number of chlorine atoms

Bicyclic alkanes

Chemical composed only of carbon, hydrogen, nitrogen, and oxygen atoms

Presence of nitro group

Number of rings

Presence of epoxy group

Primary alcohols and phenols

Molecular weight

Number of all C-O bonds

Number of tertiary amino groups

Number of quaternary carbon atoms

Number of C=C bonds

Number of aromatic amino groups

Number of acid groups

Number of ester groups

The set of seven rules was externally validated on 293 compounds from the BIODEG database. The evaluation test showed that the overall performance of the seven biodegradation rules is very good since 85% of the predictions were in agreement with the observed biodegradability. The predictions were slightly better for easily biodegradable substances, with 86.3% correct predictions vs. 83.6% correct predictions for poorly biodegradable substances. The evaluation test shows that the prediction scores on the training and test sets are very similar, and it confirms a solid predictive potential of the seven developed biodegradation rules for easily biodegradable chemicals.

In general, the inductive machine learning method develops the structural rules without human input. By the examination of data, the computer deduces sets of rules that best describe the modeled endpoint, in this case the biodegradability of chemicals. Consequently, this approach may also suggest the degradation processes, i.e. rules, which are not feasible in the natural environment. But, more importantly, such a system may lead to the discovery of new rules, i.e. the structure/biodegradability rules not previously known to experts. Today, it is also

possible to suggest the specific structural rules to the inductive learning systems and the method will test it against the available data and include it into the final set of rules if it is sufficiently relevant for biodegradability of chemicals.

A notable advantage of this approach is that a simple system of rules with a relatively small number of structural features (11 structural descriptors) could achieve such a high performance, comparable with that of far more complex models like Biodeg1 to Biodeg7 modules having from 37 to 43 structural descriptors. The main reason for such a drastic reduction (3-4 folds) of necessary structural descriptors is the fact that the structural rules can also incorporate the combinations of functional groups which are important for biodegradability of specific chemical. This was done in a simple way since the rules do not specify the relative position of relevant fragments. Nevertheless, the results show that the biodegradation of a specific fragment should be considered in the context of its molecular environment.

Another notable advantage of biodegradability rules developed by the inductive machine learning method is that besides the structural (molecular) features this artificial intelligence methodology can also handle the environmental properties like acclimation, chemical concentration, the presence and type of solids relevant for chemical bioavailability, and similar. Such environmental properties relevant for biodegradability can be also included in the future sets of logical rules either in the rule(s) of their own or combined with the structural characteristics in the common rule(s). It is reasonable to assume that the models accounting for actual environmental conditions will be more reliable in predicting biodegradability.

MultiCASE and MultiCASE/META Expert Systems

The MultiCASE program (37–39) is a fully automated expert system that analyzes the activity of a given set of compounds and automatically identifies structural features and physicochemical properties that seem to be responsible for the observed activity. This expert system generates all structural fragments with two, three, or four heavy atoms and selects those that are statistically most significant for the endpoint of interest, in this case biodegradability. The selected structural fragments associated with easy biodegradability are known as the biophores, while the structural fragments associated with poor biodegradability are the biophobes. The novelty here is that the selection of relevant structural fragments is based only on the training set chemicals and not on some predefined rules or fragment databases. The MultiCASE modeling program has been evaluated on a training set of 630 compounds (269 easily biodegradable and 361 poorly biodegradable) from the MITI-I dataset in order to investigate whether its implicit variable selection procedure will result in the correct classification of chemicals as easily or poorly biodegradable. The set of 269 compounds was searched for fragments that stimulate biodegradability in the MITI-I test (the biophores), while the second file of 361 compounds was searched for fragments that impede biodegradability in the MITI-I test (the biophobes). By this procedure program located 48 biophores that explain MITI-I data for all 269 biodegradable

compounds, as well as 10 biophobes. Finally, a multiple linear regression (MLR) model was built between the 58 selected fragments and the MITI-I data and such model was capable to correctly classify 92.5% of data in the training set.

The test set of 244 compounds not used in the model development was used to evaluate the ability of selected 58 fragments (the biophores and biophobes) to correctly classify biodegradability of the test set chemicals. First, all compounds were searched for the presence of biophores. This search resulted in 41 warnings, indicating compounds with structural fragments that may be the potential biophores but none was present in the training set. In such cases, it was not possible to make predictions since the program cannot evaluate the effect of “unknown” fragments on biodegradability. In addition, one compound was too small to contain any biophore. This reduced the test set to 202 compounds. Due to the absence of a biophore, 106 compounds were predicted as poorly biodegradable. This was a correct prediction for 95 compounds (89.6%) according to their MITI-I values. Furthermore, 96 compounds were predicted to be easily biodegradable due to the presence of a biophore, but this was correct only for 43 of those chemicals (44.8%). Thus, the presence of a biophore in a molecule does not mean that such compound will be easily biodegradable. The test set of 244 compounds was then searched for the biophobes. The second search resulted in 37 warnings on potential biophobes. Thus, the test set has to be reduced to 207 compounds. Due to the presence of a biophobe, 111 compounds were predicted to be poorly biodegradable, while 96 were predicted as easily biodegradable due to the absence of any known biophobe. According to MITI-I test data, these predictions were correct for 82 (73.9%) and 65 (67.7%) compounds, respectively. From the results of external validation, it is clear that the MultiCASE model performs very well for the prediction of poor biodegradability based on the absence of known biophores. In that case, the success rate is 89.6%, which is a very good performance for the external validation. The absence of a known biophore indicates a lack of an active site for microbial attack, and it seems to be a good indicator for a poor biodegradability of a compound. Other assumptions based on the presence or absence of biophores or biophobes result in low prediction scores (44.8–73.9%) and cannot be used in evaluation of a compound’s biodegradability. The poor performance of the model based on the presence of a biophore may be rationalized either by: (i) the presence of a biophore that will not lead to a complete biodegradation (mineralization) or (ii) the simultaneous presence of a biophobe in a molecule that will make its biodegradation difficult.

The MultiCASE approach has also been used to model anaerobic biodegradation in aquatic media (40). Only the high-quality data for 79 chemicals from the Environmental Fate database (41) has been used in this modeling effort. In such data set, 45 chemicals were easily biodegradable, 16 were inactive under anaerobic conditions while 18 were only marginally biodegradable. MultiCASE program identified aromatic and aliphatic thiols, methoxy, alcohol, and carboxylic ester groups as the anaerobic biophores, but no significant biophobes were found. The relevance of identified biophores was confirmed because all were associated with the known metabolic transformations. In the MultiCASE approach, chemicals with one or more biophores are classified as easily biodegradable unless there is one or more biophobes. Thus, the inability to identify the anaerobic

biophobes has significantly influences model ability to correctly classify poorly biodegradable chemicals. Consequently, the MultiCASE model for anaerobic biodegradation was better in classifying easily biodegradable chemicals (89% correct) than those that are poorly biodegradable (64% correct).

One of the first expert systems for biodegradability was a hybrid approach based on the combined use of MultiCASE and META (42). The MultiCASE/META system relies on the statistics to set the hierarchy and on the mechanistic understanding for development of the rules. META is an automatic rule induction program that gives qualitative predictions of the aerobic biodegradation pathway (42, 43) and it is composed of 70 transformations that match 13 biophores found by MultiCASE analysis from the literature data (39). The weights of the biophores calculated by MultiCASE are used to define the hierarchy of transformation rules for a given parent chemical structure. In the next stage of this expert system development (44) several biophobes (C-halogen, C-NO₂, C-CN, C-NH, and branched aliphatic chains) were also identified by analyzing 200 chemicals from the MITI-I database. The improved model performed very well on a small validation set and correctly classified all 34 chemicals.

The results of MultiCASE model can be easily rationalized and their mechanistic interpretation is also possible. One potential problem is that all relevant biophores and biophobes are not located during the model development since the specific structural features important for biodegradation are not present in the training set. Thus, such model may fail when used to predict biodegradability of chemicals outside applied training set. Furthermore, the MultiCASE model seems to be better suited for identifying poorly biodegradable chemicals. Namely, even the presence of a single biodegradation retarding fragment (the biophobe) can prevent mineralization, while the presence of one or more biodegradation enhancing fragments (the biophores) only indicate the possible metabolic pathways, which may not lead to the mineralization.

CATABOL Expert System

CATABOL is another expert system (45–47) that predicts the possible transformation products formed by biodegradation of the parent compound. This hybrid system consists of a knowledge-based system for predicting the biotransformation pathways and a probabilistic model that calculates the probabilities of each transformation as well as the overall biochemical oxygen demand (BOD) and/or CO₂ production. The novelties of this expert system are that (i) the biodegradation potential of parent compound is determined from all individual steps in the biodegradation pathway and (ii) it explicitly takes into account the effect of adjacent fragments before executing each transformation step. The system contains a library of more than 500 individual transformations (abiotic and enzymatic) (21) that are hierarchically ordered. The hierarchy is set according to the descending order of the individual transformation probabilities. Before any individual transformation is applied on a target fragment, the presence of adjacent inhibitory fragments is checked for since such fragments may

either completely prevent the specific transformation or significantly reduce its probability to occur. The mineralization process may be a long sequence of transformations but the number of critical steps (the rate-determining steps) for mineralization of individual chemical is small.

Based on above principles, several specific models have been developed for various biodegradability endpoints and incorporated into the CATALOGIC software suite (<http://oasis-lmc.org/products/software/catalogic.aspx>). In CATABOL 301C model, the probabilities of individual transformations were deduced from the BOD data of 745 compounds from the MITI-I database. The catabolic reactions with similar BOD and similar targets are assumed to have the same probability. Since analysis of the MITI-I data resulted in many transformations with equal probability, their hierarchy is established based on expert knowledge. The model correctly classified 85% of easily biodegradable chemicals and 91% of poorly biodegradable chemicals. In CATABOL 301B model the probabilities of individual transformations were deduced from the percentage of theoretical CO₂ release in 28 days (Modified Sturm test) of 109 compounds. This model correctly classified 88% of easily biodegradable chemicals and 73% of poorly biodegradable chemicals. Furthermore, both models also enable the identification of potentially persistent catabolic intermediates which is beyond the capability of previous biodegradability models. The applicability domains of CATABOL models are defined by the range of log K_{ow} data, molecular weights and fragments of correctly classified chemicals from their respective training sets. Although, the biodegradation pathways predicted by CATABOL models are subject to considerable uncertainty, the CATABOL models outputs can be very helpful in determining the degradation pathways of chemicals for which the critical data are missing (48).

The Multivariate PLS Model

A multivariate PLS model for classifying organic chemicals as easily or poorly biodegradable under the MITI-I test conditions was proposed by Loonen et al. (8, 49, 50). The model is based on MITI-I data for 894 substances of widely varying chemical structure of which 388 chemicals were easily biodegradable while 506 were poorly biodegradable. It was developed in several steps. A set of 127 predefined structural fragments was selected (51) and a descriptor matrix was developed indicating the absence or presence of each fragment in 894 chemicals. A model was developed in which the MITI data were correlated with the structural fragments using the PLS discriminant analysis. The developed PLS model generates predictions on a continuous scale from zero to one. Thus, a transformation was needed to compare such predictions with the original binary data for biodegradability. The continuous scale was divided into two areas, >0.55 and <0.45, corresponding to easily biodegradable and poorly biodegradable chemicals, respectively. Estimates between 0.45 and 0.55 were considered the borderline cases and as not reliable (50).

The analysis of PLS model has shown that about one third of fragments, i.e. 44 fragments, have positive regression coefficients and enhance biodegradability of chemicals. The two most important positive fragments are related to the long non-branched alkyl chains which are known to be susceptible to oxidation. Other fragments associated with a significant positive effect on the biodegradability are one or more hydroxyl group(s) attached to a chain structure, and one or more carbonyl, ester, or acid groups attached either to a chain or ring structure. Chain structures with these fragments are susceptible to the oxidation processes and the formation of carboxylic acids through the intermediate formation of aldehydes. The aromatic rings with such fragments are degraded through the formation of catechol followed by the ring opening. The majority of structural fragments in PLS model, i.e. 83 fragments, is associated with the negative regression coefficients and inhibits biodegradation. The most important inhibiting fragments are one or more aromatic rings, and fragments with one or more halogen substituents on a chain or ring structure. These findings are consistent with the observations that the aerobic biodegradation decreases with the degree of halogenation. The PLS biodegradation model has very good overall classification ability, about 85%. However, it should be noted, that this result excludes predictions made for about 10% of chemicals whose estimated values were between 0.45 and 0.55. As described earlier, this is the borderline area and such estimates are not reliable and should not be used.

The influence of interactions between fragments within the same molecule was also investigated (8, 49, 50). A two-step variable selection was performed in the development of the model with fragment–fragment interactions to keep the model size manageable. In the first step, 97 structural fragments were selected which were present in at least five chemicals. Then, the most important fragment–fragment interactions were selected on the basis of their PLS regression coefficients, i.e., the additional 706 variables. With these additional variables, the model overall classification ability increased to 89%. The improved classification ability is almost entirely related to the poorly biodegradable chemicals since their classification improved significantly, i.e. from 86% to 92%.

The PLS model could not be externally validated by the use of the MITI-I test data since all data were used as a training set. Thus, the training set of 894 MITI-I data was divided into four subsets each consisting of 25% of chemicals from the database. Consequently, the four sub-models without fragment–fragment interaction terms were developed each time using three different subsets of chemicals. For each sub-model the remaining subset was used for “external” validation. The correct classifications for easily biodegradable chemicals in four subsets were from 83% to 87% while for poorly biodegradable chemicals the range was from 77% to 83% (8, 50). These results show that classification scores of internal and “external” validation are similar and confirm a solid predictive capability of the multivariate PLS model.

The application domain of multivariate PLS model is restricted by the presence of the respective fragments in the target chemical. Thus, this PLS model can be applied to all chemicals having at least one of the 127 fragments in their molecular structure. The broad range of structural fragments used in developing the PLS model allows its application to a wide variety of chemical structures.

General QSAR Models for Biodegradability

The first general QSAR model for evaluating biodegradability of organic chemicals was developed about 25 years ago (7). This relatively simple model, 4 structural descriptors and 3 correction factors, is based on biodegradability data obtained from a survey in which 17 experts evaluated the ultimate aerobic biodegradability of 50 organic chemicals (18). Although, the training set was relatively small, it covered a wide range of structures and molecular weights, and almost all those chemicals were highly multifunctional. Two different test sets, 23 and 17 chemicals, of high quality data from BIODEG database have been used to evaluate the predictive potential of this simple QSAR model (52, 53). QSAR model was successful in correctly classifying 90% of test chemicals. This independent test demonstrated the general applicability of developed QSAR model.

In this section only the most recent efforts to develop general QSAR models for evaluating biodegradability of organic chemicals, i.e. the quantitative structure/biodegradability relationships (QSBR) models, will be evaluated since several extensive reviews are already available (8–10, 17, 21, 54, 55) that cover earlier developments. Recently, two extensive modeling studies have been made to develop the generally applicable QSBR models for predicting biodegradability of organic chemicals (15, 56). The first study by Cheng et al. (15) was published about two years ago and the largest heterogeneous training set of 1440 compounds, i.e. MITI-I data, was used to develop generally applicable QSBR models. The main idea was to develop the complete *in silico* method to estimate chemical biodegradability in the environment using 148 physicochemical descriptors and 7 types of fingerprints calculated only by the open source tools. The four different descriptors reduction methods were systemically used to develop the best combinatorial classification probability models, i.e. (i) the correlation-based selection of top ten descriptors, (ii) the classification and regression tree algorithm (57), (iii) Chi-squared automatic interaction detector (58), and (iv) the support vector machine with genetic algorithm with stepwise selecting process. The following seven fingerprints implemented in PaDEL-Descriptor (59) were tested in this study; the CDK fingerprint, CDK extended fingerprint, Estate fingerprint, MACCS keys, PubChem fingerprint, Substructure fingerprint, and Klekota-Roth fingerprint (59, 60).

The four different machine learning methods, namely the support vector machine, k-nearest neighbor, naive Bayes, and C4.5 decision tree, were used to develop the classification models for biodegradability of organic chemicals using the physicochemical descriptors and fingerprints separately. Consequently, a significant number of models with reasonably high classification power were built in this study, 16 with physicochemical descriptors and 32 with various fingerprints. More specifically, models developed with the physicochemical descriptors correctly classified from 65.9% to 100% of the training set chemicals while the range of correctly classified chemicals for the models based on fingerprints was 73.7-100%. All models with high classification power were validated by a test set consisting of 164 diverse chemicals collected from the US-EPA BIODEG database and literature (25, 29). Unfortunately, the success

of developed models was only moderate in classifying biodegradability of the external test chemicals, i.e. 61.0–84.2% for 16 physicochemical models and 65.2–82.9% for 32 fingerprints models. Even four models having the perfect score with the training set chemicals performed significantly poorer for the external test set, i.e. the respective scores were 75.6, 78.7, 84.2 and 65.2% or only 75.9% on average. Furthermore, all developed models have lower predictive power than the set of seven simple structural rules described above (8).

Due to the poor performance of the best developed models in classifying biodegradability of chemicals in the test set, the seven new models were built using all previous training and test set chemicals, i.e. 1604 compounds in the training set. The 5-fold cross-validation procedure was used to evaluate the ability of new seven models to correctly classify biodegradability of the previous test chemicals. Their respective scores were somewhat improved and ranged from 78.6% to 91.2% but those results are not the true measure of models predictive power since all test set chemicals have been used in the models development. Moreover, 27 additional chemicals without MITI-I test data were selected for the so-called blind test and their biodegradability was estimated by those seven models. Consequently, the biodegradability of those 27 chemicals was measured using the MITI-I test protocol. The comparison of newly measured data and predictions made by the seven new models has shown very good to excellent classification results for the six of those models, i.e. from 85.2 to 100% of correct classification. In addition, the consensus model using the mean method (61) was applied to the blind test chemicals and achieved a perfect score. Unfortunately, there is no proof that described exercise is a true blind test and that the experimental assays for 27 chemicals were performed *a posteriori*. Furthermore, it is quite strange that the selected test set of 27 chemicals is extremely unbalanced and that almost all selected chemicals are poorly biodegradable, i.e. 23 vs. 4 chemicals. It was also not reported which criteria were used to select 27 chemicals for the so-called blind test. Unfortunately, it was also not evaluated if this small external validation set is representative of the chemical space of the developed model, but four molecules definitively cannot cover the chemical domain of models based on 1604 chemicals. Finally, it should be noted, none of developed models was explicitly reported in this study and consequently such models are not of general use (62) and can be only applied for predicting biodegradability by the authors.

Another set of generally applicable QSBR models for predicting biodegradability of organic chemicals (56) was published in 2013. The aim of this study was also to develop the reliable classification QSAR models for ready biodegradability of chemicals by using different modeling methods and wide range of molecular descriptors. Again the experimental biodegradability values were from the MITI database and collected from the webpage of the National Institute of Technology and Evaluation of Japan (NITE). The initial data set consisted of 1309 chemicals. Data were carefully screened to ensure that each individual value is in accordance with the OECD test protocol (301 C) and that the correct chemical structures were used. The remaining 1055 chemicals, i.e. 356 easily and 699 poorly biodegradable molecules, were used for modeling. The resulting data set was split into the representative training (837 molecules) and test (218 molecules) sets before modeling. DRAGON software version 6 (63)

was used to calculate molecular descriptors. A filtering of the descriptors was performed and constant, near constant, and correlated descriptors were removed. A total of 781 descriptors were used in the subsequent modeling.

Three different classification methods were used to develop the appropriate relationships between the molecular structures, encoded in molecular descriptors, and the biodegradability of chemicals: the *k* nearest neighbors (*k*NN) (64), the partial least squares discriminant analysis (PLSDA) (65, 66), and the support vector machines (SVM) (67). The application of methods founded on different mathematical strategies aimed to fully explore the chemical space and avoid potential biases of individual modeling algorithm. Furthermore, the genetic algorithms (GAs) were applied to select the optimal subset of molecular descriptors with each classification method (68). The genetic algorithms were calculated first on each block of molecular descriptors, i.e. constitutional indices, ring descriptors, topological indices, 2D matrix-based descriptors, functional group counts, atom centered fragments, atom-type E-state indices and 2D atom pairs. Descriptors selected from each block were merged and GAs were applied again to find the most appropriate subset of all molecular descriptors to calibrate the final QSAR models. The final models were selected taking into consideration the results of cross-validation as well as balanced classification. The final classification models based on the *k*NN, PLSDA and SVM approaches had 12, 23 and 14 molecular descriptors, respectively.

The three classification models have comparable scores in fitting and cross-validation with calibration set chemicals, i.e. 86% of chemicals were correctly classified. The balanced classification is achieved for the *k*NN and PLSDA models while for the SVM model there is a significant difference (11%) between the classifications of easily and poorly biodegradable chemicals. In the case of test set chemicals the classification scores of all three models was high (85-86%) and close to the results in fitting and cross-validation. The SVM and *k*NN models showed better performance in classifying poorly biodegradable chemicals by 9%.

The consensus analysis (61) was also applied to combine classification power obtained by the three different modeling techniques. Two different consensus algorithms were used: (i) each molecule was classified to the more frequent class obtained by the classification of individual *k*NN, PLSDA and SVM models (consensus 1) and (ii) a molecule was classified only if there is a consensus between all three models; otherwise, it remained unclassified (consensus 2). In the case of consensus 1 approach classification results were improved by 3% for the calibration set chemicals (the fitting and cross-validation) and only by 1-2% for the test set chemicals. Again, the balanced classification is achieved for calibration chemicals and better performance by 10% is achieved in classifying the poorly biodegradable test set chemicals. In the case of consensus 2 approach, the classification results were significantly improved (7%) for the calibration chemicals and the balanced classification is maintained. However, the penalty for significantly improved classification score was that about 20% of chemicals were not assigned. Similar result was achieved in classifying the test set chemicals; the improved classification by 5-6%, a better performance (6%) in classifying poorly biodegradable chemicals and 15% of unassigned chemicals.

All three individual classification models and two consensus approaches were additionally validated using an external validation set consisting of 670 chemicals. This validation set contained 464 chemicals from the data set used by Cheng et al. (15) and 206 persistent and bioaccumulative compounds from the Canadian Domestic Substances List (DSL) database (69). A good classification performance (82-87%) was obtained and results of validation for the three QSAR and two consensus approaches are close to the cross-validation and test set validation. Unfortunately, the classification was not well balanced and better performance up to 17% is achieved in classifying the poorly biodegradable chemicals. Also, 13% of chemicals were not classified by the consensus 2 approach.

Altogether, 41 molecular descriptors were used in all three classification models which mean that there is a very small overlap in selected molecular descriptors between different models. Specifically, only one molecular descriptor, i.e. the leading eigenvalue from Laplace matrix, is used in all three classification models and additional six molecular descriptors were selected by the pair of models. However, the structural analysis shows that descriptors selected in each QSAR model encoded similar information, i.e. the presence of halogens, branching, nitro and amino groups, rings and some other functional groups. It is well known for years (8-10) that such structural features are related to slow biodegradability. Finally, it should be pointed out that none of three QSAR models was explicitly reported in this study and consequently such models are not of general use (62) and can be only applied for predicting biodegradability by the authors.

Partial Biodegradability and Transformation Products

Microbial degradation in natural and artificial (manmade) ecosystems normally results either in a complete removal of target pesticide or pesticide remains intact if relevant microbial populations are not present. However, in some cases biodegradation processes, i.e. biotransformation (70), may also produce stable transformation products (TPs). Whether and what type of TPs are formed in the environmental and engineered systems from a given chemical depends on the precursor's chemical structure, but also on its distribution between different environmental compartments. Due to the rather complex molecular structures of modern chemicals, it is very likely that their microbial degradation will often result in the formation of stable TPs. In general, the oxidative processes lead to TPs that are more polar and consequently more mobile and less toxic than the parent compounds (71). However, there is plenty of evidence that the biotransformation of parent molecules can also yield toxicologically relevant TPs. Typical examples are the pro-pesticides like organophosphate insecticides containing a phosphorothioate or phosphorodithioate moiety which are oxidized by cytochrome P450 monooxygenases and produce oxon metabolites that are more potent inhibitors of acetylcholinesterases than their precursors (72). Two other typical examples are the microbial transformation of triclosan to the more

bioaccumulative methyl-triclosan (73), and the microbially mediated oxidative cleavage of phenoxy herbicides that yield substituted phenols acting as uncouplers of energy-transduction (74). Furthermore, there is growing evidence that the microbial transformations producing stable TPs are important for environmental compartments such as soils or sediments as well as for the engineered systems such as activated sludge (75, 76).

Today, the transformation products are an important issue in the chemical risk assessment and environmental research since a transformation product may be even more bioaccumulative and/or toxic than the parent chemical. Consequently, the significant research efforts have been made on the detection of transformation products in the environment, on the identification of relevant transformation products and their potential adverse (toxic) effects and on evaluating environmental risk related to the transformation products (70, 77–80). The occurrence of transformation products in the environment has been recently reviewed by Kolpin et al. (81). Today, the high-resolution mass spectrometric techniques enable the fast, sensitive, and reliable detection of transformation products even in the absence of chemical reference standards (79, 82–85). The high-resolution mass spectrometry has been used by Kern et al. (79) to screen for about 2000 known and predicted transformation products of 50 pesticides, biocides, and pharmaceuticals in Swiss surface waters to obtain a more comprehensive picture of their presence in the aquatic environment. For about half of the investigated parent compounds one or two transformation products were found in the seven surface water samples analyzed. In an analogous recent study the high-resolution mass spectrometry was applied to screen the environmental samples for 150 well known pesticide transformation products as well as for various suspected transformation products (86). A more complete picture of pesticide transformation products in the environment will emerge over the next years primarily due to the major advances in mass spectrometry.

Several computational tools described earlier are currently available for predicting the aerobic, microbial transformation pathways of organic compounds and the structures of potential transformation products. Those are MultiCASE/META (39, 42, 43) and CATABOL (45–47) as well as PathPred (87) and the University of Minnesota Pathway Prediction System (UM-PPS) (88, 89). A set of 1512 potential transformation products was predicted by UM-PPS for 52 pesticides, biocides, and pharmaceuticals. The subsequent search for the predicted transformation products resulted in the identification of 19 such compounds in environmental samples (79). In another study 26 transformation products, derived from 12 parent compounds, were detected in activated sludge batch reactors by various high-resolution mass spectrometry techniques (82). Of these 26 transformation products, 21 were predicted by UM-PPS. In order to transform UM-PPS into an efficient and fast screening tool for potential environmental transformation products, the large number of pathways normally suggested by UM-PPS can be drastically reduced by a set of three simple rules (80): (i) removing analogous products, (ii) selecting only the most likely products and (iii) products generation is limited on the first two generations. The reduction scheme was tested on 22 pesticides and its average efficiency was 84% (80, 90).

The majority of biodegradability classification models described in previous sections, i.e. the BIOWIN models, the logical structural rules, the multivariate PLS model and general QSAR models, cannot distinguish between the poorly biodegradable chemical and biotransformation of parent chemical into a stable transformation product since their BOD data will be similar. However, besides parent compounds, the stable transformation products should be also used to calibrate and evaluate the quality and reliability of those biodegradability classification models.

Although important advances have been recently made in this research area, a more complete picture of pesticide transformation products in the environment will emerge over the next years based on interdisciplinary and/or multidisciplinary research combining results obtained by the application of molecular genetics methods, stable isotopes analysis, bioinformatics and sensitive mass spectrometric methods (77).

Biodegradability Modeling Recommendation and Perspectives

Today there is an array of models for classifying the biodegradability of organic chemicals and some of them can also evaluate the most important microbial degradation pathways responsible for their biodegradability. Those models range from simple group contribution models, models based on chemometric methods up to expert systems based on various artificial intelligence techniques. However, their number is quite moderate if compared to a general proliferation of QSAR models for other environmental end-points. The main reason is still, as it was pointed out more than a decade ago (8), the deficiency of standardized and uniform biodegradation data for various chemical classes. In the last ten years only the MITI-I database has been extensively amended by new data. The majority of biodegradability models presented and evaluated in this review have a classification rate in the 85-90% range, thus showing a solid classification power.

BIOWIN models are the most widely used for evaluating the biodegradability potential of organic chemicals. Consequently, BIOWIN models have been most extensively evaluated and independently validated and this is definitively their major advantage. In one of the recent evaluation studies, the BIOWIN models were also probed in predicting the biodegradability of 42 pharmaceuticals and drug intermediates (91). The main feature of BIOWIN models is that all models are more suitable for classifying the easily biodegradable chemicals. Furthermore, their applicability domain is clearly defined and their potential drawbacks and pitfalls are covered in the Biodegradation Probability Program manual. Thus, if adequately applied, BIOWIN models should supply in most cases a reliable biodegradability classification for organic chemicals. The last but not the least, the BIOWIN models are easily available and freely downloadable as a part of the EPI Suite software.

The classification model based on a set of seven logical structural rules was successful in evaluating biodegradability potential of organic chemicals in the training set (MITI-I data) as well as in the test set (BIODEG data) using only

11 structural descriptors. Its main advantages are that the binary character of biodegradability data is perfectly suited for developing the logical structural rules for easy/poor biodegradability and that the combination and/or relationship between two or more functional groups can be incorporated in any structural rule. Furthermore, each logical structural rule has a straightforward physical explanation or rationalization. Thus, it is a pity that this simple and logical classification model was not more extensively evaluated and tested by the independent research groups. In the future, the machine learning approach should be used to develop the complementary set of logical structural rules for poorly biodegradable chemicals and a new class of biodegradability rules that will also include environmental properties relevant for biodegradability.

MultiCASE, MultiCASE/META and CATABOL/CATALOGIC are fully automated expert systems that can successfully classify biodegradability of organic chemicals. Furthermore, the MultiCASE program also identifies structural features, the biophores and biophobes, which seem to be responsible for the biodegradability potential of organic chemicals. The major advantage of MultiCASE/META and CATABOL/CATALOGIC expert systems is their ability to suggest the potential microbial transformation pathways of organic compounds as well as the structures of potential intermediates and stable transformation products. Moreover, the results of those expert systems can be easily rationalized and usually have a mechanistic interpretation. The expert systems MultiCASE/META and CATABOL/CATALOGIC are commonly used for estimating the biodegradation of organic compounds for regulatory purposes.

The multivariate PLS model also seems to be useful for discriminating between easily and poorly biodegradable organic chemicals. Unfortunately, it was not extensively evaluated and validated since its development 15 years ago. Its main comparative advantage is that the effect of intra-molecular interactions between fragments is incorporated into the final model. It should be also pointed out that the large majority of important fragment-fragment interactions obstruct the potential biodegradation processes of organic chemicals and helped to improve the correct classification of poorly biodegradable chemicals.

Recently two similar sets of general *in silico* QSAR models have been developed and suggested as an accurate tool for classifying biodegradability of organic chemicals (15, 56). Both QSAR systems are developed from the large number of calculated descriptors including various fingerprints, using several machine learning methods and the most recent collection of MITI-I data. However, their biodegradability classification power is hardly better than that of much simpler classification models like the group contribution models, a simple set of structural rules and automated expert systems described above, i.e. in the 85-90% range. These results are somewhat disappointing since the application of a large arsenal of molecular descriptors and statistical tools including machine learning methods complemented by a very large set of uniform biodegradability data has not resulted in the much improved classification power of developed models. Furthermore, both studies have only confirmed the well known structural features that are relevant for the biodegradability of organic chemicals. From practical point of view, the developed *in silico* QSAR models are of little use since none was explicitly reported.

It seems that the best strategy that can be recommended for estimating biodegradability of organic chemicals is similar to one proposed about a decade ago (8), i.e. the consensus approach. Namely, it was recommended to apply all relevant and reliable models for classifying the biodegradability of organic chemicals. Today those are the appropriate BIOWIN model, the set of seven structural rules, the MultiCASE system, the appropriate CATABOL model and the multivariate PLS model. If the classification results of all five models are in agreement, such classification should be considered as very reliable. If the results of four out of five models agree, such an estimate should be considered as reliable. Finally, when only three models agree in classifying a specific chemical, such a prediction should be considered only as reasonable and used with caution. Furthermore, in the case of partial consensus the information on reliability of individual classification models should be also taken into account, i.e. that Biowin1-6 models are more accurate in classifying the easily biodegradable chemicals, that CATABOL 301C model is also more accurate in classifying the easily biodegradable chemicals, that the multivariate PLS model is more accurate in classifying the poorly biodegradable chemicals, etc.

About two decades ago the first studies were published on a detailed quantum-mechanical *ab initio* analysis of reaction mechanisms and reaction-path dynamics of the major degradation processes in the troposphere (92–95). Those studies have been primarily focused on the reactions of volatile hydrocarbons and their halogenated derivatives with the hydroxyl (OH) radicals since such chemicals are commonly present in the gas phase (96–99). In the following years similar studies have been performed for other chemical classes including various pesticides and flame retardants like polybrominated diphenyl ethers (100–103), other tropospheric oxidation species like NO₃ radicals and ozone (104, 105) as well as for the reactions of OH radicals in aqueous medium (106). Consequently, due to the continuous and fast advances in computing technology (hardware and software), today such studies are almost routine as well as the standard procedure for calculating the reliable rate constants for tropospheric degradation of organic chemicals. In the coming years we will witness the analogous developments in the area of biodegradation where the environmental relevant microbial degradation processes will be accurately modeled under the realistic environmental conditions including appropriate medium (107–111). This will be achieved by the multilayered integrated molecular orbital and molecular mechanics computational approaches developed by Morokuma and co-workers (112). The combined Quantum Mechanical/Molecular Mechanical (QM/MM) methods can be used to characterize the free energy pathway of enzymatic reactions and obtain valuable information about the reaction mechanism, intermediate or stable transformation products as well as about the kinetics and thermodynamics of enzymatic reactions (113–115). The Nobel Prize in Chemistry for 2013 was awarded for the early developments of such multiscale methods that can be applied to the complex chemical and biochemical systems.

References

1. Scheringer, M. *Environ. Sci. Technol.* **1996**, *30*, 1652–1659.
2. Webster, E.; Mackay, D.; Wania, F. *Environ. Toxicol. Chem.* **1998**, *17*, 2148–2158.
3. *UNEP Stockholm Convention on Persistent Organic Pollutants (POPs)*. United Nations Environment Programme: Stockholm, Sweden, 2001.
4. Sabljic, A. *Chemosphere* **2001**, *43*, 363–375.
5. EU Regulation (EC) No 1907/2006 of the European Parliament and of the Council of 18 December 2006 concerning the Registration, Evaluation, Authorisation and Restriction of Chemicals (REACH), establishing a European Chemicals Agency, amending Directive 1999/45/EC and repealing Council Regulation (EEC) No. 793/93 and Commission Regulation (EC) No. 1488/94 as well as Council Directive 76/769/EEC and Commission Directives 91/155/EEC, 93/67/EEC, 93/105/EC and 2000/21/EC. *Off. J. Eur. Communities: Legis.* **2006**, *L 396*, 1–849.
6. Katayama, A.; Bhula, R.; Burns, G. R.; Carazo, E.; Felsot, A.; Hamilton, D.; Harris, C.; Kim, Y. H.; Kleter, G.; Koerdel, W.; Linders, J.; Peijnenburg, J. G. M. W.; Sabljic, A.; Stephenson, R. G.; Racke, D. K.; Rubin, B.; Tanaka, K.; Unsworth, J.; Wauchope, R. D. *Rev. Environ. Contam. Toxicol.* **2010**, *203*, 1–86.
7. Boethling, R. S.; Sabljic, A. *Environ. Sci. Technol.* **1989**, *23*, 672–679.
8. Sabljic, A.; Peijnenburg, W. *Pure Appl. Chem.* **2001**, *73*, 1331–1348.
9. Jaworska, J. S.; Boethling, R. S.; Howard, P. H. *Environ. Toxicol. Chem.* **2003**, *22*, 1710–1723.
10. Pavan, M.; Worth, A. P. *QSAR Comb. Sci.* **2008**, *27*, 3240.
11. Howard, P. In *Handbook of Property Estimation Methods for Chemicals*; Boethling, R., Mackay, D., Eds.; Lewis: Boca Raton, FL, 2000; pp 281–310.
12. Aronson, D.; Howard, P. H. *Anaerobic biodegradation of organic chemicals in groundwater: A summary of field and laboratory studies*; SRC TR-97-0223F; Syracuse Research: North Syracuse, NY, 1997.
13. Aronson, D.; Citra, M.; Shuler, K.; Printup, H.; Howard, P. H. *Aerobic Biodegradation of Organic Chemicals in Environmental Media: A Summary of Field and Laboratory Studies*; U.S. Environmental Protection Agency: Athens, GA, 1998.
14. *OECD Guidelines for the Testing of Chemicals, Section 3 Degradation and Accumulation*; Organisation for Economic Co-operation and Development (OECD): Paris, France, 2010; http://www.oecd-ilibrary.org/environment/oecd-guidelines-for-the-testing-of-chemicals-section-3-degradation-and-accumulation_2074577x.
15. Cheng, F. X.; Ikenaga, Y.; Zhou, Y.; Yu, Y.; Li, W. H.; Shen, J.; Du, Z.; Chen, L.; Xu, C. Y.; Liu, G. X.; Lee, P. W.; Tang, Y. *J. Chem. Inf. Model.* **2012**, *52*, 655–669.
16. American Institute of Chemical Engineers. *Design Institute for Physical Properties, Environmental Health and Safety Data Compilation, Project 911* (<http://www.aiche.org/dippr/>).

17. Baker, J. R.; Gamberger, D.; Mihelcic, J. R.; Sabljic, A. *Molecules* **2004**, *9*, 989–1004.
18. Boethling, R. S.; Gregg, B.; Frederick, R.; Gabel, N. W.; Campbell, S. E.; Sabljic, A. *Ecotoxicol. Environ. Saf.* **1989**, *18*, 252–267.
19. Boethling, R. S.; Howard, P. H.; Meylan, W.; Stiteler, W.; Beauman, J.; Tirado, N. *Environ. Sci. Technol.* **1994**, *28*, 459–465.
20. Mulder, W.; Verhaar, H.; Hermens, J.; Peijnenburg, W.; Rorije, E.; Sabljic, A. *An Overview of QSAR for Several Important Environmental Parameters*, Report to EC DGXII, 1993.
21. Boethling, R. S.; Sommer, E.; DiFiore, D. *Chem. Rev.* **2007**, *107*, 2207–2227.
22. Tunkel, J.; Howard, P. H.; Boethling, R. S.; Stiteler, W.; Loonen, H. *Environ. Toxicol. Chem.* **2000**, *19*, 2478–2485.
23. Meylan, W.; Boethling, R. S.; Aronson, D.; Howard, P.; Tunkel, J. *Environ. Toxicol. Chem.* **2007**, *26*, 1785–1792.
24. *Biodegradation probability program (BIODEG)*, Version 3; Syracuse Research Corporation: Syracuse, NY, 1992.
25. Howard, P. H.; Boethling, R. S.; Stiteler, W. M.; Meylan, W. M.; Hueber, A. E.; Beauman, J. A.; Larosche, M. E. *Environ. Toxicol. Chem.* **1992**, *11*, 593–603.
26. Gamberger, D.; Sekusak, S.; Medven, Z.; Sabljic, A. In *Biodegradability Prediction*; Peijnenburg, W. J. G. M., Damborsky, J., Eds.; NATO ASI Series 2; Kluwer Academic Publishers: Dordrecht, The Netherlands, 1996; Vol. 23, pp 41–50.
27. Tunkel, J.; Howard, P. H.; Boethling, R. S.; Stiteler, W.; Loonen, H. *Environ. Toxicol. Chem.* **2000**, *19*, 2478–2485.
28. Shelton, D. R.; Tiedje, J. M. *Appl. Environ. Microb.* **1984**, *47*, 850–857.
29. Boethling, R. S.; Lynch, D. G.; Jaworska, J. S.; Tunkel, J. L.; Thom, G. C.; Webb, S. *Environ. Toxicol. Chem.* **2004**, *23*, 911–920.
30. European Commission. *Technical Guidance Document on Risk Assessment in support of Commission Directive 93/67/EEC on Risk Assessment for New Notified Substances, Commission Regulation (EC) No 1488/94 on Risk Assessment for Existing Substances, and Directive 98/8/EC of the European Parliament and of the Council concerning the placing of Biocidal Products on the Market*. Luxembourg, 2003.
31. ECB. *Final report of REACH Implementation Project (RIP) 3.3-2. Technical Guidance Document to Industry on the Information Requirements for REACH*. European Commission-Joint Research Centre, Ispra, Italy 2007.
32. Alexander, M. *Biodegradation and Bioremediation*, 2nd ed.; Academic Press: New York, 1999.
33. Boethling, R. S.; Costanza, J. *SAR QSAR Environ. Res.* **2010**, *21*, 415–443.
34. Gamberger, D.; Sekusak, S.; Sabljic, A. *Informatica* **1993**, *17*, 157–166.
35. Gamberger, D.; Sekusak, S.; Medven, Z.; Sabljic, A. *Environ. Sci. Pollut. Res.* **1996**, *3*, 224–228.
36. Quinlan, J. R. *IEEE Expert* **1991**, *6*, 32–37.
37. Klopman, G.; Wang, S. *J. Comput. Chem.* **1991**, *12*, 1025–1032.
38. Klopman, G. *Quant. Struct.-Act. Relat.* **1992**, *11*, 176–184.

39. Klopman, G.; Tu, M. *Environ. Toxicol. Chem.* **1997**, *16*, 1829–1835.
40. Rorije, E.; Peijnenburg, W. J. G. M.; Klopman, G. *Environ. Toxicol. Chem.* **1998**, *17*, 1943–1950.
41. Howard, P. H.; Hueber, A. E.; Mulesky, B. C.; Crisman, J. S.; Meylan, W.; Crosbie, E.; Gray, D. A.; Sage, G. W.; Howard, K. P.; LaMacchia, A.; Boethling, R. S.; Troast, R. *Environ. Toxicol. Chem.* **1986**, *5*, 977–988.
42. Klopman, G.; Dimayuga, M.; Talafous, J. *J. Chem. Inform. Comput. Sci.* **1994**, *34*, 1320–1325.
43. Klopman, G.; Zhang, Z.; Balthasar, D. M.; Rosenkranz, H. S. *Environ. Toxicol. Chem.* **1995**, *14*, 395–403.
44. Klopman, G.; Tu, M.; Talafous, J. META 3. *J. Chem. Inform. Comput. Sci.* **1997**, *37*, 329–334.
45. Jaworska, J. S.; Dimitrov, S.; Nikolova, N.; Mekenyan, O. *SAR QSAR Environ. Res.* **2002**, *13*, 307–323.
46. Dimitrov, S.; Kamenska, V.; Walker, J. D.; Windle, W.; Purdy, R.; Lewis, M.; Mekenyan, O. *SAR QSAR Environ. Res.* **2004**, *15*, 69–82.
47. Dimitrov, S.; Dimitrova, G.; Pavlov, T.; Dimitrova, N.; Patlevisz, G.; Niemela, J.; Mekenyan, O. *J. Chem. Inf. Model.* **2005**, *45*, 839–849.
48. Schenker, U.; Scheringer, M.; Hungerbühler, K. *Environ. Sci. Pollut. Res.* **2007**, *14*, 145–152.
49. Loonen, H.; Lindgren, F.; Hansen, B.; Karcher, W. In *Biodegradability Prediction*; Peijnenburg, W. J. G. M., Damborsky, J., Eds.; NATO ASI Series 2; Kluwer Academic Publishers: Dordrecht, The Netherlands, 1996; Vol. 23, pp 105–114.
50. Loonen, H.; Lindgren, F.; Hansen, B.; Karcher, W.; Niemela, J.; Hiromatsu, K.; Takatsuki, M.; Peijnenburg, W.; Rorije, E.; Struij, J. *Environ. Toxicol. Chem.* **1999**, *18*, 1763–1768.
51. Eakin, D. R.; Hyde, E.; Palmer, G. *Pestic. Sci.* **1974**, *5*, 319–326.
52. Sabljic, A. *Sci. Total Environ.* **1991**, *109/110*, 197–220.
53. Sabljic, A.; Piver, W. T. *Environ. Toxicol. Chem.* **1992**, *11*, 961–972.
54. Raymond, J. W.; Rogers, T. N.; Shonnard, D. R.; Kline, A. A. *J. Hazard. Mater.* **2001**, *84*, 189–215.
55. Rucker, C.; Kummerer, K. *Green Chem.* **2012**, *14*, 857–887.
56. Mansouri, K.; Ringsted, T.; Ballabio, D.; Todeschini, R.; Consonni, V. *J. Chem. Inf. Model.* **2013**, *53*, 867–878.
57. Breiman, L. *Classification and Regression Trees*, 1st ed.; Chapman & Hall/CRC: Boca Raton, FL, 1984.
58. Sonquist, J. A.; Morgan, J. N. *The Detection of Interaction Effects*; Survey research center, University of Michigan: Ann Arbor, MI, 1964; p 296.
59. Yap, C. W. *J. Comput. Chem.* **2011**, *32*, 1466–1474.
60. Klekota, J.; Roth, F. P. *Bioinformatics* **2008**, *24*, 2518–2525.
61. Cheng, F.; Yu, Y.; Shen, J.; Yang, L.; Li, W.; Liu, G.; Lee, P. W.; Tang, Y. *J. Chem. Inf. Model.* **2011**, *51*, 996–1011.
62. Hermens, J.; Balaz, S.; Damborsky, J.; Karcher, W.; Mueller, M.; Peijnenburg, W.; Sabljic, A.; Sjoestroem, M. *SAR QSAR Environ. Res.* **1995**, *3*, 223–236.

63. *DRAGON (Software for Molecular Descriptor Calculations)*, version 6.0.28; Talete srl: Milano, Italy, 2012 (<http://www.talete.mi.it/index.htm>).
64. Kowalski, B. R.; Bender, C. F. *Anal. Chem.* **1972**, *44*, 1405–1411.
65. Wold, S.; Sjoestrom, M.; Eriksson, L. *Chemom. Intell. Lab. Syst.* **2001**, *58*, 109–130.
66. Stahle, L.; Wold, S. *J. Chemom.* **1987**, *1*, 185–196.
67. Cortes, C.; Vapnik, V. *Mach. Learn.* **1995**, *20*, 273–297.
68. Leardi, R.; Lupianez Gonzalez, A. *Chemom. Intell. Lab. Syst.* **1998**, *41*, 195–207.
69. *Environment Canada DSL (Domestic Substances List)*; <https://www.ec.gc.ca/lcpe-cepa/default.asp?lang=En&n=5F213FA8-1> (accessed March 2, 2014).
70. Escher, B. I.; Fenner, K. *Environ. Sci. Technol.* **2011**, *45*, 3835–3847.
71. Boxall, A. B. A.; Sinclair, C. J.; Fenner, K.; Kolpin, D.; Maud, S. J. *Environ. Sci. Technol.* **2004**, *38*, 368A–375A.
72. Ternan, N. G.; Mc Grath, J. W.; Mc Mullan, G.; Quinn, J. P. *World J. Microbiol. Biotechnol.* **1998**, *14*, 635–647.
73. Balmer, M. E.; Poiger, T.; Droz, C.; Romanin, K.; Bergqvist, P. A.; Muller, M. D.; Buser, H. R. *Environ. Sci. Technol.* **2004**, *38*, 390–395.
74. Spycher, S.; Pellegrini, E.; Gasteiger, J. *J. Chem. Inf. Model.* **2005**, *45*, 200–208.
75. Kern, S.; Baumgartner, R.; Helbling, D. E.; Hollender, J.; Singer, H.; Schwarzenbach, R. P.; Fenner, K. *J. Environ. Monit.* **2010**, *12*, 2100–2111.
76. Schulz, M.; Loffler, D.; Wagner, M.; Ternes, T. A. *Environ. Sci. Technol.* **2008**, *42*, 7207–7217.
77. Fenner, K.; Canonica, S.; Wackett, L. P.; Elsner, M. *Science* **2013**, *341*, 752–758.
78. Kern, S.; Singer, H.; Hollender, J.; Schwarzenbach, R. P.; Fenner, K. *Environ. Sci. Technol.* **2011**, *45*, 2833–2841.
79. Kern, S.; Fenner, K.; Singer, H. P.; Schwarzenbach, R. P.; Hollender, J. *Environ. Sci. Technol.* **2009**, *43*, 7039–7046.
80. Ng, C. A.; Fenner, K.; Hungerbuhler, K.; Scheringer, M. *Environ. Sci. Technol.* **2010**, *45*, 111–117.
81. Kolpin, D. W.; Battaglin, W. A.; Conn, K. E.; Furlong, E. T.; Glassmeyer, S. T.; Kalkhoff, S. J.; Meyer, M. T.; Schnoebelen, D. J. In *The Handbook of Environmental Chemistry, Reaction and Processes, Part P - Transformation Products of Synthetic Chemicals in the Environment*; Boxall, A. B. A., Ed.; Springer: Berlin/Heidelberg, 2009; Vol. 2, pp 205–244.
82. Helbling, D. E.; Hollender, J.; Kohler, H.-P. E.; Fenner, K. *Environ. Sci. Technol.* **2010**, *44*, 6621–6627.
83. Celiz, M. D.; Tso, J.; Aga, D. S. *Environ. Toxicol. Chem.* **2009**, *28*, 2473–2484.
84. Krauss, M.; Singer, H.; Hollender, J. *Anal. Bioanal. Chem.* **2010**, *397*, 934–951.
85. Radjenovic, J.; Petrovic, M.; Barcelo, D. *TrAC, Trends Anal. Chem.* **2009**, *28*, 562–580.
86. Reemtsma, T.; Alder, L.; Banasiak, U. *J. Chromatogr. A* **2013**, *1271*, 95–104.

87. Moriya, Y.; Shigemizu, D.; Hattori, M.; Tokimatsu, T.; Kotera, M.; Goto, S.; Kanehisa, M. *Nucleic Acids Res.* **2010**, *38*, W138–W143.
88. Ellis, L. B. M.; Gao, J.; Fenner, K.; Wackett, L. P. *Nucleic Acids Res.* **2008**, *36*, W427–W432.
89. Gao, J.; Ellis, L. B. M.; Wackett, L. P. *Nucleic Acids Res.* **2011**, *39*, W406–W411.
90. Fenner, K.; Schenker, U.; Scheringer, M. In *Handbook of Environmental Chemistry*; Springer: Berlin, 2009; Vol. 2P, pp 121–149.
91. Steger-Hartmann, T.; Länge, R.; Heuck, K. *Environ. Sci. Pollut. Res.* **2011**, *18*, 610–619.
92. Sekusak, S.; Guesten, H.; Sabljic, A. *J. Chem. Phys.* **1995**, *102*, 7504–7518.
93. Martell, J. M.; Boyd, R. J. *J. Phys. Chem.* **1995**, *99*, 13402–13411.
94. Sekusak, S.; Guesten, H.; Sabljic, A. *J. Phys. Chem.* **1996**, *100*, 6212–6224.
95. Sekusak, S.; Liedl, K. R.; Rode, B. M.; Sabljic, A. *J. Phys. Chem. A* **1997**, *101*, 4245–4253.
96. Sekusak, S.; Liedl, K. R.; Sabljic, A. *J. Phys. Chem. A* **1998**, *102*, 1583–1594.
97. Senosiain, J. P.; Klippenstein, S. J.; Miller, J. A. *J. Phys. Chem. A* **2006**, *110*, 6960–6970.
98. Peeters, J.; Vereecken, L.; Fantechi, G. *Phys. Chem. Chem. Phys.* **2001**, *3*, 5489–5504.
99. Sekusak, S.; Sabljic, A. *J. Phys. Chem. A* **2001**, *105*, 1968–1978.
100. Vereecken, L.; Francisco, J. S. *Chem. Soc. Rev.* **2012**, *41*, 6259–6293.
101. Kovacevic, G.; Sabljic, A. *J. Comput. Chem.* **2013**, *34*, 646–655.
102. Kovacevic, G.; Sabljic, A. *Chemosphere* **2013**, *92*, 851–856.
103. Zhou, J.; Chen, J.; Liang, C.-H.; Xie, Q.; Wang, Y.-N.; Zhang, S.; Qiao, X.; Li, X. *Environ. Sci. Technol.* **2011**, *45*, 4839–4845.
104. Ljubic, I.; Sabljic, A. *J. Phys. Chem. A* **2002**, *106*, 4745–4757.
105. Mora-Diez, N.; Boyd, R. J. *J. Phys. Chem. A* **2002**, *106*, 384–394.
106. Stefanic, I.; Ljubic, I.; Bonifacic, M.; Sabljic, A.; Asmus, K.-D.; Armstrong, D. A. *Phys. Chem. Chem. Phys.* **2009**, *11*, 2256–2267.
107. Sandala, G. M.; Smith, D. M.; Radom, L. *Acc. Chem. Res.* **2010**, *43*, 642–651.
108. Hammes-Schiffer, S. *Biochemistry* **2013**, *52*, 2012–2020.
109. Orlando, A.; Jorgensen, W. L. *Acc. Chem. Res.* **2010**, *43*, 142–151.
110. Monari, A.; Rivail, J.-L.; Assfeld, X. *Acc. Chem. Res.* **2013**, *46*, 596–603.
111. Layfield, J.; Hammes-Schiffer, S. *Chem. Rev.* **2014**, *114*, 3466–3494.
112. Svensson, M.; Humbel, S.; Froese, R. D. J.; Matsubara, T.; Sieber, S.; Morokuma, K. *J. Phys. Chem.* **1996**, *100*, 19357–19363.
113. Plotnikoy, N. V.; Prasad, B. R.; Chakrabarty, S.; Chu, Z. T.; Warshel, A. *J. Phys. Chem. B* **2013**, *117*, 12807–12819.
114. Polyak, I.; Reetz, M. T.; Thiel, W. *J. Phys. Chem. B* **2013**, *117*, 4993–5001.
115. Prasad, B. R.; Plotnikov, N. V.; Lameira, J.; Warshel, A. *Proc. Natl. Acad. Sci. U.S.A.* **2013**, *110*, 20509–20514.

Chapter 5

Sorption and Quantitative Structure-Activity Relationship (QSAR)

Aleksandar Sabljic*,¹ and Yoshiaki Nakagawa²

¹Department of Physical Chemistry, Institute Rudjer Boskovic, P.O.B. 180, HR-10002, Zagreb, Croatia

²Division of Applied Life Sciences, Graduate School of Agriculture, Kyoto University, Oiwake-cho, Kitashirakawa, Sakyo-ku, Kyoto 606-8502, Japan

*E-mail: sabljic@irb.hr.

The sorption of pesticides to soils or sediments is the major factor determining their mobility, transport and bioavailability in terrestrial and aquatic environments. The organic matter is the primary sorption domain in soils or sediments and sorption is considered to be primarily a partitioning process between soil organic matter and the surrounding water. The soil sorption coefficients normalized to the sorbent organic carbon content (K_{oc}) are currently used as a quantitative measure of sorption of chemicals by soil/sediment from aqueous solution. Today, many quantitative structure–activity relationship (QSAR) models based on various physical or chemical properties and structural descriptors have been developed and are used to estimate the K_{oc} values of organic chemicals. The main objective of this chapter is to overview and evaluate the recent developments in (i) $\log K_{oc}$ vs. $\log K_{ow}$ models, (ii) poly-parameter linear free energy relationship (pp-LFER) models, (iii) models for ionized chemicals and (iv) other major modeling advances. Each QSAR modeling area is critically analyzed and advantages and/or limitations of different modeling approaches are given. In addition, recommendations are given on the application and reliability of individual QSAR models for estimating soil sorption coefficients of organic chemicals.

Introduction

To accurately assess human exposure to chemicals released into the environment and their adverse environmental effects, the environmental fate of chemicals must be known. Sorption of chemicals to soil/sediment is one of the major factors determining their mobility, transport and bioavailability in terrestrial and aquatic environments (1). For various chemical classes, organic matter (OM) is the primary constituent responsible for sorption in soil or sediment and sorption is considered as a partitioning process between soil OM and the surrounding water. This is of special relevance to the fate and behavior of pesticides, which are in continuous contact with soil particles following their application to the field. The soil sorption coefficients are currently used as a quantitative measure of the extent of sorption of chemicals by soil/sediment from aqueous solutions (2–4). They are defined as the ratios (denoted as K_d) between the concentrations of a given chemical sorbed by the soil and dissolved in soil water. In order to compare the soil sorption coefficients measured for different soils, the K_d values are often normalized either to the total organic carbon content of the soil (K_{oc}) or the organic matter content of the soil (K_{om}). These two normalizing schemes are simply related by a factor 1.724; thus, it is easy to convert soil sorption coefficients reported on either basis.

For modeling the sorption of organic compounds in soils it is typically assumed that the organic carbon/water partitioning coefficient (K_{oc}) of neutral organic chemicals can be treated as a constant property that remains unaffected by the type of soil organic matter as well as by the pH of the soil solution. The assumption of the existence of a “representative” K_{oc} value is critical to any approach used for K_{oc} estimation. There is substantial evidence suggesting that the average organic matter of many soils and sediments is of reasonably uniform quality (5–12). In an early study (13) this assumption was extensively tested on two nonpolar compounds (1,2-dichlorobenzene and carbon tetrachloride) for a large number of sorbents, i.e. 32 soils and 36 sediments. A very low variation was found in the K_{oc} values within soil samples or sediment samples and only a small difference (0.22 log units) was found in log K_{oc} values for soils relative to sediments. In a more recent review (14), the log K_{oc} values were collected from the literature for eight chemicals of varying polarity and for each of those chemicals the results were available for at least 10 and up to 73 different soils or sediments. The standard deviation of log K_{oc} values for those eight chemicals ranged from 0.13–0.24. Finally, this assumption was additionally validated in a recent study (15), where 60 chemicals were tested on four soils. It was demonstrated for this large set of neutral chemicals that their soil sorption coefficients normalized to the soil organic carbon content are practically independent of pH, ionic strength, sorbate concentration, and type of soil or organic matter, having a standard deviation of 0.25 log units. Thus, it seems that the idea of universal K_{oc} values for various types of soil organic matter, originally put forward by Kile et al. (13), holds in general.

The soil sorption coefficients normalized to the soil organic carbon content (K_{oc} -activity relationship (QSAR) models (16) based on a variety of physical or chemical properties and structural descriptors such as n-octanol/water partition

coefficients, aqueous solubility, molecular connectivity indices, molecular weight, molecular surface area and reverse-phase high-performance liquid chromatography retention time (2–4, 12, 17–22). In this chapter the following important subjects from this research area will be overviewed: (i) the $\log K_{oc}$ vs. $\log K_{ow}$ models, (ii) the poly-parameter linear free energy relationship (pp-LFER) models, (iii) the models for ionized compounds and (iv) the major modeling efforts not covered by previous sections. Each of those subjects will be critically analyzed with a focus on more recent advancements and clear description of the advantages and limitations of different modeling approaches (23, 24). Finally, specific recommendations will be given on the application and reliability of specific QSAR models for estimating soil sorption coefficients of organic compounds.

Log K_{oc} versus log K_{ow} Models

The majority of reported quantitative structure–activity relationships (QSARs) for estimating K_{oc} 's are based on the relationship between K_{oc} and the n-octanol/water partition coefficient (K_{ow}) (4, 6, 8, 17, 25–29). These linear regression models are usually expressed by relating $\log K_{oc}$ to $\log K_{ow}$ (2, 4, 27).

Although almost all published linear regression models between $\log K_{oc}$ and $\log K_{ow}$ coefficients are purely empirical, by nature it seems obvious that those coefficients should be also thermodynamically related since both are related to basic molecular properties like size, shape and polarity. For the majority of chemicals both those processes are spontaneous and mainly enthalpy–driven while the entropy can also significantly contribute to the negative free energy change (30, 31). Interaction forces that may be involved in those two processes are van der Waals interactions, electrostatic interactions, hydrogen bonding, charge transfer, ligand exchange, direct or induced dipole–dipole interactions, hydrophobic bonding, chemisorptions and partitioning. Which of those forces will be dominant for soil sorption process and octanol–water partitioning of a specific chemical will naturally depend on the properties of the solid sorbent and chemical solute. Thus, it is unrealistic to expect that there will be a general linear regression model relating $\log K_{oc}$ to $\log K_{ow}$.

There are two major obstacles that prevent reliable use of published linear $\log K_{oc}$ – $\log K_{ow}$ models for estimating soil sorption coefficients. First, there is a large variability in measured and published K_{ow} data particularly for highly hydrophobic compounds well known as POPs (persistent organic pollutants) (32, 33), which translates into large uncertainties in the soil sorption coefficients estimated by such linear $\log K_{oc}$ – $\log K_{ow}$ models. Nearly three decades ago it was pointed out for the first time that there is a large uncertainty in measured and published n-octanol/water partition coefficients (3, 34, 35) and this problem has been periodically revived in this century in the relevant literature (36, 37). Despite those clear warnings published in the relevant literature, even today, erroneous K_{ow} data are still in use and propagate through the literature (36, 38). The examples of major uncertainties in the measured K_{ow} data are shown in Table I and the sources of original data are collected in reference (35).

Table I. Range of Reported Experimental n-Octanol/Water Partition Coefficients ($\log K_{ow}$) for Some Chlorophenols, PAHs, Chlorobenzenes, PCBs, and Other Chlorinated Hydrocarbons

<i>Compound</i>	<i>Range Of $\log K_{ow}$ data</i>
Pentachlorophenol	3.32 – 5.86
Trichloroethene	2.29 – 3.30
Naphthalene	3.01 – 4.70
Chlorobenzene	2.18 – 3.79
Hexachlorobenzene	4.13 – 7.42
2,2'-Dichlorobiphenyl	4.04 – 5.00
2,4,5,2',4',5'-Hexachlorobiphenyl	6.34 – 8.18
p,p'-DDT	3.98 – 6.36
Aldrin	5.52 – 7.40

The second difficulty in using the linear $\log K_{oc}$ – $\log K_{ow}$ models for estimating reliable soil sorption coefficients is the large number and wide variety of such models in the literature, i.e. more than 100 linear $\log K_{oc}$ – $\log K_{ow}$ models have been published (2–4, 14, 17). The slopes of the linear $\log K_{oc}$ – $\log K_{ow}$ models range from 0.52 to 1.00 and their intercepts, from -0.78 to 1.14. An evaluation on 31 alkyl- and chloro-benzenes, heterocyclic and substituted polycyclic aromatic hydrocarbons, chlorinated alkanes and alkenes, and chlorinated phenols for five well known and frequently used models (5, 8, 39–41) has demonstrated that the average range of estimated soil sorption coefficients is over 1.5 units on the logarithmic scale, corresponding to a factor of 35 (3). The inaccurately estimated soil sorption coefficients may result in a false risk assessment, misguided environmental policies and finally waste of significant material and/or financial resources. Thus, in such situations, an expert judgement and evaluations are needed to estimate reliable $\log K_{oc}$ values by linear $\log K_{oc}$ – $\log K_{ow}$ relationships.

A systematic study was performed on the linear $\log K_{oc}$ – $\log K_{ow}$ relationships in order to develop a reliable and user-friendly methodology for estimating soil sorption coefficients of a large number of commercial chemicals that will avoid unfortunate side-effects described above (27). The basic principle of this systematic study was to use only the evaluated and recommended $\log K_{ow}$ ($\log P_{star}$) values from the BioByte Masterfile database which today contains measured data for more than 60,000 chemicals (42, 43) in order to avoid using erroneous or questionable $\log K_{ow}$ data. If, in a rare occasion, the evaluated and reliable $\log K_{ow}$ value was not available, the calculated ClogP value (44) was used but only if all fragment values had been determined and no approximation is used in such calculation. The result of such systematic study was a system of linear $\log K_{oc}$ – $\log K_{ow}$ models with clearly defined application domains and uncertainties of the estimated $\log K_{oc}$ values. The system of linear $\log K_{oc}$ – $\log K_{ow}$ models based on $\log K_{oc}$ data of 471 chemicals are presented in Table II through their slopes, intercepts, number of chemicals, correlation coefficients and standard errors.

Table II. List of $\log K_{oc}$ - $\log K_{ow}$ Models Represented by Their Slopes, Intercepts, Number of Compounds, Correlation Coefficients, and Standard Errors

<i>Model</i>	<i>Slope</i>	<i>Intercept</i>	<i># Comp.</i>	<i>Corr.Coeff.</i>	<i>St. Error</i>
Hydrophobic	0.81	0.10	81	0.943	0.451
Nonhydrophobic	0.52	1.02	390	0.795	0.557
Agricultural chemicals	0.47	1.09	216	0.826	0.425
Phenol type chemicals	0.63	0.90	54	0.865	0.401
Alcohols & Organic acids	0.47	0.50	36	0.850	0.388
Acetanilines	0.40	1.12	21	0.719	0.339
Alcohols	0.39	0.50	13	0.876	0.397
Amides	0.33	1.25	28	0.679	0.491
Anilines	0.62	0.85	20	0.905	0.341
Carbamates	0.365	1.14	43	0.760	0.408
Dinitroanilines	0.38	1.92	20	0.909	0.242
Esters	0.49	1.05	25	0.874	0.463
Nitrobenzenes	0.77	0.55	10	0.839	0.583
Organic acids	0.60	0.32	23	0.865	0.336
Phenols & Benzonitriles	0.57	1.08	24	0.865	0.373
Phenylureas	0.49	1.05	52	0.790	0.335
Phosphates	0.49	1.17	41	0.856	0.452
Triazines	0.30	1.50	16	0.567	0.379
Triazoles	0.47	1.405	15	0.811	0.482

In order to apply the most appropriate linear $\log K_{oc}$ - $\log K_{ow}$ model for estimating the soil sorption coefficient of a specific compound a flowchart is designed (Figure 1). The process for selecting the most appropriate linear $\log K_{oc}$ - $\log K_{ow}$ model has two stages. The first stage is the search for an appropriate class-specific model using the strict rules. If such search is not successful, at the second stage, the selection of the most appropriate model for a specific chemical is made among more general models. Each linear $\log K_{oc}$ - $\log K_{ow}$ model is defined by its chemical domain, substituents domain and K_{ow} variable domain (27). Thus, in order to make a reliable estimate of the soil sorption coefficient by the system of linear $\log K_{oc}$ - $\log K_{ow}$ models, the characteristics of a specific compound must be within the application domain of a selected model.

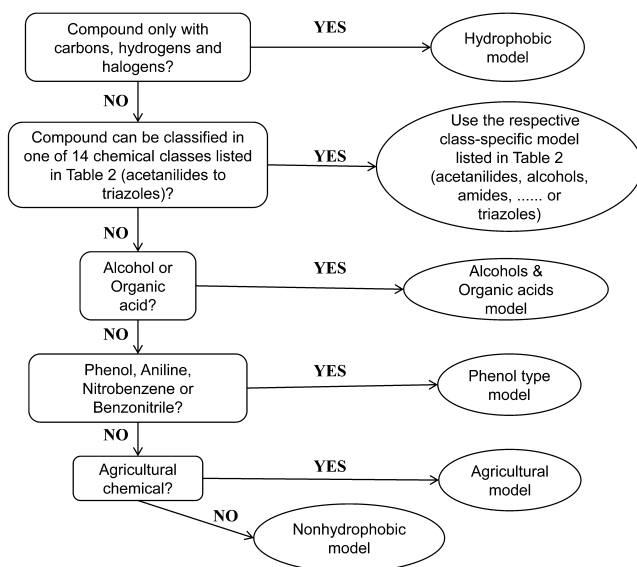


Figure 1. The flowchart for selecting the most appropriate linear $\log K_{oc}$ – $\log K_{ow}$ model.

All soil sorption data used in this systematic analysis of $\log K_{oc}$ – $\log K_{ow}$ relationships have been determined for nonionic species of respective compounds. Thus, linear $\log K_{oc}$ – $\log K_{ow}$ models listed in Table II are applicable only for nonionized chemicals. Furthermore, this approach is most appropriate for sorption systems where non-specific interactions are dominant while for compounds where specific interactions, e.g. hydrogen bonding, are significant the estimates based on $\log K_{oc}$ – $\log K_{ow}$ relationship will be less reliable. The system of linear $\log K_{oc}$ – $\log K_{ow}$ models is composed of three types of models; general, sub-general and class-specific models. General models have wide range of applicability but relatively low accuracy while on the other hand class-specific models usually have narrow application domains but high accuracy. The range of applicability and level of accuracy of sub-general models is somewhere in between. Thus, there is always a trade-off between the range of model applicability and the accuracy of estimates and by this system of models it will be possible to make reliable and accurate estimates for simple chemicals while reasonable estimates for complex chemicals that have many functional groups and large sizes. In any case, as it was pointed out in one of the recent review articles on predicting soil sorption coefficients for organic chemicals (2), the use of linear $\log K_{oc}$ – $\log K_{ow}$ relationships still provides the best return for the effort involved. Finally, the developed system of linear $\log K_{oc}$ – $\log K_{ow}$ models has been incorporated in the European Union technical guidance document for risk assessment of chemicals (45).

Polyparameter Linear Free Energy Relationship (pp-LFER) Models

In cases where the linear $\log K_{oc}$ - $\log K_{ow}$ relationships are not successful, the poly-parametric statistical approaches may be useful. The Kamlet-Taft poly-parametric approach is recognized as a powerful predictive QSAR tool (46–48) and it is based on the well-known Linear Solvation Energy Relationship concept (49, 50). More recently a more general term Linear Free Energy Relationship (LFER) is used for such type of concepts (48). The LFER concept is a general approach to describe solvation, partitioning or related properties in diverse media and Kamlet and co-workers demonstrated that many types of chemical properties depend on solute-solvent interactions (49–52). Within this approach, each such property can be described by three types of interactions: the non-specific dispersive interactions (cavity term), polar interactions (dipolarity/polarizability term) and donor or acceptor type hydrogen bonding (hydrogen-bonding terms). The poly-parameter linear free energy relationship (pp-LFER) model for partition of a chemical between a water phase and another condensed phase, in our case soil organic matter, was established by Abraham and co-workers (46) and has the following general form:

$$\log K_{oc} = eE + sS + aA + bB + vV + c \quad (1)$$

The terms in capital letters E , S , A , B , and V are sorbate (chemical) descriptors for the various types of interactions. E is excess molar refractivity which stands for the difference in polarizability compared to an alkane of the same size and accounts for Debye forces (dipole-induced dipole interactions) and London dispersive forces (induced dipole-induced dipole interactions). V is normalized McGowan volume ($(\text{cm}^3/\text{mol})/100$) of sorbate and accounts for nonspecific interactions (van der Waals interactions and cavity formation). This term is proportional to the size of molecule (sorbate) and to the Gibbs free energy necessary for cavity formation in the respective media. S refers to the dipolarity/polarizability of the sorbate but it predominantly accounts for electrostatic interactions controlled by stable charge separation, i.e. dipole-dipole interactions, while only a small fraction is related to polarizability (cross-correlation effect with E term). The remaining two descriptors A and B stand for the overall hydrogen-bond acidity (H-donor or electron acceptor) and the overall hydrogen-bond basicity (H-acceptor or electron donor), respectively.

The descriptors V and E can be estimated by fragments addition (53, 54). The descriptors S , A and B can be determined chromatographically using appropriate stationary and mobile phases (53, 55, 56) or through appropriate regressions of available data in other solvent-solvent systems. Experimentally determined substance descriptors for about one thousand compounds with mostly simple molecular structures and low molecular weights are publicly available (57–59). However, there is a lack of descriptors for more complex compounds with multiple functional groups. Thus, efforts have been made to develop methods for estimating sorbate (chemical) descriptors for chemical classes that are of

environmental concern such as modern pesticides and pharmaceuticals (60, 61). However, it was demonstrated (19) that, while pp-LFER models outperform other prediction methods for compounds for which experimentally determined sorbate (chemical) descriptors are available, the partition coefficients were predicted poorly if the sorbate descriptors had to be estimated according to the fragments method by Platts et al. (61).

Furthermore, the E descriptor for solid compounds, i.e. the majority of pesticides, cannot be calculated from experimental refractive indices but must be estimated by empirical methods from molecular structure which involves considerable uncertainty (62, 63). This problem can be by-passed by using eq 2 in which the E descriptor is replaced by L descriptor, the logarithm of the hexadecane/air partition constant of sorbate (chemical) at 25 °C in units of $[L_{\text{air}}/L_{\text{hexadecane}}]$ (64).

$$\log K_{\text{oc}} = lL + sS + aA + bB + vV + c \quad (2)$$

L can be measured for liquid and majority of solid organic chemicals (62), except for very large and very polar molecules, for which estimated L values must be used.

The coefficients e , s , a , b , and v in the eq 1 are parameters that depend on the difference in sorbate (chemical) properties between water and the soil organic matter phase. The constant c is a solvent specific free energy contribution that depends on the volume entropy effects (65). All regression coefficients and the constant c are determined by the linear multiple regression analysis against a calibration set of experimentally determined soil sorption coefficients for sorbates for which the sorbate descriptors (E or L , S , A , B , and V) must be known. If the regression coefficients are accurately calibrated, pp-LFER models can provide reasonable predictions (usually within a factor of 2-3) of partitioning coefficients over a broad range of neutral organic compounds with varying polarities.

Here we will focus only on the most recent developments in this area related to the estimation of soil sorption coefficients of organic pollutants. The first respectable and detailed pp-LFER modeling study on soil sorption coefficients was published nearly a decade ago (14). In this study a new pp-LFER was developed using 356 selected $\log K_{\text{oc}}$ values for 75 apolar, monopolar and bipolar chemicals. The first step in this modeling effort was a critical review of a data set of $\log K_{\text{oc}}$ values published in peer-reviewed literature. The following criteria were used in this critical review of K_{oc} data: (i) the sorption isotherms were measured at multiple solute (sorbate) concentrations and were approximately linear (Freundlich coefficient $n = 0.9-1.1$), (ii) data obtained by a batch experiment with clearly described procedures including control of losses, (iii) data obtained for soils with organic carbon fractions lower than 0.1% were excluded from analysis because adsorption to thermally altered carbon may dominate sorption process and (iv) data obtained with high-clay materials (clay content above 35%) were excluded from analysis too, particularly for phenolic compounds where the interactions with clay may be significant (66). In addition, only organic chemicals for which values of chemical descriptors (E , S , A , B , and V) were available in

peer-reviewed literature were used in the statistical analysis. Finally, the data presented in literature as $\log K_{om}$ were converted to $\log K_{oc}$ assuming a conversion factor of 1.72 g of soil OM/g of organic carbon (3). *E*, *S*, *A*, *B*, and *V* descriptors were taken from Abraham and Roses (67), Abraham et al. (58), Poole and Poole (68) and Platts et al. (61).

The final data set consists of 75 selected chemicals that can be classified in four groups: monoaromatic hydrocarbons without halogens (10 compounds), halogenated hydrocarbons (33 compounds—8 chlorobenzenes, 16 PCBs and 9 halogenated alkanes and alkenes), PAHs (11 compounds), and polar chemicals (21 compounds—e.g. phenols, anilines, amides and ureas). Two types of regression were performed on the above calibration set: one using all collected data (356 data points) and another using the average value for each chemical (75 data points). Regression based on the average $\log K_{oc}$ values was performed to avoid overwhelming impact of several chemical with excessive number of measured K_{oc} data from a single study (13), e.g. 1,2-dichlorobenzene with 73 data points and tetrachloromethane with 70 data points. However, regression based on all collected data provides equal weight to the entire calibration set and may better reflect the variations due to variability in soil quality, experimental precision, and different experimental bias between experimental groups. Consequently, two pp-LFER models were developed in this study represented by eq 3 (with all collected data) and eq 4 (with average values):

$$\log K_{oc} = (1.08 \pm 0.04)E - (0.83 \pm 0.09)S + (0.28 \pm 0.08)A - (1.85 \pm 0.08)B + (2.55 \pm 0.08)V - (0.12 \pm 0.05) \quad (3)$$

N = 356 $R^2 = 0.97$ average residual = 0.17 maximum residual = 0.64

$$\log K_{oc} = (1.10 \pm 0.10)E - (0.72 \pm 0.14)S + (0.15 \pm 0.15)A - (1.98 \pm 0.14)B + (2.28 \pm 0.14)V + (0.14 \pm 0.10) \quad (4)$$

N = 75 $R^2 = 0.98$ average residual = 0.18 maximum residual = 0.48

A similar quality of regression was observed for both pp-LFER models, namely their correlation coefficients and average residuals are almost identical. The most significant difference between those two pp-LFER models is in chemical descriptor *A* (hydrogen-bond acidity) since when the average values for $\log K_{oc}$ were used (eq 4) its coefficient *a* was statistically insignificant, i.e. 0.15 ± 0.15 . However, the conclusion from this study was that it is unclear which of two pp-LFER models is more appropriate.

The analysis of fractional contributions from the *eE*, *sS*, *aA*, *bB*, *vV* and *c* terms has demonstrated that for all 75 chemicals the cavity term (*vV*) has the strongest influence on $\log K_{oc}$ data. The second and third largest contributors to soil sorption data for all chemical classes were from the terms reflecting nonspecific van der Waals interactions, i.e. *eE* and *sS* terms. Finally, for group of polar chemicals, a significant contribution was also observed from H-acceptor and H-donor terms, i.e. *aA* and *bB* terms. From the mechanistic point of view those results are consistent with expectations. The dominant driving force for sorption of chemicals from water to wet soil organic matter (SOM) is the tendency of

solute molecules to escape from the bulk water phase. Wet SOM has weaker electrostatic interactions than bulk water and is a weaker hydrogen-bond acid. Consequently, polar chemicals (high S) and chemicals with significant hydrogen-bond basicity (high B) will always prefer bulk water phase. Wet SOM is a slightly stronger hydrogen-bond base compared to the bulk water phase but interactions with SOM basic sites will be only significant for chemicals with very high acidity like pentachlorophenol.

The quality and applicability of both developed pp-LFER models have been tested on insecticide carbaryl and well-known pollutant and potential endocrine disruptor 4-nonylphenol. The measured values of $\log K_{oc}$ for carbaryl range from 1.80 to 2.78, the result from a recent study on 33 soils from Australia, Pakistan and UK (69). At that time, the pp-LFER descriptors were not available for carbaryl in a peer-reviewed literature and consequently the authors have used the following commercial parameters $E = 1.512$; $S = 1.68$; $A = 0.21$; $B = 0.80$; $V = 1.5414$ distributed by Pharma Algorithms (70). Applying eqs 3 and 4 and above set of descriptors, the estimated $\log K_{oc}$ values for carbaryl were 2.64 and 2.55, i.e. within the broad range of experimental $\log K_{oc}$ data (69). The linear isotherms were reported for sorption of 4-nonylphenol on 51 terrestrial soils and respective $\log K_{oc}$ values were in a broad range of 3.47–4.39 (71). The pp-LFER descriptors were not available for 4-nonylphenol neither in the peer-reviewed literature nor commercially. Thus, the values of E , S , A , B and V descriptors had to be estimated. For cavity term, such estimation is accomplished using atomic volume contributions (54) while for other descriptors the estimation can be achieved using analogy to alkyl phenols that have fewer carbon atoms in chain. The set of estimated values for pp-LFER descriptors was $E = 0.8$; $S = 0.9$; $A = 0.55$; $B = 0.49$; $V = 2.043$. Applying eqs 3 and 4 and above set of descriptors, the estimated $\log K_{oc}$ values for 4-nonylphenol were 4.46 and 4.13, i.e. within the broad range of experimental $\log K_{oc}$ data (71). Thus, it seems that developed pp-LFER models are a reasonable choice for estimating $\log K_{oc}$ data for chemicals not included in the calibration set.

The developed pp-LFER models performed reasonably well and can estimate $\log K_{oc}$ data within 0.6 orders of magnitude for all compounds evaluated either nonpolar or polar. However, there are two important drawbacks for general application of the developed models. First, the necessary chemical descriptors are still unavailable or difficult to obtain for a large number of environmentally relevant chemicals. Fortunately, the data-base of necessary chemical descriptors is growing continuously and methods for their estimations are available. Unfortunately, in many instances the quality of estimated descriptors is not sufficient or it is difficult to judge the quality of estimated descriptors and this may significantly increase the uncertainties of $\log K_{oc}$ estimates by the developed pp-LFER models. The second important drawback of the developed pp-LFER models is that the quality of those models has not been tested on a large set of environmentally relevant chemicals and that the applicability domain of those models is not clear.

The pp-LFER models described above as well as models presented in an analogous modeling study (68) have been developed for the $\log K_{oc}$ values obtained predominantly at high sorbate concentrations (i.e. >10% of the solubility

limits). Such models may not be appropriate for estimating K_{oc} values of organic contaminants in the environment, where contaminant concentrations are typically much lower, i.e. in the nM– μ M range, since the K_{oc} values for organic compounds at environmentally relevant concentrations may be substantially different from those obtained at high sorbate concentrations. Due to the lack of a set of consistent experimental K_{oc} data measured in an environmentally more relevant concentration range, Endo et al. (72) have performed an extensive study measuring sorption isotherms at environmentally relevant concentrations and with two model sorbents (peat and lignite) for 35 selected chemicals representing various chemical classes such as apolar aliphatic (alkanes), weakly polar aliphatic (halogenated alkanes/alkenes), monopolar aliphatic (e.g. ethers, nitrile), bipolar aliphatic (alcohols), non- or weakly polar aromatic (alkyl benzenes, PAHs, thiophene, furans), monopolar aromatic (e.g. acetophenone, anisole, benzonitrile) and bipolar aromatic (phenols) compounds.

The analysis of newly measured $\log K_{oc,low}$ data for peat at environmentally relevant concentrations has clearly demonstrated that such values are up to one order of magnitude higher than literature $\log K_{oc,high}$ values obtained predominantly at high sorbate concentrations. It was also found that the literature pp-LFER models (14, 68) underestimate the measured K_{oc} values for peat at the low concentration by up to 1 order of magnitude. The extent of underestimation highly depends on the sorbate properties but primarily on the sorbate dipolarity/polarizability parameter S . More specifically, the literature pp-LFERs adequately predicted $\log K_{oc,low}$ data of apolar and weakly polar aliphatic sorbates but consistently underpredict by around one log unit $\log K_{oc,low}$ data of aromatic and some polar aliphatic sorbates. Thus, it was unambiguously proven that pp-LFER models from references (14) and (68) should not be used for estimating K_{oc} data of organic contaminants in the environment.

Therefore, it was of high importance to develop pp-LFER models for soil sorption of organic contaminants at lower, more environmentally relevant concentrations using newly measured K_{oc} data at environmentally relevant concentrations (72) complemented with analogous data for 16 sorbates on peat and 23 sorbates on lignite (73). Consequently, the final calibration sets consisted of 51 data points for peat and 58 data points for lignite. Both calibrations sets were regressed against values of chemical pp-LFER descriptors (72) and two pp-LFER models were developed represented by eq 5 (peat) and eq 6 (lignite):

$$\log K_{oc,low} = (0.32 \pm 0.20)E + (1.27 \pm 0.29)S - (0.10 \pm 0.25)A - (3.94 \pm 0.35)B + (3.71 \pm 0.22)V - (1.04 \pm 0.24) \quad (5)$$

N = 51 R² = 0.91 standard deviation = 0.34

$$\log K_{oc,low} = (0.44 \pm 0.13)E + (0.45 \pm 0.18)S - (0.26 \pm 0.17)A - (3.43 \pm 0.14)B + (3.74 \pm 0.15)V - (0.28 \pm 0.15) \quad (6)$$

N = 58 R² = 0.95 standard deviation = 0.24

The differences between calculated and measured $\log K_{oc,low}$ values for peat were within 0.3 log units for more than 82% of compounds studied. For lignite fitting was significantly better since almost 90% of compounds had deviations

below 0.3 log units. These findings show that the high quality pp-LFER models can be also developed for soil sorption of diverse chemical classes at environmentally relevant concentrations. It should be pointed out that the developed pp-LFER model for peat is significantly different from the literature pp-LFER models (14, 68) determined at near aqueous solubility limits of sorbates. The pp-LFER models developed for soil sorption of organic contaminants at environmentally relevant concentrations (eqs 5 and 6) suffer from the same deficiencies as the pp-LFER models developed for high sorbate concentrations (eqs 3 and 4) due to the lack of reliable pp-LFER descriptors for environmentally relevant chemicals. The quality of those models has not been tested on a large set of environmentally relevant chemicals and the applicability domain of those models is not clear. Predicting $\log K_{oc}$ of compounds that are out of the application domain can lead to large errors. Examples of such compounds for the pp-LFER models described by eqs 5 and 6 are (i) large hydrophobic compounds (e.g., five-ring or larger PAHs), (ii) acids, bases, and ionic compounds, (iii) highly polar, multifunctional compounds like pesticides and pharmaceuticals and (iv) perfluorinated compounds.

All pp-LFER models described up to now have been calibrated for estimating $\log K_{oc}$ data of relatively simple chemical classes like alkanes, halogenated alkanes/alkenes, PCBs, chlorobenzenes, PAHs, alcohols, ethers, phenols, anilines or similar chemicals and may not be accurate in estimating $\log K_{oc}$ data for multifunctional or complex organic chemicals like pesticides and pharmaceuticals. Chemicals of current environmental concern are often multifunctional and more polar and more complex than classical pollutants such as PCBs or PAHs and consequently there is an urgent need to develop pp-LFER model(s) that will accurately predict $\log K_{oc}$ data for pesticides, pharmaceuticals and similar type of contaminants. Recently a pp-LFER model for soil/water partitioning was calibrated with data for 79 polar and nonpolar compounds that cover a very wide range of the relevant intermolecular interactions (74). To achieve this goal the K_{oc} data had to be measured by column experiments using Pahokee peat as sorbent for majority of calibration set compounds in the nM–mM concentrations range. The K_{oc} data obtained by the column experiments using Pahokee peat as sorbent correspond nicely with data previously measured by the batch experiments with peat as sorbent at the environmentally relevant concentrations (72). Highly complex chemicals were deliberately excluded from the calibration set since LFER descriptors of pesticides and pharmaceuticals have a higher uncertainty than those of more simple chemicals and for the calibration data the reliability of the descriptors has to be high. The basic principle for selecting chemicals in the calibration set was to achieve wide range of descriptor values that will overlap as much as possible with the descriptor values of a large set of pesticides and pharmaceuticals measured by Tülp et al. (63). The only exception was the omission of chemicals with S -values higher than 2.0 to prevent significant cross-correlation between the S -values and other size-related descriptors V and L . The final calibration set consisted of 79 chemicals and produced two types of pp-LFER models (74) described by eqs 7 and 8:

$$\log K_{oc} = (0.81 \pm 0.08)E - (0.61 \pm 0.11)S - (0.21 \pm 0.14)A - (3.44 \pm 0.18)B + (2.99 \pm 0.11)V - (0.29 \pm 0.24) \quad (7)$$

N = 79 R² = 0.921 standard error = 0.25

$$\log K_{oc} = (0.54 \pm 0.05)L - (0.98 \pm 0.13)S - (0.42 \pm 0.14)A - (3.34 \pm 0.17)B + (1.20 \pm 0.20)V + (0.02 \pm 0.12) \quad (8)$$

N = 79 R² = 0.929 standard error = 0.24

The quality of the fit is very similar for both models. Nevertheless, the significant difference between *s* coefficients may result in substantial difference between estimated *K*_{oc} values for chemicals whose *S*-descriptor is higher than 1.5. The range of values for the LFER descriptors *V*, *B* and *S* of the calibration set was larger than those of previous studies (14, 68, 72). However, the fitted coefficients of eqs 7 and 8 are in the range of values reported in earlier pp-LFER models. Thus, it seems that the calibration set applied in this study span the molecular interactions space, described by the LFER descriptors, more uniformly than the previous calibration sets. It should be noted that the perfluorinated compounds are excluded from the application domain of the developed models.

The experimental *K*_{oc} data of 47 pesticides and several pharmaceuticals or hormones were used as an independent evaluation data set for the developed pp-LFER models (eqs 7 and 8) to assess their applicability to complex, environmentally relevant chemicals. Thus, the log *K*_{oc} data have been estimated for chemical from the evaluation set and compared with their measured data. The root-mean-square error (rmse) of 0.39 log units was obtained for log *K*_{oc} data estimated by eq 8 while the rmse is much higher for values estimated by eq 7, i.e. 0.59 log units. It is argued that the poor performance of the pp-LFER model described by eq 7 is due to substantial uncertainty in calculated *E* descriptors for a significant fraction of chemicals in the evaluation set, i.e. 11 pesticides and pharmaceuticals. However, the pp-LFER model described by eq 8 performs very well and can be used in estimating log *K*_{oc} data for multifunctional or complex organic chemicals like pesticides and pharmaceuticals.

The pp-LFER model described by eq 8 was additionally evaluated by comparing its estimated values with the literature *K*_{oc} data measured for Pahokee peat sorbent for 63 polar and nonpolar chemicals. A good agreement (rmse = 0.46) is found between the model predictions and the literature data. Only three chemicals have more than 1 log unit difference between the experimental and the predicted *K*_{oc} values: 2-naphthol (1.16), 2,4-dichlorophenol (1.08) and 2-octanone (1.00) and for all of them the *K*_{oc} values were underestimated. Another three chemicals also show considerable deviations: acetophenone (0.86), benzothiophene (0.78) and phenanthrene (0.70). Again, for all three chemicals, the measured *K*_{oc} values are underestimated. Another interesting point is that almost all listed chemicals with highly underestimated *K*_{oc} values are aromatic compounds. Thus, it is fair to conclude that the pp-LFER model described by eq 8 has a wide applicability for predicting *K*_{oc} values in various soils and sediments but that it should be used with caution in the case of aromatic compounds and particularly for PAHs and their derivatives.

Although, the pp-LFER model described by eq 8 has potential to correctly estimate the K_{oc} data for a wide range of apolar or polar chemical classes including multifunctional or complex organic chemicals like pesticides and pharmaceuticals there are still important drawbacks to the general applicability of developed model. As for earlier pp-LFER models, the necessary chemical descriptors are still either unavailable, difficult to obtain or have large uncertainty for a large number of environmentally relevant chemicals. Furthermore, the applicability domain of this “general” model is not clearly or explicitly defined. Although it is implicitly suggested (74) that this model can be used to accurately estimate the K_{oc} values for any type of chemicals, this is really not proven beyond the reasonable doubt.

Another effort has been made in the same year (75) to derive a more robust and more universally representative pp-LFER model for soil-water partitioning by using large sets of K_{oc} data from the literature for a more diverse set of chemicals. Two sets of K_{oc} data from the literature were used. The first set consisted of pesticides, PCBs and polyaromatic hydrocarbons (PAHs) with results for sediments and soils for 140 compounds and 740 data points. Results in this data set were limited on K_{oc} data determined by the batch method and studies in which the particle concentrations were reported. The second K_{oc} compilation, 440 compounds and data points, consisted of wider variety of chemicals with more diverse functionality (27) but included all 140 compounds from the first data set. The K_{oc} data in the second data set are the averages of measured values from the literature and no evaluation or validation has been made about the quality of those data. The solute descriptors E , S , A , B and V for all compounds were calculated with ADME Boxes 4.0 Absolv program provided by ACD Labs (76). The pp-LFER models were developed for each K_{oc} data set and respective models are described by eqs 9 and 10.

$$\log K_{oc} = (1.198 \pm 0.054)E - (0.080 \pm 0.095)S - (0.192 \pm 0.110)A - (1.807 \pm 0.074)B + (1.155 \pm 0.079)V + (0.724 \pm 0.070) \quad (9)$$

N = 740 rmse = 0.55

$$\log K_{oc} = (1.075 \pm 0.061)E - (0.277 \pm 0.083)S - (0.363 \pm 0.100)A - (1.697 \pm 0.085)B + (1.468 \pm 0.077)V + (0.670 \pm 0.088) \quad (10)$$

N = 440 rmse = 0.48

The developed pp-LFER model (eq 10) based on the more chemically diverse data set has significantly lower rmse of prediction and the smaller parameter standard errors. Furthermore, in eq 9 the regression coefficients a and s are not statistically significant. Thus, those results suggest that pp-LFER model based on the larger and more diverse data set and described by eq 10 is more appropriate. The dominant contributions in this model are from the molecular volume, vV , the dipole–dipole interaction, eE , and the hydrogen bond–donating (solute) and hydrogen bond–accepting (solvent) interaction, bB . The weak contribution by the hydrogen bond–accepting capability (aA term) is the consequence of water and organic carbon having a very similar capability of accepting hydrogen bond. It was suggested by the authors that the residual analysis for this pp-LFER model shows that there is no significant bias relative to the solute parameters except the overestimation for $\log K_{oc}$ values below 1.5. However, the plot of residuals vs.

measured K_{oc} data clearly shows that there is also a significant underestimation for log K_{oc} values above 3.0 and that there is definitively a negative trend over the whole range of this plot.

The regression coefficients of both developed pp-LFER models have been compared with the regression coefficients reported for other published pp-LFER models (14, 68, 72, 74). It was found out that the coefficients from this study differ significantly from the coefficients obtained for previous models in quantitative and sometimes even in qualitative terms. For example, the constant terms range from -1.04 to 0.724 while the s coefficients differ from -0.82 to 1.27. This means that developed pp-LFER models strongly depend on the selected calibration set and that the selection of compounds for calibration of pp-LFER model must be done with a due care and not by brute force, i.e. taking everything that is available. During this selection process the quality of K_{oc} data as well as the quality and range of solute descriptors must be taken into account. In addition, it is very important that there is no or only a weak intercorrelation between solute descriptors for compounds in the calibration set. Consequently, pp-LFER model described by eq 10 has several important weaknesses, i.e. the unknown and variable quality of log K_{oc} data, the poor quality of calculated solute descriptors (74) and the unknown and untested intercorrelations between solute descriptors. Thus, this model should not be used to estimate K_{oc} data for compounds which are outside its calibration set like pharmaceuticals, hormones, personal care products and similar.

Recently, an additional effort was made (77) to further expand the applicability domain of pp-LFER model described above by eq 8. To achieve this goal a set of new K_{oc} data has been measured for 28 non-ionized natural toxins, such as mycotoxins or phytoestrogens, which were recently identified as micropollutants in the environment (78). This test set of natural toxins is also of particular methodological interest since it is composed of compounds with a broad diversity of multifunctional groups, large molecular size and high degree of complexity. Their sorption affinity was measured with a model sorbent for soil organic matter, the Pahokee peat. The K_{oc} data for 31 mycotoxins and phytoestrogens have been determined by a dynamic HPLC-based column method and the range of experimental log K_{oc} data was 0.7 – 4.02 (77). Unfortunately, the experimentally determined LFER descriptors are only available for a single compound from the large set of studied mycotoxins and isoflavones, i.e. zearalenone. Consequently, for a subset of mycotoxins and isoflavones LFER descriptors have been calculated from molecular structure by the program ABSOLV (76).

The pp-LFER model described by eq 8 was not successful in estimating log K_{oc} data of non-ionized natural toxins since only about 40% of values were predicted within 1 log unit while more than 20% of predicted log K_{oc} values have residuals between 2-3 log units. The model was only partially successful in estimating log K_{oc} data of weakly sorbing mycotoxins, i.e. for such mycotoxins low K_{oc} values are predicted. Furthermore, for zearalenone, the only mycotoxin for which experimental pp-LFER descriptors are available, the estimated low K_{oc} (3.61) is very close to measured value of 3.42. Thus, it may be argued, that the suitability of the pp-LFER approach for mycotoxins cannot be properly assessed until experimental pp-LFER descriptors become available. However,

this also means that the ABSOLV parameters must be used with caution. These conclusions are also supported by the multiple linear regression of measured $\log K_{oc}$ values (20 toxins) with the five ABSOLV parameters which gave a poor fit ($R^2 = 0.2$) and a high rmse (0.91 log units). The $\log K_{oc}$ data of non-ionized natural toxins have been also estimated by several literature models like EPISuite's KOCWIN, SPARC and COSMOtherm (quantum-chemical based software). None of them was able to adequately predict absolute K_{oc} values either or to account for the trends observed for K_{oc} data among the various tested mycotoxins. Hence, measuring K_{oc} data for natural toxins by a dynamic HPLC-based column method seems to be the only reasonable solution for now.

The major advantage of pp-LFER approach is that it has solid and sound thermodynamic and mechanistic grounds. Furthermore, pp-LFER models developed for uniformly measured K_{oc} data have been extensively and successfully tested on broad range of various chemical classes including multifunctional and complex chemicals like pesticides and pharmaceuticals. However, there are still measured soil sorption data for hundreds of chemicals which have not been used for the evaluation of those pp-LFER models. Parenthetically, this large set of published K_{oc} data still awaits a complete and careful evaluation. At present, the lack of experimental pp-LFER descriptors is a serious limitation for the general applicability of pp-LFER models. The second important drawback of the developed pp-LFER models is that their applicability domains are not well defined. Caution is advised whenever a pp-LFER model is used outside its application domain as it was nicely demonstrated in the case of natural toxins (77).

Models for Ionized Compounds

As it was clearly stated in the previous sections, all linear $\log K_{oc}$ - $\log K_{ow}$ and pp-LFER models for estimating soil sorption coefficients (K_{oc}) described up to now are strictly applicable for non-ionized compounds. In an early study Bintein and Devillers (79) have suggested a single model for estimating the soils-water distribution coefficient (K_d) of non-ionized as well as ionized chemicals. In that quantitative model K_{ow} and ionization constants (pK_a) are molecular descriptors while pH and f_{oc} (the fraction of organic carbon) describe sorbent characteristics. The final version of that model is described by eq 11

$$\log K_d = 0.93 \times \log K_{ow} + 1.09 \times \log f_{oc} + 0.32 \times CF_a - 0.55 \times CF_b + 0.25 \quad (11)$$

N = 229 $R^2 = 0.933$ standard error = 0.433

where CF_a and CF_b are the correction factors that quantify the variation of dissociated acids or bases in the system and can be calculated by the simple expressions based on the chemical ionization constant and on the sorbent surface pH. Although, the correlation coefficient of this model was quite high, its major deficiency is that electrolytes were poorly represented in the calibration set as well as in test set (<15%). Consequently, the ability of this model in estimating the soils-water distribution coefficient (K_d) of ionized chemicals is questionable.

Recently, a significant effort has been made by two groups (80–84) to develop reliable model(s) for estimating the soil sorption coefficients (K_{oc}) of organic acids, bases and amphoters from their K_{ow} and pK_a data. The first study was published by Kah and Brown (80) where the sorption of six acidic (dicamba, metsulfuron-methyl, fluazifop-P, 2,4-D, flupyrsulfuron-methyl and fluroxypyr) and four basic (metribuzin, terbutryn, pirimicarb and fenpropimorph) pesticides was measured in nine contrasting arable soils. The measured distribution coefficients ($\log K_d$) were then submitted to statistical analyses against a wide range of soil and pesticide properties to identify the best combination of properties that describe the variation in sorption. It was observed that sorption of ionizable pesticides tends to be stronger in soils with lower pH and containing more organic carbon (OC). The influence of these two parameters was less apparent for basic compounds and indicated that different models are required for acids and bases. Consequently, the data set was split between acids and bases. When all descriptors were considered together, $\log D$ (lipophilicity corrected for pH) and OC were selected as the best predictors for the sorption of acids. However, in order to account for majority of variability in the acids sorption data an additional molecular descriptor ($GATS7v$), related to the van der Waals volume of pesticide, had to be incorporated in the regression model:

$$\log K_d = 0.06 \times \log D + 1.07 \times \log OC + 0.99 \times GATS7v + 2.45 \quad (12)$$

$$R^2 = 0.872 \quad \text{standard error} = \text{not reported}$$

$GATS7v$ is Geary autocorrelation–lag7 weighted by atomic van der Waals volumes. This regression model was then tested by predicting the distribution coefficients ($\log K_d$) on an independent dataset consisting of seven acidic pesticides. Their K_d data were measured on 36 temperate soils sampled in France and the United Kingdom and the test set included three pesticides from the calibration set (2,4-D, metsulfuron-methyl and dicamba) and four additional phenoxy acids (MCPA, 2,4,5-T, dichlorprop and mecoprop-P). Model described by eq 12 has potential to correctly predict the $\log K_d$ data of acidic pesticides since the correlation between measured and predicted values of pesticides from the test set was quite significant, i.e. $R^2 = 0.721$.

The behavior of basic pesticides was more complex since there are various mechanisms which can retain basic compounds in the soil phase. Namely, basic pesticides can bind either to the soil organic matter or to the clay through several different mechanisms. The relative importance of individual mechanism depends on various parameters such as the type and amount of soil constituents, the molecular properties of pesticide and the chemical environment of the soil phase. A large part of the variation in soil sorption for individual pesticide could be explained by the variation in the soil cationic exchange capacity and pH. However, the differences in behavior between bases could not be deduced from pesticide molecular properties alone. Relatively little experimental evidence was available for basic pesticides and, consequently, the balance between various processes is not fully understood.

Shortly after above study, the first extensive modeling study on soil sorption of ionizable organic compounds was performed by Franco and Trapp (81). A data set of 93 acids, 65 bases, and six amphoters with their K_{oc} data was collected from the literature and the averaged values from a representative variety of soils were used in statistical modeling. Their $\log K_{ow}$ and pK_a values were calculated by the ACD/Labs® software (85) and consequently the Henderson-Hasselbalch equation was used to calculate the extent of dissociation for those chemicals, i.e. neutral Φ_n , ionic Φ_{ion} , anionic Φ_- and cationic Φ_+ fractions. Only chemicals in the pK_a range 2-12 were selected for the calibration set since outside this range chemicals are in neutral form while the dissociation constants are calculated at 25°C and zero ionic strength. Three calibration sets of 62 acids, 43 bases and six amphoters were used for fitting soil sorption coefficients ($\log K_{oc}$) to $\log K_{ow}$ ($\log P_n$) and pK_a data. Consequently, the separate regression models were developed for acids (eq 13), bases (eq 14) and amphoters (eq 15):

$$\log K_{oc} = \log(\Phi_n \times 10^{0.54 \times \log P_n + 1.11} + \Phi_{ion} \times 10^{0.11 \times \log P_n + 1.54}) \quad (13)$$

N = 62 R² = 0.54 rmsd = 0.47 pH_{opt} = 5.8

$$\log K_{oc} = \log(\Phi_n \times 10^{0.37 \times \log P_n + 1.70} + \Phi_{ion} \times 10^{pK_a(0.65) \times f(0.14)}) \quad (14)$$

N = 43 R² = 0.76 rmsd = 0.55 pH_{opt} = 4.5

$$\log K_{oc} = \log(\Phi_n \times 10^{0.50 \times \log P_n + 1.13} + \Phi_- \times 10^{0.11 \times \log P_n + 1.54} + \Phi_+ \times 10^{pK_a(0.65) \times f(0.14)}) \quad (15)$$

N = 6 R² = 0.73 rmsd = 0.51 pH_{opt} = 5.0

where f is the ratio of chemical concentration in n-octanol and sum of concentrations in n-octanol and water, i.e. $f = K_{ow}/(K_{ow}+1)$ while rmsd is root mean square deviation between estimated and measured data. The pH_{opt} terms were calculated by fitting to the experimental data of calibration sets. The developed models are applicable for the whole pK_a range of acids, bases and amphoters and particularly useful for strong bases and amphoters since those are the first predictive methods for such chemicals.

Randomly selected test sets of 31 acids and 22 bases were used to test the quality of regression eqs 13 and 14, respectively, in estimating $\log K_{oc}$ of ionic chemicals. The developed models have been quite successful in estimating the $\log K_{oc}$ values of various acids (rmsd = 0.44) and bases (rmsd = 0.51) in large test sets. The only exceptions are two bases, acridine and benzo[f]quinoline, whose residuals are in the range 1.4–1.8 log units. Anyhow, it may be concluded that the developed quantitative models are successful in calculating reliable $\log K_{oc}$ of ionic chemicals and that those models should be generally applicable. Furthermore, the four parameters used in the above models, pK_a and $\log P_n$ for molecules and organic carbon and pH for the soil, all have a major impact on the sorption of ionizable chemicals.

In the follow-up study Franco et al. (82) have tried to modify above models (eqs 13, 14 and 15) by replacing their constant terms pH_{opt} by a variable, i.e. a varying pH range, and to derive models that will predict pH-dependent sorption

for ionic chemicals. To account for pH dependence, the Henderson-Hasselbalch equation (eq 16) for calculating the fraction of neutral species, where a is 1 for acids and -1 for bases, was modified and the constant term pH_{opt} is substituted by variable $(\text{pH} + \delta)$, i.e. the bulk soil pH adjusted by a corrective factor δ . The aim was to describe speciation at the sorbing surface as a function of the bulk soil acidity. Consequently, Φ_n term in eqs 13 and 14 is now calculated by eq 17.

$$\Phi_n = 1/(1 + 10^{a(\text{pH}_{\text{opt}} - \text{pK}_a)}) \quad (16)$$

The soil sorption coefficients (K_{oc}) determined at different soil pH values were collected from the literature for 10 acids (2,3,5-trichlorophenol, 2,4,6-tetrachlorophenol, 2,3,5,6-tetrachlorophenol, nitrophenol, pentachlorophenol, 2,4-dichlorophenoxyacetic acid, prosulfuron, monesin, lasalocid and sulphachloropyridazine) and 12 bases (aniline, p-toluidine, n-methylaniline, 2-methylpyridine, pyridine, quinoline, isoquinoline, quinaldine, ametrine, prometryne, atrazine and tylosin). None of those data were used in previous study (81). The data set included K_{oc} values measured on several soils of different pH and values obtained on a single soil at different pH. The reported pH data correspond to the soil solution pH at equilibrium, also known as bulk pH.

The model described by eq 13 correctly predicted the pH-dependent variation of K_{oc} data for 9 out of 10 acids. Thus, the curves are fit to the measured data, for the δ_{opt} that minimized the rmsd for individual compound. The optimal correction factor δ_{opt} ranged from -1.7 for pentachlorophenol to 1.4 for 2-nitrophenol and the mean value of δ_{opt} was -0.6. This confirms that the pH_{opt} is, on average, somewhat lower than the bulk soil pH. The corrected pH is the pH at the soil surface and it depends only on the soil properties. Consequently, the modified Henderson-Hasselbalch equation (eq 18) for calculating the neutral fraction of organic acids in soils is

$$\Phi_n = 1/(1 + 10^{a(\text{pH} + \delta - \text{pK}_a)}) \quad (17)$$

By replacing Φ_n term in eq 13 by expression from eq 18, a quantitative model is derived for reliable estimation of pH-dependent K_{oc} data of organic acids. This regression model enables prediction of pH-dependent K_{oc} values from chemical's pK_a and $\log P_n$ data and the soil bulk pH. The model developed for acids was additionally tested on a new data set of pH-specific K_{oc} values measured in different soils for seven organic acids: 4-methylbenzoic acid, trichlorophenoxyacetic acid, bromoxynil, dicamba, fluroxypyr, fluzifop P and flupysulfuron-methyl. This test set consisted of 44 K_{oc} values and rmsd between estimated and measured $\log K_{\text{oc}}$ values was only 0.32. It may be concluded that the modified model performs significantly better than the original model for organic acids (eq 13). Finally, the applicability domain for both models seems to be 0 – 12 for pK_a , -2.2 – 8.5 for P_n and 3 – 7.7 for bulk soil pH.

Unfortunately, it was not possible to develop the analogous modified model for bases. For bases, the trend of pH-dependent K_{oc} data was complex. The trend predicted by eq 14 qualitatively agreed with the data for nine compounds but underestimated the sorption data of five pyridines and quinolines. The regression was also unable to correctly describe the observed trend for three weak bases. Thus, no statistically significant adjustment of the K_{oc} models was possible for bases by using eq 14 and considering the variability in soil pH.

At the same time, another major study on pH dependent soil sorption coefficients (K_{oc}) of 32 diverse organic acids (86) has demonstrated that the main factor driving the sorption of the anionic species of organic acids is their hydrophobicity. It was found out that the ratio between observed soil sorption coefficients of neutral and anionic species of organic acids is independent of their K_{ow} values and this is in contrast to the postulated log linear function of K_{ow} by Franco et al. (81, 82). Several other studies have also concluded that anion sorption into organic matter is very similar to those of the neutral species and that it is governed by free energy contributions for hydrophobic sorption (87, 88). On a practical side, this means that hydrophobic organic acids (e.g. PCP or 2,4-DB), despite being present predominantly in their anionic form, are subject to significant retardation in aquifers as well as to partial removal by sorption in sewage treatment plants.

Other Major Efforts in Modeling K_{oc}

In this section several thermodynamic approaches for the direct calculation of soil sorption coefficients will be presented (89–92). In addition, a general statistical QSAR model for estimating soil sorption coefficients will be described due to its wide applicability domain and its extensive evaluation and validation procedure (19).

Universal Solvation Models

The first serious attempt to directly calculate the soil sorption coefficients by a thermodynamic approach was performed more than a decade ago (90). In that study, the SM5.42R and SM5CR quantum mechanical universal solvation models (93) were used to predict K_{oc} values of organic compounds. A set of effective solvent descriptors for the organic phase of soil has been developed for the SM5.42R model to directly compute soil/air partitioning free energies and consequently the partitioning of solutes between soil and air. In this procedure the soil organic phase was treated as a continuous medium with homogeneous, isotropic properties while in reality it is a highly heterogeneous system. By combining this set of solvent descriptors with the solute atomic surface tension parameters developed for water/air and organic solvent/air partitioning it is possible to calculate the partition coefficients of any solute between soil and water. The root-mean-square error for log K_{oc} values calculated by SM5.42R/AM1 model for 440 compounds is 1.39 log units. Unfortunately, the systematic analysis of the quality of calculated K_{oc} data was not performed. Even the

scatter plot, calculated vs. measured data, is missing in this study. Without such information it is impossible to evaluate the quality of developed models and eventually recommend their use. Our brief analysis of about 20% of calculated K_{oc} data has revealed several serious problems concerning their quality. First, there is a significant number of calculated log K_{oc} values with deviations of about 2 or more log units such as aldicarb sulfone (3.6 – 3.8), aldrin (1.7 – 2.0), 4-aminobenzoic acid (1.2 – 1.8), asulam (6.2 – 6.5), α -BHC (2.0 – 2.2), β -BHC (1.9 – 2.0), γ -BHC (2.1), 3-bromophenylurea (1.7 – 2.2), sec-bumeton (1.1 – 2.0), carbendazim (1.8 – 1.9), carbophenothion (1.6 – 2.4), α -chlordane (2.0 – 2.1), chlorfenvinphos (1.0 – 2.0) and chlorimuron (5.2 – 5.6). Second, in a number of cases the differences in the calculated log K_{oc} values between models SM5.42R/AM1 and SM5.42R/HF/MIDI! are 1 log units or more (e.g. benz[a]anthracene, benzo[a]pyrene, bromacil, 1-butanol and chlorfenvinphos). For the smaller set of 53 compounds used to test the robustness of parametrizations for SM5.42R/AM1 and SM5.42R/HF/MIDI! models, about 25% of compounds has calculated log K_{oc} values that deviate 1.7 – 3.8 log units from the measured data. Since there is no obvious pattern in the poorly estimated values, there is no way to tell when the estimates by SM5.42R/AM1 or SM5.42R/HF/MIDI! models will be reliable even within 1 log unit range. Thus, at present, it seems that there is no practical use for those universal solvation models.

SPARC Online-Calculator

The computer program, SPARC, uses the computational algorithms based on fundamental chemical structure theory to estimate a large number of chemical reactivity parameters and physical properties for a wide range of organic molecules strictly from molecular structure (89, 94–96). The core of SPARC computational approach is a set of mechanistic perturbation models that describe the intra/intermolecular interactions between molecules as a function of environmental conditions. Furthermore, models have been developed that quantify the various “mechanistic” descriptions commonly utilized in structure–activity analysis, such as induction, resonance and field effects. Resonance models were developed and calibrated using measured UV/vis spectra, whereas electrostatic interaction models were developed using the pK_a values measured in water. Solvation models (i.e., dispersion, induction, H-bonding, etc.) have been developed using various measured physical properties data. SPARC’s physical property models can predict vapor pressure and heat of vaporization (as a function of temperature), boiling point (as a function of pressure), diffusion coefficient (as a function of pressure and temperature), activity coefficient, solubility, partition coefficient and chromatographic retention time as a function of solvent and temperature. Today, SPARC is implemented as an online Web application (<http://archemcalc.com/sparc/>). It can explicitly calculate sorbate-sorbent interactions and consequently the soil sorption coefficients by using various empirical molecular descriptors that are derived explicitly from molecular structure (89, 94–96). Again no experimental data are required in such calculations and only a suitable molecular structure (or combination of molecular structures) is needed to represent the sorbing phase. Furthermore, it

should be pointed out that SPARC does not consider effects of the solute 3D structure on partition coefficients, and thus it calculates the identical K_{oc} values for stereoisomers (e.g. HCHs).

Although, it is believed that the SPARC calculator is a reliable estimation method for various environmentally relevant properties of any compound (e.g. (89, 97)), there is only one extensive evaluation study for soil sorption coefficients (98). In that study the structures of 15 different humic or fulvic acids (99) have been used to mimic the structure of sorbing phase and the SPARC method was used to calculate the K_{oc} values of 438 compounds on each model sorbent. Calculations could not be performed for azoxybenzene and 3-chloro-4-methoxyaniline which contain functional groups not supported by SPARC. The root-mean-square error for SPARC calculated $\log K_{oc}$ values range from 1.05 to 1.96. There is a general trend for SPARC to overestimate the $\log K_{oc}$ values irrespectively of the model sorbent used. The range of SPARC $\log K_{oc}$ calculated values for individual chemical (0.75–6.13) is unreasonably high compared with the measured variability. Even for the moderately hydrophobic chemicals, i.e. $\log K_{oc}$ 1–4, the spread of calculated values is about 4 log units and strongly depends on the selected model of sorbent. Unfortunately, the systematic analysis, on the class by class bases, of the quality of SPARC calculated $\log K_{oc}$ data was not performed and, consequently, there is no information in which case the calculated $\log K_{oc}$ values by SPARC will be reliable and in which case the SPARC should not be used to calculate $\log K_{oc}$ data. Such analysis must be performed before the SPARC calculator can be recommended for either general or specific use in estimating $\log K_{oc}$ data.

Recently, the SPARC online-calculator was also evaluated (77) on calculating the soil sorption coefficients for a set of 28 non-ionized natural toxins, such as mycotoxins or phytoestrogens, which were recently identified as micropollutants in the environment (78). This set of natural toxins is also of methodological interest since it is composed of compounds with a broad diversity of multifunctional groups, large molecular size and high degree of complexity. Due to the time and hardware constrains, SPARC calculations were limited to the smallest sorbent models, and K_{oc} values were therefore calculated for the models representing leonardite, two terrestrial humic acids and three aquatic humic acids. To assess the influence of sorbent structure, the K_{oc} values were calculated for a set of eight “simple” nonpolar and polar neutral toxins. The $\log K_{oc}$ range for the eight simple compounds on the six different sorbent models is from 0.5 to 2.1. Not only is the $\log K_{oc}$ range for mycotoxins among the different sorbent models relatively wide, the different affinities between two sorbent models are not necessarily following the same trend. The $\log K_{oc}$ values for all neutral toxins were only calculated for the leonardite and for all compounds predicted sorption affinities were far above the experimental values. Notably, the non-retaining compounds were predicted among the values with strongest affinities. Clearly, the present version of SPARC online-calculator is not suitable for calculating the K_{oc} values of non-ionized natural toxins, i.e. compounds with large molecular size and high degree of complexity. It should be noted that none of the other models/methods, i.e. EPIsuite’s KOCWIN, COSMOtherm and pp-LFER, were successful in estimating the K_{oc} values for this set of highly complex organic compounds.

COSMO-RS and COSMOtherm Approaches

Commercial software COSMOtherm calculates partition coefficients between desired phases based on the quantum chemical and statistical thermodynamic calculations (91, 92). COSMO-RS and COSMOtherm approaches combine quantum theory, dielectric continuum models, the concept of surface interactions and statistical thermodynamics (100). Here a liquid system is considered to be an ensemble of molecules of different type, including solvent and solute. For solvent and solute molecule, a density functional calculation with the dielectric continuum solvation model COSMO (101) is performed to get the total energy and the polarization charge COSMO density that the dielectric continuum produces on the molecular surface. For an efficient statistical thermodynamics calculation, the solvent is considered to be an ensemble of pair-wise and interacting molecular surfaces and new and efficient statistical thermodynamics procedure is developed to calculate the chemical potentials of compounds in the solvent (91). The only information needed as input for calculating the soil sorption coefficients is the molecular structure of the solute and solvent while the natural organic matter, i.e. the sorption phase, is treated as an undefined phase (91). The only input needed by COSMOtherm software is a computationally cheap quantum-chemical COSMO-calculation of the regarded molecules. The only other input needed is a small set of parameters which depend only on the quantum-chemical method. At present parametrizations are available for the quantum-chemical/density functional program packages DMOL³ and Turbomole, while for the semi-empirical program MOPAC and for the quantum-chemical program packages ORCA and GAMESS-US parametrizations are in preparation.

The first evaluation of this thermodynamical approach for calculating soil sorption coefficients was performed by its authors about a decade ago (91). In that study the sorbent phase, i.e. soil, is treated as a pseudo-liquid. The geometries of 440 compounds have been optimized by the semiempirical AM1/COSMO (101) method using the MOPAC2000 program (102). For the optimized geometries the COSMO polarization charge densities on the molecular surfaces have been computed on the density functional level with the COSMO extension of the Turbomole program package (103, 104) with the split-valence polarization basis set. Finally, the corresponding σ moments have been calculated from the polarization charge densities using the COSMOtherm program (92) and the multilinear regression of five calculated σ moments (M_0 , M_2 , M_3 , M_{acc} and M_{don}) vs. the experimental log K_{oc} data for a training set of 387 compounds yielded the following model:

$$\Phi_n = 1/(1 + 10^{a(\text{pH}-0.6-\text{pKa})}) \quad (18)$$

On the second stage derived model described by eq 19 was evaluated on an independent test set of 53 compounds. In general the quality of calculated log K_{oc} data was similar for the training set and for the test set, i.e. rmse was 0.72 for the test set. Furthermore, the systematic analysis of COSMOtherm calculated log K_{oc} data has shown that some chemical classes have systematic deviations.

For example, the polycyclic aromatic hydrocarbons (18 compounds) and their aza-derivatives (10 compounds) are systematically underestimated and for the majority of compounds the deviations are in the 1–2 log units range. On the other hand, the calculated log K_{oc} data for simple alcohols are systematically overestimated by approximately 0.8 log units. Finally, for 35 phosphates in the dataset the calculated soil sorption coefficients are significantly overestimated, in some cases up to 2 log units, e.g. phosalone. Thus, it is fair to conclude that the above model described by eq 19 in general gives reasonable estimates for log K_{oc} data but that it should not be used to estimate soil sorption coefficients of phosphates while a caution should be exercised in applying this model to alcohols, polycyclic aromatic hydrocarbons and their aza-derivatives.

Recently, COSMO-SAC (Conductor-like Screening Model–Segment Activity Coefficient) (105) model, a variant of the COSMO-RS model developed by Klamt and colleagues (91, 100), has been evaluated on the same set of log K_{oc} data for 440 organic compounds (98). In that study the structures of 16 different humic or fulvic acids (99) have been used to mimic the structure of sorbing phase and the soil organic matter is modeled as an organic solvent composed of humic or fulvic acid molecules. The only other input information needed for COSMO-SAC model to calculate log K_{oc} data is the molecular structures of water and that of the solutes. The COSMO-SAC model uses the density functional QM methods combined with the dielectric continuum solvation model COSMO (101) to calculate the energy of each solute or solvent molecule and the charge density on its surface. Methods based on statistical thermodynamics are then applied using the surface-charge distributions on the molecules to predict the activity coefficients for solutes in a given solvent. The soil sorption coefficients are then calculated as the ratio of the activity coefficients in the two phases. Thus, in this approach there is no fitting procedure to the experimental data as in the model described by eq 19. The log K_{oc} values were calculated by the COSMO-SAC model for a set of 440 diverse, environmentally relevant chemicals. The calculated log K_{oc} data, using 19 diverse models for organic matter phase, agree generally well with the experimental data since rmse is 0.84–1.08. That is, the COSMO-SAC method can predict log K_{oc} values for a diverse set of compounds within an order of magnitude without adhering to any calibration of the model by experimental K_{oc} data. For 76% of the compounds the log K_{oc} data are predicted within 1 log unit of the measured values and only for eight compounds predictions deviated from the measured log K_{oc} by more than 2 log units (amitrole, asulam, 3,5-dinitrobenzamide, tricyclazol, benzo[f]quinoline, urea, thiabendazole, 7H-dibenzo[c,g]carbazole). Thus, if the precision of 1 log unit for estimated log K_{oc} data is acceptable, the COSMO-SAC model may be a method of choice.

The quality of quantum-chemical COSMOtherm software was also evaluated recently (77) by calculating soil sorption coefficients for a set of 28 non-ionized natural toxins, such as mycotoxins or phytoestrogens, recently identified as micropollutants in the environment (78). Those natural toxins are also of methodological interest due to their significant size and high functional complexity. Due to the time and hardware limitations, COSMOtherm calculations have been made only for the smallest sorbent natural organic matter (NOM)

model and $\log K_{oc}$ values were calculated only for the model representing Leonardite humic acid. It should be also noted that the COSMOtherm values were not calibrated to a set of known sorption coefficients, but are solely based on statistical-thermodynamics using quantum-chemical properties. The COSMOtherm predicted $\log K_{oc}$ values for 28 non-ionized natural toxins are in the same range as experimental values, though the scatter with experimental data is significant. For 12 out of 20 neutral mycotoxins the predicted K_{oc} values are within a factor 10 of the measured data. While aflatoxins and most alternaria toxins were accurately predicted, i.e. within 0.5 log units, alternariol methylether, the zearalenol isomers and the trichothecenes were all estimated to have a significantly stronger sorption than observed. However, only half of all weakly sorbing mycotoxins were also among the lowest predicted $\log K_{oc}$ values. The linear fit of data for predicted $\log K_{oc}$ vs. experimental $\log K_{oc}$ values with a fixed slope of one resulted in a regression with rmse of 1.03. This result is comparable to the findings of previous extensive evaluation study (98) in which COSMO-SAC approach was applied to calculate the K_{oc} values for 440 neutral compounds spanning 6 orders of magnitude and for several NOM models. It should be also noted that all other models/methods, i.e. EPISuite's KOCWIN, SPARC and pp-LFER, were far less successful in estimating the K_{oc} data for the set of natural toxins, i.e. highly complex organic compounds. At present, it seems that COSMOtherm or COSMO-SAC is the only method of choice for estimating the K_{oc} data of highly complex organic compounds but only if the precision of 1 log unit for estimated $\log K_{oc}$ data is acceptable.

The General Statistical QSAR Model

A new model to estimate the soil-water partition coefficient of non-ionic organic compounds normalized to soil organic carbon, K_{oc} , from the two-dimensional molecular structure has been developed recently (19). This general statistical QSAR model is unique since all literature soil/Swater partition coefficients available for organic compounds have been used in its development, testing and/or evaluation as well as due to its extensive evaluation procedure. Literature data of $\log K_{oc}$ for 571 organic chemicals were collected and fitted to the large set of parameters restricted to 2D structural information. The final multilinear model for predicting $\log K_{oc}$ contains three continuous and size related variables P_i (molecular weight MW, bond connectivity ϵ and molecular E-state), 21 fragment correction factors F_j , four structural indicator variables I_k , and one regression constant and is described by eq 20:

$$\log K_{oc} = 0.0168(\pm 8) \times M_0 - 0.017(\pm 2) \times M_2 - 0.040(\pm 4) \times M_3 + 0.19(\pm 5) \times M_{acc} - 0.27(\pm 5) \times M_{don} + 0.37(\pm 14) \quad (19)$$

N = 387 R² = 0.71 rmse = 0.62

The predictive capacity of this general statistical model is evaluated through cross-validation (10 runs, each leaving out 10% of the compounds), permutation (12 runs with varying degrees of target value scrambling (106)) and external

prediction with three test sets. For each quality test the predictive squared correlation coefficient q^2 and its associated standard error (se) and bias are reported. First, the cross-validation was performed and the resultant statistics are $q^2 = 0.830$, $se = 0.503$, and $bias = -0.002$, which is similar to the initial prediction set statistics ($q^2 = 0.834$, $se = 0.512$). Second, a permutation test was performed with varying degrees of scrambling ranging from about 12.5% up to 100% permutation. The results show that by increasing permutation the calibration and prediction performances decrease systematically up to near 100% permutation and scrambling q^2 becomes negative. Moreover, the difference between calibration and prediction increases with increased scrambling. Thus, both statistical tests indicate the high statistical quality of developed model.

Three mostly external data sets were used for testing the predictive performance of this model. The first external set consisted of 41 compounds from study by Nguyen et al. (14) and none was included in the calibration set. Results for the new model were slightly better than for the calibration set or leave-10%-out cross-validation statistics, i.e. $q^2 = 0.934$ and $se = 0.379$. The second external test set comprised data for 48 nonpolar or weakly polar monofunctional compounds (35) that have not been used in development of present model. For these relatively simple and typically hydrophobic compounds, the developed model is more accurate since standard error is significantly reduced ($se = 0.307$) if compared with the calibration set results. The third test set (107) is only partially external since 63 of 93 compounds have been used in the calibration set but their reported values are quite different. As expected the standard error for this test set is significantly higher ($se = 0.613$) if compared with the results obtained for calibration set. It is fair to conclude, based on the results of extensive evaluation procedure, that the general statistical model has significant predictive capabilities and that its application domain is very broad.

However, there are still some potential drawbacks of this general statistical model which have not been rationalized yet. First, all three continuous and size related variables P_1 (molecular weight MW, bond connectivity ϵ and molecular E-state) are highly inter-correlated, i.e. ϵ vs. MW ($r^2 = 0.72$), E-state vs. MW ($r^2 = 0.67$) and E-state vs. ϵ ($r^2 = 0.73$). This is clearly an undesirable property for the independent variables in a multilinear model. However, it is not clear when and how will such statistical weakness affect the quality of predicted soil sorption coefficients. Furthermore, there are several significant outliers in the calibration set. The largest outlier is 2,3,7,8-tetrachlorodibenzodioxin (TCDD) whose experimental $\log K_{oc}$ (6.50) is underestimated by 1.88 log units. Another major outlier is benzo(ghi)perylene whose reported $\log K_{oc}$ (4.61) is overestimated by 1.76 log units. Two other outliers hexabromobiphenyl and 2,6-dichlorobenzamide are also overestimated by 1.50 and 1.47 log units, respectively. Thus, it seems that developed model may have a problem in predicting $\log K_{oc}$ data for some large PAHs or halogenated aromatics. This is particularly disturbing since simple models based on $\log K_{ow}$ (5, 27) or the first-order molecular connectivity index (108–110) are more accurate in predicting the soil sorption coefficients for those outliers and such type of chemicals (8, 17, 27, 35, 111).

K_{oc} Modeling Summary and Perspectives

This critical analysis of recent developments in modeling soil sorption coefficients (K_{oc}) has shown that there are reliable QSAR models for every taste, i.e. for log K_{ow} fans, for thermodynamics enthusiasts and for statistics aficionados. The simplest, oldest and still the most widely used methods to predict K_{oc} values of organic compounds are well established linear correlations between log K_{oc} and log K_{ow} . Today, the most reliable model from this class is the system of QSAR models (27) that is incorporated into the European Union technical guidance document for risk assessment of chemicals (45). The major prerequisite for reliable estimates is the use of measured and evaluated K_{ow} data. The BioByte Masterfile database now contains such K_{ow} data for more than 60,000 chemicals (42, 43), a number that is continuously increasing. A recent study on the use of calculated K_{ow} values in modeling soil sorption coefficients (112) has stressed once more the well-known problem that calculated K_{ow} values introduce additional and significant uncertainty in estimating the K_{oc} data (3, 35). Namely, depending on the model, i.e. algorithm, the estimated K_{ow} values regularly vary by 1 log unit and in some cases even 2 log units or more, e.g. triallate (2.17), aldrin (2.6), dieldrin (2.44), endosulfan (3.5), disulfoton (2.52), ethion (4.44), ethoprophos (2.5), fonofos (2.4), malathion (2.2), phorate (2.5), phosalone (2.7), terbufos (2.9), tricyclazole (2.0), leptophos (2.6), methidathion (2.7), piperophos (2.6), etc. Consequently, the large variability in calculated K_{ow} data translates directly into the large uncertainties in soil sorption coefficients estimated by linear log K_{oc} -log K_{ow} models. Thus, whenever possible, the calculated K_{ow} data should be avoided for calculating the soil sorption coefficients. Unfortunately, the system of linear log K_{oc} -log K_{ow} models (27) has not yet been evaluated on the emerging pollutants like pharmaceuticals, primarily antibiotics, and personal care products (PCPs). Therefore, one of primary objectives for this research area is to evaluate the quality of estimates by this system of linear log K_{oc} -log K_{ow} models for pharmaceuticals and personal care products and, if necessary, extend the system of linear models to cover these two important classes of environmental pollutants.

The major advances in developing pp-LFER models for estimating soil sorption coefficients have been made during the last 10 years. As pointed out earlier, the most appealing feature of pp-LFER approach seems to be its solid and sound thermodynamic and mechanistic grounds. An additional attribute for the majority of the developed pp-LFER models is the use of uniformly measured K_{oc} data for their calibration and successful evaluation on various chemical classes. However, despite such a careful stepwise procedure, recent comparative analysis (75) has demonstrated that the regression coefficients of published pp-LFER models differ significantly and for the constant term range from -1.04 to 0.724 while for the s coefficient range from -0.82 to 1.27. This means that the developed pp-LFER models strongly depend on the selected calibration data set and this should not be the case for models with solid and sound thermodynamic and mechanistic grounds. Therefore, the selection of compounds for calibration of pp-LFER model must be done carefully, particularly considering the quality and reliability of their relevant experimental data. Besides using only the high quality K_{oc} data for calibration, the quality and range of solute descriptors must be also

evaluated. At present, the lack of experimental pp-LFER descriptors and the poor quality of calculated pp-LFER descriptors for a large number of environmentally relevant chemicals are the major obstacles for developing generally applicable pp-LFER model. Another major drawback in developing the general pp-LFER model for soil sorption is the potential inter-correlation between solute descriptors for the calibration set chemicals which has not been evaluated in number of developed models. Therefore, the primary future objective for this research area should be to evaluate the quality of experimental K_{oc} values since a large set of published K_{oc} data still awaits complete and careful evaluation. Finally, it should be also considered that the “one size fits all” assumption, i.e. one pp-LFER model for all chemicals, may not work for soil sorption coefficients.

As pp-LFER models, the SPARC online-calculator and COSMO modules are also based on thermodynamic and mechanistic grounds. Nevertheless, those two approaches are much less successful in estimating the soil sorption coefficients. Two evaluation studies (77, 98) have demonstrated that the root-mean-square errors for SPARC calculated $\log K_{oc}$ values range from 1.05 to 1.96 and that there is a general trend to overestimate the $\log K_{oc}$ values. Thus, if the precision of 1 log unit or more is acceptable, the SPARC online-calculator may be an acceptable method for estimated $\log K_{oc}$ data. An analogous situation also pertains to the K_{oc} estimates produced by various COSMO modules. The systematic analysis of COSMOtherm-calculated $\log K_{oc}$ values (91) has shown that the polycyclic aromatic hydrocarbons and their aza-derivatives are systematically underestimated by 1–2 log units while the simple alcohols are systematically overestimated by about 0.8 log units. Furthermore, phosphates were also significantly overestimated, in a number of cases by up to 2 log units. An extensive evaluation study of COSMO-SAC module (98) has shown that about 75% of compounds have calculated $\log K_{oc}$ values within 1 log unit of the measured values. However, for more than 100 chemicals, predictions deviate from the measured $\log K_{oc}$ values by more than 1 log unit and the root-mean-square error is close to 1. The COSMOtherm had a similar score in estimating $\log K_{oc}$ values for 28 non-ionized natural toxins (77). Thus, if the precision of 1 log unit for estimated $\log K_{oc}$ data is acceptable, the COSMO modules may also be a reasonable choice but not for phosphates.

The main advantage of the general statistical QSAR model (19) is its wide applicability domain since all up to date literature soil-water partition coefficients available for organic compounds have been used in its development, testing and/or evaluation. However, due to the statistical nature of the QSAR model, it should not be used outside its applicability domain. Namely, outside the applicability domain, each estimated $\log K_{oc}$ value can be either reasonable or wrong by orders of magnitude and there is no way to know which will be the case for any specific chemical. Thus, the application of statistical QSAR models outside their applicability domains is like flipping a coin and is best characterized by the famous movie quote “Do I (you) feel lucky?”. Furthermore, as pointed out earlier, all three size related variables (molecular weight, bond connectivity and molecular E-state) are highly inter-correlated and it is not clear when and how will this affect the quality of estimated soil sorption coefficients for chemicals that are within the applicability domain. This may be the reason why there are several

significant outliers even in its calibration set, i.e. 2,3,7,8-tetrachlorodibenzodioxin (TCDD), benzo(ghi)perylene, hexabromobiphenyl and 2,6-dichlorobenzamide. Another disadvantage of the general statistical QSAR model is that it was not evaluated on the emerging pollutants like pharmaceuticals, personal care products and similar highly complex chemicals.

Pharmaceuticals and personal care products (PPCPs) are emerging as a new class of global pollutants. Thus, it will be highly desirable to have a reliable QSAR model for estimating their soil sorption coefficients. Unfortunately, only a limited effort has been made either to develop the specific QSAR models for PPCPs or to evaluate the quality and/or reliability of existing QSAR models for estimating the soil sorption coefficients of PPCPs. The experimental K_{oc} data of several pharmaceuticals and hormones were compared with those estimated by the two pp-LFER models (eqs 7 and 8) to assess their applicability to complex, environmentally relevant chemicals. A root-mean-square error of about 0.4 log units was obtained for log K_{oc} data estimated by eq 8. Thus, it seems that this pp-LFER model performs very well and may be used for estimating log K_{oc} data of hormones and pharmaceuticals. The prospective candidates for estimating the log K_{oc} data of PPCPs are also the models for ionized compounds (eqs 13–15), since PPCPs frequently comprise several easily ionizable functional groups. Furthermore, a number of pharmaceuticals, primarily antibiotics, have been used in the calibration sets for those models and the average error of their K_{oc} estimates was 0.36 log units. Thus, it seems that the models for ionized compounds are also a reasonable choice for estimating log K_{oc} data of pharmaceuticals.

Thus, to summarize, the two main objectives for this research area are (i) to evaluate the quality of experimental K_{oc} values since a large fraction of published K_{oc} data still awaits careful evaluation and, consequently, to derive the standard data set(s) for evaluating and/or testing the quality of available and future QSAR models and (ii) to evaluate the available QSAR models in estimating the soil sorption coefficients of emerging pollutants like pharmaceuticals, personal care products or similar highly complex chemicals.

References

1. Katayama, A.; Bhula, R.; Burns, G. R.; Carazo, E.; Felsot, A.; Hamilton, D.; Harris, C.; Kim, Y. H.; Kleter, G.; Koerdel, W.; Linders, J.; Peijnenburg, J. G. M. W.; Sabljic, A.; Stephenson, R. G.; Racke, D. K.; Rubin, B.; Tanaka, K.; Unsworth, J.; Wauchope, R. D. *Rev. Environ. Contam. Toxicol.* **2010**, *203*, 1–86.
2. Doucette, W. J. *Environ. Toxicol. Chem.* **2002**, *22*, 1771–1788.
3. Sabljic, A. *Environ. Health Perspect.* **1989**, *83*, 179–190.
4. Wauchope, R. D.; Yeh, S.; Linders, J. B. H. J.; Kloskowski, R.; Tanaka, K.; Rubin, B.; Katayama, A.; Kordel, W.; Gerstl, Z.; Lane, M.; Unsworth, J. B. *Pest Manage. Sci.* **2002**, *58*, 419–445.
5. Karickhoff, S. W.; Brown, D. S.; Scott, T. S. *Water Res.* **1979**, *13*, 241–248.
6. Karickhoff, S. W. *Chemosphere* **1981**, *10*, 833–846.

7. Chiou, C. T.; Peters, L. J.; Freed, V. H. *Science (Washington, D.C.)* **1979**, *206*, 831–832.
8. Chiou, C. T.; Porter, P. E.; Schmedding, D. W. *Environ. Sci. Technol.* **1983**, *17*, 227–231.
9. Allen-King, R. M.; Grathwohl, P.; Ball, W. P. *Adv. Water Resour.* **2002**, *25*, 985–1016.
10. Grathwohl, P. *Environ. Sci. Technol.* **1990**, *24*, 1687–1693.
11. Chiou, C. T. *Partition and Adsorption of Organic Contaminants in Environmental Systems*; John Wiley & Sons: New York, 2002.
12. Gerstl, Z. *J. Contam. Hydrol.* **1990**, *6*, 357–375.
13. Kile, D. E.; Chiou, C. T.; Zhou, H.; Li, H.; Xu, O. *Environ. Sci. Technol.* **1995**, *29*, 1401–1406.
14. Nguyen, T. H.; Goss, K. U.; Ball, W. P. *Environ. Sci. Technol.* **2005**, *39*, 913–924.
15. Bronner, G.; Goss, K. U. *Environ. Sci. Technol.* **2011**, *45*, 1307–1312.
16. Fujita, T.; Nishimura, K.; Takayama, C.; Yoshida, M.; Uchida, M. In *Handbook of Pesticide Toxicology, Volume 1. Principles*; Krieger, R. I., Ed.; Academic Press: San Diego, CA, 2001; pp 649–670.
17. Gawlik, B. M.; Sotiriou, N.; Feicht, E. A.; Schulte-Hostede, S.; Kettrup, A. *Chemosphere* **1997**, *34*, 2525–2551.
18. Delle Site, A. *J. Phys. Chem. Ref. Data* **2001**, *30*, 187–439.
19. Schüürmann, G.; Ebert, R. U.; Kühne, R. *Environ. Sci. Technol.* **2006**, *40*, 7005–7011.
20. Gramatica, P.; Giani, E.; Papa, E. *J. Mol. Graphics Modell.* **2007**, *25*, 755–766.
21. Baker, J. R.; Mihelcic, J. R.; Sabljic, A. *Chemosphere* **2001**, *45*, 213–221.
22. Razzaque, M. M.; Grathwohl, P. *Water Res.* **2008**, *42*, 3775–3780.
23. Hermens, J.; Balaz, S.; Damborsky, J.; Karcher, W.; Mueller, M.; Peijnenburg, W.; Sabljic, A.; Sjoestroem, M. *SAR QSAR Environ. Res.* **1995**, *3*, 223–236.
24. Sabljic, A.; Peijnenburg, W. *Pure Appl. Chem.* **2001**, *73*, 1331–1348.
25. Kenaga, E. E.; Goring, C. A. I. In *Aquatic Toxicology*; Eaton, J. C., Parrish, P. R., Hendricks, A. C., Eds.; STP 707. American Society for Testing and Materials: Philadelphia, PA, 1980; pp 78–115.
26. Briggs, G. G. *J. Agric. Food Chem.* **1981**, *29*, 1050–1059.
27. Sabljic, A.; Guesten, H.; Verhaar, H.; Hermens, J. *Chemosphere* **1995**, *31*, 4489–4515.
28. Yang, F.; Qu, R. J.; Wang, M.; Tang, Y. Q.; Feng, M. B.; Wang, Z. Y. *Geoderma* **2013**, *193*, 140–148.
29. Wen, Y.; Su, L. M.; Qin, W. C.; Fu, L.; He, J.; Zhao, Y. H. *Chemosphere* **2012**, *86*, 634–640.
30. van Wenzel, A. P.; Opperhuizen, A. *Chemosphere* **1995**, *31*, 3605–3615.
31. Opperhuizen, A.; Serne, P.; Van der Steen, J. M. D. *Environ. Sci. Technol.* **1988**, *22*, 286–292.
32. Wania, F.; Mackay, D. *Environ. Sci. Technol.* **1996**, *30*, 390A–396A.
33. Sabljic, A. *Chemosphere* **2001**, *43*, 363–375.
34. Sabljic, A. *J. Agric. Food Chem.* **1984**, *32*, 243–246.

35. Sabljic, A. *Environ. Sci. Technol.* **1987**, *21*, 358–366.
36. Pontolillo, J.; Eganhouse, R. P. *The Search for Reliable Aqueous Solubility (Sw) and Octanol-Water Partition Coefficient (K_{ow}) Data for Hydrophobic Organic Compounds: DDT and DDE as a Case Study*; U. S. Geological Survey Water-Resources Investigations Report 01-4201; USGS: Reston, VA, 2001.
37. Renner, R. *Environ. Sci. Technol.* **2002**, *36*, 411A–413A.
38. Linkov, I.; Ames, M. R.; Crouch, E. A. C.; Satterstrom, F. K. *Environ. Sci. Technol.* **2005**, *39*, 6917–6922.
39. *KOCWIN 2.00 (EPI-Suite v.4.1)*; Syracuse Research Corporation: Syracuse, NY, 2010.
40. Wen, Y.; Su, L. M.; Qin, W. C.; Fu, L.; He, J.; Zhao, Y. H. *Chemosphere* **2012**, *86*, 634–640.
41. Means, J. C.; Wood, S. G.; Hassett, J. J.; Banwart, W. L. *Environ. Sci. Technol.* **1982**, *16*, 93–98.
42. Weininger, D. *MedChem User's Manual V 3.54*; Daylight Chemical Information Systems, Inc.: Irvine, CA, 1989; <http://www.daylight.com/daycgi/clogp>.
43. BioByte Corp., Clermont, CA 91711-4707, <http://www.biobyte.com/bb/prod/bioloom.html>.
44. *PCModels*. Daylight Chemical Information Systems, Inc., P.O. Box 7737, Laguna Niguel, CA 92677; <http://www.daylight.com/products/pcmodels.html>.
45. European Commission. *Technical guidance document in support of Commission Directive 93/67/EEC on risk assessment for new notified substances*; Commission Regulation (EC) No 1488/94 on risk assessment for existing substances and Directive 98/8/EC of the European Parliament and of the Council concerning the placing of biocidal products on the market. EUR 20418/EN/3. Luxembourg, Luxembourg, 2003.
46. Abraham, M. H. *Chem. Soc. Rev.* **1993**, *22*, 73–83.
47. Abraham, M. H.; Chadham, H. S. In *Lipophilicity in Drug Action and Toxicology*; Pliska, V., Testa, B., van de Waterbeemd, H., Eds.; Methods and Principles in Medicinal Chemistry; VCH: Weinheim, Germany, 1996; Vol. 4, pp 311–337.
48. Goss, K. U.; Schwarzenbach, R. P. *Environ. Sci. Technol.* **2001**, *35*, 1–9.
49. Kamlet, M. J.; Doherty, R. M.; Veith, G. D.; Taft, R. W.; Abraham, M. H. *Environ. Sci. Technol.* **1986**, *20*, 690–695.
50. Kamlet, M. J.; Abraham, M. H.; Doherty, R. M.; Taft, R. W. *J. Am. Chem. Soc.* **1984**, *106*, 464–466.
51. Kamlet, M. J.; Doherty, R. M.; Carr, P. W.; Mackay, D.; Abraham, M. H.; Taft, R. W. *Environ. Sci. Technol.* **1988**, *22*, 503–509.
52. Kamlet, M. J.; Doherty, R. M.; Abraham, M. H.; Marcus, Y.; Taft, R. W. *J. Phys. Chem.* **1988**, *92*, 5244–5255.
53. Abraham, M. H.; Poole, C. F.; Poole, S. K. *J. Chromatogr., A* **1999**, *842*, 79–114.

54. McGowan, J. C.; Mellors, A. *Molecular Volumes in Chemistry and Biology—Application Including Partitioning and Toxicity*; Ellis Horwood: Chichester, U.K., 1986.
55. Abraham, M. H.; Ibrahim, A.; Zissimos, A. M. *J. Chromatogr., A* **2004**, *1037*, 29–47.
56. Abraham, M. H.; Whiting, G. S.; Doherty, R. M.; Shuely, W. J. *J. Chromatogr.* **1991**, *587*, 213–228.
57. Abraham, M. H.; Chadha, H. S.; Whiting, G. S.; Mitchell, R. C. *J. Pharm. Sci.* **1994**, *83*, 1085–1100.
58. Abraham, M. H.; Andonianhaftvan, J.; Whiting, G. S.; Leo, A.; Taft, R. S. *J. Chem. Soc., Perkin Trans. 2* **1994**, 1777–1791.
59. Torres-Lapasio, J. R.; Garcia-Alvarez-Coque, M. C.; Roses, M.; Bosch, E.; Zissimos, A. M.; Abraham, M. H. *Anal. Chim. Acta* **2004**, *515*, 209–227.
60. Hickey, J. P.; Passino-Reader, D. R. *Environ. Sci. Technol.* **1991**, *25*, 1753–1760.
61. Platts, J. A.; Abraham, M. H.; Butina, D.; Hersey, A. *J. Chem. Inf. Comput. Sci.* **2000**, *40*, 71–80.
62. Atapattu, S. N.; Poole, C. F. *J. Chromatogr., A* **2008**, *1195*, 136–145.
63. Tülp, H. C.; Goss, K. U.; Schwarzenbach, R. P.; Fenner, K. *Environ. Sci. Technol.* **2008**, *42*, 2034–2040.
64. Goss, K. U. *Fluid Phase Equilib.* **2005**, *233*, 19–22.
65. Goss, K. U. *J. Phys. Chem. B* **2003**, *107*, 14025–14029.
66. Haderlein, S. B.; Schwarzenbach, R. P. *Environ. Sci. Technol.* **1993**, *27*, 316–326.
67. Abraham, M. H.; Roses, M. *J. Phys. Org. Chem.* **1994**, *7*, 672–684.
68. Poole, S. K.; Poole, C. F. *J. Chromatogr., A* **1999**, *845*, 381–400.
69. Ahmad, R.; Kookana, R. S.; Alston, A. M.; Bromilow, R. H. *Aust. J. Soil Res.* **2001**, *39*, 893–908.
70. Pharma Algorithms Inc., 591 Indian Road, Toronto, ON, Canada, M6P 2C4.
71. During, R. A.; Krahe, S.; Gath, S. *Environ. Sci. Technol.* **2002**, *36*, 4052–4057.
72. Endo, S.; Grathwohl, P.; Haderlein, S. B.; Schmidt, T. C. *Environ. Sci. Technol.* **2009**, *43*, 3094–3100.
73. Endo, S.; Grathwohl, P.; Haderlein, S. B.; Schmidt, T. C. *Environ. Sci. Technol.* **2008**, *42*, 5897–5903.
74. Bronner, G.; Goss, K. U. *Environ. Sci. Technol.* **2011**, *45*, 1313–1319.
75. Kipka, U.; Di Toro, D. M. *Environ. Toxicol. Chem.* **2011**, *30*, 2013–2022.
76. *ABSOLV ACD/ADME Suite*, version 4; Advanced Chemistry Development: Toronto, ON, Canada; http://www.acdlabs.com/products/pc_admet/.
77. Schenzel, J.; Goss, K. U.; Schwarzenbach, R. P.; Bucheli, T. D.; Droge, S. T. *J. Environ. Sci. Technol.* **2012**, *46*, 6118–6126.
78. Schenzel, J.; Schwarzenbach, R. P.; Bucheli, T. D. *J. Agric. Food Chem.* **2010**, *58*, 11207–11217.
79. Bintein, S.; Devillers, J. *Chemosphere* **1994**, *28*, 1171–1188.
80. Kah, M.; Brown, C. D. *J. Agric. Food Chem.* **2007**, *55*, 2312–2322.
81. Franco, A.; Trapp, S. *Environ. Toxicol. Chem.* **2008**, *27*, 1995–2004.

82. Franco, A.; Fu, W. J.; Trapp, S. *Environ. Toxicol. Chem.* **2009**, *28*, 458–464
Erratum *Environ. Toxicol. Chem.* **2009**, *28*, 2018.
83. Franco, A.; Trapp, S. *Environ. Toxicol. Chem.* **2010**, *29*, 789–799.
84. Franco, A.; Trapp, S.; MacKay, D. *Environ. Sci. Technol.* **2010**, *44*, 6123–6129.
85. *ACD/I-Lab*, ver 6.01; Advanced Chemistry Development: Toronto, ON, Canada.
86. Tülp, H. C.; Fenner, K.; Schwarzenbach, R. P.; Goss, K. U. *Environ. Sci. Technol.* **2009**, *43*, 9189–9195.
87. Hyun, S.; Lee, L. S. *Environ. Sci. Technol.* **2004**, *38*, 5413–5419.
88. Higgins, C. P.; Luthy, R. G. *Environ. Sci. Technol.* **2007**, *41*, 6316–6316.
89. Hilal, S. H.; Saravanaraj, A. N.; Whiteside, T.; Carreira, L. A. *J. Comput.-Aided Mol. Des.* **2007**, *21*, 693–708.
90. Winget, P.; Cramer, C. J.; Truhlar, D. G. *Environ. Sci. Technol.* **2000**, *34*, 4733–4740.
91. Klamt, A.; Eckert, F.; Diedenhofen, M. *Environ. Toxicol. Chem.* **2002**, *21*, 2562–2566.
92. Eckert, F.; Klamt, A. *COSMOtherm*, Version C2.1; COSMOlogic GmbH & Co. KG; Leverkusen, Germany, 2009; <http://www.cosmologic.de/index.php>.
93. Dolney, D. M.; Hawkins, G. D.; Winget, P.; Liotard, D. A.; Cramer, C. J.; Truhlar, D. G. *J. Comput. Chem.* **2000**, *21*, 340–366.
94. Hilal, S. H.; Karickhoff, S. W.; Carreira, L. A. *QSAR Comb. Sci.* **2003**, *22*, 565–574.
95. Hilal, S. H.; Karickhoff, S. W.; Carreira, L. A. *QSAR Comb. Sci.* **2004**, *23*, 709–720.
96. Karickhoff, S. W.; Carreira, L. A.; Hilal, S. H. *SPARC On-line Calculator*, version 4.5; <http://archemcalc.com/sparc/>.
97. Zhang, X. M.; Brown, T. N.; Wania, F.; Heimstad, E. S.; Goss, K. U. *Environ. Int.* **2010**, *36*, 514–520.
98. Phillips, K. L.; Di Toro, D. M.; Sandler, S. I. *Environ. Sci. Technol.* **2011**, *45*, 1021–1027.
99. Atalay, Y. B.; Carbonaro, R. F.; Di Toro, D. M. *Environ. Sci. Technol.* **2009**, *43*, 3626–3631.
100. Klamt, A.; Eckert, F. *Fluid Phase Equilib.* **2000**, *172*, 43–72.
101. Klamt, A.; Schüürmann, G. *J. Chem. Soc., Perkin Trans. 2* **1993**, 799–805.
102. Fujitsu. 2002. *MOPAC2000 Program*. Tokyo, Japan.
103. Schäfer, A.; Klamt, A.; Sattel, D.; Lohrenz, J. C. W.; Eckert, F. *Phys. Chem. Chem. Phys.* **2000**, *2*, 2187–2193.
104. Ahlrichs, R.; Bär, M.; Häser, M.; Horn, H.; Kölmel, C. *Chem. Phys. Lett.* **1989**, *162*, 165–169.
105. Wang, S.; Sandler, S. I.; Chen, C. C. *Ind. Eng. Chem. Res.* **2007**, *46*, 7275–7288.
106. Kühne, R.; Ebert, R. U.; Schüürmann, G. *Environ. Sci. Technol.* **2005**, *39*, 6705–6711.
107. Baker, J. R.; Mihelcic, J. R.; Luehrs, D. C.; Hickey, J. P. *Water Environ. Res.* **1997**, *69*, 136–145.
108. Sabljic, A.; Protic, M. *Bull. Environ. Contam. Toxicol.* **1982**, *28*, 162–165.

109. Sabljic, A. *Sci. Total Environ.* **1991**, *109/110*, 197–220.
110. Sabljic, A.; Piver, W. T. *Environ. Toxicol. Chem.* **1992**, *11*, 961–972.
111. Sabljic, A.; Horvatic, D. *J. Chem. Inf. Comput. Sci.* **1993**, *33*, 292–295.
112. dos Reis, R. R.; Sampaio, S. C.; de Melo, E. B. *Water Res.* **2013**, *47*, 5751–5759.

Chapter 6

Evaluations of Regulatory Kinetics Analysis Approaches

**Jane Tang,^{*,1} Russell L. Jones,¹ Michael Huang,² Wenlin Chen,³
Richard Allen,⁴ Sue Hayes,³ and Robin Sur¹**

**¹Bayer CropScience LLC, 2 TW Alexander Drive,
Research Triangle Park, North Carolina 27709**

²DuPont Crop Protection, 1090 Elkton Road, Newark, Delaware 19711

**³Syngenta Crop Protection, LLC, 410 Swing Road,
Greensboro, North Carolina 27409**

⁴Valent U.S.A. Corporation, 6560 Trinity Court, Dublin, California 94568

***E-mail: Jane-zhenxu.tang@bayer.com.**

Degradation of crop protection products is often described by first-order kinetics. Surface and ground water models currently used by regulatory agencies to regulate these products require a first order degradation rate constant. However, single first order kinetics may not appropriately describe the degradation behavior over an experimental period. In these cases, the use of non-first order kinetics can be useful in fitting degradation data to determine rate constants for exposure models. Different kinetics analysis procedures can result in vastly different degradation rates for exposure modeling input, leading to very different predictions of exposure levels. Regulatory agencies have developed guidance to standardize the analysis procedure to support agrochemical registrations. This paper presents a comparison of kinetics analysis procedures between a guidance used by European Union and a guidance used by USA and Canada, and an evaluation of the two approaches using several data sets.

Introduction

Environmental exposure assessment depends on environmental fate properties of an agrochemical, such as degradation and sorption behaviors. Current water exposure models, including surface and ground water models, often describe degradation by first order kinetics. However in many cases degradation behavior of a chemical in field or laboratory is better described by non-first order kinetics. Therefore, the choice to derive an appropriate first-order degradation half-life from first or non-first order data is very critical to exposure and risk assessment. Different kinetics analysis procedures can result in very different degradation rate for exposure modeling input. A number of factors could contribute to this uncertainty. Examples are kinetics model selection, goodness of fit criteria, statistical approach used for parameter optimization, and expert assumptions and judgments.

Pesticide regulatory agencies have published guidance documents to standardize kinetics analysis approaches. The FOCUS group in Europe (the FORum for Co-ordination of pesticide fate models and their Use) developed a kinetics guidance document in 2006, and the approach defined in this document is used for estimating degradation kinetics from environmental fate studies of agrochemicals in EU (European Union) registration (EU FOCUS guidance hereafter) (1). For the similar purpose, a NAFTA (North American Free Trade Agreement) kinetics guidance document was also developed in 2011, and is used by US EPA (US Environmental Protection Agency) and Canada PMRA (Pest Management Regulatory Agency) for registration evaluations (NAFTA guidance hereafter) (2). The purpose of this paper is to 1) compare kinetics procedures used by the EU FOCUS guidance and NAFTA guidance; 2) evaluate the two kinetics analysis approaches using several common data sets by deriving and comparing kinetic endpoints (degradation half-life) according to the respective guidance. This paper focuses on the recently released NAFTA guidance, because the FOCUS guidance has been used since 2006.

Materials and Methods

The EU FOCUS guidance has proposed approaches for calculating degradation kinetics for both parent and metabolites for field and laboratory degradation studies. This includes DT_{50} and DT_{90} values for triggering additional studies and degradation rates for use in models for estimating environmental exposure. The approaches defined in the NAFTA guidance are to estimate kinetic endpoints for the use in exposure models, not for triggering higher tier testing, as this is not part of the NAFTA registration review process. In addition, the NAFTA guidance only applies to parent substance, a guidance document to estimate metabolite degradation kinetics is not yet available in US and Canada. Therefore, the scope of this paper is limited to evaluating the kinetics analysis approaches for use in water exposure models for parent substances.

Kinetics Models

Degradation of organic compounds in soil and water is often described by first order kinetics. However, single first order kinetics (SFO) may not appropriately describe the degradation behavior over an experimental period as a compound may undergo strong binding, or other confounded reactions in environmental media. In these cases, the use of other kinetic models including FOMC (First Order Multi-Compartment), IORE (Indeterminate Order Rate Equation, mathematically equivalent to FOMC), DFOP (Double First Order in Parallel), and HS (Hockey- Stick) can be useful in fitting degradation data to determine kinetic endpoints such as DT_{50} and DT_{90} , from which a degradation rate to be used in exposure assessments can be estimated. The kinetic models are presented as following in the form of differential equations. The parameter optimization requires solving these equations by integration.

Single First-Order (SFO) is used by both the EU FOCUS guidance and the NAFTA guidance. The SFO kinetics essentially assumes that degradation in soil is a homogeneous process (i.e., uniform rate in all phases of the bulk porous system). The reaction equation for the SFO degradation kinetics may be written as

$$\frac{dM}{dt} = -k M \quad (1)$$

where M is the amount of the compound considered, t is time, and k is the rate constant. Half-life (DT_{50}) and DT_{90} values are calculated from a SFO rate constant k as $DT_{50} = \ln(2) / k$ and $DT_{90} = \ln(10) / k$, respectively.

First-Order Multiple-Compartment (FOMC) is used by the EU FOCUS guidance. This model was first proposed by Gustafson and Holden (3), which assumes that there is a continuous distribution of first-order reaction rate constants in the heterogeneous soil porous media. Further assuming a gamma probability distribution function (γ -pdf) for the rate constant k , the corresponding reaction equation for the overall population of all first-order degradation rates may be written as

$$\frac{dM}{dt} = -\frac{\alpha}{\beta} M \left(\frac{t}{\beta} + 1 \right)^{-1} \quad (2)$$

where M is the amount of the compound considered, t is time, and α and β are coefficients of the γ -pdf of the first order rate constant k . The FOMC model contains two kinetic parameters and is suitable to describe bi-phasic degradation behavior. DT_{50} and DT_{90} values can be calculated using the following equation:

$$DT_x = \beta \left[\left(\frac{100}{100-x} \right)^{\left(\frac{1}{\alpha} \right)} - 1 \right] \quad (3)$$

Double-First-Order in Parallel (DFOP) is used by both the EU FOCUS guidance and the NAFTA guidance. This model assumes that there are two distinct SFO compartments operating in parallel, each with a specific relative size g and $1-g$, and degradation rate constants k_1 and k_2 , respectively. This model can be written as

$$\frac{dM}{dt} = -\frac{k_1 g e^{-k_1 t} + k_2 (1-g) e^{-k_2 t}}{g e^{-k_1 t} + (1-g) e^{-k_2 t}} M \quad (4)$$

where M is the amount of the compound considered and t is time. The DFOP model contains three kinetic parameters and is suitable to describe bi-phasic degradation behavior. DT_{50} and DT_{90} values can only be estimated by using an iterative procedure.

Hockey-Stick (HS) is another kinetics model used by the EU FOCUS guidance. This model assumes two sequential first-order degradation rates that change from k_1 to k_2 at a certain breakpoint t_b . The corresponding reaction equation may be written as

$$\begin{aligned} \frac{dM}{dt} &= -k_1 M && \text{for } t \leq t_b \\ \frac{dM}{dt} &= -k_2 M && \text{for } t > t_b \end{aligned} \quad (5)$$

DT_{50} and DT_{90} values can be calculated using the following equation:

$$\begin{aligned} DT_x &= \frac{\ln \frac{100}{100-x}}{k_1} && \text{for } DT_x \leq t_b \\ DT_x &= t_b + \frac{\left(\ln \frac{100}{100-x} - k_1 t_b \right)}{k_2} && \text{for } DT_x > t_b \end{aligned} \quad (6)$$

Indeterminate Order Rate Equation (IORE) is used by the NAFTA guidance. The degradation rate equation is generalized to allow fractional exponent (or reaction order). Although there is no obvious physical reason why degradation may possess a fractional reaction order, the IORE model can be parameterized to be mathematically equivalent to the FOMC model described in the EU FOCUS guidance. The IORE model is defined by:

$$\frac{dM}{dt} = -k_{IORE} M^N \quad (7)$$

where is degradation rate, and the N parameter determines how fast the degradation rate declines with decreasing concentration and is an indicator of how far the data deviate from a first order model (where $N = 1$).

The detailed parameter conversions between IORE and FOMC can be found in the NAFTA guidance (2).

Half-Life Selection Criteria

Figure 1 and 2 present the decision chart of model selection defined by EU-FOCUS guidance and NAFTA guidance, respectively. The similarity of both approaches is that they start with SFO kinetics. If an SFO fit is acceptable, then both use the calculated SFO half-life for exposure models. When SFO kinetics does not provide an acceptable fit to the data, a half-life for exposure models is calculated from the results of non-first order kinetic models. The methods used to estimate an SFO half-life from non-first order models are different in the procedures described in the EU FOCUS guidance and NAFTA guidance.

In the EU FOCUS procedures, the half-life for modeling is calculated by dividing the estimated DT_{90} from the FOMC model fit by 3.32 if the DT_{90} is reached in the experimental studies. This approach assumes that the derived half-life is based on a SFO model passing through a hypothetical DT_{90} which is the same as the DT_{90} of the FOMC model fit. If the DT_{90} is not reached in the experimental studies, the half-life of the slow phase of the HS model or the slow compartment of the DFOP model (whichever gives the better fit) is considered the half-life to be used in exposure modeling.

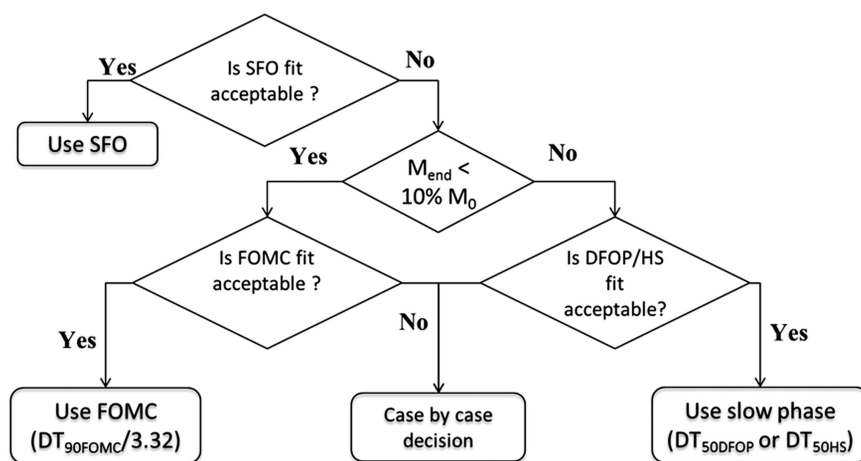


Figure 1. A simplified flow chart for selecting a half-life of parent for exposure models based on the EU FOCUS guidance (1).

In the NAFTA procedures, when SFO kinetics does not adequately describe the data, two half-life values are derived. The first one is referred as a representative half-life ($t_{R\ IORE}$), which is calculated from the DT_{90} by the IORE model fit divided by 3.32, assuming the half-life calculated from a SFO model that would pass through a hypothetical DT_{90} of the IORE fit. A $t_{R\ IORE}$ value is calculated using the following equation:

$$t_{IORE} = \frac{\lg(2)}{\lg(10)} \frac{C_0^{1-N}(1-0.1^{1-N})}{(1-N)k_{IORE}} \quad (8)$$

The second half-life is determined from the slow compartment of the DFOP model fit to the data. The shorter of the two calculated half-lives is then considered as the half-life to be used for modeling according to the NAFTA guidance.

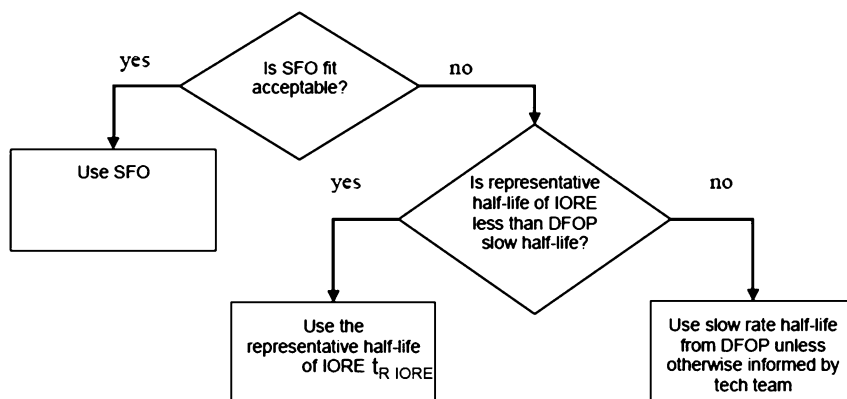


Figure 2. Process for selecting half-life for exposure models in the NAFTA guidance (2).

One of the major differences between the EU FOCUS procedure and the NAFTA procedure is the acceptability criterion for the SFO model fit. This paper presents a brief summary of the criterion. The details of the acceptability criteria for the SFO model fit can be found in the respective guidance documents.

The EU-FOCUS guidance uses two criteria for the goodness of fit: visual inspection and an error criterion based on chi-square (χ^2) significance test. The visual inspection focuses on the residuals which should not be distributed systematically but randomly, and whether the DT_{90} is adequately described by the model. However in the case of systematic but sufficiently small deviations a fit is still qualified as visually acceptable. A chi-square error percentage value of less than 15% usually indicates an acceptable fit, but the final determination is based on the visual inspection.

A χ^2 error percentage value is calculated from chi-square statistics. The model that produces the smallest “err” is considered the best fit.

$$\text{err} = 100 \cdot \sqrt{\frac{1}{\chi^2_{\text{tabulated}}} \cdot \sum \frac{(C-O)^2}{O^2}} \quad (9)$$

where, C = calculated value, O = observed value, \bar{O} = mean of all observed values, err = measurement error. The calculated χ^2 for a specific fit may be compared to $\chi^2_{m, \alpha}$ ($\chi^2_{\text{tabulated}}$) where m is degrees of freedom and α is the probability that one may obtain the given or higher χ^2 by chance.

The NAFTA guidance tests if the exponent N of a non-first order IORE model is significantly different from 1. If the IORE exponent does not deviate significantly from 1, the data are deemed to be adequately represented by SFO. The procedure adopted by the NAFTA guidance is taken from Draper and Smith (4) and Motulsky and Chistopoulus (5). The significant test procedure is described below

$$S_{\text{model}} = \sum (M_{\text{model}} - M_d)^2 \quad (10)$$

where S_{model} is objective function for SFO (S_{SFO}) or IORE (S_{IORE}), M_{model} is modeled value, and M_d is measured value

$$S_c = S_{\text{IORE}} \left(1 + \frac{p}{n-p} F(p, n-p, \alpha) \right) \quad (11)$$

where S_c is the critical value that defines the confidence contours, p is number of parameters, (3 in this case), α is the confidence level specified at 0.50 for this guidance, and F(a,b,c) is F distribution with a and b degrees of freedom and level of confidence c.

If S_{SFO} is less than S_c , the SFO model is used to describe kinetics for modeling. If not, use IORE or DFOP for modeling.

It should be noted that by setting the confidence level at $\alpha=0.5$ (not at the conventional 0.05), the NAFTA guidance for the F test is much more prone to reach false positive conclusions, i.e., rejecting the simpler model SFO while accepting the more complicated models IORE or DFOP. Unlike the FOCUS guidance, visual inspection is not considered in the NAFTA guidance for testing goodness of fit. Another major difference is that, unlike the EU FOCUS procedure, the NAFTA procedure does not perform the goodness of fit and model parameter significant test for each model fitting.

Kinetics Modeling Tools

The mathematical software tool MATLAB with a user shell “KinGUI” ((6) and (7)) were used for kinetics characterization defined in the FOCUS guidance document. PESTDF, developed by PMRA as a package of the statistical software tool R ((8) and (9)), were used to implement the NAFTA kinetic approach. ModelMaker (10) from Modelkinetix (originally developed and published by Cherwell Scientific Ltd., UK) was used to further examine one data set.

Data Sets Evaluated

Twenty data sets from actual experimental studies were used for the evaluations. All the data sets were taken from the EU approved registration documents, and the half-lives for exposure models derived from these data sets have been accepted by the EU. The data sets were divided into three classes based on the EU FOCUS guidance: eleven data sets fit SFO, three data sets fit FOMC, and six data sets fit DFOP. The half-lives were therefore calculated using the corresponding acceptable kinetics models. The same data sets were characterized using the NAFTA procedure in this paper.

Results and Discussions

The data sets used in the evaluation follow SFO degradation or bi-phasic degradation modeled by both the EU FOCUS approach and the NAFTA approach. However, for the same data sets, the derived degradation half-life for exposure models can be very different, depending on the kinetics models that each approach uses to fit the data sets. The consequence can be vastly different predictions of exposure levels in the two regulatory systems.

Table 1 summarizes evaluations for the data sets for which the EU FOCUS procedures have determined that the SFO kinetics were acceptable. The same data sets fitted the SFO model based on the EU FOCUS guidance were all determined unacceptable based on the NAFTA guidance except one data set #11 with a very short half -life (2 days). The half-lives calculated using the non-first order model IORE or DFOP determined by the NAFTA guidance are longer than those calculated using the SFO model by the EU FOCUS guidance. The magnitude of the difference is within a factor of two except data set #5 which shows more than 4 times difference. This evaluation demonstrates that the NAFTA guidance is more strict in accepting SFO model than the EU FOCUS guidance, therefore tends to give longer half lives. This overestimation is expected as the NAFTA guidance sets the model comparison F test at a very high level ($\alpha=0.5$) for the significance test. Conventionally, significance test is often specified at $\alpha=0.05$ to minimize false positive conclusions, which in this case is to minimize the errors that the simpler model is in fact correct but rejected. Another observation is that for the IORE fitting, N , as an exponent, is much more mathematically sensitive to small variations in data than the k value in the IORE model (equation 7). Whether this is a critical factor in the selection of IORE compared to SFO needs to be further evaluated.

Table 1. Comparison of Half-Life (in Days) Determined by EU FOCUS and NAFTA Guidance for Data Sets Which FOCUS Procedures Determined That SFO Kinetics Were Acceptable

Data set	FOCUS		NAFTA	
	Half-life	Model	Half-life	Model
#1	60	SFO	94	DFOP (slow phase)
#2	39	SFO	53	IORE t_R
#3	55	SFO	102	IORE t_R
#4	211	SFO	282	DFOP (slow phase)
#5	232	SFO	1,070	DFOP (slow phase)
#6	62	SFO	97	IORE t_R
#7	66	SFO	94	DFOP (slow phase)
#8	41	SFO	74	IORE t_R
#9	43	SFO	87	IORE t_R
#10	2.9	SFO	2.5	IORE t_R
#11	2.2	SFO	2.2	SFO

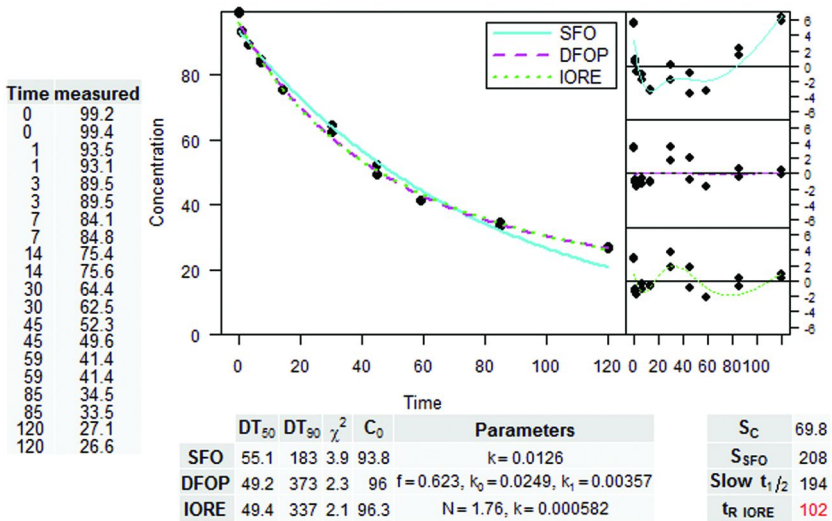


Figure 3. Output by the NAFTA PESTDF tool for data set #3.

Figure 3 presents the output by the NAFTA PESTDF tool for data set #3. According to the NAFTA guidance, the SFO model was rejected, because it did not provide the best fit based on the guidance-specified statistical criterion. However, in laboratory experiments, degradation rates often slow down near the end of the experiment, sometimes at least partially as a result of the changes in the conditions (biological activity) in the incubation flasks, which would not be representative of behavior under field conditions. This effect is particularly noticeable in longer studies, such as 365-day laboratory studies required by previous guidelines for US and PMRA. In addition, degradation in laboratory conditions can slow down due to other factors, such as decreased bio-availability as a result of increasing sorption to soil, which may be representative of behavior under field conditions, or increased sorption with time. Because of the potential for slowing of degradation due to changes in the incubation flasks, the FOCUS procedure allows SFO kinetics to be used for data sets that appear to sufficiently follow SFO kinetics through the main portion of the degradation, even though a statistically better fit might be obtained with another kinetic model. The reason FOCUS selects SFO model for such cases is because FOCUS procedure allows the use of visual inspection criteria.

Table 2. Comparison of Half-Life (in Days) Determined by FOCUS and NAFTA Guidance for Data Sets Which FOCUS Procedures Determined That Non-First Order Kinetics Were Preferred

<i>Data set</i>	<i>FOCUS</i>		<i>NAFTA</i>	
	<i>Half-life</i>	<i>Model</i>	<i>Half-life</i>	<i>Model</i>
#12	57	FOMC	46	DFOP (slow phase)
#13	30	FOMC	30	IORE t_r
#14	65	FOMC	58	DFOP (slow phase)
#15	158	DFOP (slow phase)	160	DFOP (slow phase)
#16	169	DFOP (slow phase)	170	DFOP (slow phase)
#17	210	DFOP (slow phase)	210	DFOP (slow phase)
#18	142	DFOP (slow phase)	143	DFOP (slow phase)
#19	90	DFOP (slow phase)	91	DFOP (slow phase)
#20	434	DFOP (slow phase)	434	DFOP (slow phase)

Table 2 summarizes evaluations for data sets which the EU FOCUS procedures determined that the SFO kinetics was not acceptable, therefore non-first order kinetics was used. Data sets (#12 to #14) fitting the FOMC model based on the EU FOCUS guidance, were described by the IORE model which is mathematically equivalent to FOMC, and the DFOP model based on the NAFTA

guidance. The derived half-lives from the NAFTA tool are comparable or slightly shorter. The data sets (#15 to #20) were described by the DFOP model according to both EU FOCUS and NAFTA guidance, the derived half-lives are comparable as expected.

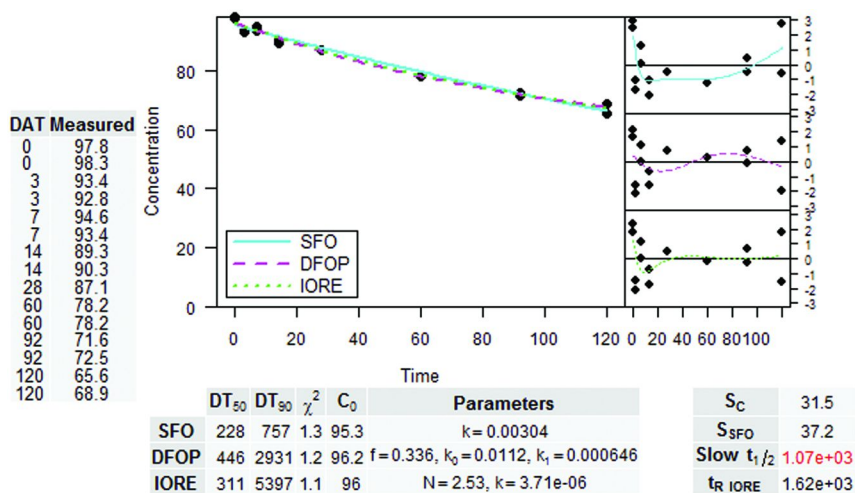


Figure 4. Output by the NAFTA PESTDF tool for data set #5.

Additional Evaluation of Data Set #5

For data set #5, as shown in Figure 4, the output from the NAFTA PESTDF tool shows that the fitting quality of SFO and IORE/DFOP were similar. However, the resulted half-life from IORE is 4 times higher than SFO. Because of this significant discrepancy, additional work was done on this data set using the KinGUI (Version 2.2012.209.845) (7) and ModelMaker (10) software programs for estimating kinetic fits. Figure 5 shows the results for SFO and DFOP kinetics from KinGUI and the results for IORE and DFOP kinetics from ModelMaker. Kinetic endpoints for these fits are provided in Table 3. Both the NAFTA tool and KinGUI predicted essentially the same good fit for SFO kinetics, with a half-life of about 228 days and a χ^2 error of 1.3%. For DFOP kinetics the estimated DT₅₀ in the slow compartment was the same with KinGUI and ModelMaker, although the optimization procedure was somewhat different, especially for the fast compartment, probably reflecting the different optimization routines (iteratively weighted non-linear least squares for KinGUI and non-linear least squares for ModelMaker). However, NAFTA tool fit was worse (χ^2 error of 1.2% compared to 0.84% and 0.93% for KinGUI and ModelMaker, respectively), indicating that the optimization routine may have become stuck in a local minimum. In addition for the IORE fits, there was a significant difference in the representative

half-life ($t_{R\ IORE}$) calculated with the NAFTA tool (1620 days) and ModelMaker (754 days). The parameters describing DFOP are not significant as shown by the FOCUS parameter significance test. More work is needed to understand why the NAFTA tool produced such different results compared to other standard software packages.

Table 3. Comparison of Kinetic Endpoints for Data Set #5 Obtained Using Different Software Packages

<i>Model</i>	<i>SFO</i>	<i>DFOP</i>		<i>IORE</i>	
<i>Tool</i>	$t_{1/2}$ (d)	<i>Overall DT₉₀</i> (d)	<i>Slow-phase (k₂) t_{1/2}</i> (d)	<i>Overall DT₉₀</i> (d)	$t_{R, IORE}$ (d)
KinGUI	228	779	238	-	-
ModelMaker	-	778	238	2503	754
NAFTA	228	2931	1070	5397	1620

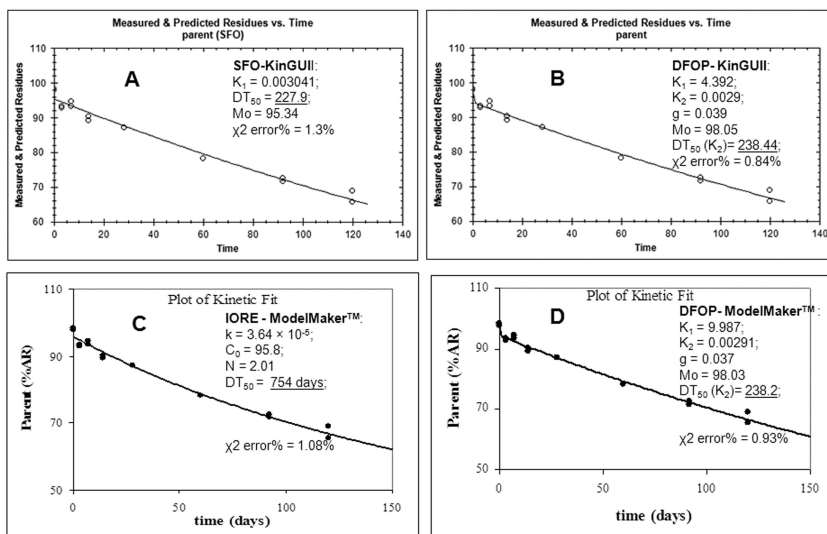


Figure 5. Kinetic fits for data set #5 obtained with ModelMaker™ and KinGUI comparing to the fit with NAFTA tool in Figure 2. Note that in the lower left hand graph, the DT₅₀ provided is actually the t_R (representative half-life).

Conclusions and Recommendations

Regulatory exposure modeling is used to estimate environmental concentrations of crop protection products in the risk assessment process. Reliable data analysis to derive the critical degradation rate for modeling is therefore fundamental to sound regulatory decision making. The main difference between the EU FOCUS guidance and the NAFTA guidance is the acceptance criteria of the SFO model fit. The NAFTA guidance is more strict in accepting SFO model due to the criteria restricted to only significant test of N value, therefore it determines that the half-lives for exposure models are calculated from non-first order model (IORE/DFOP) more often than the EU FOCUS guidance. Consequently, the use of the NAFTA tool will often result in slower degradation rates (longer half-lives) than the values determined using the kinetic guidance from FOCUS. The magnitude of the difference of datasets presented in this study is within 4 times difference. To our knowledge, the difference can be higher (e.g. one order of magnitude higher). The difference will be even greater after the EPA exposure assessment approach adjusts the degradation rate to be the upper bound of the 90th percentile confidence interval (FOCUS guidance specifies the use of the geometric mean or median, depending on the number of values). Further examination of the acceptance criteria for the first order kinetics in the NAFTA tool is recommended (such as choice of α value for the significance test). When SFO kinetics provides an adequate fit of the data, user should be able to select SFO model based on visual inspection and its use should be considered for the principle of simplicity and chemical and biological basis, even if an improved fit is obtained with more complicated kinetics.

For data sets described by non-first order model (DFOP or FOMC) according to FOCUS guidance, similar half-lives are obtained with the EU FOCUS and the NAFTA guidance. However, it is recommended that the NAFTA guidance should perform a model parameter significance test to reject or accept non-first order models, and avoid half-lives determined from a model fit with non-significant parameters. Significance test results of the model parameters should be reported as part of the results. If goodness of fit for both SFO and non-first order models is statistically significant, preference should be given to SFO as outlined in the decision charts (Figure 1 and 2).

While the use of first-order half-lives in exposure models is appropriate for screening level assessments, the ability to conduct higher tier exposure assessments considering degradation patterns that do not follow SFO kinetics should be maintained as a higher tier option. In some cases, especially for ecological assessments, the initial rapid degradation can be sufficient to reduce exposure levels such that the risk quotient does not exceed regulatory levels of concern. One approach that can be used with existing models is the use of DFOP kinetics by modeling the compound as two substances, one with a faster and the other with a slower degradation rate. Consideration of time-dependent sorption in higher tier exposure assessment should be also helpful to address non-first order degradations.

References

1. FOCUS. Guidance Document on Estimating Persistence and Degradation Kinetics from Environmental Fate Studies on Pesticides in EU Registration, Report of the FOCUS Work Group on Degradation Kinetics, EC Document Reference Sanco/10058/2005, version 2.0, 2006; 434 pp, <http://focus.jrc.ec.europa.eu/dk/docs/finalreportFOCDegKin04June06linked.pdf>.
2. EPA; PMRA. NAFTA Guidance for Evaluating and Calculating Degradation Kinetics in Environmental Media, NAFTA Technical Working Group on Pesticides, 2012; 7 pp. http://www.epa.gov/oppefed1/ecorisk_ders/degradation_kinetics/NAFTA_Degradation_Kinetics.htm.
3. Gustafson, D. I.; Holden, L. *Environ. Sci. Technol.* **1990**, *24*, 1032–1038.
4. Draper, N.; Smith H. *Applied Regression Analysis*; John Wiley & Sons: New York, 1981.
5. Motulsky, H.; Christopoulos, A. *Fitting Models to Biological Data using Linear and Nonlinear Regression. A Practical Guide to Curve Fitting*; Graph Pad Software Inc.: San Diego, CA, 2003; www.graphpad.com.
6. MatLab. *MatLab Version 7.0.4.365 (R14) Service Pack 2. Optimisation Toolbox, Statistics Toolbox, MatLab Compiler*; The Mathworks Inc.: Natick, MA, 2005.
7. Bramley, Y. Verification of the Kinetic Modelling Software KinGUI 1.1. Report KGUIV01, 2007.
8. NAFTA. *PestDFV1*. 2012; http://www.epa.gov/oppefed1/ecorisk_ders/degradation_kinetics/NAFTA_Degradation_Kinetics.htm.
9. R-2.15.0-win. *A Programming Environment for Data Analysis and Graphics* <http://www.r-project.org/>.
10. ModelMaker. Modelkinetix: Reading, Berkshire, U.K.

Chapter 7

Principles of the Use of Aged Sorption Studies in EU Regulatory Exposure Assessments

Sabine Beulke* and Wendy van Beinum

The Food and Environment Research Agency, Sand Hutton,
York YO41 1LZ, United Kingdom

*E-mail: sabine.beulke@fera.gsi.gov.uk.

Regulatory exposure assessments for pesticides assume in the first instance that pesticide sorption is constant. Equilibrium sorption coefficients are used to predict environmental concentrations in groundwater. In Europe, the calculations can be refined considering an increase in sorption over time ('aged sorption'). The U.K. Chemicals Regulation Directorate (CRD) commissioned research to underpin the development of a regulatory guidance document on aged sorption. The draft guidance proposes how to measure aged sorption of parent compounds in laboratory studies, outlines procedures to fit kinetic models to the experimental data and suggests criteria to test the goodness of fit and acceptability of the parameters. Options for use of the parameters in EU regulatory groundwater exposure assessments are highlighted. A description of the principles of the draft guidance is given in this chapter.

Introduction

The characterization of sorption of a pesticide to soil is a key requirement of the regulatory process that pesticides must undergo before being placed on the market in the EU. Sorption data are used in the environmental risk assessment to calculate predicted environmental concentrations in groundwater using mathematical pesticide leaching models. The calculated long-term annual average concentrations in groundwater are compared with regulatory triggers. In the first instance, sorption is measured in standard laboratory batch studies (*I*) and the sorption coefficient is determined as the ratio between sorbed and dissolved

pesticide. It is assumed that sorption coefficients are constant over time and that sorption is fully reversible ('sorption equilibrium'). However, adsorption has frequently been observed to increase over and above the batch sorption value the longer the contact time between the substance and soil (2–5). This phenomenon will be referred to as 'aged sorption' in this chapter, other expressions are also used, such as 'time dependent sorption', 'kinetic sorption' and 'non-equilibrium sorption'.

Companies wishing to register a new compound in Europe have the option to account for the increase in pesticide sorption over time within the calculation of predicted environmental concentrations in groundwater. For this purpose, experimental laboratory studies are undertaken that demonstrate aged sorption. Conceptual models that describe the mechanisms of aged sorption are fitted to the experimental data and the model parameters are optimized. Pesticide leaching models that include the same description of aging are then employed to simulate pesticide movement to groundwater, with the aged sorption parameters set to those optimized against the experimental observations.

The U.K. Chemicals Regulation Directorate (CRD) commissioned a research project funded by the Department of Environment, Food and Rural Affairs (DEFRA) to develop guidance on methodologies for aged sorption experiments and modeling in the regulatory context. A literature review, experimental work and modeling were undertaken to investigate approaches for assessing aged sorption of pesticides (6). A guidance document was drafted based on the findings of the research project. After discussion with stakeholders and testing by an independent consultancy (sponsored by the European Crop Protection Association), and following further DEFRA funded research (7), a revised guidance document was compiled (8). The general procedure proposed in the draft guidance document is depicted in Figure 1. This chapter presents the principles of each step and outlines the key recommendations. More detail is available in the documents published on the DEFRA website (6–8).

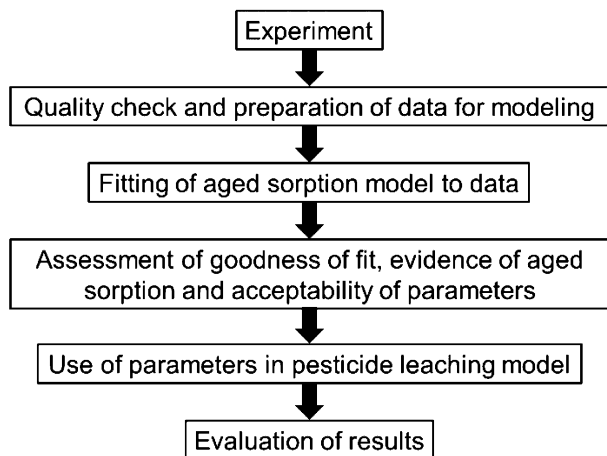


Figure 1. Schematic representation of the procedure to account for aged sorption in the calculation of predicted environmental concentrations in groundwater.

It is important to remember that there are differences in the environmental risk assessment procedure in the EU and US/Canada. The option to account for aged sorption in regulatory exposure assessments for pesticides currently only exists in Europe. The recommendations summarized in this chapter are therefore applicable to Europe only, although the general principles could be useful in a wider context.

Disclaimer

It should be noted that the U.K. CRD recommends “that the draft guidance is **NOT** used for registration purposes until after EFSA PPR Panel scrutiny and until the guidance document has been ‘**noted**’ by the EU Standing Committee on the Food Chain and Animal Health (SCFCAH). If applicants wish to use the guidance as part of a regulatory submission, it is strongly recommended that they discuss this first with the appropriate regulatory authority.”

Experiments To Quantify Aged Sorption of Pesticides in Soil

Experimental methods to measure aged sorption parameters of parent compounds in laboratory studies were reviewed (6). A standardized protocol was recommended in the draft guidance (8). Standardization is desirable, in order to enhance the reproducibility of the experimental results and maximize the reliability of derived model parameters. The test substance is added to sieved soil which is then incubated in the dark at constant temperature and soil moisture. Samples are taken at intervals, extracted for 24 hours with aqueous solution (0.01 molar CaCl₂) to determine the concentration in the liquid phase of the soil, and extracted with organic solvent to determine the total extractable pesticide residue. The procedure is similar to that recommended by OECD guideline 307 for aerobic and anaerobic transformation in soil (9) except that an aqueous extraction step is added for measuring the quantity that is not adsorbed. An example dataset is shown in Figure 2.

Conceptual Model

An overview of mathematical models that describe slow pesticide sorption is given by Suddaby *et al.* in Chapter 11 of this book. Two broad categories, mass transfer models and diffusion models, can be differentiated. Mass transfer models assume that the soil can be conceptualized as compartments with different properties. Solute movement between the compartments follows the first-order reaction kinetics with transfer rate coefficients. There are several types of mass-transfer models: mobile-immobile models assume that there is a rate-limited transfer between mobile and immobile regions of soil pore water. Multi-site models conceptualize the rate-limited process as a solute transfer between sorption sites of different characteristics. Aged sorption is caused by slow movement of

pesticide molecules to less accessible sorption sites and slow desorption from these sites. The ratio of sorbed to dissolved pesticide thus increases over time. Stochastic models account for heterogeneities of soil characteristics and their affinity for pesticides. They do not explicitly consider multiple compartments, but assume that there is a continuum of possible first-order desorption rate constants. The rate constants are distributed according to a probability density function.

The mass-transfer models described above approximate the slow transfer using the first-order kinetics. Diffusion models (*e.g.* (10, 11)) use mechanistic descriptions of diffusion of the pesticide against a concentration gradient which leads to rate-limited transport in soils. Intra-aggregate pore diffusion and intra-organic diffusion through micropores of soil organic matter are possible processes.

The selection of a time-dependent sorption model for regulatory use needs to strike a balance between the ability of the model to describe aged sorption under a range of situations, and the feasibility to determine the model parameters from experiments with reasonable effort. In addition, it must be possible to implement the aged sorption routine into pesticide leaching models that simulate the transport of pesticides through the soil profile. The research that underpins the guidance development considered only the simplest form of the multi-site models (two-site model) to be a viable option (6). Two-site models assume that sorption reactions are fast on one fraction of the sorption sites and slow on the remaining sites (*e.g.* (12–14)). The fast sites could be easily accessible sites on the outer surface of soil aggregates whereas the slow sites might comprise less accessible binding sites within soil organic matter. The fast reaction cannot be distinguished from instantaneous processes and is thus described by equilibrium partitioning. The transfer between the fast and slow – or non-equilibrium – sites is described by the first-order reactions. The rates of adsorption and desorption that describe this transfer are identical in some models and different in others. Degradation can occur in some or all of the three phases (liquid, equilibrium, non-equilibrium). The rates of degradation can be identical or differ between the compartments.

Boesten *et al.* (15) implemented the two-site model proposed by Leistra *et al.* (16) for a laboratory system in the PEARLNEQ software. This two site model and a very similar formulation (14) are the most common mathematical descriptions of time-dependent sorption that are currently used in the regulatory context. They are integrated into the FOCUS versions of the pesticide leaching models PEARL, MACRO, PELMO and PRZM used in European registration (17). A summary of the assumptions and the parameters used by PEARLNEQ are given below:

- Extraction of the soil with aqueous solution for 24 hours characterizes the equilibrium fraction. The sorbed equilibrium domain can be calculated from the aqueous concentration and the total amount. Pesticide that is not available in the equilibrium fraction (dissolved + sorbed) over this timescale is considered to be in the non-equilibrium fraction.
- Sorption on the equilibrium sites is instantaneous with a sorption coefficient $K_{OM,EQ}$. Adsorption-desorption on the non-equilibrium sites is described by the first-order mass transfer. PEARLNEQ makes the

simplifying assumption that adsorption onto the non-equilibrium site occurs at the same rate as desorption with an ad- and desorption rate constant k_{des} (note that in reality adsorption and desorption rates can be different). The ratio of non-equilibrium sorption to equilibrium sorption is f_{NE} .

- When the ultimate sorption equilibrium is attained (*i.e.* when the non-equilibrium sites reach equilibrium), sorption on the equilibrium and the non-equilibrium sites can be described by a Freundlich isotherm. The ratio of sorbed to dissolved pesticide on both sites is concentration dependent, this non-linearity is characterized by the Freundlich exponent $1/n$. The Freundlich exponent is the same for the equilibrium and non-equilibrium domain.
- Irreversibly sorbed pesticide is not considered explicitly in the model. It is assumed that all pesticide that is either degraded or irreversibly bound is 'lost' from the system (*i.e.* not available for desorption and leaching). The two processes are thus lumped together.
- Degradation occurs only in the liquid phase and on the equilibrium sorption sites and follows the first-order kinetics with a degradation half-life $DegT50$. Molecules sorbed on the slow non-equilibrium sorption sites are considered not to degrade.
- The equations that are commonly used to correct degradation in the bulk soil for effects of soil moisture and temperature on degradation (18, 19) are valid for degradation in the two-site model.
- The adsorption-desorption rate and the parameter that characterizes the ratio of equilibrium to non-equilibrium sorption are considered to be independent of soil moisture and temperature over the environmental ranges of these conditions in soil.

Parameters Estimation

The draft guidance document recommends that the two-site aged sorption model should be fitted against the experimental data using optimization tools (8). The parameters that give the best match to the data are recorded. The model is fitted to measurements of the total extractable mass of pesticide in soil (*i.e.* the sum of the mass sorbed plus the mass in the liquid phase) and the aqueous concentration, measured at several points in time. The model has six parameters: the initial concentration of the pesticide $M_{p\ i\ i}$, the degradation half-life $DegT50$, the equilibrium (*i.e.* initial) sorption coefficient $K_{OM,EQ}$, the Freundlich exponent $1/n$, the ratio of non-equilibrium sorption to equilibrium sorption f_{NE} and the desorption rate constant k_{des} . The extent and speed of the increase in sorption over time is determined by f_{NE} and k_{des} . The Freundlich exponent is fixed during optimization. For new studies, an independently measured batch Freundlich exponent should be available for each soil used in the aged sorption experiment. In older studies where this is not the case, an average of the Freundlich exponents for the substance measured in other soils could be used.

The handling of the data before and during the fitting influences the robustness of the parameters. Comprehensive research was undertaken to identify requirements that will help investigators to design experiments in an efficient way and maximize the potential for robust parameter estimation. The recommended principles of the data requirements and data handling are summarized here, more detail can be found elsewhere (6–8). The recommended time for extraction of the soil samples with an aqueous solution is 24 hours. Short-term adsorption, precipitation and dissolution influence the measurements during the first two days after pesticide application. The two-site model is not able to describe the rapid reactions immediately after application, as well as the slower processes operating at a time scale of weeks or months, because it contains only one kinetic sorption site. Elimination of samples of total mass and aqueous concentration taken less than 2 days after application gives a better description of the long-term behavior. Measurements below the limit of quantification (LOQ) are also discarded. It is proposed that at least six sampling times later than day 1 should remain following elimination of data below LOQ and any outliers, with at least one sampling time point any time during day 2 or day 3. A minimum of 2 replicates per sampling date is recommended. Replicate measurements are used individually in the model fitting. The research concluded that weighting of the measurements by the inverse of the measured value during the optimization is advantageous because it accounts for the fact that absolute values for the total mass are often much larger than the concentrations in the liquid phase. It is proposed that at least 10% of the total mass should be sorbed at each time point. Otherwise, instantaneous equilibrium sorption data should be used in the exposure assessment. Relaxed criteria are outlined for legacy studies that were undertaken before the guidance was made available (8).

Visual and Statistical Assessment of the Goodness of Fit

The DEFRA-funded research identified criteria for accepting or rejecting the fit of the two-site model to experimental data (6–8). The recommendations are summarized below. Consequences of failing the criteria are outlined in the draft guidance (8).

It is important that the model gives a good visual fit to the measured data for total mass (sorbed + dissolved; extractable with organic solvent) and aqueous concentration (extractable with CaCl_2) plotted versus time. Figure 2 shows measured and simulated data for an example dataset. The model matches the data well. Weighted residuals (simulated minus observed value divided by observed) are a useful means to detect systematic deviations (patterns of over- or under-predictions). In this example, the residuals are small and randomly distributed around the zero line.

Figure 2 also shows apparent K_d values ($K_{d,app}$) at each sampling time. These illustrate the increase in sorption over time. Apparent K_d values are the ratios of sorbed pesticide per mass unit soil to the concentration in the liquid phase per volume liquid. Apparent K_d values should show a clear increase in sorption over

time that can be distinguished from the scatter in the data. In Figure 2, $K_{d,app}$ increases over time until the end of the experiment and this is matched well by the model.

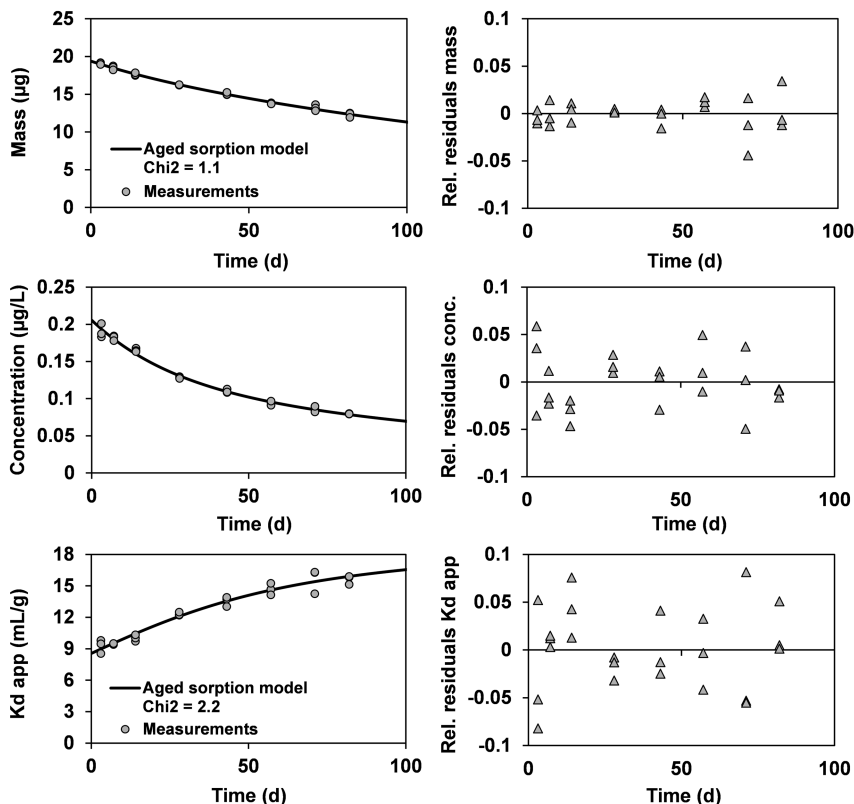


Figure 2. Example of fitted vs measured total mass (sorbed + dissolved) and liquid phase concentrations, apparent K_d values and residuals for the non-equilibrium sorption model (8).

The visual assessment is intended to be used in conjunction with a statistical assessment. The proposed guidance (8) selected a χ^2 error value as the statistical criterion. This is calculated for total mass and concentration data together. The smaller the error value, the better the fit. The χ^2 error should ideally be <15% although this is not a cut-off. The small χ^2 error values of 1.1% for the total mass and concentration data shown in Figure 2 confirm that the model gives a very good fit to the measurements.

Evidence for Aged Sorption

The aim of the modeling is to estimate parameters that characterize aged sorption. It is, therefore, important that the experimental data show sufficient evidence that aged sorption is relevant. The draft guidance proposes that the decision could be based on a comparison between the aged sorption model and an equilibrium model that ignores aged sorption (8). This can be achieved by setting f_{NE} and k_{des} to zero during model fitting. The equilibrium model includes degradation. Figure 3 shows the total mass and concentration data and apparent K_d values for both models plotted against time (the left hand side of Figure 3 is identical with that in Figure 2).

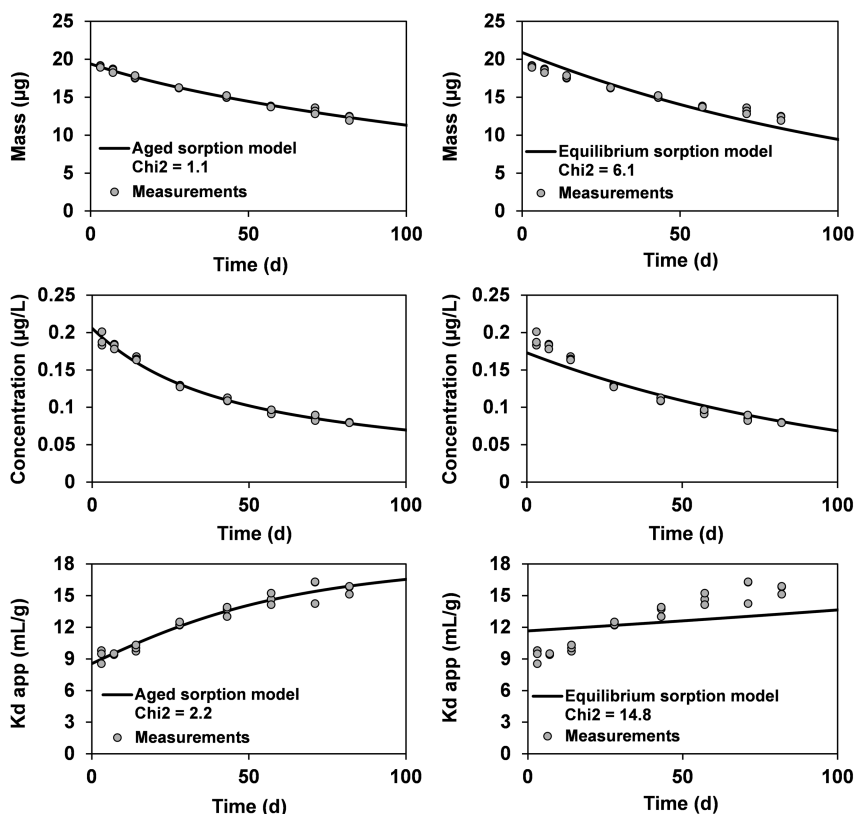


Figure 3. Example of fitted vs measured total mass (sorbed + dissolved) and liquid phase concentrations, apparent K_d values and residuals for the non-equilibrium (left) and equilibrium (right) sorption model (8).

A comparison between the two models shows clear evidence for aged sorption in this example. There is a systematic deviation of the equilibrium model from the data. The equilibrium model simulates a slight increase in sorption over time.

This is due to the use of a Freundlich sorption isotherm with a $1/n$ value <1 , as the pesticide degrades over time, the ratio of sorbed to dissolved pesticide is shifted more and more towards the sorbed state. But the increase in sorption due to Freundlich sorption is not sufficient to match the observed increase. Total mass and concentration, and particularly the apparent K_d values, are described much better when aged sorption is considered. The χ^2 error is much smaller (2.2% compared with 14.8% for the apparent K_d).

Acceptability of the Parameters

Research has been undertaken to identify suitable criteria for the acceptability of the optimized aged sorption parameters (20). This aimed at reducing uncertainties in groundwater assessments based on these parameters without being too restrictive. Actions that should be taken in case the criteria are not met are described in the draft guidance (8).

Optimization tools usually give the optimized parameter values together with the standard error or the 95% confidence interval for each parameter. Confidence intervals reflect the uncertainty around the parameter estimates. Uncertainty can be caused by scatter in the measurements, a small number of measurements, interdependency between two or more parameters and the lack of sensitivity of the model parameters. The relative standard error (RSE) is a statistical criterion derived from the confidence interval. The RSE can be approximated by dividing the 95% confidence interval by $4 \times$ the parameter value to calculate the RSE. This is because the width of the 95% confidence interval equals ~ 4 times the standard deviation (or standard error) based on a normal distribution (the fitted value plus or minus $2 \times$ the standard deviation). The research suggested that the confidence interval or the RSE could be used as an indication for the reliability of the fitted parameters. The draft guidance proposes that the RSE for any of the parameters should not be greater than 0.40. This implies that the width of the 95% confidence interval must not be greater than 160% (i.e. $\pm 80\%$ of the parameter estimate).

In addition, it was suggested that the fitted $K_{OM,EQ}$ value should be compared with the $K_{OM,EQ}$ value that is calculated from the measured total mass and concentration in the liquid phase on day 0. A discrepancy of 20% or less between the fitted and average measured initial K_{OM} is acceptable. The fitted value of the parameter f_{NE} must be <10 and the fitted k_{des} must be $<0.5 \text{ day}^{-1}$.

Use of Aged Sorption in Regulatory Leaching Assessments

The analysis outlined above will have to be undertaken for each individual laboratory aged sorption experiment. Fitted parameters can only be accepted if all criteria are met. If a study meets the data requirements and goodness of fit criteria, but the RSE is too large, then default parameters (0.3 for f_{NE} and 0.01 for k_{des}) can be used, provided aged sorption is relevant. It should be noted that the guidance applies to new studies. Relaxed criteria are outlined for legacy studies that were undertaken before the guidance became available.

Once the appropriate parameters have been identified for each study, a leaching assessment can be carried out that accounts for aged sorption ('higher tier assessment'). Chapters 16, 17, and 18 of this book illustrate how aged sorption can significantly influence predicted environmental concentrations.

The proposed guidance suggested that four studies should be undertaken for each new compound, using different soils. Aged sorption should only be accounted for in the groundwater assessment if at least two datasets result in either default or fitted parameters. There are, in principle two options for the use of the parameters from the four (or more) studies in calculations of predicted environmental concentrations in groundwater (PEC GW):

1. Each parameter combination (f_{NE} , k_{des} , $K_{OM,EQ}$, $DegT50$ and the Freundlich exponent used in the optimization) is used individually in the leaching model. PEC GW are derived for each combination and the median PECs is calculated thereafter.
2. The parameters are averaged over all soils (arithmetic mean $K_{OM,EQ}$, $1/n$ and f_{NE} , geometric mean $DegT50$ and k_{des} . The average is entered into the leaching model, *i.e.* a single PEC GW is calculated.

At lower tiers of the leaching assessment where aged sorption is ignored, degradation and sorption properties are averaged over all available studies and the mean, median or geomean is used in the calculations. For consistency between the lower and higher tier, option 2 would be the preferred choice. But the parameters of the aged sorption model seem to be correlated with each other (δ), and averaging prior to use in the leaching modeling may not be appropriate. The choice of option 1 or 2 does not necessarily affect the calculated concentrations in groundwater, but differences cannot be ruled out at this stage. For the time being, the best option may be to use both methods alongside each other in higher tier leaching assessments that account for aged sorption to gain more experience.

There is a general understanding that risk assessments at the higher tier should not ignore the information generated at the lower tier. It is also accepted that the degree of conservatism should be reduced at the higher tier assessments relative to the lower tier. The use of parameter combinations from the aged sorption studies in the higher tier leaching modeling, without consideration of the lower tier data on degradation and sorption would conflict with these principles. Both, degradation and equilibrium sorption parameters derived from the aged sorption studies could differ considerably from those based on standard OECD 307 and 106 studies at the lower tier. Regarding degradation, the study conditions and design of the aged sorption study are practically identical to the lower tier OECD 307 studies. But even if the same soils were used in the lower and higher tier studies, differences in degradation cannot be excluded. For example, these could arise from differences in microbial activity in soils taken at different times. At the lower tier, laboratory degradation data are often allowed to be combined with field DT50 values where degradation is often faster than in the laboratory. If the lower tier data are ignored, then the higher tier leaching assessment with inclusion of aged

sorption may result in a larger PEC_{GW} than the lower tier. Further analysis and review of the implications of these procedures for exposure estimation is needed to explore if and how these issues could be resolved.

It is also often assumed that higher tier assessments reduce the uncertainty in the calculated estimates of pesticide exposure. Leaching assessments that include aged sorption do not always lead to less uncertainty, because the optimized aged sorption parameters can have wider confidence intervals (or perhaps reveal for the first time that a false degree of certainty has been associated with leaching assessments based upon instantaneous sorption studies). But, aged sorption is definitely a relevant phenomenon for pesticides, and a degree of uncertainty will have to be accepted in the interest of an increased realism of the assessment. The proposed procedures (8) aim at limiting the uncertainty without being too restrictive.

Outlook

CRD has submitted the draft guidance and relevant reports to the European Food Safety Authority (EFSA). EFSA will explore the potential for further refinement and adoption of the guidance at European level.

The draft guidance that is published on the DEFRA website (8) only considers laboratory aged sorption studies with directly dosed parent compounds. Current research commissioned by CRD is exploring the options for estimating aged sorption parameters for metabolites formed from dosed parent substances and for pesticides in field studies. Two options are being considered for field studies. The first option aims at estimating all aged sorption parameters (f_{NE} , k_{des} , $K_{OM,EQ}$, $DegT50$) by fitting the two-site model against the field data. The second option is to use aged sorption parameters from the laboratory in the modeling of the field study and optimize only the $DegT50$ against the field experiment. The intention would be to use the field $DegT50$ in combination with laboratory aged sorption parameters in pesticide leaching modeling for EU regulatory assessments.

Chapter Summary

Pesticide leaching modeling at the first tier of EU regulatory environmental exposure assessments assumes that pesticide sorption is instantaneous and fully reversible. This implies that the strength of sorption is constant with time. In reality, sorption has frequently been observed to increase after longer times of interaction with the soil, thereby reducing the risk for leaching. This phenomenon is referred to as ‘aged sorption’ in this chapter. Aged sorption can be accounted for within the calculation of pesticide leaching in the regulatory context in the EU. For this purpose, experiments are carried out over extended timescales in the laboratory and the results are described with mathematical models that account for the mechanisms of aged sorption. The estimated parameters are entered into pesticide leaching models that use the same mathematical concepts.

The U.K. Chemicals Regulation Directorate (CRD) commissioned a research project (funded by DEFRA) to address a lack of agreed and clear guidance on how experimental aged sorption studies should be conducted and interpreted and how the results should be implemented in regulatory exposure assessments in Europe (6). A draft guidance document was developed. This was presented and discussed at a workshop with representatives of European regulatory authorities, academia, consultancies and industry. Feedback was collated. After testing of the guidance against real datasets by an independent consultancy (sponsored by the European Crop Protection Association) and further DEFRA funded research, the guidance was revised (7). The revised guidance (8) was submitted to the European Food Safety Authority (EFSA) for scrutiny. EFSA will explore the potential for developing a guidance document at EU level. The principles of the draft guidance document (8) are presented in this chapter. The key recommendations are:

- The recommended experimental procedure is very similar to an OECD 307 laboratory degradation study with an additional aqueous extraction step
- A two-site model that assumes rapid binding on some sorption sites and slow adsorption-desorption on the remaining sites is considered the best option in the context of the regulatory environmental exposure assessment.
- Methodologies for data handling and data requirements were proposed (*e.g.* at least six time points, two replicates, eliminate data <LOQ), in order to increase the likelihood of robust parameter estimation and obtain maximum benefit from the experimental effort.
- The goodness of fit of the model to the data is assessed using a combination of visual assessment and a statistical test. The observed total mass (sorbed + liquid) and liquid phase concentration over time should be matched well by the model, without systematic deviations from the measured data. The guidance proposes a χ^2 error value as the statistical criterion.
- The acceptability of the model parameters is based on the relative standard error with a current suggestion that this should not exceed 0.4. It is further proposed that the fitted $K_{OM,EQ}$ value should be within $\pm 20\%$ of the $K_{OM,EQ}$ value that is calculated from the measurements on day 0.
- It should be checked whether there is evidence for aged sorption in the dataset by comparing the fit of the aged sorption model with that of an equilibrium model.
- For new studies, the fitted aged sorption parameters are accepted for use in leaching modeling if all criteria set out in the guidance are met. Default aged sorption parameters can be used under some circumstances. Relaxed criteria for legacy studies that were undertaken before the guidance became available are outlined in the draft guidance document.
- Experiments with four or more soils should be undertaken for each substance. Options for use of the parameters from these studies in the regulatory groundwater exposure assessment are discussed.

Acknowledgments

This work was funded by DEFRA within projects PS2235 and PS2244. We are grateful to stakeholders from industry, European regulatory authorities, research organizations and consultancies for their input into the guidance development.

References

1. OECD. *OECD Guidelines for the Testing of Chemicals*, Test No 106: “Adsorption-Desorption using a Batch Equilibrium Method”; Organization for Economic Cooperation and Development, 2000.
2. Walker, A.; Jurado-Exposito, M. *Weed Res.* **1998**, *38*, 229–238.
3. Cox, L.; Walker, A. *Chemosphere* **1999**, *38*, 2707–2718.
4. DEFRA. *Time-dependent sorption processes in soil*, report for DEFRA project PS2206; Warwick HRI, 2004; URL: http://randd.defra.gov.uk/Document.aspx?Document=PS2206_3831_FRP.doc.
5. DEFRA. *Characterisation and modelling of time-dependent sorption of pesticides*, report for DEFRA project PS2228; The Food and Environment Research Agency, 2009; URL: http://randd.defra.gov.uk/Document.aspx?Document=PS2228_7878_FRP.doc.
6. DEFRA. *Development of guidance on the implementation of aged soil sorption studies into regulatory exposure assessments*, report for DEFRA project PS2235; The Food and Environment Research Agency, 2010.
7. DEFRA. *Consideration of additional experimental datasets to support the development of the revised guidance on aged sorption studies*, report for DEFRA project PS2244; The Food and Environment Research Agency, 2012.
8. Beulke, S.; van Beinum, W. *Guidance on how aged sorption studies for pesticides should be conducted, analysed and used in regulatory assessments*, funded by DEFRA within projects PS2235 and PS2244, 2012; URL: <http://www.pesticides.gov.uk/guidance/industries/pesticides/topics/pesticide-approvals/pesticides-registration/data-requirements-handbook/Draft-guidance-on-time-dependent-soil-adsorption-of-pesticides>.
9. OECD. *OECD Guidelines for the Testing of Chemicals*, Test No 307: Aerobic and anaerobic transformation in soil; Organization for Economic Cooperation and Development, 2002.
10. van Beinum, W.; Beulke, S.; Brown, C. D. *Environ. Sci. Technol.* **2006**, *40*, 494–500.
11. Altfelder, S.; Streck, T. *J. Contam. Hydrol.* **2006**, *86*, 279–298.
12. Karickhoff, S. W. In *Contaminants and Sediments*; Baker, R. A., Ed.; Ann Arbor Science Publishers Inc: Ann Arbor, MI, 1980; Vol. II, pp 193–204.
13. Van Genuchten, M. Th.; Wagenet, R. J. *Soil Sci. Soc. Am. J.* **1989**, *53*, 1303–1310.
14. Streck, T.; Poletika, N.; Jury, W. A.; Farmer, W. J. *Water Resour. Res.* **1995**, *31*, 811–822.

15. Boesten, J. J. T. I.; Tiktak, A.; van Leerdam, R. C. *Manual of PEARLNEQ V4*, 2007; URL: http://www.pearl.pesticidemodels.eu/pdf/usermanual_pearl_neq_4.pdf.
16. Leistra, M.; Van der Linden, A. M. A.; Boesten, J. J. T. I.; Tiktak, A.; Van den Berg, F. *PEARL model for pesticide behaviour and emissions in soil-plant systems. Description of processes*, Alterra report 013, Alterra, Wageningen; RIVM report 711401009, Bilthoven, The Netherlands, 2001; URL: <http://www.pearl.pesticidemodels.eu>.
17. FOCUS. *Assessing the Potential for Movement of Active Substances and their Metabolites to Ground Water in the EU*, report of the FOCUS Ground Water Work Group, EC Document Reference Sanco/13144/2010 version 1, 2010; 604 pp.
18. FOCUS. *FOCUS groundwater scenarios in the EU pesticide registration process*, report of the FOCUS Groundwater Scenarios Workgroup, EC Document Reference Sanco/321/2000 rev 2, 2000; 202 pp.
19. FOCUS. *Generic Guidance for FOCUS groundwater scenarios*, version 1.1, 2002; 61 pp.
20. ter Horst, M. M. S.; Boesten, J. J. T. I.; van Beinum, W.; Beulke, S. *Environ. Model. Software* **2013**, *46*, 260–270.

Chapter 8

Biphasic Behaviors of Pesticide Degradation in Soils: Verification via Pathway Kinetic Fits

Michael Xiao Huang*

DuPont Crop Protection, 1090 Elkton Road, Newark, Delaware 19711

*E-mail: Michael-Xiao.Huang@dupont.com.

The biphasic behavior of pesticide degradation in soil is currently determined by fitting the parent compound degradation data to a simple first-order (SFO) model and a set of biphasic kinetic models, such as FOMC (the first-order in multi-compartments), DFOP (the double first-order in parallel), and IORE (the in-determined order rate equation). If SFO fit is rejected by visual and statistical assessment, degradation is considered biphasic, and a degradation half-life that represents the slow phase degradation is selected for exposure modeling. However, in some cases, SFO fit is acceptable although FOMC and DFOP provide a better fit. The use of a biphasic fit may result in a much longer estimated degradation half-life than warranted. Thus, appropriate identification of biphasic behavior is critical in determining a conservative but realistic degradation rate for a pesticide. In this study, we explore the feasibility of verifying biphasic behavior by fitting both parent compound and metabolite data with SFO-SFO and DFOP-SFO kinetic pathway models. For the three datasets explored, we demonstrate that pesticide biphasic degradation in soil could be due to an artifact, reduced microbial activities, and/or aged sorption. The impact on selection of degradation rate of a pesticide for modeling is also discussed.

Introduction

The degradation rate of a pesticide in soil is one of the most important environmental fate properties used in exposure modeling and risk assessment. In regulatory models, pesticide degradation is usually simulated by the simple first-order kinetics (SFO). However, pesticide degradation in soil is often biphasic or more suitably represented by non-first order kinetic models such as FOMC (the first-order in multi-compartments), DFOP (the double first-order in parallel), and IORE (the in-determined order rate equation). Mechanistically, pesticide degradation is considered biphasic if degradation is fast initially but slows down as it becomes more tightly bound to soil. As a conservative approach, a degradation half-life *DegT50* that represents the slow phase degradation of a pesticide in soil is determined by fitting parent compound data to a biphasic model and this value is used in regulatory models that assume the first-order kinetics of degradation. In this discussion, *DegT50* is used to represent the degradation half-life selected for exposure modeling, while *DT50/DT90* denotes the time taken for 50% or 90% of parent pesticide to degrade.

In the current European kinetics guidance (1), degradation is considered biphasic and the SFO fit to the parent compound data is rejected when one of the following three criteria are met: 1) the χ^2 -test error > 15%; 2) the degradation rate (*k*) t-test fails, and 3) visual assessment is unacceptable. For biphasic degradation, if > 90% of parent compound has degraded at the end of study, then FOMC *DT90/3.32* is selected as the slow phase *DegT50*. If < 90% of parent compound has degraded, DFOP slow phase degradation rate (*k*₂) (as defined in the equation $M = M_0 (g e^{-k_1 t} + (1-g) e^{-k_2 t})$; *M* and *M*₀ = pesticide residue at time *t* and *t* = 0; *k*₁ and *k*₂ are the fast and slow phase degradation rates respectively; *g* is the fraction of *M*₀ in the fast degradation phase) is converted by the equation $\ln(2)/k_2$ to *DegT50* and used for exposure modeling.

In the NAFTA kinetics guidance (2), the parent compound data are fit to the IORE model ($dM/dt = -k_{IORE} \times M^N$; *M* = pesticide residue at time *t* and *k*_{IORE} is the rate constant of degradation; *N* is the exponent). The SFO fit is rejected if the exponent *N* is significantly larger than 1. If the SFO fit is rejected, the IORE representative half-life (*t*_{1/2}) and DFOP slow phase *DegT50* ($\ln(2)/k_2$) are calculated and whichever is shorter is selected to represent the slow phase degradation of pesticides in soil.

The evaluation by Tang et al (3) in this book indicates that the SFO fit could be rejected by the NAFTA guidance (2) even when it is acceptable by the FOCUS kinetic guidance (1). There is also a trend in regulatory review that SFO fit is rejected when FOMC and DFOP provide a better fit. In these cases, the selected *DegT50* could be 2-4 times longer than the actual half-life (*DT50*) of pesticide degradation. Thus, verification of a biphasic behavior is critical in determining the actual degradation rate of a pesticide in soil.

Theoretically, biphasic degradation could result only from aged sorption, but experimentally it could also arise from an experimental artifact or reduced microbial activities (1). For aged sorption, pesticides transfer gradually to a more tightly bound phase, causing the appearance of biphasic degradation. In this case, a *DegT50* that represents the slow phase degradation is justified for

use in modeling. However, if biphasic behavior is an experimental artifact or due to reduced microbial activities, then a certain deviation from the SFO fit should be allowed before SFO is rejected since no slow degradation phase actually exists. Thus, without verification of biphasic degradation, it is likely that over-conservative degradation rates could be selected for exposure modeling.

In this study, we explore the feasibility of verifying biphasic degradation by fitting both parent compound and metabolite data to a SFO-SFO or DFOP-SFO kinetic pathway model, with SFO or DFOP for parent compound and SFO for metabolites. Pesticide degradation in soil is usually conducted with ¹⁴C-labeled compound to quantify both parent compound degradation and metabolite formation, and to determine degradation pathway. Experimentally, the kinetics of degradation of parent compound in soil must be consistent with the kinetics of formation of all metabolites. Thus, if parent compound degradation is indeed biphasic, the DFOP-SFO pathway model is required to describe both parent compound degradation and formation of metabolites.

In this study, three datasets are selected to represent degradation under normal and reduced microbial activities and under the influence of aged sorption, respectively. With these datasets, we demonstrate that biphasic behavior could be due to an experimental artifact, reduced microbial activities, and/or aged sorption, and the impact on determination of degradation rate of a pesticide in soil is discussed.

Materials and Methods

Datasets Evaluated

Three datasets that represent the degradation of one pesticide in soil under normal and reduced microbial activities, and another pesticide behavior under the influence of aged sorption were selected for analyses. The degradation studies were conducted with ¹⁴C-labeled compound at a temperature of 20°C and a moisture content of 40-50% maximum water holding capacity. The metabolites were identified and quantified, with the degradation pathway for one pesticide experimentally confirmed by monitoring the degradation products of each metabolite and the pathway for the other pesticide confirmed by regulatory review. The bound residues, CO₂, and minor unidentified metabolites were also quantified, with a total recovery of 90-110%. The OECD guideline for these experiments was followed.

Kinetics Analyses

The kinetics of degradation in soils for the pesticide was examined following the European FOCUS kinetics guidance (1). The data for parent compound only were fit with SFO and DFOP kinetic models, respectively. The SFO *DegT50* and DFOP slow phase *DegT50* ($\ln(2)/k_2$) were calculated as two extreme degradation rates that may be selected for modeling if degradation is considered biphasic. The goodness of fit was visually and statistically examined and the significance of degradation rate was analyzed with the t-test.

The pathway kinetics fit when both parent compound and metabolites were considered was conducted by using a step-wise approach, as recommended in the FOCUS guidance (1). At Step 1, the parent compound and Stage 1 metabolites (i.e., the metabolites formed directly from parent compound) were included in the kinetic fits with SFO-SFO or DFOP-SFO models, respectively. A sink term was included for parent compound and metabolites but was removed if its formation fraction was optimized to 0.

At the subsequent steps, more metabolites were added until all metabolite were included in the metabolic pathway for kinetic analysis. For all the datasets, pathway kinetic fits were first simulated with SFO and then DFOP for the parent compound to obtain optimal degradation rate constants. SFO was used for all the metabolites in the SFO-SFO and DFOP-SFO fits. However, for the dataset with reduced microbial activities, the metabolites (particularly those with formation peaks observed) were simulated with FOMC, under the assumption that reduced microbial activities impact degradation of parent compound and metabolites.

All the pathway kinetic models were set up and rate constants were optimized using ModelMaker™ (4), as suggested in the FOCUS guidance (1). The goodness of fit was examined visually and also statistically. The optimized parameters were analyzed by the t-test.

Aged Sorption

Mechanistically, aged sorption can often yield behavior that looks like biphasic degradation. Several two-site sorption models for aged sorption have been developed, with variations in assumed degradation mechanisms (5–7). In this study, we assume that degradation only occurs in soil pore water. Pesticide is partitioned instantaneously between soil pore water and Site 1 (i.e., equilibrium site) of the partition coefficient K_d . Pesticide is gradually transferred with time via soil pore water (or transformed directly) to Site 2 to which pesticide is more tightly bound at a partition coefficient approximated as $N_{neq} \times K_d$, where N_{neq} is the ratio of the partition coefficient for Site 2 to Site 1. Linear sorption is assumed. The degradation of pesticide under the influence of aged sorption can be represented in the following equations:

$$\frac{d}{dt} [\theta C + \rho(S_1 + S_2)] = -\mu_l \theta C \quad [1]$$

$$S_1 = K_d C \quad [2]$$

$$S_2 = N_{neq} K_d C \quad [3]$$

$$\frac{dS_2}{dt} = \alpha [N_{neq} S_1 - S_2] \quad [4]$$

where t is time (days), θ is soil water content ($\text{cm}^3 \text{cm}^{-3}$), ρ is soil bulk density (g cm^{-3}), S_1 is concentration on the equilibrium Site 1 ($\mu\text{g g}^{-1}$), S_2 is concentration on the non-equilibrium Site 2 ($\mu\text{g g}^{-1}$), C is concentration in soil pore water ($\mu\text{g mL}^{-1}$), μ_l is the degradation rate in soil pore water (day^{-1}), α is the desorption rate constant from Site 2 (day^{-1}).

This two-site model, as illustrated in Figure 1, is implemented using ModelMaker™, with the initial conditions of $C(t=0) = C_o$, $S_1(t=0) = K_d C_o$, $S_2(t=0) = 0$, respectively.

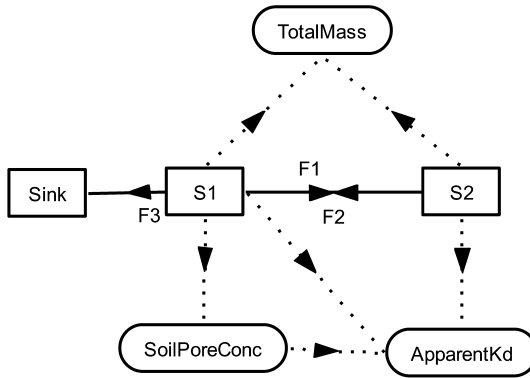


Figure 1. Implementation of the two-site aged sorption model on ModelMaker™ (F_1 , F_2 , and F_3 represent the mass flow rates between compartments of S_1 , S_2 and Sink as represented in eqs (1) and (4); the variables $TotalMass$ (S in eq (5)), $SoilPoreConc$ (C in eq (6)), and $ApparentKd$ (K_{d_app} in eq (6)) are defined to: (1) fit the data for parent compound quantities in soils to the aged sorption model and (2) calculate the apparent K_{d_app} from soil pore water concentration C , S_1 , and S_2 as shown in eq (6)).

The total mass (S) ($\mu\text{g g}^{-1}$) in soils and apparent partition coefficient K_{d_app} are defined as follows:

$$S = S_1 \times \left(\frac{\theta}{K_d \rho} + 1 \right) + S_2 \quad [5]$$

$$K_{d_app} = \frac{S_1 + S_2}{C} \quad [6]$$

The parameters θ , ρ , and K_d were experimentally determined for the soils used in the degradation studies. Thus, the sorption data ($Total\ mass\ vs.\ time$) can be fit to the two-site aged sorption model, with S_o ($\mu\text{g g}^{-1}$) as an initial condition and the parameters N_{neq} , α , and μ_l set for optimization. The goodness of fit was examined following the FOCUS guidance (1), with the parameters also tested for significance.

The apparent partition coefficient $K_{d, App}$ was generated as a function of time (t) and compared to those measured for the soils with similar properties to verify if the aged sorption is indeed responsible for biphasic degradation.

Results and Discussions

Artifacts

Biphasic degradation of pesticides in soil is usually characterized by the initial rapid decrease from Day 0 followed by a slow decline near the end of the study. SFO fit frequently misses the data point for Day 0 and the last 2-3 data points near the end of the study, while DFOP fit can catch those data points, leading to improved kinetic fit.

As shown in Figure 2, for Dataset # 1, the SFO fit describes the degradation well from Day3 to Day 63, in which 80% of parent compound degraded, with a χ^2 -test error of 11%. The degradation rate also passes at the t-test. The data point at Day 0 is slightly missed, and the degradation at the last two sampling points is overpredicted. However, SFO fit is arguably acceptable. Following the FOCUS kinetics guidance, the estimated SFO $DegT_{50}$ of 25.7 days can be accepted for modeling.

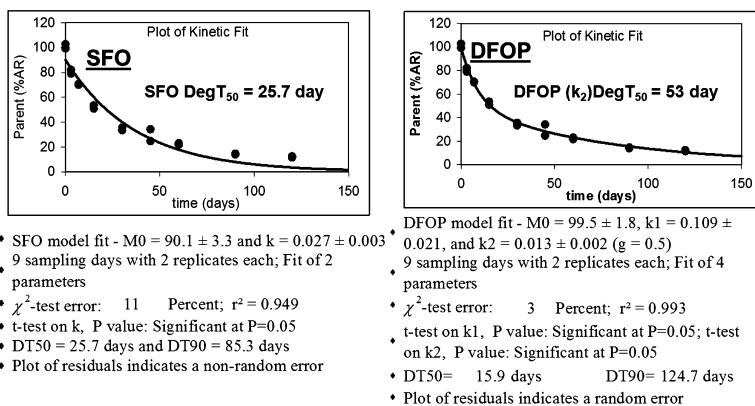


Figure 2. SFO and DFOP kinetic fit for Dataset # 1.

However, the kinetic fit with DFOP is improved, with the data points at Day 0, Day 90, and Day 120 simulated. The error at which the χ^2 test passes decreases from 11% (SFO fit) to 3% (DFOP fit). The optimized degradation rates for k_1 and k_2 for the DFOP model also pass at the t-test. The DFOP slow phase $DegT_{50}$ (i.e., $\ln(2)/k_2$) of 53 days is nearly twice the SFO $DegT_{50}$, and it will be selected for modeling following the FOCUS guidance if degradation is considered biphasic since the DT_{90} was not reached in the experiment.

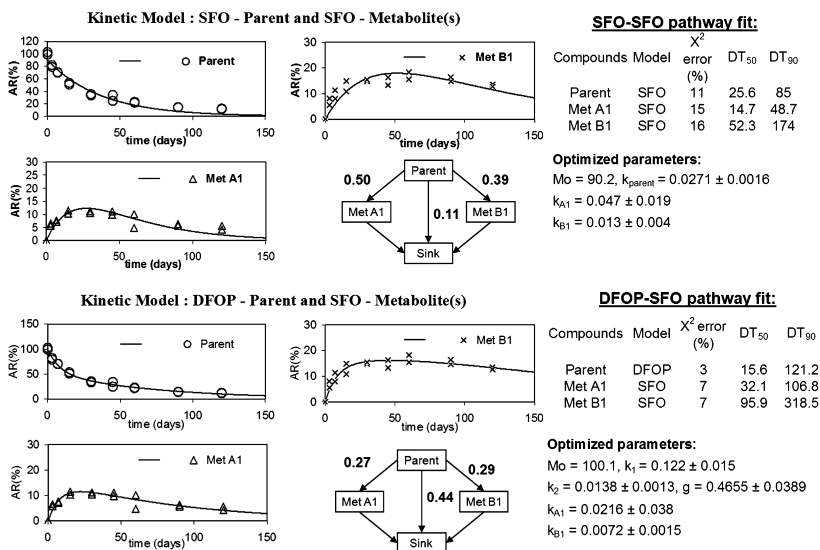


Figure 3. SFO-SFO and DFOP-SFO kinetic fit with Stage 1 Metabolites for Dataset # 1.

In the pathway kinetic fit with Stage 1 metabolites (i.e., the metabolites formed directly from parent compound), parent compound and metabolites are visually well simulated by the SFO-SFO model, with a χ^2 error of 11-16% (Figure 3). However, the kinetic fit for both parent compound and metabolites was improved with DFOP-SFO model, with a χ^2 error decreasing to 3% for parent compound and 7% for the metabolites (Figure 3).

Thus, DFOP does provide a better fit for the parent compound than SFO, either with the data for parent compound only or the data for the parent compound and Stage 1 metabolites in the pathway fit (Figure 3). However, a contradiction with the experimental observation is noticed in the DFOP-SFO pathway fit in Figure 3, when the formation fraction of the sink for the parent compound is compared to the combined radioactivity of bound residues, CO₂, and un-identified minor metabolites observed at the end of degradation study, or when the formation fractions of Stage 1 metabolites are compared to the maximum combined radioactivity of a Stage 1 metabolite and its further degradation products.

In the DFOP-SFO fit with the parent compound and its Stage 1 metabolites, 44% of parent compound goes to the sink, while 27% and 29% degrade to the Stage 1 metabolites Met A1 and Met B1 respectively (Figure 3). This prediction contradicts with the experimental observation. First, the formation fraction of 0.44 for the sink term of parent compound far exceeds the combined radioactivity of 23% AR (AR = applied radioactivity) for the bound residue (19% AR), CO₂ (0%AR), and un-identified minor metabolites (4%AR) at the end of the study.

Second, the formation fractions of 27% for Met A1 and 29% for Met B1 are less than the maximum combined radioactivity of 41% AR for Met A1 and its products (Met A2 and Met A3), and 31% AR for Met B1 and its products (Met B2 and Met B3) observed in the study. This indicates that DFOP overpredicts the parent compound degradation rate (as indicated by its shorter DT_{50} than SFO DT_{50} in Figure 3) so that the mass generated from parent compound is more than what the formation pattern of a Stage 1 metabolite could indicate. As a result, the excess of mass generated from parent compound is forced to the sink, but not enough mass goes to Stage 1 metabolites so that their degradation products can be predicted.

Thus, if DFOP is selected for parent compound degradation, the degradation products of Stage 1 metabolites, particularly Met A1 because more degradation products are formed due to its short DT_{50} , may not be simulated in the full pathway fit when all metabolites are included.

In the SFO-SFO fit with the parent compound and its Stage 1 metabolites, only 11% of parent compound goes to the sink, while 50% and 39% degrade to the Stage 1 metabolites Met A1 and Met B1. This prediction is consistent with the experimental observation, as discussed earlier. Note that the formation fraction of the sink from the parent compound can be lower than the combined radioactivity of bound residues, CO_2 , and un-identified minor metabolites observed at the end of study, as the latter can come from degradation of metabolites as well. Thus, parent compound and its metabolites should be simulated by the SFO-SFO pathway fit when all the metabolites are included.

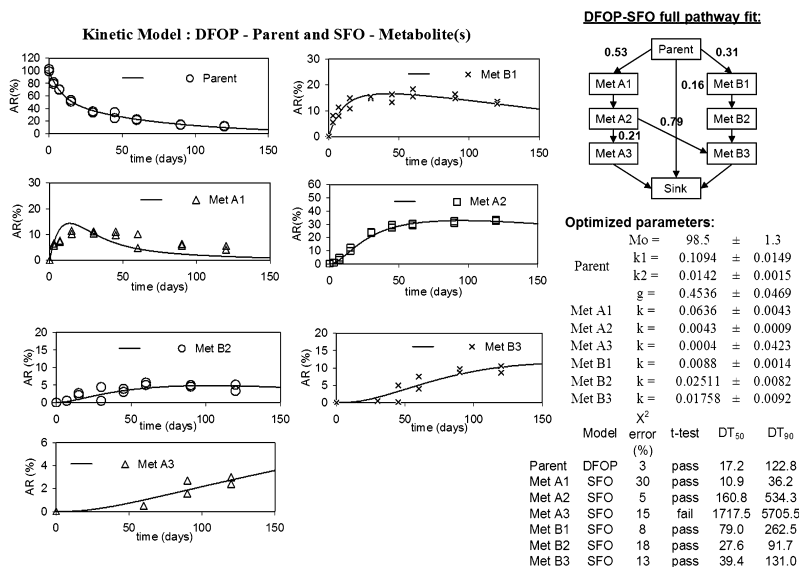


Figure 4. DFOP-SFO pathway kinetic fit with all metabolites for Dataset # 1.

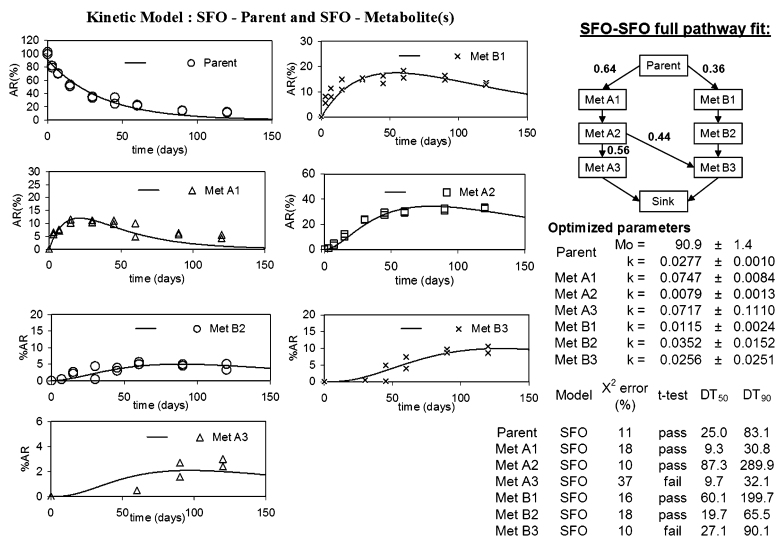


Figure 5. SFO-SFO full pathway kinetic fit with all metabolites for Dataset # 1.

Just as expected, as illustrated in Figure 4, Met A1, as the precursor to Met A2 and Met A3, was not simulated with a χ^2 error of 30%, when all metabolites were included in the DFOP-SFO full pathway fit. Although the formation fraction of Met A1 increased from 0.27 (in the DFOP-SFO fit with Stage 1 metabolites in Figure 3) to 0.53, the mass flow through Met A1 is not enough to account for Met A1 and its degradation products at the same time. This result clearly indicates that DFOP overpredicts initial parent compound degradation rate (by capturing the pesticide residue at Day 0) and the excessive mass of parent compound forced to the sink is not correctable even when all the degradation products of the Stage 1 metabolite such as Met A1 are included.

In the SFO-SFO full pathway kinetic fit with all metabolites included, parent compound and all metabolites (including Met A1) are well simulated, with an acceptable χ^2 error of 18% for Met A1 (Figure 5). Note that the formation fraction for the sink from the parent compound in the full pathway SFO-SFO fit was always optimized to zero; thus, the sink term for the parent compound was removed in the final step of optimization (Figure 5). The poor fit to the metabolite Met A3 is expected due to its low concentration of <5% AR.

The above discussion indicates that the use of SFO for parent compound in the pathway kinetic fit not only provides acceptable description of parent compound degradation but also formation of its metabolites. The selection of DFOP for parent compound, however, fails to predict the formation of metabolites. Thus, SFO should be considered the more reasonable model for description of parent compound degradation than DFOP. The acceptable degradation half-life to use in environmental fate simulations should be the SFO $DegT_{50}$ of 25.7 days, as the existence of a slow degradation phase is not supported in the full pathway fit with all metabolites included.

The initial sudden drop in the quantity of a pesticide from Day 0 to the next sampling point seems to be the main reason for the slightly biphasic behavior of parent compound degradation in this dataset, but it is not accompanied by the simultaneous formation of the same quantities of metabolites. The biphasic behavior, as shown by the parent degradation data alone, is likely due to an experimental artifact, such as the initial quick transformation of parent compound into non-extractable residue in soil. Thus, the DFOP slow phase *DegT*₅₀ of 53 days should not be used in exposure modeling.

Microbial Activities

Reduced microbial activities could also be the reason for biphasic degradation observed in the laboratory studies. Data set # 2 was collected with the same pesticide as for Data set # 1 but in a different soil. The study period of 365 days was also much longer than the period of 120 days for Dataset # 1. During this study, the microbial biomass dropped from 43 at Day 0 to 29 mg carbon per 100 g soil at Day 126, but remained at 28 mg carbon per 100 g soils at Day 365. However, >90% of parent compound degraded by Day 63. Thus, the impact of reduced microbial activity on degradation of parent compound and metabolites is expected.

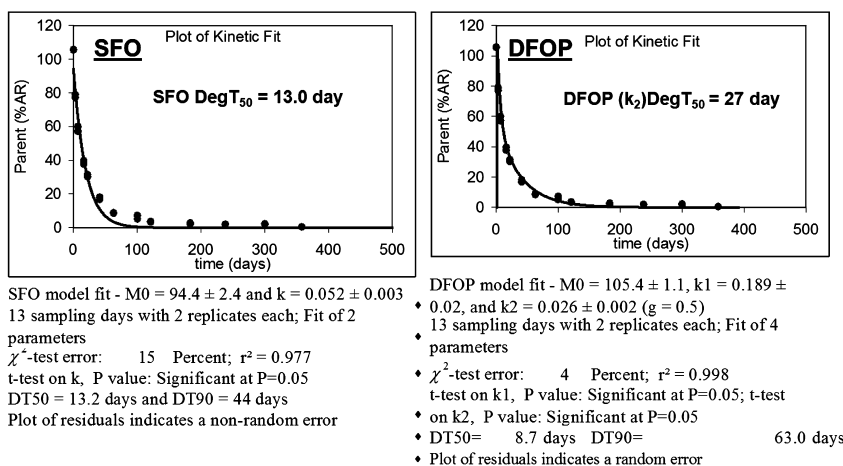


Figure 6. SFO and DFOP kinetic fit for Dataset # 2.

In the SFO fit with Dataset # 2, parent compound degradation is well simulated from Day 3 to Day 63 (Figure 6). Visually, the value at Day 0 is slightly missed and data points in the six sampling points after Day 63 were underpredicted. However, >90% of parent compound has degraded at Day 63. Thus, the SFO *DT*₅₀ of 13.2 days can be accepted for modeling, following the FOCUS guidance (1).

In the DFOP fit, the data points at Day 0 and those after Day 63 are well simulated, with a χ^2 -test error of only 4% (Figure 6). The DFOP slow phase (*k*₂) *DegT*₅₀ of 27 days is nearly twice the SFO *DegT*₅₀, and it would be selected for modeling if degradation is considered biphasic.

To determine if biphasic behavior is due to reduced microbial activities, we first conducted the full pathway fits with SFO-SFO (Figure 7) and DFOP-SFO fits (not provided). In the pathway fit with SFO-SFO, all the metabolites were reasonably well simulated, except for the Stage 1 metabolite with a short DT_{50} (e.g., Met A1). However, the deviation for the metabolites with a local maximum - Met A2 and Met A3 is also significant. The metabolites with monotonically increasing mass over time are reasonably well simulated. Note that the pathway for Met A1 to Met B2 is theoretically possible and included for improved kinetic fit.

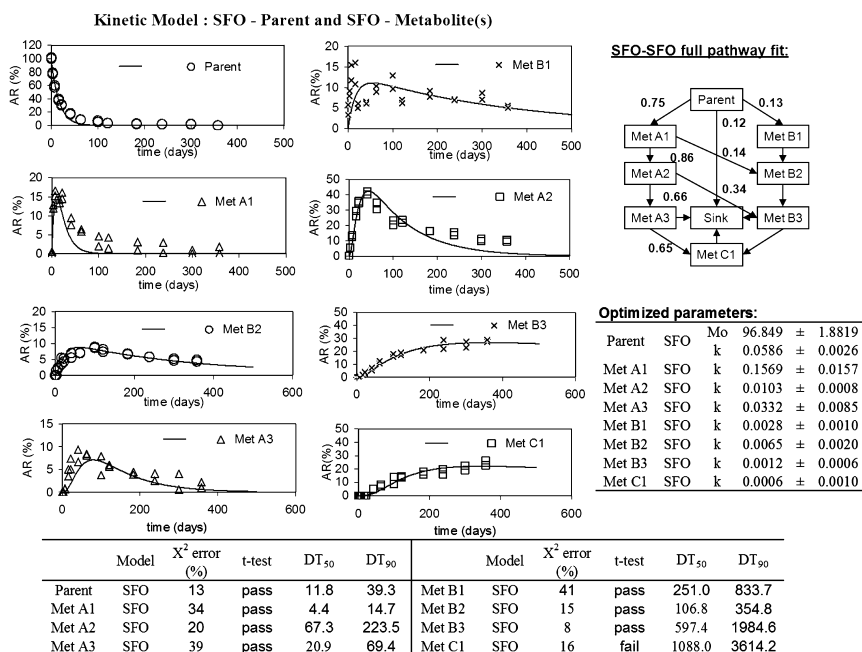


Figure 7. SFO-SFO kinetic fit with all metabolites included for Dataset # 2.

However, in the DFOP-SFO fit, the kinetic fits for parent compound and all metabolites were not improved. This is expected as reduced microbial activities affect not only degradation of parent compound but also metabolites. Thus, we conducted additional kinetic fits with FOMC-FOMC-SFO. FOMC was used for parent compound and metabolites with formation peaks observed (Met A1, Met A2, and Met A3). Note that DFOP for metabolites is difficult in the pathway fit. Thus, FOMC was selected for both parent compound and metabolites (1). For the metabolites Met B1, Met B2, Met B3, and Met C1, SFO was still used, as they are more persistent and impact of reduced microbial activities should be much less significant.

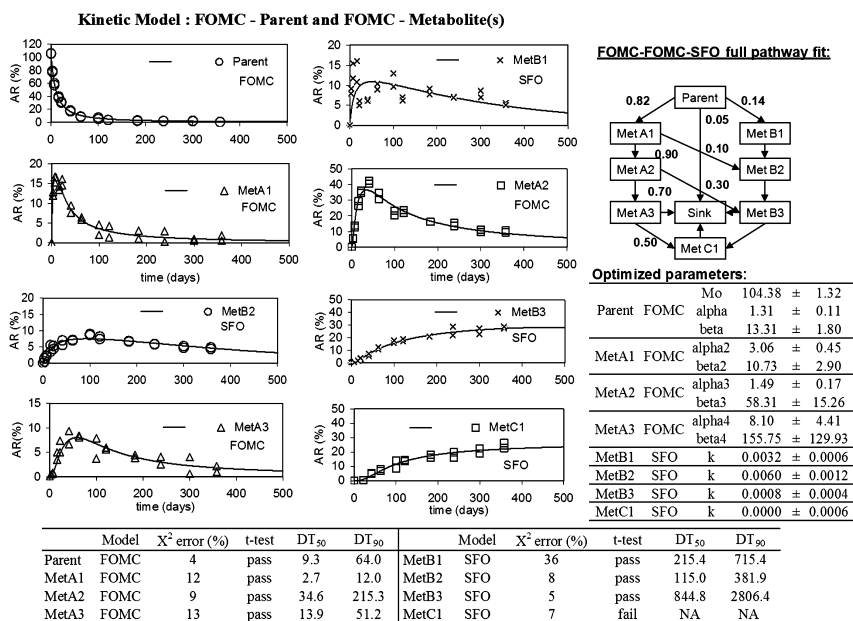


Figure 8. FOMC-FOMC-SFO kinetic fit with all metabolites included for Dataset # 2.

For the FOMC-FOMC-SFO pathway fit for Dataset #2, parent compound and all metabolites were well simulated, with χ^2 -test errors of 4% for parent compound, 5-13% for the metabolites except for Met B1, and 36% for Met B1, as shown in Figure 8. The higher χ^2 -test error for Met B1 is expected due to the high variability in replicate samples.

The results in Figure 8 clearly indicate that biphasic behavior of parent compound degradation in Dataset # 2 is due to reduced microbial activities. SFO *DegT50* should be longer under the influence of reduced microbial activities than under the normal microbial activities. Thus, SFO *DegT50* should be adequate for description of pesticide degradation in exposure modeling, if SFO fit is acceptable by the FOCUS criteria. For Dataset # 2, SFO *DegT50* of 13 days should be selected for modeling, as >90% of parent compound has degraded before the deviation from SFO fit becomes noticeable. On the other hand, the DFOP slow phase *DegT50* of 27 days, which mainly reflects the influence of reduced microbial activity rather than the existence of slow phase degradation of a pesticide, should be eliminated for consideration in exposure modeling.

Aged Sorption

Mechanistically, aged sorption is the main cause for biphasic degradation of pesticides in soil. If it is confirmed, the DFOP slow phase DegT50 is justified for the slower degradation of more tightly bound pesticides in soil. However, the impact of aged sorption on ground water leaching risk can also be simulated as a higher-tiered option in the regulatory models (4). Thus, whether SFO *DegT50* is adequate for conservative exposure modeling can be examined.

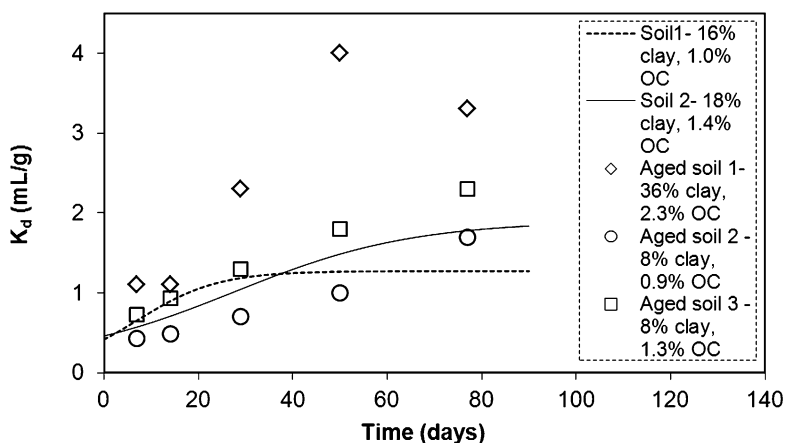
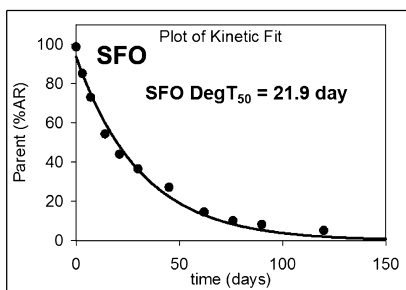


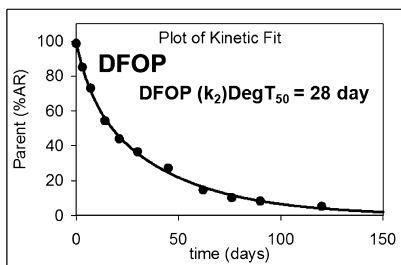
Figure 9. Apparent K_d as a function of time for the three soils as measured in the aged sorption study (data points), in comparison with those calculated (dash and solid lines) from the 2-site aged sorption model from degradation studies with the two soils in Dataset # 3.

In this study, we selected a pesticide which shows significant aged sorption behavior. The apparent K_d for the pesticide in the three soils with 8-36% clay and 0.9-2.3% OC increases by 2.8-5.3 times in 77 days, as shown in Figure 9.

We reviewed the SFO-SFO and DFOP-SFO kinetic full pathway fits for the degradation in five soils. We found that in all five soils, DFOP-SFO always provide improved kinetic fits for both parent compound and metabolites, as compared to the SFO-SFO fit. In the two soils with different ^{14}C -labeled compound, DFOP for parent compound is even required for all the metabolites to be simulated. Thus, the data for these two soils in Dataset # 3 were further evaluated to assess the impact of aged sorption on degradation behaviors.



- SFO model fit - $M_0 = 93.6 \pm 2.5$ and $k = 0.032 \pm 0.002$
- 11 sampling days with 1 replicates each; Fit of 2 parameters
- χ^2 -test error: 7 Percent; $r^2 = 0.988$
- t-test on k, P value: Significant at $P=0.05$
- $DT_{50} = 21.9$ days and $DT_{90} = 72.7$ days
- Plot of residuals indicates a non-random error



- DFOP model fit - $M_0 = 99 \pm 1.6$, $k_1 = 0.131 \pm 0.043$, and $k_2 = 0.024 \pm 0.002$ ($g = 0.3$)
- 11 sampling days with 1 replicates each; Fit of 4
- χ^2 -test error: 3 Percent; $r^2 = 0.998$
- t-test on k_1 , P value: Significant at $P=0.05$; t-test on k_2 , P value: Significant at $P=0.05$
- $DT_{50} = 17.9$ days $DT_{90} = 83$ days
- Plot of residuals indicates a random error

Figure 10. SFO and DFOP kinetic fit for Soil 1 in Dataset # 3.

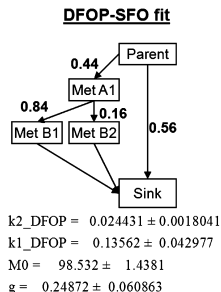
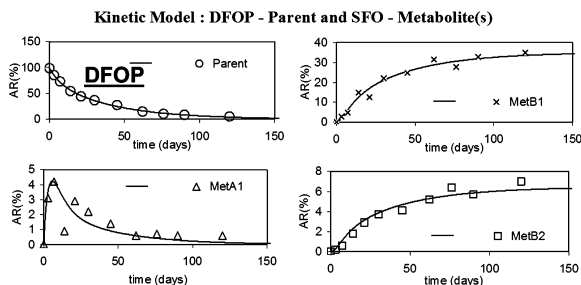
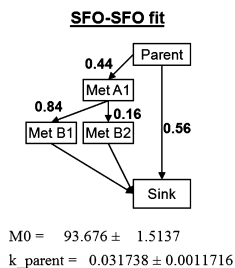
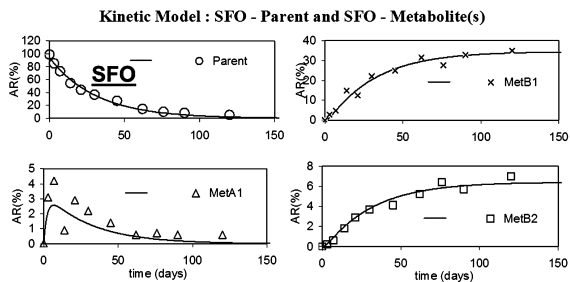


Figure 11. SFO-SFO and DFOP-SFO pathway fit for Soil 1 in Dataset # 3.

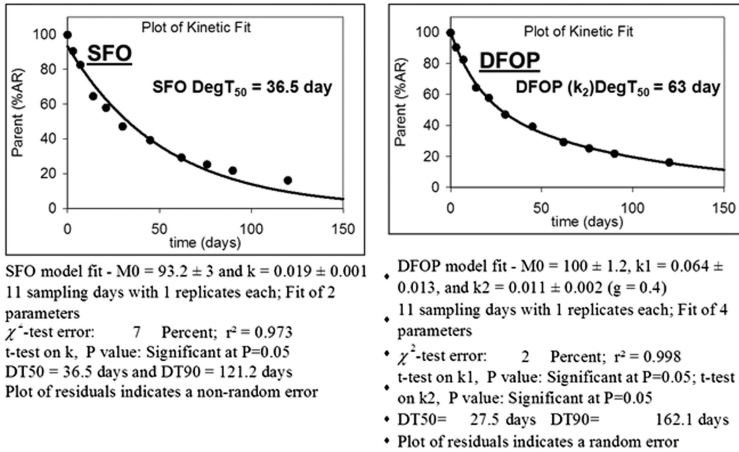


Figure 12. SFO and DFOP kinetic fit for Soil 2 in Dataset # 3.

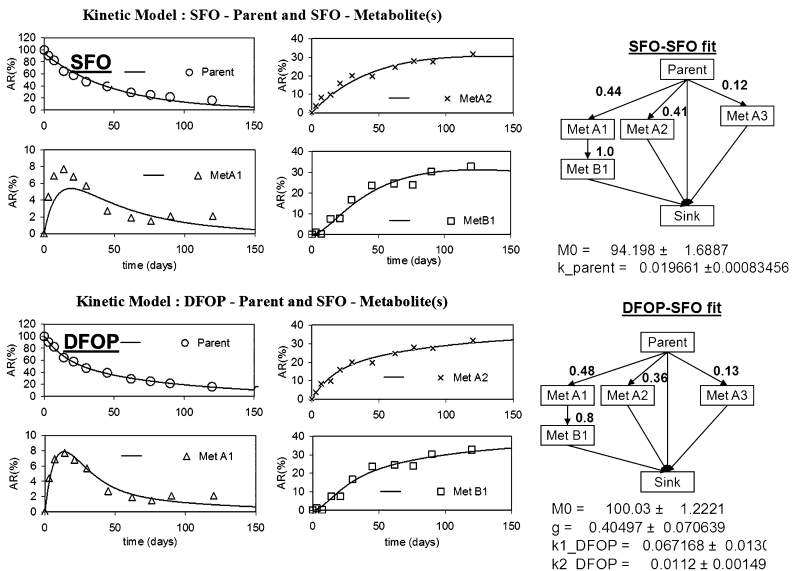


Figure 13. SFO-SFO and DFOP-SFO pathway fit for Soil 2 in Dataset # 3.

As shown in Figure 10, in the SFO fit for Soil 1 in Dataset # 3, parent compound degradation is well simulated, with a χ^2 -test error of 7%. However, the value at Day 0 is slightly missed and the last five data points were slightly but consistently underpredicted. The SFO fit is acceptable by FOCUS criteria; and SFO *DegT50* of 21.9 days can be accepted for modeling. However, in the pathway fit with SFO-SFO model, the Stage 1 metabolite Met A1 is not simulated (Figure 11).

DFOP provides an improved kinetic fit to the parent compound data for Soil 1, notably with the data point at Day 0 and the last five data points simulated, with a χ^2 -test error of 3% (Figure 10). In addition, all metabolites are simulated in the pathway fit with DFOP-SFO model (Figure 11). This indicates that degradation is slightly biphasic in Soil 1, although the DFOP slow phase *DegT50* of 28 days is only slightly longer than the SFO *DegT50* of 21.9 days.

Similar kinetic observations were made with Soil 2 in Dataset # 3 but with a larger deviation from the SFO fit with parent compound data (Figure 12). The metabolite Met A1 is not described either in the SFO-SFO pathway fit (Figure 13). However, the DFOP for parent compound not only provides a better fit to the parent compound data (Figure 12) but also allows both parent compound and metabolites to be simulated in the DFOP-SFO pathway fit (Figure 13). This confirms that degradation is also slightly biphasic in Soil 2.

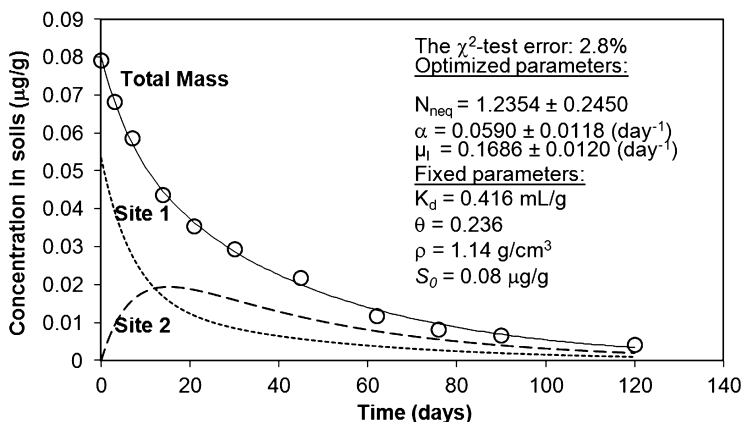


Figure 14. The degradation of the pesticide in Soil 1 in Dataset # 3 as predicted by the two-site aged sorption model.

To further demonstrate if biphasic behavior indeed arises from aged sorption, we also fit the parent compound dataset to the two-site aged sorption model described earlier. The partition coefficient K_d (mL/g) was calculated from the clay content, as the sorption of this compound is clay-dependent. Moisture content θ (cm³/cm³) was calculated from 50% maximum water holding capacity used in the study and a bulk density ρ (g/cm³) was also measured experimentally. Thus, the parameters of K_d , θ , and ρ were fixed during optimization. The two-site aged sorption model is then fit to the parent compound data for Soil 1 and Soil 2,

respectively, with the parameters of N_{neq} , α , and μ_l set for optimization. The total mass S_0 at Day 0 of 0.08 $\mu\text{g/g}$ was used to set up the initial condition of modeling fitting.

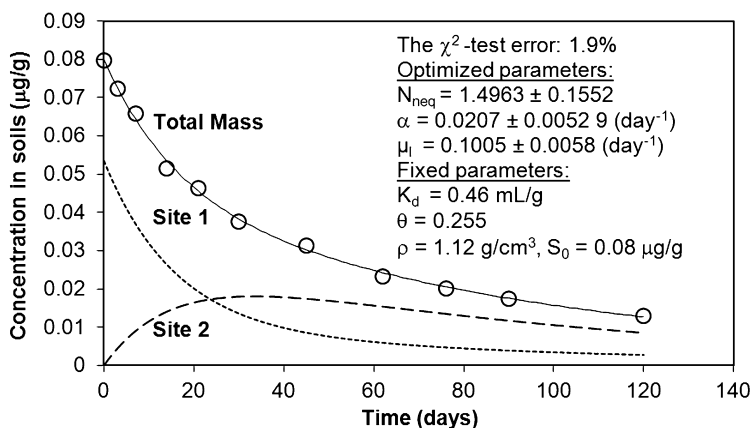


Figure 15. The degradation of the pesticide in Soil 2 in Dataset # 3 as predicted by the two-site aged sorption model.

As shown in Figure 14 and Figure 15, degradation of parent compound in Soil 1 and Soil 2 is well simulated with the two-site aged sorption model, with a χ^2 -test error of 2.8% and 1.9% respectively. The N_{neq} of 1.5 for Soil 2 is higher than the value of 1.2 for Soil 1, indicating stronger sorption at Site 2 in Soil 2.

In addition, the apparent K_d values for Soil 1 and Soil 2 as predicted from the aged sorption model are between those for the soils with similar clay (8%) and organic carbon contents (1-1.4%) used in the aged sorption (Figure 9). This confirms that slight biphasic behavior results from aged sorption.

Based on this verification, it seems that the slow phase DFOP $DegT50$ of 28 days for Soil 1 and 63 days for Soil 2 should be selected for exposure modeling, as they are more or less representative of degradation rate of more tightly bound pesticide residues. However, aged sorption not only slows down degradation, but it also significantly increases K_d values. Thus, the impact of aged sorption on leaching risk as a higher-tier option should be assessed before the SFO $DegT50$ is rejected.

The two-site aged sorption model used in this study assumes that degradation occurs only in the soil pore water, but the regulatory ground water model allows degradation to occur for the pesticide not only in soil pore water but also bound to Site 1. Thus, using the equations in the FOCUS guidance (1), we calculated the values for the parameters of F_{neq} (i.e., $F_{neq} = \Phi ((1 + \rho K_d)/(\rho K_d))$; $\Phi = (g(1-g) \times (k_1 - k_2)^2 / (k_1 k_2))$, k_t (i.e., $k_t = g k_1 + (1-g) k_2$) and k_{des} (i.e., $k_{des} = (k_1 k_2) / (g k_1 + (1-g) k_2)$) from the DFOP parameters of k_1 , k_2 , and g , the partition coefficient K_d , moisture content θ , and bulk density ρ . Note that F_{neq} , k_t , and k_{des} are equivalent to but they are not the same as N_{neq} , μ_l and α in the two-site aged sorption model in this study.

For Soil 2, the parameters of F_{neg} , k_t , and k_{des} for the aged sorption model used in the regulatory ground water model are calculated to be 1.499, 0.0339 (day^{-1}) ($DT50 = 20.5$ days), and 0.0222 (day^{-1}). We then calculated PEC_{gw} with this set of parameters ($1/n = 0.94$ in the Freundlich equation) with aged sorption considered in the simulation, SFO $DegT50$ of 36.5, and DFOP slow phase $DegT50$ of 63 days with no aged sorption considered, respectively. The results indicate that PEC_{gw} for the aged sorption is 4 times lower than PEC_{gw} for the SFO $DegT50$ and 10 times lower than PEC_{gw} for the DFOP slow phase $DegT50$. This result indicates that the SFO $DegT50$ is protective of ground water leaching risk and should be selected as realistic but conservative endpoint for exposure modeling, when the SFO fit is acceptable by the FOCUS criteria.

Conclusions and Recommendations

It has been shown in this study that biphasic degradation of pesticides in soil could result from an experimental artifact, reduced microbial activities, and aged sorption. The causes for biphasic behavior can be clarified by fitting parent compound and metabolite data into a SFO-SFO, DFOP-SFO, or FOMC-FOMC-SFO kinetic pathway model. As a result, conservative but realistic degradation rates of pesticides can be selected for exposure modeling.

The analyses in this study also indicate that a certain degree of deviation from SFO should be allowed in deriving the degradation rate for exposure modeling, particularly when the SFO fit is acceptable by the FOCUS criteria (1). The use of biphasic model such as DFOP as an option to calculate the slow phase degradation rate, when SFO fit is acceptable by FOCUS criteria, is likely to lead to unnecessarily over-conservative exposure assessment.

References

1. FOCUS. *Guidance Document on Estimating Persistence and Degradation Kinetics from Environmental Fate Studies on Pesticides in EU Registration, Report of the FOCUS Work Group on Degradation Kinetics*; EC Document Reference SANCO/10058/2005 Version 2.0; June, 2006; pp 110, 112.
2. NAFTA. *NAFTA Guidance for Evaluating and Calculating Degradation Kinetics in Environmental Media*; NAFTA Technical Working Group on Pesticides; December 17, 2012; p 2, http://www.epa.gov/oppefed1/ecorisk_ders/degradation_kinetics/NAFTA_Degradation_Kinetics.htm.
3. Tang, J.; Russell, L. J.; Huang, X. M.; Chen, W. L.; Allen, R.; Hayes, S.; Sur, R. In *Non-First Order Degradation and Time-Dependent Sorption of Organic Chemicals in Soil*; Chen, W. L., Sabljic, A., Cryer, S. A., Kookana, R., Eds.; ACS Symposium Book 1174; American Chemical Society: Washington DC, 2014; pp 119–132.
4. *ModelMaker™*. Modelkinetix: Reading, Berkshire, U.K., 2002.
5. Beulke, S.; van Beinum, W. *Guidance on how aged sorption studies for pesticides should be conducted, analysed and used in regulatory assessments*;

The Food and Environment Research Agency; Sand Hutton, York, YO41 1LZ, U.K., revised version, May 2012.

6. Shaner, D.; Brunk, G.; Nisse, S.; Westra, P.; Chen, W. L. *J. Environ. Qual.* **2012**, *41*, 170–178.
7. Guo, L.; Jury, W. A.; Wagenet, R. J.; Flury, M. *J. Contam. Hydrol.* **2000**, *43*, 45–62.

Chapter 9

Nonlinear Soil Dissipation Kinetics: The Use of a Set of Simple First-Order Processes To Describe a Biphasic Degradation Pattern

John R. Purdy*,¹ and Mark Cheplick²

¹Abacus Consulting Services Ltd., Campbellville, Ontario, Canada L0P1B0

²Waterborne Environmental, Leesburg, Virginia U.S.A. 20175

*E-mail johnrpurdy@gmail.com.

The analytical results for a pesticide compound in a set of laboratory soil dissipation studies with a variety of different soil types from North America and Europe show a range of behavior from linear simple first-order to a pronounced biphasic pattern. Using a set of three simple first-order equations, representing reversible movement between two compartments in the soil, and irreversible degradation from one of the two compartments, it was possible to fit the data from all sites. The output was a set of three simultaneously optimized rate constants for each soil type, along with the goodness of fit statistics. The physical interpretation of this model was found to be unrelated to soil physical properties but associated with the movement of residues between a compartment in which the degradation processes occur, and a compartment in which they do not. The former compartment resembles what has been called the bioaccessible compartment in soil. This model, identified as the SFO3 model, is useful for calculation of rate constants for parent compound and intermediate metabolites, comparison of lab and field results, correction for changes in soil temperature or moisture content, identification of outlier data, and development of parameters for modelling input. The utility of the resulting rate constants for predictive modelling for environmental risk assessment depends on the availability of measurable soil properties that can be used to predict them, such as bioaccessibility.

Introduction

The rate of decline of the concentration of a pesticide in the soil environment after application is an essential factor in environmental risk assessment. It is a key input value for models that are used to estimate the persistence and movement of pesticides in the environment. This process can be approximated by a simple exponential decay equation that is equivalent to the first-order (SFO) equation for chemical reactions (1, 2). While this remains the main equation used in modelling, it has long been recognized that it does not give a good fit to all experimental soil dissipation data sets; much effort has been expended to find equations that are more generally applicable to both lab and field study data (2, 3). In this work, the modelling of a series of 11 data sets for laboratory aerobic soil degradation of chlorpyrifos in soil were used to develop an alternate approach to nonlinear soil dissipation kinetics and to generate soil dissipation rate constants for use in PRZM-EXAMS modeling to support environmental risk assessments of chlorpyrifos (4, 5). The possible use of measured bio-accessibility to parameterize models such as PRZM/EXAMS for modelling environmental behavior of compounds is discussed. The potential for analysis of data from field soil dissipation studies for use in risk assessment was also considered using an example data set.

The degradation of chlorpyrifos in soil leads to formation of 3,5,6-trichloropyridinol. The results from a number of studies show that this step can be either abiotic or biotic, and the rate is 1.7 to 2-fold faster in biologically active soils (5, 6). Both modes of hydrolysis can occur in aerobic soil. The rate of abiotic hydrolysis is pH dependent and is faster under alkaline conditions. Under aerobic conditions, the major terminal degradate of chlorpyrifos is CO₂ (6).

The 11 laboratory data sets used in this modelling work were from studies of the degradation of ¹⁴C-chlorpyrifos in soil under aerobic conditions. The properties of the soils are listed in Table 1. The results from all soils showed good mass balance. There were some notable effects of soil properties: The originally reported DT50's in Table 1 show that the degradation of chlorpyrifos is slower at low temperatures or in dry soil near the wilting point (10% Field Moisture Capacity (FMC)). Sterile conditions reduced the production of CO₂, but did not reduce the degradation rate. Overall however, the DT50 values from all soils were not correlated with soil properties well enough to allow the DT50 to be predicted for use in modelling. It is possible that the soils that show a faster hydrolysis rate are those with a microbiome capable of biologically accelerated hydrolysis and that the biologically mediated degradation is less influenced by pH (5, 6). In this section, the application of a reversible binding kinetic model is investigated to evaluate its usefulness and physical significance using the available dissipation data sets as examples.

Table 1. Reported DT50 and Soil Properties For Laboratory Dissipation

<i>Soil ID</i>	<i>Texture</i>	<i>Source</i>	<i>pH</i>	<i>%OC</i>	<i>Moisture Content (%FMC)</i>	<i>75% F.M.C.</i>	<i>SFO DT50 (days)</i>	<i>Comment</i>
Barnes	Loam	ND	7.1	3.6	75	20.6	22	
Catlin	Silty Clay Loam	IL	6.1	2.01	75	21.02	34	
Charentilly	Silty Clay Loam	FRANCE	6.1	1	40	33.2	95	
Commerce	Loam	MS	7.4	0.68	75	13.5	11	
Cuckney	Sand	UK	6	1.2	40	26.2	111	
German Std 2:3	Sandy Loam	Germany	5.4	1.01	75	10.8	141	
Marcham	Sandy Clay Loam	UK	7.7	1.7	40	34.2	43	
Marcham	Sandy Clay Loam	UK	7.7	1.7	40	34.2	80	Cold 10°C
Marcham	Sandy Clay Loam	UK	7.7	1.7	10	34.2	126	Dry
Marcham sterile	Sandy Clay Loam	UK	7.7	1.7	40	34.2	21	Sterile
Miami	Silt Loam	IN	6.6	1.12	75	17.92	24	
Norfolk	Loamy Sand	VA	6.6	0.29	75	4.66	102	Very low moisture
Stockton Clay	Clay	CA	5.9	1.15	75	25.75	107	

Continued on next page.

Table 1. (Continued). Reported DT50 and Soil Properties For Laboratory Dissipation

<i>Soil ID</i>	<i>Texture</i>	<i>Source</i>	<i>pH</i>	<i>%OC</i>	<i>MoistureContent (%FMC)</i>	<i>75% F.M.C.</i>	<i>SFO DT50 (days)</i>	<i>Comment</i>
Thessaloniki	Loam	GREECE	7.9	0.8	40	32.6	46	
Tranent	Silt loam	UK	n.r	n.r	25	22	12.6	

Kinetic Modelling

The degradation of chlorpyrifos does not fit a simple first-order kinetic model (6) (See example in Figure 1). There was no evidence of a rapid initial volatilization under laboratory aerobic soil metabolism test conditions that would contribute to the initial faster decline in concentration of chlorpyrifos. Two-compartment kinetics gave an improved fit, but this involves use of an empirical model with no physical reality assigned to the two compartments. A mechanistic kinetic model was set up based on the assumption that the nonlinear behavior is caused by a transition from dissolved parent compound to adsorbed residues over time (5). The kinetic model consists of 3 compartments as shown in the schematic diagram in Figure 2:

- 1. M1 -a compartment in which the chlorpyrifos present is immediately available for biodegradation
- 2. M2 -a compartment in which no degradation occurs (nonbioavailable)
- 3. M3 -a compartment for metabolites and terminal degradation products

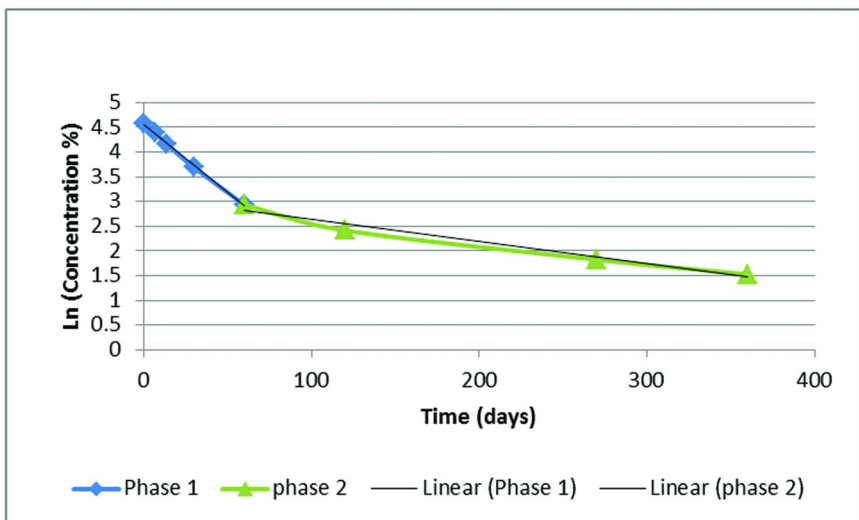
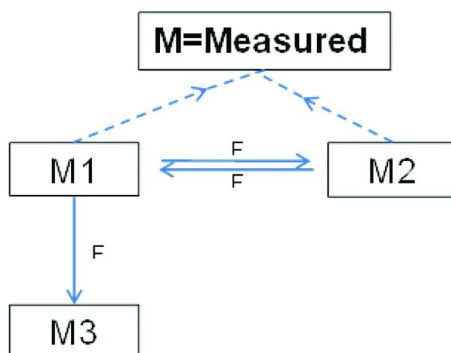


Figure 1. Biphasic Degradation of Chlorpyrifos in Aerobic Soil.

Flows of material between these compartments are shown by arrows in the schematic diagram. These flows are represented by simple first-order differential equations with rate constants k . The rate constant for movement into the non-active compartment is defined as k_1 . Competing with this process is the degradation of chlorpyrifos with rate constant k_m . The third process, with rate constant k_2 , is the reverse of the first; the movement from the inactive or non-labile compartment to the labile compartment from which degradation can occur.



Parameter definitions and equations

Main Equations

compartment: M2 Status: Unconditional, Universal, Initial Value = 0.0

$$dM2/dt = +F1-F2$$

compartment: M1 Status: Unconditional, Universal, Initial Value = 98.3

$$dM1/dt = -F1+F2-F3$$

compartment: M3 Status: Unconditional, Universal, Initial Value = 0.0

$$dM3/dt = +F3$$

flow: F1 Flow from M1 to M2, Status: Unconditional,
Universal

$$F1 = k_1 * M1$$

flow: F2 Flow from M2 to M1, Status: Unconditional

$$F2 = k_2 * M2$$

flow: F3 Flow from M1 to Metabolites, Status: Unconditional

$$F3 = k_m * M1$$

variable: M measured chlorpyrifos , Status:

Unconditional

$$M = M1+M2$$

Notes:

1. Assignment of unconditional status to a parameter in ModelMaker software makes it accessible from anywhere in the model.
2. The value of an unconditional component is defined using a single equation which is always used when evaluating the component.
3. Additional components to correct for temperature or soil moisture or multiple applications can be added.

ModelMaker Version 4, Cherwell Scientific

Figure 2. SFO3 Conceptual kinetic model for nonlinear soil dissipation kinetics.

During the development of this reversible binding model, the M1 compartment was thought to be the dissolved phase and M2 was thought to correspond to the adsorbed phase in the soil (5).

The FOCUS review describes a similar system for the SFORB model, in which the two compartments are considered to be dissolved and adsorbed parent compound respectively (2). The SFORB model is described in terms of two

differential equations, with a combined algebraic solution. In this work, the system was described in terms of three SFO equations, with rate constants k_1 , k_2 , and k_m . No assumption of equilibrium is made. In addition, it was assumed that the analytical results for the concentration vs time represent the sum of the material in both compartments M1 and M2, since the analytical extraction method is known to recover all but the bound residues present in the soil sample. These three equations are simultaneously optimized to obtain a dissipation curve that fits the concentration vs time data for each soil. For convenience, it will be referred to as the SFO3 kinetic model.

A schematic diagram and a list of parameters and equations are provided in Figure 2. As an overview of how this model works, initially the chlorpyrifos is readily bioavailable and degradation is limited only by the rate of metabolism (k_m). The linear trend in concentration vs time is described by the balance of the three rate constants k_1 , k_2 and k_m . The transfer between M1 and M2 is reversible, but the degradation is irreversible. In systems where k_m is less than or equal to k_2 , metabolism is the rate limiting step and the system behaves like a SFO process. But if k_2 is slower, the proportion of the parent compound that is in M1 will be depleted and k_2 will become the rate limiting step over time. This results in nonlinear kinetics. Nonlinear behavior can also occur when k_m is slower than k_1 . It is assumed that all degradation, including both abiotic and metabolic degradation and formation of bound residues occurs from M1. The model was set up using ModelMaker Version 4, from Cherwell Scientific Software, UK, which is a matrix based modelling software application of Matlab.

Model Setup

As input data, the measured amount of parent compound was entered as the sum of the amounts in compartments M1 and M2. In the ModelMaker software, this is represented by setting the measured concentration as a variable M, connected to M1 and M2 by “influences” shown in Figure 2 by dashed arrow lines. The influence is the equation $M = M1+M2$. The input data is not log-transformed. For the laboratory results, the first data point concentration value was entered for the initial value of M1 because the concentration measurements are relatively accurate and the mass balance was good. The initial values of M2 and M3 were set to zero. Estimated values were manually entered for the rate constants for the first trial runs based on approximations from the SFO rate of dissipation given in Table 1. These values were adjusted in some of the trial runs to be close enough for the optimization routine to converge on a solution for the input data from each soil. When the model is run, the software first integrates the set of differential equations using the Marquardt method, and then optimizes the rate constants selected to provide the best fit for the data. Five integration methods (Euler, Mid-Point, Runge-Kutta, Bulirsch-Stoer and Gear’s method) are available in the software. The default Runge-Kutta method was used for all sites since the differential equations are straightforward. Examples of the parameter optimization results for the 11 laboratory data sets are shown in Figures 3-5, and the optimization results are listed in Table 2.

Table 2. Optimization Results and DT50 Values

<i>Soil</i>	<i>Optimization Results</i>									<i>Degrees of Freedom^{a)}</i>
	<i>k₁</i> <i>DT50</i>	<i>Estimation</i> <i>Error</i>	<i>k₂</i> <i>DT50</i>	<i>Estimation</i> <i>Error</i>	<i>k_m</i> <i>DT50</i>	<i>Estimation</i> <i>Error</i>	<i>R</i> ²	<i>F</i>	<i>p</i>	
Laboratory Studies										
Barnes	0.00344	0.00097	0.00245	0.00148	0.0310	0.00110	0.9989	2350	0.104	7
	201.5		282		22.4					
Catlin^{b)}	0.00315	0.00118	0.00386	0.00133	0.02457	0.00229	0.9904	259	0.695	7
	220.3		179.6		28.2					
Charentilly	0.529	0.275	0.0573	0.00976	0.0758	0.0290	0.9931	503	0.039	9
	1.3		12.1		9.1					
Commerce	0.00753	0.00103	0.00702	0.00144	0.0613	0.00125	0.9997	7342	0.718	7
	92.1		99.0		11.3					
Cuckney	0.529	c	0.0573	c	0.0758	c				9
	1.3		12.1		9.1					
German 2:3	0.0124	0.01428	0.0211	0.0143	0.007	0.00148	0.9973	918	0.066	7
	55.9		32.9		99.1					
Marcham	0.0908	0.0211	0.0154	0.00446	0.0789	0.00855	0.9894	374	0.013	10
	7.6		45		8.8					
Miami	0.0181	0.0164	0.0312	0.0246	0.0395	0.00544	0.9966	737	0.027	7

<i>Soil</i>	<i>Optimization Results</i>									
	k_1 DT50	<i>Estimation</i> <i>Error</i>	k_2 DT50	<i>Estimation</i> <i>Error</i>	k_m DT50	<i>Estimation</i> <i>Error</i>	R^2	F	p	<i>Degrees of</i> <i>Freedom</i> ^(a)
Norfolk	38.4		22.2		17.5					
	0.0129	0.0046	0.0125	0.00309	0.0122	0.00108	0.9987	1883	0.106	7
Stockton	53.7		55.5		57					
	0.0031	0.00128	0.0021	0.00219	0.0072	0.00042	0.9987	1871	0.706	7
Thessaloniki	227.3		338.1		96.7					
	0.0206	0.0116	0.00467	0.0113	0.02256	0.0029	0.9873	310	0.012	10
	33.6		148.4		30.7					
Field Study										
Tranent	0.12515	0.01788	0.01751	0.01407	0.01315	0.0168	0.9847	226	0.000313	9
(Arrhenius)	5.5		39.6		52.7					
Tranent	0.1333	0.01859	0.01482	0.01009	0.00878	0.0092	0.9845	222	0.000297	9
(Q10)	5.2		46.8		79.0					

^{a)} Notes: Total degrees of freedom: Model accounts for 2 degrees of freedom. ^{b)} Catlin soil data required weighted least squares regression, all others were run with Ordinary Least Squares. ^{c)} The model did not converge. Values for Charentilly were used and they fit very well.

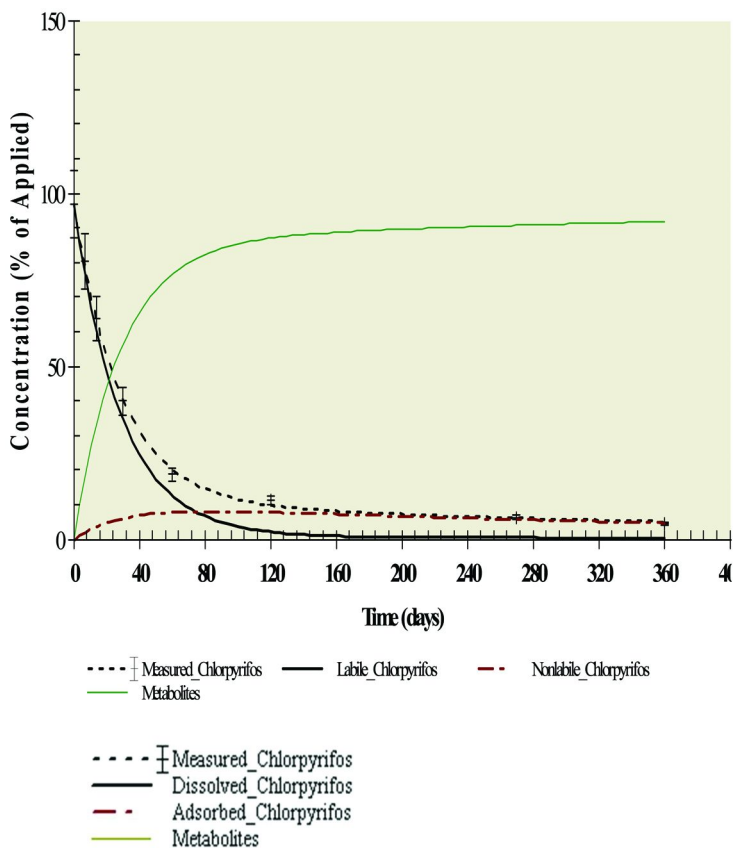


Figure 3. Model Results - Barnes Soil.

Application to Field Dissipation Studies

Given that the model gave a good fit to the laboratory data which represents a closed system at constant temperature, it was then possible to apply it to the field dissipation study results by assuming that volatility, runoff and leaching losses were minimal, and adding a daily temperature correction factor based on either a direct Arrhenius equation (3) or the Q10 method (2).

The schematic diagram and model setups are shown in Figure 6. The results obtained using the temperature records from a field soil dissipation soil with chlorpyrifos in Tranent, Scotland is shown in Figure 7 and 8 for the Arrhenius and Q10 methods respectively. The daily mean temperatures used are shown in Figure 9. A correction factor to normalize the moisture content is also available (2), but was not used for this work.

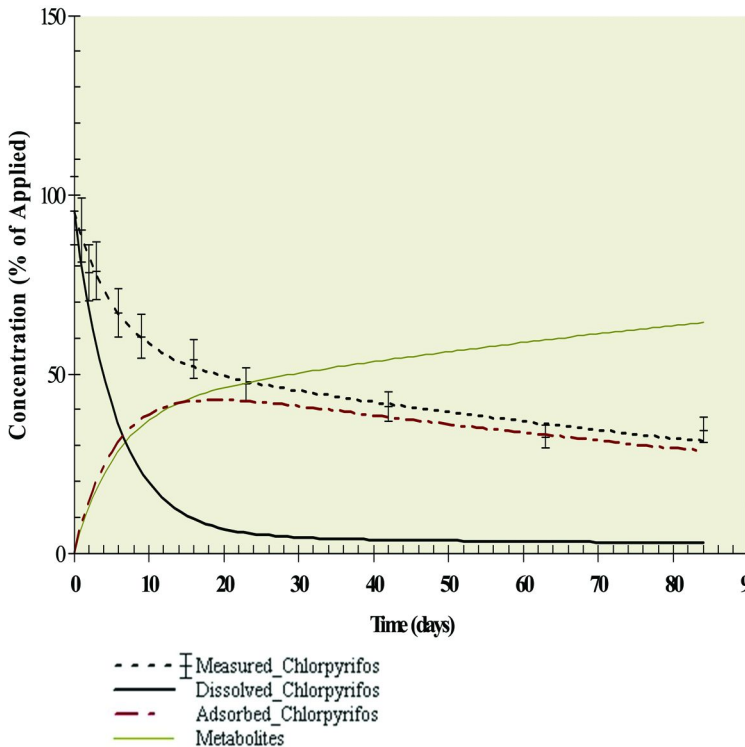


Figure 4. Model Results - Marcham Soil.

The Arrhenius equation for the effects of temperature T on the rate constant k is shown in eq 1.

$$k_T = k_0 e^{-E/RT} \quad (1)$$

where: k_T = rate constant at temperature T in degrees Kelvin.

- k_0 = frequency factor
- E = activation energy
- R = universal gas constant = 8.315 J mol^{-1}
- $e = 2.718$

If the rate at one temperature is known, the rate at another temperature can be estimated if the activation energy is also known. As an initial approximation, the activation energy, E , was given an approximate value of 40 kJ mol^{-1} (3), since this was sufficient to demonstrate the effectiveness of the model. This activation energy can be measured for a compound of interest by measuring degradation rates at a series of temperatures. Although the processes involved in

the reversible movement between compartments M1 and M2 are likely different from the degradation, a simplifying assumption was made that the same value of E would apply to all three rate constants. It was originally felt that adsorption onto an enzyme active site might be similar to adsorption onto a surface, and this assumption was retained when the compartments were seen as labile and non-labile compartments. The correction factor A for time t in days after application was defined as in eq 2 below:

$$A_t = k_{T1}/k_{T2} = e^{(E/RT1-E/RT2)} \quad (2)$$

For T1 = 20°C, this gives eq 3:

$$A_t = e^{(16.4-4811/T2)} \quad (3)$$

Since this relationship fails in living systems when the temperature drops below 4°C or in inorganic systems when the temperature drops below freezing, the model was set up with timed events to set A = 0 when the mean air temperature dropped below 0°C and to return to equation 3 when it warmed up again.

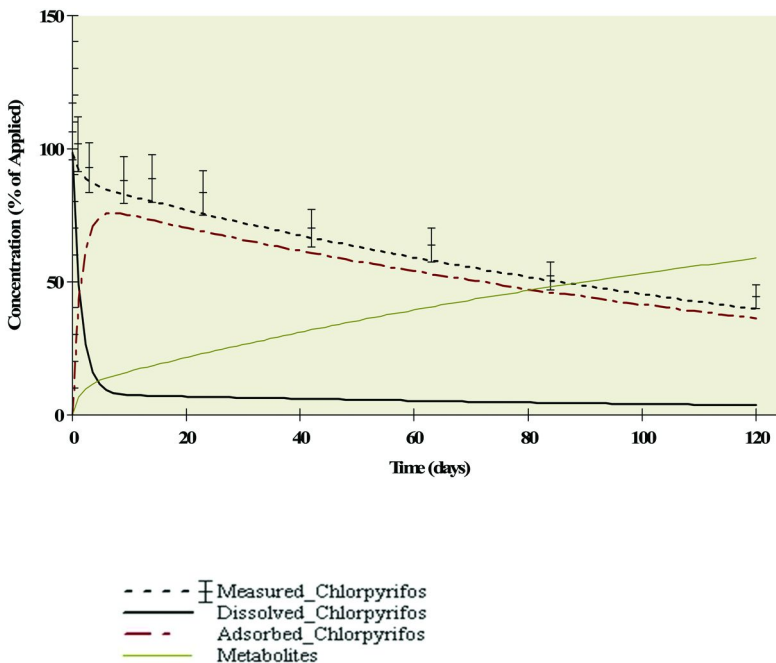
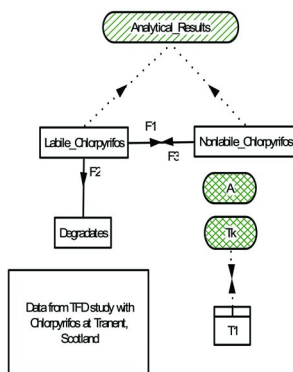


Figure 5. Model Results - Charentilly Soil.



Model Details:

Main

Variable: A

Status: Conditional, Universal

A =

$\exp(16.4-4811/Tk)$ for $(t \leq 258)$
 0 for $(t > 258)$ and $(t \leq 336)$
 $\exp(16.4-4811/Tk)$ for $(t > 336)$
 $\exp(16.4-4811/Tk)$ by default

Variable: Analytical_Results Status: Unconditional, Global

Analytical_Results = Labile_Chlorpyrifos + Nonlabile_Chlorpyrifos

compartment: Degradates Status: Unconditional

$d\text{Degradates}/dt = +F2$

Initial Value = 0.0

flow: F1 Status: Unconditional

Flow from Labile_Chlorpyrifos to Nonlabile_Chlorpyrifos

$F1 = k_1 * \text{Labile_Chlorpyrifos} * A$

flow: F2 Status: Unconditional

Flow from Labile_Chlorpyrifos to Degradates

$F2 = k_m * \text{Labile_Chlorpyrifos} * A$

flow: F3 Status: Unconditional

Flow from Nonlabile_Chlorpyrifos to Labile_Chlorpyrifos

$F3 = k_2 * \text{Nonlabile_Chlorpyrifos} * A$

compartment: Labile_Chlorpyrifos Status: Unconditional

$d\text{Labile_Chlorpyrifos}/dt = -F1 - F2 + F3$

Initial Value = 111.2

compartment: Nonlabile_Chlorpyrifos Status: Unconditional

$d\text{Nonlabile_Chlorpyrifos}/dt = +F1 - F3$

Initial Value = 0.0

lookup table: T1

t Control

Temperature Data Status: Universal

variable: Tk Status: Unconditional Universal

Temperature in degrees Kelvin

$Tk = 258 + \text{LOOKUP}(\text{Temperature}, t)$ Temperature relative to Day 0

Notes:

1. The factor A for the Q10 method was replaced by Q, where

$Q = \exp(0.09478 * (T2 - 20))$ for $(t \leq 258)$
 0 for $(t > 258)$ and $(t \leq 336)$
 $\exp(0.09478 * (T2 - 20))$ for $(t > 336)$
 $\exp(0.09478 * (T2 - 20))$ by default

and variable Tk was replaced by $T2 = \text{Temperature in degrees Celsius}$.

2. The initial concentration value was optimized to best fit for the field data. Both calculation methods gave an initial value of 111.2%. The concentrations in the lab data were done by ^{14}C and were more accurate, so the time zero value was used as the initial value in the model.

Figure 6. SFO3 Model With Temperature Normalisation Factor.

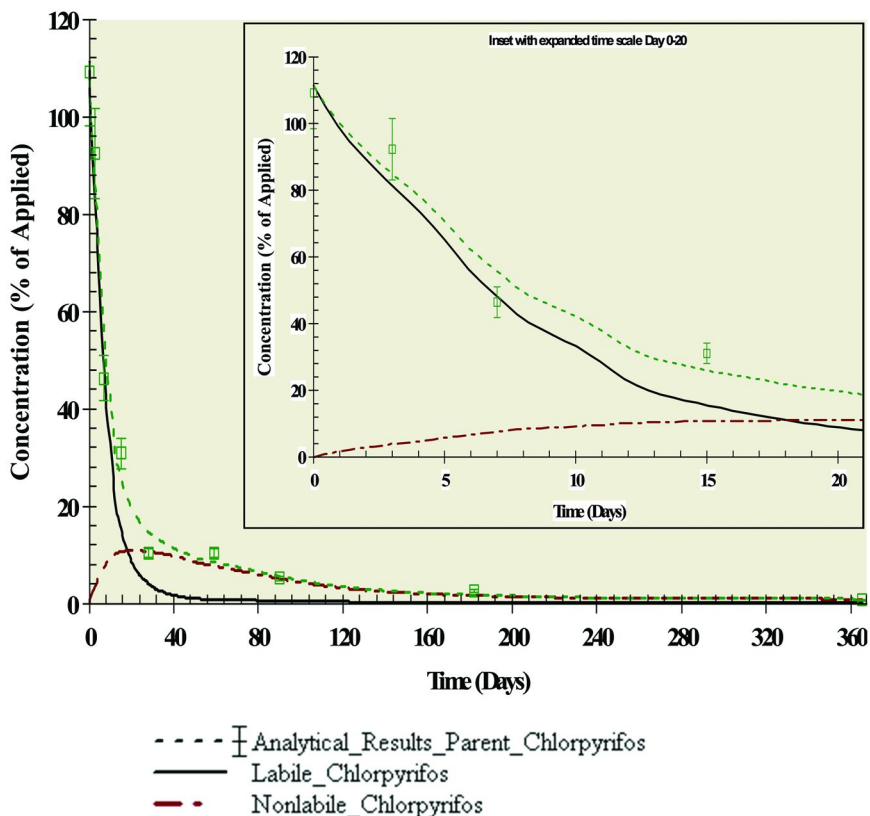


Figure 7. Optimized Fit Using Arrhenius Equation For Field Dissipation Data.

With the Q_{10} calculations, the Correction Factor Q at time t in days after application is used to normalize the temperature to a standard value, T_0 , typically 20°C (2) as in eq 4 below:

$$Q_t = Q_{10}^{(T-T_0)/10} \quad (4)$$

The standard value of $Q_{10} = 2.58$ was used (2). Substituting this value and 20°C in eq 4 and rearranging gives eq 5:

$$Q_t = \exp(0.09478 \cdot (T - 20)) \quad (5)$$

This relationship also fails below 4°C . This was dealt with as described above for the Arrhenius method.

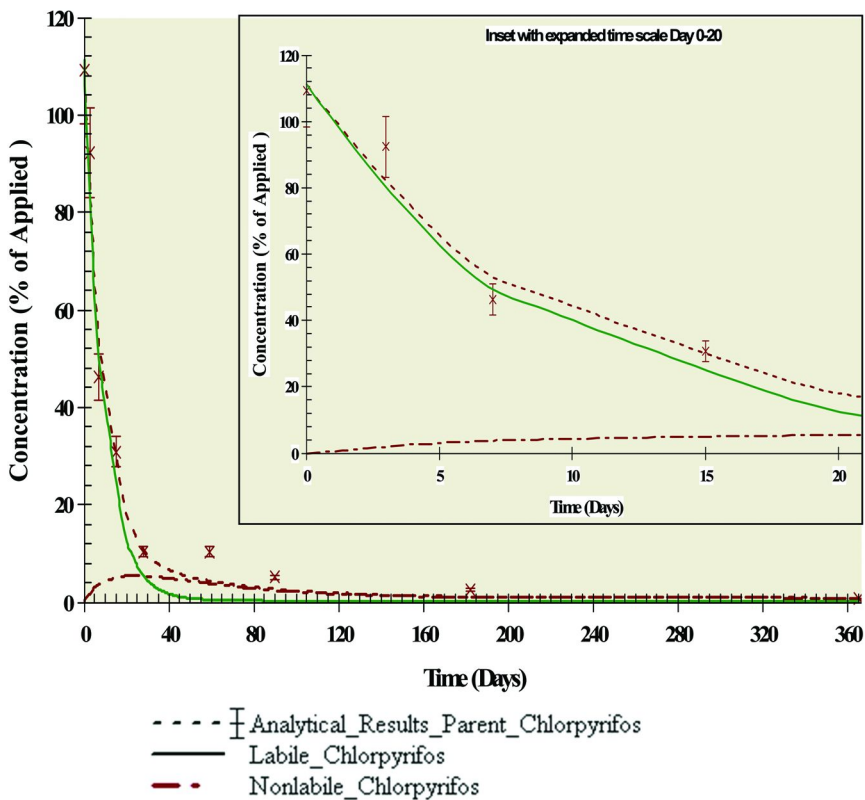


Figure 8. Optimized Fit Using Q10 Temperature Correction For Field.

Results From Laboratory Data

The 11 laboratory aerobic metabolism data sets available for chlorpyrifos were run in the model. The optimized rate constants with corresponding DT50 and DT90 values are listed in Table 2. The statistical data for the curve fitting are included in Table 2. The statistics show an excellent fit to the model in all cases, except that the data from the Cuckney soil could not be successfully optimized by computer due to the very brief time for the desorption process to become dominant. However, the data were very similar to those for the Charentilly soil 3 and the parameter values optimized in the Charentilly data gave a very good fit for the Cuckney data (Table 2). The Catlin soil data required weighted least squares regression; all others were run with ordinary least squares optimization. Some of the p values indicate that additional data points would improve the goodness of fit.

The excellent visual fit to the data throughout the soil types and climatic conditions is illustrated in Figure 3-5. These graphs exemplify soils in which the onset of the slower phase of dissipation occurred after approximately 60, 20 and <10 days respectively.

As noted above, our first assumption was that the nonlinear behavior of chlorpyrifos is caused by a rapid dissipation of residues from soil pore water followed by a slow dissipation phase in which the rate of degradation is limited by the rate of desorption i.e. that in Figure 2, M1 corresponds to the dissolved phase and M2 to the adsorbed phase. The graphs in Figure 3-5 include lines for the total amount of parent as well as the proportions in M1 and M2 and it is apparent that the slow phase corresponds to the rate of decline of concentration in M2 after the residues in M1 are depleted, which fit the assumption very well. However, the time scale for the change to the slower degradation process is much longer than the time taken for soil adsorption and desorption processes to reach equilibrium, which is on the scale of hours (7). In the data illustrated in Figure 1, the transition takes more than 30 days.

From Figure 1, the ratio of k_1 and k_2 appears to be related to the equilibrium adsorption coefficient, K_d (3), but the system is not at equilibrium. Since K_d or its organic carbon corrected version K_{oc} are expected to be related to soil properties (3), considerable effort was expended to find a relationship between the soil properties in Table 1 and the optimized values found for k_1 and k_2 , or the ratio of these values. Such a relationship could be used to predict values of these parameters for modeling soils in a continent-wide exposure assessment (5). However no such relationship was found. For example, the proportion of parent compound that remains in compartment M1 after 20 days is close to 50% in Figure 3. From the value of K_{oc} , which ranges from 973 to 31000 (5), the proportion in the dissolved phase should be very small and consistent with the lack of leaching movement observed for chlorpyrifos. It is clear from high proportion of residues in both M1 and M2 that the material in these compartments does not move with soil pore water. Therefore, M1 and M2 cannot be interpreted as the dissolved and adsorbed compartments in the soil. They are instead, bioavailable and nonbioavailable compartments (8) and in addition, abiotic hydrolysis occurs only from M1. To represent this, the compartments were called labile and non-labile. It follows that the half-life that is relevant for modelling should be obtained from k_m , which is the rate of actual elimination of the parent compound when it is in a labile form.

Considerable effort was also expended to find a way to estimate the rate constant, k_m , from the properties of soils so that modelling could be done on a wider range of soils. The values of k_m did not show a correlation with soil pH but as was found for the reported SFO DT50 values (5), the results could be divided into two groups. The group including the German Standard soil, Cuckney, Stockton and Thessaloniki have longer DT50 values and have a significant correlation to pH. The contribution from abiotic hydrolysis, which is sensitive to pH may be larger in these soils, while the soils with shorter DT50 values have more biological degradation, which occurs where pH is regulated inside living cells. This remains unproven since the grouping by the DT50 vs pH in Table 1 and 2 are similar, but not the same. From the results in Table 2, the SFO3 model was equally successful in handling both groups of soils, and this provides further support for the assumption that degradation, including both transformation and formation of bound residues, takes place only from M1.

The average and Std. Dev. of DT50 values based on k_m were 35.4 days and 33.9 days respectively. The upper 95% confidence limit of the mean DT50 was 58.9 days. This value tracks the bioavailable portion of the residues in soil that would be toxic for risk assessment purposes, and could be used in worst case modelling for most soil studies.

To give rise to nonlinear kinetics, there must be at least one compartment in the soil from which degradation does not occur and another from which it does. A second assumption is based on the recognition that measured concentrations in soil are not the same as the concentration available for biotic or abiotic reaction; and to have analytical recoveries approaching 100%, the analytical results must represent the sum of both compartments. A third assumption, that the applied material is initially in the labile compartment, is based on the fact that the applied material moves into the soil in the pore water that is on the surface of every particle. These assumptions are consistent with the independently developed concepts of bioaccessibility and the distinction between accessibility and chemical activity in the soil. It has been shown that accessibility is correlated to the rate of biodegradation, but not to the partition or movement of materials in the soil, which depend on the balance of the activity in the various soil components and that for some compounds, the accessibility can be measured. (9-11). While Mayer and Reichenberg proposed that accessibility operates at the macro level of uptake and biodegradation, it is evident that for bioaccumulation to occur, they also operate within the living organism and even within the cell. It may be possible to use measured accessibility to parameterize models such as PRZM/EXAMS for modelling environmental behavior of compounds.

The proposed SFO3 model uses only simple first-order kinetics, but explains the nonlinear kinetics over a wide range of data sets. The model reduces the number of assumptions required and simplifies the mathematics; the adsorption and desorption equilibrium, which operates on a much shorter time. It provides insight into processes that drive the changes in degradation rate and bioavailability of the active ingredient with time.

There are some cautionary notes for the use of the model. For data sets such as Charentilly where the nonlinear transition occurs soon after application the SFO3 model approaches a simple first-order model. Consideration of the schematic diagram shows that it is also possible to approach SFO kinetics if the nonlinear transition occurs late in the time interval. This shows that there may be more than one optimum in the regression, and care is needed to avoid unrealistic values of the three rate constants when running the model. The data from the Cuckney site did not converge on a solution in the ModelMaker software. This could be caused by insufficient data and degrees of freedom. From a visual assessment, the values appeared close to those from Charentilly and a good fit to the data was obtained using the rate constants from the latter site.

Field Dissipation Study Modelling Results

Among the field soil dissipation data sets available for chlorpyrifos, the data from a site in Tranent Scotland had the most sample dates and the most useful range of temperatures to illustrate the use of the model. The rainfall data showed no significant dry periods, so the moisture content correction was not done. The set-up for such a calculation is a simple extension of the set-up for the temperature correction (See schematic and model set-up in Figure 6). Both the Arrhenius temperature correction and the Q10 calculation gave an optimized initial total concentration of 111.2% relative to the planned application rate. With this initial value the optimized DT50 for degradation was 5.3 days in the faster phase followed by 66.0 days in the slow phase. The corresponding values for the Q10 method were 4.9 days and 69.3 days. The regression coefficients were above 0.98. Further details are listed in Table 2. The dissipation rates were faster than the average under laboratory conditions, which indicates that modelling based on laboratory rate constants would be conservative. The goodness of fit can also be seen in the dissipation graphs in Figure 8 and 9. These graphs also illustrate the ability of the model to identify outlier data points and other inconsistencies in nonlinear data sets. For an example of an outlier, see the data for Day 273 in Figure 7 and 9.

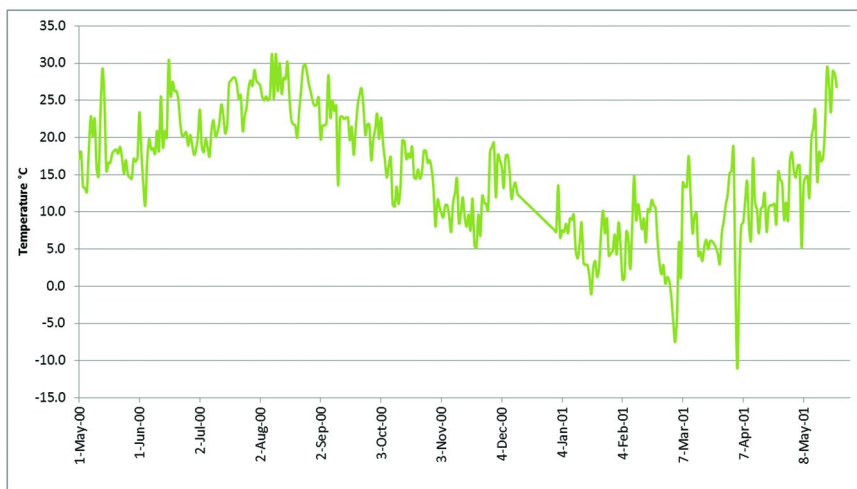


Figure 9. Daily Mean Temperature Data From Tranent, Scotland.

Conclusions

A kinetic model was set up using 3 simple first-order equations with reversible movement of parent compound into a compartment in which degradation does not occur. Residues in both labile and non-labile compartments are readily extractable for analysis, but are not mobile in the soil and are not related to the adsorption/desorption processes.

The modelling results show that such a conceptual model accounts for a very high proportion of the variability of the data and explains the nonlinear behavior of chlorpyrifos without making assumptions about equilibrium or other relationships among the rate constants.

The model fit the concentration vs time data from aerobic soil dissipation data for ¹⁴C-chlorpyrifos in 11 different soils very well, but the resulting rate constants were not correlated to physical soil properties and could not be predicted from these properties as was found with the rate constants originally reported for these soils.

The degradation rate from the bioavailable compartment is the first-order rate constant to be used for environmental fate modeling. The lack of degradation, either biotic or abiotic, in this compartment shows that the material in it is not bioavailable and non-bioavailable residues are not hazardous.

The SFO3 model is versatile and related to the physical behavior of the compound in the soil environment. It provides a good fit to nonlinear concentration versus time data. It can be used for lab or field data and corrections for soil moisture or temperature can be applied. It is possible to include timed events such as multiple applications. The applications for SFO3 include calculation of rate constants for parent and intermediate metabolites, comparison of lab and field results, correction for changes in soil temperature or moisture content, identification of outlier data, and development of parameters for modelling input.

Acknowledgments

The authors would like to thank the DowAgrosciences LLC for access to the data used in this assessment.

References

1. Hoskin, W. M. *Plant Proc. FAO* **1961**, *9*, 163–168.
2. FOCUS. Guidance Document on Estimating Persistence and Degradation Kinetics from Environmental Fate Studies on Pesticides in EU Registration. Report of the FOCUS Work Group on Degradation Kinetics, 2006, EC Document; p 434.
3. Nash, R. *Environmental Chemistry of the Herbicides*; Grover, R., Ed.; CRC Press: Boca Raton FL, 1988; pp 131–170.
4. Giesy, J. P.; Solomon, K. R.; Cutler, G. C.; Giddings, J. M.; MacKay, D.; Moore, D. R. J.; Purdy, J.; Williams, W. M. *Rev. Environ. Contam. Toxicol.* **2014**, *231*, 1–12.
5. Solomon, K. R.; Williams, W. M.; MacKay, D.; Purdy, J.; Giddings, J. M. *Rev. Environ. Contam. Toxicol.* **2014**, *231*, 13–34.
6. Racke, K. D. *Rev. Environ. Contam. Toxicol.* **1993**, *131*, 1–154.
7. OECD. *Test No. 106: Adsorption -- Desorption Using a Batch Equilibrium Method in OECD Guidelines for the Testing of Chemicals, Section 1 Physical-Chemical properties*; OECD Publishing: Paris, 2000,

8. Hance, R. J. *Environmental Chemistry of the Herbicides*; Grover, R., Ed.; CRC Press: Boca Raton FL, 1988; pp 1–19.
9. Mayer, P.; Reichenberg, F. *Environ. Toxicol. Chem.* **2006**, *47*, 1239–1245.
10. Gan, J.; Cui, X.; Bao, J. *J. Environ. Sci. Technol.* **2013**, *47*, 9833–9840.
11. Katayama, A.; Bhula, R.; Burns, G. R.; Carazo, E.; Felsot, A.; Hamilton, D.; Harris, C.; Kim, Y.-H.; Kleter, G.; Koerdel, W.; Linders, J.; Peijnenburg, J. G. M. W.; Sabljic, A.; Stephenson, R. G.; Racke, D. K.; Rubin, B.; Tanaka, K.; Unsworth, J.; Wauchope, R. D. *Rev. Environ. Contam. Toxicol.* **2010**, *203*, 1–86.

Chapter 10

Statistical Means for Proper Determination of Kinetic Half-lives

Scott H. Jackson*

BASF Corporation, 26 Davis Drive,
Research Triangle Park, North Carolina 27709

*E-mail: scott.jackson@basf.com. Phone: (919) 547-2349.

In the NAFTA regulatory community, a consistent methodology for estimating dissipation times for environmental fate data is not applied. This work presented here demonstrates that the inappropriate use of pseudo-first-order degradation model can result in inaccurate estimates of soil degradation rates. A statistical tool is presented that can be used to identify an appropriate statistical model to best describe a particular environmental fate dataset. Methods are also proposed to identify if transforming datasets are required to a more appropriate scale. Additionally statistical testing procedures have been proposed to select the appropriate model within that scale. Results from this work indicate that, unless the proposed diagnostic and statistical procedures are used, inaccurate estimates of dissipation times may result.

Introduction

The regulatory community requires that pesticide manufacturers conduct and submit a series of physical-chemical and environmental fate studies in support of the registration granting process. The studies submitted allow evaluation of a molecule's behavior in various environmentally relevant matrices such as soil, water, and sediment. The studies are intended to allow the quantification of different degradation mechanisms in the matrices due to the influences of both biotic and abiotic processes. One of the most important endpoints generated

from the studies is the determination of compound degradation time, or the time required for concentration to decline in the various study matrices. Normally the time required for 50% of the compound to dissipate or degrade (the DT_{50}) is of primary interest, but other endpoints may be of interest such as the time required for 90% of the molecule to dissipate or degrade (a DT_{90}).

More recently there have been shifts in regulatory decision processes toward a more hazard-based process to categorize persistence. Hazard-based persistence decisions compare a study-based endpoint to a pre-determined criterion or trigger. For example, a soil degradation half-life of greater than 180 days might be judged by a hazard-based categorization as a persistent molecule, while a risk-based method would consider other environmentally relevant facts before suggesting the molecule was persistent. While hazard-based regulatory decisions allow for a more readily understood decision, the assessments typically provide a superficial characterization assessment.

One problem for users of various regression approaches is the implementation of a regression fit criterion. Is the coefficient of determination a good regression selection criterion? Is the coefficient of determination plus the examination of residuals a good selection criterion? Are there other more statically based methods that are better for selecting regression approaches? The goal for looking at fit criterion is eliminating user bias, and to ensure the best description of the data. It has been pointed out in the literature (1) that inaccurate first-order kinetics are often used to describe data. The typical cost of an environmental fate laboratory study is about \$200-400 thousand dollars. The goal for any type of calculation should be to reflect the data being characterized as accurately as possible. In the regulatory community (regulated/regulator), initial attempts to specify an appropriate regression model selection has been based on the coefficient of determination, r^2 or R^2 . In the text *Organic Chemicals in the Soil Environment* (2), Hamaker proposed a series of empirically based equations for determination of half-lives in a pseudo systematic approach.

This pseudo-first- order (PFO) equation has historically been used as a first attempt to analyze data sets. This familiar equation is defined as

$$C_t = C_0 \exp(-kt), \quad (1)$$

where C_t is the concentration at time t , C_0 is the initial concentration, and k is the proportionality coefficient. Unfortunately, many researchers using this approach stopped regression analyses if they obtained an r^2 or R^2 value that seemed reasonable. The Hamaker equation in the log scale can be written as

$$\ln(C_t) = \ln(C_0) - kt. \quad (2)$$

If the data are linear in the log scale, equation 2 may be an appropriate model for that scale. However, few current generation agrochemicals exhibit linear degradation patterns in the log scale.

As a result, Hamaker (2) proposed a power-rate model that allowed a better description of nonlinear data sets as:

$$C_t = \frac{C_0}{(1 + \alpha C_0^\alpha kt)^{1/\alpha}}, \quad (3)$$

where α is an unknown parameter, and the other parameters are defined as in (eq. 1).

Timme–Frehse–Laska Equation

In a similar approach to Hamaker, Timme et al. (3) proposed six functions that were also empirically based. However, they took the additional step of suggesting that the choice of the equation should be based on the value R^2 . The approach prescribed using the Timme equations was to start with a linear equation, and then to progress to increasingly nonlinear equations in sequence until an R^2 value of 0.7 was reached in an effort to improve fit. While this approach was useful in that it added the start of a systemic framework, the coefficients of determination cannot be used to determine the adequacy of a model.

$$y = \left(\frac{\log x}{\log b} \right)^2 \quad 1^{\text{st}} \text{ Order} \quad (4)$$

$$y = \left[\frac{a}{b} (\sqrt{x} - 1) \right]^2 \quad 1.5 \text{ Order} \quad (5)$$

$$y = \left[\frac{a}{b} (x - 1) \right]^2 \quad 2^{\text{nd}} \text{ Order} \quad (6)$$

However, choice, as discussed previously, was based on an arbitrary decision to use a coefficient of determination of 0.7. Some in the regulatory community have suggested that all data set analysis should be based on a rate-constant ($t_{1/2}$) determination. It is important that a clear distinction be made between DT_{50} and $t_{1/2}$ values. A DT_{50} implies that the value describes the time required for 50% of the starting concentration to dissipate or degrade. A $t_{1/2}$ result implies that the number is derived from a rate constant, which may or may not describe where 50% of the starting concentration has dissipated or degraded.

However, one problem with this assumption is that few data sets are actually described well by a linear relationship in a natural or log scale. This would mean that most data sets characterized by the use of a rate constant calculation are poorly described. This mis-description is especially a concern when a compound is classified for persistence for example. Additionally, when the half-life is a model input, this miss-characterization is carried through to predicted environmental exposures. Mojasevic et al. (1) and Leake et al. (4) have pointed out that when

examining factors influencing degradation half-life values, inaccurate first-order kinetics are often used to describe the relationship. The goal for any type of calculation should be to reflect the processes being characterized as accurately as possible. Further details regarding the implications of using DT_{50} and $t_{1/2}$ approaches may be found in Massey et al (5).

As researchers continued to examine the use of regression models for use in describing data sets, they were not satisfied with empirical fits to data with little statistical basis.

Gustafson-Holden Equation

One approach, which was theoretically based and worked computationally well, was proposed by Gustafson and Holden (9). The Gustafson–Holden equation (eq. 7) was a unique approach that allowed both linear and nonlinear data sets to be solved since it is based on the flexible gamma distribution. The equation was described by the authors as being first-order and solved for three unknowns (C_0 , α , and β):

$$C_t = C_0(1 + \beta t)^\alpha, \quad (7)$$

Using a log scale, this equation (8) can be written as:

$$\ln(C_t) = \ln(C_0) + \alpha \ln(1 + \beta t). \quad (8)$$

Goodness of Fit Testing

Since historically in a regulatory context there has not been a single systematic justification for applying regression models to data sets appropriately. The question remains, what is an acceptable means for judging goodness of fit. Basic statistical conventions would suggest evaluating the coefficient of determination (r^2 or R^2). Next an examination of residuals should be conducted. However, examining residues and acceptance of the coefficient of determination is subjective. An overused axiom in science is the principle of parsimony or Occam's Razor. This fundamental principle of the scientific method roughly states that the simplest plausible explanation should be used in any scientific endeavor. Or Occam's razor is used to decide between "theories" that have already passed theoretical scrutiny tests, and which are equally well supported by evidence. This axiom would argue for the use of residuals and the coefficient of determination. However, a more quantitative approach was desirable.

The goal of this presentation is to propose a method whereby regression models may be correctly applied and evaluated for goodness of fit.

Table 1. Example Dataset with Two Replicate Samples Per Sampling Interval. The Observations Are Presented as a Percent of a Nominal Applied Dose.

<i>Days</i>	<i>Observation (% of Dose)</i>
0	102.5
0	96.7
1	78.6
1	71.2
3	69.4
3	51
7	42.7
7	41.5
14	28.5
14	22.4
28	18.6
28	14.3
42	10.3
42	8.4
61	6.3
61	5.6
91	6
91	2.8
118	3
118	2.9

Statistical Considerations for Model Selection

The nature of environmental fate data requires that an appropriate regression model be selected and simultaneously an appropriate transformation function should be selected so that the data is in the appropriate scale. While this manuscript will not go into the selection of transformation functions, it has been shown that log or natural log transformation is typically used with environmental fate data. However, the regression model and data scale (transformation) should be selected so that the residuals do not exhibit any systematic behavior. The variability of the residuals should be similar across the time axis. The data also need to be normally distributed which is especially important if an F-test is to be used. When comparing several regression models for fit to a data set, one very useful method is the application of an F-test. A description of an appropriate

F-testing procedure has been described by Aldworth and Jackson (6) and therefore will not be explained in this paper. However the implementation of the method will be used to determine if the selected models are descriptive.

Use of Visual Inspection

An analysis of data is incomplete without a visual inspection of data. Normally, a plot of the raw data should be used to get an initial idea of which approach should be used. Fitted values should be plotted against the data as a check for goodness of fit. Residuals should be plotted to check for goodness of fit and to evaluate the appropriateness of transformation function or scale used.

Example

As an illustration of the principles of analysis, an example dataset will be used and analyzed. Additionally, an Excel tool has been developed for performing various determinations including F-tests. This Excel tool can be found at <http://www.stone-env.com/agchem/agres.php> (7). The time scale in the example are days after dosing (DAT) and are plotted as the X axis, while observed percent of dose will be plotted as the Y axis. Similarly they shall serve as the corresponding X,Y pairs for analysis (Table 1).

Normally the first step in analysis would be to simply regress the data. The results of regressing both the simple regression and the G-H equation are presented.

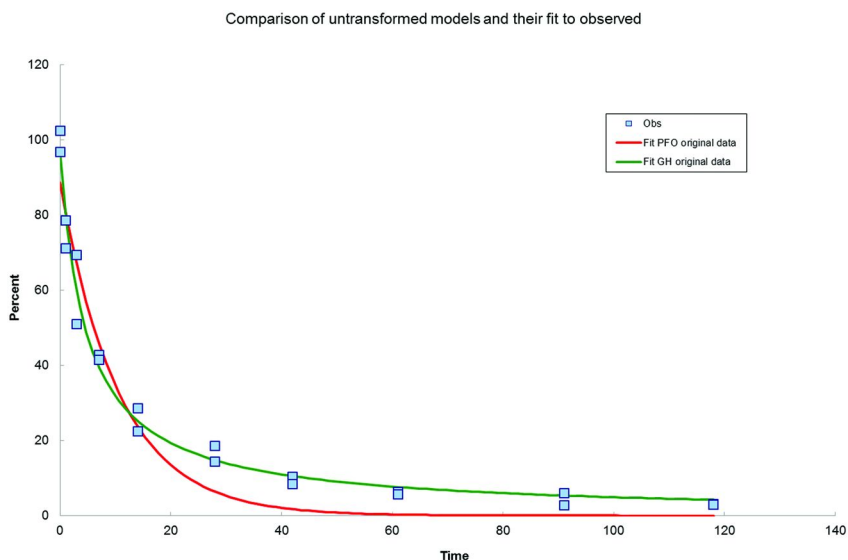


Figure 1. A presentation of the pseudo first-order and G-H fits to the data. (see color insert)

From an examination of Figure 1, it is evident that the G-H method intersected the data points reasonably well, while the pseudo-first-order regression fit did not. Surprisingly, the r^2 for the pseudo-first-order regression is 0.96, while the R^2 for the G-H regression was 0.98. This example points out two concerns when fitting regressions to data A) relying on a coefficient of determination, and B) failing to critically examine the regression fit to data. If an examination is made of the residuals in Figure 2, it is also evident that the simple regression did not describe the data well since the residuals are not distributed either side of the mean (zero line).

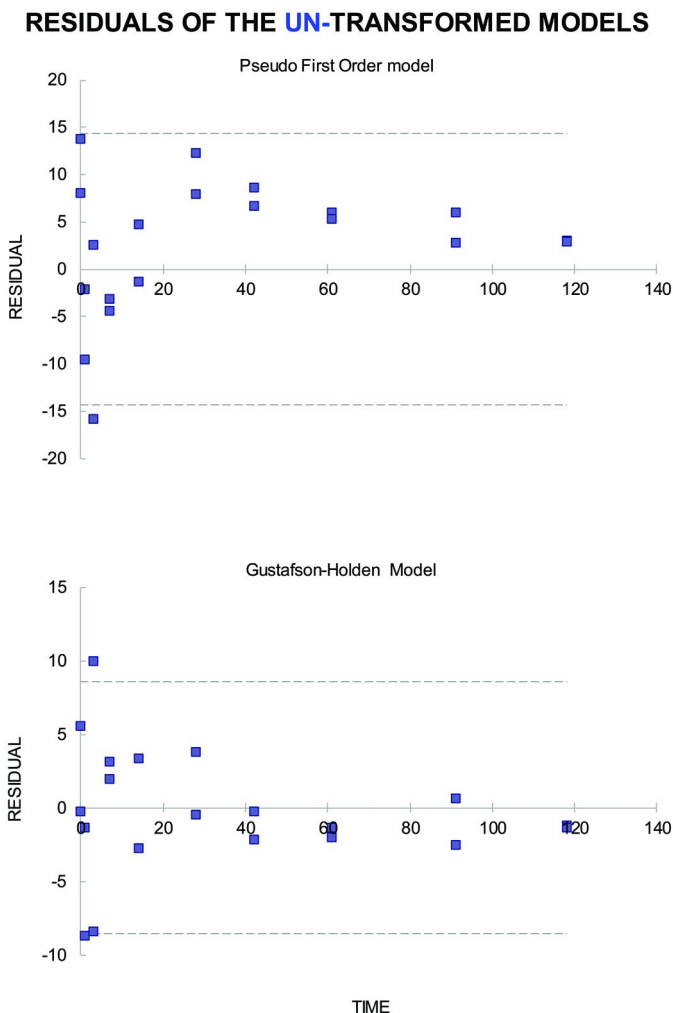


Figure 2. Presentation of untransformed residuals for both regression models.

However if the analyst simply looked at 50% or 90% dissipation times (DT), they might be satisfied with the results. The DT₅₀ for the pseudo-first-order (PFO) and G-H were 4.8 and 7.4 days respectively. The DT₉₀ values were 24.5 and 46.3 for the PFO and G-H regressions respectively. The next step typically performed is to log transform data that is not fully linear.

RESIDUALS OF THE LOG-TRANSFORMED MODELS

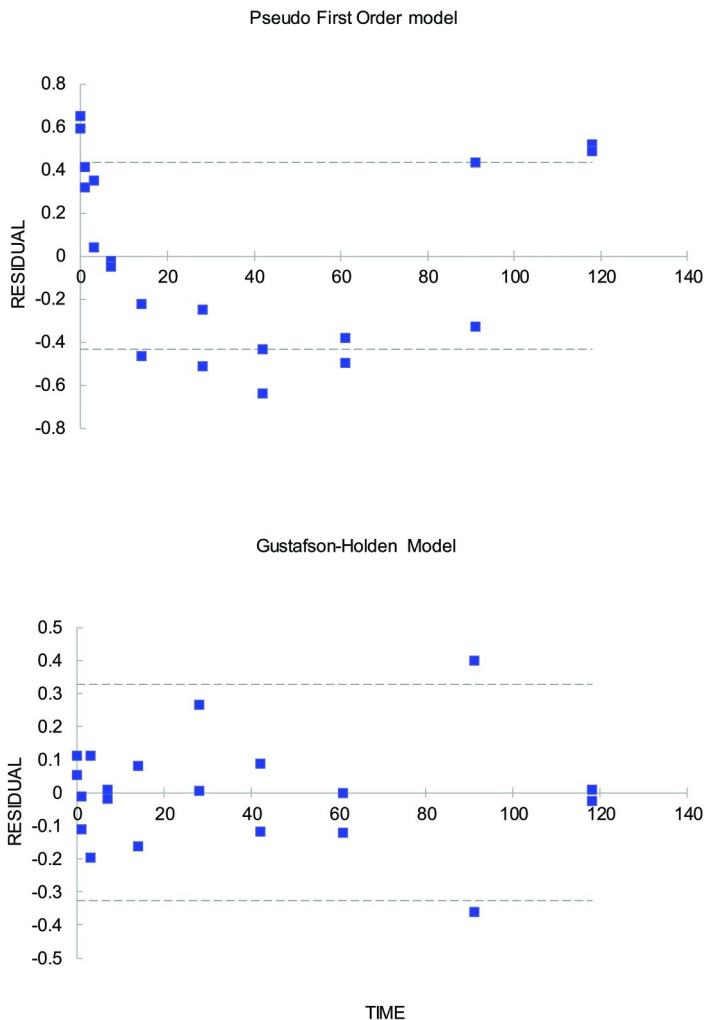


Figure 3. Presentation of transformed residuals for both regression models.

In Figure 3 compared to Figure 2, the GH model does restrict residual scatter after data transformation (or the residuals are equally distributed around the mean). The DT₅₀ for the PFO and G-H were 24.1 and 6.0 days respectively. The DT₉₀ values were 79.9 and 43.2 for the PFO and G-H regressions respectively.

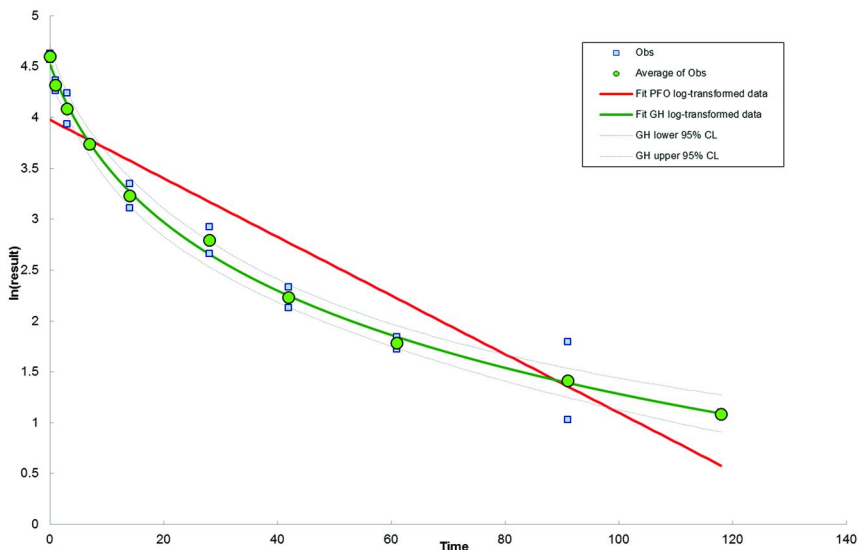


Figure 4. A presentation of the pseudo-first-order and G-H fits to the data log transformed. (see color insert)

From an examination of Figure 4, it is evident that the G-H method intersected the data points reasonably well, while the simple regression fit did not. Surprisingly, the r^2 for the pseudo-first-order regression is 0.88, while the R^2 for the G-H regression was 0.98. This example points out concerns comparing several models with different data treatment methods. If we simply examined r^2 , then a conclusion might be that the PFO method with untransformed data was a good approach. Examining residuals helps to inform a decision between models and data transformation methods. Examining the coefficient of determination and DT_{50} results might seem a good selection criterion when judging between regression models and data treatment. However confoundingly, it appears that transforming the data made results worse for the PFO model, while marginally improving the GH model result. After an examination of results comparing transformed data and models, a great deal of subjectivity could bias the proper basis for choosing a model and data treatment. However, the implementation of an F-test for selecting models would help decisions when comparing multiple models and several data treatment methods. Since there is a desire for a more robust decision process for selecting models, the use of an F-test metric is appealing. A useful statistical testing procedure to select between two competing models using the F-test has been well described (8). Greater statistical detail on using an F-test for regulatory study data analysis can be found in Aldworth and Jackson (6). To help implement and understand the F-test process, a Microsoft Excel application has been developed that

calculates the statistics discussed in this presentation. The tool can be found at URL <http://www.stone-env.com/agchem/agres.php#agdownload> (7). There are versions for Excel 2003, 2007, and 2010.

Table 2 is a summary of the various combinations possible using two models and a transformation method.

Table 2. A Summary of Statistic Results Based on Various Analysis Combination

<i>Goodness-of-fit test</i>	<i>log-transformed data</i>		<i>untransformed, original data</i>	
	PFO	GH	PFO	GH
F_{LOF}	8.94	0.23	4.36	0.56
P	0.001	0.964	0.0166	0.769
r^2 or R^2	0.878	0.982	0.960	0.983
Compare Models				
F for model comparison	101.75		37.74	
P for model comparison	1.36E-08		1.08E-05	
	PFO	GH	PFO	GH
DT_{50}	24.1	6.0	7.4	4.8
DT_{75}	48.1	16.6	14.7	14.8
DT_{90}	79.9	43.2	24.5	46.3
Confidence Limits				
DT_{90LCL}	–	33.3	–	–
DT_{90UCL}	–	53.1	–	–

Summary

There are straightforward steps for evaluating a model or several models as predictive tools in kinetic analysis. The first step is the resulting coefficient of determination. Is the r^2 or R^2 high enough? Next step would be an ocular examination of the regression and its fit to the data. As observed with the PFO regression and the transformed data, the coefficient of determination seems reasonable but the fit to data was poor. The next step in evaluation is to look at the plot of residuals. The problem with looking at the coefficient of determination and residuals is that they are both analyst subjective. It has been presented that the coefficients of determination may seem adequately descriptive (numerically

high) but still can be a poor description of the data. However an F-test provides a statistical basis without bias for selecting between competing models and data treatment methods. To further aid readers and users in their understanding of the F-test methodology, a Microsoft Excel calculator has been developed and is publically available for download.

References

1. Mojasevic, M.; Helling, C. S.; Gish, T. J.; Doherty, M. A. Persistence of seven pesticides as influenced by soil moisture. *J. Environ. Sci. Health* **1996**, *B31*, 469–476.
2. Hamaker J. W. Decomposition: quantitative aspects. in *Organic Chemicals in the Soil Environment*; Goring C. A. I., Hamaker J. W., Eds.; Marcel Dekker, Inc.: New York, 1972; pp 253–340
3. Timme, G.; Freshe, H.; Laska, V. Statistical interpretation and graphic representation of the degradation behavior of pesticides residues. II. *Pflanzenschutz-Nachr. Bayer* **1986**, *39*, 187–203.
4. Leake, C. R.; Humphreys, S. P.; Austin, D. J. *Factors influencing the modeling of pesticide degradation in soil and the estimate of half-life (DT50) and DT90 values*; British Crop Protection Council Monograph, 62; Farnham: Surrey, U.K., 1995
5. Massey, J.; Jackson, S.; Saha, M.; Zietz, E. Monitoring of agrochemical residues in soil: Best practices for conducting soil residue studies. In *Handbook of residue analytical methods for agrochemicals*; Roberts, T. R., Ed.; John Wiley & Sons, Ltd.: Chichester, U.K., 2004; Vol. 2.
6. Aldworth, J.; Jackson, S. H. A Systematic Approach for Determining Proper Selection of Regression Models for Analysis of Environmental Fate Datasets. *Pest Manage. Sci.* **2008**, *64*, 536–543.
7. Aldworth-Jackson Fitting Tool is an Excel-based tool created as a teaching tool for EPA. The method follows that outlined in the paper by Jeremy Aldworth and Scott Jackson in *Pest Manage. Sci.* **2008**, *64*, 536–543; <http://www.stone-env.com/agchem/agres.php#agdownload>.
8. Neter, J.; Wasserman, W.; Kutner, M. H. *Applied Linear Statistical Models*, 3rd ed.; Irwin: Homewood, IL, 1990
9. Gustafson, D. I.; Holden, L. Nonlinear pesticide dissipation in soil: a new model based on spatial variability. *Environ. Sci. Technol.* **1990**, *24*, 1032–1038.

Chapter 11

Experiments and Modeling To Quantify Irreversibility of Pesticide Sorption-Desorption in Soil

Laura Suddaby,^{*,1} Sabine Beulke,² Wendy van Beinum,²
Robin Oliver,³ Sui Kuet,³ Rafael Celis,⁴ William Koskinen,⁵
and Colin Brown⁶

¹TSGE Consulting Limited, Concordia House, St. James Business Park,
Grimbald Crag Court, Knaresborough, North Yorkshire, HG5 8QB, U.K.

²The Food and Environment Research Agency, Sand Hutton, York,
North Yorkshire, YO41 1LZ, U.K.

³Syngenta, Jealott's Hill International Research Centre,
Bracknell, Berkshire, RG42 6EY, U.K.

⁴Instituto de Recursos Naturales y Agrobiología de Sevilla (IRNAS), CSIC,
Avenida Reina Mercedes 10, 41012 Sevilla, Spain

⁵Department of Soil, Water and Climate, University of Minnesota,
439 Borlaug Hall, 1991 Upper Buford Circle,
St. Paul, Minnesota, 55108. U.S.A.

⁶Environment Department, University of York, Heslington, York,
North Yorkshire, YO10 5DD, U.K.

*E-mail: laura.suddaby@tsgeurope.com.

Pesticide sorption behavior is a complex process. The importance of extremely slow retention and release has superseded the notion that sorption of pesticides to soil is an instantaneous and reversible process. A fraction of sorbed pesticide is also often reported to bind irreversibly to the soil matrix. Irreversible sorption has potentially significant implications for reducing pesticide mobility and bioavailability. However, an accepted experimental method with the ability to quantify irreversible sorption does not exist due to procedural difficulties in identifying slowly reversible and irreversible

fractions relevant at the field scale. Use of isotopes, generally ^{14}C , is a promising means of quantifying irreversible sorption and providing crucial parameters and data for pesticide fate modeling.

Introduction

Sorption is recognized as a key mechanism controlling the distribution of pesticide between solid and aqueous phases in the soil environment. Sorption thus controls both the amount of pesticide available for leaching and the amount available for uptake by target and non-target organisms (1). The study of sorption itself however, provides complex experimental challenges. Sorption and desorption are dynamic processes and are often observed to increase and decrease respectively as a function of contact time with the soil. The sorption kinetics controlling these time-dependent interactions typically involve multiple sorption domains ranging from instantaneous to extremely slow and months or years may be required to approach true equilibrium (2). There is also considerable evidence to suggest that pesticide sorption to soil is only partially reversible. Pesticide desorption can often be observed to ultimately occur at a negligible rate, thus leaving behind a fraction of sorbed pesticide that is apparently desorption-resistant (3). This fraction is described by a range of terms within the literature, of which non-extractable residue, bound residue or irreversible sorption are the most commonly used.

The ability to quantify the amount of pesticide available for desorption and that which is desorption-resistant would significantly improve our understanding of pesticide sorption-desorption in soil as well as the power of models for predicting pesticide fate. At present however, a standard procedure to quantify readily-desorbable, slowly-desorbable and non-desorbable pesticide does not exist. Northcott and Jones (11) were the last to review the state-of-the-art regarding experimental approaches and instrumental methods used to quantify and/or characterize fractions of non-desorbable pesticide. Classically, exhaustive extraction techniques were used with the sole aim of recovering as much of the pesticide as possible (12). The definition of non-desorbed pesticide proposed by Führ *et al.* (13) stipulated that “the extraction method must not substantially change the compounds themselves or the structure of the matrix”; methodology has since seen a shift towards more natural methods of extraction and the use of isotopes, generally ^{14}C (3, 11).

The first part of this chapter reviews the nomenclature used in the literature to describe desorption-resistant pesticide and discusses mechanisms of formation. The second part discusses experiments and modeling approaches used to quantify irreversibility in pesticide sorption-desorption in soil.

Nomenclature: Bound Residues, Non-Extractable Residues, and Irreversible Sorption

The descriptive terms “free” and “bound” residue are used to differentiate between pesticide residues that can be readily extracted from the soil and those that remain resistant to such an extraction (7). The most widely used definition provided to date was proposed by Roberts *et al.* (8) who described non-desorbable or “bound” residue as *“chemical species originating from pesticides, used according to good agricultural practice, that are unextracted by methods which do not significantly change the chemical nature of these residues.”* Although this definition has been modified many times, it has not changed substantially (4). The most notable addition was provided by Calderbank (9) who introduced the concept that the environmental significance of non-desorbed pesticide hinges on its bioavailability and biological effect, rather than the extent to which it can or cannot be extracted or released by chemical methods: *“clearly the important matter is not so much how the residue is defined but the question of its biological availability”*. The last agreed definition for non-desorbable pesticide was provided by Führ *et al.* (6) who also considered the structure of the soil matrix: *“Bound residues represent compounds in soil, plant or animal, which persist in the matrix in the form of the parent substance or its metabolite(s) after extraction. The extraction method must not substantially change the compounds themselves or the nature of the matrix.”*

Although the aforementioned definitions of “bound” residues have been widely acknowledged, non-desorbable pesticide residue is described by a variety of terms within the literature; therefore some clarifications will be made as to their use and meaning. Firstly, the term non-extractable residue (sometimes referred to as unextractable residue) is used commonly throughout the literature. Use of the term non-extractable residue reflects its operationally-defined nature by which the majority of non-desorbable pesticide residues are measured experimentally (1, 5, 10–12). Thus, considering that the definition of a bound residue relates to the fraction of sorbed pesticide resistant to extraction, a bound residue is a non-extractable residue (1). Conversely, a non-extractable residue is not necessarily a bound residue. The fraction of non-extractable residue that has been quantified is entirely dependent on the experimental conditions, method and solvent used to perform the extraction and obtain the reported results (7). The decision to discontinue a given extraction is usually an arbitrary choice and additional amounts of the bound chemicals can normally be recovered by increasing the time or intensity of extraction (13). The classification of compound residues by these definitions can be misleading due to the range of methods used to quantify such fractions (4). Thus, the non-extractable fraction can result in overestimation of the true bound residue fraction due to its operationally-defined nature.

Secondly, the term irreversible sorption is used in certain circumstances. To further complicate matters numerous variations of this term exist within the literature, the meanings of which are essentially equivalent to that of irreversible sorption, though worded differently (Table 1).

Table 1. Variation for the term irreversible sorption in the literature

<i>Terminology used</i>	<i>Reference</i>
Irreversibly sorbed Irreversibly bound Irreversible behavior Irreversibility in pesticide adsorption-desorption Irreversible sites	Celis and Koskinen (14)
Sorption irreversibility Irreversible sorption behavior Non-desorbable Irreversible component	Celis and Koskinen (15)
Irreversible compartment	Chen <i>et al.</i> (3)
Irreversible binding	Burgos <i>et al.</i> (16)
Desorption irreversibility	Yu <i>et al.</i> (17)
Irreversible effects Desorption resistant	Sander and Pignatello (18)

Use of the descriptor “irreversible” implies that the sorbed pesticide is irretrievably bound to the soil matrix, i.e. it can never be recovered. In some studies however, the authors have instead defined their own terms. For instance, Sander and Pignatello (19) have used the term irreversible sorption in a thermodynamic context “*that does not necessarily imply an irretrievably bound state.*” In their later paper Sander and Pignatello (18) explain that “*the term “irreversible” does not necessarily imply the generation of irretrievable (unextractable) residues, although it does not exclude this possibility.*” What is clear, is that the inconsistency in choice of descriptors, and study-dependent definitions of irreversible sorption, limits the ability to make direct comparisons between studies and results in confusion or misinterpretation of their meaning. There is a need, therefore, for the standardization of the terms and definitions used to describe desorption-resistant pesticide residues.

Typically, the term irreversible sorption appears to be used in circumstances where a permanent change in the adsorbate/adsorbent system is proposed i.e. a mechanical or structural rearrangement (20). For instance, Yu *et al.* (17) consider the highly irreversible sorption of pyrimethanil to soils amended with high-microporosity biochar to be the result of adsorption and desorption occurring from different physical environments. Chen *et al.* (3) believe the hysteresis phenomenon observed in their study was partially caused by the irreversible sorption (by physical entrapment) of pentachlorophenol to lipids. Furthermore, Sander and Pignatello (18, 19) have discussed in detail the irreversible deformation of micropores by the sorbate such that adsorption and desorption follow different pathways; a mechanism thought to result in irreversibility in pesticide sorption.

The following definitions are provided for the meanings of the terms used in this chapter: (i) the term irreversible sorption is used to refer to pesticide residue that cannot be recovered from the soil matrix and is thus not available for

degradation or to soil microbes; (ii) the term non-extractable residue is used to define the fraction of pesticide resistant to desorption by the chosen extraction method i.e. extractable where it is possible to use a harsher extraction conditions; and (iii) the term bound residue is used to describe the irreversibly sorbed fraction of pesticide in addition to a fraction of non-equilibrium sorbed pesticide, which may not have been extracted within the time-scale of the experiment. Irreversible sorption and bound residues are hence differentiated in terms of potential for remobilization. Irreversibly sorbed pesticide will never be released from the soil matrix under any circumstance, and may be thought of as essentially removed from the environmental system. Bound residues are not considered permanently bound. Thus, using the term non-extractable residue or bound residue suggests that the potential for remobilization of the residue is unknown. This is the result of the procedural difficulties in reliably establishing desorption endpoints.

The formation of soil-bound pesticide residues has gained significant attention for its importance for the fate and transport of organic contaminants in environmental systems through limiting the bioavailability of pesticides in surface soil systems and having the potential to reduce pesticide mobility in the environment (21). As a consequence, bound residue phenomena have been reviewed in detail on several occasions (1, 8, 11, 22–25). The subject is explored in a greater detail in the following sections.

Formation of Bound Residues: Abiotic and Biogenic Mechanisms

The key mechanisms involved in the formation of bound residues are covalent bonding and physical entrapment (21, 26–28). Both mechanisms of formation may involve the parent molecule and/or its metabolite(s). Covalent bonding and physical entrapment are the direct result of abiotic interactions (i.e. physical and chemical binding). However, biotic interactions (microbial action) have the ability to indirectly or artificially augment the formation of bound residues.

There is strong evidence in the literature to suggest that microbial activity plays a significant role (via biodegradation) in bound residue formation. The majority of this information comes from studies that have tried to identify the parent compound or metabolite(s) by applying different degradation techniques (4). For example: (i) Reuter *et al.* (29) found that the formation of bound residues for the herbicide ¹⁴C-isoproturon was largely dependent on the prior degradation of ¹⁴C-isoproturon to the metabolite 4-isopropylaniline; (ii) Wang *et al.* (30) observed that degradation of the parent compound (new herbicide ZJ0273) was accompanied by formation of bound residues and mineralization to CO₂; and, (iii) Chilom *et al.* (31) found that bound residue formation of naphthalene was low, but formation was 5-20 times higher for its primary metabolite *cis*-naphthalene-1,2-dihydrodiol.

It is well known that the presence of hydroxyl and carboxyl groups greatly enhances the chemical reactivity of metabolites, and thus their ability to form bound residues (24, 32). In addition to this effect, it is also possible for the soil microbial community to influence soil bound residue formation via another route.

Microorganisms degrading parent material are also able to assimilate the derived carbon into their cellular components (e.g. fatty acids and amino acids), which in turn becomes stabilized within the soil organic matter (33). Thus, a proportion of soil bound residue is likely biogenic in nature. A recent publication by Nowak *et al.* (33) showed that after 64 days of incubation, 44% of initially-applied 2,4-D had been converted to microbial biomass and finally to biogenic residues. Since such residues would not pose any ecotoxicological hazard and this clearly has important implications for risk assessment. Biogenic residues are not considered in the definition of bound residues and their exclusion may lead to overestimation of the risk bound residues pose to the environment (33, 34).

The effects of microbial activity may also depend on the pesticide in question. Irreversible sorption has been reported to occur in a number of studies in which sodium azide (NaN_3) was applied to minimize bacterial growth and biodegradation (3, 17, 18). As no degradation was found to occur during the experimental time-frames of these studies, this suggests that the fractions of irreversible sorption reported refer only to parent material. All three studies attributed the occurrence of irreversible sorption to some form of physical entrapment or matrix deformation, such that adsorption and desorption were occurring to and from different physical environments. However, Chen *et al.* (3) and Yu *et al.* (17) used only very short adsorption and desorption times (24 and ≤ 96 hours, respectively), suggesting that the irreversible fractions observed are unlikely to be truly irreversible. Sander and Pignatello (18) used considerably longer adsorption (140 days) and desorption (87 days) periods, however they concluded that although a small fraction of pesticide desorbs extremely slowly, it is too early to conclude that it is permanently trapped. Therefore, this evidence suggests that at this stage it is necessary to include both parent and non-parent materials in the definition of bound residues. As bound residues can only be quantified using ^{14}C -labelled compounds, little knowledge of their chemical identity is ever revealed (23, 34). Therefore the chemical identity of bound residues is still uncertain as is their irreversible status. Relative to the parent material, non-parent material may be more likely to take part in similar irreversible binding reactions, although this will depend on the chemical structure of the pesticide in question.

Experiments To Quantify Irreversibility in Pesticide Sorption-Desorption in Soil

The study of irreversible sorption behavior presents complex experimental challenges. Quantifying irreversible sorption first requires identifying the fraction of pesticide taking part in slowly reversible (non-equilibrium or kinetic) sorption, ideally by methods that do not result in an operational definition or alter the structure of the soil matrix. Quantification of the slowly reversible fraction also typically requires prohibitive experimental time-frames to be observed in order to reach desorption endpoints. Secondly, degradation of the parent material is a further complicating factor due to the protracted time-scales often involved, and must be measured in order to generate an accurate mass balance. There is no scientific consensus that recognizes a standard experimental method to

address these complex experimental challenges. An approach with the ability to differentiate between the two sorption processes would be a valuable tool for improving the accuracy of pesticide fate models and development of such a method has been the subject of much research and discussion.

Experimental methods and techniques to quantify and/or characterize non-desorbed pesticide residue have been discussed in detail by Northcott and Jones (4). The authors categorized the techniques into the following groups: (i) quantitative methods e.g. solvent extraction procedures that aim to extract pesticide residues from the soil and provide numerical estimates of the irreversible fraction; (ii) diagnostic methods e.g. electron spin resonance (ESR), fourier transform infra-red (FTIR) and nuclear magnetic resonance (NMR) that aim to qualitatively determine the nature of bound residue interactions rather than the amount; and (iii) indirect experimental methods e.g. hydrolysis methods, derivatisation extraction, model compound investigations, pyrolysis and thermal desorption techniques used for isolation and fractionation of soil humic substances in order to characterize the nature of the non-desorbed pesticide residue (4). Some examples of such studies are summarized in the following section.

Experimental Examples

Burauel and Führ (10) used outdoor lysimeter studies to observe the formation and long-term fate of non-extractable residues. They separately applied three pesticides, two polycyclic aromatic hydrocarbons (PAHs) and two polychlorinated biphenyls (PCBs) to orthic luvisols that contained either post-emergent winter wheat, pre-emergent maize or post-emergent summer wheat. They then used an optimal extraction method for each compound, always starting with a 24-hour extraction using 0.01M CaCl₂ and then using progressively harsher solvent extractions. A microcosm study carried out by Mordaunt *et al.* (11) characterised the formation of bound residues over 91 days for atrazine, dicamba, isoproturon, lindane, paraquat and trifluralin. The extractability of the adsorbed pesticide was determined using a sequential extraction procedure, with increasing strength of solvent (0.01M CaCl₂ < acetonitrile:water (9:1) < methanol < dichloromethane) to simulate readily available and potentially available fractions. The soils were finally combusted to complete the mass balance.

Gevao *et al.* (35) assessed the bioavailability of non-extractable (bound) pesticide residues to earthworms using a Soxhlet extraction. Soils treated with ¹⁴C-labelled atrazine, dicamba and isoproturon were incubated for 100 days and then subjected to exhaustive Soxhlet extractions with methanol and dichloromethane. Clean soil was then added to the extracted soil in the ratio of 7:1 to increase the volume. After earthworms had lived in these previously extracted soils for 28 days, 0.02-0.2% of previously bound ¹⁴C activity was adsorbed into earthworm tissue, showing that soil-bound residues can be bioavailable to earthworms, albeit at very low percentages. This supports speculation that soil-bound residues are not excluded from environmental interactions and processes. The authors also found that the presence of earthworms in soils suppressed the formation of bound residues.

A study by Dec *et al.* (27) used a silylation procedure and $^{13}\text{C-NMR}$ -spectroscopy to measure bound residue formation for the fungicide cyprodinil. Soils were incubated with either a low-concentration ($3 \mu\text{g mL}^{-1}$) or high-concentration ($500 \mu\text{g mL}^{-1}$) of cyprodinil for 6 months; the bound residue fractions amounted to approximately 50% and 18% of the initial radioactivity, respectively. The isolated humic acid fraction and the NaOH-extracted soil (the humin fraction) were suspended in chloroform and silylated by overnight shaking with trimethylchlorosilane. Analysis of the silylated extracts by $^{13}\text{C-NMR}$ revealed that the formation of bound residue in the $500 \mu\text{g mL}^{-1}$ samples involved: (i) sequestration of the unaltered or slightly altered fungicide in the humin fraction; and, (ii) cleavage of the cyprodinil molecule between the aromatic rings with subsequent covalent binding of the separated moieties to humic acid.

Loiseau and Barriuso (28) characterised the formation of bound residues for atrazine using fractionation techniques for soil organic matter. The authors incubated soil samples in the laboratory for 56 days. Soil samples were either sterilized (i.e. soil microflora absent) or unsterilized (i.e. soil microflora present). The fraction of bound residue formed ranged from 10-40%, with the greater fractions of bound residue formed in the soil samples where the soil microflora was present. Soil size fractionation was followed by alkaline extraction, before and after treatment with hydrogen fluoride; acid hydrolysis with 2M hydrochloric acid in reflux conditions was then applied to the soils containing bound residues. Most of the bound residue was found to be in the finest fraction ($< 20 \mu\text{m}$) that contained the humified organic matter (from 61-77% of the total bound residue), and between 78 and 89% was solubilized during the different steps of the chemical fractionation procedure. Between 20-50% of the bound residue fraction was identified as intact atrazine and its main derivatives, indicating that this proportion of the bound residue was probably formed by entrapment in voids of the soil organic matter. Between 13 and 30% of the bound residue was associated with humic acids. The ability of microorganisms to mineralize the triazine ring augments the formation of bound residues via generation of reactive transformation products. A soil $\text{pH} < 6$ favours the formation and stabilization of hydroxylated derivatives of atrazine and a high content of humic acids favours the formation of chemically bound residues.

Many experiments quantifying bound residues, non-extractable residues and irreversible sorption have used exhaustive extraction procedures of varying harshness. There is a general consensus that although the results of such solvent-extraction studies reflect potential behaviors of the compounds and their metabolites in the environment, the fraction of non-extractable compound still remains operationally-defined by the chosen extraction procedure (11). Thus, it will always be possible to obtain better recoveries of compound where availability of technique, time and cost is of no consideration. The soil used in the experimental system no longer represents natural soil as the use of organic solvents in soil extractions dramatically change the soil structure (11). This occurs due to the removal of both soil water and a large part of the organic matter (usually the more soluble humic acids) from the soil matrix. Therefore, the non-extractable fraction determined using such methods may only be of limited relevance to natural soils. A more sensible approach would be to adopt a more

“natural” extraction (i.e. one that mimics solutions likely to be present in the soil), giving a resultant bound residue likely to be representative of field conditions (35). Thus, the use of isotopes, mainly ^{14}C , have played an important role in characterizing pesticide exchange kinetics.

Isotope Exchange

A promising experimental method developed by Celis and Koskinen (14, 15) and later adopted by Sander and Pignatello (19) is the isotope exchange technique, which characterizes pesticide exchange kinetics *in-situ*. The isotope exchange technique involves the use of both ^{12}C - and ^{14}C -labelled pesticide, which are initially applied to soils separately. Following the adsorption period, ^{12}C - and ^{14}C -pesticide supernatants are then exchanged between corresponding samples (Figure 1).

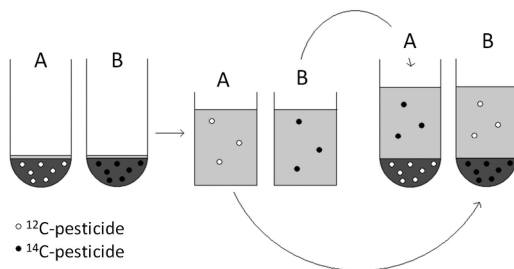


Figure 1. The isotope exchange technique.

The subsequent exchange between ^{12}C - and ^{14}C -pesticide is then observed during a specific length of time in order to characterize the kinetics of pesticide exchange and provide an estimation of the amount of sorbed pesticide that was not taking part in the exchange. Celis and Koskinen’s method eliminates inherent experimental artifacts of other approaches such as the specific effectiveness of the extracting method and changes to the sorption matrix. However, taking into account the recent advances in knowledge in both sorption-desorption kinetics and irreversibility in the sorption-desorption process, it would seem unlikely that true irreversible sorption could be measured after the three-day period considered by the authors. Sander and Pignatello (18, 19) also carried out isotope exchange experiments, which they considered a promising method to unequivocally establish whether sorbate entrapment occurs during a sorption-desorption cycle. Sander and Pignatello (18, 19) used equilibration times of up to 140 days with the objective of ensuring sorption equilibrium in their forward isotope exchange experiment with the persistent hydrocarbons naphthalene and 1,4-dichlorobenzene.

An isotope exchange experiment was also carried out by Suddaby (36) using three test compounds and soils to establish whether isotope exchange techniques are an effective measure of physical irreversibility in pesticide sorption-desorption to soils over time; and if present, whether the irreversibly bound fraction of pesticide changes over time, or is influenced by pesticide and soil type. The three pesticides were selected to have a range in sorption properties; they comprised chlorotoluron (equilibration time of up to 56 days, 14-day isotope exchange), prometryn (equilibration time of up to 168 days, 14-day isotope exchange), and hexaconazole (equilibration time of up to 168 days, 14-day isotope exchange). The experiments were carried out with three soils (Blackwood, Andover, Salop series) with different clay contents and pH. The soils were sterilized to control degradation, thus only the parent compound was taking part in the exchange between the soil and solution. Sorption equilibrium was not reached during the equilibration time for all pesticide-soil systems studied, even after 168 days. As a result, further adsorption was observed rather than isotope exchange during the 14-day exchange period. Thus the isotope exchange method is not powerful enough to discriminate between slowly reversible and irreversible sorption due to the protracted time-scales involved in reaching true equilibrium.

A new forced isotope exchange procedure, involving the addition of a high-concentration ^{12}C -pesticide solution was developed by Suddaby (36) and tested for the same pesticide-soil combinations. The forced isotope exchange technique aims to characterize the fraction of irreversible sorption that is relevant under field conditions. Forced isotope exchange was carried out over extended time scales following adsorption up to 168 days and the 14-day isotope exchange phase. The procedure assumes that the capacity of a soil to adsorb a pesticide has a saturation point. Repeated influx of high-concentration ^{12}C -pesticide over time ensures that competition for sorption to soil between ^{12}C - and ^{14}C -pesticide is increasingly biased towards the former. The supply of ^{12}C -pesticide to the soil surface to take part in sorption is essentially instantaneous with desorption the rate-limiting step. Thus, as ^{12}C -pesticide occupies all available sorption sites by out-competing any available ^{14}C -pesticide, it is possible to identify, through measurement of ^{14}C -pesticide in solution, the proportion of sorbed ^{14}C -pesticide available for desorption and hence the proportion of ^{14}C -pesticide not taking part in the sorption-desorption process.

All compounds showed a similar desorption profile and that of chlorotoluron is shown as an example. The bulk of total recoverable ^{14}C -chlorotoluron was extracted with the first addition of ^{12}C -chlorotoluron (average 25% Blackwood, 42% Andover and 21% Salop after 1 d; Figure 2). This was followed by a gradual decline in ^{14}C -chlorotoluron recovery over time, which finally reached <1% recovery of initial for the Blackwood and Andover soils and 2% for the Salop soil between 161 and 204 days. It should also be noted that in each case the forced exchange was still releasing small amounts of ^{14}C -pesticide from soil (particularly the Salop soil) at the end of the process, albeit at very slow rates. Thus, desorption endpoints had still not been reached even after 204 days.

At the end of the desorption procedure, soils were extracted with solvent and then combusted. The mass balance for chlorotoluron is shown in Figure 3. The three extractable fractions characterized by Figure 3 show the relative amounts

of ^{14}C -chlorotoluron desorbed from the soil when the harshness of the extraction was increased in the order: solvent > forced isotope exchange > isotope exchange. Further analysis revealed the irreversible fraction, proportion of metabolite(s) and a fraction unaccounted for by the chemical analyses.

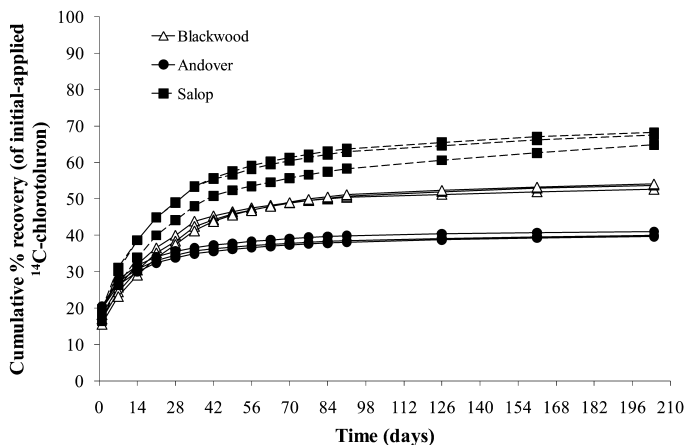


Figure 2. Cumulative percentage recovery of initial ^{14}C -chlorotoluron applied using the forced isotope exchange method. Samples are initially ^{14}C with 56-days sorption and isotope exchange for 14-days (3 replicates per soil).

A three-site sorption model was also developed to assess whether the data generated by isotope exchange and forced isotope exchange experiments is sufficient to disentangle non-equilibrium and irreversible sorption, and is discussed in the following section.

Modeling Approaches To Quantify Irreversibility in Pesticide Sorption-Desorption in Soil

Mathematical modeling provides an important means to anticipate, and thereby minimize, potentially adverse impacts to non-target environmental compartments. The development and validation of mathematical models with the power to accurately assess pesticide fate in the environment is a complicated task. The sorption of organic chemicals in soils is kinetically controlled by rate-limiting processes. As a consequence, a number of attempts have been made to model non-equilibrium and irreversible sorption processes mathematically. These will be summarized in the following sections, building on existing literature reviews (37–41).

Irreversible sorption cannot be modeled without instantaneous and/or non-equilibrium sorption sites. Therefore, the following modeling section discusses the most commonly used approaches for modeling non-equilibrium sorption and irreversible sorption.

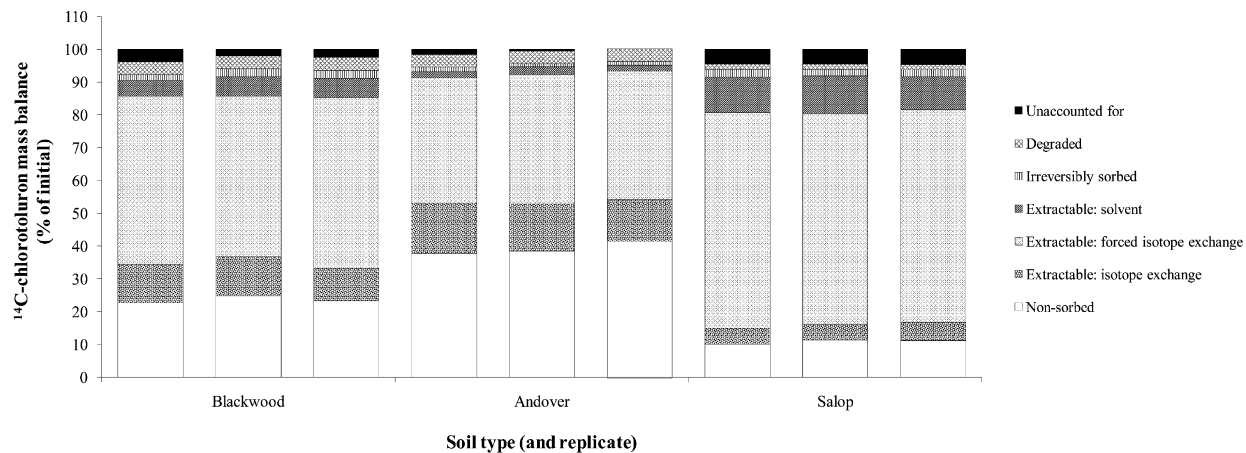


Figure 3. Mass balance of initially-applied ^{14}C -chlorotoluron to nine soil samples adsorbed for 56-days. Three replicate samples per soil type are shown. The non-sorbed fraction reflects ^{14}C -chlorotoluron present in the aqueous phase after the adsorption period, whilst that which partitioned to the soil is collectively represented by the three extractable fractions and irreversibly sorbed fraction.

Mass Transfer Models

Mass transfer models assume that the sorbent is comprised of one or multiple sorption sites or domains (42). Solute movement between the different sites or domains is usually assumed to follow first-order reaction kinetics, though second-order kinetics have also been used (43). Rate-limited transfer processes are generated by either: (i) transport-related (physical) non-equilibrium; or (ii) sorption-related non-equilibrium (44). Transport-related (physical) non-equilibrium is caused by heterogeneous flow domains (e.g. aggregates and macropores); their rate-limited effect on solute transport has been well documented (44–46). Sorption-related non-equilibrium results from either chemical non-equilibrium (e.g. chemisorption) or rate-limited diffusive mass transfer processes (44). Since the sorption of several organic compounds is usually driven by partitioning between the soil solution and soil organic matter, chemical non-equilibrium effects are usually disregarded (44).

Two major mass transfer modeling approaches have been established: (i) mobile-immobile (two-region) models; and, (ii) two-site and multi-site models. Modeling approaches used to incorporate irreversible sorption will also be considered.

Mobile-Immobile (Two-Region) Models

Mobile-immobile (two-region) models explain non-equilibrium behavior by assuming that the soil matrix consists of two types of regions: (i) a region where the soil water is mobile; and, (ii) a region where the soil water is immobile. Deans (47) was amongst the earliest to conceptualize the soil matrix in terms of mobile and immobile regions. van Genuchten and Wierenga (48) also proposed a model where the soil water is divided into mobile and immobile regions. Convective-dispersive solute transport is limited to the mobile soil water region and diffusive mass transfer processes control the rate of pesticide adsorption-desorption within the immobile soil water region (49). Ma and Selim (37) have also provided equations to describe solute movement in mobile and immobile regions of the soil water. The difficulty in using mobile-immobile (two-region) models however, is the uncertainty involved in defining the relative size of mobile and immobile domains (37).

Two-Site Models and Multi-Site Models

Two-site models (or two-stage models) are the simplest form of a multi-site model. It should be noted that two-site models are mathematically indistinguishable from mobile-immobile (two-region) models, described in the previous section. In a two-site model, the soil matrix is divided into two types of sorption sites: (i) sites where sorption reactions occur instantaneously (equilibrium sorption); and, (ii) sites where sorption reactions are rate-limited

and occur kinetically, proceeding as a first-order reaction (40, 50). The faster sorption reactions are assumed to occur on easily accessible sites e.g. the outer surface of soil aggregates, with the slower sorption reactions postulated to occur on less accessible sorption sites situated within the soil organic matter (41). Solute transfer between the fast and slow sorption sites is described by kinetically-controlled reactions (50–52). Degradation may also be integrated into two-site models, operating at either one or both types of sorption sites (53).

The two-site approach has been used in the leaching model PEARL (54) and in the PEARLNEQ software for predicting parameters to describe long-term sorption kinetics (55). Solute sorbed at equilibrium sites is assumed to be constantly at equilibrium and the solute sorbed at non-equilibrium sites is described by a pseudo first-order sorption rate equation (55). Degradation is only assumed to affect the solute sorbed at equilibrium sites. A similar approach to non-equilibrium sorption has also been implemented into the pesticide leaching model MACRO (56), though degradation in this model is described by four separate first-order kinetic rate coefficients (solid and liquid, micro- and macropores).

The assumption of only two sorption sites oversimplifies soil systems. Boesten *et al.* (57) for example, found it was necessary to include three sorption sites in order to adequately describe their data: (i) sites where sorption reactions occur instantaneously; (ii) sites where sorption reactions occur kinetically using a time-scale of days; and, (iii) sites where sorption reactions occur kinetically using a time-scale of hundreds of days. Saffron *et al.* (58) considered three types of desorption regimes: (i) a fast or instantaneous regime, where desorption occurs at rates not captured by the first few sampling points; (ii) a dynamic regime in which rates are well measured by the sampling scheme; and, (iii) a slow regime where rates are slower than can be measured given the combination of data uncertainty and duration of sampling. They found that although naphthalene desorption was best described by two regimes, all three regimes were required to adequately describe the desorption behavior of atrazine. Although in reality there are multiple sorption sites, each with different rates of sorption, obtaining sufficient experimental data to adequately parameterize such models is challenging (41).

Irreversible Sorption Models

In an irreversible sorption model, the rate of desorption from one type of sorption site is set to zero. Selim and Amacher (43) proposed the use of a second-order kinetic approach to describe solute retention during transport in soils; their model incorporated three different sorption sites, two reversible (S_1 , S_2) and one irreversible (S_{irr}). They used five adsorption-desorption rate constants in total (though the rate of desorption from the irreversible site (S_{irr}) is zero). Prata *et al.* (59) fitted atrazine breakthrough curves with a three-site chemical non-equilibrium convective-dispersive transport model considering irreversible sorption. The three-site non-equilibrium model predicted that around 40% of the applied atrazine was irreversibly sorbed at the end of the leaching experiment, which corresponded with the sum of their measured extractable and non-extractable fractions.

Celis and Koskinen (14, 15) also considered irreversible sorption in their two-site model. They assumed that sorption occurred on either easily desorbable sites or irreversible sites. When the authors fitted the model to the data from the isotope-exchange experiments described above, the model estimated that approximately 10% of sorbed pesticide was irreversibly bound. Suddaby *et al.* (60) re-analysed Celis and Koskinen's data using a three-site sorption model (Figure 4). Its purpose was to simulate: (i) instantaneous exchange between solution and soil in the equilibrium phase; (ii) slow but reversible binding on non-equilibrium sites and (iii) slow movement from non-equilibrium sites to irreversible sites.

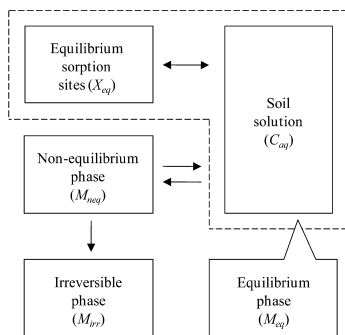


Figure 4. Schematic representation of the three-site model. The equilibrium phase (M_{eq}) includes both the concentration ($\mu\text{g mL}^{-1}$) of pesticide in the soil solution (C_{aq}) and the pesticide sorbed ($\mu\text{g g}^{-1}$) at equilibrium sites (X_{eq}). Reproduced with permission from Suddaby *et al.* (60). Copyright 2013 American Chemical Society.

The equations used to apply the three-site sorption model to Celis and Koskinen's isotope exchange data are described in detail in Suddaby *et al.* (60); only an outline of the mathematical is described here. The quantity of pesticide sorbed at equilibrium sites (X_{eq}) was derived using the following equation:

$$X_{eq} = K_{feq} C_{aq}^{1/n}$$

where K_{feq} is the Freundlich sorption distribution coefficient and $1/n$ is the Freundlich exponent, describing sorption nonlinearity with increasing solute concentration. The quantity of pesticide sorbed at equilibrium sites (X_{eq}) is then used to determine the mass of pesticide in the equilibrium phase (M_{eq}):

$$M_{eq} = (V_{sol} C_{aq}) + (M_{soil} X_{eq})$$

where the parameters V_{sol} and M_{soil} , respectively refer to the volume of solution and mass of soil used in the experimental system. The following differential equations were used to calculate the masses of pesticide in the nonequilibrium (M_{neq}) and irreversible phases (M_{irr}) of sorption:

$$\frac{dM_{\text{neq}}}{dt} = (k_{\text{des}}F_{\text{neq}}K_{\text{feq}}C_{\text{aq}}^{1/n}) - (k_{\text{des}}M_{\text{neq}}) - (k_{\text{irr}}M_{\text{neq}})$$

$$\frac{dM_{\text{irr}}}{dt} = k_{\text{irr}}M_{\text{neq}}$$

where k_{des} is the desorption or exchange rate, F_{neq} is the ratio of sorption in the nonequilibrium phase to sorption in the equilibrium phase and k_{irr} is the rate of irreversible sorption. The experimental method necessitates that the three-site model is applied four times per pesticide in order to predict the behavior of both ^{12}C and ^{14}C isotopes individually during the sorption phase and then simultaneously after supernatant exchange. Application of the three-site model to Celis and Koskinen's data showed that experimental observations could be described by instantaneous and non-equilibrium sorption behavior alone and without the need to invoke an additional irreversible sorption component (60).

However, the irreversible sorption model was also applied to the adsorption, isotope exchange and forced isotope exchange datasets described earlier, obtained for chlorotoluron, prometryn and hexaconazole by Suddaby (36). For these datasets, the irreversible sorption sites had to be included to describe the data (Figure 5). Furthermore, the fraction of irreversible sorption at the end of the experiments estimated by the model was larger than the measured fraction. This highlights the difficulty in including irreversible sorption in pesticide sorption models, as it is difficult to obtain detailed experimental data accurate enough to support the necessary additional model parameters.

Diffusion Models

These models are based on the assumption that sorption can be described in terms of diffusion through the spherical geometry of the sorbent, usually based on Fick's law (40, 42). Ma and Selim (42) have established complex diffusion equations based on several aggregate geometries (rectangular, solid and hollow cylindrical aggregates) by introducing a time-dependent phase transfer constant in addition to the diffusion coefficient. van Beinum *et al.* (61) and Altfelder and Streck (2) have both used diffusion models to simulate time-dependent sorption. van Beinum *et al.* (61) were able to effectively describe the radial diffusion of pesticide into lignin particles and its subsequent desorption. Altfelder and Streck (2) compared a first-order and spherical diffusion model to describe and predict the long-term sorption and desorption processes of chlorotoluron in two soils; they found that the spherical diffusion model performed better than the first-order model. Diffusion models based on well-defined geometry are difficult to apply to a field situation, since they require information relating to the geometry of structural units, which are rarely available (42).

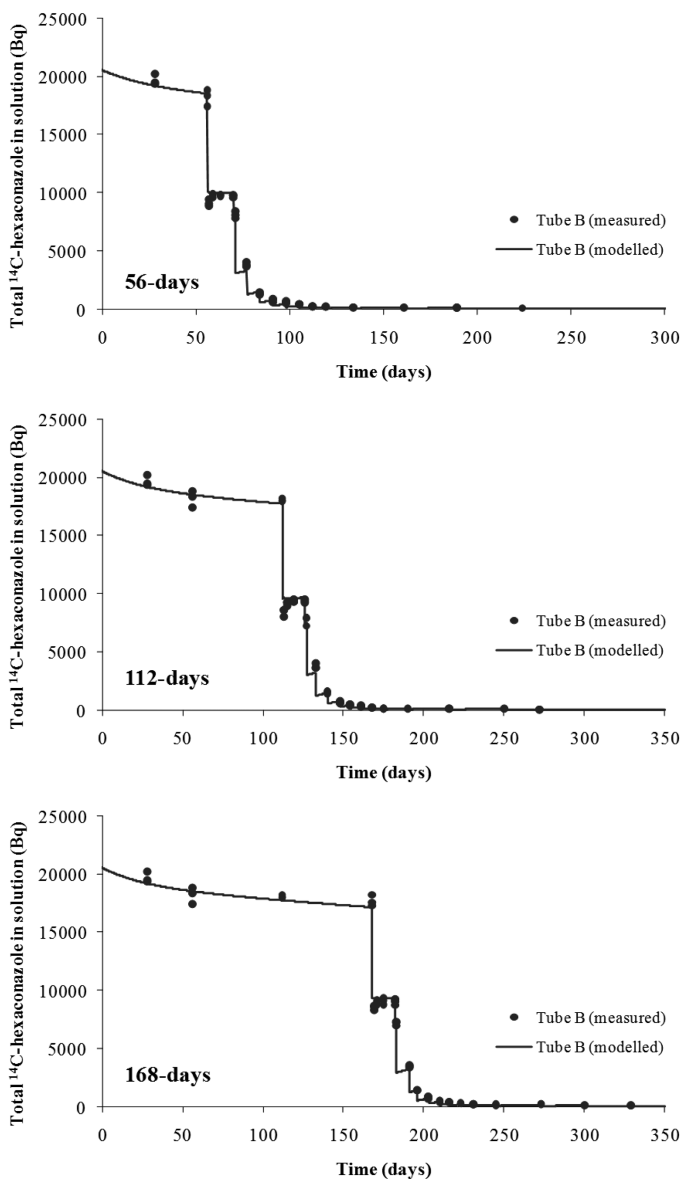


Figure 5. Example of irreversible model fit to the hexaconazole adsorption, isotope exchange and forced isotope exchange data for the Blackwood soil, after 56, 112 and 168 days of adsorption, 14 days isotope exchange and 147 days for forced isotope exchange. Data are plotted in triplicate.

Chapter Summary

Adsorption-desorption is not a simple instantaneous equilibrium process as previously thought, or assumed by many contaminant transport models. As well as time-dependent sorption interactions, some sorbed pesticide has been observed to exist in an irretrievable, soil-bound state. This fraction has important implications for pesticide leaching and bioavailability. Although this fraction of sorbed pesticide is termed irreversible sorption in principle, many variations of this term exist within the literature. This is the result of the operational definition of such residues, which means that their quantification is dependent on the method of extraction. Therefore, the terms bound residue and non-extractable residue are commonly used in order to express uncertainty in the true fraction of irreversibly sorbed pesticide. The mechanisms responsible for irreversible sorption are proposed to include covalent bonding and physical entrapment and a proportion may also be biogenic in nature.

Irreversible sorption is not considered in any of the existing regulatory models to determine predicted environmental pesticide concentrations in soil and water due to difficulties in deriving the parameters. Slowly reversible sorption and irreversible sorption are difficult to separate experimentally (41). Very slow desorption kinetics can give the impression that the sorbed pesticide is irreversibly bound, though it is instead an effect of an experimental time-frame that is not long enough to observe desorption end-points (41). Time-dependent sorption can be used at higher tiers of the regulatory risk assessment but no harmonized methodology exists.

Although many experimental methods and techniques to quantify and/or characterize non-desorption pesticide residue exist, a standardized procedure to adequately distinguish between slowly reversible and irreversible sorption has not yet been accepted within the scientific community. The isotope exchange technique, developed by Celis and Koskinen (14, 15) was repeated by Suddaby *et al.* (36, 60) who found that the method is not powerful enough to differentiate between slowly reversible and irreversible sorption as a result of the long time scales required to reach true sorption equilibrium. Suddaby *et al.* (36, 60) developed a new forced isotope exchange technique and tested the method for three pesticides and soils. Forced isotope exchange is a promising technique for estimating the proportion of sorbed pesticide taking part in irreversible sorption. However, for the tested compounds and soils the forced isotope exchange method showed that under abiotic conditions sorption is largely reversible, but desorption occurred over exceptionally long time-scales. Irreversible sorption is likely to occur to a greater extent in the presence of an active soil microbial community.

Acknowledgments

Part of this manuscript was undertaken as part of a PhD at the University of York funded by EPSRC and Syngenta (Jealott's Hill International Research Centre).

References

1. Barriuso, E.; Benoit, P.; Dubus, I. G. *Environ. Sci. Technol.* **2008**, *42*, 1845–1854.
2. Altfelder, S.; Streck, T. *J. Contam. Hydrol.* **2006**, *86*, 279–298.
3. Chen, Y.-X.; Chen, H.-L.; Xu, Y.-T.; Shen, M.-W. *Environ. Int.* **2004**, *30*, 31–37.
4. Northcott, G. L.; Jones, K. C. *Environ. Pollut.* **2000**, *108*, 19–43.
5. Gevao, B.; Jones, K. C.; Semple, K. T. *Environ. Pollut.* **2005**, *133*, 17–24.
6. Führ, F.; Ophoff, H.; Burauel, P.; Wanner, U.; Haider, K. In *Modification of Definition of Bound Residues*; Fuhr, F., et al., Eds.; Wiley-VCH: Weinheim, 1998; pp 175–176.
7. Roberts, T. R.; Klein, W.; Still, G. G.; Kearney, P. C.; Drescher, N.; Desmoras, J.; Esser, H. O.; Aharonson, N.; Vonk, J. W. *Pure Appl. Chem.* **1984**, *56*, 945–956.
8. Gevao, B.; Semple, K. T.; Jones, K. C. *Environ. Pollut.* **2000**, *108*, 3–14.
9. Calderbank, A. *Rev. Environ. Contam. Toxicol.* **1989**, *108*, 72–103.
10. Burauel, P.; Führ, F. *Environ. Pollut.* **2000**, *108*, 45–52.
11. Mordaunt, C. J.; Gevao, B.; Jones, K. C.; Semple, K. T. *Environ. Pollut.* **2005**, *133*, 25–34.
12. Wanner, U.; Führ, F.; deGraaf, A. A.; Burauel, P. *Environ. Pollut.* **2005**, *133*, 35–41.
13. Alexander, M. *Environ. Sci. Technol.* **1995**, *29*, 2713–2717.
14. Celis, R.; Koskinen, W. C. *J. Agric. Food. Chem.* **1999a**, *47*, 782–790.
15. Celis, R.; Koskinen, W. C. *Soil Sci. Soc. Am. J.* **1999b**, *63*, 1659–1666.
16. Burgos, W. D.; Novak, J. T.; Berry, D. F. *Environ. Sci. Technol.* **1996**, *30*, 1205–1211.
17. Yu, X.; Pan, L.; Ying, G.; Kookana, R. S. *J. Environ. Sci.* **2010**, *22*, 615–620.
18. Sander, M.; Pignatello, J. J. *Environ. Toxicol. Chem.* **2009**, *28*, 447–457.
19. Sander, M.; Pignatello, J. J. *Environ. Sci. Technol.* **2005**, *39*, 7476–7484.
20. Kan, A. T.; Fu, G.; Tomson, M. B. *Environ. Sci. Technol.* **1994**, *28*, 859–867.
21. Huang, W.; Weber, W. J. *Environ. Sci. Technol.* **1997**, *31*, 2562–2569.
22. Reid, B. J.; Jones, K. C.; Semple, K. T. *Environ. Pollut.* **2000**, *108*, 103–112.
23. Barraclough, D.; Kearney, T.; Croxford, A. *Environ. Pollut.* **2005**, *133*, 85–90.
24. Kan, A. T.; Chen, W.; Tomson, M. B. *Environ. Pollut.* **2000**, *108*, 81–89.
25. Katayama, A.; Bhula, R.; Burns, G. R.; Carazo, E.; Felsot, A.; Hamilton, D.; Harris, C.; Kim, Y.-H.; Kleter, G.; Koedel, W.; Linders, J.; Peijnenburg, J. G. M. W.; Sabljic, A.; Stephenson, R. G.; Racke, D. K.; Rubin, B.; Tanaka, K.; Unsworth, J.; Wauchope, R. D. *Rev. Environ. Contam. Toxicol.* **2010**, *203*, 1–86.
26. Barriuso, E.; Benoit, P. Available: http://www.eu-footprint.org/downloads/FOOTPRINT_DL5.pdf; 2006.
27. Dec, J.; Haider, K.; Schäffer, A.; Fernandes, E.; Bollag, J. M. *Environ. Sci. Technol.* **1997**, *31*, 2991–2997.
28. Loiseau, L.; Barriuso, E. *Environ. Sci. Technol.* **2002**, *36*, 683–689.

29. Reuter, S.; Ilim, M.; Munch, J. C.; Andreux, F.; Scheunert, I. *Chemosphere* **1999**, *39*, 627–639.
30. Wang, H.; Ye, Q.; Yue, L.; Yu, Z.; Han, A.; Yang, Z.; Lu, L. *Chemosphere* **2009**, *76*, 1036–1040.
31. Chilom, G.; Bestetti, G.; Sello, G.; Rice, J. A. *Chemosphere* **2004**, *56*, 853–860.
32. Richnow, H. H.; Seifert, R.; Hefter, J.; Link, M.; Francke, W.; Schaefer, G.; Michaelis, W. *Org. Geochem.* **1997**, *26*, 745–758.
33. Nowak, K. M.; Miltner, A.; Gehre, M.; Schäffer, A.; Kästner, M. *Environ. Sci. Technol.* **2010**, *45*, 999–1006.
34. Kästner, M.; Streibich, S.; Beyrer, M.; Richnow, H. H.; Fritsche, W. *Appl. Environ. Microbiol.* **1999**, *65*, 1834–1842.
35. Gevao, B.; Mordaunt, C. J.; Semple, K. T.; Pearce, T. G.; Jones, K. C. *Environ. Sci. Technol.* **2001**, *35*, 501–507.
36. Suddaby, L. A. PhD. Thesis, University of York, York, 2012.
37. Ma, L.; Selim, H. M. In *Advances in Agronomy*; Sparks, D. L., Ed.; Academic Press: San Diego, 1997; pp 95–150.
38. Scow, K. M.; Johnson, C. R. In *Advances in Agronomy*; Sparks, D. L., Ed.; Academic Press: San Diego, 1997; pp 1–56.
39. Pignatello, J. J. In *Advances in Agronomy*; Sparks, D. L., Ed.; Academic Press: San Diego, 2000; pp 1–73.
40. Maraqa, M. A. *J. Contam. Hydrol.* **2001**, *53*, 153–171.
41. van Beinum, W.; Beulke, S.; Boesten, J.; ter Horst, M. *Research report for DEFRA project PS2235*; Food and Environment Research Agency (FERA) and Alterra: York, U.K./Wageningen, The Netherlands, 2010.
42. Fortin, J.; Flury, M.; Jury, W. A.; Streck, T. *J. Contam. Hydrol.* **1997**, *25*, 219–234.
43. Selim, H. M.; Amacher, M. C. *Water Resour. Res.* **1988**, *24*, 2061–2075.
44. Brusseau, M. L.; Jessup, R. E.; Rao, P. S. C. *Environ. Sci. Technol.* **1991**, *25*, 134–142.
45. Brusseau, M. L.; Rao, P. S. C. *Geoderma* **1990**, *46*, 169–192.
46. Jarvis, N. J. *Eur. J. Soil Sci.* **2007**, *58*, 523–546.
47. Deans, H. H. *Soc. Petrol Eng. J.* **1963**, *3*, 49–52.
48. van Genuchten, M. T.; Wierenga, P. J. *Soil Sci. Soc. Am. J.* **1976**, *40*, 473–480.
49. Rao, P. S. C.; Jessup, R. E. *Ecol. Model.* **1982**, *16*, 67–75.
50. van Genuchten, M. T.; Wagenet, R. J. *Soil Sci. Soc. Am. J.* **1989**, *53*, 1303–1310.
51. Streck, T.; Poletika, N.; Jury, W. A.; Farmer, W. J. *Water Resour. Res.* **1995**, *31*, 811–822.
52. Heistermann, M.; Jene, B.; Fent, G.; Feyerabend, M.; Seppelt, R.; Richter, O.; Kubiak, R. *Pest. Manage. Sci.* **2003**, *59*, 1276–1290.
53. Guo, L.; Jury, W. A.; Wagenet, R. J.; Flury, M. *J. Contam. Hydrol.* **2000**, *43*, 45–62.
54. Leistra, M.; van der Linden, A. M. A.; Boesten, J. J. T. I.; Tiktak, A.; van den Berg, F. *PEARL model for pesticide behaviour and emissions in soil-plant systems*; Description of processes; Alterra report 13, RIVM report 711401009; Alterra: Wageningen, 2001; pp 1–117.

55. Boesten, J. J. T. I.; Tiktak, A.; van Leerdam, R. C. 2007 available at http://www.pearl.pesticidemodells.eu/pdf/usermanual_pearl_neq_4.pdf.
56. Larsbo, M.; Jarvis, N. *Emergo: Studies in the Biogeophysical Environment*; Swedish University of Agricultural Sciences: Uppsala, Sweden, 2003; pp 1–52.
57. Boesten, J. J. T. I.; Van Der Pas, L. J. T.; Smelt, J. H. *Pestic. Sci.* **1989**, *25*, 187–203.
58. Saffron, C. M.; Park, J.-H.; Dale, B. E.; Voice, T. C. *Environ. Sci. Technol.* **2006**, *40*, 7662–7667.
59. Prata, F.; Lavorenti, A.; Vanderborght, J.; Burauel, P.; Vereecken, H. *Vadose Zone J.* **2003**, *2*, 728–738.
60. Suddaby, L. A.; Beulke, S.; van Beinum, W.; Celis, R.; Koskinen, W.; Brown, C. D. *J. Agric. Food. Chem.* **2013**, *61*, 2033–2038.
61. van Beinum, W.; Beulke, S.; Brown, C. D. *Environ. Sci. Technol.* **2006**, *40*, 494–500.

Chapter 12

Sorption of Pesticides and its Dependence on Soil Properties: Chemometrics Approach for Estimating Sorption

Rai S. Kookana,^{*,1} Riaz Ahmad,^{2,3} and Annemieke Farenhorst⁴

¹CSIRO Land and Water, and University of Adelaide, PMB No. 2,
Glen Osmond, SA 5064, Australia

²Department of Soil Science & Soil Water Conservation,
Pir Mehr Ali Shah Arid Agriculture University,
Rawalpindi, Punjab, Pakistan

³Punjab Agricultural Research Board, Lahore, Punjab, Pakistan

⁴Department of Soil Science, University of Manitoba,
Winnipeg, MB R3T 2N2, Canada

*E-mail: Rai.Kookana@csiro.au.

Sorption is one of the major processes that determine the fate, effects, efficacy and ecological risks of pesticides in terrestrial and aquatic environments. In this chapter we provide an overview of sorption and its dependence on soil properties. Soil solid phase consists of mineral and organic matter; both in strong association with each other make a contribution towards sorption of pesticides, depending on their relative abundance in soil/sediments, chemistry and the chemical nature of the pesticide molecule. We discuss the roles of organic matter and clay contents as well their chemistries in determining sorption of pesticides, and assess the partition theory in terms of its adequacy in describing the observed sorption behavior of pesticides in soil. The complex interactions and heterogeneities associated with the soil solid phase contribute to the large degree of variation in K_{oc} , a parameter that is often used to extrapolate the pesticide sorption estimate, among soils. A more comprehensive approach incorporating soil organic matter as well as soil minerals (both contents as well as their chemistries) is therefore desirable to fully incorporate

the role of soil surfaces in sorption of organic compounds. Therefore, we introduce some emerging approaches based on chemometrics and infrared spectroscopy that appear promising for comprehensive representations of the combined role of organic matter, mineralogy and other soil properties in estimating pesticide sorption in soil.

Introduction

Sorption is one of the major processes that determine the fate, effects, and ecological risks of pesticides in terrestrial and aquatic environments. The sorption process commences as soon as a pesticide molecule comes in contact with soil/sediment and occurs mainly in the scale of hours. Other processes such as movement, persistence, efficacy, bioavailability, and ecotoxicity in the environment are often relatively slower and are affected by the sorption process. Therefore, the sorption parameter of a pesticide in soil is of fundamental importance in considering not only its effectiveness (and choosing appropriate application rate for a given soil type) but its potential risk to the environment.

In this chapter, we provide an overview of sorption and its dependence on soil properties. We discuss the role of organic matter and clays, their contents and chemistries in determining sorption behavior of pesticides. We scrutinize the validity of the partition theory in describing sorption behavior of pesticides purely on the basis of soil organic carbon content (SOC) alone. We also introduce emerging approaches, especially those based on chemometrics and infrared spectroscopy, that appear promising for comprehensive representations of the combined role of soil organic matter (SOM) and mineralogical properties of soils.

Pesticide Sorption Processes in Soil and Sediments

Uptake of organic molecules by a solid phase from a gaseous or liquid phase is generally referred to as adsorption. However, some organic compounds including non-ionic pesticides are also believed to exhibit a phase-partitioning process (absorption), akin to liquid-type interactions of two immiscible solvents. This is based on the assumption that the macromolecular SOM acts as an immiscible solvent leading to a partitioning process, similar to that between *n*-octanol and water. The octanol-water partitioning coefficient (K_{ow}) is commonly used to represent the hydrophobicity of a compound. Since the two processes (adsorption/absorption) are difficult to distinguish experimentally in soils and sediments, the term ‘sorption’ is preferred, which makes no distinction between absorption, adsorption and precipitation of organic compounds (1).

In addition to neutral compounds, many pesticides are ionic or ionizable in nature. Due to the presence of multiple functional groups, pesticide molecules can donate or accept protons depending on environmental conditions. The cationic, anionic or zwitterionic species are formed depending on the chemistry of the molecule and/or the pH of the surrounding environment. Sorption of pesticides

on a solid phase can involve a variety of mechanisms, ranging from London-van der Waals forces, hydrogen bonding, ligand exchange, ion exchange, cation-water bridging, covalent bonding and even physical trapping (1). Sorption from the perspective of sorbate as well as sorbent has been discussed by Pignatello (2), especially on organic carbon and black carbon in soils.

The extent of sorption by a solid phase is determined by the nature and properties of both sorbate (e.g. a pesticide) and sorbent (soil or sediment) as well as ambient conditions during the equilibrium process (e.g. temperature, water content). Chemical characteristics of the aqueous phase which are important for sorption processes include pH, ionic strength, and redox status, all of which affect surface properties of sorbent, interactions between liquid and solid phases, and the ionization state and reactivity of the sorbate. Indeed, liquid-solid interface characteristics can have important impact on sorbate-sorbent interactions.

Important Soil Properties Affecting Sorption

A number of soil properties including its chemistry, mineralogy, SOM, and pH, and environmental factors such as soil water content and temperature can influence pesticide sorption in soil. These soil properties are very important in determining the mechanisms of sorption and thereafter mobility of a pesticide in soil. Due to close association between the mineral and organic matter, it is often difficult to treat these as separate properties, in the context of sorption. Soils are inherently heterogeneous in nature and how variation of soil parameters influences the sorption interactions of pesticides is discussed below.

Organic Matter

Soil organic matter has been recognized as one of the most relevant soil properties in regulating sorption of non-ionizable pesticides (3, 4). Strong correlation has been frequently observed between sorption of non-ionizable pesticides and the SOM content (5). However, ionizable pesticides such as weakly basic triazines can be sorbed to both SOM and clay minerals, and the sorption is pH dependent (4). For non-ionic pesticides, the humified materials in soil, due to their oxygen-containing functional groups such as $-\text{COOH}$, phenolic, aliphatic, enolic, $-\text{OH}$, and $\text{C}=\text{O}$, have often been found to be good sorbents (6).

The content and the chemistry of SOM vary from soil to soil in terms of its polarity, elemental composition, aromaticity, condensation, and degree of diagenetic evolution from a loose polymer to condensed coal-like structures (7–10). Both the type and the age of SOM may affect sorption of pesticides. The type of vegetation from which the SOM originates affects its chemical composition and degree of decomposition (11). For example, humic materials of grassland soils are rich in humic acids, whereas fulvic acids dominate in forest soils (12). The O-alkyl C tends to decrease with decomposition, while the proportion of alkyl C tends to increase and aromatic C may increase or decrease, depending on the conditions (13–15).

Soils around the world have been found to contain different amounts of black carbon such as charcoal (16), a highly aromatic condensed ring structure. In addition, biochar (charcoal produced specifically for agricultural use) is attracting increasing attention as a soil amendment to sequester carbon and enhance soil fertility (17). Black carbon or biochars have been noted to have very high affinity for organic compounds including pesticides (18–20). Yang and Sheng (18) reported that biochar produced from wheat and rice residues was 400–2500 times more effective than soil in sorbing diuron herbicide. The high specific surface area and aromatic nature of carbon in biochars may be responsible for their extraordinary sorption properties (2, 21). However, the capacity of biochars to sorb pesticides may depend on soil types. For example, Ahmad and colleagues (unpublished data), recently studied the sorption behavior of carbaryl in two contrasting soils from New Zealand previously amended with biochars produced from corn stover at 350 °C and 550 °C. They found that while the amendment of soils with biochar at an agronomic application rate of 7.2 t C ha⁻¹ enhanced the sorption of carbaryl significantly; the magnitude of this effect varied considerably depending on soil type and the pyrolysis temperature used to produce the biochar.

Soil Mineralogy

Clay minerals can sorb organic compounds that are cationic in nature (e.g. diquat and paraquat herbicides) or those containing polar functional groups (23–25). The clays in highly weathered soils are dominated by kaolinite (1:1 type of clay minerals) and have lower capacity for pesticide sorption than 2:1 type clay minerals such as montmorillonite and vermiculite (26). The high surface acidity of hydroxyinterlayerd clays and their complexes can increase the protonation of weakly-basic herbicides such as atrazine and, consequently their sorption by ionic bonds at low pH, and their sorption by physical forces (H-bonds) at near-neutral pH (22). Many soils, especially in the tropical regions, contain variable-charge minerals (e.g. iron oxides, gibbsite) with distinct physical and chemical properties (27). For example, Oxisols can carry net positive charge at ambient pH and can effectively sorb anionic pesticides (28).

Other Soil Properties

Unlike hydrophobic non-ionic compounds, sorption of ionizable pesticides is highly sensitive to variations in the soil pH. This relationship mainly originates from different proportion of ionic and neutral form of the pesticide present at each pH level and also from the presence of surfaces with pH-dependent charges in soils. Soil pH regulates the electrostatic charge of soil colloids (organic matter and oxides) and protonation or chemical dissociation of pesticide molecules. Basic pesticide molecules become protonated at lower pH and therefore, more strongly sorbed to the soil colloids. On the contrary, the acidic pesticides ionize and become anions as pH increases (one or more pH units above the pK_a) and exhibit lower sorption (28, 29). Soil pH varies markedly among soils of different regions. The soils in wet tropics are generally acidic, whereas those in arid regions

are highly alkaline leading to markedly different sorption behavior. This effect makes direct extrapolation of pesticide sorption data, particularly for ionizable compounds, between acidic and alkaline soils difficult.

Soil temperature and water content are other important environmental parameters that may influence pesticide sorption. The effect of soil temperature on pesticide sorption has been noted to be highly variable. Valverde-Garcia et al. (30) and Khan et al. (31) noted that the elevation of temperature favoured sorption of pesticides in soils. They attributed this enhanced sorption to the increased number of active sites on humus. For 2,4-D sorption by 41 wetland sediments, Gaultier et al. (32) observed a significant increase in the 2,4-D sorption parameter when the experimental temperature was at 25°C rather than 5°C. By contrast, studies on sorption of cyanazine on different homoionic peats by Dios-Cancela et al. (33) showed decreasing sorption with increasing temperature, which was attributed to either a decrease in the attractive forces between the pesticide and the peat or a change in the solubility of the pesticide. In another study on sorption of atrazine on kaolinite and montmorillonite clays, Fruhstorfer et al. (34) postulated that since a rise in temperature causes an increase in the kinetic energy of the molecules with constant electrostatic attraction, this leads to a decrease in sorption of pesticides.

Sorption may also be influenced by soil moisture status, but this effect is not well understood. Several studies by Koskinen and co-workers (e.g. (35, 36)) show that sorption of herbicides may increase with soil water content. Roy et al. (37) reported significant effects of water content on the sorption of five fungicides and these effects were found to be dependent on the properties of the chemicals and the sorption mechanism. Berglöf et al. (35) proposed that at higher water contents, more pesticide solution is in contact with a large surface area of soil particles, which facilitates the accessibility of the pesticide to sorption sites. Methods, such as the one proposed by Ahmad et al. (38), may help better understand the role of soil water content in sorption of pesticides.

Conventional Approaches of Estimating Sorption of Pesticides in Soils

Pedotransfer Functions

Pedotransfer functions based on soil properties have been developed to describe the sorption of pesticides in soils. For example, Weber et al. (39) correlated the literature reported pesticide K_d values for 57 pesticides from different chemical classes with the key soil properties (such as SOM, clay content and /or soil pH) and developed equations for estimation of K_d values for improved soil mobility predictions. Ahmad and Rahman (40) carried out a study examining the effect of soil properties mentioned above on sorption of two commonly used herbicides, atrazine (weak base) and imazethapyr (weak acid), in 101 allophanic and non-allophanic soils of New Zealand. A wide variation in the sorption affinities of the soils was found, as the K_d values of atrazine and imazethapyr ranged from 0.7 to 52.1 L kg⁻¹ and 0.1 to 11.3 L kg⁻¹, respectively. For atrazine, the sorption affinities for the allophanic set of soils (mean K_d , 8.5 L kg⁻¹) were

greater than for the non-allophanic set of soils (mean K_d , 7.5 L kg⁻¹). However, no effect of allophanic status was found on imazethapyr sorption. None of the measured soil properties could alone explain adequately the sorption behavior of the herbicides. Multiple regression analyses revealed that SOC content, pH and, to a lesser extent sand were the primary soil properties. The authors compared their calculations with Weber et al. (39) models and found limited congruence between the two (as shown in Figure 1). The above examples show that while pesticide sorption in soils can be correlated well to soil properties, it may not be easy to transfer the functions based on soils from one region to another.

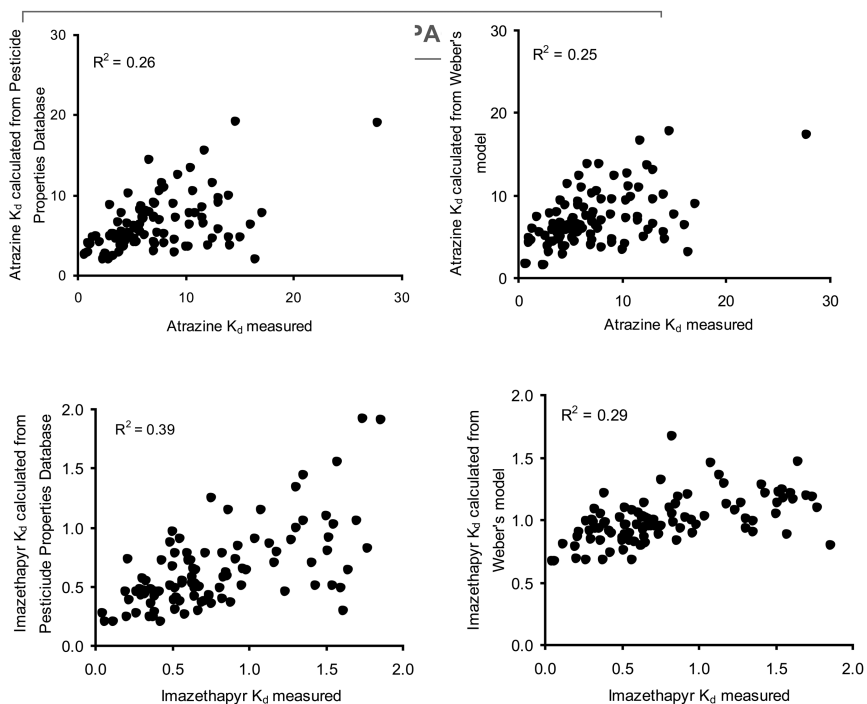


Figure 1. Relationships between measured K_d values of atrazine and imazethapyr and corresponding K_d values calculated from Pesticides Properties Database (42) and Weber's models (39). Reprinted with permission from Ahmad and Rahman, (40). Copyright (2009) American Chemical Society.

Quantitative Structure-Activity Relationship (QSAR)

There are several indirect methods of estimating sorption based on chemical characteristics of compounds, ranging from solubility, K_{ow} , retention factor in reverse-phase liquid chromatography and molecular structure. So called Quantitative Structure-Activity Relationship (QSAR) based approaches rely on molecular properties, such as molecular size descriptors, solvation energy relationships, molecular connectivity indices and other properties. These methods

have been discussed by Wauchope et al. (42) and by others cited in their review. Another chapter in this book (43) describes the QSAR approach in detail and applies QSAR for pesticide sorption. The appropriateness of the choice of a particular QSAR approach depends on the chemical structure and properties of the molecule (44) and their utility on the objective of the exercise (42).

Partitioning Theory (K_{oc} Model)

Partitioning processes on SOM from aqueous systems have been widely accepted as a major contributing factor, especially for non-ionic pesticides (45). Consequently, organic carbon content of soil is often used to normalise the sorption coefficient (K_d) of pesticides to obtain K_{oc} , such that $K_{oc} = K_d / f_{oc}$, where f_{oc} is the fraction of organic carbon in soil. Assuming that K_{oc} is a constant (i.e. sorption per unit carbon in various soils is the same), one can extrapolate K_{oc} value from one soil to other. This approach has been widely accepted and used in various pesticide fate models. However, partitioning is a historic paradigm for sorption on SOM for non-polar solutes and, in most cases, it is a simplification for the purposes of modelling rather than driven by the evidence from sorption studies (2).

A large body of evidence in literature shows that K_{oc} , despite the users' tendency to assume this as a constant, is a highly variable parameter. As early as in 1972, Hamakar and Thompson (46) and subsequently, Minglegrin and Gerstl (47) and Gerstl (48) highlighted the variability associated with K_{oc} (K_{OM} based on bulk SOM was used in some of these studies). More recently, Ahmad et al. (49) measured sorption of two pesticides (carbaryl and phosalone) on 48 soils collected from tropical and temperate regions involving three countries (Australia, Pakistan and the U.K.). They found only about half the variance (46-53 %) in K_d was explainable from the f_{oc} alone. Similarly, using 101 soils from southern Australia, Forouzangohar et al. (50) noted that while sorption of diuron showed dependence on SOM, only 42% of the variation in K_d was explained by f_{oc} . The sorption data reported by Ahmad et al. (49) for carbaryl measured in soils from various countries have been presented in Figure 2. The figure demonstrates that contrary to assumption of K_{oc} being constant, the parameter shows strong dependency on the chemistry of SOC rather than its concentration in soil.

Wauchope et al. (42), in a most comprehensive analysis, assessed thousands of K_{oc} values of a large number of pesticides from a database (41) and identified the extent of variations in the parameter and factors contributing to this. They noted that typical coefficients of variation (CV) among reported values of K_{oc} were in the range of 40-60%. The ratios between maximum and minimum values reported for the same compound from a single database were found to vary from 3 to 10 (Figure 3). The variation was found to be independent of the magnitude of K_{oc} (i.e. low or high K_{oc} reflecting hydrophilic or hydrophobic compounds). The authors ascribed about half of the observed variability in K_{oc} to experimental errors plus the variability in measuring SOM and the remainder to the variability in organic matter itself, such as its chemistry. However, we believe that soil minerals (organo-mineral interactions) may also have contributed to the observed variability in K_{oc} and should be taken into considerations.

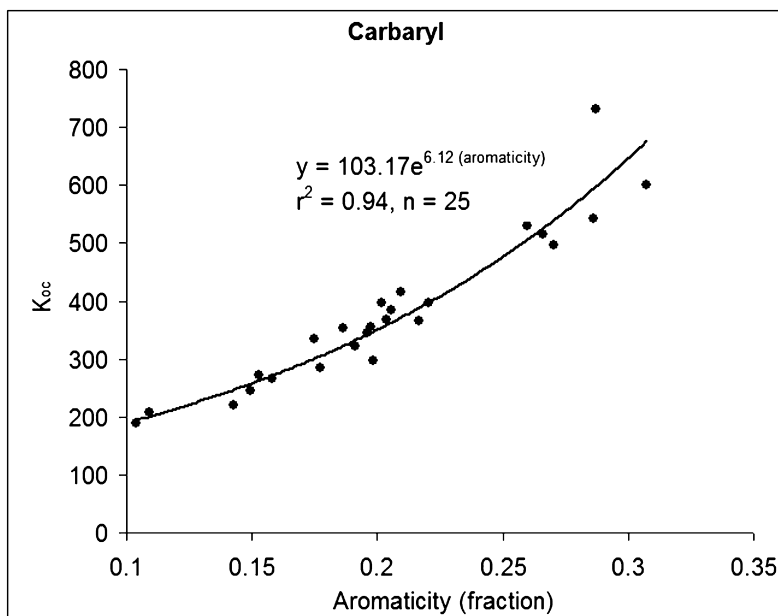


Figure 2. Dependence of sorption (K_{oc}) of carbaryl insecticide in soils on the chemistry of soil organic carbon. Reprinted with permission from Ahmad et al. (49). Copyright (2001) American Chemical Society.

Disproportionate Reliance on Soil Organic Matter Content in Prediction of Sorption

As discussed above, it is generally assumed that the sorption behavior of organic compounds is largely moderated by the content of organic matter in soils/sediments, and the role of clay minerals is generally ignored, especially during risk assessment (51). This is despite the fact that often soils are much richer in the mineral matter, i.e. its content in soils is often an order of magnitude higher than that of organic matter. Besides, numerous studies over the years have demonstrated that clay minerals, especially expandable smectites, do have a strong affinity for a variety of organic compounds such as pesticides and nitroaromatic compounds. For example, Laird et al. (52) studied sorption of atrazine on soil smectite clays and showed that relatively pure smectites were quite effective sorbents of the herbicide, depending on their compositions. Similarly, clay minerals were found to be good sorbents for nitroaromatic compounds (e.g. (53)). Despite the large body of literature, the role of clays in determining the sorption behavior of organic compounds in soils/sediments, and consequently

their ecological risks, is still not fully appreciated and incorporated in the risk assessment models. Soil organic matter and clay minerals are often closely associated and the type of precursors of humic substances and chelating organic acids associated with hydroxyinterlayered clays also have a pronounced impact on the sorption of pesticides by clays (22). Hence, the impact of clay minerals on pesticide sorption needs to be studied by considering this association.

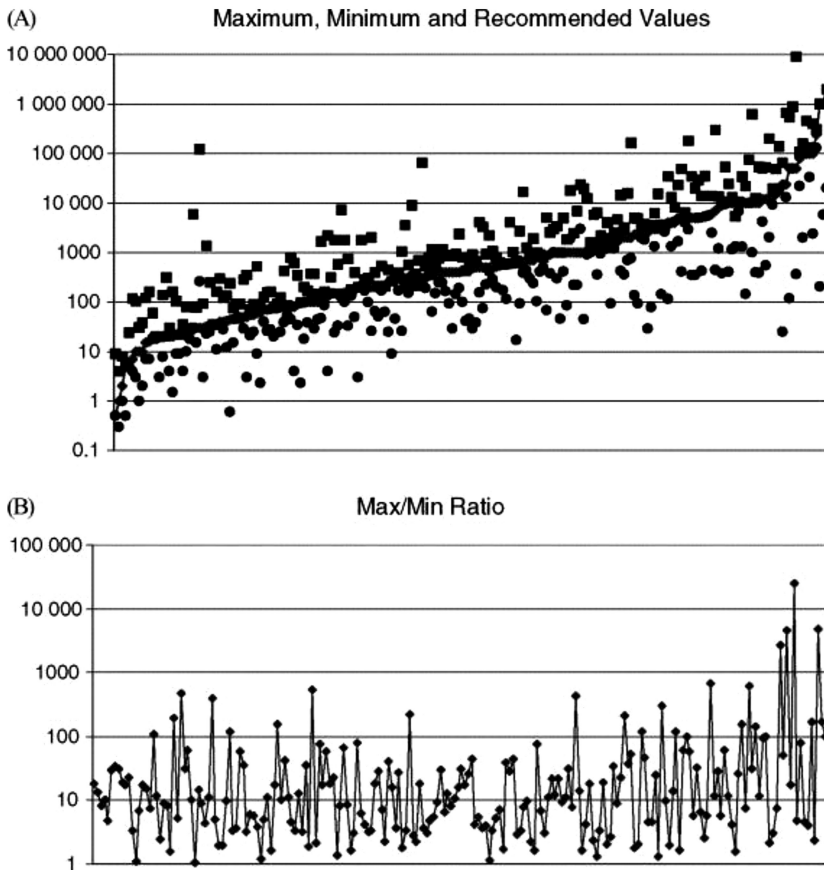


Figure 3. The observed values (A) and the variations in K_{oc} values (B) as indicated by the ratio of maximum to minimum values for a range of pesticide active ingredients in soils. Reproduced with permission from Wauchope et al. (42). Copyright (2002) Society of Chemical Industry.

One of the major developments that led to a disproportionate dominance of the role of organic matter in sorption of organic compounds in soils is the introduction of the “partition theory” (45), mentioned earlier in this paper. This theory allowed an easy extrapolation of sorption measured on one soil to another based on its carbon content alone, using the K_{oc} parameter. The simplicity of the concept led to models which could account for sorption of organic compounds in soil/sediments by a universal parameter K_{oc} , applicable to all soils/sediments. However, as discussed earlier, this concept is a simplification based on the sorption behavior of non-ionic organic compounds, while a substantial proportion of pesticides are ionic or ionizable (weakly basic, acidic) in nature. For example, the most used herbicide glyphosate is a zwitterion, the bypridilium herbicides (paraquat and diquat) are cationic in nature and the triazines (e.g. atrazine) are weakly basic compounds. Indeed the low ecological risk profiles of most commonly used herbicides glyphosate, paraquat and diquat are due to their strong adsorption on clay minerals. But for the ability of soil clays to “detoxify” them rapidly, the environmental safety of these herbicides may not have been the same.

Furthermore, the measured sorption isotherms of organic compounds in soils/sediments are more commonly non-linear in nature, contrary to the assumption of the partition theory (2). The non-linearity of sorption isotherms is indicative of complex organo-mineral interactions reflecting the role of chemistry of organic matter and/or clays in determining the sorption behavior of organic compounds in soils.

As discussed above, our studies (49, 54, 55) and those by many others (42, 56–58) observed that the organic matter content alone fails to adequately describe the sorption behavior of a wide range of pesticides in soils. Due to strong association between the two, the minerals and organic matter in soils are essentially inseparable (59) and organo-mineral interactions in soil may play a major role in sorption of organic compounds including pesticides (57). A more comprehensive approach incorporating soil organic as well as mineral matter (both contents as well as their chemistries) is therefore desirable to fully incorporate the role of soil surfaces in sorption of organic compounds.

Recent Advances in Estimating Pesticide Sorption Based on Integrated Soil Properties

The recent developments in application of infrared spectroscopy (IR) in characterization of soils and sediments open a window of opportunity to estimate the sorption of organic compounds based on the overall contributions of mineral as well as organic matter in soils. Chemometric approaches, especially partial least squares (PLS) regression, with infrared spectroscopy have been found to be particularly effective in characterizing soils in terms of a range of soil properties, such as organic carbon content, clay content, cation exchange capacity etc. (60). Application of a couple of these approaches in estimating the sorption of pesticides has been discussed below.

Prediction of Soil Properties by Infrared Spectroscopy

Several statistical measures can be used to evaluate how well IR predicts soil properties. The coefficient of determination (R^2) and the root mean square error of prediction (RMSEP) or the standard error of prediction (SEP) are the most consistent parameters reported in studies. Using the SEP and bias separately is preferred to using RMSEP which integrates the bias in its value (61). The ratio of prediction to deviation (RPD) and the ratio of the SEP to the range (RER) are also commonly used to evaluate the accuracy of IR measurements (62). In general, it is understood that a larger R^2 , smaller SEP or RMSEP, and larger RPD indicate a more successful application of IR when measuring soil properties (63). While Dunn et al. (64) suggested 3 categories for RPD as poor, <1.6 ; acceptable, $1.6-2.0$; and excellent, >2.0 for soil analysis. Malley et al. (2004) proposed that values of RPD >4 be judged as indicating excellent calibrations, >3 as successful, and between 2.25 to 3.0 as moderately successful.

Near-infrared spectroscopy (NIR) is a technique that has long been recognized as having practical applications in agricultural and food industries. Its potential in soil research has also been demonstrated. For example, it has been used to successfully predict total carbon, or fractions of carbon in soils obtained from regions in Canada (62, 65, 67), United States (63, 67, 68), Australia (64), Uruguay (69), and Germany, Norway, and Denmark (70). NIR has also been used to predict soil textural characteristics (sand, silt or clay), pH, cation exchange capacity (CEC), CaCO_3 content, and the total or exchangeable macronutrients (i.e., N, K, Ca, Mg, and P), micronutrients (Fe, Mn, Zn, Cu, Mo, and Ni), and metals (Pd, Co, Cd, Ag, V, Hg, Cr) (65, 66, 69, 71). The accuracy of these predictions ranged from less than successful to excellent calibrations. For the same parameter, one data set of soil samples may show successful calibrations (e.g. CEC shows $R^2 = 0.89$ and RPD = 3.0 for Duck Mountain Provincial Park samples [$n=108$] in Malley et al. (71), while another data set of soil samples demonstrates poor calibrations (e.g. CEC shows $R^2 = 0.51$ and RPD = 1.4 for agro-Manitoba samples [$n=1,000$] in Malley et al. (71). When small (e.g. $n=100$) or large (e.g. $n=1,000$) data sets are used, moderately to excellent NIR calibrations are common when measuring SOC and clay (63, 71, 72).

Similarly, mid-infrared spectroscopy (MIR) combined with PLS regression approach has also been successfully used to estimate the content of soil major oxides, pH, sum of cations, Ca, Mg, K, Na, total N, clay content, and organic carbon content (60, 73). The technique has been particularly successful in predicting the SOC. Furthermore, both NIR and MIR techniques have also been applied to predict the chemistry of organic carbon. For example, Cozzolino and Moron (69) and Zimmermann et al. (74) showed that both MIR and NIR not only can estimate SOC in bulk soils but also in different particle-size fractions. Janik et al. (75) and Bornemann et al. (76) demonstrated that MIR could also be used for effective estimations of black carbon in soils. They employed MIR-PLS approach in analyzing the f_{oc} and black carbon contents in 309 soils collected from different depths in soils from America, Europe and Asia. In this study benzene polycarboxylic acid (BPCAs) was used as a specific marker of black carbon. The

prediction of BPCA carbon in the full set of soils ($n=309$) resulted in a R^2 of 0.84 and an RPD close to 2.5, both indicating a secure predictive capability of the approach.

Prediction of Pesticide Sorption in Soils by Near- and Mid-Infrared Spectroscopy and Chemometrics

Bengtsson et al. (77) were the first to demonstrate that NIR could be used to determine sorption coefficients (K_d) in soils. Their reference data consisted of K_d values of lindane (an organochlorine insecticide) and linuron (a substituted urea herbicide) determined for 27 soil samples by batch equilibrium experiments. Spectral data was collected between 1100 to 2500 nm at 2 nm intervals using a NIR 4600 scanning monochromator. The reference and NIR data demonstrated good agreement with R^2 being 0.85 for lindane and 0.84 for linuron. Both pesticides showed good correlations that were even greater than the reported linear relation between SOC and lindane ($R^2=0.82$) or linuron ($R^2=0.74$) K_d values. Both lindane and linuron are neutral pesticides whose sorption in soil linearly increases with increasing SOC (77).

Farenhorst and collaborators further investigated the feasibility of NIR as a tool for estimating K_d values for pesticides and related compounds (Singh et al. (66, 78)). Their study included the herbicides 2,4-D (a weakly-acidic), atrazine (a weakly-basic), and glyphosate (a zwitterion), as well as a natural steroid hormone, 17 β -estradiol. They determined the K_d values of these compounds in 609 horizons collected from 70 soil profiles in two irregular undulating to hummocky agricultural landscapes in the Canadian Prairies. Spectral data were obtained by scanning the 609 soil samples in 5 cm diameter glass Petri dishes to a 45VISNIR Zeiss Corona spectrometer using a wavelength range 380–1690 at 2 nm intervals, and to a Foss NIR Systems 6500 spectrometer with a wavelength range 1100–2500 at 2 nm intervals. The noisy region (380–700 nm) of the Corona spectra was removed so that, for the Corona, there was a wavelength range of 700–1690 nm. For both the Corona and Foss spectrometers, excellent to moderately successful calibrations were found for SOC and K_d values of 2,4-D, atrazine and 17 β -estradiol, with R^2 ranging from 0.80 to 0.96, and the RPD ranging from 2.22 to 5.34 (Table 1). In contrast, the calibrations for glyphosate, pH and soil textural characteristics were largely unsuccessful in both landscapes and with both spectrometers (Table 1). These and the results of Bengtsson et al. (77) suggest that for herbicides such as atrazine, 2,4-D and linuron, whose soil retention is largely controlled by SOC, NIR is a good tool for quantifying sorption coefficients in soil, but it has limited value for measuring sorption coefficients for glyphosate, which is not significantly correlated with SOC (79) or may even decrease with increasing SOC (80).

Table 1. Calibration Results of 2,4-D, Atrazine, Glyphosate and 17 β -Estradiol Kd Values and Selected Soil Properties in Soil Samples Presented in Petri Dishes to Two NIR Spectrometers (Data from Ref. (66), Farenhorst, Unpublished Data)

	<i>R</i> ²	<i>SEP</i>	<i>Bias</i>	<i>RPD</i>	<i>RER</i>	<i>R</i> ²	<i>SEP</i>	<i>Bias</i>	<i>RPD</i>	<i>RER</i>
<i>Parameter</i>	<i>Landscape A (n=313)</i>					<i>Landscape B (n=295)</i>				
	<i>Foss NIR Systems 6500 spectrometer</i>									
2,4-D	0.92	0.39	-3.07E-07	3.96	17.24	0.86	0.34	-9.79E-06	2.53	11.40
Atrazine	0.93	1.93	-2.38E-05	4.18	16.58	0.91	0.60	-7.08E-07	3.35	14.01
Glyphosate	0.54	16.91	-2.35E-04	1.40	6.97	0.58	60.44	-2.04E-05	1.76	9.01
17 β -estradiol	0.92	2.71	8.75E-07	3.78	14.77	0.84	2.42	-4.42E-07	2.53	10.89
SOC%	0.96	0.26	3.89E-07	5.34	18.89	0.91	0.29	-1.86E-06	3.21	12.16
pH	0.67	0.19	2.76E-06	1.70	8.22	0.65	0.39	-2.32E-05	1.71	6.55
Sand%	0.51	10.9	5.48E-06	1.25	6.39	0.70	5.89	-8.01E-06	1.76	10.00
Silt%	0.43	5.51	-6.90E-05	1.35	7.17	0.51	5.92	1.36E-04	1.44	9.03
Clay%	0.48	6.83	4.12E-06	1.05	4.83	0.79	3.28	-6.04E-05	2.13	8.87
	<i>45VISNIR Zeiss Corona spectrometer</i>									
2,4-D	0.88	0.51	4.84E-06	3.02	14.91	0.82	0.38	-4.51E-09	2.22	10.03
Atrazine	0.85	3.12	1.23E-07	2.42	9.28	0.80	0.87	1.04E-07	2.31	9.68
Glyphosate	0.41	19.19	-1.08E-06	1.34	8.41	0.57	56.22	-7.90E-05	1.90	9.68
17 β -estradiol	0.93	2.69	8.06E-05	3.75	15.27	0.81	2.58	-6.99E-07	2.37	10.21

Continued on next page.

Table 1. (Continued). Calibration Results of 2,4-D, Atrazine, Glyphosate and 17 β -Estradiol Kd Values and Selected Soil Properties in Soil Samples Presented in Petri Dishes to Two NIR Spectrometers (Data from Ref. (66), Farenhorst, Unpublished Data)

	<i>R</i> ²	<i>SEP</i>	<i>Bias</i>	<i>RPD</i>	<i>RER</i>	<i>R</i> ²	<i>SEP</i>	<i>Bias</i>	<i>RPD</i>	<i>RER</i>
<i>Parameter</i>	<i>Landscape A (n=313)</i>					<i>Landscape B (n=295)</i>				
SOC%	0.92	0.37	2.14E-08	3.49	13.04	0.90	0.31	-5.60E-08	2.98	11.26
pH	0.76	0.16	-1.80E-07	2.08	9.18	0.76	0.33	-2.88E-07	2.05	7.83
Sand%	0.55	9.37	7.41E-05	1.83	9.99	0.52	7.31	2.22E-05	1.39	8.06
Silt%	0.49	5.2	-4.03E-05	1.64	10.6	0.41	6.59	3.24E-05	1.29	8.12
Clay%	0.59	5.25	-1.20E-05	1.93	9.09	0.73	3.69	-7.35E-06	1.91	7.89

MIR spectroscopy has been successfully employed to predict sorption of pesticides. Forouzangohar et al. (50) tested this approach on a set of 101 surface soils, collected along a 400 km longitudinal transect from south-eastern South Australia. The soils were characterized using diffuse reflectance infrared Fourier transform (DRIFT) technique. Sorption coefficients of a non-ionic pesticide, diuron [3-(3,4-dichlorophenyl)-1,1-dimethylurea], were measured on these soils by a batch method. The K_{oc} approach was compared against the MIR-PLS approach for prediction of K_d values. They developed and validated the MIR-PLS model by dividing the initial data set into four validation sets. Calibrations were developed using leave-one-out cross-validation which estimates prediction error by removing samples from the calibration set one by one, and predicting them as unknown samples using the remaining calibration samples (81). The model resulted in a coefficient of determination (R^2) of 0.69, standard error (SE) of 5.57 and RPD of 1.63. The K_{oc} approach, on the other hand, was found to be inferior with values of R^2 , SE and RPD of 0.42, 7.26 and 1.25, respectively (Figure 4). To detect spectral outliers, principal component analysis (PCA) was performed on the spectra. It was noted that the significant statistical difference between the two models was mainly due to the outliers detected via PCA . While, the performance of the two models was essentially similar for the rest of the calibration set, this was only true when the best fit K_{oc} was obtained from the measured sorption data on these 101 soils and not taken from the literature. For another herbicide, atrazine, Kookana et al. (82) tested the same approach on a smaller set of surface and subsurface soils (total of 31 samples) and found that compared to the K_{oc} model based on f_{OC} alone, the predictions using MIR-PLS were significantly superior with improved correlation coefficients and lower standard error of estimation.

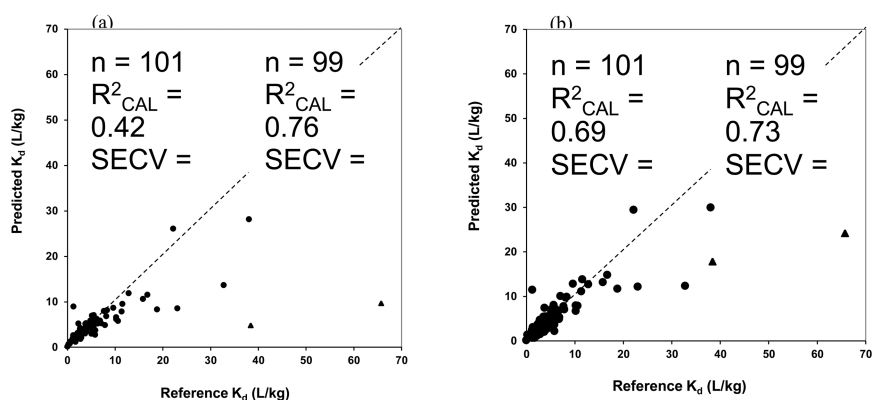


Figure 4. Measured versus predicted sorption parameter (K_d) using K_{oc} approach (a) and using mid infrared spectroscopy incorporating various soil types (b). Reprinted with permission from Forouzangohar et al., (50). Copyright(2008) American Chemical Society.

Forouzangohar et al. (83) also made a direct comparison between MIR and visible-NIR (VNIR) for prediction of sorption of diuron on 112 Australian soils (including the 101 soils used in the earlier study). For VNIRS, the spectral data were collected from 400 to 2500 nm with an interval of 2 nm on a NIR 6500 (NIRSystems, Silver Spring, USA) and for MIR spectroscopy, the spectral data were collected for 60 s in the frequency range of 4000 to 500 cm^{-1} (2500-20000 nm) at 8 cm^{-1} resolution on Perkin Elmer Spectrum-One FTIR (Perkin Elmer Inc., Mass. USA). A comparison of the performances of VNIR and MIR spectroscopy for predicting both f_{oc} and K_d of diuron was made using PLS regression. In this study, MIR outperformed VNIR for predictions of both of the parameters. MIR-PLS model provided a better prediction for diuron K_d values in their calibration set. The key indices R^2 and RPD for K_d prediction were 0.8 and 2.3 for the MIR-PLS model and 0.4 and 1.3 for the VNIR-PLS model, respectively.

Concluding Remarks

Soil solid phase consists of mineral and organic matters, which are strongly associated with each other and are often difficult to fully separate, despite the common efforts by many workers to isolate one from the other. Both phases contribute towards sorption of pesticides depending on their relative abundance in soil/sediments, their chemistries and the chemical nature of the pesticide molecules. The complex interactions and heterogeneities associated with the soil solid phase contribute to the large degree of variation in the K_{oc} parameter often used to extrapolate the pesticide sorption estimate between soils. One reason for popularity of the K_{oc} model has been ease of its use and absence of any other similar approach that is more comprehensively based on soil properties. Therefore, despite the general recognition in literature of the role of organo-mineral interactions in determining sorption of pesticide, sorption estimates based on a broad range of soil properties have been missing. In this regard, the IR with chemometrics may be worth exploring.

The examples presented in this paper show that both MIR and NIR spectroscopy are attractive approaches for rapid assessment of pesticides sorption in soils. In several studies, the assessment by IR-PLS was found to be superior to the K_{oc} model, on the basis of not only the accuracy of prediction, but also being a direct estimation of K_d based on the integrated properties of organic and mineral matter. The K_{oc} approach on the other hand uses an intervening parameter, which considers only one soil property i.e. f_{oc} . Furthermore, IR-PLS approach is attractive not only because it allows integration of a range of soil properties (amount and nature of organic carbon as well as mineral matter) in K_d estimation, but also being a relatively high-throughput, cost-effective and easy-to-use technique. While the IR-PLS approach is promising, its broad-based applicability is yet to be demonstrated fully. Further work is needed to assess the transferability of the sorption data predicted by this approach between soils from different regions.

Acknowledgments

RK acknowledges the contributions of several students and colleagues, including Riaz Ahmad, Mohsen Forouzangohar, Ahmad Ahangar, Les Janik, Ronald Smernik, for their research over the years, leading to this chapter. Thanks are also due to the anonymous reviewers for their constructive comments on the manuscript.

References

1. Koskinen, W. C.; Harper, S. S. In *Pesticides in the Soil Environment: Processes, Impacts and Modeling*; Cheng, H. H.; Ed.; Soil Science Society of America: Madison, WI, 1990; pp 51–78.
2. Pignatello, J. J. Interactions of anthropogenic organic chemicals with natural organic matter and black carbon in environmental particles. In *Biophysical-Chemical Processes of Anthropogenic Organic Compounds in Environmental Systems*; Xing, B. Senesi, N., Hunag, P. M., Eds.; Wiley: New York, 2011; pp 3–50.
3. Bollag, J. M.; Myers, C. J.; Minard, R. D. *Sci. Total Environ.* **1992**, *123/124*, 205–217.
4. Weber, J. B.; Wilkerson, G. G.; Linker, H. M.; Wilcut, J. W.; Leidy, R. B.; Senseman, S.; Witt, W. W.; Barrett, M.; Vencill, W. K.; Shaw, D. R.; Mueller, T. C.; Miller, D. K.; Becke, B. J.; Talbert, R. E.; Peeper, T. F. *Weed Sci.* **2000**, *48*, 75–88.
5. Karickhoff, S. W.; Brown, D. S.; Scott, T. A. *Water Res.* **1979**, *13*, 241–248.
6. Hance, R. J. Adsorption and bioavailability. In *Environmental Chemistry of Herbicides*; Grover, R., Ed.; CRC Press: Boca Raton, Florida, 1988; Vol. 1 pp 1–20.
7. Theng, B. K. G. Clay-humic interactions and soil aggregate stability. In *Soil Structure and Aggregate Stability*; Rengasamy, P., Ed.; Seminar Proceedings; Institute of Irrigation and Salinity Research: Tatura, Australia, 1987; pp 32–73.
8. Grathwohl, P. *Environ. Sci. Technol.* **1990**, *24*, 1687–1693.
9. Kögel-Knabner, I. *Soil Biochem.* **1993**, *8*, 101–105.
10. Karapanagioti, H. K.; Kleinedam, S.; Sabatini, D. A.; Grathwohl, P.; Ligouis, B. *Environ. Sci. Technol.* **2000**, *34*, 406–414.
11. Krosshavn, M.; Southon, T. E.; Steinnes, E. *J. Soil Sci.* **1992**, *43*, 485–493.
12. Stevenson, F. J. Organic matter reactions involving pesticides in soil. In *Humus Chemistry, Genesis, Composition, Reactions*, 2nd ed.; John Wiley and Sons, Inc.: New York, 1994; pp 453–471.
13. Inbar, Y.; Chen, Y.; Hadar, Y. *Soil Sci. Soc. Am. J.* **1989**, *53*, 1695–1701.
14. Lessa, A. S. N.; Anderson, D. W.; Chatson, B. *Plant Soil* **1996**, *184*, 207–217.
15. Baldock, J. A.; Oades, J. M.; Nelson, P. N.; Skene, T. M.; Golchine, A.; Clark, P. *Aust. J. Soil Res.* **1997**, *35*, 1061–1083.
16. Schmidt, M. W. I.; Noack, A. G. *Global Biogeochem. Cycles* **2000**, *14*, 777–794.
17. Lehmann, J. *Nature* **2007**, *447*, 143–144.

18. Yang, Y. N.; Sheng, G. Y. *Environ. Sci. Technol.* **2003**, *37*, 3635–3639.
19. Cornelissen, G.; Gustafsson, O. *Environ. Sci. Technol.* **2004**, *38*, 148–155.
20. Kookana, R. S. *Aust. J. Soil Res.* **2010**, *48*, 627–637.
21. Kookana, R. S.; Sarmah, A. K.; van Zwieten, L.; Krull, E.; Singh, B. *Adv. Agron.* **2011**, *112*, 103–143.
22. Indraratne, S. P.; Farenhorst, A.; Goh, T. B. *J. Environ. Sci. Health, Part B* **2008**, *43*, 21–26.
23. Weber, J. B. *Soil Sci. Soc. Am. Proc.* **1970**, *34*, 401–404.
24. Kookana, R. S.; Baskaran, S.; Naidu, R. *Aust. J. Soil Res.* **1998**, *36*, 715–764.
25. Li, H.; Sheng, G.; Teppen, B. J.; Johnston, C. T.; Boyd, S. A. *Soil Sci. Soc. Am. J.* **2003**, *67*, 122–131.
26. Bailey, G. W.; White, J. L. *Residue Rev.* **1970**, *32*, 29–92.
27. Quafoku, N. P.; Van Ranst, E.; Noble, A.; Baert, G. *Adv. Agron.* **2004**, *84*, 159–215.
28. Regitano, J. B.; Alleoni, L. R. F.; Vidal-Torrado, P.; Casagrande, J. C.; Tornissielo, V. L. *J. Environ. Qual.* **2000**, *29*, 894–900.
29. Sarmah, A. K.; Kookana, R. S.; Alston, A. M. *Aust. J. Agric. Res.* **1998**, *49*, 775–790.
30. Valverde-Garcia, A.; Gonzalez-Pradas, E.; Villafranca-Sanchez, M.; Del Rey Bueno, F.; Garcia-Rodriguez, A. *Soil Sci. Soc. Am. J.* **1988**, *52*, 1571–1574.
31. Khan, Z. A.; Misra, B. M.; Raghu, K. *J. Environ. Sci. Health* **1996**, *31*, 1015–1027.
32. Gaultier, J.; Farenhorst, A.; Kim, S. M.; Saiyed, I.; Cessna, A. J.; Glozier, N. E. *Wetlands* **2009**, *29*, 837–844.
33. Dios-Cancela, G.; Romero, T. E.; Sánchez-Rasero, F. *Soil Sci.* **1990**, *150*, 836–843.
34. Fruhstorfer, P.; Schneider, R. J.; Niessner, R. *Sci. Total Environ.* **1993**, *138*, 317–328.
35. Berglöf, T.; Koskinen, W. C.; Brücher, J.; Kylin, H. *J. Agric. Food Chem.* **2000**, *48*, 3718–3721.
36. Berglöf, T.; Koskinen, W. C.; Duffy, M. J.; Norberg, K. A.; Kylin, H. *J. Agric. Food Chem.* **2003**, *51*, 3598–3603.
37. Roy, C.; Gaillardon, P.; Montfort, F. *Pest Manage. Sci.* **2000**, *56*, 795–803.
38. Ahmad, R.; Katou, H.; Kookana, R. S. *J. Environ. Qual.* **2005**, *34*, 1045–1054.
39. Weber, J. B.; Wilkerson, G. G.; Reinhardt, C. F. *Chemosphere* **2004**, *55*, 157–166.
40. Ahmad, R.; Rahman, A. *J. Agric. Food Chem.* **2009**, *57*, 10866–10875.
41. Hornsby, A. G.; Wauchope, R. D.; Herner, A. E. *Pesticide Properties in the Environment*; Springer Verlag: New York, 1996.
42. Wauchope, R. D.; Yeh, S.; Linders, J. B. H. J.; Kloskowski, R.; Tanaka, K.; Rubin, B.; Katamaya, A.; Kordel, W.; Gerstl, Z.; Lane, M.; Unsworth, J. B. *Pest. Manage. Sci.* **2002**, *58*, 419–445.
43. Sabljic A.; Nakagawa, Y. In *Non-First Order Degradation and Time-Dependent Sorption of Organic Chemicals in Soil*; Chen, W., Cheplick, M., Reinken, G., Jones, R. L. Eds.; ACS Symposium Series 1174; American Chemical Society: Washington, DC, 2014; pp 85–118.

44. Sabljic, A.; Gusten, H.; Verhaar, H.; Hermens, J. *Chemosphere* **1995**, *31*, 4489–4514.
45. Chiou, C. T.; Peters, L. J.; Freed, V. H. *Science* **1979**, *206*, 831–832.
46. Hamaker, J. W.; Thompson, J. M. In *Organic Chemicals in the Soil Environment*; Goring, C. A. I., Hamaker, J. W., Eds.; Marcel Dekker Inc.: New York, 1972; pp 49–143.
47. Mingelgrin, U.; Gerstl, Z. *J. Environ. Qual.* **1983**, *12*, 1–11.
48. Gerstl, Z. *J. Contam. Hydrol.* **1990**, *6*, 357–375.
49. Ahmad, R.; Kookana, R. S.; Alston, A. M.; Skjemstad, J. O. *Environ. Sci. Technol.* **2001**, *35*, 878–884.
50. Forouzangohar, M.; Kookana, R. S.; Forrester, S. T.; Smernik, R. J.; Chittleborough, D. J. *Environ. Sci. Technol.* **2008**, *42*, 3283–3288.
51. Ahmad, R.; Kookana, R. S. In *Rational Environmental Management of Agrochemicals*; Kennedy, I., Solomon, K. R., Gee, S. J., Crossan, A. N., Wang, S., Sánchez-Bao, F., Eds.; ACS Symposium Series 966; American Chemical Society: Washington, DC, 2007; pp 100–119.
52. Laird, D. A.; Barriuso, E.; Dowdy, R. H.; Koskinen, W. C. *Soil Sci. Soc. Am. J.* **1992**, *56*, 62–67.
53. Haderlien, S. B.; Schwarzenbach, R. P. *Environ. Sci. Technol.* **1993**, *27*, 316–322.
54. Singh, N.; Kookana, R. S. *J. Environ. Sci. Health, Part B.* **2009**, *44*, 214–219.
55. Ahangar, A. G.; Smernik, R. J.; Kookana, R. S.; Chittleborough, D. J. *Chemosphere* **2008**, *70*, 1153–1160.
56. Boyd, S. A.; Johnston, C. T.; Laird, D. A.; Teppen, B. J.; Li, H. Comprehensive Study of Organic Contaminant Adsorption by Clays: Methodologies, mechanisms and environmental implications. In *Biophysical-Chemical Processes of Anthropogenic Organic Compounds in Environmental Systems*; Xing, B., Senesi, N., Hunag, P. M., Eds.; Wiley: New York, 2011; pp 51–72.
57. Simpson, M. J.; Simpson, A. J. The role of organic matter-mineral interactions in the sorption of organic contaminants. In *Biophysical-Chemical Processes of Anthropogenic Organic Compounds in Environmental Systems*; Xing, B., Senesi, N., Hunag, P. M., Eds.; Wiley: New York, 2011; pp 73–90.
58. Farenhorst, A.; McQueen, D. A. R.; Saiyed, I.; Hilderbrand, C.; Li, S.; Lobb, D. A.; Messing, P.; Schumacher, T. E.; Papiernik, S. K.; Lindstrom, M. J. *Geoderma* **2009**, *150*, 267–277.
59. Kleber, M.; Sollins, P.; Sutton, R. *Biogeochemistry* **2007**, *85*, 9–24.
60. Janik, L. J.; Skjemstad, J. O. *Aust. J. Soil Res.* **1995**, *33*, 637–650.
61. Williams, P. *Near-infrared Technology - Getting the best out of light, A short course in the practical implementation of near-infrared spectroscopy for the user*, 5.4 ed.; PDK Grain, PDK Projects, Inc.: Winnepeg, MB, 2009; 182 pp.
62. Martin, P. D.; Malley, D. F.; Manning, G.; Fuller, L. *Can. J. Soil Sci.* **2002**, *82*, 413–422.
63. Chang, C. W.; Laird, D. A. *Soil Sci.* **2002**, *167*, 110–116.
64. Dunn, B. W.; Batten, G. D.; Beecher, H. G.; Ciavarella, S. *Aust. J. Exp. Agric.* **2002**, *24*, 607–614.

65. Malley, D. F.; Martin, P. D.; Ben-Dor, E. Application in analysis in soils. In *Near-Infrared Spectroscopy in Agriculture*; Roberts, C. A., Workman, J., Jr., Reeves, J. B., III, Eds.; Agronomy Monograph No. 44; American Society of Agronomy, Crop Sciences Society of America, Soil Science Society of America: Madison, WI, 2004; Chapter 26, pp 729–784.
66. Singh, B.; Malley, D. F.; Farenhorst, A.; Williams, P. *J. Agric. Food Chem.* **2012**, *60*, 9948–9953.
67. McCarty, G. W.; Reeves, J. B., III; Reeves, V. B.; Follett, R. F.; Kimble, J. M. *Soil Sci. Soc. Am. J.* **2002**, *66*, 640–646.
68. Reeves, J. B., III; McCarty, G. W.; Mimmo, T. *Environ. Pollut.* **2002**, *116*, S277–S284.
69. Cozzolino, D.; Morón, A. *Soil Tillage Res.* **2006**, *85*, 78–85.
70. Terhoeven-Urselmans, T.; Kerstin, M.; Helfrich, M.; Flessa, H.; Ludwig, B. *J. Plant Nutr. Soil. Sci.* **2006**, *169*, 168–174.
71. Malley, D. F.; Martin, P. D.; McClintock, L. M.; Yesmin, L.; Eilers, R. G.; Haluschak, P. Feasibility of analyzing archived Canadian prairie agricultural soils by near infrared reflectance spectroscopy. In *Near-Infrared Spectroscopy*; Davies, A. M. C., Giangiacomo, R., Eds.; Proceedings of the 9th International Conference; NIR Publications: Norwich, U.K., 2000; pp 579–585.
72. Sorensen, L. K.; Dalsgaard, S. *Soil Sci. Soc. Am. J.* **2005**, *69*, 159–167.
73. Janik, L. J.; Skjemstad, J. O.; Raven, M. D. *Aust. J. Soil Res.* **1995**, *33*, 621–636.
74. Zimmermann, M.; Leifeld, J.; Fuhrer, J. *Soil Biol. Biochem.* **2007**, *39*, 224–231.
75. Janik, L. J.; Skjemstad, J. O.; Shepherd, K. D.; Spouncer, L. *Aust. J. Soil Res.* **2007**, *45*, 73–81.
76. Bornemann, L.; Welp, G.; Brodowski, S.; Rodionov, A.; Amelung, W. *Org. Geochem.* **2008**, *39*, 1537–1544.
77. Bengtsson, S.; Berglof, T.; Kylin, H. *Bull. Environ. Contam. Toxicol.* **2007**, *78*, 295–298.
78. Singh, B.; Farenhorst, A.; Malley, D. *NIR News* **2010**, *21*, 8–10.
79. Farenhorst, A.; Papiernik, S. K.; Saiyed, I.; Messing, P.; Stephens, K. D.; Schumacher, J. A.; Lobb, D. A.; Li, S.; Lindstrom, M. J.; Schumacher, T. E. *J. Environ. Qual.* **2008**, *37*, 1201–1208.
80. Gerritse, R. G.; Beltran, J.; Hernandez, F. *Aust. J. Soil Res.* **1996**, *24*, 599–607.
81. Naes, T.; Isaksson, T.; Fearn, T.; Davies, T. *A user-friendly guide to multivariate calibration and classification*; NIR Publications: Chichester, 2002.
82. Kookana, R. S.; Janik, L. J.; Forouzanoghar, M.; Forrester, S. T. *J. Agric. Food Chem.* **2008**, *56*, 3208–3213.
83. Forouzanoghar, M.; Cozzolino, D.; Kookana, R. S.; Smernik, R. J.; Forrester, S. T.; Chittleborough, D. J. *Environ. Sci. Technol.* **2009**, *43*, 4049–4055.

Chapter 13

Quantifying Transient Sorption Behavior of Agrochemicals Using Simple Experiments and Modeling

Steven A. Cryer*

Enabling Capabilities Technology Center, Dow AgroSciences LLC,
9330 Zionsville Road, Indianapolis, Indiana 46268

*E-mail: sacryer@dow.com.

Sorption and desorption of an organic chemical to/from vegetation or soil manifest different behavior over time. Pesticide mobility in soil and/or released to the atmosphere is strongly coupled to the chemical's sorption characteristics, altering the pesticide transport in various environmental matrices (soil, air, water). A modified soil column batch experiment was designed to measure the transient sorption and desorption nature for a wide variety of pesticides in soil. This experimental system minimizes many shortcomings associated with obtaining sorption parameters through fitting saturated soil column observations with an advective–dispersive transport equation. Experimental observations are used to explore different sorption/desorption algorithms, offering insight and recommendations for appropriate algorithms that capture the transient sorption nature for a specific pesticide. For example, a second-order soil sorption kinetic model and the two-site kinetic/equilibrium model were found to yield reasonable comparisons to experimental observations for a highly sorbed insecticide (chlorpyrifos). Although the two-site model can give excellent agreement between experiment and model predictions, this may just be a consequence of the additional free parameter used to “curve fit” the solution to experimental data. It's possible other simpler non-equilibrium sorption-desorption models offer similar comparison to experiment, and the basic experimental system used here can yield insight into

the applicability of different proposed sorption-desorption mechanisms. Mechanistic models for environmental fate often incorporate many different sorption algorithms for the user to choose from. However, the robustness and versatility of the 2-site model, with its ability to recover equilibrium sorption in the appropriate limit, indicate this popular algorithm should be standardized in mechanistic and regulatory pesticide fate models. Examples of the modeling impact of transient sorption on pesticide leaching using the one-dimensional finite element HYDRUS model are provided.

Introduction

Field studies are often used to provide guidance and insight into the fate of a pesticide. However, field studies are expensive and are limited in scope with respect to the semi-infinite edaphic, climatic, and agronomic parameter combinations that are inherent from regional variability. A cost effective alternative to understand pesticide fate under parametric uncertainty is the use of mechanistic modeling. Here the chemistry and physics of the processes are appropriately characterized by mathematical representations of these phenomena. Models often account for complex mechanisms such as non-linear chemical degradation and/or transient sorption and desorption of the pesticide to/from soil, pore-water, leaf surfaces, and so on, while providing insights for pesticide transport and exposure to organisms.

Sorption is the process for a pesticide to partition or bind to environmental matrices via chemical and physical mechanisms. The most common experiment for sorption is to spike a pesticide into the water phase for a system containing water and soil. Following agitation over a prescribed time period (e.g., 24-hrs), the pesticide mass in the aqueous phase (C_{outer}) is measured, and by difference the pesticide partitioned into the soil phase (C_{sorbed}) is determined. Over the time scale of the experiments, pesticide degradation is often negligible and therefore sorption is characteristic of the partitioning between the bulk aqueous phase/soil pore water with that of soil solids, Figure 1.

Many common environmental fate and modeling practices often assume the simplest of algorithms such as i) pesticide dissipation is governed by first order kinetics, ii) instantaneous equilibrium sorption, and iii) soil properties are uniform with depth. Many of the commonly used pesticide dissipation models account for this simplistic analysis but often require more complex algorithms to be implemented if realistic predictions of pesticide fate are to be made. Sorption is one of the many mechanisms responsible for overall dissipation, and coefficient(s) characterizing sorption can be used for qualitative comparison with other compounds to rank the importance of appropriate environmental pathways. Pesticide mobility is strongly tied to the pesticide's sorption and degradation characteristics, and the real benefit from incorporating generic and refined algorithms is in selecting the "right" mechanism for use in predictive, mechanistic modeling for the fate of the pesticide.

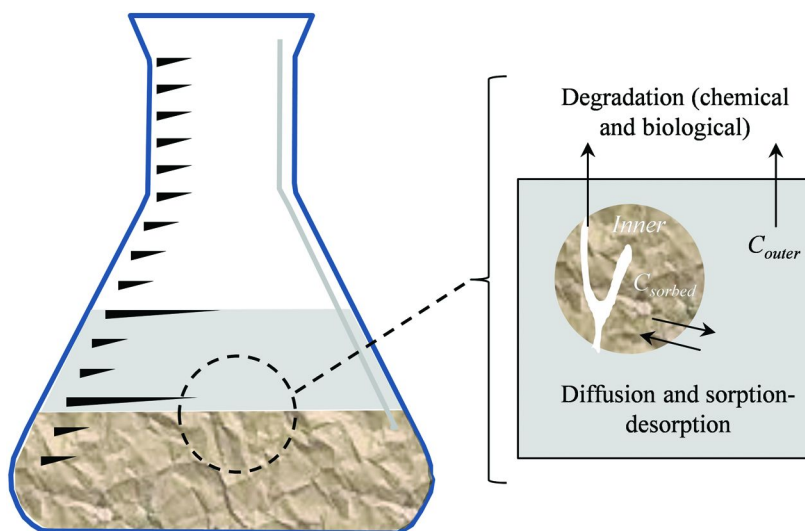


Figure 1. Pesticide sorption experiment for water-soil matrices.

For a conventional soil column experiment, a cylindrical column is packed with soil and capped at both ends. The soil is saturated via a continuously flowing volume of water, entering at one end of the column and exiting out the other end. A chemical is injected at the entrance over a certain injection time to create a finite chemical pulse. Analysis for this type of experiment includes: i) concentration of the chemical leaving in the effluent and ii) following the experiment, the sectioning and analysis of chemical residues at various depths in the soil column. If no sorption or degradation occurs within the soil, then the entering chemical pulse will remain unchanged as the pulse propagates through the column. Pesticide dispersion, sorption and dissipation alter the shape and concentration levels of the initial pulse to something different as the pulse propagates through the soil column, Figure 2. Sorption characteristics of the pesticide in soil can alter the breakthrough times of the solute pulse and the pulse shape as it exits the column. Thus, knowledge of the various mechanisms involved with pesticide sorption/desorption can be inferred through algorithm choice and mechanistic models to match experimental observations.

A realistic prediction of pesticide environmental fate in various environmental matrices is dependent upon both the correct mathematical descriptions of the mechanisms and in the availability of accurate transport properties that characterize the mathematical expressions. Even complex models can be partially parameterized using curve fitting tools such as CXTFIT (1, 2) where input parameters are adjusted until experimental observations match simulation predictions through minimization of the sum of squared error. If the number of degrees of freedom is large, then using an optimization routine such as CXTFIT is appropriate. However, often physicochemical properties associated with

degradation and sorption can be measured in independent lab experiments. This work describes an experimental setup where transient sorption and desorption can be addressed that minimizes several of the shortcomings of traditional soil column experiments. These measured sorption parameters can be used in many existing pesticide fate models or easily incorporated into others.

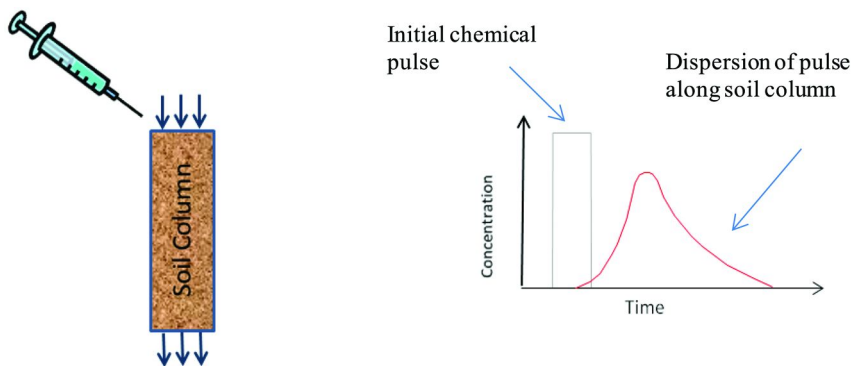


Figure 2. Characteristic soil column experiment with typical solute effluent concentration measurements leaving the column.

Methods and Materials

Sorption and desorption of an organic chemical from a solid substrate such as soil or foliage is expressed as the rate of chemical change between various environmental compartments. A simple material balance for each compartment can be written as

$$\text{Rate of mass change} = \text{input} - \text{output} + \text{generation} - \text{consumption.} \quad (1)$$

These material balance equations lead to a coupled system of ordinary differential equations (ODEs). For typical air/soil environments, the environmental compartments are soil (solid), pore water (aqueous), and vapor, with the generation and consumption terms of eq. 1 are often zero. If transport into the air (e.g., volatility) from soil and water is small, then the environmental compartments where pesticide mass can move is summarized in Figure 3(a). Often the soil is broken down into two regions where one region is governed by equilibrium sorption (I) while the other has transient sorption governed by kinetic algorithms (II), Figure 3(b). The arrows in Figure 3 are indicative of mass movement between compartments.

For the aqueous compartment of Figure 3(a), eq. 1 can be written as

$$\frac{dc}{dt} = -k_1g_1(C) + k_2g_2(S) \quad (2)$$

where C is the concentration of the solute in water, S the concentration in the soil (solid) and $g_1(C)$ and $g_2(S)$ are functions dependent upon the concentrations C and S , while k_1 and k_2 are the rate constants that parameterize the magnitude of mass transfer between the aqueous and solid compartments, respectively. By overall mass balance

$$S = C_0 + S_0 - C \quad (3)$$

where C_0 and S_0 are the initial concentration of pesticide in the aqueous and solid phase, respectively. The other compartment transient solute concentration can be determined once C (or S) is known.

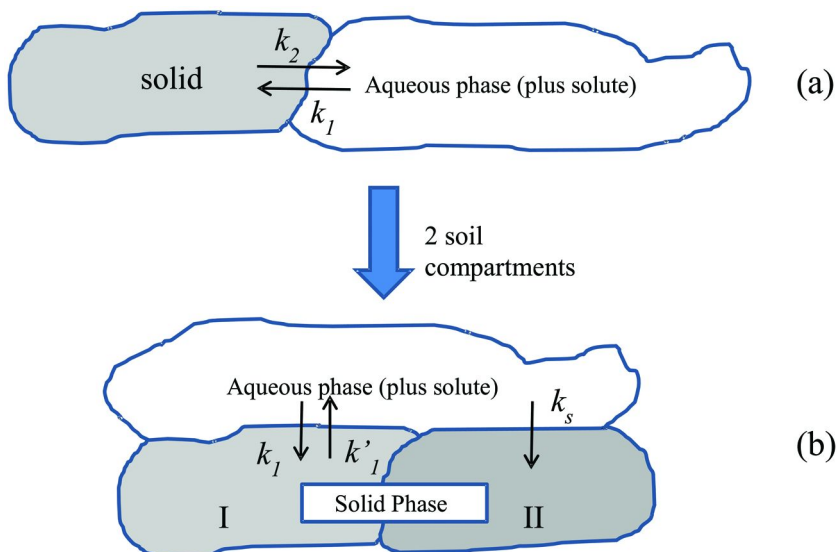


Figure 3. Environmental compartments for pesticide transport assuming volatility is negligible.

Simple functional forms for $g_1(C)$ and $g_2(S)$ are assumed as summarized in Table I, where the material balance equations for solute the aqueous phase, representing transient sorption and desorption, can be written as

$$\frac{dC}{dt} = -k_1 C^m + k_2 S^n \quad (4)$$

where m and n are specific integers used in this analysis, and k_1 and k_2 represent the rate constants for sorption and desorption, respectively (Figure 3 (a)).

More complex sorption/desorption algorithms have been proposed (3, 4). Several of these sorption models are now incorporated into current environmental fate modeling tools. Here, the soil is broken into two regions where it has been postulated one region is governed by equilibrium partitioning (sorption) and the other region kinetically governed, Figure 3 (b). Material balance equations are

written for both sites in the 2-site kinetic/equilibrium sorption model. Thus, the mass transfer system of equations for sorption/desorption for each site can be written as

$$\frac{dS_I}{dt} = f_I k_d \frac{dC}{dt} \quad (5)$$

$$\frac{dS_{II}}{dt} = \frac{k_s}{k_d} [(1 - f_I)k_d C - S_{II}] \quad (6)$$

subject to $S_I(0) = S_{II}(0) = 0$.

Here,

k_d = equilibrium partition coefficient for sorption sites (which is the ratio of the rate constants k_l to k'_l at equilibrium)

k_s = rate constant for kinetically governed sorption sites

f_I = fraction of type I (equilibrium sorption) sites [and $(1-f_I)$ is the number of type II (kinetically governed sorption sites)].

Table I. Descriptions of Kinetic Sorption/Desorption Algorithms Explored

<i>Algorithm</i>	$g_1(C)$	$g_2(S)$
1 st order sorption	C	0
2 nd order sorption	C ²	0
1 st order sorption w/ 1 st order desorption	C	S

All of the sorption/desorption material balance differential equations described herein (Table I, Equations 2-6) can be integrated analytically, with results summarized in Table II.

Experiment

A modified soil column batch experiment is proposed to measure sorption characteristics. The experiment consists of a 500 mL three neck flask where the aqueous phase is continually recirculated through a small soil column (i.d. 2.4 cm), Figure 4. In contrast to a traditional soil column experiment where the effluent leaving the columns is analyzed for solute and discarded, here the solution is being mixed and recirculated back to the top of the column. The aqueous phase is sampled over time via the septum port on the vessel, with aliquots analyzed for pesticide residues. This experiment is somewhat analogous to a traditional batch chemical reactor, but instead of a chemical reaction, sorption and desorption is acting as sources and sinks that impact the availability of the solute in the bulk aqueous system. Pesticide is initially supplied to the aqueous bulk phase (i.e., injected at $t=0$) and subsequently decreases with time as governed by the sorption/desorption processes occurring in the short soil column.

Table II. Analytical Solutions to the Various Sorption/Desorption Algorithms Used in This Analysis

Description	Solution
first-order sorption ($m = 1, n = 0$)	$\frac{C}{C_0} = e^{-k_1 t}$
second-order sorption ($m = 2, n = 0$)	$\frac{C}{C_0} = \frac{1}{1 - k_1 C_0 t}$,
first-order sorption with first-order desorption ($m = 1, n = 1$)	$\frac{C}{C_0} = \frac{e^{-k_1(k_s+1)t} - k_s}{k_s + 1}$, $\frac{C}{C_0} = 1 - \frac{S}{C_0}$
two site kinetic/equilibrium sorption model	$\frac{S_I}{C_0} = -\frac{k_d^2 f_I \{e^{-\lambda t} (f_I - 1) - f_I - 1\}}{1 + k_d}$, $\frac{C}{C_0} = 1 - \frac{S_I}{C_0} - \frac{S_{II}}{C_0}$ $\frac{S_{II}}{C_0} = \frac{k_d}{1 + k_d} [(f_I^2 k_d - f_I k_d + f_I - 1)e^{-\lambda t} - f_I^2 k_d - f_I + 1]$

The advection-dispersion equation is traditionally used to back calculate the sorption parameters based upon the experimentally observed solute breakthrough curve from large soil columns. Short residence times for the effluent transporting through the soil column minimizes many of the shortcomings of traditional, full size soil columns while simplifying model fitting. Specifically, the small volume of soil (~12.9 cm³) in this experimental apparatus provides a higher likelihood for homogeneous dispersion of the soil than much larger columns could afford (e.g., minimizes regions within the soil where preferential flow may occur). A small soil column also lowers the delay time for effluent entering and leaving the column (~ 1 minute) which is several orders of magnitude faster than conventional sorption kinetic experiments. Examples and observations for the insecticide (chlorpyrifos) sorption characteristics in Cecil soil are provided. Additional details of the experimental procedure are found elsewhere (5).

Transport Modeling

Quantification of experimental observations for sorption provides insight into appropriate mechanisms and necessary mathematical descriptions used to describe the phenomena. Many of the regulatory pesticide soil fate models have algorithms for equilibrium (Freundlich linear/nonlinear isotherms) and time dependent sorption. FOCUS (6) models PELMO (7, 8) and PEARL (9, 10) both contain time dependent sorption algorithms. The current incarnation of the U.S. regulatory model PRZM3 (11) only has the option for equilibrium

sorption mechanism for water/soil systems, but does allow for different pesticide degradation descriptors. However, PRZM3 has been modified for European use to include time dependent sorption and can be found elsewhere [FOCUS PRZM (GW)], <http://focus.jrc.ec.europa.eu/gw/models/PRZM/download.html>].

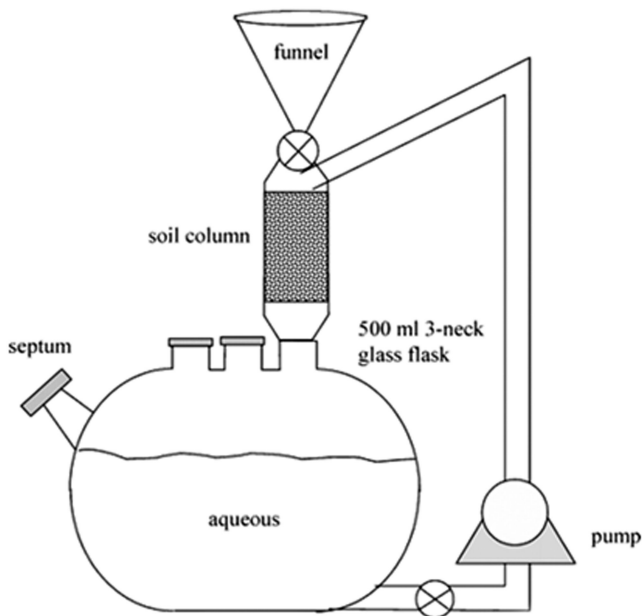


Figure 4. Experimental apparatus used to quantify chlorpyrifos sorption. Reproduced with Permission from *J. Agric. Food Chem.* Vol 53, No. 10, 2005.

An alternative approach for analyzing experimental sorption data is using the HYDRUS model. HYDRUS (<http://www.pc-progress.com/en/Default.aspx?hydrus-1d>), a public domain soil physics model, solves the conservation equations of water, heat and solute transport in variable-saturated media (12). HYDRUS sorption models include equilibrium and multiple non-equilibrium routines, and also uses a discretized version of the Richards equation, a more realistic representation for water movement than the simplistic tipping bucket water balances of other models. HYDRUS has been shown to adequately address the transient flow of water through soil (13, 14). Simulation results using simple and complex forms for degradation and sorption illustrate the dynamic range of results that ensue and suggest what can be gained through

refinement in mechanistic predictions over simpler approaches. Additional work involving HYDRUS can be found elsewhere (15). HYDRUS-1D is used to simulate solute flow for a hypothetical pesticide in a saturated soil column, Figure 5.

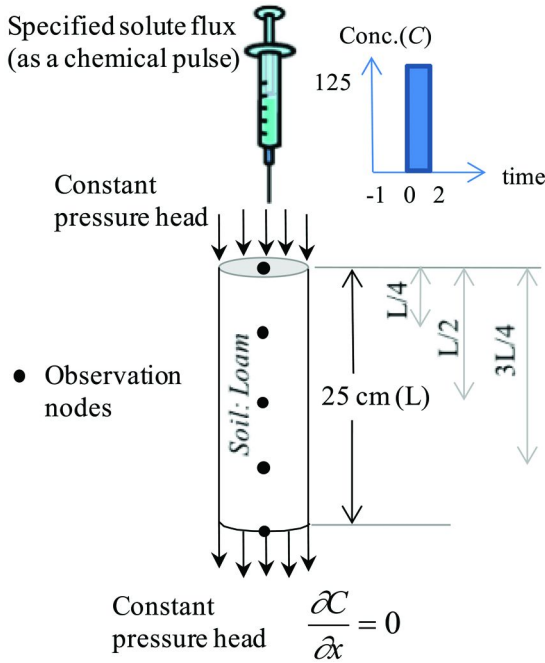


Figure 5. Geometry and boundary conditions for example problem in saturated flow through a soil column.

The equilibrium partition coefficient for chlorpyrifos (k_d) for a soil/water system is large (16); indicating chlorpyrifos is immobile in soil. Thus, a hypothetical pesticide was defined that has the propensity to be transported through saturated soil pores of a soil column leaching experiment to illustrate differences in leaching potential that can arise should an incorrect sorption mechanism be assumed via using the HYDRUS 1-D model.

In the present study, five locations from the soil column entry to exit are defined as observation points where solute concentrations, as it passes through the soil column, are simulated and recorded by HYDRUS. Physicochemical properties of the hypothetical pesticide and soil column experimental geometry, used for HYDRUS simulations, are summarized in Table III for saturated flow through soil.

Table III. Physicochemical Properties of a Hypothetical Solute and Column for the Saturated Column Solute Transport Example Problem

<i>Parameter</i>	<i>Magnitude (or model)</i>
Porosity Model	van Genuchten-Mualem
Column Length (<i>L</i>)	25 cm
Soil Type	Loam
Residual soil water content	0.078
Saturated soil water content	0.0448
Parameter “ α ” in soil water retention function	0.036 [cm ⁻¹]
Parameter “ n ” in soil water retention function	1.56
Saturated hydraulic conductivity [LT ⁻¹]	2.65 [cm d ⁻¹]
Soil bulk density	1.32 g cm ⁻³
Adsorption isotherm coefficient (k_d)	0.25 [g ⁻¹ cm ³]
Solute Diffusion Coefficient	0.696 [cm ² d ⁻¹]
Solute Concentration of Pulse	125 [g d ⁻¹]
Solute Pulse Duration	2 [d]

Results

Experimental

Comparison between the sorption/desorption algorithms and experimental observations for chlorpyrifos are seen in Figure 6, where it is found that chlorpyrifos readily sorbs quickly over the first 6-h interval. The transient sorption/desorption algorithm that most closely approximates experimental observations is the 2nd order sorption only model. The worst comparison is between transient Freundlich like algorithms (e.g., 1st order sorption, 1st order sorption with 1st order desorption) which overestimate the sorption magnitude for chlorpyrifos. A compromise that predicts the correct equilibrium sorption behavior while slightly over predicting the sorption potential early on for chlorpyrifos is the two-site kinetic-equilibrium sorption model. Data obtained from this novel experimental apparatus can be used to easily infer or select the best sorption/desorption algorithms for a specific combination of solute/soil properties. Thus, mechanistic environmental fate modeling can be refined by using the appropriate sorption/desorption algorithms that best describe experimental observations.

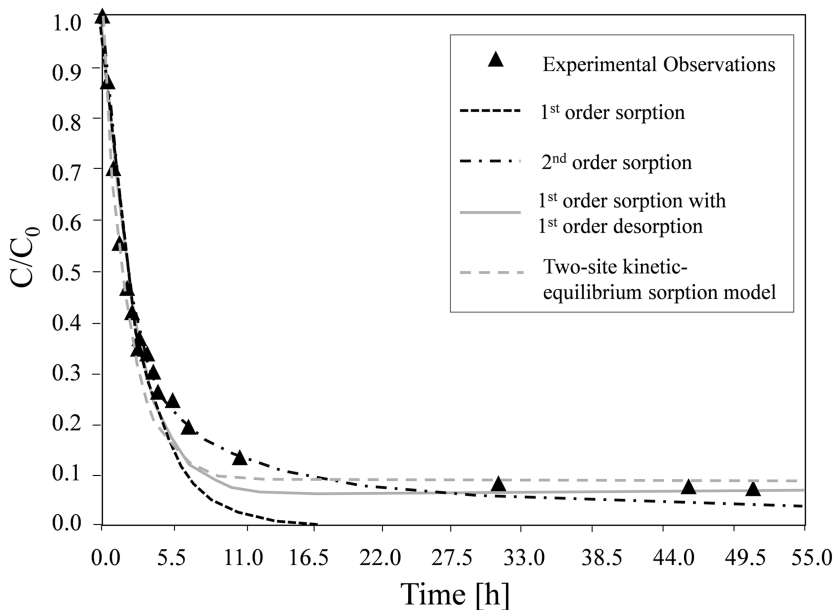


Figure 6. Comparison of experimental observations obtained from the recirculation apparatus to multiple proposed sorption mechanisms.

Modeling

Simulation results of HYDRUS-1D, using the properties summarized in Table III for a saturated soil column, are provided in Figures 7-8. Figure 7(a) represents simulation results when equilibrium sorption is assumed. The solute peak disperses uniformly through the soil column from top to bottom. Figure 7(b) illustrates the impact of kinetically governed sorption (2-site model), both in impacting the breakthrough time for the solute pulse ($x=L$) and the non-symmetric dispersion characteristics of the pulse throughout the column.

A representative simulated result for the breakthrough pulse of solute is provided in Figure 8. Clearly the choice of sorption/desorption algorithms impact the movement of the solute through saturated soil as seen by the predicted solute breakthrough curves leaving the column. This example illustrates the importance of using the correct sorption algorithm(s) if a realistic prediction of environmental transport (leaching) of a solute is sought. Experimental observations are necessary to address appropriate sorption algorithms specific for the soil and pesticide being investigated.

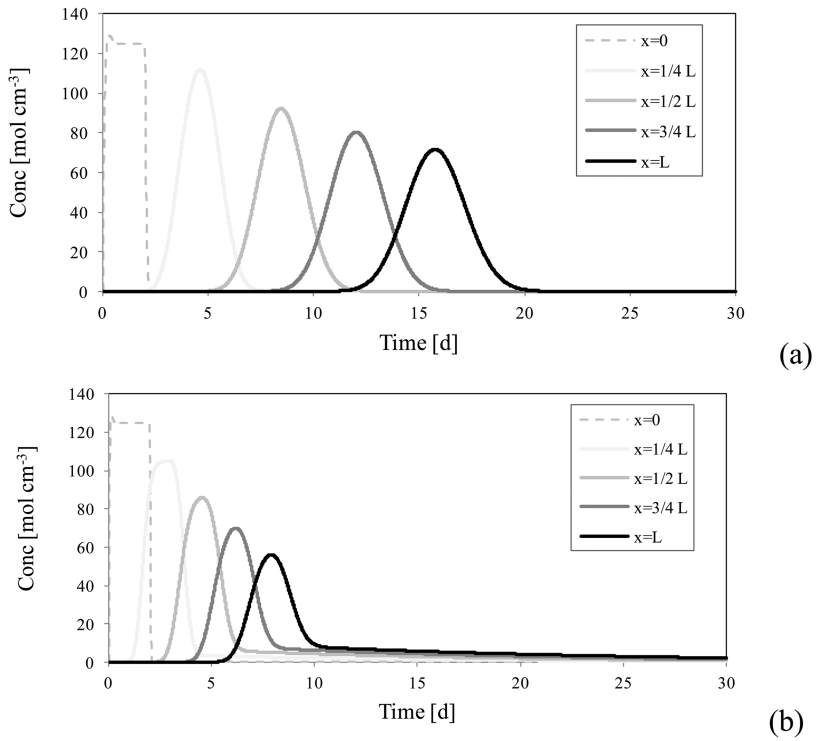


Figure 7. Breakthrough curves for the hypothetical pesticide (Table III) when equilibrium sorption (a) and the 2-site model (b) are assumed. The equilibrium soil/water partition coefficient (k_d) is constant for all simulations (a), and $f_1 = 0.25$, $k_s = 0.1 \text{ d}^{-1}$ for the 2-site model (b).

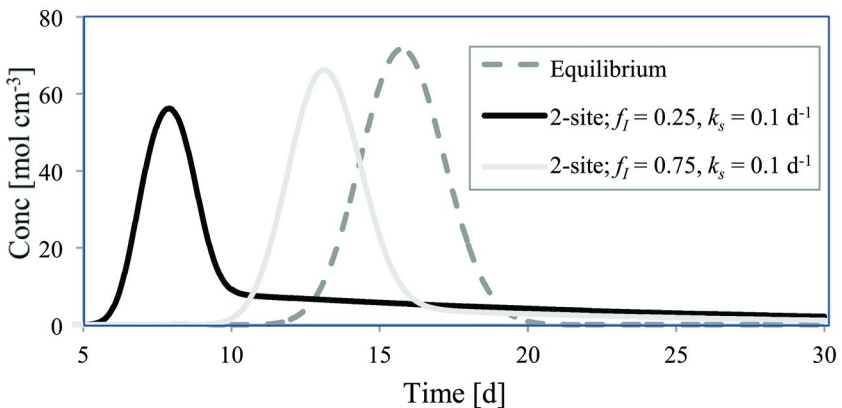


Figure 8. Simulated soil column breakthrough curves given different sorption algorithms for the hypothetical pesticide. 2-site model, f_1 = fraction of sorption sites (equilibrium), k_s = rate constant for kinetically governed sorption sites [d^{-1}].

Conclusions

Chlorpyrifos clearly demonstrates non-equilibrium sorption/desorption behavior as observed from a modified soil column batch experiment designed for this analysis. Multiple soil sorption/desorption models were proposed that include the 2-site kinetic/equilibrium (most versatile but having 3 free parameters), a 1st order sorption with first order desorption (2 free parameters), a second and first order kinetic sorption (1 free parameter) with no desorption, and equilibrium sorption. For many/most of the proposed sorption/desorption models, analytical solutions to the governing material balance equations exist or can be easily obtained. Thus, incorporation of more refined algorithms for sorption/desorption can easily be implemented into existing pesticide environmental fate models (should they not currently exist), and a robust environmental fate model, properly parameterized, can lead to better, more refined predictions of pesticide fate.

The 2-site kinetic/equilibrium sorption model has been around for decades and should be considered in the sorption algorithms that are available in regulatory models should simpler algorithms prove inadequate. Even though the experimental and sorption modeling results for chlorpyrifos described here suggests sorption is a 2nd order kinetic process, most studies have focused on first or near first order approximations for the modeling of sorption. This is true for the two-site kinetic/equilibrium sorption model. The two site algorithm does increase the number of parameters by 1 (e.g., the fraction of sorption sites that are governed by kinetic behavior, f_i). However, f_i can be set to one to recover the traditional equilibrium sorption algorithm. The PRZM3 model has been modified to incorporate the 2-site/kinetic sorption algorithm (PRZM3-Kinetic and the FOCUS model PRZM-GW) (17), but this sorption algorithm is now standard for most realistic pesticide fate and transport models (e.g., HYDRUS). PRZM3 alternative models are probably a better choice than the original PRZM3 since these models offer more representative sorption algorithms than what the original PRZM3 equilibrium sorption approximation can provide.

References

1. Toride, N.; Leij, F. J.; van Genuchten, M. Th. Research Report No. 137, U.S. Salinity Laboratory, USDA, ARS, Riverside, California, 1995.
2. Parker, J. C.; van Genuchten, M. Th. Bull. 84-3, Virginia Agril. Exp. Stn., Blacksburg, 1984; 96 pp.
3. van Genuchten, M. Tn.; Wagenet, R. J. *Soil Sci. Soc. Am. J.* **1989**, *53*, 1303–1310.
4. Gamedainger, A. P.; Wagenet, R. J.; van Genuchten, M. Th. *Soil Sci. Soc. Am. J.* **1990**, *54*, 957–963.
5. Cryer, S. A. *J. Agric. Food Chem.* **2005**, *53*, 4103–4109.
6. FOCUS. EC Document Reference Sanco/321/2000 rev 2, 2000; pp 1–202.
7. Klein M. PELMO. Report from Fraunhofer-Institut für Umweltchemie und Ökotoxikologie, D57392 Schmallenberg, Germany, 1995.

8. Jene B. Report from Staatliche Lehr- und Forschungsanstalt für Landwirtschaft, Weinbau und Gartenbau, D-67435, Neustadt an der Weinstrasse, Germany, 1998.
9. Tiktak A.; Van den Berg, F.; Boesten, J. J. T. I.; Van Kraalingen, D.; Leistra M.; Van der Linden, A. M. A. RIVM Report 711401008, Alterra Report 28, RIVM, Bilthoven, The Netherlands, 2001; 144 pp, available at www.alterra.models/pearl.
10. Leistra M.; Van der Linden, A. M. A.; Boesten, J. J. T. I.; Tiktak A.; Van den Berg F. Alterra Report 013, RIVM Report 711401009, Alterra Wageningen UR, Wageningen, The Netherlands, 2001; 115 pp, available at www.alterra.models/pearl.
11. Carsel, R. F.; Imhoff, J. C.; Hummel, P. R.; Cheplick, J. M.; Donigan, A. S., Jr. National Exposure Research laboratory, Office of Research and Development, U.S. Environmental Protection Agency, Athens, GA, 1995.
12. Šimůnek, J.; van Genuchten, M. Th.; Šejna, M. *Vadose Zone J.* **2008**, 7 (2), 587–600 DOI: 10.2136/VZJ2007.0077, Special Issue “*Vadose Zone Modeling*..
13. de Jong, R.; Bootsma, A. *Can. J. Soil Sci.* **1996**, 76, 263–273 DOI: 10.4141/cjss96-033.
14. Ranatunga, K.; Natin, E. R.; Barratt, D. G. *Environ. Model. Softw.* **2008**, 23, 1182–1206 DOI: 10.1016/j. envsoft.2008.02.003.
15. Šimůnek, J.; Köhne, J. M.; Kodešová, R.; Šejna, M. *Soil Water Res.* **2008**, 3 (Special Issue 1), S42–S51.
16. Racke, K. D. *Rev. Environ. Contam. Toxicol.* **1993**, 131, 1–154.
17. Chen, W.; Cheplick, M.; Reinken, G.; Jones, R. In *Non-First Order Degradation and Time-Dependent Sorption of Organic Chemicals in Soil*; Chen, W., Sabljic, A., Cryer, S. A., Kookana, R., Eds.; ACS Symposium Series 1174; American Chemical Society: Washington, DC, 2014; pp 277–299.

Chapter 14

Spatial Variability of Pesticide Sorption: Measurements and Integration to Pesticide Fate Models

**Annemieke Farenhorst,^{*,1} Ross McQueen,¹ Rai S. Kookana,²
Baljeet Singh,¹ and Diane Malley³**

¹Department of Soil Science, University of Manitoba,
Winnipeg, Manitoba, R3T 2N2, Canada

²CSIRO Land and Water, University of Adelaide Waite Campus,
South Australia, 5064, Australia

³PDK Projects, Inc., Nanaimo, British Columbia, V9V 1L6, Canada

*E-mail: annemieke.farenhorst@umanitoba.ca

Pesticide fate models are useful in testing the impact of agricultural management practices on the quality of water resources. The sorption parameter is among the most sensitive of the input parameters used by pesticide fate models. Numerous pesticide sorption experiments have been conducted in the past 75 years, but mainly focussed on surface soils. The batch equilibrium procedure is a conventional technique to quantify sorption parameters. In this chapter, we summarize selected batch equilibrium studies to demonstrate that sorption parameters vary widely among sampling points within soil-landscapes. We recognize that probability density functions (PDFs) have been incorporated into stochastic simulations of pesticide fate to help account for sorption spatial variability, but also show that PDFs can vary widely for different pesticides and/or soil depth. We propose that near-infrared spectroscopy (NIRS) can be used in combination with batch equilibrium techniques to more rapidly quantify the sorption variability of herbicides. We demonstrate that NIRS can be integrated into the Pesticide Root Zone Model version 3.12.2 to improve spatial resolutions for calculating the mass of herbicide leached to depth at the field scale. Better quantification of herbicide

sorption variability and hence leaching potential will provide greater confidence in using pesticide fate models in regulatory practices, as well as in management programs that promote both sustainable agriculture and adequate environmental protection of water resources.

Introduction

Pesticides have the potential to move from their application target into the atmosphere, surface water and groundwater (Table 1). Pesticides may become airborne through application drift (1) post-volatilization losses from land, water, or vegetative surfaces (2) and on wind-eroded soil (3). Pesticide loadings to surface waters are due to atmospheric wet and dry deposition (4–6), storm-induced surface runoff (7, 8) and groundwater recharge (7). Many factors can influence the risk of groundwater contamination by pesticides (9). Multivariate statistics on water quality data collected at a national scale in the United States have shown that the likelihood of detecting a specific pesticide in shallow groundwater is greater for pesticides that have small sorption parameters (10).

Table 1. Number of Studies That Tested for a Given Herbicide (# Studies) in Environmental Samples (Surface Water, Groundwater, Rain, or Air) and the Percent of Studies That Reported Detecting That Herbicide in Their Study (% Detect)

<i>Pesticide</i>	<i># studies</i>	<i>% detect</i>	<i>References</i>
2,4-D	19	100	(4, 6, 7, 12–27)
2,4-DB	4	67	(14, 15, 19, 26)
alachlor	3	67	(6, 16, 23)
atrazine	7	83	(6, 14, 16, 19, 23–25)
bromoxynil	16	100	(4, 6, 7, 12, 14, 15, 18, 19, 21–28)
clopyralid	6	100	(6, 19, 21, 24, 26, 27)
dicamba	18	100	(4, 6, 7, 12–15, 18–28)
dichlorprop	8	100	(14–19, 21, 22, 24, 26)
diclofop-methyl	3	80	(13, 18, 21)
ethalfluralin	7	83	(6, 16, 19, 21, 23, 25, 27)
ethametsulfuron methyl	1	100	(24)
fenoxaprop-p-ethyl	3	67	(13, 19, 21)
glufosinate ammonium	2	50	(6, 26)

Continued on next page.

Table 1. (Continued). Number of Studies That Tested for a Given Herbicide (# Studies) in Environmental Samples (Surface Water, Groundwater, Rain, or Air) and the Percent of Studies That Reported Detecting That Herbicide in Their Study (% Detect)

<i>Pesticide</i>	<i># studies</i>	<i>% detect</i>	<i>References</i>
glyphosate	3	100	(6, 26, 29)
imazamethabenz	3	100	(13, 18, 24)
imazethapyr	2	100	(19, 24)
MCPA	16	100	(6, 12–19, 21–28)
MCPB	5	100	(14, 15, 22, 24, 27)
mecoprop	7	100	(6, 18, 19, 21, 24, 26, 27)
metolachlor	5	100	(6, 14, 16, 23, 25, 27)
metribuzin	4	100	(21, 22, 24, 27)
metsulfuron-methyl	2	100	(24, 27)
picloram	5	100	(13, 14, 22, 24, 27)
quinclorac	1	100	(19)
simazine	3	100	(14, 24, 27)
sulfosulfuron	2	100	(24, 27)
thifensulfuron methyl	2	100	(24, 27)
trallate	14	100	(4, 6–8, 12–14, 16, 19, 21–25, 27)
tribenuron-methyl	1	100	(24)
trifluralin	15	93	(6, 7, 12–16, 18, 19, 21–25, 27, 28)

Data retrieved from Western Canadian studies published in refereed journals over a twenty year time span (1991-2011) (modified from Wilson (11)).

Pesticide concentrations measured in groundwater samples are usually reported to be below the level of concern to the health of organisms, although compound specific levels have exceeded the European groundwater quality standard of 0.1 µg/L (30, 31). Groundwater contamination is concerning, as more than 2.7 billion people rely on groundwater for potable water, including 75% of the population in Europe (32). A common pragmatic approach to assessing the spatial and temporal risk of potential water contamination by pesticides is to use pesticide fate models. For example, when the region of interest is large such as the agricultural land base of Canada, pesticide fate models are useful in assessing the effectiveness of beneficial agricultural management practices in protecting ground water resources (33). Pesticide fate models can augment large-scale water monitoring programs in the regulatory practices of pesticide environmental exposure assessments (34).

It is well known that sorption parameters are among the most sensitive input parameters in calculating pesticide transport to depth (35–37). Hence, field-specific data on sorption parameters have been found to be more important to the refinement of risks assessments than the choice of the pesticide fate model itself (38). Accurately quantifying the spatial variability of sorption parameters is important for better understandings of the uncertainty in the application of pesticide fate models over multiple spatial scales (e.g., from field to regions). In this chapter, we discuss the spatial variability of sorption parameters as reported by studies operating at the field, catchment and regional scales. We also provide an example of how to use near-infrared spectroscopy (NIRS) to estimate sorption variability for simulation inputs into the Pesticide Root Zone Model version 3.12.2 at the field scale.

Measurement and Quantification of Sorption

Sorption is a general term that refers to an increase in the concentration of a pesticide in the solid phase resulting from a reduction in the concentration of a pesticide in the liquid or gas phase. Pesticide sorption by soil is most commonly estimated using the batch equilibrium method (39), which provides for a measurement K , that is referred to as either the sorption parameter or partition constant, and has been used for more than five decades (40). Sorption of pesticides by soil is a rapid process, particularly in batch experiments (41), with the greatest sorption occurring within minutes to a few hours, and then decreasing over time with the majority of studies using 24 h as a default time for reaching equilibrium (39). In reality, sorption continues to increase slowly over time for most pesticides with studies showing an increase in sorption parameters by a factor up to 3.8 over 100 days (42). The OECD guideline 106 (43) gives a detailed description of the batch equilibrium method. In essence, a pesticide solution is added to air-dried soil in a test tube. The pesticide solution is usually prepared in 0.01 M CaCl₂ to minimize the dispersion of organoclay complexes (44) and to allow easy separation of solid and liquid phases, and the test tube is rotated to establish chemical equilibrium in the slurry. The concentration of the pesticide in the equilibrium solution (C_e) is measured, while the concentration of the pesticide in soil at equilibrium (C_s) is usually calculated using the difference between the pesticide mass in the initial solution and the pesticide mass in the solution at equilibrium.

When the batch equilibrium procedure is carried out using a single pesticide concentration, the distribution constant K_d , is calculated by C_s/C_e . K_d values can be influenced by the pesticide concentration used and tend to decrease as the concentration of the initial pesticide solution increases because the competition by pesticide molecules limits available sorption sites (45). In this case, the measured isotherm at different equilibrium concentrations displays a nonlinear pattern, often described by the Freundlich equation.

A sorption isotherm is applied, when a range of initial pesticide concentrations are used, to yield a single sorption parameter. Four (46) to seven (47) initial pesticide concentrations are typically used with the best fit to the sorption isotherm

often being the Freundlich rather than the Langmuir equation (48). The K_f (Freundlich constant) is calculated by nonlinear regression using the Freundlich equation in its log transformed form: $\text{Log } C_s = \log K_f + 1/n \log C_e$, where $1/n$ is the slope describing nonlinearity. Linear sorption is observed when $1/n = 1$, and it is only in this case that $K_d = K_f$. The exponent $1/n$ is usually greater than 0.7 (39), and very few experimental studies have reported values of $1/n$ greater than 1 for soils (49). Units of C_e and C_s should be chosen so that that isotherm lines cross at $C_e = 1$, which is the point where K_f is evaluated (50), as non-linear and linear isotherms intersect at $C_e = 1$. The unit of K_f varies depending on which units are chosen for C_e and C_s . This makes it difficult to compare K_f values among different studies, although a method has been developed to overcome this challenge (51).

K_d can be divided by the fraction of organic carbon in soil to calculate the soil organic carbon normalised sorption coefficient, K_{oc} . Researchers have proposed methods that allow K_{oc} to be measured independent of soil such as by high-performance liquid chromatography (52). K_{oc} can also be calculated using empirical regression equations that include, as the dependent variables, the n-octanol-water partition coefficient (K_{ow}) or water solubility (S) of the pesticide (53). The slope and intercept in these equations are influenced by the type of pesticides included in the regression (54). Even when the same equation is used, the calculated K_{oc} may not be consistent among studies because for each pesticide, there is a surprisingly wide variation in the data reported for K_{ow} and S (55).

With few exceptions, pesticide sorption parameters have been almost exclusively determined without considering the competition of other pesticides for sorption sites in soil. Nevertheless, studies have demonstrated that the sorption of some pesticides is reduced when other pesticides are competing for sorption sites in soil (48, 56–58). Inorganic chemicals can also compete with pesticides for sorption sites in soil, which has been observed for the herbicides diquat + paraquat and calcium (59), glyphosate and phosphorus (60, 61), glyphosate and cadmium (62), and propisochlor and copper (63).

Sorption Spatial Variability and Influencing Factors

Realization that the pesticide sorption varies among soil types arose as part of experimental work that tested differential pesticide bioactivity between soils (64–66). Numerous pesticide sorption experiments have been conducted in the past 75 years with most focussing on surface soils. Surprisingly, relatively few studies have defined the spatial variability in sorption parameters, and these studies have predominantly focussed on herbicides at the field scale (Table 2). The field scale variation in sorption parameters can be as large as that observed for the regional scale. For example, for soils in the Canadian Prairies, K_d values for 2,4-D ranged from 0.6 to 12.5 L/kg ($n=72$) in surface horizon samples taken along a 360-m long slope in an agricultural field (67) and from 0.6 to 14.5 L/kg ($n=41$) in surface horizon samples taken within a series of ecozones spanning a 660,000 km² area (68).

When examining the spatial variability of herbicide sorption in fields, catchments or regions, it is common for studies to evaluate whether the coefficient of variation (CV) of K_{oc} is smaller than that of K_d . By normalizing for organic carbon, it was hypothesized that K_{oc} should have a smaller coefficient of variation (CV) among soil types than K_d (78), but in only 55% of the comparable cases reported in Table 2 this is true. In fact, it is seldom the case for glyphosate whose sorption is weakly or not significantly associated with soil organic carbon (SOC) (37, 69).

Table 2. Studies Examining the Spatial Distribution of Herbicide Sorption Parameters. Mean and Coefficient of Variation (CV%) Values As Reported in the Reference Stated with the Exception of Singh (69) for Which the Values Were Calculated Based on Spreadsheets Containing Raw Data. H = Horizon, Which Can Be A, B or C Horizons, n=Number of Samples, F=Field, U=Upper Slopes, M=Mid Slopes, L=Lower Slopes. The Label A-Horizon Is Treated as Synonymous to Surface Soil. S = Subsurface Soil Which Is 40-50 Depth in Oliver (70) and 50-60 cm Depth in Rodrigues-Cruz (71).

<i>Sampling protocol</i>	<i>H</i>	<i>n</i>	<i>K_d mean</i>	<i>K_d CV%</i>	<i>K_{oc} mean</i>	<i>K_{oc} CV%</i>	<i>Reference</i>
2,4-dichlorophenoxy acetic acid							
F transect	A	72	4.21	50	211	26	(67)
	B	72	0.92	113	176	131	
	C	72	0.33	55	89	34	
F landform	A	121	2.90	48	82	30	(69)
	B	80	0.60	84	40	56	
	C	116	0.29	76	30	69	
F landform	A	110	1.98	42	98	30	(37)
	B	75	71.39	180	118	58	
	C	113	4.36	45	256	182	
F grid - U	A	98	0.9	44	91	37	(37)
F grid - M	A	128	1.0	50	108	48	
F grid - L	A	61	1.6	25	140	30	
Regional	A	123	5.8	89	235	59	(68)

Atrazine

Continued on next page.

Table 2. (Continued). Studies Examining the Spatial Distribution of Herbicide Sorption Parameters. Mean and Coefficient of Variation (CV%) Values As Reported in the Reference Stated with the Exception of Singh (69) for Which the Values Were Calculated Based on Spreadsheets Containing Raw Data. H = Horizon, Which Can Be A, B or C Horizons, n=Number of Samples, F=Field, U=Upper Slopes, M=Mid Slopes, L=Lower Slopes. The Label A-Horizon Is Treated as Synonymous to Surface Soil. S = Subsurface Soil Which Is 40-50 Depth in Oliver (70) and 50-60 cm Depth in Rodrigues-Cruz (71).

<i>Sampling protocol</i>	<i>H</i>	<i>n</i>	<i>K_d mean</i>	<i>K_d CV%</i>	<i>K_{oc} mean</i>	<i>K_{oc} CV%</i>	<i>Reference</i>
F landform	A	121	16.73	51	476	37	(69)
	B	80	3.87	62	270	32	
	C	116	2.42	49	259	46	
F landform	A	110	4.36	45	213	33	
	B	75	1.14	39	247	49	
	C	113	0.76	42	568	233	
F grid	A	241	5.2	35	181	21.2	(72)
Catchment	A	51	0.80	29	-	-	(73)
Regional	A	19	2.67	121	191	116	(70)
	S	18	0.84	132	119	114	
Bentazone							
F grid	A	20	0.06	26	-	-	(71)
	S	20	0.11	44	-	-	
Carbaryl							
F grid	A	27	10.50	115	522	147	(74)
Diuron							
Regional	A	43	9.6	161	407	63	(75)
Regional	A	101	6.49	140	315	84	(76)
Glyphosate							
F landform	A	121	43.37	65	1561	91	(69)
	B	80	61.04	51	5217	82	
	C	116	48.09	38	5445	52	
F landform	A	110	71.39	180	4903	187	
	B	75	94.51	136	20,540	130	
	C	113	73.87	84	65,411	322	

Continued on next page.

Table 2. (Continued). Studies Examining the Spatial Distribution of Herbicide Sorption Parameters. Mean and Coefficient of Variation (CV%) Values As Reported in the Reference Stated with the Exception of Singh (69) for Which the Values Were Calculated Based on Spreadsheets Containing Raw Data. H = Horizon, Which Can Be A, B or C Horizons, n=Number of Samples, F=Field, U=Upper Slopes, M=Mid Slopes, L=Lower Slopes. The Label A-Horizon Is Treated as Synonymous to Surface Soil. S = Subsurface Soil Which Is 40-50 Depth in Oliver (70) and 50-60 cm Depth in Rodrigues-Cruz (71).

<i>Sampling protocol</i>	<i>H</i>	<i>n</i>	<i>K_d mean</i>	<i>K_d CV%</i>	<i>K_{oc} mean</i>	<i>K_{oc} CV%</i>	<i>Reference</i>
F grid - U	A	98	108.2	28	11,183	30	(37)
F grid - M	A	128	133.6	36	14,863	43	
F grid - L	A	61	118.7	29	10,891	33	
Imazethapyr							
F grid	A	35	1.56	69.2	-	-	(70)
Isoproturon							
Catchment	A	51	0.85	30.0	-	-	(73)
F grid	A	20	1.32	7	-	-	(71)
	S	20	0.34	50	-	-	
Mecoprop							
F grid	A	20	0.26	26	-	-	(71)
	S	20	0.07	24	-	-	
Metamitron							
Catchment	A	51	0.96	30.0	-	-	(73)
Napropamide							
F grid	A	36	2.01	31	363	38	(77)
Phosalone							
F grid	A	27	172.18	131	9504	162	(74)

For the twelve different herbicides examined in various studies (Table 2), the reported CV of K_d has ranged from 7 to 180% but that of K_{oc} from 21 to 322%. For herbicides whose sorption is significantly associated with SOC, soil organic matter (SOM) characteristics largely determine the amount of herbicide sorbed per unit organic carbon. Techniques, ranging from conventional chemical fractionation methods to solid state Cross Polarization and Magic-Angle Spinning ^{13}C -Nuclear Magnetic Resonance applied on whole soils, have been used to derive SOM chemical, physical and structural parameters for correlation analyses

with K_{oc} values. For non-ionic herbicides, e.g. carbaryl, phosalonema (74) and diuron (79) but also for ionisable herbicides such as 2,4-D (80) an increased SOM aromaticity results in increasing K_{oc} values.

Pesticide sorption parameters in farm fields vary because sorption processes respond to the heterogeneity of soil properties that exists across slope positions and with soil depth. Intrinsic factors, such as irregularities in parent material deposition and weathering, as well as vertical pedological processes of leaching and bioturbation, induce variations in these soil properties in fields (81, 82). Thus, for a given herbicide, there can be large differences in the CV of K_d depending on the field sampled (e.g., glyphosate (69)), the slope position sampled (e.g., 2,4-D (37)), and the sampling depth (e.g., 2,4-D (67)) (Table 2). Sorption parameters are significantly associated with SOC content (37, 67, 72, 73, 83, 84), soil pH and clay content (37, 67, 72, 83). Also, in two field studies (67, 69), variations in 2,4-D K_d were particularly strong in the B-horizon (Table 2), possibly because the presence of iron oxides is known to increase 2,4-D sorption in soil (85, 86). Such redoximorphic features only occur in soil profiles that showed evidence of poor drainage and periodic reduction.

Extrinsic factors such as the cultivation of fields can influence soil properties variations due to the redistribution of topsoil from upper slope to lower slope positions by tillage (87). Soil redistribution by tillage can have a profound impact on soil profile characteristics (88–90) and herbicide sorption (84, 90). For example, in calcareous prairie landscapes that have been subjected to intensive tillage practices for decades, soil profiles in upper slopes are usually entirely low in SOC, but high in soil carbonate content and soil pH. In these landscapes, for herbicides 2,4-D, glyphosate (84) and saflufenacil (90) K_d and K_{oc} values have shown to vary less with depth in soil profiles of upper slopes than lower slopes.

Topography is a soil-forming factor and affects the redistribution of water and soil in soil-landscape and hence influences soil development and the characteristics of the soil layers particularly the surface soil. Digital terrain modelling can be used for quantitative morphometric characterization of landscapes with examples of terrain attributes being slope gradient, slope aspect, horizontal, vertical and mean curvatures (91) topographic and stream power index, and specific catchment area (60, 92). It has been shown that the strongest dependence of soil properties on topography arises within the surface layer to a depth of 30 cm (93). The r^2 values of regression equations describing the relation between topographic variables and soil properties have been shown to vary from 0.39 to 0.82 in landscapes, with predictions being most successful for SOC but also adequate for clay and soil pH in several landscapes (94–98). Digital terrain models have been shown in some cases to improve the predictions of fate parameters of herbicides in surface soils of fields. Terrain attributes can explain 50 to 56% of the spatial variability of 2,4-D K_d values in some landscapes (37, 98), but for landscapes in which the discharge of solute-rich water from wetlands is a major soil-forming factor, the association between terrain attributes and sorption parameters have been shown to be very weak (69). In these cases, soil development is less controlled by surface processes.

The variation of pesticide sorption parameters in landscapes remains difficult to predict because of the large variations in K_d and K_{oc} values. Probability density functions have been incorporated in stochastic pesticide fate simulations to help

account for spatial variations in sorption input parameters. Modelers typically assume that a normal (99), log-normal (100), or uniform (101) distribution to describe variability in sorption parameters at the large scale. In reality, nevertheless, the appropriate distribution for a particular pesticide in a particular spatial unit is not well understood. We utilized data reported in a study by Singh (69) in which 70 soil profiles were collected in an undulating to hummocky terrains under grain and oilseed rotation and zero-tilled (16 ha). These profiles were sampled by horizon, yielding 314 samples in total. These data show that distributions vary widely among pesticides and mineral horizons (Figure 1). Thus the best fit to distributions resulted in a range of probability density functions (Table 3). The log-normal function provided a better fit to K_d and K_{oc} data than normal and uniform PDFs across all pesticides and mineral horizons (Table 3).

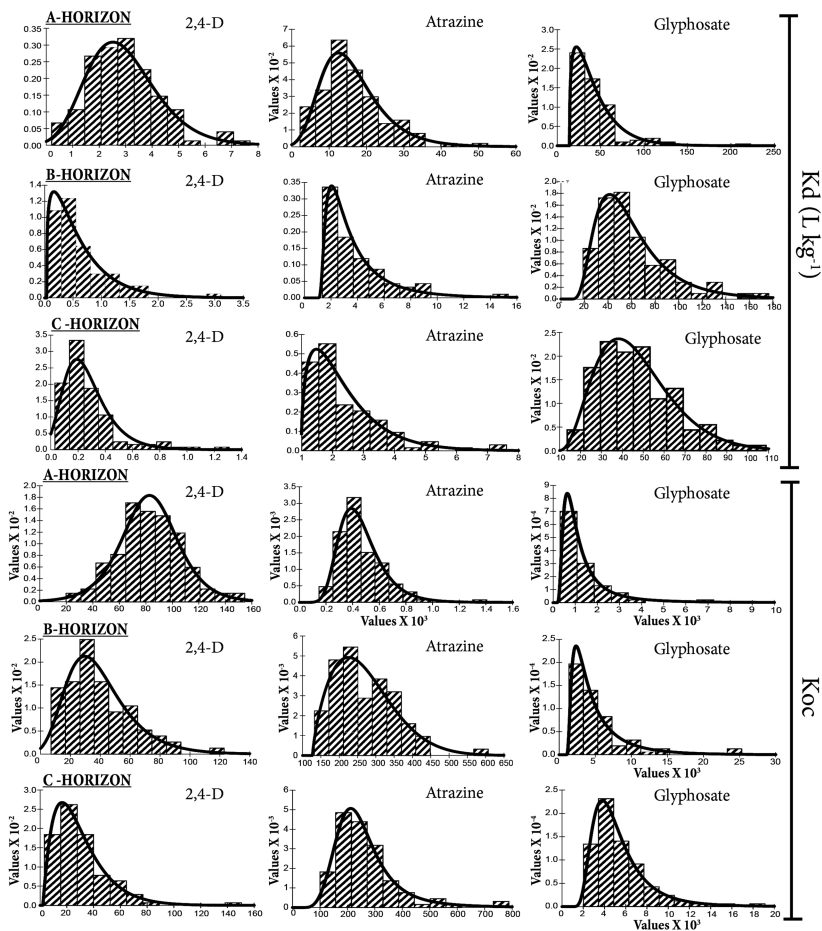


Figure 1. Probability distributions for 2,4-D, atrazine and glyphosate K_d and K_{oc} values by soil mineral horizon in a undulating to hummocky terrain in Manitoba, Canada. Data described in Singh (69).

Pesticide Fate Models

Siimes Kämäri (102) described 54 pesticide fate models. Thirteen of these are one-dimensional deterministic models designed for the simulation of pesticide fate at the field scale. These models are simpler than those that simulate pesticide fate in two- or three-dimensions and thus have the advantage of requiring fewer input data, and being more computationally efficient. One-dimensional models are more readily used in regulatory and policy assessment at the large scale (33, 34, 103). Examples include the Pesticide Root Zone Model [1984], Groundwater Loading Effects of Agricultural Management Practices [1987], Leaching Estimation and Chemistry Model [1987], the Root Zone Water Quality Model [1992], and Pesticide Emission Assessment at Regional and Local scales [2000]. Although designed as a deterministic model, one can incorporate probability distribution to, for example, the Pesticide Root Zone Model, to account for input parametric uncertainty (33).

Spatial variations in sorption parameters are not often considered in fate modeling due to lack of quantitative data describing appropriate input parameters. For example, batch equilibrium techniques are time-consuming and expensive and this information is often unavailable. Thus, when deterministic modeling approaches are used at the large-scale, sorption parameters are often estimated from generic databases (103) or from regression equations based on soil properties data (104). Alternatively, stochastic modeling utilizes probability density functions often under the assumption that sorption parameters are independent of soil properties (105), leading to large uncertainties in risk assessments (106).

Uncertainties in risk assessment could be more accurately accounted for by using more efficient methods that, at a more reasonable cost, can rapidly measure the sorption coefficients of large numbers of soil samples. NIRS is molecular spectroscopy operating in the wavelength range 780 to 2500 nm. Substances absorbing light in this region are generally those with covalent bonds between O, H, C, and N. NIRS correlates the spectral data from a set of representative samples with the chemical analytical data in the form of calibrations that are utilized to predict future samples of the same type (107). NIRS is successful in predicting a range of soil properties, including strong predictions for SOC content and clay (108, 109). Hence, for fields and regions, NIRS has been successfully used to estimate sorption coefficients for herbicides lindane, diuron (110), atrazine and 2,4-D (111), illustrating the main strength of NIRS in estimating sorption parameters of both nonionic and ionisable pesticides. Nevertheless, there are exceptions such as the poor applicability of NIRS for estimating the sorption of glyphosate whose sorption is often poorly correlated with SOC (Farenhorst unpublished data). The application of NIRS and other spectroscopic techniques in estimating sorption coefficients is further discussed in detail in Chapter 12 (112) in this volume.

Table 3. Variation in Sorption Parameters and Soil Organic Carbon Content in A, B and C Horizons and the Goodness of Fit (Chi-Square with $P < 0.05$) for Probability Distributions (Best Fitted Distribution, Normal Distribution and Log-Normal Distribution) Fitted to Data

<i>Parameter</i>	<i>Mean</i>	<i>StDev</i>	<i>CV</i>	<i>Best fit</i>	<i>Best Fit</i>	<i>Normal</i>	<i>Log-Normal</i>
<i>K_d</i> in A-horizon							
2,4D	2.9	1.4	48	Pearson5	2.6	4.6	3.4
glyphosate	43.4	28.3	65	Gamma	4.6	78.6	7.6
Atrazine	16.7	8.5	51	ExtValue	1.8	12.2	3.0
<i>K_{oc}</i> in A-horizon							
2,4D	81.7	24.4	30	logistic	4.6	8.0	8.6
glyphosate	1560.7	1426.5	91	Pearson5	7.0	104.4	13.8
Atrazine	475.7	175.5	37	ExtValue	13.8	19.4	17.0
<i>K_d</i> in B-horizon							
2,4D	0.6	0.5	84	Gamma	5.2	31.5	6.7
glyphosate	61.0	31.4	51	Lognorm	1.6	19.6	1.6
Atrazine	3.9	2.4	62	InvGauss	2.4	45.9	3.2
<i>K_{oc}</i> in B-horizon							
2,4D	39.8	22.2	56	ExtValue	6.7	12.0	9.0
glyphosate	5216.5	4276.6	82	InvGauss	2.1	65.4	67.0
Atrazine	270.2	85.4	32	Weibull	9.0	13.3	13.3
<i>K_d</i> in C-horizon							
2,4D	0.3	0.2	76	ExtValue	2.8	43.1	8.0
glyphosate	48.1	18.5	38	BetaGeneral	2.6	18.3	19.1
Atrazine	2.4	1.2	49	Gamma	5.3	51.9	9.1
<i>K_{oc}</i> in C-horizon							
2,4D	29.5	20.4	69	Gamma	3.9	24.9	9.1
glyphosate	5444.7	2807.1	52	Pearson5	6.6	41.6	10.5
Atrazine	258.9	117.8	46	LogLogistic	5.7	29.3	7.4

(Data from Singh (69))

Here we provide an example of one of our recent studies (113) in which we tested the feasibility of using NIRS to measure a large number of 2,4-D K_d values for use as input parameters in Pesticide Root Zone Model version 3.12.2 (PRZM3). The study utilized samples from 309 soil horizons. In the example

provided, spectra were recorded in triplicate for each 25 g soil sample using the Foss NIRS Systems model 6500 spectrophotometer (Carl Zeiss, Jena, Germany) equipped with a Rapid Content Sampler (RSC). Soil was presented in 5 cm diameter glass petri dishes to collect data over the wavelength range of 1100 to 2500 nm at 2 nm intervals. This results in 700 absorbance values for each spectrum. Triplicate spectra were obtained for each sample by rotating the petri dish 120 degrees between scans. The triplicate spectra for each sample were imported into Unscrambler® multivariate statistical analysis software version 9.8 (2008, CAMO Process ASA) and averaged. Then 2,4-D Lab- K_d values, determined by batch equilibrium procedures in the laboratory for each sample, were added to the Unscrambler file to become the constituent. Partial least squares regression (PLS1) was used to develop calibrations for 2,4-D Lab- K_d values. Calibrations used the test set method in which all the samples were sorted from low to high values for the constituent and were divided into calibration (two-thirds of the total samples) and validation (one-third of the total samples) by selecting every third sample for the validation set. This results in approximately the same distribution of values in the calibration and validation sets. A total of 37 trial calibrations were developed the constituent by performing mathematical pretreatments on the raw spectra by smoothing over 5, 11, 21, or 41 wavelength points. This was followed by transformation of the spectra to the first or second derivative using derivative gaps of 5, 11, 21, or 41 wavelength points. The best calibration for the constituent was selected based on the highest coefficient of determination (r^2) between the laboratory-measured values of the constituent and the NIRS predicted values for the constituent, the lowest standard error of prediction (SEP), and the highest RPD. The RPD value is the ratio of the SD of the constituent values in the validation set to SEP. In soil and environmental analysis, values of RPD >3 are considered successful (108) or excellent (114) calibrations.

Using the best calibration, 2,4-D distribution constants were predicted (2,4-D NIRS- K_d values) for all samples in the validation set. Results (Table 4) indicate that NIRS is an excellent tool to determine 2,4-D K_d values. An added benefit is the non-destruction of samples and the rapid nature of the NIRS analysis, leading to quick throughput for many samples used to characterize spatial and regional variability.

Subsequently, the predicted NIRS- K_d were used as input parameters in PRZM3 to calculate the herbicide mass leached (kg/ha) in the 103 soil horizons from the validation set. Lab- K_d measured by conventional batch equilibrium techniques were also used as input parameters in PRZM3 to calculate the herbicide mass leached (kg/ha) in the same soil horizons. As shown in Table 5, the correlation coefficient (r) between Lab- L_m (herbicide mass calculated by PRZM3 using Lab- K_d) and NIRS- L_m (herbicide mass calculated by PRZM3 using NIRS- K_d) was strong. The regression equation shows how NIRS- L_m can be used to calculate the herbicide mass leached that would have been predicted when using the conventional batch equilibrium procedure and PRZM3 (Table 5). As such, better quantification of pesticide sorption variability through NIRS may provide greater confidence in pesticide fate modelling by improving on the assessment of pesticide leaching potential in soil-landscapes.

Table 4. Accuracy of Prediction and Mathematical Treatment for the Prediction of the 2,4-D distribution coefficient (K_d) by near-infrared spectroscopy (NIRS). r^2 , SEP, bias and RPD Values Are for Data Derived from Evaluation of the Validation Sample Set.^a

<i>n</i>	r^2	SEP	bias	RPD	math treatment
103	0.90	0.47	0.03	3.17	s13d13

^a n = number of samples in the validation set; r^2 = coefficient of determination; SEP = standard error of prediction; bias = difference between mean of the NIRS-predicted data (2,4-D NIRS- K_d values) and the reference data (2,4-D lab- K_d values); RPD = ratio of standard deviation of values in the validation set to SEP; for mathematical treatment, the segment = number of wavelength points over which the spectra were smoothed and designated as “s”; gap = number of wavelength points over which the derivative was calculated, in this case “d” for the first derivative.

Table 5. Correlation and Relationship between Lab- L_m (Herbicide Mass Calculated by PRZM3 Using Lab- K_d) and NIRS- L_m (Herbicide Mass Calculated by PRZM3 Using NIRS- K_d) for Data Derived from Evaluation of the Validation Sample Set^a

<i>n</i>	<i>r</i>	Regression equation	RMSE	<i>p</i> -value
103	0.89	Lab- L_m = $8.33 \times 10^{-3} + 9.02 \times 10^{-1}(\text{NIRS- } L_m)$	5.78×10^{-4}	<0.001

^a n = number of samples in the validation set; r = correlation coefficient; RMSE = root mean square error of regression.

Concluding Remarks

Pesticide sorption parameters have been determined using batch equilibrium procedures in numerous studies for the past 75 years, although few studies have allowed for detailed descriptions of the spatial variations of sorption parameters at field and regional scales. However, it is now well understood that such variations are caused by differences in soil properties resulting from natural processes of soil formation as well as human impacts such as cultivation. Pesticide use can only be sustainable when agricultural management practices are designed to minimize the potential off-site transport of pesticides from its application area into the broader environment where, depending on estimated environmental concentrations and toxicological profiles, may pose a risk to ecological systems and drinking water resources.

Many governments are attempting to improve how agricultural pesticides are used. These attempts are often founded on decisions based on the outcome of pesticide fate models under assumed worst case conditions. Useful assessments aimed to understand pesticide off-target movement should be conducted to test

hypothetical as well as realistic scenarios of pesticide transport using measured sorption variability data under defined farm management and climatic conditions.

Sorption parameters are among the most sensitive input parameters in pesticide fate models. Therefore, the usefulness of these models will depend on the accuracy of the sorption parameter data. As a result, the difficulty of accurately describing the variability of sorption input parameters at the field and regional scales poses an enormous challenge when developing government policy and program recommendations concerning optimal pesticide use to safeguard both agricultural productivity and the environment. As outlined in this chapter, NIRS extends conventional analytical capacity with a method that is rapid and non-destructive to determine the K_d values in numerous samples collected in a field for integration into pesticide fate modeling.

Acknowledgments

All references by Farenhorst cited in the chapter were made possible through funding from the Natural Sciences and Engineering Research Council of Canada.

References

1. Caldwell, D. *Quantification of spray drift from aerial applications of pesticide*; University of Saskatchewan: Saskatoon, Saskatchewan, 2007.
2. Grover, R.; Shewchuk, S. R.; Cessna, A. J.; Smith, A. E.; Hunter, J. H. *J. Environ. Qual.* **1985**, *14*, 203–210.
3. Larney, F. J.; Cessna, A. J.; Bullock, M. S. *J. Environ. Qual.* **1999**, *28*, 1412–1421.
4. Waite, D. T. G. R.; Westcott, N. D.; Irvine, D. G.; Kerr, L. A.; Sommerstad, H. *Environ. Toxicol. Chem.* **1995**, *14*, 1171–1175.
5. Jantunen, L. M.; Helm, P. A.; Ridal, J. J.; Bidleman, T. F. *Atmos. Environ.* **2008**, *42*, 8533–8542.
6. Messing, P. G.; Farenhorst, A.; Waite, D. T.; McQueen, D. A. R.; Sproull, J. F.; Humphries, D. A.; Thompson, L. L. *Atmos. Environ.* **2011**, *5*, 7227–2734.
7. Waite, D. T.; Grover, R.; Westcott, D. *Environ. Toxicol. Chem.* **1992**, *11*, 741–748.
8. Donald, D.; Hunter, F.; Sverko, E.; Hill, B.; Syrgiannis, J. *Environ. Toxicol. Chem.* **2005**, *24*, 2–10.
9. Barbash, J. E.; Thelin, G. P.; Kolpin, D. W.; Gilliom, R. J. *J. Environ. Qual.* **1997**, *30*, 831–845.
10. Kolpin, D. W.; Barbash, J. E.; Gilliom, R. J. *Environ. Sci. Technol.* **1998**, *32*, 558–566.
11. Wilson, J. L. *Agricultural Pesticide Use Trends in Manitoba and 2,4-D Fate in Soil*; University of Manitoba: Winnipeg, Manitoba, 2012.
12. Grover, R.; Waite, D. T.; Cessna, A. J.; Nicholaichuk, W.; Irvin, D.; Kerr, L. A.; Best, K. *Environ. Toxicol. Chem.* **1997**, *16*, 638–643.
13. Anderson, A.-M.; Saffran, K. A.; Byrtus, G. *Pesticides in Alberta surface waters*; T/833; Alberta Environment: Edmonton, AB, 1997.

14. Wood, J. A.; Anthony, D. H. J. *J. Environ. Qual.* **1997**, *26*, 1308–1318.
15. Donald, D. B.; Syriannis, J.; Hunter, F.; Weiss, G. *Sci. Total Environ.* **1999**, *23*, 1173–1181.
16. Rawn, D. F. K.; Halldorson, T. H. J.; Woychuk, R. N.; Lawson, B. D.; Muir, D. C. G. *Water Qual. Res.* **1999a**, *34*, 183–219.
17. Rawn, D. F. K.; Halldorson, T. H. J.; Lawson, B. D.; Muir, D. C. G. *J. Environ. Qual.* **1999b**, *28*, 898–906.
18. Donald, D. B.; Gurprasad, N. P.; Quinnett-Abbott, L.; Cash, K. *Environ. Toxicol. Chem.* **2001**, *20*, 273–279.
19. Hill, B.; Harker, K.; Hasselback, P.; Moyer, J.; Inaba, D.; Byers, S. *Phenoxy herbicides in Alberta rainfall as affected by location, season, and weather patterns*; Final Technical Report No. 990059; AAFC Lethbridge Research Centre: Lethbridge, AB, 2002; pp 1–109.
20. Waite, D. T.; Sproull, J. F.; Quiring, D. V.; Cessna, A. J. *Anal. Chim. Acta.* **2002**, *467*, 245–252.
21. Cessna, A. J.; Elliott, J. A. *J. Environ. Qual.* **2004**, *33*, 302–315.
22. Donald, D. B.; Hunter, F. G.; Sverko, E.; Hill, B. D.; Syrgiannis, J. *Environ. Toxicol. Chem.* **2005**, *24*, 2–10.
23. Yao, Y.; Tuduri, L.; Harner, T.; Blancard, P.; Poissant, L.; Murphy, C.; Belzer, W.; Aulagnier, F.; Li, Y.-F.; Sverko, E. *Atmos. Environ.* **2006**, *40*, 4339–4351.
24. Donald, D. B.; Cessna, A. J.; Sverko, E.; Glozier, N. *Environ. Health Perspect.* **2007**, *115*, 1183–1191.
25. Yao, Y.; Harner, T.; Blancard, P.; Tuduri, L.; Waite, D.; Poissant, L.; Murphy, C.; Belzer, W.; Aulagnier, F.; Sverko, E. *Environ. Sci. Technol.* **2008**, *42*, 5931–5937.
26. Glozier, N. E.; Struger, J.; Cessna, A. J.; Gledhill, M. R.; Ernst, W. R.; Sekela, M. A.; Cagampan, S. J.; Sverko, E.; Murphy, C.; Murray, J.; Donald, D. B. *Environ. Sci. Pollut. Res.* **2012**, *19*, 821–834.
27. Environment Canada. *Presence and levels of priority pesticides in selected aquatic ecosystems*; Water Science and Technology Directorate, Environment Canada: Ottawa, ON, 2011; Cat. No: En14-40/2011E=PDF, 103 pp.
28. Waite, D. T.; Cessna, A. J.; Grover, R.; Kerr, L. A.; Snihura, A. D. *J. Environ. Qual.* **2004**, *33*, 1116–1128.
29. Humphries, D.; Byrtus, G.; Anderson, A. M. *Glyphosate residues in Alberta's atmospheric deposition, soils and surface waters*; Alberta Environment: Edmonton, AB, 2005; Pub. No. T/806, 43 pp.
30. Loos, R.; Locoro, G.; Comero, S.; Contini, S.; Schwesig, D.; Werres, F.; Balsaa, P.; Gans, O.; Weiss, S.; Blaha, L.; Bolchi, B.; Gawlik, B. M. *Water Res.* **2010**, *44*, 4115–4126.
31. Toccalino, P. L.; Gilliom, R. J.; Lindsey, B. D.; Rupert, M. G. *Groundwater* **2014** DOI:10.1111/gwat.12176.
32. Morris, B. L.; Lawrence, A. R. L.; Chilton, P. J. C.; Adams, B.; Calow, R. C.; Klinck, B. A. *Groundwater and its Susceptibility to Degradation: A Global Assessment of the Problem and Options for Management*; RS. 03-3; United Nations Environment Programme, 2003.

33. Gagnon, P.; Sheedy, C.; Farenhorst, A.; McQueen, D. A. R.; Cessna, A. J.; Newlands, N. K. *Integr. Environ. Assess. Manage.* **2004** DOI:10.1002/ieam.1533.
34. Dubus, I. G.; Colin, D.; Brown, C. D.; Beulke, S. *Pest Manage. Sci.* **2003**, *59*, 962–982.
35. Villeneuve, J. P.; Lafrance, P.; Banton, O.; Frechette, P.; Robert, C. J. *Contam. Hydrol.* **1998**, *3*, 77–96.
36. Boesten, J. J. T. I.; van der Linden, A. M. A. *J. Environ. Qual.* **1991**, *20*, 425–435.
37. Farenhorst, A.; Papiernik, S. K.; Saiyed, I. M. P.; Stephens, K. D.; Schumacher, J. A.; Lobb, D. A.; Li, S.; Lindstrom, M. J.; Schumacher, T. E. *J. Environ. Qual.* **2008**, *37*, 1201–1208.
38. Dann, R. L.; Close, M. E.; Lee, R.; Pang, L. *J. Environ. Qual.* **2006**, *35*, 628–640.
39. Wauchope, R. D.; Yeh, S.; Linders, J.; Kloskowski, R.; Tanaka, K.; Rubin, B.; Katayama, A.; Kordel, W.; Gerstl, Z.; Lane, M.; Unsworth, J. B. *Pest Manage. Sci.* **2002**, *58*, 419–445.
40. Yuen, Q. H.; Hilton, H. W. *J. Agric. Food Chem.* **1962**, *10*, 386–392.
41. Kookana, R. S.; Aylmore, L. A. G.; Gerritse, R. G. *Soil Sci.* **1992**, *154*, 214–225.
42. Oi, M. *J. Agric. Food Chem.* **1999**, *47*, 327–332.
43. OECD/OCDE. *OECD guideline for the testing of chemicals*; 2000.
44. Hinds, A. A.; Lowe, L. E. *Can. J. Soil Sci.* **1980**, *60*, 329–335.
45. Gaultier, J.; Farenhorst, A.; Kim, S. M.; Saiyed, I.; Cessna, A. J.; Glozier, N. E. *Wetlands* **2009**, *29*, 837–844.
46. Indraratne, S. P.; Farenhorst, A.; Goh, T. B. *J. Environ. Sci. Health, Part B* **2008**, *43*, 21–26.
47. Vallée, R.; Dousset, S.; Billet, D.; Benoit *Environ. Sci. Pollut. Res. Int.* **2013**, *21*, 4895–4905.
48. Jin, X.; Ren, J.; Wang, B.; Lu, Q.; Yu, Y. *Environ. Sci. Pollut. Res. Int.* **2013**, *20*, 6282–6289.
49. Piwowarczyk, A. A.; Holden, N. M. *Chemosphere* **2013**, *90*, 535–541.
50. Bowman, B. E. *J. Environ. Sci. Health* **1981**, *816*, 113–123.
51. Bowman, B. T. *Soil Sci. Soc. Am. J.* **1982**, *46*, 740–743.
52. Hodson, J.; Williams, N. A. *Chemosphere* **1988**, *17*, 67–77.
53. Briggs, G. G. *J. Agric. Food Chem.* **1981**, *29*, 1050–1059.
54. Brown, D. S.; Flagg, E. W. *J. Environ. Qual.* **1981**, *10*, 382–387.
55. Pontolillo, J.; Eganhouse, R. P. *The Search for Reliable Aqueous Solubility (Sw) and Octanol-Water Partition Coefficient (Kow) Data for Hydrophobic Organic Compounds: DDT and DDE as a Case Study*; U.S. Geological Survey Water-Resources Investigations 01-4201, 2001.
56. Turin, H. J.; Bowman, R. S. *J. Environ. Qual.* **1997**, *26*, 1282–1287.
57. Farenhorst, A.; B.T., B. *J. Environ. Sci. Health, Part B* **1998**, *33*, 671–681.
58. Farenhorst, F.; Prokopowich, B. *J. Environ. Sci. Health, Part B* **2003**, *B38*, 713–721.
59. Best, J. A.; Weber, J. B.; Weed, S. B. *Soil Sci.* **1972**, *114*, 444–450.

60. de Jonge, H.; de Jonge, L. W.; Jacobsen, O. H.; Yamaguchi, T.; Moldrup, P. *Soil Sci.* **2001**, *166*, 230–238.
61. Dion, H. M.; Harsh, J. B.; Hill, H. H. *J. Radioanal. Nucl. Chem.* **2001**, *249*, 385–390.
62. Wang, B.; Zhou, D.; Luo, X.; Sun, R. *J. Environ. Sci. (China)* **2004**, *16*, 881–884.
63. Xu, X.; Huang, M.; Gu, Q.; Wanga, Y.; Cao, Y.; Du, X.; Xu, D.; Huang, Q.; Li, F. *J. Colloid Interface Sci.* **2005**, *287*, 422–427.
64. Shipinoy, N. A. *Bull. Plant Prot.* **1940**, *1-2*, 192–199.
65. Barlow, F.; Hadaway, A. B. *Bull. Entomol. Res.* **1955**, *46*, 547–559.
66. Bailey, G. W.; White, J. J. *Agric. Food Chem.* **1964**, *12*, 324–332.
67. Gaultier, J.; Farenhorst, A.; Crow, G. *Can. J. Soil Sci.* **2006**, *86*, 89–95.
68. Gaultier, J.; Farenhorst, A.; Cathcart, J.; Goddard, T. *J. Environ. Qual.* **2008**, *37*, 1825–1836.
69. Singh, B.; Farenhorst, A.; Gaultier, J.; Pennock, D.; Degenhardt, D.; McQueen, R. *Geoderma* **2014** (accepted to with revisions).
70. Oliver, D. P.; Kookana, R. S.; Salama, R. B.; Correll, R. *Aust. J. Soil Res.* **2003**, *41*, 861–874.
71. Rodriguez-Cruz, S. M.; Jones, J. E.; Bending, J. D. *Soil. Biol. Biochem.* **2006**, *38*, 2910–2918.
72. Novak, J. M.; Moorman, T. B.; Cambardella, C. A. *J. Environ. Qual.* **1997**, *26*, 1271–1277.
73. Coquet, Y.; Barriuso, E. *Agronomie* **2002**, *22*, 389–398.
74. Ahmad, R.; Kookana, R.; Alston, A.; Skjemstad, J. *J. Environ. Sci. Technol.* **2001**, *35*, 878–884.
75. Liyanage, J. A.; Watawala, R. C.; Aravinna, P. G. P.; Smith, L.; Kookana, R. S. *J. Agric. Food Chem.* **2006**, *54*, 1784–1791.
76. Forouzangohar, M.; Kookana, R. S.; Forrester, S. T.; J., S. R.; Chittleborough, D. J. *J. Environ. Sci. Technol.* **2008**, *42*, 3283–3288.
77. Elabd, H.; Jury, W. A. *J. Environ. Sci. Technol.* **1986**, *20*, 256–260.
78. Gerstl, Z. *J. Contam. Hydrol.* **1990**, *6*, 357–375.
79. Ahangar, G. A.; R.J., S.; Kookana, R. S.; Chittleborough, D. J. *Chemosphere* **2008**, *70*, 1153–1160.
80. Farenhorst, A.; Saiyed, I.; Goh, T. B.; McQueen, P. *J. Environ. Sci. Health, Part B* **2010**, *45*, 204–213.
81. Goderya, F. S. *J. Soil. Contam.* **1998**, *7*, 243–264.
82. Park, S. J.; Vlek, P. L. G. *Geoderma* **2002**, *109*, 117–140.
83. Oleivera, R. S.; Koskinen, W. C.; Ferreira, F. A.; Khakural, B. R.; Mulla, D. J.; Robert, P. J. *Weed Science* **1999**, *47*, 243–248.
84. Farenhorst, A.; McQueen, D. A. R.; Saiyed, I.; C. Hilderbrand, C.; Li, S.; Lobb, D. A.; Messing, P.; Schumacher, T. E.; Papiernik, S. K.; Lindstrom, M. J. *Geoderma* **2009**, *150*, 267–277.
85. Reddy, K.; Gambrell, R. *Agric. Ecosyst. Environ.* **1987**, *18*, 231–241.
86. Celis, R.; Hermosin, M. C.; Cox, L.; Cornejo, J. *J. Environ. Sci. Technol.* **1999**, *33*, 1200–1206.
87. Gregorich, E.; Anderson, D. *Geoderma* **1985**, *36*, 343–354.

88. Lindstrom, M. J.; Nelson, W. W.; Schumacher, T. E. *Soil Tillage Res.* **1992**, *24*, 243–255.
89. Li, S.; Lobb, D. A.; Lindstrom, M. J.; Farenhorst, A. *Catena* **2007**, *70*, 493–505.
90. Papiernik, S. K.; Koskinen, W. C.; Barber, B. L. *Agric. Food Chem.* **2012**, *60*, 10936–10941.
91. Evans, I. S. Z. *Geomorph. Suppl-Bd.* **1980**, *36*, 274–295.
92. Martz, L. W.; De Jong, E. *Comput. Geosci.* **1988**, *14*, 627–640.
93. Florinsky, I. V.; Eilers, R. G.; Manning, G. R.; Fuller, L. G. *Environ. Modell. Software.* **2002**, *17*, 295–311.
94. Pennock, D. J.; Zebarth, B. J.; De Jong, E. *Geoderma* **1987**, *40*, 297–315.
95. Moore, I. D.; Grayson, R. B.; Ladson, A. R. *Hydrol. Proc.* **1991**, *5*, 3–30.
96. Gessler, P. E.; Moore, I. D.; McKenzie, N. J.; Ryan, P. J. *Int. J. Geogr. Inform. Sci.* **1995**, *9*, 421–432.
97. Florinsky, I. V.; Arlashina, H. A. *Geoderma* **1998**, *82*, 359–380.
98. Farenhorst, A.; Florinsky, I. V.; Monreal, C. M.; Muc, D. *Can. J. Soil Sci.* **2003**, *83*, 557–564.
99. Nofzigers, D. L.; Chena, J.; Haana, C. T. *J. Environ. Sci. Health, Part A* **1994**, *29*, 1133–1155.
100. Dubus, I. G.; Brown, C. D. *J. Environ. Qual.* **2002**, *31*, 227–240.
101. Warren-Hicks, W.; Carbone, J. P.; Havens, P. L. *Environ. Toxicol. Chem.* **2002**, *21*, 1570–1577.
102. Siimes, K.; Kamari, J. *Boreal Environ. Res.* **2003**, *8*, 35–51.
103. Cessna, A. J.; Sheedy, C.; Farenhorst, A.; McQueen, D. A. R. *Environmental Sustainability of Canadian Agriculture: Agri-Environmental Indicator Report Series - Pesticides*; Agriculture and Agri-Food Canada: Ottawa, Ontario, 2010; pp 101–107.
104. Weber, J. B.; Wilkerson, G. G.; Reinhardt, C. F. *Chemosphere* **2004**, *55*, 157–166.
105. Heuvelink, G. B. M.; Burgers, S. L. G. E.; Tiktak, A.; Van Den Berg, F. *Geoderma* **2010**, *155*, 186–192.
106. Dubus, I. G.; Brown, C. D.; Beulke, S. *Sci. Total Environ.* **2003**, *317*, 53–72.
107. Williams, P.; Norris, K. *Near-Infrared Technology in the Agricultural and Food Industries*; American Association of Cereal Chemists, Inc: St. Paul, Minnesota, 2001; p 296.
108. Malley, D. F.; Martin, P. D.; Ben-Dor, E. Application in analysis of soils. In *Near-Infrared Spectroscopy in Agriculture*; Roberts, C. A., Workman, J. J., Reeves, J. B., Eds.; American Society of Agronomy-Crop Science Society of America-Soil Science Society of America: Madison, WI, 2004; Vol. Agronomy Monograph No. 44, pp 729–784.
109. Reeves, J. B.; McCarty, G. W.; Mimmo, T. *Environ. Pollut.* **2002**, *116*, S277–S28.
110. Bengtsson, S.; Berglof, T.; Kylin, H. *Bull. Environ. Contam. Toxicol.* **2007**, *78*, 295–298.
111. Singh, B.; Farenhorst, A.; Malley, F. *Near Infrared Spectrosc. News* **2010**, *21*, 7–9.

112. Kookana, R. S.; Ahmad, R.; Farenhorst, A. Sorption of pesticides and its dependence on soil properties: Chemometrics approach for estimating sorption. In *Non-First Order Degradation and Time-Dependent Sorption of Organic Chemicals in Soil*; Chen, W., Cheplick, M., Reinken, G., Jones, R. L., Eds; ACS Symposium Series 1174; American Chemical Society: Washington, DC, 2014; Chapter 14.
113. Singh, B.; Farenhorst, A.; McQueen, R.; Malley, F. Unpublished data.
114. Dunn, B. W.; Batten, G. D.; Beecher, H. G.; Ciavarella, S. *Aust. J. Exp. Agric.* **2002**, *24*, 607–614.

Chapter 15

Implementation of Sorption Kinetics Coupled with Differential Degradation in the Soil Pore Water System for FOCUS-PRZM

Wenlin Chen,^{*}¹ Mark Cheplick,² Gerald Reinken,³ and Russell Jones⁴

¹Syngenta Crop Protection, LLC, Greensboro, North Carolina 27409, U.S.A.

²Waterborne Environmental, Inc., Leesburg, Virginia 20175, U.S.A.

³Bayer CropScience, Monheim 6690, Germany

⁴Bayer CropScience, Research Triangle Park, North Carolina 27709, U.S.A.

^{*}E-mail: wenlin.chen@syngenta.com.

This chapter describes the development of the coupled sorption and degradation kinetics in the soil-water system and the implementation of the kinetics into FOCUS-PRZM (Pesticide Root Zone Model), which is used in European pesticide registrations for assessing the leaching potential under proposed use conditions (1, 2). New codes of the kinetics were verified by the analytical solution (assuming linear sorption isotherm) and a well-established model LEACHP. Several field measured data sets were used to evaluate the new version of FOCUS-PRZM. Results demonstrate that the new version was able to reasonably predict the soil residue levels for many orders of magnitude over the entire time scale of field experiments. Parameters of the sorption kinetics can be converted to the ones adapted in FOCUS-PEARL, one of the other EU regulatory models for pesticide groundwater exposure assessment. Model simulations showed high sensitivity of sorption kinetics to the predicted groundwater concentrations in all nine EU groundwater scenarios.

Introduction

Time-dependent sorption of pesticides and other anthropogenic organic compounds by soil solid constituents is a widely observed environmental fate process. There is a large amount of research that has been published and extensive literature reviews are available (3–5). The kinetic behavior commonly exhibits a pattern of fast initial adsorption (or release in desorption experiments) of molecules in the aqueous phase by soil particles (appears within minutes to hours or “instantaneously”) followed by a much slower process lasting for days to months. This two-step process is widely described mathematically by a two-site sorption model, which assumes two soil fractions (sites) coexisting in a soil representative elementary volume, with one adsorbing chemicals instantaneously and the other time-dependently (6–11).

The kinetic nature of sorption has shown rate-limiting effects on biodegradation due to reduced bio-availability of the adsorbed chemicals to microorganisms which perform metabolism primarily in soil pore water (12, 13). Mathematical models with variable mechanistic specifications have been proposed to describe the interrelated processes of sorption and biodegradation (8, 14–17). These coupled sorption and degradation kinetics with certain variations in parameter definition have been used in several environmental fate and transport models (e.g., LEACHP, RZWQM, PEARL, and MACRO) for regulatory assessment and management purposes (18–21).

FOCUS-PRZM and FOCUS-PELMO are two of the four leaching computer models officially used within the EU for pesticide registration evaluations (1). The core modules of FOCUS-PRZM and PELMO (i.e. water flow and solute fate and transport) are based on the Pesticide Root Zone Model (PRZM), with the sorption module assumed as a simple equilibrium partition process described by the Freundlich equation between the aqueous and solid phases in the soil-water system (22). Sorption kinetics, however, were implemented in the other two EU models, PEARL and MACRO. In order to harmonize the environmental fate processes among the EU regulatory models, there is a desire to develop a time-dependent sorption algorithm in FOCUS-PRZM and PELMO so that higher tier assessment can be conducted on the same scientific basis with refined parameterization. Since the same algorithms are applicable to FOCUS-PELMO, only FOCUS-PRZM is mentioned in the following sections of this chapter.

The objective of this chapter is to document the development of the sorption kinetics in FOCUS-PRZM and to evaluate performance of the new module by comparing model-predicted results with measured soil residue data obtained from two terrestrial field dissipation studies, one conducted in California, U.S.A. and the other in Guiseniers, France. Solutions to the coupled sorption and degradation kinetics have been proposed by several authors (8, 16). However, these solutions do not distinguish degradation rates in soil pore water, and/or on different sorbed sites (labile or more tightly bound). We thus present here a “generalized” form of the coupled sorption and degradation kinetics with an analytical solution that can be reduced to the same equations used in other regulatory models such as LEACHP and PEARL. This analytical solution is then implemented in FOCUS-

PRZM to achieve numerical accuracy for the daily time-step used in the numerical schemes of the water flow and solute transport modules. The codes are verified by comparing the FOCUS-PRZM simulation results to the results obtained by the established LEACHP model.

Materials and Methods

Theory

Coupled Sorption and Degradation Kinetics

A common mathematical model for sorption and the interrelated biodegradation kinetics is the two-site/two-region model (6–9, 16, 17), which separates soil sorption into two types of sites (or regions), with one site type reaching sorption equilibrium instantaneously and the other time-dependently. The basis for this simplification is the common two-stage pattern exhibited in experimental data where initial sorption proceeds faster at time scales ranging from minutes to hours and then continues in a much slower phase for days to months (11). The initial sorption can be simplified as an instantaneous step on the soil fraction where sorption equilibrium is attained quickly. This simplification is justifiable considering the generally slow leaching process in soil. Sorption continues on the other soil fraction at a slower rate. A schematic representation of the kinetics model is provided in Figure 1.

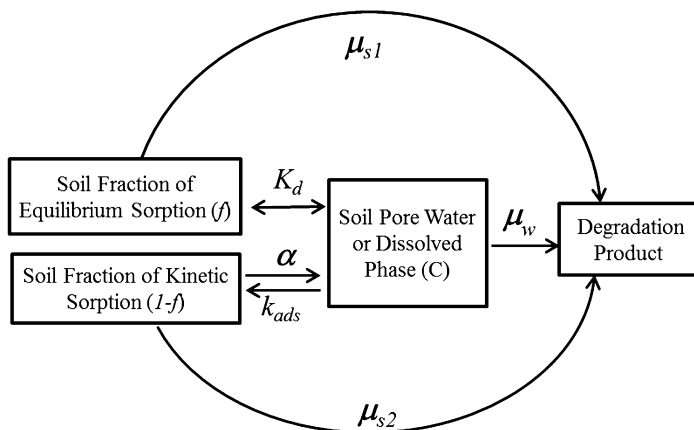


Figure 1. Schematic representation of the two-site sorption and degradation kinetic model in the soil-water system.

Considering different degradation rates on the equilibrium and time-dependent fractions and in the soil pore water, the system of differential equations of the kinetic model can be expressed as below:

$$\frac{d}{dt}[\theta C + \rho(S_1 + S_2)] = -\mu_w \theta C - \rho\mu_{s1}S_1 - \rho\mu_{s2}S_2 \quad (1)$$

$$\frac{dS_1}{dt} = fK_d \frac{dC}{dt} \quad (2)$$

$$\frac{dS_2}{dt} = \alpha[(1-f)K_d C - S_2] - \mu_{s2}S_2 \quad (3)$$

Where

C	Concentration in the dissolved phase; $\mu\text{g/L}$.
S_1	Concentration in the instantaneous (equilibrium) adsorbed phase, $\mu\text{g/g}$.
S_2	Concentration in the kinetic adsorbed phase, $\mu\text{g/g}$. Total sorption $S = S_1 + S_2$.
K_d	Total partition coefficient when sorption equilibrium is achieved at both sorption sites, mL/g . Thus, by definition: $K_d = (S_1 + S_2)/C = K_{d1} + K_{d2}$, where K_{d1} and K_{d2} are individual partition coefficients at both types of sorption sites, respectively.
f	Soil fraction of the instantaneous adsorbed phase, dimensionless. By definition, $f = S_1/(S_1 + S_2)$ when sorption equilibrium is reached, or $f = K_{d1}/K_d$.
α	First-order desorption rate constant (or mass transfer coefficient) in the kinetic adsorbed phase, day^{-1} ; (note it can be shown that $\alpha = k_{ads}/K_d$, k_{ads} is first-order adsorption rate constant in the kinetic adsorbed phase, day^{-1}).
μ_{s1}	Degradation rate constant on the equilibrium adsorption site, day^{-1} .
μ_{s2}	Degradation rate constant on the kinetics adsorption site, day^{-1} .
μ_w	Degradation rate constant in the soil pore water or liquid phase, day^{-1} .
θ	Soil moisture content, cm^3/cm^3 .
ρ	Soil bulk density, g/cm^3 .
t	Time, day.

With the initial conditions: $C(0) = C_0$, $S_1(0) = fK_d C_0$, and $S_2(0) = S_0$, Eqs. 1-3 can be solved analytically assuming sorption is linearly related to concentration in soil pore water when complete equilibrium is achieved (i.e. $1/n=1$ and $K_d = K_f$ in the general Freundlich equation $S=K_f C^{1/n}$). The analytical solutions are provided in Eqs. 4-7 below with the dummy variables defined in Eqs.8-15.

$$C = \frac{C_0}{(\lambda_1 - \lambda_2)} [(\alpha + \mu_{s_2} + \lambda_1) \exp(\lambda_1 t) - (\alpha + \mu_{s_2} + \lambda_2) \exp(\lambda_2 t)] + \frac{\alpha S_0}{(\lambda_1 - \lambda_2)} [\exp(\lambda_1 t) - \exp(\lambda_2 t)] \quad (4)$$

$$S_1 = fK_d C \quad (5)$$

$$S_2 = \frac{\alpha(1-f)K_d C_0}{(\lambda_1 - \lambda_2)} [\exp(\lambda_1 t) - \exp(\lambda_2 t)] + \frac{S_0}{(\lambda_1 - \lambda_2)} [(\alpha + \mu_{s_2} + \lambda_1) \exp(\lambda_2 t) - (\alpha + \mu_{s_2} + \lambda_2) \exp(\lambda_1 t)] \quad (6)$$

And

$$C_t = (\theta + \rho f K_d) C + \rho S_2 \quad (7)$$

Eq. 7 is for the total concentration both in the adsorbed phase and in the soil pore water. The dummy parameters in Eqs. 4 to 6 are defined below.

$$\lambda_1 = \frac{1}{2}(-b + \sqrt{b^2 - 4c}) \quad (8)$$

$$\lambda_2 = \frac{1}{2}(-b - \sqrt{b^2 - 4c}) \quad (9)$$

$$b = \gamma + \mu_{s_2} + \mu_e \quad (10)$$

$$c = \mu_e (\alpha + \mu_{s_2}) + \mu_{s_2} (\gamma - \alpha) \quad (11)$$

$$\mu_e = \frac{\mu_w + (R_1 - 1)\mu_{s_1}}{R_1} \quad (12)$$

$$\omega = \frac{\alpha \rho}{R_1 \theta}, \quad \gamma = \frac{\alpha R}{R_1} \quad (13)$$

$$R_1 = 1 + \frac{f \rho K_d}{\theta} \quad (14)$$

$$R = 1 + \frac{\rho K_d}{\theta} \quad (15)$$

Note that the analytical solutions have a mathematical singularity at $\alpha = 0$, and $\mu_w = \mu_{s_1} = \mu_{s_2}$ as the two macro rate constants be equal (i.e., $\lambda_1 = \lambda_2$). As a result, setting $\alpha = 0$ should not be allowed in the PRZM codes in case of no sorption kinetics and no differential degradation between soil pore water and the two sorbed phases. These constraints should be taken into account when fitting the model to data. In addition to the overall equilibrium sorption partition coefficient K_d (or equivalently, the soil organic carbon-normalized partition coefficient K_{oc}),

five new parameters are introduced in the coupled kinetics: the fraction of the soil equilibrium sorption (f); desorption rate constant (α), degradation rate constant in soil pore water (μ_w); degradation rate constants on the equilibrium sorption phase (μ_{s1}) and the kinetic sorption domain (μ_{s2}).

Implementation in FOCUS-PRZM

Solute transport in the soil porous media is described by the Convection-Dispersion Equation (CDE) (22). For simplicity, the terms of fate and transport in gaseous phase and via runoff/erosion and other processes are not duplicated here in the equations below but will be added in the PRZM codes. The CDE after incorporating the two-site sorption kinetics (Eqs. 1-3) is expressed as:

$$\frac{\partial [C(\theta + f_{eq}K_d\rho)]}{\partial t} = D \frac{\partial^2(C\theta)}{\partial z^2} - \frac{\partial C\theta V}{\partial z} - C[\mu_w\theta + \mu_{s1}fK_d\rho] - \rho \frac{dS_2}{dt} \quad (16)$$

Where D is solute diffusion-dispersion coefficient, cm/day²; z is distance in soil profile, cm; V is soil pore water velocity, cm/day. Other variables and coefficients are defined in Eqs. 1-3.

The CDE with the kinetic sorption term would require adjustment in the coefficients of the tridiagonal matrix. Following the backward difference in PRZM (22), Eq. 16 can be discretized in both time and space using the numerical scheme:

$$\frac{\partial C}{\partial t} \approx \frac{C_i^j - C_i^{j-1}}{\Delta t} \quad (17)$$

$$\frac{\partial^2 C}{\partial z^2} \approx \frac{C_{i+1}^j - C_i^j}{0.5\Delta z_i(\Delta z_{i+1} + \Delta z_i)} - \frac{C_i^j - C_{i-1}^j}{0.5\Delta z_i(\Delta z_i + \Delta z_{i-1})} \quad (18)$$

$$\frac{\partial C}{\partial z} \approx \frac{C_i^j - C_{i-1}^j}{\Delta z_i} \quad (19)$$

$$\frac{dS_2}{dt} \approx \frac{S_i^j - S_i^{j-1}}{\Delta t} \quad (20)$$

Where the superscript j represents the current status at time t and $j-1$ represents the previous time step at time $t-\Delta t$; similarly the subscript i denotes space of soil compartment i .

Writing each concentration term for time step j and substituting Eqs. 17-20 into Eq. 16 leads to a system of algebra equations for soil compartment i ($i \neq 1$ and n , the upper and lower boundary compartments):

$$A_i C_{i-1}^j + B_i C_i^j + E_i C_{i+1}^j = F_i C_i^{j-1} \quad (21)$$

Where

$$A_i = \left(-\frac{D_{i-1}^j \theta_{i-1}}{0.5\Delta z_i (\Delta z_i + \Delta z_{i-1})} - \frac{V_{i-1} \theta_{i-1}}{\Delta z_i} \right) \Delta t \quad (22)$$

$$B_i = \left(\theta_i + f_{eq_i} K_{di} \rho_i \right) + \left(\frac{D_i^j \theta_i}{0.5\Delta z_i (\Delta z_i + \Delta z_{i-1})} + \frac{D_i^j \theta_i}{0.5\Delta z_i (\Delta z_i + \Delta z_{i+1})} + \frac{V_i \theta_i}{\Delta z_i} \right) \Delta t + \left(\mu_{w_i} \theta_i + \mu_{s1i} f_{eq_i} K_{di} \rho_i \right) \Delta t \quad (23)$$

$$E_i = -\frac{D_{i+1}^j \theta_{i+1}}{0.5\Delta z_i (\Delta z_i + \Delta z_{i+1})} \Delta t \quad (24)$$

$$F_i = \left(\theta_i + f_{eq_i} K_{di} \rho_i \right) C_i^{j-1} - \rho_i (S_{2i}^j - S_{2i}^{j-1}) \quad (25)$$

Sorption on the kinetic site S_{2i}^j (Eq. 25) is updated before the solution of the CDE. Since the rate of degradation (liquid and/or solid phases) and the mass transfer process (α) can be relatively large within the daily time-step adopted by PRZM, an integration of these coupled terms over the time step is necessary. This is done by using the analytical solution of the coupled sorption and degradation kinetics (Eq. 6). Specifically, at the beginning of each day, S_{2i}^j is estimated via Eq. 6 with previous day's values as initial conditions for each soil compartment, the CDE is then subsequently solved (Figure 2). Note that when $S_2 = 0$, and $f=1$ (no kinetic sorption), the above equations reduce to the original version of the PRZM fate model.

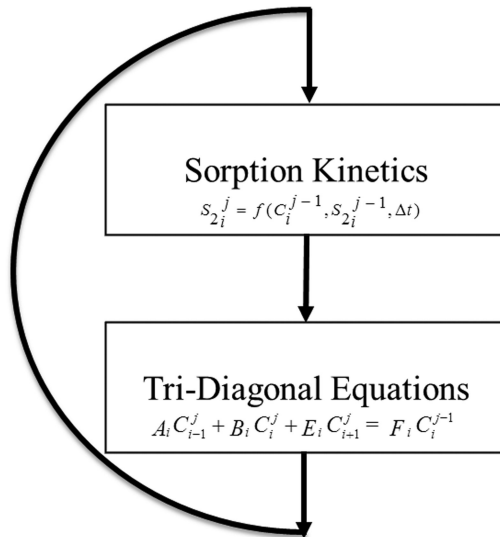


Figure 2. Diagram of the numerical scheme within a daily time-step implemented on FOCUS-PRZM. Symbols in equation: C is concentration in soil pore water ($\mu\text{g/L}$); subscript indicates soil profile compartment number; superscript indicates time, day; A_i , B_i , E_i , and F_i are coefficients of the tri-diagonal equations of the solute transport convection-dispersion model, S_2 is the sorbed mass on the kinetic site, $\mu\text{g/g}$; and Δt is time-step (1 day).

For non-linear sorption (i.e., the exponent $1/n$ of the Freundlich equation is not 1), a new K_d is adjusted each day by the equation:

$$K_{d_i}^j = \frac{K_f C_i^{j1/n}}{C_i^j} \quad (26)$$

Where K_f is the Freundlich sorption coefficient. Other variables are defined previously. Note that the K_d for the Freundlich type sorption is a function of C in Eq. 26. As such, potential improvement for estimating the mass distribution coefficient between C and S may be expected via iterative loops in the numerical solution. This iterative refinement, however, is not currently adapted to maintain reasonable model execution speed.

Relationship between FOCUS-PRZM and PEARL Parameters

Sorption kinetics in the FOCUS PEARL model is adapted slightly differently in compartment definition and its associated mathematical formulations (Figure 3). It is a two-site sorption kinetics model assuming no degradation on the non-equilibrium sorption (NES) domain. Degradation in the soil pore water and equilibrium sorption domain is the same with a uniform decay rate constant (k_t). Both equilibrium (eq) and non-equilibrium (neq) compartments are described by the Freundlich isotherm with individual distribution coefficients $K_{f,eq}$ and $K_{f,neq}$.

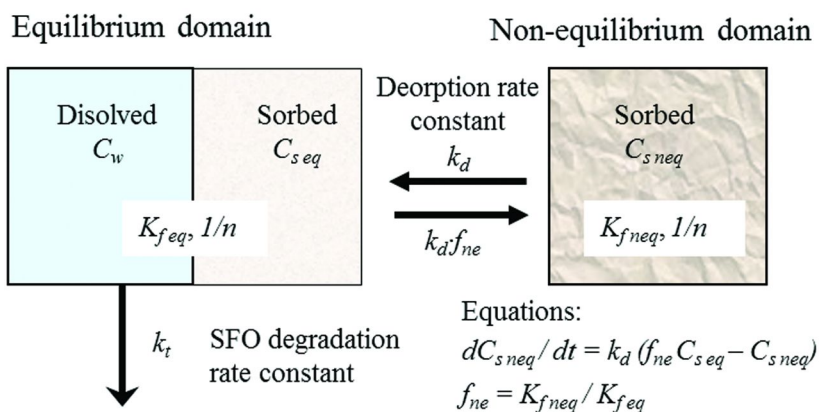


Figure 3. Diagram of the sorption kinetics formulated in FOCUS PEARL.

Comparing to the sorption kinetics defined in FOCUS-PRZM model, the difference is that PEARL defines the fraction of the NES domain (f_{ne}) as the ratio:

$$f_{ne} = \frac{K_{f_neq}}{K_{f_eq}} \quad (27)$$

Regardless whether the Freundlich isotherm is linear or not, it can be shown that

$$f_{ne} = \frac{1-f}{f} \quad (28)$$

Similarly, it can be shown that the desorption rate coefficient denoted as k_d in PEARL is equivalent to α in FOCUS-PRZM. Rewriting Eq. 3 of the kinetics for the NES site assuming Freundlich sorption isotherm and no degradation gives:

$$\frac{dS_2}{dt} = \alpha[(1-f)K_d C^{1/n} - S_2] \quad (29)$$

Using Eq. 28 and recognizing $K_d = K_{f_eq} + K_{f_neq}$ by definition, Eq. 29 can be written:

$$\frac{dS_2}{dt} = \alpha[K_{f_neq} C^{1/n} - S_2] \quad (30)$$

Eq. 30 is the same as Eq. 4.2 in PEARL (20) when setting the reference concentration to unity and using the same symbols for other variables (e.g., $C=C_w$, $S_1=C_{s\ eq}$, and $S_2=C_{s\ neq}$ per Figure 3).

As discussed above, assuming no degradation on the NES domain (i.e. $\mu_{s2}=0$) and a uniform degradation rate constant for the soil pore water and the equilibrium sorbed phase (i.e. $\mu_w = \mu_{s1}$), the effective degradation $DT50_{eq}$ can be approximated from the total soil system $DT50_{tot}$ using the following equation:

$$DT50_{eq} = \frac{DT50_{tot}}{1 + f_{ne}} \quad (31)$$

where variables are defined previously. Note that Eq. 31 is not an accurate relationship but an approximation based on several assumptions (e.g. linear sorption isotherm, a slow degradation rate coefficient compared to sorption rate constant α and a small f_{ne}). Boesten and van der Linden have published a similar but more complex approximation equation (2, 23).

Field Data

U.S. Data

Soil residue data of a sulfonylurea herbicide from a US EPA guideline terrestrial field dissipation study was used to calibrate the model for the required kinetic parameters. The study was conducted in a loamy sand soil in Madera, CA, USA, from June, 1999 to January, 2001. Soil characteristics are listed in Table 1. The study consisted of two treated plots (bare soil and cotton cropped, each

measured 41 m by 14 m) and a control (41 m by 5 m). Each of the treated plots was further divided into three replicate subplots. Three applications at 60 g a.i./ha were broadcast to the two treated plots on June 25, July 9, and July 23, 1999. The cotton was approximately 8 to 13 cm tall when the first application occurred. Daily weather data (air temperature, rainfall, wind speed etc.) and sprinkler irrigation amount were recorded on site. The cumulative total water input (sum of rainfall and irrigation; cm) and average daily temperature were plotted in Figure 4a for the course of the terrestrial field dissipation study.

Table 1. Soil Chemical-Physical Properties at the Terrestrial Field Dissipation Site, Madera, California, U.S.A.

<i>Soil Depth (cm)</i>	<i>USDA Soil Texture</i>	<i>BD (g/cm³)</i>	<i>Moisture Content at 33 kPa (cm³/cm³)</i>	<i>OM (%)</i>	<i>Soil pH (H₂O)</i>	<i>CEC (meq./100g)</i>
0 – 15	LS	1.49	11.2	1.3	6.7	7.8
15 – 30	LS	1.58	10.5	0.8	7.4	6.3
30 – 45	LS	1.60	8.9	0.6	7.6	5.7
45 – 60	LS	1.60	10.6	0.5	7.8	6.4

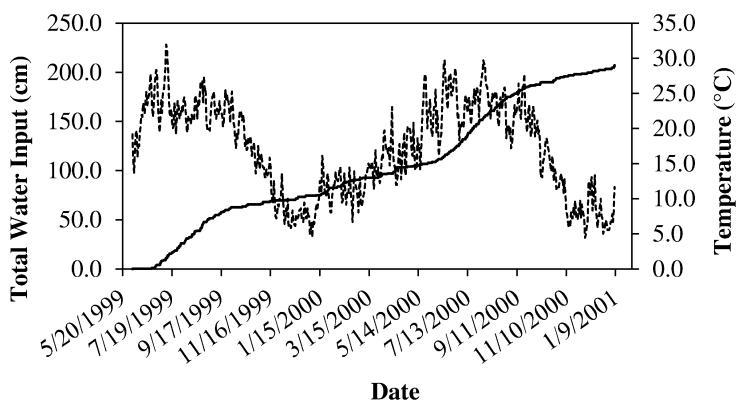
NOTE: LS=Loamy Sand. BD=Bulk density; OM=Organic Matter Content. CEC=Cation Exchange Capacity. Bulk density and 33 kPa moisture content were measured on undisturbed soil cores taken from the field plots.

Soil samples were taken to a depth of 120 cm below ground in 15 cm increment from the treated and control plots before each chemical application, 7 days after the first and second applications, and then at 1, 3, 7, 14, 21, 28, 61, 91, 119, 182, 271, 357, 451, and 536 days following the third application. Five soil core samples were collected, combined, and thoroughly mixed to create a composite sample for each depth and replicate of the treated plots. The composite soil samples were extracted with 70% methanol/water (v/v) one time and 70% methanol/water (v/v) with 2% ammonium hydroxide two times at room temperature for 30 minutes each. The combined extracts were analyzed for determining the total residue concentrations of the test compound using high performance liquid chromatography (HPLC). The limit of quantification (LOQ) was 0.5 ppb (or µg/Kg).

The calibrated model was then applied to a second data set consisting of field soil samples taken from 17 field locations in ten states (AR, CA, FL, MS, NC, PA, OH, SC, TN, and TX) between 1998 and 2002. Unlike the EPA guideline terrestrial field dissipation study, these were general biological field trials and in most cases

there were only 2 to 3 soil samples taken during the entire trial. Site-specific soil properties were characterized for the surface layer 0-15 cm. Daily weather data were obtained from the nearby weather stations of the National Oceanic and Atmospheric Administration (NOAA). Application rate varied from 6.4 to 60 g/ha mostly with a single application (only two trials had 3 applications) between March and July. All samples were cored from the 0-15 cm soil layer. The limit of detection (LOD, 0.01 ppb) was used for the laboratory analytical method.

a. Cumulative total water input (rainfall + irrigation; cm) and daily average temperature, Madera, CA, USA, June 1999-January 2001.



b. Daily rainfall (bars) and mean monthly air temperature (dashed line) of the terrestrial field dissipation study at Guiseniers, France, April, 1998 – April, 2000.

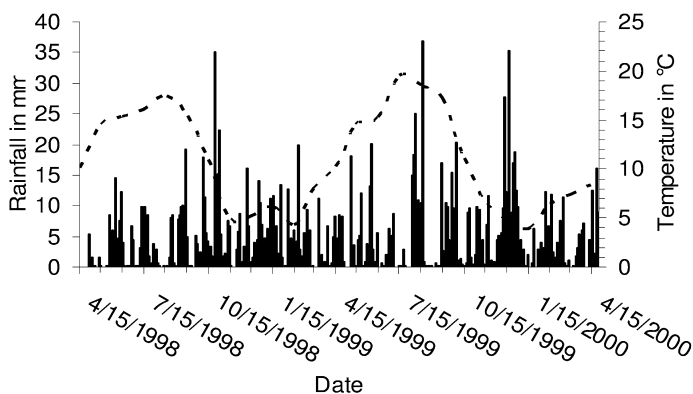


Figure 4. Water inputs and temperature at the two terrestrial field dissipation study sites used for evaluating FOCUS-PRZM.

EU Data

The third field data set used for model comparison was obtained from a field dissipation study conducted with a neonicotinoid in northern France (F-27700 Guiseniers, Haute-Normandie, Eure) from April, 1998 to May, 2000. This study was one of the six European trials and is used as example for model evaluation in this chapter. The soil was a silty loam with detailed characteristics listed on Table 2. The mean annual rainfall during the experimental period totaled 954 mm with mean annual temperature of 11.0 °C. Daily rainfall and monthly average air temperature were presented in Figure 4b. The test substance was sprayed to bare soil at an application rate 150 g a.i./ha on the 27th of May 1998. The trial was cropped with spring wheat sown shortly before application. In the autumn after spring wheat harvest, grass was sown and then cut several times when the grass reached a height of approximately 10 cm. Soil samples were taken at eleven intervals following the day of treatment (DAT 15, 28, 56, 91, 135, 199, 270, 360, 480, 599, 729). At each sampling time point 20 soil core samples were collected, combined, and thoroughly mixed to create a composite sample for each depth and replicate of the treated plots. On DAT 0, samples were taken using the "Piercer" (diameter of 5 cm) to a depth of 10 cm. On the other sampling dates, a pushing sampling system ("Wacker Hammer", diameter of 4.8 -5 cm) was used to take soil cores down to a depth of 50 cm.

Table 2. Soil Chemical-Physical Properties at the Terrestrial Field Dissipation Site, Guiseniers, France

<i>Soil Depth (cm)</i>	<i>USDA Soil Texture</i>	<i>MWHC (cm³/cm³)</i>	<i>OM (%)</i>	<i>Soil pH (CaCl₂)</i>	<i>CEC (meq./100g)</i>
<i>0 – 30</i>	SL	44.4	1.9	5.2	13
<i>30 – 50</i>	SL	49.3	0.9	6.2	10

NOTE: SL=Silty Loam. MWHC=Maximum Water Holding Capacity. OM=Organic Matter Content. CEC=Cation Exchange Capacity.

Model parameters of the sorption kinetics were independently determined for two soils (silt loam and sandy loam) in the laboratory. An aged sorption protocol was used where the test compound was incubated with soil for 0, 2, 7, 14, 27, 55 and 99 days under constant soil moisture at 40% of the maximum water holding capacity and temperature of 20 °C. After aging of the soil, 200 ml of 0.01 M aqueous CaCl₂ solution was added and equilibrium was established after shaking for 24 hours at 20 °C. After centrifugation, the supernatant (desorption solution) was removed and analyzed. The residual soil was extracted once with 80 ml

methanol and then three times with 80 ml acetonitrile. For each extraction cycle, the soil was shaken for 30 min and centrifuged. The extracts were combined for analysis (cold organic extract). After cold organic extraction, the moist soil residue was hot-extracted under reflux with acetonitrile/water (50:50) for 2 hours and centrifuged (hot organic extract).

For the model evaluation, both organic extracts (cold and hot) were taken to determine the amount of the non-equilibrium fraction (S_2) (Figure 5). The total mass extracted by the aqueous CaCl_2 solution was distributed between the dissolved soil pore water concentration (C) and the sorbed at the equilibrium sites (S_1) using the Freundlich isotherm measured separately in a batch sorption equilibrium study. The Freundlich isotherm parameters were: $K_f = 0.657 \text{ L/kg}$ for the silt loam ($\text{OC} = 0.83\%$); $K_f = 1.133 \text{ L/kg}$ for the sandy loam ($\text{OC} = 1.02\%$); and mean $1/n = 0.83$. Results of the sorption parameters were obtained by fitting the kinetics model to the measured data and provided in Figure 5 for the two soils. Averaged values of the fitted parameters were used to evaluate the field trial.

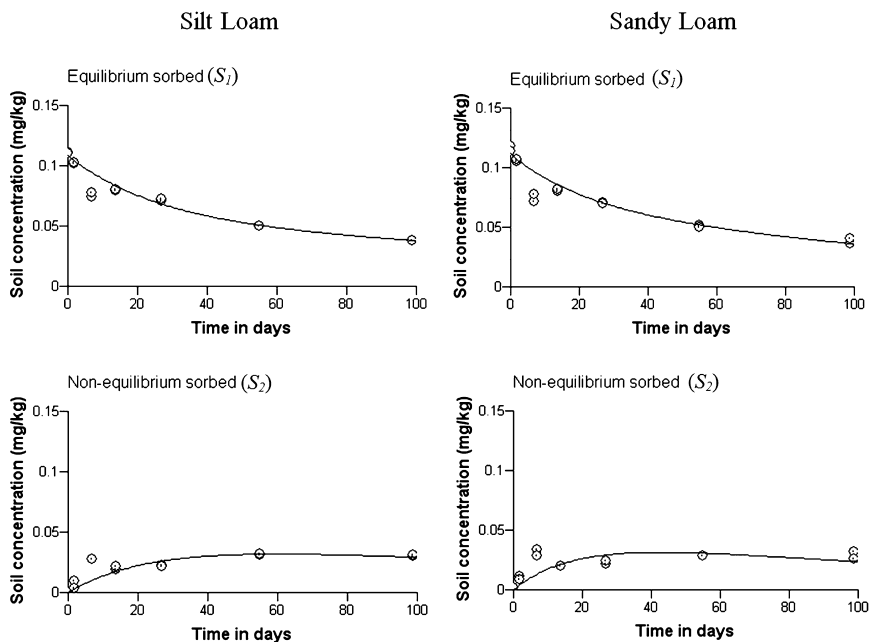


Figure 5. Laboratory measurements and determination of sorption parameters in two European soils: modeled (solid line) and measured (symbols) concentrations on the equilibrium sorption sites (top) and the non-equilibrium sorption (NES) sites (bottom). Fitted parameters were in the table below.

Results and Discussion

Code Verification

The new codes implemented in FOCUS-PRZM were verified by comparing the model predictions with the analytical solutions of the coupled kinetics (Eqs. 4-7) and with the results by LEACHP modeling (Figure 6). A hypothetical case without rainfall and evapotranspiration (i.e. no water flow) was simulated with the new codes and LEACHP. Parameters used in the synthetic case were: application rate: 1.0 Kg a.i./ha (assuming perfect mixing in 10 cm soil after application), soil bulk density = 1.45 g/cm³, soil moisture content = 0.45 cm³/cm³. The kinetic and fate parameters are indicated on Figure 6. As shown in the model comparison, the new codes in FOCUS-PRZM give almost identical results as the analytical solution and LEACHP-predicted concentrations, suggesting that the codes implemented in the model are programed accurately.

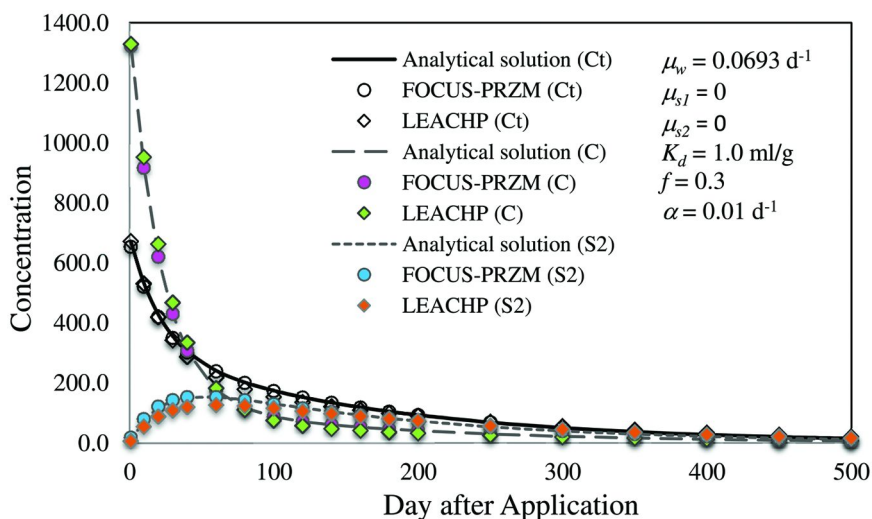


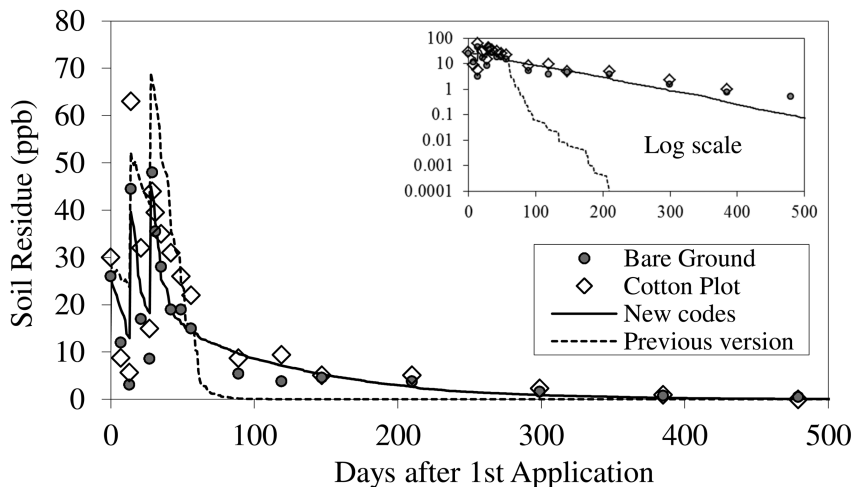
Figure 6. Comparison of FOCUS-PRZM and LEACHP to the analytical solution of the coupled sorption and degradation kinetics (Eqs. 4-7). (see color insert)

Comparison with Field Data from U.S.

The measured soil concentration data obtained from the CA terrestrial field dissipation study were used to calibrate (manual tuning) the required parameters in the new FOCUS-PRZM implemented with the NES algorithm. For comparison purpose, the previous version of FOCUS-PRZM which assumes local equilibrium sorption (LES) in the soil-water system was also calibrated. Results of the modeled and measured dissipation data are provided in Figures 7a and b for the soil depth 0-15 cm and 15-30 cm, respectively. Comparisons for other soil depths were not made because only a few sporadic detectable concentrations near the LOQ (0.5 ppb) were found at depths between 30 and 61 cm and no detectable

residues below 61 cm in the soil profile. Site-specific information was used in the model calibration, including soil, weather (rainfall, temperature, and potential evapotranspiration), irrigation, application, and field agronomic activities.

a. 0-15 cm soil layer



b. 15-30 cm soil layer

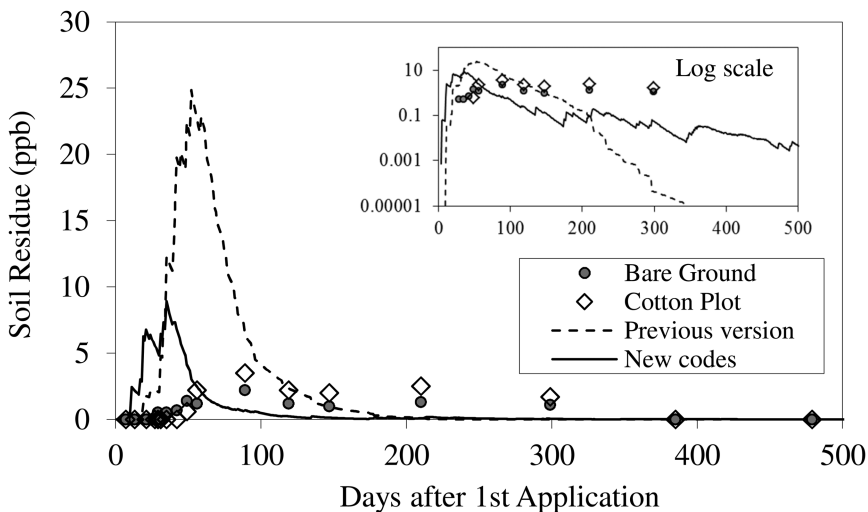


Figure 7. Model calibration results using measured soil concentrations from a terrestrial field dissipation study on a loamy sand soil, Madera, CA. Three applications were made at 60 g ai/ha in a 14 day interval (6/25, 7/9, 7/23, 1999). Soil core samples were taken to the depth 120 cm below ground. A few sporadic detections around LOQ (0.5 ppb) were found in 30-60 cm and no detectable concentration at depth below 61 cm in the study.

For the new version of FOCUS-PRZM with NES, the calibrated fate parameters were $\alpha=0.013\text{ d}^{-1}$, $\mu_w=0.139\text{ d}^{-1}$, $\mu_{s1}=\mu_{s2}=0.003\text{ d}^{-1}$, $K_{oc}=100\text{ mL/g}$, and $f=0.2$. Parameter adjustments were initially made from a laboratory aged sorption study with treated soil samples incubated for 85 days at 25 °C and 75% field soil moisture holding capacity (data not shown). The field data-calibrated f value was found to be slightly lower than the ratio (0.22) of the measured apparent K_d ($=S/C$) between Day 0 and Day 85 after treatment. The measured apparent K_d on Day 85 was found to overestimate the ultimate sorption equilibrium K_d based on the field data. This was likely due to the effect of the concurrent degradation in the aged sorption study. As shown in Chen et al. (24), apparent K_d generally increases with incubation time and may eventually reach a plateau. However, a plateaued apparent K_d does not necessarily suggest sorption equilibrium when degradation co-occurs in the soil-water system.

For the previous version of FOCUS-PRZM with LES, a K_{oc} value ($=78\text{ mL/g}$) and a bulk soil degradation half-life of 7.1 days (i.e., both in pore water and on the sorbed phases) were found to best fit the observed data in the beginning 60 days after the first application but noticeably underestimate the later observations (dash line in Figure 7a). A longer half-life value could fit the later decline data better but would grossly over-predict the earlier peak concentrations (results not shown). The K_{oc} ($=78\text{ mL/g}$) was directly taken from the median value determined from a laboratory batch equilibrium sorption study. This value was not further adjusted as it paired reasonably well with the half-life (7.1 days) to predict the peak residue concentrations in the topsoil layer (Figure 7a). Although noticeable over-prediction was observed in the subsoil layer (Figure 7b), suggesting the need of increasing K_{oc} (i.e., reducing mobility), an increase in K_{oc} would result in over-prediction of the topsoil residue levels. This mutual constraint of data fitting is indicative of lacking flexibility in the LES model to better predict fate and transport at various spatial and temporal scales.

The new FOCUS-PRZM (solid line in Figures 7a and b) clearly outperformed its previous version in predicting both the peak and the aged soil residue levels over the full time scale despite some underestimation at the end of the field study. The observed dissipation in the topsoil showed a bi-phasic pattern where initial decline was fast and then followed by lingering low soil residue concentrations. While predictions for the subsoil deserved more improvement, the overall better fit by the new NES model appeared to support the hypothesis that compounds were more bioavailable to degradation shortly after application. In this case, 20% sorption (i.e., $f=0.2$) was instantaneous, thus leaving 80% sorption being time-dependent. Molecules not instantaneously sorbed would be highly bioavailable for rapid degradation in the soil pore water ($\mu_w=0.139\text{ d}^{-1}$). In a later stage, chemical bioavailability decreased as residues became sorbed and subsequent desorption was slow ($\alpha=0.013\text{ d}^{-1}$), thus limiting the rate of degradation in the soil pore water. These interrelated, simultaneously operating, and time-dependent processes (i.e., adsorption, desorption, and degradation) were simulated reasonably well by the new NES codes implemented in FOCUS-PRZM. In comparison, the previous version of the model assuming full local sorption equilibrium with a K_{oc} (78 mL/g) not much different from the new NES model-calibrated K_{oc} (100 mL/g), failed to predict the prolonged

dissipation pattern due to its lacking mechanism to account for the rate-limiting effect of time-dependent sorption on degradation.

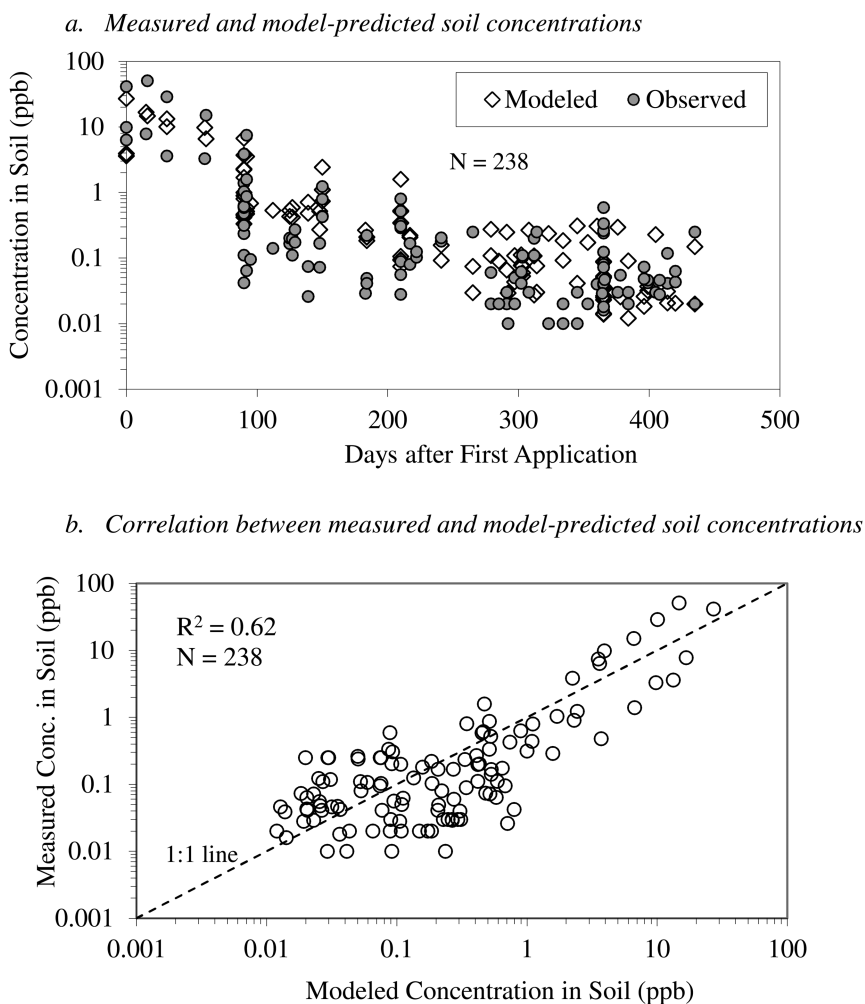


Figure 8. Comparison of model independent predictions with measured soil samples taken from 17 field locations in nine states (AR, CA, FL, MS, NC, PA, OH, SC, TN, and TX) between 1998 and 2002. Application rate varied from 6.4 to 60 g/ha. All samples were cored from the 0-15 cm soil layer.

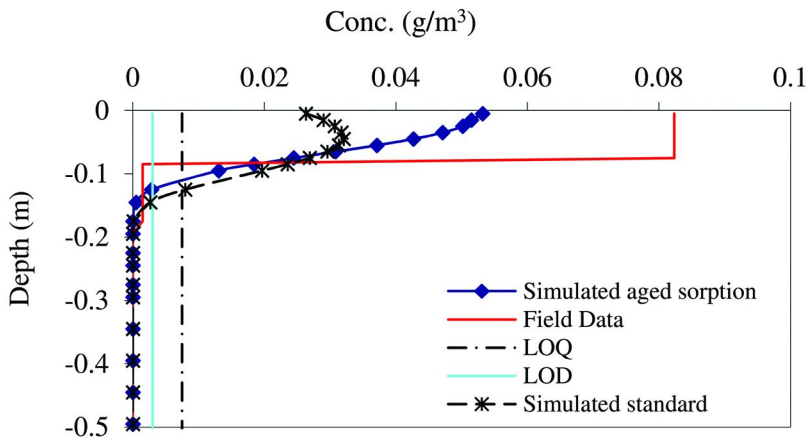
The calibrated new FOCUS-PRZM was independently evaluated against a set of field collected soil residue data from 17 geographical locations in 10 states (Figures 8a and b). The independent evaluation means that the model was used to predict the 17 data sets independent of the CA field dissipation study with which the kinetic fate parameter values were calibrated from. Recognizing the potential soil-dependency of kinetic fate parameters, we focused on the model predictability for the overall trend measured from the 17 sites. For this purpose, site-specific data-model comparisons were not plotted. Instead, all measured residue soil concentration data were first organized and plotted by days after the first application at each site (Figure 8a). In this plot, scatter in the measured data points on a given day would represent the differences in geographical conditions, application rates, and the potential variability in the environmental fate processes (i.e., sorption and degradation). Two observations can be made from this general comparison. First, it is interesting that the overall dissipation pattern of the combined data sets appeared bi-phasic albeit high variability. Second, although the model assumes no variability in the kinetics fate parameters, the predicted magnitudes were in the same range of the data scatter, indicating dominant geographical variability predicted by the model.

The measured soil residue concentrations are compared with the corresponding modeled results on a site-specific basis in Figure 8b. As shown, the model was able to predict the 238 measured soil residue data points with $R^2=0.62$. Clearly, scatter in the collected data sets was large and was reflective of the variability in the wide geography and different environmental conditions under which these measurements were made. The model responded reasonably well to the inherent field location variability as well as the range of almost 5 orders of magnitude in the measured concentrations. It is expected that the model-data scatter could be reduced if site-specific environmental fate parameters were known and used for model predictions.

Comparison with EU Data

Data from a field dissipation study at Guiseniers, France, was used to further evaluate the kinetic sorption model as implemented in FOCUS-PRZM under European conditions. Model parameters of the sorption kinetics were independently measured in the laboratory for two soils and the mean values of these parameters were used (Figure 5). These include the three kinetic sorption parameters characterizing the sorption capacity (f and K_d) and the desorption rate constant (α) for the NES domain. Assuming no degradation on the NES domain (i.e. $\mu_{s2}=0$), the degradation rate constant in the soil pore water and on the equilibrium sorbed phase (i.e. assuming $\mu_w = \mu_{s1}$) was determined by fitting the time- and depth-dependent field residue data. The fitted $DT50$ value is termed effective degradation $DT50_{eq}$ as it takes into account only the soil water and the equilibrium sorption phase. It can be shown that $DT50_{eq}$ is systematically smaller than the total system $DT50_{tot}$ (see Eq. 31 below) for the bulk soil.

a. *Soil residue depth profile field dissipation (Day 135)*



b. *Soil residue depth profile field dissipation (Day 729)*

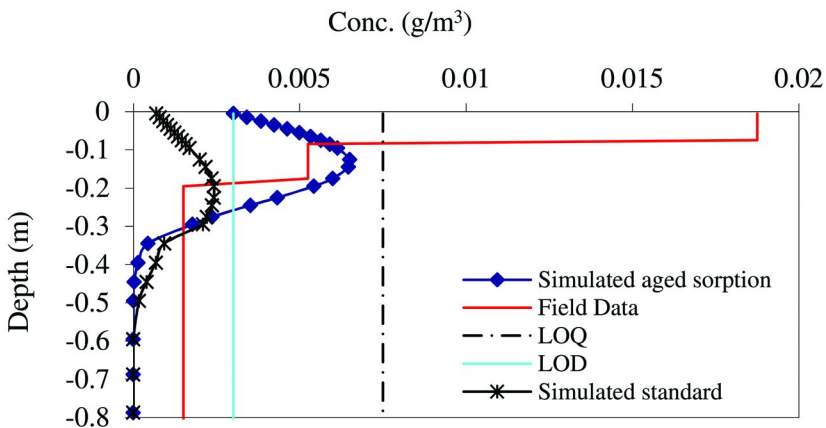


Figure 9. Model comparisons to field soil residue data of a neonicotinoid obtained from a terrestrial field dissipation study conducted at Guiseniers, France after bare soil spray application of 150 g ai/ha during spring 1998. Examples of predicted concentration distributions in soil profiles on Day 135 (a) and Day 729 (b) after application, respectively. Model simulations were made with two options: with kinetic sorption parameterized using aged sorption data from laboratory experiments, and with “standard” assumptions (i.e., no kinetic sorption).

Measured and modeled concentration distributions in the soil profile on Day 135 and Day 729 after application were compared in Figures 9a and b, respectively. FOCUS-PRZM with the NES kinetics predicted the measured residue mass much closer than the model without sorption kinetics (indicated as “Simulated standard” on the figure) even though the downward transport was still

over-predicted and the top soil residue under-predicted by the NES model. One of the reasons could be the tipping bucket water transport mechanism adopted in FOCUS-PRZM which does not allow upward movement of either water or solutes as it does occur in reality due to surface evapotranspiration. Similar to the US study results, FOCUS-PRZM without NES kinetics more pronouncedly over-predicted leaching while under-predicted the residue levels on the surface soil layer (Figs 9a and b). Such discrepancy became more obvious as time elapsed from Day 135 to Day 729. This effect of sorption kinetics on predicted drain flow concentrations was further illustrated in Figure 10, where a standard FOCUS_{SW} drainage scenario was simulated by the MACRO model with the kinetic sorption parameters above. Consistent with the predicted soil residue patterns in the field dissipation study by FOCUS-PRZM, higher and earlier concentration “breakthrough” was predicted when sorption kinetics was not considered in the MACRO model (blue color).

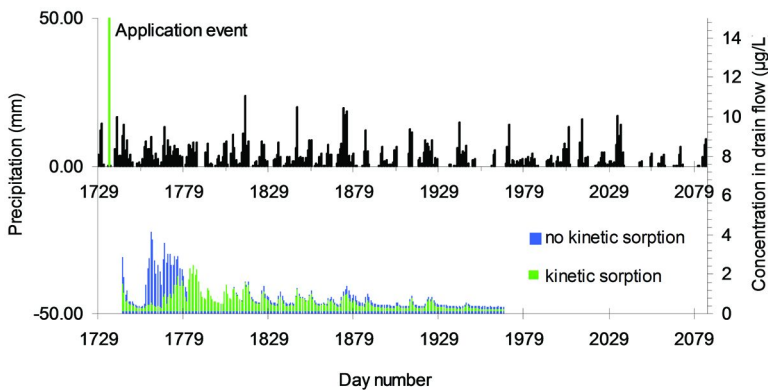


Figure 10. Effects of kinetic sorption on predicted drain flow concentrations in a standard FOCUS drainage scenario simulated by the MACRO model (using input parameters as in Figure 9). (see color insert)

Example Simulations for the Nine FOCUS Scenarios

A simulation series was conducted with three variations of the FOCUS example pesticide (or Pesticide D, with $K_{om}=35$ L/kg, Freundlich exponent $1/n=0.9$) for the nine FOCUS groundwater scenarios (Figure 11). An annual application in winter cereals (1 Kg/ha one day before crop emergence, CAM = 1, Q10= 2.58, no runoff) was assumed. The following variations were considered with respect to the sorption kinetics:

- A. Without kinetic sorption;
- B. Default kinetic sorption (PEARL: $f_{ne} = 0.3$, $\alpha = 0.01 \text{ d}^{-1}$);
- C. Extreme kinetic sorption (PEARL: $f_{ne} = 0.5$, $\alpha = 0.5 \text{ d}^{-1}$).

The effective degradation $DT50_{eq}$ of the equilibrium sorption phase (which is always smaller than $DT50_{tot}$ of the total bulk soil) was calculated based on Eq. 31 using the standard soil $DT50_{tot}$ (i.e. 20 days for FOCUS Pesticide D) and the applicable kinetic sorption parameter. The following effective DT50 values corresponding to the three sets of different sorption kinetics above were calculated as model inputs for degradation:

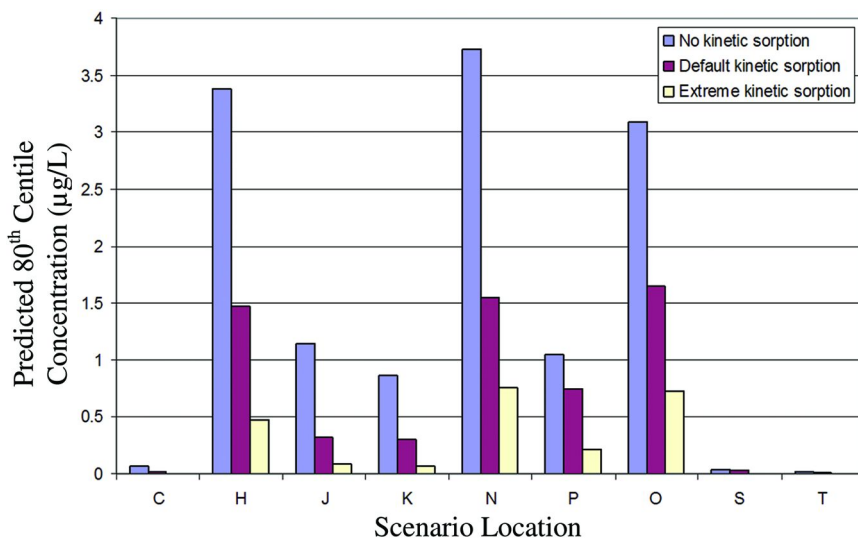


Figure 11. Comparison of FOCUS-PRZM simulated annual average concentrations (80th percentile) for three different kinetic sorption cases at the nine FOCUS groundwater scenario locations: C=Châteaudun; H=Hamburg; J=Jokioinen; K=Kremsmünster; O=Okehampton; P=Piacenza; N=Porto; S=Sevilla; T=Thiva. (see color insert)

The simulation results of the three different sorption kinetics assumptions for the nine FOCUS groundwater scenarios are provided in Figure 11. As shown, the sensitivity of the annual concentrations to kinetic sorption is clearly demonstrated for all nine scenarios. Kinetic sorption tended to reduce the mobility of the test compound in these cases and had a significant effect on simulated leaching concentrations.

Conclusions

This chapter described the development of the coupled sorption and degradation kinetics in the soil-water system and the implementation of the kinetics into FOCUS-PRZM. New codes of the kinetics were verified by the analytical solution (assuming linear sorption isotherm) and a well-established model LEACHP. Several field measured data sets were used to evaluate the new version of FOCUS-PRZM. Results demonstrated that the new model was able to reasonably predict the soil residue levels in many orders of magnitude over the entire time scale of field experiments. Parameters of the sorption kinetics can be converted to the ones adapted in FOCUS PEARL, one of the other EU regulatory models for pesticide groundwater exposure assessment. Model simulations showed high model sensitivity of sorption kinetics to predicted groundwater concentrations in all nine EU groundwater scenarios.

References

1. FOCUS. *FOCUS groundwater scenarios in the EU review of active substances*, report of the FOCUS Groundwater Scenarios Workgroup, EC Document Reference, Sanco/321/2000 rev. 2, 2000; pp 202
2. FOCUS. *Assessing Potential for Movement of Active Substances and their Metabolites to Ground Water in the EU*, report of the FOCUS Ground Water Work Group, version 1, 2009; pp 594.
3. Pignatello, J. J. *Adv. Agron.* **2000**, *69*, 1–73.
4. Wauchope, R. D.; Yeh, S.; Linders, J. B. H. J.; Kloskowski, R.; Tanaka, K.; Rubin, B.; Katayama, A.; Kördel, W.; Gerstl, Z.; Lane, M.; Unsworth, J. B. *Pest Manage. Sci.* **2002**, *58*, 419–445.
5. Brusseau, M. L.; Rao, P. S. C.; Gillham, R. W. *Crit. Rev. Environ. Control* **1989**, *19*, 33–99.
6. Selim, H. M.; Davidson, J. M.; Rao, P. S. C. *Soil Sci. Soc. Am. J.* **1977**, *41*, 3–10.
7. Cameron, D. A.; Klute, A. *Water Resour. Res.* **1977**, *13*, 183–188.
8. van Genuchten, M. T.; Wagenet, R. J. *Soil Sci. Soc. Am. J.* **1989**, *53*, 1303–1310.
9. Streck, T.; Poletika, N. N.; Jury, W. A.; Farmer, W. J. *Water Resour. Res.* **1995**, *31*, 811–822.
10. Chen, W.; Wagenet, R. J. *Environ. Sci. Technol.* **1995**, *29*, 2725–2734.
11. Chen, W.; Wagenet, R. J. *Soil Sci. Soc. Am. J.* **1997**, *61*, 360–371.
12. Scow, K. M. In *Sorption and degradation of pesticides and organic chemicals in soil*; Linn, D. M., Carski, F. H., Brussenu, M. L., Chang, F. H., Eds.; SSSA Spec. Publ. 32; Soil Science Society of America: Madison, WI, 1993; pp 73–114.
13. Alexander, M. *Environ. Sci. Technol.* **2000**, *34*, 4259–4265.
14. Scow, K. M.; Hutson, J. *Soil Sci. Soc. Am. J.* **1992**, *56*, 119–127.
15. Shelton, D.; Doherty, M. A. *Soil Sci. Soc. Am. J.* **1997**, *61*, 1078–1084.
16. Guo, L.; Jury, W. A.; Wagenet, R. J.; Flury, M. *J. Contam. Hydrol.* **2000**, *43*, 45–62.

17. Shaner, D.; Brunk, G.; Nissen, S.; Westra, P.; Chen, W. *J. Environ. Qual.* **2012**, *41*, 170–178.
18. Hutson, J. L.; Wagenet, R. J. *LEACHM: Leaching Estimation and Chemistry Model*, version 3; Research Series No. 92-3; Cornell University: Ithaca, New York, 1992.
19. Wauchope, R. D.; Rojas, K. W.; Ahuja, L. R.; Ma, Q.; Malone, R. W.; Ma, L. *Pest Manage. Sci.* **2004**, *60*, 222–239.
20. Leistra, M.; van der Linden, A. M. A.; Boesten, J. J. T. I.; Tiktak, A.; van den Berg, F. *PEARL model for pesticide behavior and emissions in soil-plant systems: Description of the processes in FOCUS PEARL*, v1.1.1. RIVM report 711401 009, Alterra-rapport 013. ISSN 1566-7197; Alterra: Wageningen, Netherlands, 2001.
21. Jarvis, N. *MACRO 5.2 - Water and solute transport in macroporous soils*; 2010. Available online: <http://www.slu.se/en/collaborative-centres-and-projects/centre-for-chemical-pesticides-ckb1/areas-of-operation-within-ckb/models/macro-52/>.
22. Suárez, L. A. *PRZM-3, A Model for Predicting Pesticide and Nitrogen Fate in the Crop Root and Unsaturated Soil Zones: Users Manual for Release 3.12.2*; EPA/600/R-05/111; U.S. Environmental Protection Agency (EPA): Washington, DC, 2005.
23. Boesten J. J. T. I.; van der Linden, A. M. A. 2001 BCPC Symposium Proceedings No 78: Pesticide behaviour in soils and water, 2001; pp 27–32.
24. Chen, W.; Laabs, V.; Kookana, A. C.; Koskinen W. C. In *Non-First Order Degradation and Time-Dependent Sorption of Organic Chemicals in Soil*; Chen, W., Sabljic, A. Steven, A. C., Kookana, R.; Eds.; ACS Symposium Series 1174; American Chemical Society: Washington, DC, 2014; Chapter 5–37.

Chapter 16

Effect of Refined Environmental Fate Properties on Groundwater Concentrations Calculated With PRZM

**Robin Sur,* Jane Tang, Russell L. Jones, Daniel G. Dyer,
and Peter N. Coody**

**Bayer CropScience LP, 2 TW Alexander Drive, Research Triangle Park,
North Carolina 27709, United States**

***E-mail: robin.sur@bayer.com.**

Non-linear sorption and time-dependent sorption (TDS) are common compound properties that allow for a more realistic description of the transport and degradation of agrochemicals in the vadose zone of the soil. The EU groundwater model FOCUS-PRZM 3.5.2 includes these soil processes following intensive evaluation and technical dialog among European stakeholders (regulatory authorities, academia, consultants, and industry). This approach is used in the EU regulatory process and therefore, laboratory data needed to describe the enhanced binding processes are often available. The PRZM-GW model (by US-EPA) considers only linear sorption. Non-linear and time-dependent sorption can be included in FOCUS-PRZM 3.5.2 with the EPA environmental scenarios to demonstrate the effect on the predicted groundwater concentrations. In many cases significant reductions in the predicted groundwater concentrations can be obtained. In this study the existence and extent of time-dependent sorption has additionally been confirmed in the field by evaluating the solute downward movement in two long-term field accumulation studies. These studies were conducted over 6 to 8 years, a time period much longer than used for laboratory studies. The TDS effect was at least as pronounced as measured in the laboratory. The results suggest that incorporation of Freundlich sorption and time-dependent sorption into the exposure assessments for plant

protection products would result in more realistic estimates of groundwater concentrations. Often the necessary studies to derive reliable Freundlich and TDS sorption parameter are available. It is therefore recommended to consider this approach in drinking water exposure assessments for North America.

Introduction

US-EPA has released the numerical leaching model PRZM-GW in December 2012 to estimate concentrations of pesticides in drinking water (1) as a supplement to the long-standing screening level model SCI-GROW (2). Main reasons have been to evaluate concentrations in groundwater based on repetitive multiple year applications of pesticides and to assess the effect of different agronomic practices and use restrictions on the outcome, e.g. applications only every other year. SCI-GROW contains a regression equation, based on the evaluation of prospective groundwater monitoring studies of ten compounds at twelve sites vulnerable to leaching, and thus providing a conservative estimate of the expected groundwater concentration representing the upper 95% to 99% confidence interval of monitoring results. PRZM-GW, however, is based on PRZM 3.12.2, i.e. a one-dimensional finite difference numerical model to predict water and solute movement in the root zone of the soil (3). Hydrology is estimated by the field capacity or ‘tipping-bucket’ model, i.e. water in a soil compartment exceeding field capacity drains into the next lower compartment within one day (4). Solute transport is described by the Convection-Dispersion Equation. EPA has developed six environmental standard scenarios at the Tier-1 level to be used with PRZM-GW that represent vulnerable soil and climatic conditions at sites on the US east coast and in the upper Midwest. In some cases the PRZM-GW derived groundwater concentrations are up to orders of magnitude higher than the corresponding SCI-GROW results that are based on measurements of real-world concentrations. This is partly due to the very conservative standard environmental fate input parameters used on Tier-1. The present paper deals with refinement options based on non-linear (Freundlich) and time-dependent (non-equilibrium) sorption to obtain a more realistic groundwater exposure assessment. Generally, compound sorption is higher at lower concentrations due to the Freundlich effect and with longer residence time in soil due to time-dependent sorption. These sorption processes are established environmental fate properties of pesticides and their metabolites in soil and have been described in numerous studies for many different compounds (5).

Material and Methods

Test Compound

The test compound under investigation was a pesticide named BCS-01 for the purpose of anonymity. The methods applied to derive the environmental fate characteristics relevant for leaching modeling are described in the following sections.

Laboratory Batch Adsorption Study

The laboratory batch equilibrium adsorption experiments were conducted in accordance with guidelines from OECD (6), US-EPA (7), Canadian PMRA (8), and Japanese MAFF (9).

The equilibrium adsorption of BCS-01 was measured on five different soils with initial concentrations of BCS-01 at about 1, 0.3, 0.1, 0.03, and 0.01 mg/L in 0.01 molar aqueous calcium chloride solutions with a soil/solution ratio of 1 to 4. Adsorption took place in the dark at 20°C by shaking for 48 hours. Afterwards, the aqueous supernatant was separated by centrifugation and the a.i. residues in the supernatant were analyzed by liquid scintillation counting (LSC). After a further desorption step with 0.01 molar aqueous calcium chloride solutions, the soil was extracted with acetonitrile at ambient conditions and analyzed by LSC.

Adsorption parameters were calculated using the Freundlich adsorption isotherm. The Freundlich sorption coefficients and exponents were derived from linearized isotherms with equilibrium concentrations over two orders of magnitude from 600 µg/L to 2 µg/L, which covered the expected range of drinking water concentrations. To illustrate the effect of increased sorption at lower concentrations the soil-water distribution coefficient ($K_{OC,D}$; eq 4) was calculated as a function of the concentration in the liquid phase c_L . This was achieved by dividing the sorbed equilibrium concentration X_{EQ} as expressed by the Freundlich equation (1) by the concentration in the liquid phase c_L according to the following formulae:

$$X_{EQ} = m_{OC} K_{OC,EQ} c_{L,R} \left(\frac{c_L}{c_{L,R}} \right)^{1/n} \quad (1)$$

with

$$K_{F,EQ} = m_{OC} K_{OC,EQ} \quad (2)$$

X_{EQ}	Concentration sorbed at equilibrium sites (mg/kg)
$K_{OC,EQ}$	Equilibrium Freundlich sorption coefficient on organic carbon (L/kg)
$K_{F,EQ}$	Equilibrium Freundlich sorption coefficient (L/kg)
c_L	Concentration in liquid phase (mg/L)
$c_{L,R}$	Reference concentration in the liquid phase (1 mg/L)
$1/n$	Freundlich exponent
m_{OC}	Mass fraction of organic carbon in soil

Distribution coefficient:

$$K_D = \frac{X_{EQ}}{\frac{c_L}{c_{L,R}} c_{L,R}} = m_{OC} K_{OC,EQ} \left(\frac{c_L}{c_{L,R}} \right)^{1/n-1} \quad (3)$$

Distribution coefficient on organic carbon:

$$K_{OC,D} = \frac{K_D}{m_{OC}} = K_{OC,EQ} \left(\frac{C_L}{C_{L,R}} \right)^{1/n-1} \quad (4)$$

Time-Dependent Sorption Study

Experimental Setup

Two time-dependent sorption (TDS) studies with BCS-01 were conducted on five different soils. The purpose was to investigate changes of the sorption parameter K_D of BCS-01 due to aging in soil. In these studies the soils were prepared and incubated in accordance with typical aerobic soil metabolism/degradation methods, according to OECD test guideline 307 (10) and US EPA Subdivision N, Section 162-1 (11). The specific feature of these TDS studies was that an aqueous desorption was conducted as the first soil extraction step according to the procedure described in the OECD guidance on adsorption/desorption measurements (6) and in EPA Subdivision N, Section 163-1 (7). The entire soil sample was subjected to desorption using a 0.01 molar calcium chloride solution at a soil-to-solution ratio of 1:4 until equilibrium between the concentration of BCS-01 in solution and the adsorbed portion had been established, i.e. shaking for 24 h. Further extraction steps with organic solvents at ambient temperature and at 70°C were additionally conducted. Eight samples were taken between 0 d (2 h), 1 d, 2 d/3 d, 7 d, 14 d/15 d, 30 d, 58 d/62 d, and 121 d/128 d after incubation. Two individual flasks (true replicates) per soil were analyzed at each sampling interval. For each sample, distribution coefficients K_D were calculated according to the following formulae:

$$K_D = \frac{X_{EXTR}}{C_{L,SUS}} \quad (5)$$

where

$$C_{L,SUS} = \frac{AI_{SUP}}{V_{SUP}} \quad (6)$$

$$X_{EXTR} = \frac{AI_{ORG} + AI_{HOT} - (C_{L,SUS} \times V_{INT})}{M_S} \quad (7)$$

$$V_{INT} = V + V_{ADD} - V_{SUP} \quad (8)$$

Symbols and Units

V	Original porewater volume of soil (moist soil) (L)
V_{ADD}	Added volume of desorption solution (L)
V_{SUP}	Volume of desorption solution (L) after centrifugation (supernatant)
V_{INT}	Interstitial water (porewater), volume of water remaining in soil after desorption and centrifugation (L)
$C_{\text{L,SUS}}$	Concentration of test item in desorption solution at equilibrium (mg/L)
X_{EXTR}	Total concentration of test item sorbed at the end of the shaking period related to soil dry weight (mg/kg)
M_{s}	Dry mass of soil (kg)
AI_{SUP}	Mass of test item in desorption solution (supernatant) (mg)
AI_{ORG}	Mass of test item in organic extract (cold extraction) (mg)
AI_{HOT}	Test item in aggressive organic extract (hot extraction) (mg)

The interstitial water volume V_{INT} is the remaining aqueous solution still present in the soil, after adding the desorption solution volume V_{ADD} to the original porewater volume V in the moist soil, then shaking, centrifuging and then decanting the supernatant volume V_{SUP} (eqs 7 and 8).

According to OECD guideline 106 (6), the amount of test item contained in the interstitial water (needed in eq 7), is calculated by subtraction the volume of desorption solution V_{SUP} (supernatant after centrifugation) from the original volume of solution employed to soil ($V + V_{\text{ADD}}$), multiplied by the measured concentration of test item in the desorption solution $C_{\text{L,SUS}}$.

Time-Dependent Sorption Model

The two-site TDS model described by Leistra et al. (12) was used to derive the model parameters for BCS-01 based on the laboratory TDS study. The conceptual model is depicted in Figure 1. The model assumes two different kinds of sorption sites, the one for equilibrium and the other for non-equilibrium sorption. Sorption at the equilibrium sites takes place instantaneously. This process is operationally defined as being completed within 24 h of shaking a soil-water suspension (13) and can therefore be measured within the OECD guideline study 106 on adsorption/desorption measurements (6). Sorption at the non-equilibrium sites proceeds slower and this is measured in the TDS laboratory study. Non-equilibrium sorption is rate limited and characterized by the so-called desorption rate constant k_{des} . Sorption to both types of sites follows Freundlich isotherms assuming the same exponent $1/n$ but different Freundlich coefficients. The model parameter f_{NE} defines the ratio of Freundlich sorption coefficients in the non-equilibrium ($K_{\text{F,NE}}$) and the equilibrium compartments ($K_{\text{F,EQ}}$). Degradation is assumed to follow single first-order kinetics and only to occur in the equilibrium compartment including equilibrium sorption sites and

the liquid phase. This approach was extensively evaluated by industry, academia and regulatory authorities in Europe over the past 10 years and has been used for groundwater assessments in the European regulatory process (14, 15).

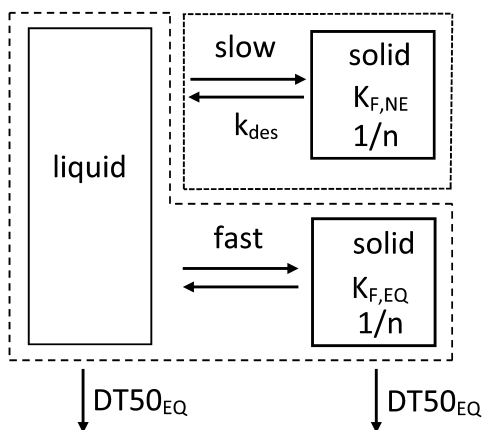


Figure 1. Two-site time-dependent sorption model. The dashed line encloses the equilibrium compartment consisting of the liquid and the equilibrium sorption phase. The dotted line shows the non-equilibrium soil compartment. Model parameters are explained in the text.

Tools To Derive TDS Model Parameters

The program PEARLNEQ (13) contains the TDS model as described in Leistra et al. (12) along with the optimization package PEST (16). It was used to derive the TDS model parameters for BCS-01 based on the laboratory TDS studies. Besides experimental conditions, e.g. soil dry mass and water content, the main model inputs are total compound mass in the system M_p and compound concentration in the liquid phase c_L as a function of time. The following assumptions and equations are part of the program. The total mass of a pesticide in each test vessel of a TDS laboratory study is the sum over the amounts in the liquid phase, the equilibrium sorbed and the non-equilibrium sorbed phases:

$$M_p = Vc_L + M_s(X_{EQ} + X_{NE}) \quad (9)$$

with:

M_p	Total mass of pesticide in each jar (mg)
V	Volume of water in soil incubated in each jar (porewater) (L)
C_L	Concentration in liquid phase (mg/L)
M_s	Dry mass of soil incubated in each jar (kg)
X_{EQ}	Concentration sorbed at equilibrium sites (mg/kg)
X_{NE}	Concentration sorbed at non-equilibrium sites (mg/kg)

Sorption both at the equilibrium and non-equilibrium sites is described by Freundlich type isotherms. The Freundlich exponent $1/n$ from the batch adsorption/desorption study is assumed to be equally valid for the equilibrium and non-equilibrium domain. Both isotherms are related to each other by the dimensionless factor f_{NE} :

$$X_{EQ} = K_{F,EQ} C_{L,R} \left(\frac{C_L}{C_{L,R}} \right)^{1/n} \quad (10)$$

$$f_{NE} = \frac{K_{F,NE}}{K_{F,EQ}} \quad (11)$$

with:

$C_{L,R}$	Reference concentration in the liquid phase (1 mg/L)
$K_{F,EQ}$	Equilibrium Freundlich sorption coefficient (L/kg)
$K_{F,NE}$	Non-equilibrium Freundlich sorption coefficient (L/kg)
$1/n$	Freundlich exponent

The sorption rate equation for the non-equilibrium sites is described as follows:

$$\frac{dX_{NE}}{dt} = k_{des} \left(K_{F,NE} C_{L,R} \left(\frac{C_L}{C_{L,R}} \right)^{1/n} - X_{NE} \right) \quad (12)$$

Since soil degradation with the rate constant k_t is assumed to occur only in the equilibrium domain of the soil system, liquid and equilibrium sorbed compound, the following rate law applies:

$$\frac{dM_p}{dt} = -k_t (V C_L + M_s X_{EQ}) \quad (13)$$

with:

$$DT50_{EQ} = \frac{\ln 2}{k_t} \quad (14)$$

The half-life of a compound in the equilibrium domain of the soil system ($DT50_{EQ}$) has to be faster by the relative size of the equilibrium domain compared to the total soil domain ($DT50_{TOT}$), i.e. the sum of equilibrium and non-equilibrium domain (17). By this, it is assured that the overall half-life in the total system of the soil stays the same, irrespective whether the TDS model is used or not:

$$DT50_{EQ} \approx \frac{DT50_{TOT}}{1 + f_{NE}} \quad (15)$$

PEARLNEQ solves both differential equations (12 and 13) numerically using Euler's method for integration of the state variables M_p and X_{NE} . The concentration in the liquid phase c_L is calculated via an iteration procedure as described in Appendix 2 of Leistra et al. (12) and in Appendix 4 of FOCUS (18).

Concentration was measured in the desorption solution of the TDS laboratory studies after adding a measured volume of calcium chloride solution V_{ADD} . Thus, the concentration measured in the supernatant of the soil-water suspension was used rather than the concentration in the soil porewater before desorption.

It is generally assumed that during the desorption period of 24 h full equilibrium is reached and that desorption from the non-equilibrium sites in this period of time can be ignored. Therefore, using the mass balance eq (9) the following relationship (16) is obtained. It presumes mass conservation and equal concentrations sorbed at the non-equilibrium sites in the moist soil and in the soil-water suspension:

$$Vc_{L,MS} + M_s(X_{EQ,MS} + X_{NE}) = (V + V_{ADD})c_{L,SUS} + M_s(X_{EQ,SUS} + X_{NE}) \quad (16)$$

with:

Subscript MS	Moist soil system
Subscript SUS	Soil-water suspension system
V_{ADD}	Volume of calcium chloride solution added to the soil at each sampling point just before starting the 24 h desorption experiment (mL)

Eq (16) was solved by PEARLNEQ at each time point for $c_{L,SUS}$ using eq (10) and $c_{L,SUS}$ was provided as output along with the total mass in the system.

As an additional output the distribution coefficient was calculated, which generally varies with time. To differentiate this distribution coefficient from the Freundlich coefficients used by the model it is also called apparent sorption coefficient. The increase of this variable over time may serve as additional evidence for time-dependent sorption:

$$K_D = \frac{X_{EQ,SUS} + X_{NE}}{c_{L,SUS}} \quad (17)$$

Details how K_D was calculated in the laboratory TDS study are given in eqs 5-8. In total, five TDS model parameters were optimized (Table 1).

Table 1. TDS Model Parameters to Be Optimized

Desorption rate constant	k_{des}
Ratio of Freundlich coefficient in non-equilibrium to equilibrium domain	$f_{NE} = \frac{K_{F,NE}}{K_{F,EQ}}$
Freundlich sorption coefficient for the equilibrium compartment normalized to organic matter content	$K_{OM,EQ} = \frac{K_{OC,EQ}}{1.724}$
Initial substance mass in the total system (t = 0)	M_{ini}
Degradation half-life in the equilibrium domain of soil including water	$DT50_{EQ} = \frac{\ln 2}{k_t}$

For three out of five TDS study soils measurements of the Freundlich exponent $1/n$ were available on the same soils from the batch adsorption study. These were used in the optimization runs ('paired data'). For the remaining two soils average Freundlich exponents calculated from all soils were used.

Leaching Models

PRZM-GW

Tier 1 groundwater estimated drinking water concentrations (EDWCs) for BCS-01 after soil application were derived with PRZM-GW (Pesticide Root Zone Model for Groundwater, version 1.1, January 23, 2014), using the GW-GUI (Graphical User Interface, version 1.07, January 23, 2014) and EPA standard scenarios (revision February 19, 2014). PRZM-GW is a one-dimensional, finite-difference model that estimates the concentrations of pesticides in groundwater. It accounts for pesticide fate in the crop root zone by simulating pesticide transport and degradation through the soil profile after a pesticide is applied to an agricultural field. PRZM-GW permits the assessment of multiple years of pesticide application (up to 100 years) on a single site. Six standard scenarios, each representing a different region known to be vulnerable to groundwater contaminations, were available for use with PRZM-GW for risk assessment purposes. In PRZM-GW simulations, each of these standard scenarios was used. PRZM-GW output values represent pesticide concentrations in a vulnerable groundwater supply that is located directly beneath a rural agricultural field (19).

FOCUS-PRZM 3.5.2

FOCUS-PRZM is a numerical leaching model officially used within the EU pesticide registration process (20). It is a one-dimensional finite difference numerical model to predict water and solute movement in the root zone of the soil (3). Hydrology is estimated by the field capacity or ‘tipping-bucket’ model, i.e. water in a soil compartment exceeding field capacity drains into the next lower compartment within one day (4). Solute transport is described by the Convection-Dispersion Equation.

FOCUS-PRZM 3.5.2 also contains a two-site time-dependent sorption model similar to that used in PEARLNEQ (21). Both the PEARLNEQ and the PRZM models are mathematically equivalent, but the TDS model parameters are expressed slightly differently. However, they can be converted using simple mathematical operations (14, 22). The difference between PEARLNEQ and PRZM are the parameters used to express the sorbed concentration on the equilibrium and non-equilibrium sites. The following equations are used by PRZM:

$$X_{EQ} = f_{EQ} K_{F,TOT} C_{L,R} \left(\frac{C_L}{C_{L,R}} \right)^{1/n} \quad (18)$$

with

$$K_{F,TOT} = K_{F,EQ} + K_{F,NE} \quad (19)$$

$$f_{EQ} = \frac{K_{F,EQ}}{K_{F,TOT}} \quad (20)$$

$$\frac{dX_{NE}}{dt} = \alpha \left((1 - f_{EQ}) K_{F,TOT} C_{L,R} \left(\frac{C_L}{C_{L,R}} \right)^{1/n} - X_{NE} \right) \quad (21)$$

f_{EQ}	Fraction of instantaneous equilibrium sorption sites in soil
$K_{F,TOT}$	Freundlich coefficient for total sorption in soil (equilibrium + non-equilibrium)
A	First-order desorption rate constant (d ⁻¹)

Comparing PEARLNEQ equations (10 and 12) and PRZM equations (18 and 21), the following conversion has to be used (Table 2). When using the input shell of FOCUS-PRZM 3.5.2 the user is required to enter the TDS parameters as used in the PEARLNEQ definition. The program does the parameter conversion

internally when creating the PRZM input file for the simulation run. However, if the user directly edits the ASCII input file (as was done for the BCS-01 work), the PEARLNEQ TDS parameters need to be converted to the FOCUS-PRZM parameters manually before entering into the input file.

Table 2. Relationship between PEARL and FOCUS-PRZM TDS Model Parameters

<i>PEARLNEQ definition (required by FOCUS-PRZM 3.5.2. input shell)</i>	<i>FOCUS-PRZM definition (as appears in FOCUS-PRZM 3.5.2 input file)</i>
k_{des}	$\alpha = k_{des}$
f_{NE}	$f_{EQ} = \frac{1}{1 + f_{NE}}$
$K_{F,EQ}$	$K_{F,TOT} = K_{F,EQ}(1 + f_{NE})$
$DT50_{EQ} = \frac{\ln 2}{k_t}$	$DT50_{EQ} = \frac{\ln 2}{k_t}$

Parameter Conversion for Model Input

1. Temperature Normalization

Normalization of the half-lives of BCS-01 from 20°C to 25°C was conducted in accordance with EPA guidance using a Q_{10} of 2 and the following formula (23):

$$DT_{50}(25^{\circ}\text{C}) = DT_{50}(T) Q_{10}^{\frac{T - T_{ref}}{10K}} \quad (22)$$

T: actual study temperature (K)
 T_{ref} : reference temperature (here: 298.15 K)
 DT_{50} : half-life (d)

2. Calculation of Soil Half-Life

The final soil half-life for model input was the 90th percentile confidence bound on the arithmetic mean half-life calculated according to (25):

$$DT_{50,input} = DT_{50,average} + \frac{t_{90,n-1}s}{\sqrt{n}} \quad (23)$$

where,

$DT_{50,input}$ = half-life input value (d)

$DT_{50,average}$ = mean of sample half-lives (d)

s = sample standard deviation (d)

n = number of half-lives available

$t_{90,n-1}$ = one-sided Student's t value for $\alpha = 0.1$ (i.e., 1.0-0.9)

Hydrolysis Study

Data from a hydrolysis study with BCS-01 at 50°C were additionally used in the exposure assessment. The study had been conducted for 120 h and showed the formation of an unknown hydrolysis product increasing with time. A hydrolysis half-life of 219 d at 50°C was evaluated. This degradation rate was significantly different from zero (t-test probability <0.05). The hydrolysis half-life was normalized to a temperature of 25°C ($Q_{10} = 2$) resulting in 1240 d, which is usable in exposure assessments.

Terrestrial Field Accumulation Studies

Experimental Setup

The long-term terrestrial field accumulation (TFA) behavior of BCS-01 at two sites in Germany and Southern France with 6 to 8 annual applications each at 250 g/ha has been studied to investigate mobility under outdoor conditions. The topsoil layers (0-30 cm) were of sandy loam or silt loam texture and organic carbon contents ranged from 0.7% to 0.9%. Applications had been repeated until plateau concentrations in soil were reached, i.e. until a steady state between soil loading and degradation was reached and in turn the lower part of the so-called 'saw tooth' curve did not increase anymore over time.

Soil samplings were performed with a 'Wacker Hammer' and related coring accessories (\varnothing 48 to 50 mm) to a depth of 75 cm. At each sampling interval, a total of 20 soil cores were taken from treated plots. The sampling spots were distributed randomly over the plots to obtain representative samples. Soil samples were taken at three sampling intervals per year as determined by the events, i.e. before application (= at the end of the winter period), after application, and in autumn before winter dormancy.

Evaluation of Terrestrial Field Accumulation Studies

The field residue data was used in the present study to derive a Freundlich sorption coefficient and TDS model parameters being representative for the long-term sorption behavior of BCS-01 in the field.

The evaluation of each TFA site consisted of two levels:

- Level 1: Optimization of long-term equilibrium sorption parameters, $DT50_{TOT}$ and of $K_{OC,TOT}$, with Freundlich exponent fixed to batch laboratory value ($1/n < 1$)
 - $K_{OC,TOT}$ is the long-term equilibrium sorption coefficient, finally containing
 - Equilibrium sorption
 - Non-equilibrium sorption (TDS), although all sites are assumed to be equilibrium sites, valid for sufficiently long times, for equilibration
- Level 2: Optimization of full TDS model parameters (k_{des} , f_{NE} , $DT50_{EQ}$) with K_{OC} and Freundlich exponent fixed to batch laboratory value ($1/n < 1$)
 - K_{OC} ($=K_{OC,EQ}$) contains equilibrium sorption only

The results of Level 1 and Level 2 were used to quantify the extent of TDS in the field and to compare it to the laboratory TDS parameters to assess the conservatism of groundwater modeling on Tier-2.

The comparison with the short-term batch laboratory Freundlich coefficient should demonstrate the extent of TDS actually occurring under more realistic field conditions. The evaluation was conducted using the leaching model PEARL, which is considered equivalent to PRZM in terms of the description of soil hydrology and solute transport in the vadose zone (14, 24). For the TFA sites PEARL scenarios were developed in compliance with the North American guidance on PRZM-GW (25):

- Change of degradation rate with temperature according to $Q_{10} = 2$
- No dependency of degradation rate on soil moisture
- Increasing depth dependent dispersivities
 - 1 cm from 0 – 10 cm depth
 - 5 cm from 10 – 20 cm depth
 - 20 cm from 20 – 100 cm depth
- Linear decrease of degradation rate with depth down to zero at 1 m

The scenarios representing the two TFA sites were parameterized using site specific soil data and weather information from nearby weather stations. Mualem - van Genuchten soil hydraulic parameters (θ_r , θ_s , α , n , λ , K_s) were calculated based on texture using the ROSETTA class pedotransfer functions (26). Daily weather data were taken from nearby weather stations (minimum and maximum

temperature, precipitation, humidity, solar radiation, wind speed). Potential evapotranspiration was calculated with PEARL using the Penman-Monteith model.

The measured depth distributions at the different sampling dates of BCS-01 were fitted against simulated residues in total soil of a PEARL simulation run for the respective TFA scenario. For this purpose, the input parameters for half-life and sorption coefficient (or TDS parameters, depending on the type of 'level', see above) were iteratively adjusted to obtain the optimum fit. This parameter estimation process was automated with the PEST software tool for inverse modeling (16). Residues were inversely weighted ($1/x^2$). The 'obs2obs' utility of this package was additionally used to average PEARL output concentrations over a soil layer thickness of 10 cm to match the depth increment of the measured residue data.

Field residues C_{soil} reported in units of $\mu\text{g}/\text{kg}$ were converted to C_{soil} expressed as kg m^{-3} prior to optimization to match the unit of the PEARL parameter 'ConSys' describing the concentration in different soil depths:

$$C_{soil} \left[\frac{\text{kg}}{\text{m}^3} \right] = C_{soil} \left[\frac{\mu\text{g}}{\text{kg}} \right] \times \rho_{soil\ layer} \left[\frac{\text{kg}}{\text{L}} \right] \times 10^{-9} \left[\frac{\text{kg}}{\mu\text{g}} \right] \times 10^3 \left[\frac{\text{L}}{\text{m}^3} \right] \quad (24)$$

As measured values were not available the dry soil bulk density ρ of each soil layer was calculated from its organic carbon fraction (f_{OM} in g/g) by the following pedo transfer function which is also implemented in FOCUS-PEARL (12):

$$\rho_{soil\ layer} = 1.800 + 1.236 \times f_{OM} - 2.910 \times \sqrt{f_{OM}} \quad (25)$$

Finally, for graphical representation the results were converted to concentrations C_{soil} in units of g/ha according to the following formula:

$$C_{soil} \left[\frac{\text{g}}{\text{ha}} \right] = C_{soil} \left[\frac{\text{kg}}{\text{m}^3} \right] \times h_{soil\ layer} [\text{m}] \times 10^4 \left[\frac{\text{m}^2}{\text{ha}} \right] \times 10^3 \left[\frac{\text{g}}{\text{kg}} \right] \quad (26)$$

with:

$$h_{soil\ layer} = 0.1 \text{ m (thickness of soil layer)}$$

Results and Discussion

Freundlich Sorption Parameters

In the laboratory adsorption study BCS-01 exhibited a pronounced non-linear sorption isotherm with an arithmetic mean Freundlich exponent of 0.83 (Table 3). Figure 2 shows the adsorbed concentration plotted against the liquid concentration at equilibrium, which assumes the typically curved shape of the Freundlich isotherm. This curvature is responsible for the fact that at lower concentrations

sorption, i.e. the distribution coefficient, is higher than at higher concentrations. For comparison, the linear isotherm that PRZM-GW assumes by default is also depicted. It is evident that for liquid concentrations below one mg/L the actual sorption as indicated by the Freundlich isotherm is considerably stronger than the value according to the linear isotherm used by PRZM-GW. Another way to highlight the difference between both curves is looking at the actual soil-water distribution coefficient as a function of liquid concentration at equilibrium. Figure 3 is obtained by plotting the normalized soil-water distribution coefficient $K_{OC,D}$ of BCS-01 against its equilibrium concentration in the aqueous phase.

Two lines are depicted, one for non-linear Freundlich sorption using the average Freundlich coefficient $K_{OC,EQ}$ and the average Freundlich exponent $1/n$ of 279 L/kg and 0.83, respectively. The other line shows linear sorption assuming the same Freundlich coefficient but an exponent of 1 (to represent no concentration dependency). The curves only intersect at the reference concentration $c_{L,R}$ of 1 mg/L. At lower concentrations the Freundlich sorption effect increases the distribution coefficient $K_{OC,D}$ whereas for linear sorption no increase in sorption takes place. The plotted data points of binding coefficient $K_{OC,D}$ at different soil solution concentrations derived from five laboratory soils show how Freundlich sorption with an exponent of 0.83 much better represents the sorption behavior of BCS-01 than linear sorption assumed in Tier-1 modeling. At the lowest measured concentration of 2 $\mu\text{g/L}$ the actual soil-water distribution coefficient is about 3-times larger than assuming linear sorption.

Table 3. Laboratory Batch Freundlich Adsorption Coefficients and Exponents of BCS-01 on Different Soils (Adsorption Time 48 h, 20°C)

<i>Soil</i>	$K_{OC,EQ}$ (L/kg)	$1/n$
AXXa	233.2	0.765
HF	260.5	0.838
WW	233.7	0.849
PV	267.3	0.846
ST	399.7	0.837
Average	278.9	0.827

Time-Dependent Sorption Parameters

Time-Dependent Sorption Behavior

On average, a 2.1-fold increase of the distribution coefficient $K_{OC,D}$ was observed over the approximately 120 days of incubation in the time-dependent sorption study (Figure 4) compared to the $K_{OC,D}$ obtained after 2 d or 3 d of incubation. The actual Freundlich sorption coefficient $K_{OC,EQ}$ increased by a

factor of 1.8. Freundlich coefficients were calculated at each point in time from $K_{OC,D}$ and the liquid concentration C_L by inversion of eq (4). The difference between both curves is shown exemplary for soil AXXa in Figure 5. Compared to the batch equilibrium sorption study the Freundlich sorption coefficient $K_{OC,EQ}$ increased by a factor of 1.4.

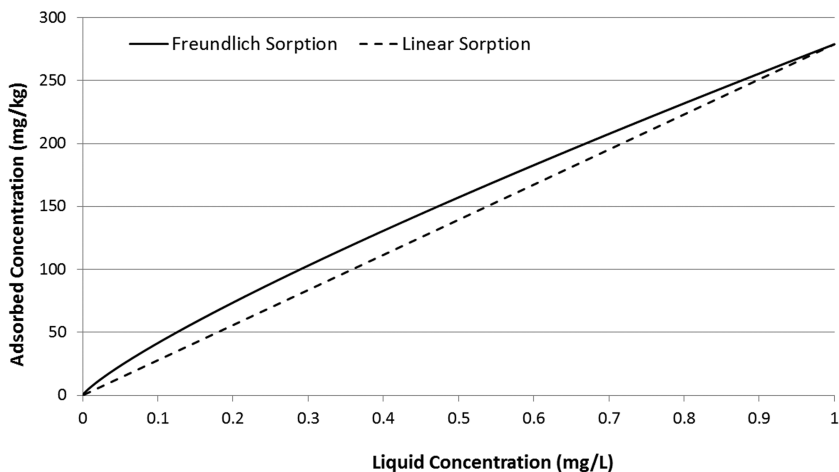


Figure 2. Sorption behavior for linear and non-linear Freundlich isotherms. Compound BCS-01 exhibits a pronounced non-linear sorption with a mean Freundlich exponent of 0.83.

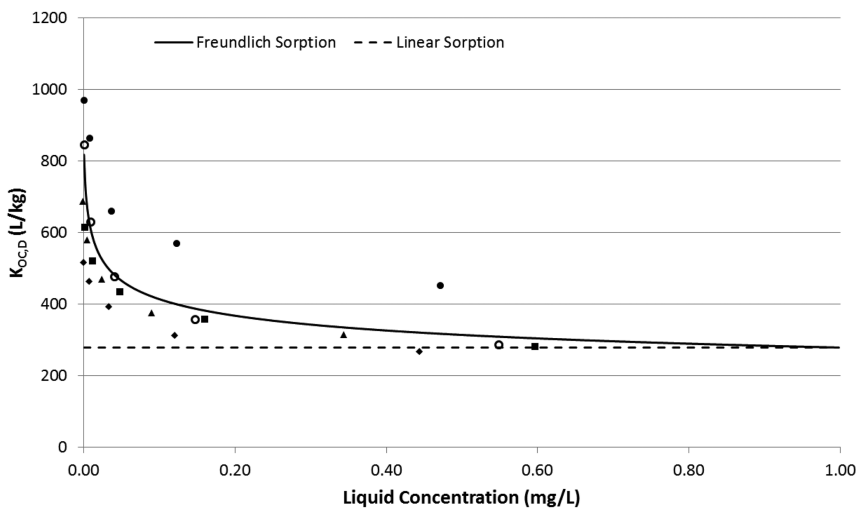


Figure 3. Soil-water distribution coefficient $K_{OC,D}$ of BCS-01 normalized to soil organic carbon content, as a function of equilibrium concentration of BCS-01 in the aqueous phase of a laboratory batch adsorption/desorption study. The symbols represent measured values on five different soils.

A time dependency of chemical binding to soil over several months is common for crop protection products. It is an important compound property that should be included in a refined, i.e. Tier-2, groundwater exposure assessment, because the travel time to groundwater is comparatively long and therefore exposure is driven by the long-term sorption behavior as shown in Figure 4.

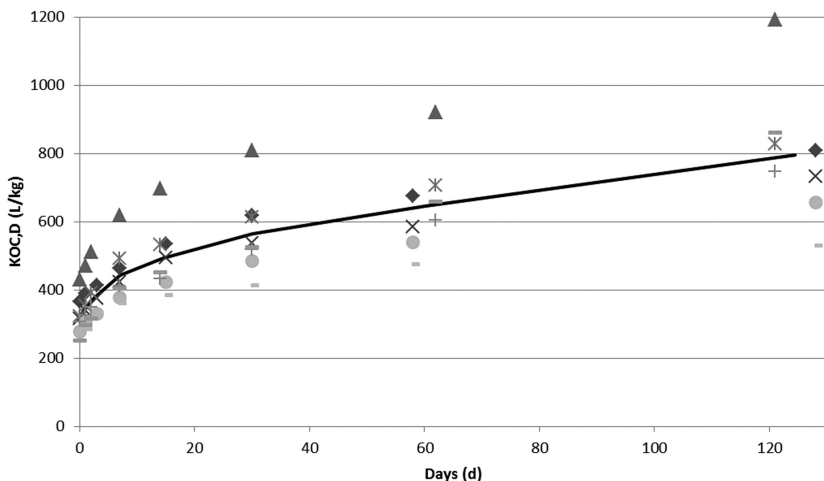


Figure 4. Increase of sorption coefficient $K_{OC,D}$ over time on five soils. Average increase was 2.1-fold compared to day 2 or 3. Symbols represent measurements on different soils. The solid line is an interpolation through all data points.

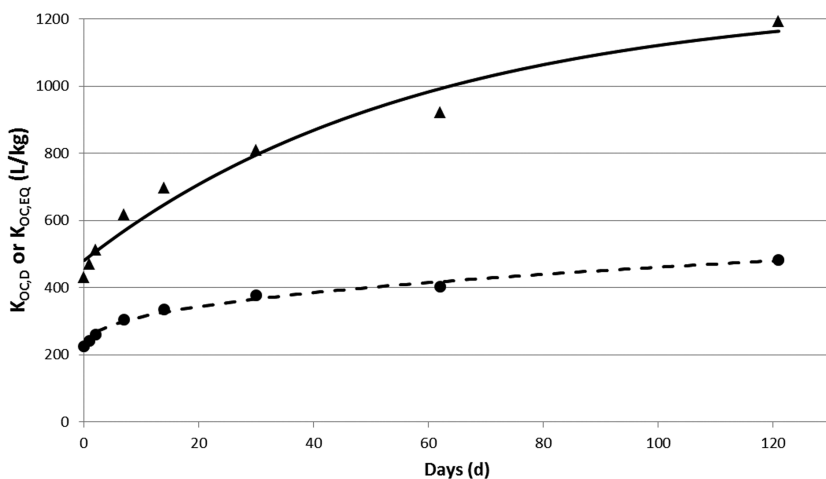


Figure 5. Distribution coefficient $K_{OC,D}$ (triangles) and Freundlich coefficient $K_{OC,EQ}$ (dots) for soil AXXa over time in the time-dependent sorption study. $K_{OC,D}$ and $K_{OC,EQ}$ increase by a factor of 1.9 and 2.4, respectively between 2 days and 121 days after application. Solid and dashed lines are best fits through data points.

Total Soil Degradation in Time-Dependent Sorption Study

As the TDS study was a combined degradation and time-dependent sorption study, single-first order half-lives for the total soil compartment $DT50_{TOT}$ were also evaluated, which ranged from 210 d to 464 d (Table 4).

Table 4. Laboratory Single-First Order Soil Degradation Half-Lives $DT50_{TOT}$ (in Days) of BCS-01 at 20°C in the TDS Study

Soil	Study 1	Study 2
HF	210	221
AXXa	464	231
WW	250	339
AIIIa/DD	162	165
Average	255	

Note: These half-lives were derived based on degradation in the total compartment of the soil; no TDS model was applied.

Time-Dependent Sorption Model Parameters

The TDS model parameters for BCS-01 were derived based on the experimental data provided in two laboratory studies on five different soils. As an example the results for soil HF are discussed here. Figure 6 shows the decline of the total mass of BCS-01 from soil including the liquid phase (top) and of the concentration in the liquid phase (bottom). The first two data points (days 0 and 1) have not been used for the fit in order to focus the optimization on the long-term sorption behavior. The apparent distribution coefficient K_D at each time point was calculated based on observed and simulated concentrations (Figure 7). The agreement between measured and calculated K_D was very close demonstrating that the chosen TDS model was capable of capturing the increased sorption with time very well.

In addition, a standard equilibrium optimization was carried out without TDS, assuming that only equilibrium sorption sites are available (i.e., $f_{NE} = 0$ and $k_{des} = 0$). In this case only three parameters were optimized ($K_{OM,EQ}$, M_{ini} , and $DT50_{EQ} = DT50_{TOT}$). It became obvious from visual assessment of total mass and concentration in the liquid phase that the assumption of equilibrium sorption alone could not account for the biphasic decline behavior of BCS-01 in both compartments (Figure 8). The TDS model, however, was capable of describing well the slowdown of degradation with time. Furthermore, the increase in K_D over time could not be captured without TDS (Figure 9). In contrast, the almost threefold increase of K_D was well captured by the TDS model (Figure 7). The five TDS parameters obtained by optimization for all five soils are compiled in Table 5.

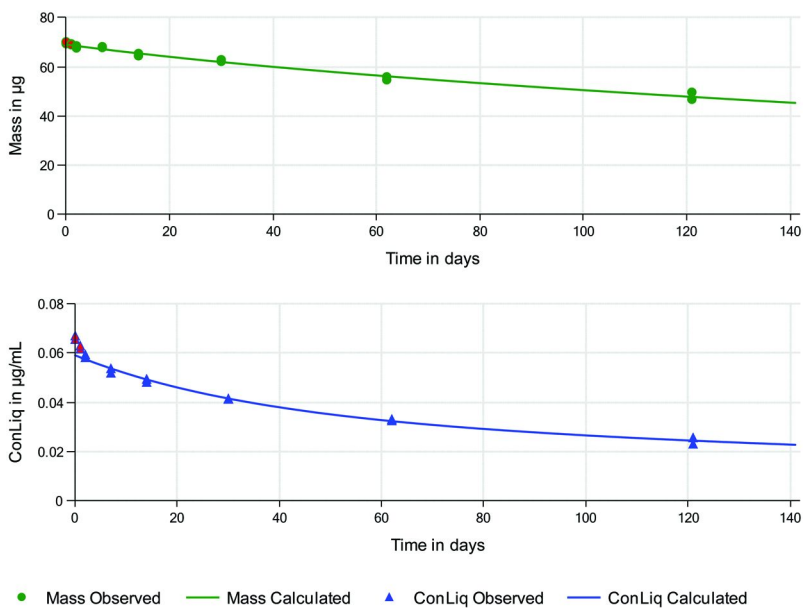


Figure 6. Observed vs. calculated total mass (top) and concentration in the liquid phase (bottom) for soil HF; TDS model fitted for f_{NE} , k_{des} , $K_{OM,EQ}$, $DT50_{EQ}$, M_{ini} with PEARLNEQ.

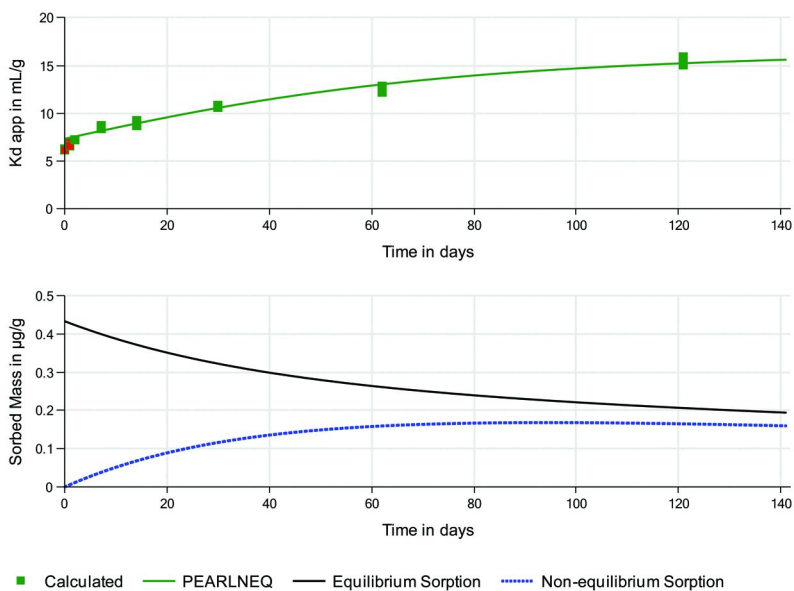


Figure 7. Observed vs. calculated soil-water partitioning coefficient K_D (top) and calculated mass sorbed at equilibrium and non-equilibrium sites (bottom) for soil HF; TDS model fitted for f_{NE} , k_{des} , $K_{OM,EQ}$, $DT50_{EQ}$, M_{ini} with PEARLNEQ.

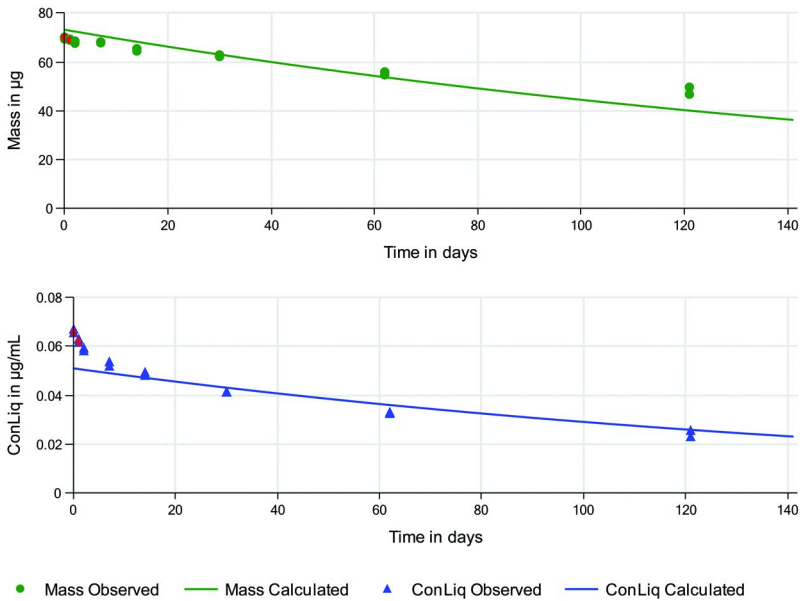


Figure 8. Observed vs. calculated total mass (top) and concentration in the liquid phase (bottom) for soil HF; no TDS model used, fitted only for $K_{OM,EQ}$, $DT50_{TOT}$, M_{ini} with PEARLNEQ.

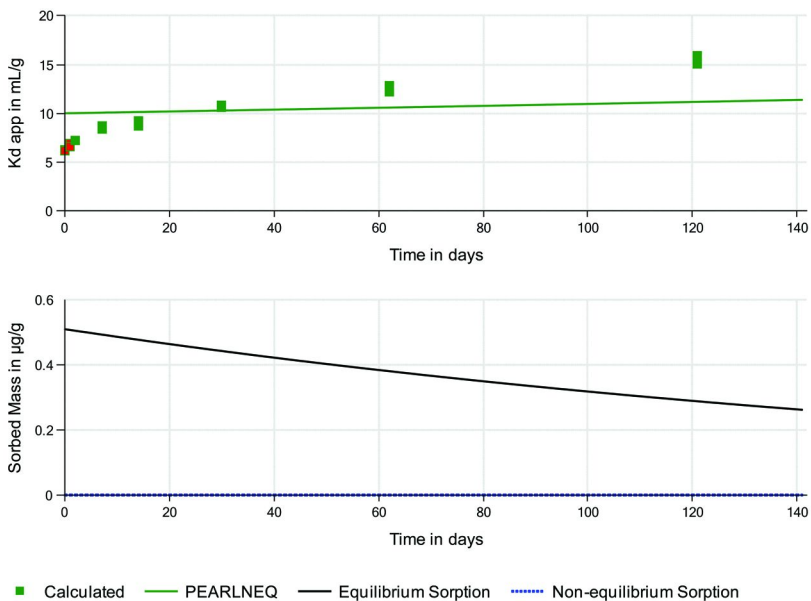


Figure 9. Observed vs. calculated soil-water partitioning coefficient K_D (top) and calculated mass sorbed at equilibrium and non-equilibrium sites (bottom) for soil HF; no TDS model used, fitted only for $K_{OM,EQ}$, $DT50_{TOT}$, M_{ini} with PEARLNEQ.

In contrast to the equilibrium sorption model alone, only the TDS model was able to describe the results of the TDS study with BCS-01, i.e. total concentration in soil, concentration in the liquid phase and the soil-water distribution coefficient. Especially, the increase of the apparent sorption coefficient K_D at each time point, experimentally apparently increasing by a factor of about 3 could be well explained by the TDS model (Figure 7).

As sorption of organic compounds to soil is a determining factor of their mobility in the environment, the refined approach using TDS is considered appropriate for higher-tier groundwater exposure assessment.

Table 5. Fitted Time-Dependent Sorption (TDS) Model Parameters for BCS-01 Using PEARLNEQ Software

<i>Soil</i>	f_{NE}	$k_{des} (d^{-1})$	$DT50_{EQ} (20^{\circ}C) (d)$	$M_{ini} (\mu g)$	$K_{OM,EQ} (L/kg)$
HF	0.51	0.0178	171.1	69.1	128.7
AXXa	0.49	0.0174	167.2	70.2	161.5
WW	0.47	0.0234	235.9	69.4	156.6
AIIIa	0.57	0.0114	124.9	70.0	130.9
HF	0.44	0.0227	157.6	65.2	120.8
AXXa	0.48	0.0346	312.6	62.7	110.0
WW	0.43	0.0238	190.3	66.0	143.2
DD	0.28	0.0296	140.4	62.4	102.8
Average	0.46	0.0226	187.5	66.9	131.8

Leaching Modeling

Tier-1 Groundwater Exposure Assessment with Linear Freundlich Sorption

The Tier-1 PRZM-GW calculations were based on the input parameters for the Freundlich sorption coefficient and laboratory soil degradation half-lives following the general guidance on PRZM-GW. The input parameters are compiled in Table 6. Resulting estimated drinking water concentrations (EDWCs) are given in Table 7.

Due to the only slight differences between highest daily and post breakthrough concentrations, the following higher-tier exposure assessments were only evaluated for the former type of concentration.

Table 6. Input Parameters for Tier-1 PRZM-GW Calculations of BCS-01

<i>Input Parameter (Unit)</i>	<i>Value</i>
Aerobic soil degradation half-life DT50 _{TOT} (25°C) (d), 90 th percentile confidence bound on the average half-life	215
Hydrolysis half-life (25°C) (d)	1240
Adsorption coefficient (L/kg)	279
Application date (dd-mm)	19-05
Application method	1 (ground)
Application rate (g/ha)	140
Number of applications	1
Application retreatment	annually
Duration of simulation (y)	100

Table 7. Results of Tier-1 PRZM-GW Estimated Drinking Water Concentrations (EDWCs) of BCS-01, Soil Application, 140 g/ha, 100 Years of Simulation

<i>EPA Scenario</i>	<i>Highest Daily Value (µg/L)</i>	<i>Post Breakthrough Average (µg/L)</i>	<i>Average Simulation Breakthrough Time (d)</i>
Wisconsin	16.5	14.2	6104
North Carolina	7.38	5.92	4604
Georgia	3.04	2.79	5821
Florida - Potato	0.466	0.329	6641
Florida - Citrus	10.8	9.37	3509
Delmarva	9.73	8.62	4447

Equivalence of models PRZM-GW and FOCUS-PRZM 3.5.2

To ensure modeling compliance with North American regulatory methods, the output concentrations of PRZM-GW and FOCUS-PRZM 3.5.2 were compared for all six EPA standard scenarios using 100 years of weather data. Freundlich sorption and TDS were turned off in FOCUS-PRZM 3.5.2 to be consistent with the standard PRZM-GW requirements ($1/n = 1.0$, $f_{NE} = 0$, $k_{des} = 0$). The model input parameters were taken from Tier-1 modeling (Table 6).

Small differences of highest daily concentrations between both models were observed. The model output concentration of FOCUS-PRZM 3.5.2 was always slightly higher compared to PRZM-GW. Deviations ranged from 0.3% to 4.2% (Table 8). As an example, the concentration-to-time curves for the North Carolina and the Wisconsin EPA standard scenarios are depicted in Figure 10 and Figure 11, respectively.

Table 8. Highest Daily Concentrations of BCS-01 in 6 EPA Standard Scenarios Calculated with PRZM-GW and FOCUS-PRZM 3.5.2 (Soil DT50_{TOT} 215 Days, Hydrolysis DT50 1240 Days, K_{OC,EQ} 279 L/kg, 140 g/ha, 100 Years of Simulation)

EPA Scenario	Highest Daily Value BCS-01 (ug/L)		% Deviation
	PRZM-GW	FOCUS-PRZM 3.5.2	
WI	16.5	17.2	4.2
NC	7.38	7.46	1.2
GA	3.04	3.08	1.1
FL-potato	0.466	0.473	1.6
FL-citrus	10.8	10.8	0.3
Delmarva	9.73	9.98	2.5

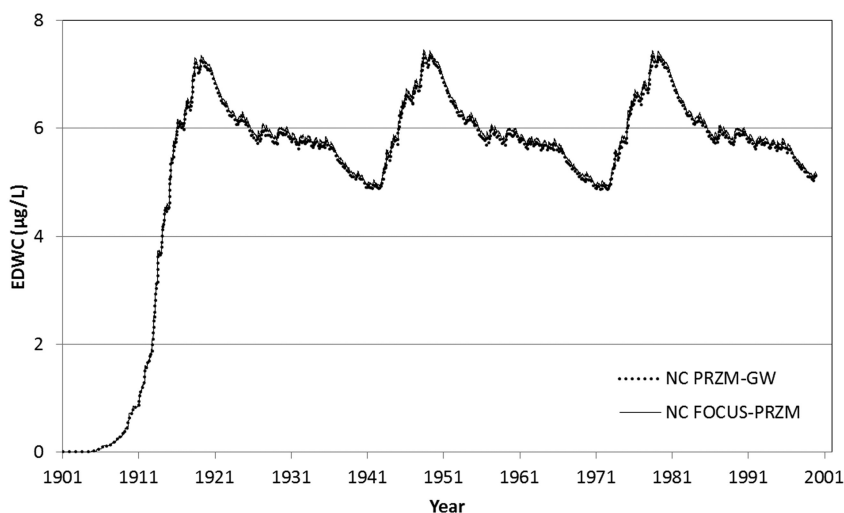


Figure 10. Concentration of BCS-01 in groundwater at North Carolina EPA standard scenario using 100 year weather data calculated with PRZM-GW and FOCUS-PRZM 3.5.2. Freundlich and time-dependent sorption were turned off in FOCUS-PRZM 3.5.2. Annual soil loading 140 g/ha, soil DT50_{TOT} 215 d, hydrolysis DT50 1,240 d, K_{OC,EQ} = 279 L/kg.

As PRZM-GW as currently released does not support Freundlich or time-dependent sorption, FOCUS-PRZM 3.5.2 was used for all calculations with refined sorption assumptions (Tier-2) based on the similarity of both models.

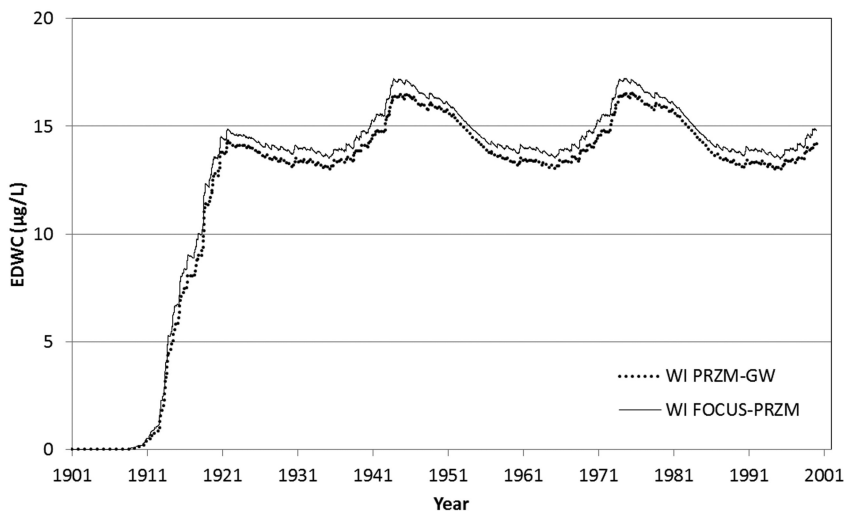


Figure 11. Concentration of BCS-01 in groundwater at Wisconsin EPA standard scenario using 100 year weather data calculated with PRZM-GW and FOCUS-PRZM 3.5.2. Freundlich and time-dependent sorption were turned off in FOCUS-PRZM 3.5.2. Annual soil loading 140 g/ha, soil $DT50_{TOT}$ 215 d, hydrolysis $DT50$ 1,240 d, $K_{OC,EQ} = 279$ L/kg.

Tier-2 Groundwater Exposure Assessment with Time-Dependent Freundlich Sorption

A higher-tier groundwater exposure assessment for the six EPA standard scenarios was conducted, applying laboratory non-linear Freundlich sorption and time-dependent sorption (TDS) parameters, using FOCUS-PRZM 3.5.2. The standard batch equilibrium sorption coefficient of 279 L/kg was used along with the Freundlich exponent of 0.83 (Table 3). The TDS model parameters f_{NE} , k_{des} and $DT50_{EQ}$ were taken from the evaluation of the laboratory TDS study (Table 5). For f_{NE} and k_{des} arithmetic mean values were used. For the equilibrium $DT50_{EQ}$ the 90th percentile on the average of the individual $DT50_{EQ}$, normalized to 25°C, was selected for model input (Table 9). Estimated drinking water concentrations (EDWCs) with FOCUS-PRZM 3.5.2, taking into account Freundlich sorption and time-dependent Freundlich sorption, are given in Table

10. Comparing these Tier-2 results to the Tier-1 EDWCs, with linear Freundlich sorption, shows a significant reduction of the groundwater exposure. The median reduction of the highest daily values for all 6 scenarios can be described by a factor of 3 applying Freundlich sorption only and by a factor of 5 with combined Freundlich and time-dependent sorption. As an example, the effect of non-linear Freundlich sorption and of non-linear Freundlich sorption with TDS on drinking water concentration at the Georgia scenario is depicted in Figure 12. Non-linear Freundlich sorption reduces the drinking water concentration by a factor of 4 compared to Tier-1 (linear sorption) and with additional TDS the reduction is 10-fold. Generally, reduction factors on Tier-2 become higher with decreasing concentrations on Tier-1. Both compound properties, Freundlich sorption and TDS, reduce mobility of the compound, thus leaving more residence time for BCS-01 in the upper soil layers where most of the degradation actually occurs. As can be seen from Figure 12, breakthrough of BCS-01 in the Georgia scenario takes about 15 years on Tier-1, 45 years on Tier-2 with Freundlich sorption and 65 years with Freundlich sorption and TDS. Highest concentrations of BCS-01 are predicted for the Wisconsin scenario (Table 10) due to the smallest organic carbon content in topsoil (0.46% from 0 – 20 cm) and the lowest annual average temperature (8°C) of all scenarios. These environmental conditions lead to an increased mobility in soil and slowdown of degradation, respectively.

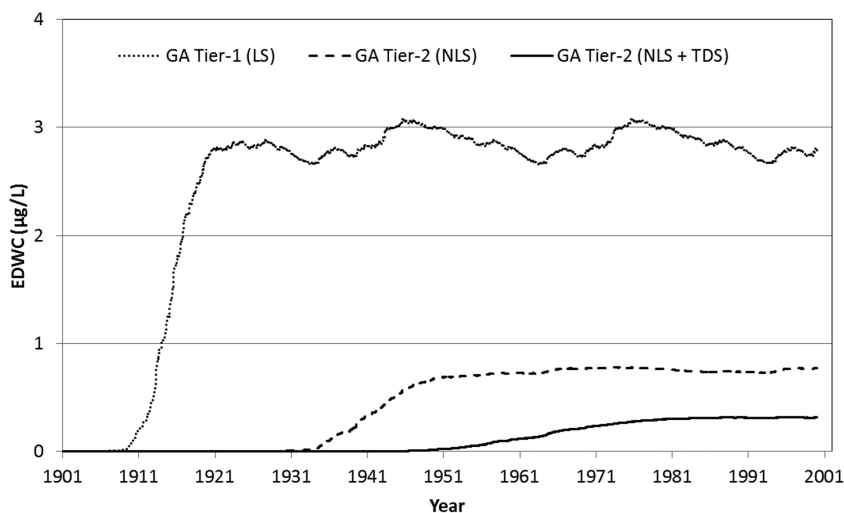


Figure 12. Estimated drinking water concentration at the Georgia EPA standard scenario based on different tiers of the exposure assessment (LS: linear sorption, NLS: non-linear Freundlich sorption, TDS: time-dependent sorption).

Table 9. Input Parameters for Tier-2 FOCUS-PRZM 3.5.2 Calculations of BCS-01

<i>Input Parameter (Unit)</i>	<i>Tier-1, linear sorption</i>	<i>Tier-2, non-linear sorption</i>	<i>Tier-2, non-linear sorption and TDS</i>
Aerobic soil degradation half-life in total compartment DT50 _{TOT} (d)	215	215	n/a
Aerobic soil degradation half-life in equilibrium compartment DT50 _{EQ} (d) *	n/a	n/a	154
Ratio of Freundlich coefficient at non-equilibrium and equilibrium sites f _{NE}	n/a	n/a	0.46
Desorption rate constant k _{des} (d ⁻¹)	n/a	n/a	0.023
Hydrolysis half-life (d)	1,240	1,240	1,240
Freundlich adsorption coefficient in equilibrium compartment K _{OC,EQ} (L/kg)	279	279	279
Freundlich exponent 1/n	1	0.83	0.83
Application date (dd-mm)	19-05	19-05	19-05
Application method	1 (ground)	1 (ground)	1 (ground)
Application rate (g/ha)	140	140	140
Number of applications	1	1	1
Application retreatment	annually	annually	annually
Duration of simulation (y)	100	100	100

* The DT50_{EQ} is only valid in combination with the TDS model as degradation is – by definition – confined to the equilibrium compartment of the soil.

Evaluation of Time-Dependent Sorption in the Field

Optimization of Long-Term Sorption Coefficient

In a first step (Level 1), the long-term (effective) Freundlich sorption coefficient, normalized to the organic carbon content, K_{OC,TOT} and the corresponding degradation half-life DT50_{TOT} of BCS-01 at the German and French TFA sites were optimized using PEARL and PEST. The Freundlich exponent 1/n was fixed to 0.807 for the German site, which is the average of the two laboratory values obtained for the corresponding soils ‘AXXa’ and ‘WW’ (Table 3). It was fixed to 0.827 for the French site, which was the average of the five laboratory values obtained in the batch equilibrium sorption study as no measurements on comparable laboratory soils were available (Table 3).

Table 10. Results of Tier-1 PRZM-GW and Tier-2 FOCUS-PRZM 3.5.2 Estimated Drinking Water Concentrations (EDWCs) for BCS-01, Soil Application 140 g/ha (Highest Daily Values)

<i>EPA Scenario</i>	<i>Tier-1, linear sorption</i>	<i>Tier-2, non-linear sorption</i>	<i>Tier-2, non-linear sorption and TDS</i>
	<i>FOCUS-PRZM (µg/L)</i>	<i>FOCUS-PRZM (µg/L)</i>	<i>FOCUS-PRZM (µg/L)</i>
Wisconsin	17	10	8.3
North Carolina	7.5	2.1	1.4
Georgia	3.1	0.78	0.31
Florida - Potato	0.47	9×10 ⁻⁵	1×10 ⁻⁶
Florida - Citrus	11	4.4	3.0
Delmarva	10	3.9	2.2

Visual fits to the observed data can be seen in Figure 13 to Figure 17 for the total soil profile as well as for individual layers for the German site and in Figure 18 to Figure 22 for the French site. Layers beyond 40 cm, i.e. 40 cm – 50 cm, 50 cm – 60 cm, and 60 cm – 75 cm were included in the fit. However, these are not depicted here, due to the low residues found (all below LOQ). So, leaching of BCS-01 was minimal under real-world field conditions.

The topmost layer (0-10 cm) shows some inconsistencies in the experimental residue data. Residues in the German and the French trial increased substantially in April 2010 without application. It is assumed that the application had not been conducted homogeneously and sampling was not representative enough to compensate for it. In addition, in some years (e.g. for German trial in 2005, 2006, 2011, 2012; French trial: 2006, 2008, 2009) the increase of residues due to application did not match the nominal application rate (250 g/ha). Presumably the actual application rate was smaller than the nominal.

In the topmost layers (0-10 cm) the simulated residues were lower than observed ones, because the model attributed more material into the second layer (10 cm – 20 cm) as actually observed and thus overestimated the downward movement of BCS-01. Also the increase of the residues above LOQ in the third soil layer (20 cm – 30 cm) at the end of the study was well captured by the model for both field sites. Residues in the fourth layer (30 cm – 40 cm) were mostly below LOD (1.5 µg/kg), i.e. a concentration range by definition too unreliable to include in a visual assessment. In conclusion, the model predicted more leaching in the field than was actually observed.

The results of the parameter optimization are compiled in Table 11. The estimated $K_{OC,TOT}$ of 587 L/kg and 414 L/kg from the long-term TFA studies in Germany and France are about 2.5- and 1.5-fold greater than the average laboratory batch $K_{OC,EQ}$ of 233 L/kg (Table 3, soils ‘AXXa’ and ‘WW’) and 279 L/kg (Table 3, all soils), respectively. This provides evidence for an actually

much stronger sorption under long-term field conditions than under short-term laboratory conditions. In addition, a significantly smaller half-life $DT50_{TOT}$ of 184 days was determined under German field conditions compared to the average of 321 days on both corresponding laboratory soils (Table 4, soils ‘AXXa’ and ‘WW’). The field half-life of 211 days derived for the French site was comparable to the average $DT50_{TOT}$ of 255 days in all laboratory soils (Table 4).

Table 11. Fitting Results of $K_{OC,TOT}$ and $DT50_{TOT}$ of BCS-01 in German and French Terrestrial Field Accumulation (TFA) Trials, Assuming Nonlinear Sorption (95% Confidence Limit)

<i>TFA Site</i>	<i>Optimized, fitted, at field</i>		<i>Fixed</i>
	$K_{OC,TOT}$ (L/kg)	$DT50_{TOT}$ (d)	<i>1/n</i>
Germany	587 (536-642)	184 (158-213)	0.807
France	414 (398-430)	211 (205-217)	0.827

Table 12. Effect of Initial Values for $K_{OC,TOT}$ and $DT50_{TOT}$ on the Result of Optimization for the German Terrestrial Field Dissipation Trial (SSQ: Sum of Squared Weighted Residuals)

<i>Initial Values</i>		<i>Optimized Values</i>		
$K_{OC,TOT}$ (L/kg)	$DT50_{TOT}$ (d)	$K_{OC,TOT}$ (L/kg)	$DT50_{TOT}$ (d)	<i>SSQ</i>
172	200	587	184	1.237×10^{13}
345	100	587	184	1.237×10^{13}
517	300	587	184	1.237×10^{13}
50	50	29	25	1.284×10^{13}

PEST determined a rather high correlation coefficient of 0.90 between both parameters $K_{OC,TOT}$ and $DT50_{TOT}$ for the German site suggesting that the optimization result may not be a unique solution. Therefore, the effect of different sets of initial parameters on the outcome of the optimization was evaluated to ensure that the global minimum of the objective function was actually found by PEST (Table 12). Finally, the parameter combination with the smallest sum of squared weighted residuals (SSQ) was chosen. The correlation coefficient between both parameters at the French site, however, was moderate (0.77).

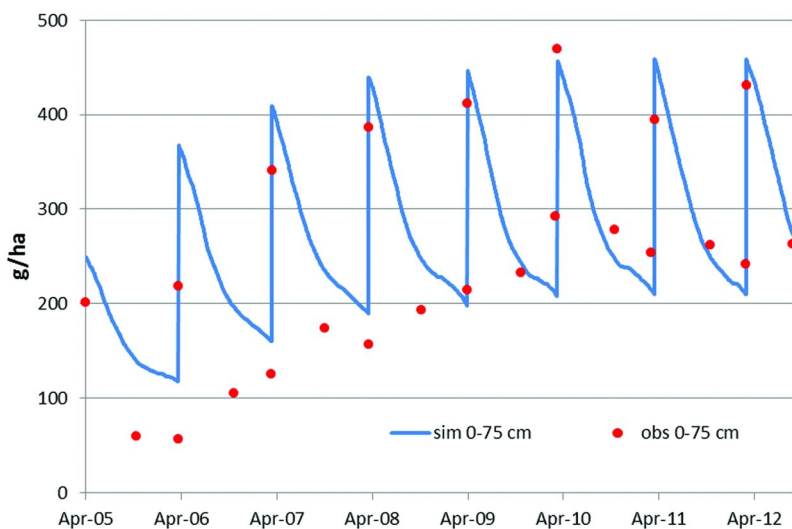


Figure 13. Simulated vs. observed total soil residue of BCS-01 in German TFA study (entire soil profile, 0-75 cm). Sorption coefficient $K_{OC,TOT}$ with non-linear Freundlich isotherm and soil half-life $DT50_{TOT}$ were optimized.

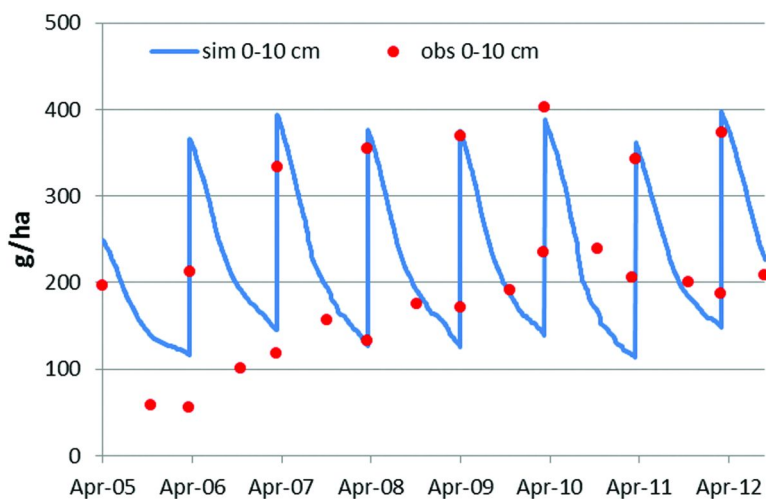


Figure 14. Simulated vs. observed total soil residue of BCS-01 in German TFA study (layer 0-10 cm). Sorption coefficient $K_{OC,TOT}$ with non-linear Freundlich isotherm and soil half-life $DT50_{TOT}$ were optimized.

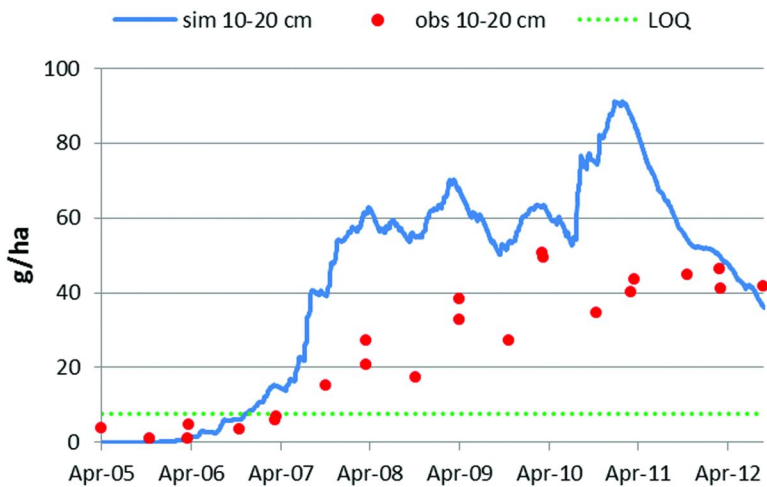


Figure 15. Simulated vs. observed total soil residue of BCS-01 in German TFA study (layer 10-20 cm). Sorption coefficient $K_{OC,TOT}$ with non-linear Freundlich isotherm and soil half-life $DT50_{TOT}$ were optimized.

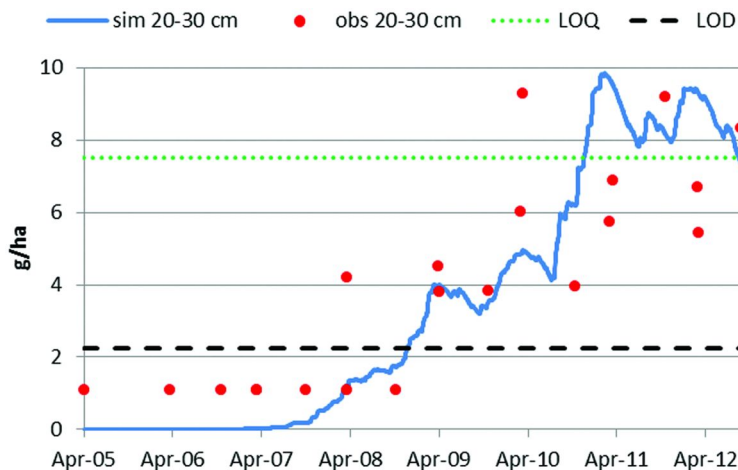


Figure 16. Simulated vs. observed total soil residue of BCS-01 in German TFA study (layer 20-30 cm). Sorption coefficient $K_{OC,TOT}$ with non-linear Freundlich isotherm and soil half-life $DT50_{TOT}$ were optimized.

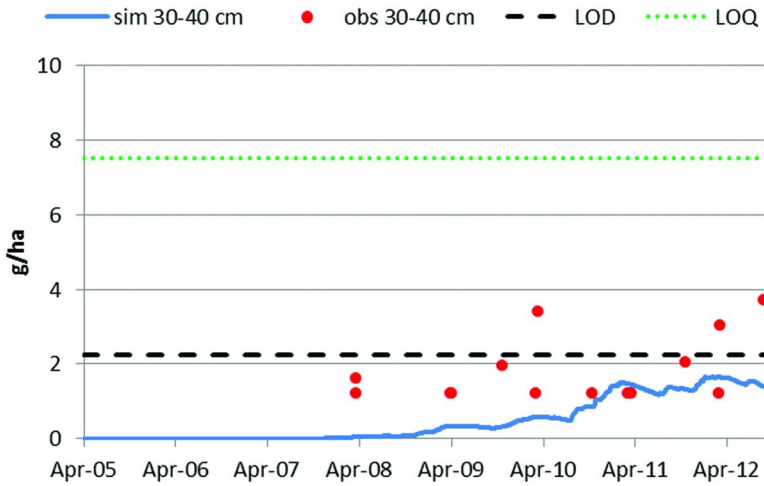


Figure 17. Simulated vs. observed total soil residue of BCS-01 in German TFA study (layer 30-40 cm). Sorption coefficient $K_{OC,TOT}$ with non-linear Freundlich isotherm and soil half-life $DT50_{TOT}$ were optimized.

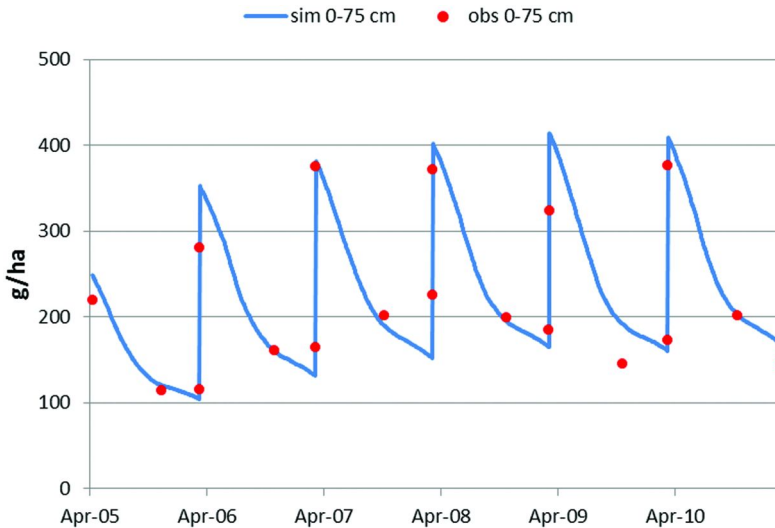


Figure 18. Simulated vs. observed total soil residue of BCS-01 in French TFA study (entire soil profile, 0-75 cm). Sorption coefficient $K_{OC,TOT}$ with non-linear Freundlich isotherm and soil half-life $DT50_{TOT}$ were optimized.

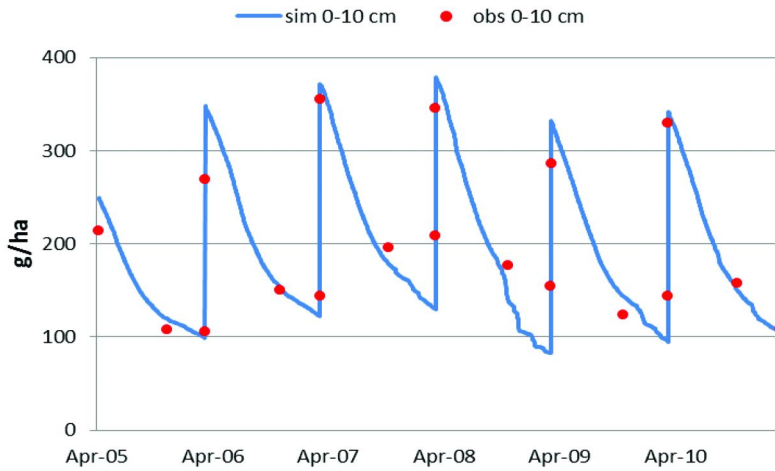


Figure 19. Simulated vs. observed total soil residue of BCS-01 in French TFA study (soil layer 0-10 cm). Sorption coefficient $K_{OC,TOT}$ with non-linear Freundlich isotherm and soil half-life $DT50_{TOT}$ were optimized.

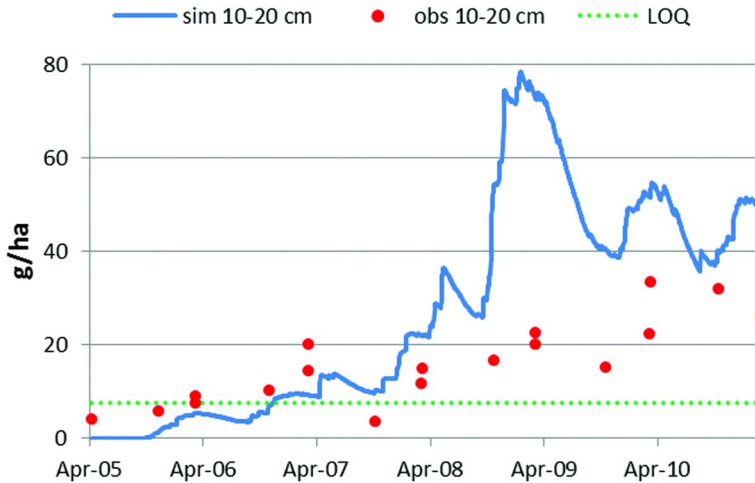


Figure 20. Simulated vs. observed total soil residue of BCS-01 in French TFA study (soil layer 10-20 cm). Sorption coefficient $K_{OC,TOT}$ with non-linear Freundlich isotherm and soil half-life $DT50_{TOT}$ were optimized.

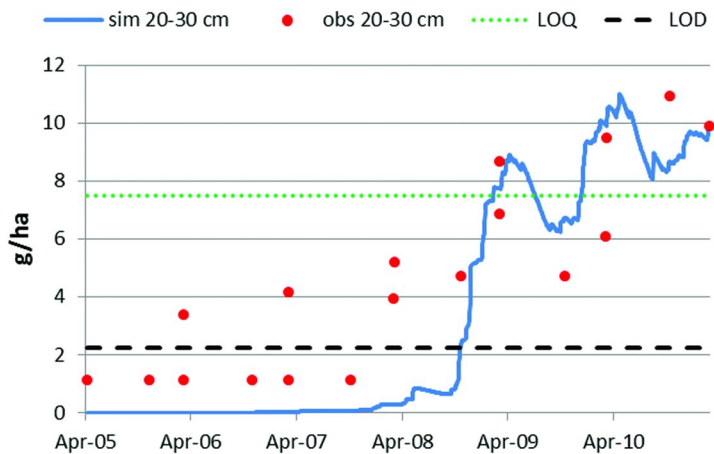


Figure 21. Simulated vs. observed total soil residue of BCS-01 in the French TFA study (soil layer 20-30 cm). Sorption coefficient $K_{OC,TOT}$ with non-linear Freundlich isotherm and soil half-life $DT50_{TOT}$ were optimized.

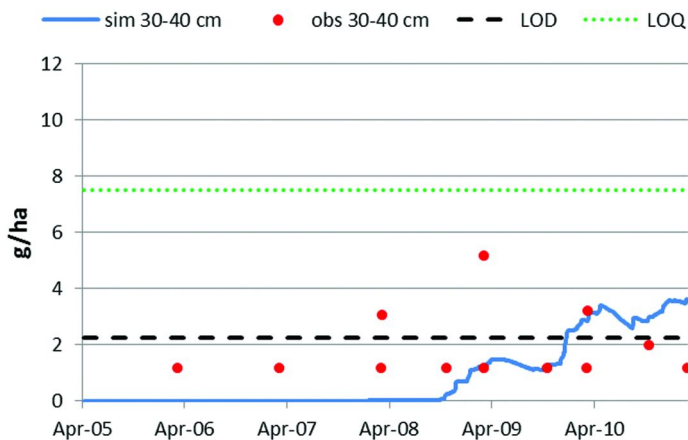


Figure 22. Simulated vs. observed total soil residue of BCS-01 in French TFA study (soil layer 30-40 cm). Sorption coefficient $K_{OC,TOT}$ with non-linear Freundlich isotherm and soil half-life $DT50_{TOT}$ were optimized.

Optimization of TDS Parameters

In a second step (Level 2), the TDS parameters f_{NE} , k_{des} , and $DT50_{EQ}$ of BCS-01 were evaluated from the German and French field accumulation trials, using PEARL and PEST software. In parallel, the Freundlich parameters $K_{OC,EQ}$ and $1/n$ were fixed to average data of the laboratory batch adsorption study (German site: average for soil AXXa, WW; French site: average all soils, Table 3). The results are compiled in Table 13. The model fits to the observed data points were very similar to those obtained when fitting the adsorption coefficient (previous paragraph) and were therefore not depicted here. This similarity suggests that both approaches are equivalent, which is discussed at the end of this chapter.

Table 13. Fitting Results of TDS Parameters of BCS-01 in German and French Terrestrial Field Accumulation (TFA) Trials, Assuming Time-Dependent Freundlich Sorption (95% Confidence Limit)

TFD Trial	Optimized			Fixed	
	f_{NE}	k_{des} (d^{-1})	$DT50_{EQ}$ (d)	$1/n$	$K_{OC,EQ}$ (L/kg)
Germany	1.6 (1.3-1.9)	0.1 (0.02-0.5)	70 (63-77)	0.807	233
France	0.47 (0.41-0.54)	0.035 (0.002-0.7)	142 (138-146)	0.827	279

A pronounced TDS effect was found at the German site as indicated by an f_{NE} of 1.6 (Table 13). This would mean that the time-dependent non-equilibrium sorption capacity is 160% of the instantaneous, equilibrium sorption capacity (eq 11) or, in other respects, 62% of the total sorption capacity is due to time-dependent non-equilibrium sorption sites (eq 19 and Table 2, relation between Freundlich coefficient for total sorption in soil $K_{F,TOT}$ and f_{NE}). The TDS at the French site was smaller but still significant with f_{NE} of 0.47. Here, the time-dependent non-equilibrium sorption capacity was 47% of the instantaneous sorption capacity or still 32% of the total sorption capacity was due to time-dependent non-equilibrium sorption sites.

The f_{NE} parameter determined in the German field is significantly greater than estimated in corresponding laboratory soils (average of soils AXXa, WW, 0.47, Table 5). This indicates a stronger TDS effect under long-term field conditions than under short-term laboratory conditions. The f_{NE} value for the French site is comparable to the laboratory derived value of 0.46 (average of all soils, Table 5).

The desorption rate constants k_{des} in the field amounted to 0.1 d^{-1} and 0.035 d^{-1} at the German and French site, respectively (Table 13), which corresponds to a half-lives for the exchange between equilibrium and non-equilibrium sorbed substance of about 7 days and 20 days. However, the large 95% confidence intervals showed that this parameter could not be determined reliably in the field experiment. In the corresponding laboratory soils it amounted to 0.025 d^{-1} and 0.023 d^{-1} , which equals a half-life of 28 d and 30 d for the exchange between equilibrium and non-equilibrium sorbed substance (Table 5, German site: average of soils AXXa, WW; French site: average of all soils).

Time-dependent sorption takes place at a certain time scale, which is characterized by desorption rate constant k_{des} . If the time scale studied is much longer, time-dependent sorption effects cannot be detected anymore. The sampling intervals were half years, which also explains k_{des} could not be determined reliably in the inverse modelling.

The fitted half-life in the equilibrium domain at the German and French sites, DT50_{EQ} , was 70 days and 142 days, respectively. Corresponding soils in the time-dependent laboratory study resulted in higher DT50_{EQ} of 227 days and 188 days (Table 5, German site: average of soils AXXa, WW; French site: average of all soils). This half-life DT50_{EQ} is valid only in combination with the TDS model.

Equivalence of a Long-Term Equilibrium Sorption Model and TDS Model

The approaches used on Level 1 (optimization of long-term equilibrium sorption coefficient $K_{\text{OC,TOT}}$ and DT50_{TOT}) and Level 2 (Optimization of TDS model parameters, f_{NE} , k_{des} , DT50_{EQ}) were found to be equivalent in describing the mobility of BCS-01 in soil. On Level 1, the fitted field- $K_{\text{OC,TOT}}$ contains contributions, both from (short-term) equilibrium and long-term non-equilibrium sorption, although all sorption sites are assumed to be equilibrium sorption sites. This might be valid, especially in case of long times (long experimental duration), for equilibration.

On Level 2 the $K_{\text{OC,EQ}}$ was fixed to the laboratory derived value accounting for equilibrium sorption only. Then, all information on non-equilibrium sorption in the field is added by fitting the TDS model parameters f_{NE} and k_{des} to experimental field data.

Both approaches are interrelated. The Freundlich sorption coefficient $K_{\text{OC,TOT}}$ obtained on Level 1 can be calculated from f_{NE} optimized on Level 2, according to the relationship given in Table 2. The additional TDS model parameter, the desorption rate constant k_{des} , could not be derived reliably and was not sensitive to describe the downward movement of BCS-01. Time-dependent sorption takes place at a certain time scale which is characterized by k_{des} and is usually, and also in this study, in the order of only a few weeks. If the time scale studied is much longer, time-dependent sorption effects cannot be detected anymore. The sampling intervals were half years. This also explains why it was not possible to identify k_{des} in the inverse modelling.

Table 14 shows that the resulting sorption parameters on Levels 1 and 2 are very similar.

Table 14. Comparison of Fitted Sorption Parameters of BCS-01 at the Field Obtained with Equilibrium Sorption (Level 1) or Time-Dependent Sorption (Level 2) (95% Confidence Limit)

<i>TFA Site</i>	<i>Level 1, long-term equilibrium sorption</i>	<i>Level 2, time dependent equilibrium and non-equilibrium sorption</i>
	$K_{OC,TOT}$	$K_{OC,EQ} \times (1+f_{NE})$
Germany	587 (536-642)	606 (536-676)
France	414 (398-430)	410 (393-430)

Table 15 shows that the back calculation of the half-life for the total soil domain on Level 2 (eq 15) gives almost the same values as obtained on Level 1.

Table 15. Comparison of Fitted Half-Lives of BCS-01 at the Field Obtained with Equilibrium Sorption (Level 1) or Time-Dependent Sorption (Level 2) (95 % Confidence Limit)

<i>TFA Site</i>	<i>Level 1, long-term equilibrium sorption</i>	<i>Level 2, time dependent equilibrium and non-equilibrium sorption</i>
	$DT50_{TOT}$	$DT50_{EQ} \times (1+f_{NE})$
Germany	184 (158-213)	182 (161-203)
France	211 (205-217)	209 (200-219)

Based on the comparison of these parameters, K_{OC} and $DT50$, (Table 14 + Table 15), it can be seen, that the model approaches seem to be equivalent to describe the mobility of BCS-01 in soil:

1. Long-term equilibrium sorption, with an effective $K_{OC,TOT}$ and $DT50_{TOT}$.
2. Time dependent sorption (TDS) model, with f_{NE} , k_{des} , $DT50_{EQ}$ and $K_{OC,EQ}$.

Conclusions

The groundwater exposure assessment for compound BCS-01 with PRZM-GW and Tier-1 assumptions has been shown to be overly conservative. The use of laboratory non-linear Freundlich sorption on Tier-2 makes the assessment more realistic (median 3-fold reduction in EDWC across all 6 EPA standard scenarios

compared to PRZM-GW and Tier-1), yet still conservative. Additional laboratory time-dependent sorption further increases the realism of the assessment while still maintaining its conservatism (median 5-fold reduction in EDWC across all 6 EPA standard scenarios compared to PRZM-GW and Tier-1).

Based on field data it was furthermore demonstrated that the use of a long-term Freundlich sorption coefficient was equivalent to using the mechanistic time-dependent sorption model to describe the mobility of BCS-01. Dynamic TDS parameters (k_{des}) are less relevant for long-term behavior. That is, a simplified model may be sufficient to describe long-term sorption behavior under field conditions. The TDS effect in the field was at least as high as in the laboratory.

References

1. Brady, D. *Approval of PRZM-GW for Use in Drinking Water Exposure Assessments*; Memorandum, Office of Chemical Safety and Pollution Prevention; U.S. Environmental Protection Agency: Washington, DC, Dec 11th, 2012.
2. Barrett, M. *Initial Tier Screening of Pesticides for Groundwater Concentration Using the SCI-GROW Model*; U.S. Environmental Protection Agency: Washington, DC, 1997.
3. Suárez, L. A. *PRZM-3, A Model for Predicting Pesticide and Nitrogen Fate in the Crop Root and Unsaturated Soil Zones: User's Manual for Release 3.12.2*; U.S. Environmental Protection Agency: Washington, DC; EPA/600/R-05/111. September 2006, revision a.
4. Carsel, R. F.; Smith, C. N.; Mulkey, L. A.; Dean, J. D.; Jowise, P. *User's manual for the pesticide root zone model (PRZM) Release 1*; U.S. Environmental Protection Agency, Athens, GA, 1984; EPA - 600 / 3-84-109.
5. Sur, R.; Menke, U.; Dalkmann, P.; Paetzold, S.; Keppler, J.; Goerlitz, G. *Proceedings of the Conference on Pesticides in Soil, Water and Air*; 12-14 September 2009, York, U.K.
6. *OECD Guideline for Testing of Chemicals No. 106*; Adsorption/Desorption (2000-01-21).
7. *EPA Pesticide Assessment Guidelines, Subdivision N, Chemistry: Environmental Fate § 163-1, Leaching and Adsorption/Desorption Studies*; (1982-10-18).
8. *Environmental Chemistry and Fate, Guidelines for registration of Pesticides in Canada*; PMRA DACO No. 8.2.4.2 (1987)
9. *Japanese MAFF New Test Guidelines for Supporting Registration of Chemical Pesticides*.
10. *OECD Guideline 307. Aerobic and Anaerobic Transformation in Soil*; April 24, 2002.
11. *Pesticide Assessment Guidelines, Subdivision N Chemistry: Environmental Fate § 162-1 Aerobic soil metabolism studies*; U.S. Environmental Protection Agency: Washington, DC, Oct. 18th, 1982.

12. Leistra, M.; Van der Linden, A. M. A.; Boesten, J. J. T. I.; Tiktak, A.; Van den Berg, F. *Alterra report 013, Alterra, Wageningen, RIVM report 711401009; Bilthoven, The Netherlands, 2001.*
13. Boesten, J. J. T. I.; ter Horst, M. M. S. *Manual of PEARLNEQ v5. Working Document 304; Alterra, Wageningen, The Netherlands, 2012.*
14. *Report of the FOCUS Ground Water Work Group, EC Document Reference Sanco/13144/2010 version 1; 13 June 2009.*
15. Beulke, S.; van Beinum, W. *Guidance on how aged sorption studies for pesticides should be conducted, analysed and used in regulatory assessments; FERA: York, U.K., 2012.*
16. Doherty, J. *PEST. Model-independent parameter estimation, 5th ed.; Watermark Numerical Computing: Brisbane, Australia, 2005.*
17. Boesten, J. J. T. I.; van der Linden, A. M. A. Symposium Proceedings No 78; British Crop Protection Council: Brighton, U.K., November 13–15, 2001; p 27–32.
18. *Report of the FOCUS Work Group on Degradation Kinetics, EC Document Reference Sanco/10058/2005 version 2.0; June 2006.*
19. Baris, R.; Barrett, M.; Bohaty, R. F. H.; Echeverria, M.; Villanueva, P.; Wolf, J.; Young, D. *Guidance for Using PRZM-GW in Drinking Water Exposure Assessments; U.S. Environmental Protection Agency: Washington, DC, Oct. 15, 2012.*
20. *Report of the FOCUS Groundwater Scenarios Workgroup, EC Document Reference Sanco/321/2000 rev.2; November 2000; 202 pp.*
21. *Non-First Order Degradation and Time-Dependent Sorption of Organic Chemicals in Soil; Chen, W., Cheplick, M., Reinken, G., Jones, R. L., Eds; ACS Symposium Series 1174; American Chemical Society: Washington, DC, 2014.*
22. Chen, W.; Wagenet, R. J. *Soil Sci. Soc. Am. J.* **1997**, *61*, 360–371.
23. *Guidance for Selecting Input Parameters for Modeling Pesticide Concentrations in Groundwater Using the Pesticide Root Zone Model; U.S. Environmental Protection Agency: Washington, DC; Health Canada, Ottawa, Version 1.0, 2012.*
24. Baris, R.; Barrett, M.; Bohaty, R. F. H.; Echeverria, M.; Kennedy, I.; Malis, G.; Wolf, J.; Young, D. *Identification and Evaluation of Existing Models for Estimating Environmental Pesticide Transport to Groundwater; Health Canada & USEPA: Ottawa and Washington, DC, Oct. 15th, 2012.*
25. *Scenarios and Metadata for Estimating Pesticide Concentrations in Groundwater Using the Pesticide Root Zone Model; retrieved December 26, 2013, from http://www.epa.gov/oppefed1/models/water/przm_gw/wqtt_przm_gw_scenarios_metadata.htm.*
26. Schaap, M. G.; Leij, F. J. *Soil Sci.* **1998**, *163*, 765–779.

Chapter 17

The Significance of Time-Dependent Sorption on Leaching Potential - A Comparison of Measured Field Results and Modeled Estimates

Timothy Negley,^{*,1} Richard Allen,² Jane Tang,³ Daniel Dyer,³
and Kacie Gehl¹

¹ARCADIS U.S., Inc., 6723 Towpath Road, Syracuse, New York 13214

²Valent U.S.A. Corporation, 6560 Trinity Court, Dublin, California 94568

³Bayer CropScience, 2 T.W. Alexander Drive,
Research Triangle Park, North Carolina 27709

*E-mail: timothy.negley@arcadis-us.com.

A growing literature base provides evidence that the assumption of linear, or “instantaneous equilibrium,” sorption is inadequate for modeling the leaching potential of crop-protection products. Clothianidin is one example of a product that possesses non-linear and time-dependent sorption characteristics. Standard batch equilibrium sorption coefficients are expected to underestimate the binding of clothianidin to soil and, therefore, do not adequately represent how clothianidin behaves in the environment. This chapter presents the results of a modeling assessment to evaluate the importance of considering non-linear and time-dependent sorption in leaching modeling for compounds with measured time-dependent sorption characteristics. The results of field measurements are compared to modeled estimates for three sorption isotherm scenarios: 1) linear adsorption, 2) non-linear Freundlich isotherm, and 3) time-dependent sorption. Results indicate that using time-dependent sorption in the environmental fate model more accurately represents field observations than the other two sorption scenarios investigated.

Introduction

One sorption characteristic that can be particularly important in assessing leaching potential of crop-protection products is time-dependent sorption (TDS), also referred to as “kinetic sorption.” TDS is an important mechanism affecting the fate and transport of crop-protection products, and a growing literature base indicates that the assumption of linear, or “instantaneous equilibrium,” sorption is inadequate to simulate the leaching potential for many compounds (1–6). Research indicates sorption kinetics for some compounds are not in equilibrium and can vary over multiple time frames. Although a number of pesticide leaching models include the ability to model sorption using non-linear and kinetic sorption approaches, current regulatory models used to assess the leaching potential of crop-protection products in North America do not presently account for TDS properties in risk assessment (7).

Simulation models used for risk-assessment purposes by both the United States (US) Environmental Protection Agency (USEPA) and Canada’s Pest Management Regulatory Agency (PMRA) assume that the partition coefficient describing soil adsorption of pesticides is both independent of concentration of the pesticide adsorbed to the soil surface and constant over time. These assumptions are conservative and considered by regulatory authorities to be appropriate for the initial tiers of risk assessment (7). However, when data are available to compare environmental fate predictions with field observations, as in the case study presented in this chapter, it is possible to evaluate if the behavior in the field can be associated with either or both of these two established pesticide sorption phenomena.

A useful case study for assessing the significance of time-dependent sorption on modeled leaching behavior is clothianidin (E)-1-(2-chloro-1,3-thiazol-5-ylmethyl)-3-methyl-2-nitroguanidine (IUPAC), an insecticide for a wide range of seed treatment, soil, and foliar uses in the US and Canada. Consistent with a tiered approach to assess the risk to groundwater resources, many field studies have been conducted and submitted to both the USEPA Environmental Fate and Effects Division (EFED) and Canada’s PMRA to examine the dissipation of clothianidin under field conditions (8). Laboratory degradation studies indicate that clothianidin degrades slowly and batch adsorption/desorption studies indicate the compound is moderately adsorbed to soil (8). Residues measured in the field from ten terrestrial field dissipation (TFD) studies indicate limited mobility of clothianidin, with most of the residues in soil observed in the top 45 centimeters (cm) of surficial soil with infrequent observations at depth (8). Specific data showing the increasing sorption of clothianidin with time have also been documented (9).

The purpose of this chapter is to present an assessment of the leaching potential of a compound with measured TDS characteristics under three sorption scenarios: 1) linear or “instantaneous equilibrium” sorption; 2) non-linear Freundlich sorption; and 3) time-dependent or “kinetic” sorption. The complete set of ten field studies for clothianidin was evaluated and is summarized in this chapter. Simulation results from field trials conducted in Ontario and

Wisconsin are discussed in depth as examples of the modeling exercise; however, results from an additional seven field sites modeled are also summarized (the tenth site was not modeled as discussed later). Examination of the modeled versus measured results from the field studies indicates that current regulatory models, which assume linear adsorption, can significantly over-predict potential leaching for compounds that demonstrate non-linear and time-dependent sorption properties. However, as discussed in this chapter, models are available that can account for the non-linear and time-dependent sorption properties of compounds, and these models can more accurately predict the potential fate of compounds that demonstrate time-dependent sorption characteristics.

Materials and Methods

Regulatory models used for this assessment were developed by the USEPA, PMRA, and the FORum for Co-ordination of pesticide fate models and their USE (FOCUS). Models were parameterized based on site-specific data obtained from nine of ten TFD studies conducted in North America. Six bare-soil treated trial sites were evaluated in the U.S. and Canada, including California, Georgia, North Dakota, Ohio, Washington, Wisconsin, Ontario, and Saskatchewan (8) to determine the residue levels of clothianidin and its degradates, and to provide estimates of the dissipation time and mobility of clothianidin under field conditions. Two turf dissipation studies were also conducted in the U.S. at test sites located in Illinois and Mississippi. Sorption inputs in the modeling were obtained from batch equilibrium, as well as time-dependent sorption studies.

Terrestrial Field Dissipation Studies

Table 1 summarizes location, soil texture, application rates and the calculated field dissipation half-life (DT_{50}) of the ten TFD studies conducted in North America. The soil types ranged from sand to clay loam. Target application rates ranged from 225 to 660 grams of active ingredient per hectare (g a.i./ha). Clothianidin was applied to established turf at two sites, at target application rates of 449 g a.i./ha. Study durations at the turf trial sites were 4 months; however, the bare-soil treated plot studies were conducted for 21 to 32 months. Due to typical variations of day zero mass values from the target values in TFD studies, the initial day zero mass (M_0) from the kinetics assessment is also reported and was used in the environmental fate modeling assessment.

Table 1. Terrestrial Field Dissipation Studies for Clothianidin Conducted in North America

<i>Location</i>	<i>Depth Obs.(cm)</i>	<i>Mass (g a.i./ha)</i>	<i>Target M₀</i>	<i>Soil 0-15 cm</i>	<i>Soil 15-100 cm</i>	<i>Duration (d)</i>	<i>DT₅₀ (d)</i>
<i>CA</i>	15 - 30	225	118	L	L / SL	982	n.a.
<i>GA</i>	0 - 15	225	139	SL	SL / SCL	730	925
<i>IL Turf</i>	15 - 30	449	593	SiL	SiL, CL	120	67.6
<i>MS Turf</i>	60 - 75	449	474	CL	L, SL, CL	120	238
<i>ND</i>	30 - 45	243	166	CL	CL, SiCL, SiC	864	838
<i>OH</i>	45 - 60	660	515	SiCL	SiCL, C, CL, SiC	735	295
<i>ONT</i>	15 - 30	660	536	SiL	L / SiL	798	349
<i>SK</i>	30 - 45	243	n.a.	CL	SiCL, C, CL, SiC	857	n.a.
<i>WA</i>	15 - 30	225	177	LS	LS / SL	623	206
<i>WI</i>	45 - 60	660	565	S	S	823	399

NOTE: *DT₅₀* values and study lengths are days, depth observed (Depth Obs.) is the maximum depth interval at which residues were observed in the field above the limit of quantitation (5 micrograms per kilogram). *DT₅₀* values for California and Saskatchewan were not available (n.a.) based on limited observed degradation. C = clay, CL = Clay Loam, L = loam, LS = loamy sand, SiC = Silty Clay, SiCL = Silty Clay Loam, SiL = Silt Loam, S = sand, SCL = Sandy Clay Loam, SL = Sandy Loam.

Field studies indicated that detectable residues of clothianidin were limited to the upper 30 centimeters (cm) of soil at four dissipation sites, with most of the mass retained in the upper 15 cm over the duration of the studies (4 to 32 months). Even under a high vulnerability situation encountered during a study conducted in Wisconsin on a sandy soil (92 to 96% sand) with high water input (260 cm of rainfall/irrigation), no crop, and minimal evapotranspiration (ET), the study showed only low concentrations of clothianidin near the limit of quantitation (LOQ) of 5 micrograms per kilogram ($\mu\text{g}/\text{kg}$) at the 45-60 cm soil depth. Turf studies showed that residues were confined to the 0-30 cm soil depth at the Illinois test site and were primarily located in the 0-45 cm soil depth at the Mississippi test site, though low level detections were observed from 45-75 cm (8).

Calculated field-dissipation half-lives ranged from 67.6 days at the Illinois site to 925 days at the Georgia trial site. At the California and Saskatchewan test sites, the DT_{50} could not be calculated under field conditions due to limited dissipation over the trial duration.

Laboratory Studies

Table 2 summarizes the laboratory-derived aerobic soil half-life values for a variety of different soil types. Soil organic carbon-water partitioning coefficients (K_{oc}), including sorption values calculated using a linear isotherm as commonly used in PMRA groundwater risk assessments, are provided. At 20 degrees Celsius, clothianidin degraded in two soils with first-order half-lives of 148 and 239 days (Höfchen and Laacher Hof soil series; USEPA/EFED calculated values). In seven soils ranging in texture from sand to silt loam, half-life values ranged from 495 to 1,155 days (BBA 2.2, Quincy, Sparta, Crosby, Gardena, Howe, and Elder soil series). In the tenth (Fuquay) soil series, degradation was too slow to accurately calculate the degradation rate over the 1-year study period. Half-life values presented are consistent with USEPA's calculations (8) based on the studies performed by Bayer CropScience.

In laboratory batch equilibrium studies, K_{oc} values ranged from 84 to 345 liters per kilogram (L/kg) (8). A key observation in these studies was the Freundlich exponent ($1/n$) values less than 1.0 (ranging from 0.809 to 0.865), indicating a non-linear sorption attribute of clothianidin. The recalculated 20th percentile K_{oc} value, typically used by PMRA for groundwater risk assessments and used in this environmental fate modeling assessment, was 98 L/kg assuming a linear isotherm.

A laboratory time-dependent sorption study for Clothianidin conducted with two soils (Laacher Hof AXXa and Laacher Hof A III) showed that sorption of clothianidin (as measured by the value of K_{oc}) increased by a factor of 2.1 to 3.5 after incubation for 99 days (9), as illustrated on Figure 1. In contrast, OECD Guideline 106, which is commonly used to determine K_{oc} , allows for only a 48-hour test period. Therefore, an assumption of linear sorption will underestimate the binding of clothianidin to soil and fail to accurately represent how clothianidin behaves in the environment.

Table 2. Laboratory Half-Life Values and Adsorption Coefficients of Clothianidin

Soil	Origin	Texture	Half-Life (d)	K_{oc} (L/kg)		1/n
				Freundlich	Linear	
Höfchen	Germany	Si	148			
Laacher Hof	Germany	SiL	239	84	78	0.815
BBA 2.2	Germany	LS	495	119	103	0.865
Quincy	Washington	LS	533	129	109	0.835
Sparta	Wisconsin	S	533			
Gardena	N. Dakota	SiL	693			
Crosby	Ohio	SiL	578	123	109	0.822
Howe	Indiana	SL	990			
Elder	California	L	1,155	345	345	0.809
Fuquay	Georgia	LS	Stable			

NOTE: Half-life values reported in days derived by USEPA (8). Laboratory calculated K_{oc} values in liters per kilogram (L/kg) were calculated based on Freundlich sorption isotherm. Freundlich exponent expressed as 1/n. L = loam, LS = loamy sand, S = sand, Si = silt, SiL = silt loam, SL = Sandy Loam.

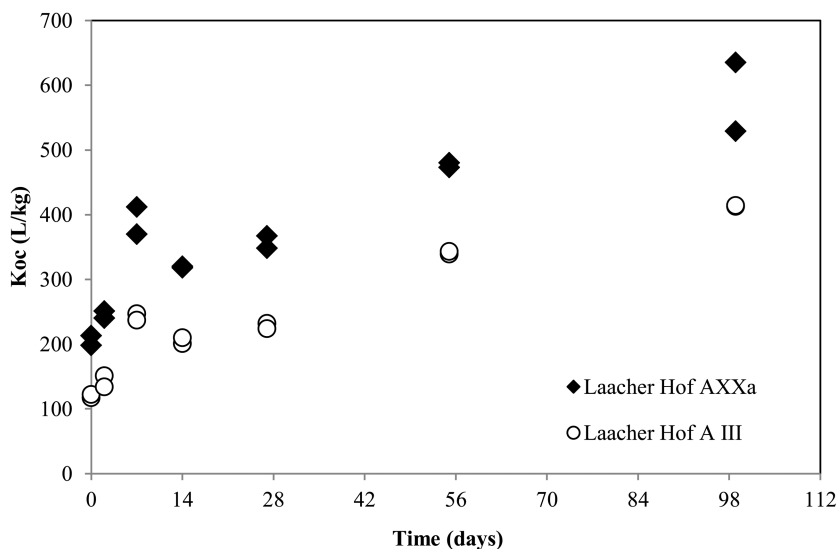


Figure 1. Results of time-dependent sorption study of clothianidin on two different soils.

Table 3. Summary of Soil Characteristics used for Modeling

<i>Location</i>	<i>Maximum Water Content</i>			<i>Wilting Point</i>			<i>Percent Organic Carbon</i>			<i>Bulk Density</i>		
	<i>A</i>	<i>B</i>	<i>C</i>	<i>A</i>	<i>B</i>	<i>C</i>	<i>A</i>	<i>B</i>	<i>C</i>	<i>A</i>	<i>B</i>	<i>C</i>
California	0.27	0.24	0.21	0.13	0.11	0.10	1.38	1.03	0.55	1.36	1.33	1.33
Georgia	0.17	0.22	0.26	0.07	0.13	0.17	0.32	0.16	0.08	1.78	1.60	1.61
Illinois	0.34	0.34	0.34	0.15	0.19	0.21	2.55	1.33	0.41	1.09	1.12	1.15
Mississippi	0.35	0.30	0.24	0.21	0.17	0.11	0.93	0.61	0.29	1.12	1.13	1.14
North Dakota	0.37	0.38	0.40	0.23	0.23	0.25	3.44	1.06	0.33	1.06	1.15	1.15
Ohio	0.38	0.40	0.34	0.21	0.26	0.21	1.53	0.58	0.33	1.67	1.55	1.44
Ontario	0.33	0.29	0.38	0.14	0.13	0.14	1.83	0.50	0.08	1.36	1.47	1.51
Saskatchewan	0.36	0.40	0.37	0.22	0.26	0.21	2.15	0.54	0.39	1.29	1.25	1.23
Washington	0.09	0.10	0.15	0.04	0.04	0.06	0.35	0.13	0.09	1.60	1.61	1.69
Wisconsin	0.08	0.06	0.06	0.04	0.03	0.02	0.79	0.16	0.03	1.49	1.55	1.59

NOTE: Maximum water contents and wilting points are $\text{cm}^3\text{cm}^{-3}$, bulk densities are g/mL . Values are averaged across key depth intervals for simplicity (A = 0 to 15 cm, B = 15 to 100 cm, C = greater than 100 cm).

Modeling Approach

Two fate and transport models were used for modeling the potential movement of clothianidin in soil. The first model, Pesticide Root Zone Model for Groundwater (PRZM-GW), was developed by the USEPA and PMRA (10) under the North American Free Trade Agreement (NAFTA) to estimate potential pesticide concentrations in groundwater. FOCUS PRZM (11), a similar model developed by FOCUS, was used in this assessment, as it has the capability to simulate non-linear Freundlich sorption and kinetic sorption (12), while PRZM-GW can only simulate linear sorption. Both models are essentially the same conceptually and rely on the Pesticide Root Zone Model as the primary engine (13), and only differ in the representation of the different sorption mechanisms assumed. PRZM-GW and FOCUS PRZM predictions were evaluated side-by-side to confirm that both models produced the same results when parameterized by identical linear sorption algorithms. Once it was confirmed that FOCUS PRZM reproduces PRZM-GW results under the assumption of linear sorption, all subsequent model simulations were completed using FOCUS PRZM.

Site-specific meteorological input files were created for each TFD trial site for the duration of the TFD study as described below. Total daily water inputs from each TFD were set to daily rainfall plus daily irrigation. In addition, the runoff curve number was set to a low value to eliminate potential surface runoff as per the NAFTA approach for leaching assessments (7). Daily evapotranspiration provided in the TFD studies was incorporated directly into the meteorological file. As discussed earlier, application rates used in the model were based on the initial mass value (M_0) estimated from the TFD kinetics assessments as summarized in Table 1.

Table 3 summarizes key soils inputs obtained from the TFD studies. Maximum water content and wilting point were based on the moisture holding capacity at 1/10 bar calculated using the Soil Water Characteristic Estimates by Texture and Organic tool (14). Organic matter and bulk density were obtained from TFD soil characterization results. As eight of the ten TFD sites were bare soil, crop parameters were not used in the model. For the Illinois and Mississippi turf scenarios, basic turf crop parameters were based on USEPA Florida turf scenario (15).

Table 3 illustrates the overall vulnerability of the trial locations based on soil properties. For example, the California, Georgia, Washington, and Wisconsin soils were overall the most vulnerable based on a combination of low organic carbon content and coarse texture (reflected by lower maximum water content).

Sorption Parameterization

All model inputs were held constant at each TFD trial site, except for the sorption input parameters for each of the three sorption scenarios. Sorption scenarios included a linear isotherm, a non-linear Freundlich isotherm, and both

non-linear and time-dependent sorption. Linear sorption modeling was based on the 20th percentile K_{oc} and maximum K_{oc} values (98 and 345 L/kg, respectively) calculated based on a linear isotherm.

Non-linear sorption parameters were calculated based on laboratory batch equilibrium studies assuming a Freundlich isotherm. Non-linear Freundlich K_{oc} values ranged from 84 to 129 L/kg for four test soils, and 345 L/kg for a fifth soil with Freundlich exponent ($1/n$) values ranging from 0.809 to 0.865 for both the adsorption and desorption phases. The minimum K_{oc} (84 L/kg), arithmetic mean (160 L/kg), and maximum K_{oc} (345 L/kg) values from the batch adsorption/desorption studies (8) were selected to evaluate predicted soil residues within the bounds of the measured laboratory data. In addition, a conservative upper-bound Freundlich exponent (0.86) was selected from the laboratory studies.

TDS was modeled in FOCUS PRZM version 3.5.2 (11). FOCUS PRZM implements the well-established Streck model for TDS (11, 12, 16, 17). The model requires the user to input the f_{ne} , which is the ratio of the Freundlich coefficients for the non-equilibrium sorption phase ($K_{f,neq}$) and the equilibrium sorption phase ($K_{f,eq}$). The user must also enter the first-order desorption rate in the non-equilibrium domain (K_{des}). Finally, because the model assumes that a compound residing in the non-equilibrium domain is not subject to transformation (i.e., is generally not available for microbial degradation), the user must also specify an appropriate DT_{50} (Kt) for the equilibrium phase (aqueous phase only). All values used for modeling are listed in Table 4.

Table 4. Sorption Parameters used for Modeling

<i>Sorption Scenario</i>	<i>Lower Bound K_{oc}</i>	<i>Central Tendency K_{oc}</i>	<i>Upper Bound K_{oc}</i>	<i>Freundlich Exponent</i>	<i>f_{ne}</i>	<i>K_{des}</i>
LS	98	n.a.	345	1.0	n.a.	n.a.
NLS	84	160	345	0.86	n.a.	n.a.
NLS/TDS	84	160	345	0.86	0.6	0.0313

NOTE: Linear sorption (LS) coefficients are based on a linear isotherm with a 20th percentile K_{oc} value equal to 98 L/kg. Non-linear sorption (NLS) and time-dependent sorption (TDS) parameters are based on laboratory-calculated values in Table 2 and a conservative upper-bound Freundlich exponent.

ACSL Optimize version 1.2 was used to optimize the f_{ne} and K_{des} values for the two available soils (Laacher Hof AXXa and Laacher Hof A III) that were evaluated in the laboratory TDS study (9, 18). ACSL Optimize uses the maximum likelihood, that describes the probability to obtain a given set of data assuming that model and model parameter are correct, for the objective function. Goodness of fit was assessed by visual observation, the Chi-square (χ^2) percent error test, and the coefficient of determination (r^2).

The f_{ne} values ranged from 0.541 to 0.660 with an arithmetic mean of 0.60 that was used in this modeling study (9, 18). The K_{des} values were also optimized in ACSL for the same two soils and ranged from 0.0241 to 0.0385 with an arithmetic mean of 0.0313 that was used in this modeling study (9, 18).

Degradation Parameterization

Table 5 lists the degradation parameters used for site-specific modeling at each TFD trial site. For linear and non-linear sorption modeling, the DT_{50} calculated from each of the TFD studies was used for modeling dissipation from 0 to 1 meter below ground surface. Beyond 1 meter, degradation was assumed negligible, consistent with NAFTA modeling approaches for compounds stable to hydrolysis (7).

As noted earlier, PRZM assumes degradation is restricted to the equilibrium sorption phase (aqueous) and that degradation does not occur in the non-equilibrium (solid) phase due to the compound being unavailable for microbial degradation. Because degradation is always more rapid in the equilibrium phase than the degradation DT_{50} in bulk soil (12), the user must also specify an appropriate DT_{50} for the equilibrium condition (aqueous phase only). When modeling TDS in FOCUS PRZM using DT_{50} values based on bulk soil studies, the residue decline data must be reevaluated and a DT_{50eq} recalculated. The recalculation procedure depends on the type of studies (laboratory or field degradation studies) and the nature of the substance (parent or metabolite). An approximation (11, 12, 19) has been developed that scales the DT_{50} for the total system (DT_{50tot}) to estimate the DT_{50} in the equilibrium phase (DT_{50eq}):

$$DT_{50eq} = \frac{DT_{50tot}}{1 + f_{ne}}$$

where,

f_{ne} = ratio of non-equilibrium Freundlich coefficient and equilibrium coefficient

DT_{50eq} = DT_{50} for the equilibrium condition (aqueous phase only)

Table 5. Degradation Parameters used for Modeling

<i>Sorption Scenario</i>	<i>GA</i>	<i>IL</i>	<i>MS</i>	<i>ND</i>	<i>OH</i>	<i>WA</i>	<i>WI</i>	<i>ON</i>
LS / NLS ^a	925	67.6	238	838	295	206	399	349
TDS ^b	578	42	149	524	184	129	249	218

^a NOTE: Dissipation half-lives in days for each field trial site used in the modeling of linear and non-linear sorption. ^b For TDS modeling, DT_{50} values are for the equilibrium condition (aqueous phase only). California was assumed stable based on limited dissipation observed in the TFD. Saskatchewan was not modeled based on limited movement and dissipation.

Goodness of Fit

Modeled results were assessed for goodness-of-fit to observed results using the Chi-square (χ^2) percent error test and the coefficient of determination (r^2). The χ^2 test considers the sum of the residuals and the measurement errors as

$$\chi^2 = \sum \frac{(C - O)^2}{\left(\frac{err}{100} \times \bar{O}\right)^2}$$

where,

C = calculated value

O = observed value

\bar{O} = mean of all observed values

err = measurement error percentage

The r^2 value indicates how well the observed data are replicated by the model.

The r^2 value is calculated as follows:

$$r^2 = \frac{[\sum_{i=1}^n (pred_i - \overline{pred})(obs_i - \overline{obs})]^2}{\sum_{i=1}^n (pred_i - \overline{pred})^2 \sum_{i=1}^n (obs_i - \overline{obs})^2}$$

where,

$pred_i$ = predicted mass at time i

\overline{pred} = mean of all predicted values

obs_i = observed mass at time i

\overline{obs} = mean of all observed values

n = number of observations

Generally, the best model to represent the observed data is one that visually agrees well with observed data, has the lowest χ^2 percent error, and has the highest r^2 value. These methods of assessing goodness of fit are commonly employed by pesticide regulatory authorities in Europe (20) and North America (21).

Results and Discussions

Site-specific modeling was performed for nine of the ten dissipation studies (Saskatchewan was not modeled due to limited movement and dissipation). The Ontario and Wisconsin test sites are discussed in detail to illustrate the importance of TDS for predicting the behavior of clothianidin in the environment. The Ontario and Wisconsin test sites represent a range of soil textures, with relatively long DT_{50} values, and sufficient residue mobility to test the influence of TDS on fate and transport of clothianidin in the environment. In fact, the Wisconsin trial site demonstrated the highest clothianidin mobility among all the bare-soil test sites. Results are also summarized for the remaining seven sites modeled, which show similar trends.

Ontario Trial Site

One key observation at the Ontario site is that residues observed in the field were confined to 0-30 cm soil interval. However, leaching below 30 cm was significantly over-predicted by the model when assuming linear sorption (LS) and a conservative K_{oc} value as shown in Figure 2. The over-prediction of leaching at 15-30 cm is evident by the much higher residue predicted than observed after approximately 100 days. In addition, by the end of the 798-day study, the model estimated zero residues in the surface layer (i.e., residues had leached), whereas nearly 100 grams per hectare (g/ha) still remained in the surface layer in the field study.

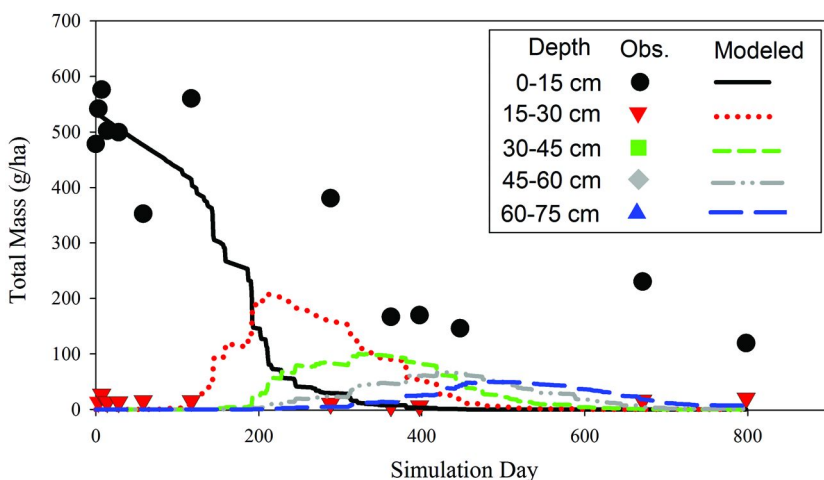


Figure 2. Modeled versus observed residues for the Ontario trial site based on linear sorption and K_{oc} of 98 L/kg.

In contrast, the best fit to the Ontario field data was achieved using non-linear and time-dependent sorption with the mean K_{oc} value of 160 L/kg. Figure 3 illustrates good visual agreement between modeled and measured residues in the 0-15 cm soil depth, with some over-prediction of the low-level residues observed in the 15-30 cm interval by the end of the study.

Table 6 summarizes the model results for all eight sorption scenarios considered at the Ontario trial site for the duration of the study, ranging from linear sorption and a lower-bound K_{oc} value to non-linear and TDS with increasing K_{oc} values. The table provides a mass balance of the mass (M) applied in the model. The percent of the applied mass used on day zero of the model was divided into the percent predicted to decay over the entire soil profile, the percent retained in the interval where residues were observed in the TFD study (e.g., 0-30 cm in Ontario) and, the percent that was estimated to leach below the maximum depth of observed residues in the TFD (e.g., >30 cm).

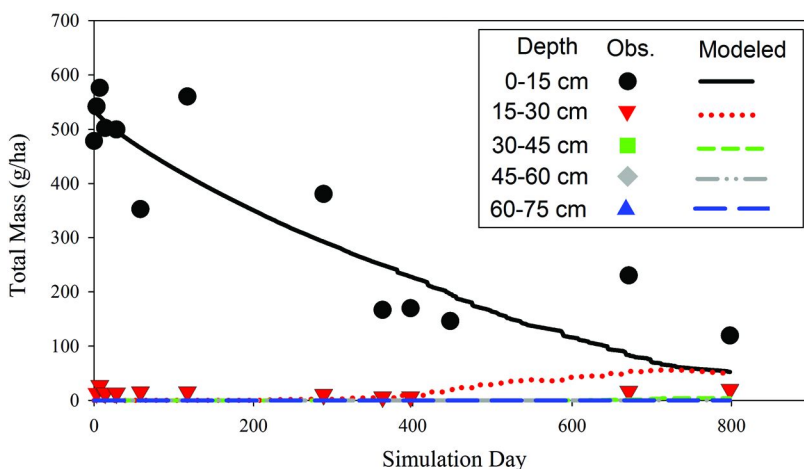


Figure 3. Modeled versus observed residues for the Ontario trial site based on non-linear sorption and time-dependent sorption with a K_{oc} of 160 L/kg.

Table 6. Summary of Fate and Transport Results for Clothianidin Sorption Scenarios in Ontario for the Depth of Maximum Observed Residue (0-30 cm) (Presented as Percent of Day Zero Mass)

Scenario:	TFD	LS		NLS			TDS	
		98	345	84	160	345	84	160
M, Applied	100	100	100	100	100	100	100	100
M, Decayed	74.0	68.7	79.6	73.6	79.6	79.9	80.9	80.1
M, Retained ^a	26.0	0	16.2	0.2	6.9	20.5	5.6	19.2
M, Leached ^b	0	31.3	4.2	26.1	13.5	0	13.4	0.8
χ^2	n.a.	27.0	17.7	24.4	19.9	17.2	20.2	17.4
r^2	n.a.	0.840	0.777	0.833	0.743	0.785	0.765	0.784

^a NOTE: Mass (M) retained is the percent of the applied mass retained in the depth interval observed in the field (0-30 cm). ^b Mass leached is the percent of the applied mass predicted to leach below the maximum observed residue depth (30 cm) in the TFD study. No runoff occurred based on the conservative curve number used in NAFTA groundwater scenarios to promote infiltration and prevent runoff. TFD = Terrestrial field dissipation study, LS = linear sorption, NLS = non-linear sorption, TDS = non-linear and time-dependent sorption.

In general, Table 6 illustrates less ability of linear sorption to accurately predict clothianidin mobility using conservative K_{oc} values. For the linear sorption scenario and K_{oc} of 98 L/kg, 31.3% of the applied mass leached below 30 cm; however, no mass was observed in the field below the 30-cm depth. Conversely, for the same scenario, the model estimated no mass remaining in the 0-30 cm

interval at the end of the 798-day study; however, 26% of the original mass was observed in the field at the end of the study. These results show the inability of equilibrium sorption to capture field observations when all other parameters are held fixed. The relatively lower χ^2 percent error for the 0-30 cm TDS modeling results further illustrates the better fit to the observed data than when simulating linear sorption only. Based on the χ^2 test and comparison of the amount leached to the actual observed leaching, linear sorption is only a reasonable fit when using the maximum K_{oc} value obtained from the batch equilibrium studies.

Non-linear and time-dependent sorption using the mean K_{oc} of 160 L/kg, as well as non-linear sorption with the upper-bound K_{oc} value of 345 L/kg, predicted less than 1% clothianidin leached below 30 cm, which is consistent with field observations. The mass remaining in the 0-30 cm profile also matched the observed data well. Specifically, 20% of the applied mass was estimated to remain in the 0-30 cm profile, which is consistent with the 26% that remained in the same interval in the field.

Wisconsin Trial Site

Linear sorption resulted in a poor model fit to the observed data based on visual inspection of predicted versus observed residues (Figure 4). Residues measured at the Wisconsin site were detected only in the 0-60 cm soil interval; however, modeled residues clearly over-predicted potential leaching observed in the field early in the study. For example, when assuming linear sorption and a K_{oc} of 98 L/kg, by 180 days, the model estimated that almost all of the clothianidin had leached from the entire depth profile, in contrast to the field study where residues remained in the upper 60 cm of soil for the entire study duration (823 days).

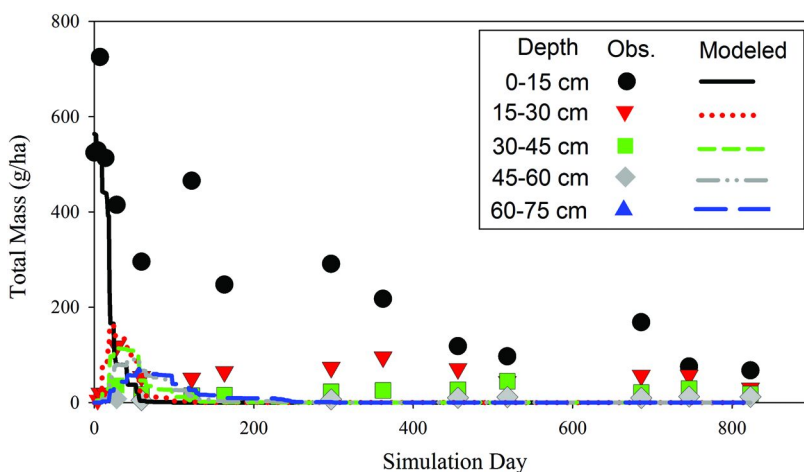


Figure 4. Modeled versus observed residues in the soil profile for the Wisconsin trial site based on linear sorption and a K_{oc} of 98 L/kg.

In contrast, the best fit to the data from the Wisconsin site was achieved using non-linear and time-dependent sorption. Figure 5 illustrates that good visual agreement was achieved between measured and modeled results for all of the intervals using the upper-bound K_{oc} value of 345 L/kg.

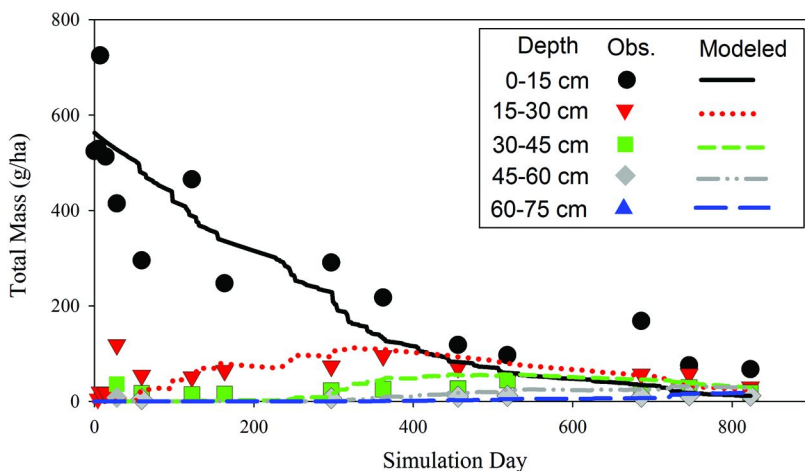


Figure 5. Modeled versus observed residues in the soil profile for the Wisconsin trial site based on non-linear sorption and time-dependent sorption with a K_{oc} of 345 L/kg.

Table 7 summarizes the model results for all eight sorption mechanisms examined for the Wisconsin site for the duration of the study. In general, the table shows the improvement in observed versus modeled results across the full range of K_{oc} values and sorption mechanisms.

Table 7 highlights the inability of linear sorption and conservative K_{oc} values to accurately predict the leaching potential compared to measured results in the field (TFD). For example, in the field, 77.5% of the day zero mass decayed by the end of the TFD with 22.5% remaining in the 0-60 cm soil interval. In contrast, modeling based on linear sorption (LS) and the 20th percentile K_{oc} (98 L/kg) predicted that 86.9% of the initial mass leached to a depth below 60 cm, even though no residues were observed below 60 cm in the TFD. In addition, the amount of clothianidin that degraded in the full soil profile varied significantly across the model approaches. The limited decay for the linear sorption scenarios is due to rapid leaching past 100 cm, where the model artificially assumed zero degradation (7). As the residence time in the biotic zone increased across the sorption scenarios, the overall clothianidin decayed mass also increased, eventually to 76% when considering non-linear and time-dependent sorption, which is consistent with the 77.5% observed in the TFD.

Table 7. Summary of Fate and Transport Results for Clothianidin Sorption Scenarios in Wisconsin for the Depth of Maximum Observed Residue (0-60 cm) (Presented as Percent of Day Zero Mass)

Scenario: <i>K_{oc}</i> :	TFD	<u>LS</u>		<u>NLS</u>			<u>TDS</u>		
		98	345	84	160	345	84	160	345
M, Applied	100	100	100	100	100	100	100	100	100
M, Decayed	77.5	13.1	50.7	16.4	36.1	68.0	32.1	56.4	76.0
M, Retained ^a	22.5	0	0	0	0	2.1	0.1	1.5	16.5
M, Leached ^b	0	86.9	49.3	83.6	63.9	29.9	67.7	42.1	7.5
χ^2	n.a.	53.1	31.6	51.1	42.9	22.86	41.2	28.4	16.5
<i>R</i> ²	n.a.	0.639	0.781	0.660	0.716	0.802	0.758	0.793	0.808

^a NOTE: Mass (M) retained is the percent of the applied mass retained in the depth interval observed in the field (0-60 cm). ^b Mass leached is the percent of the applied mass predicted to leach below the maximum observed residue depth (60 cm) in the TFD study. TFD = Terrestrial field dissipation study, LS = linear sorption, NLS = non-linear sorption, TDS = non-linear and time-dependent sorption.

The lower χ^2 percent error and higher r^2 value for the TDS modeling further illustrates the better fit to the observed data than when simulating linear sorption only. For example, the χ^2 percent error of 31.6% assuming linear sorption and the maximum K_{oc} value decreased by nearly a factor of two when accounting for TDS. For TDS modeling using the upper-bound K_{oc} the good visual fit, low χ^2 percent error, and high r^2 value confirm the importance of including the TDS characteristics of clothianidin, particularly on the most vulnerable soils.

All Sites

Table 8 illustrates the best fit models for the nine modeled trial sites for the range of K_{oc} values measured and the three sorption mechanisms, including linear sorption, non-linear sorption, as well as non-linear and time-dependent sorption. The table shows the percent of the applied mass predicted that leached below the maximum observed residue depth from each TFD trial site. Zeroes in the table indicate good agreement between the predicted and the observed maximum depth of residue reached in soil profile. In contrast, high values indicate the model over-predicted a significant amount of the applied mass leached below the maximum depth of observed residues in the field (see Table 1 for depth of maximum leaching). For example, the 91% in Georgia (linear sorption and K_{oc} of 98 L/kg) indicates the model predicted 91% of the applied mass to leach below 15 cm; however, no residues were observed below 15 cm in the field.

Table 8. Summary of Modeled Leaching Potential below Maximum Observed Depth for Clothianidin Sorption Scenarios (Expressed as Percent of Applied)

<i>Scenario: Koc:</i>	<i>LS</i>		<i>NLS</i>			<i>TDS</i>			<i>Soil Texture</i>	<i>Excess Water</i>
	<i>98</i>	<i>345</i>	<i>84</i>	<i>160</i>	<i>345</i>	<i>84</i>	<i>160</i>	<i>345</i>		
<i>Illinois</i>	<u>0.1</u>	0	0	0	0	0	0	n.a.	M	H
<i>Mississippi</i>	<u>0.1</u>	0	0	0	0	0	0	n.a.	F/M	H
<i>N. Dakota</i>	26.6	0	<u>2.3</u>	0	0	0	0	n.a.	F/M	M
<i>Ohio</i>	<u>14.9</u>	0	<u>7.5</u>	0	0	<u>0.2</u>	0	n.a.	F/M	M
<i>Ontario</i>	31.3	<u>4.2</u>	26.1	<u>13.5</u>	0	<u>13.4</u>	<u>0.8</u>	n.a.	M	M
<i>California</i>	100	96.3	99.9	96.6	<u>8.7</u>	95.9	52.5	0	C	H
<i>Wisconsin</i>	86.9	49.3	83.6	63.9	29.9	67.8	42.1	<u>7.5</u>	C	H
<i>Washington</i>	82.4	42.5	78.0	56.0	26.0	57.5	33.7	<u>13</u>	C	H
<i>Georgia</i>	91.0	57.3	88.7	81.6	65.7	80.9	69.8	<u>57.3</u>	C	H

NOTE: Percent leached is the percent of the applied mass that leached below the maximum observed residue depth in the field study (Table 1) for linear sorption (LS), non-linear sorption (NLS), and non-linear and time-dependent sorption (TDS). **Scenarios with less than 15% predicted to leach below the maximum observed depth (underlined) are in reasonable agreement with predicted and observed maximum leaching depth.** Soil texture abbreviations: M= medium, F/M = fine to medium, C = coarse. Excess moisture inputs indicated as medium (M) to high (H) based on less than or greater than 2 millimeters per day of excess moisture input on average, respectively.

In general, the linear sorption scenario as used in PRZM-GW performs reasonably well for certain scenarios (e.g., fine to medium soil texture and higher organic carbon content), but over-predicts leaching at the high vulnerability sites (less than 1% organic carbon, coarse-textured soils, and high excess moisture input). For example, for the turf trial sites in Illinois and Mississippi, reasonable agreement was achieved for all sorption scenarios and the full range of K_{oc} values under the linear sorption scenario. Observed residues in Ohio and North Dakota bare-soil treated plots were also comparable to modeled estimates under the non-linear Freundlich sorption scenarios, even with a conservative K_{oc} value of 84 at the Ontario site.

For the most vulnerable sites—including Wisconsin, Washington, and Georgia where organic carbon was less than 1%, soils were coarse-textured, and excess moisture input was relatively high—the model over-predicts leaching potential compared to observed when equilibrium sorption is assumed, but more closely approximates field observations when NLS and TDS are assumed. The Georgia site illustrates lower sensitivity to TDS at sites with negligible organic carbon and coarse soil texture. For example, organic carbon in Georgia was generally 0.3% or less; therefore, inclusion of non-linear and TDS sorption characteristics had less influence due to the comparatively lower organic carbon content than the remaining sites. The poor comparison of modeled and measured values at this site indicates that other factors may have retarded the leaching of clothianidin.

Conclusions

Results of laboratory environmental fate studies revealed that clothianidin possesses time-dependent and non-linear sorption characteristics. The higher binding of clothianidin to soil than predicted by assuming equilibrium conditions over a relatively short time period lowers the potential mass available for leaching. The standard batch equilibrium sorption coefficients underestimate the binding of clothianidin to soil and, therefore, do not accurately represent how clothianidin behaves in the environment. The time-dependent sorption mechanism is critical to a complete understanding and evaluation of the potential leaching of clothianidin. Model simulations of nine studies indicate that models that do not account for non-linear sorption will tend to over-predict the mobility of clothianidin in the field. This is especially true when a lower-bound K_{oc} value is selected for linear sorption modeling and for coarse-textured soils. For coarse-textured soils with low organic matter, use of kinetic sorption and use of the upper-bound K_{oc} , achieved good model agreement with field observations of clothianidin residues. When kinetic sorption was accounted for in the FORum for Co-ordination of pesticide fate models and their USE (FOCUS) Pesticide Root Zone Model, estimated residues were in good agreement with observed residues. This underscores the importance of considering non-linear and time-dependent sorption characteristics in assessing leaching potential when sufficient data are

available to characterize these phenomena, and that using linear sorption may significantly over-predict the potential for leaching for a variety of different scenarios. Measurement of sorption parameters in a specific soil is required to better predict mobility behavior, especially in vulnerable soils under high water-input conditions.

Acknowledgments

Assistance from colleagues S. Sweeney and A. Newcombe of ARCADIS U.S., Inc. is much appreciated.

References

1. Boesten, J. J. T. I.; van der Pas, L. J. T.; Smelt, J. H. *Pestic. Sci.* **1989**, *25*, 187–203.
2. Guo, L.; Wagenet, R. J.; Jury, W. A. *Soil Sci. Soc. Am. J.* **1999**, *63*, 1637–1644.
3. Green, R. E.; Karickhoff, S. W. Sorption Estimates for Modeling. In *Pesticides in the Soil Environment: Processes, Impacts and Modeling*; Cheng, H. H., Ed.; Book Series 2; Soil Science Society of America: Madison, WI, 1990.
4. Ma, Q. L.; Selim, H. M. *Soil Sci. Soc. Am. J.* **2005**, *69*, 318–327.
5. Ma, Q. L.; Rahman, A.; Holland, P. T.; James, T. K.; McNaughton, D. E. *J. Environ. Qual.* **2004**, *33*, 930–938.
6. Ma, Q. L.; Rahman, A.; James, T. K.; Holland, P. T.; McNaughton, D. E.; Roja, K. W.; Ahuja, L. R. *J. Environ. Qual.* **2004**, *68*, 1491–1500.
7. U.S. Environmental Protection Agency. *Model and Scenario Development Guidance for Estimating Pesticide Concentrations in Groundwater Using the Pesticide Root Zone Model*; Washington, DC, 2012.
8. U.S. Environmental Protection Agency. *Clothianidin Registration of Prosper T400 Seed Treatment on Mustard Seed (Oilseed and Condiment) and Poncho/Votivo Seed Treatment on Cotton*; November 2, 2010; Docket EPA-HQ-OPP-2011-0865.
9. Stupp, H. P. *Time Dependent Sorption of TI-435 in two Different Soils*; Bayer AG Report 110121; Monheim, Germany, 2001.
10. U.S. Environmental Protection Agency. *The Pesticide Root Zone Model for GroundWater (PRZM-GW)*; Washington, DC, 2013.
11. Forum for Co-ordination of Pesticide Fate Models and their Use. *Assessing Potential for Movement of Active Substances and their Metabolites to Ground Water in the EU*; Sanco/13144/2010, European Union, 2009.
12. Cheplick, M.; Chen, W.; Jones, R.; Reinken. G. *Implementation of Kinetic Sorption into PRZM*; http://focus.jrc.ec.europa.eu/gw/par/FOCUS_PRZM_parameter2.0.pdf (accessed June 10, 2012).
13. Carousel, R. F.; Imhoff, J. C.; Hummel, P. R.; Cheplick, J. M.; Donigian, A. S., Jr.; Suárez. L. A. *PRZM-3, A Model for Predicting Pesticide and Nitrogen*

Fate in the Crop Root and Unsaturated Soil Zones: Users Manual for Release 3.12.2; EPA/600/R-05/111; Washington, DC, 2005.

14. Saxton, E. K.; Rawls, W. *Soil Water Characteristic Estimates by Texture and Organic Matter for Hydrologic Solutions*; <http://hydrolab.arsusda.gov/soilwater/Index.htm> (accessed June 10, 2012).
15. U.S. Environmental Protection Agency. *Metadata for the PE5 Standard Surface Water Modeling Scenario for Florida Turf*; <http://www.epa.gov/oppefed1/models/water/> (accessed Jun 10, 2012).
16. Streck, T.; Poletika, N. N.; Jury, W. A.; Farmer, W. J. *Water Resour. Res.* **1995**, *31*, 811–822.
17. van Genuchten, M. Th.; Wagenet, R. J. Two-site/two-region Models for Pesticide Transport and Degradation: Theoretical Development and Analytical Solution. *Soil Sci. Soc. Am. J.* **1989**, *53*, 1303–1310.
18. Hammel, K. *Evaluation of the Time-dependent Sorption of Clothianidin Based on Batch Equilibrium Experiments in Two Soils*. Bayer AG Report MEF-04/281; MRID Number 46913101; Monheim, Germany, 2004.
19. Boesten, J. J. T. I.; van der Linden, A. M. A. In *Long-term Sorption Kinetics on Leaching as Calculated with the PEARL Model for FOCUS scenarios*; Walker, A., Ed.; Proceedings Number 78 of Pesticide Behaviour in Soils and Water, Brighton, United Kingdom, November 13–15, 2001.
20. Forum for Co-ordination of Pesticide Fate Models and their Use. 2006. *Guidance document on estimating persistence and degradation kinetics from environmental fate studies on pesticides in EU registration*; Sanco/10058/2005 version 2.0, European Union, 2006.
21. U.S. Environmental Protection Agency. *Standard Operating Procedure for Using the NAFTA Guidance to Calculate Representative Half-life Values and Characterizing Pesticide Degradation*; Washington, DC, 2012.

Chapter 18

Evaluation of the FOCUS-PRZM Model for Predicting Acetochlor Leaching and Persistence in Soil

Qingli Ma,^{*,1} A. Rahman,² P. T. Holland,³ T. K. James,²
and D. E. McNaughton³

¹Exponent, Inc., 1150 Connecticut Avenue, NW, Suite 1100,
Washington, DC 20036, U.S.A.

²AgResearch, Ruakura Research Centre, P.B. 3123, Hamilton, New Zealand

³HortResearch, Ruakura Research Centre, P.B. 3123,
Hamilton, New Zealand

*E-mail: qma@exponent.com.

Sorption of pesticides in soil is often time-dependent, with increasing adsorption with time. This time-dependent sorption kinetics can lead to groundwater concentrations that are significantly different from those predicted using an equilibrium adsorption model such as that employed in the U.S. EPA PRZM-GW model. Currently, the U.S. EPA is revising PRZM-GW to incorporate the time-dependent sorption kinetics that is used in FOCUS-PRZM3.5.2 model. While PRZM-GW with such time-dependent sorption kinetics is not yet available, the influence of the two sorption hypotheses on predicted acetochlor leaching and persistence in soil was evaluated using the FOCUS-PRZM3.5.2 model. This model is capable of simulating both equilibrium and time-dependent sorption processes, with the latter being modeled by a two-site, equilibrium and kinetic sorption model. The FOCUS-PRZM3.5.2 model was parameterized separately with the equilibrium adsorption model as well as the time-dependent sorption model. The equilibrium adsorption coefficient (K_d) was obtained from a laboratory batch equilibrium study, while the kinetic sorption parameters for the two-site, time-dependent

sorption model were obtained by model calibration by minimizing the root mean square errors between measured and simulated acetochlor mass in the soil profile. The optimized kinetic sorption site is 4% of the total sorption site, indicating that acetochlor was primarily in equilibrium over the course of the study. Still, the calibrated time-dependent sorption model much better predicted the persistence and distributions of acetochlor in the soil profile than the equilibrium adsorption model did. This is especially obvious for the later periods after acetochlor application. Limited leaching of acetochlor in the soil makes it difficult to look further into the capability of the sorption models for leaching prediction. A sensitivity analysis indicates that the FOCUS-PRZM-predicted concentration distributions of acetochlor in the soil profile are sensitive to kinetic sorption parameters.

Introduction

Sorption of pesticides in soil has frequently been shown to increase with time (1–3). This sorption characteristic has often been referred as time-dependent sorption or nonequilibrium sorption. Time-dependent sorption kinetics have been reported to better describe pesticide behavior (1, 3, 4). It has also been used to refine estimates of predicted environmental concentrations in groundwater in Europe (5). As more evidence emerges to indicate that pesticide sorption is often time-dependent rather than in equilibrium, there is a need to incorporate time-dependent sorption kinetics into the current groundwater models to better estimate pesticide concentrations in groundwater. However, the time-dependent sorption kinetics has yet to be incorporated into the U.S. Environmental Protection Agency's (EPA's) groundwater models such as the PRZM-GW model, although work is currently underway to expand the capability of the model with such a kinetic sorption feature as used in the FOCUS-PRZM3.5.2 model. As such, the FOCUS-PRZM3.5.2 model is used to evaluate the leaching and persistence of acetochlor in soil as affected by equilibrium and kinetic sorption models.

Acetochlor [2-chloro-N-(ethoxymethyl)-N-(2-ethyl-6-methylphenyl)acetamide] is a herbicide that is widely used to control a wide spectrum of weeds. Data on acetochlor equilibrium adsorption and degradation under controlled laboratory conditions and dissipation under field conditions have been reported previously (4). These data were used for the current study. The time-dependent sorption of acetochlor is unavailable. Thus, the optimized kinetic sorption parameters by model calibration were used for the current study.

The objective of this study was to evaluate the performance of the FOCUS-PRZM3.5.2 model for estimating acetochlor persistence and concentration distributions in the soil profile as affected by equilibrium and kinetic sorption models.

The FOCUS-PRZM3.5.2 Model

The FOCUS-PRZM3.5.2 was developed based on the EPA's Pesticide Root Zone Model (PRZM) (6). PRZM is a one dimensional finite-difference model for prediction of the vertical movement of chemicals in soil by chromatographic leaching. PRZM3.12.2 is currently used by U.S. EPA for exposure assessment. The FOCUS-PRZM3.5.2 was developed from PRZM3.12 with expanded capabilities for using the nonlinear Freundlich equilibrium adsorption model, the ability to make the degradation rate a function of soil moisture, the capability to consider increasing sorption with time and implementation of exact first-order kinetics for metabolites. The time-dependent sorption model is based on a two-site sorption model (1, 7), which assumes that sorption in a fraction (f) of the sorption sites is in equilibrium, while sorption in the remaining sites is in non-equilibrium and time dependent, as follows:

$$\text{Sorption on equilibrium sites: } S1 = fK_dC \quad (1)$$

$$\text{Sorption on non-equilibrium sites: } \frac{dS2}{dt} = \alpha[(1 - f)K_dC - S2] \quad (2)$$

where $S1$ and $S2$ are the concentrations on equilibrium and kinetic sorption sites, respectively; K_d is equilibrium adsorption coefficient; C is the concentration in soil solution; α is the first-order desorption rate constant; and t is time.

FOCUS-PRZM3.5.2 does not use f as a model input parameter, but rather it defines a parameter, f_{ne} as an input. The f_{ne} is defined as the ratio of non-equilibrium sites to equilibrium sites. In addition, when the time-dependent sorption model is employed, FOCUS-PRZM3.5.2 uses the half-life in the equilibrium phase ($DT50_{eq}$) to determine pesticide degradation in soil. Thus, the degradation half-life derived from the laboratory degradation study ($DT50_{tot}$) needs to be adjusted using the following equation:

$$DT50_{eq} = \frac{DT50_{tot}}{1+f_{ne}} \quad (3)$$

Materials and Methods

Terrestrial Field Dissipation Study

Dissipation of acetochlor in the field of a Hamilton clay loam (Humic Hapludull, illuvial spadic) was determined in nine field plots (including three untreated plots) at two application rates (2.5 and 5.0 kg a.i./ha) near Hamilton, New Zealand. The top soil (0-20 cm) consisted of 25%, 33%, and 2.7% of sand, clay, and soil organic carbon, respectively. Details were provided in (4). Briefly, Roustabout® (0.84 kg a.i./L) was applied in 300 L of water per hectare to the soil surface at the targeted application rates, with each application rate having three replicates. Soil cores were collected up to 100 cm below the surface to determine acetochlor residues in the soil on the day of treatment and at 7, 14, 21, 28, 41, 55, 84, 117, and 147 days after the treatment.

Equilibrium Adsorption Measurements

The equilibrium adsorption coefficient (K_d) was determined using the modified Organization for Economic Co-operation and Development (OECD) (8) procedure. The determined K_d value is 3.3 L/kg (4).

Estimates of Kinetic Sorption Parameters

The time-dependent sorption study was not conducted for acetochlor. As a result, the kinetic sorption parameters (f_{ne} and α) were obtained by model calibration by minimizing the root mean square errors between measured and simulated acetochlor mass in the soil profile at 2.5 kg a.i./ha application rate and then examined whether or not the calibrated model improved the predictions of the measured acetochlor mass at high application rate (5.0 kg a.i./ha). The optimized fraction of the equilibrium adsorption sites (f) is 0.96. Thus, f_{ne} is 0.042. The optimized desorption rate constant (α) is 0.012 d⁻¹. The uncertainty of these calibrated parameters on predicted acetochlor persistence and distributions in the soil profile was evaluated in the sensitivity analysis, as described later.

Degradation Study

Degradation of acetochlor was determined in the laboratory under a range of temperature (10 °C, 22 °C, and 30 °C) and soil moisture (40%, 60% and 80% maximum water holding capacity) regimes. The half-life at 22 °C and 60% maximum water holding capacity (DT50_{tot}) was 19.5 days. The degradation half-life in equilibrium phase (DT50_{eq}) for FOCUS-PRZM3.5.2 model is calculated to be 18.7 days according to eq 3. The soil moisture correction factor (Walker's constant) for degradation half-life adjustment is 0.14.

Modeling Acetochlor Persistence and Leaching in Soil Using the FOCUS-PRZM3.5.2 Model

The FOCUS-PRZM3.5.2 model was parameterized with parameters (e.g., K_d and DT50 values) determined in the laboratory studies under well controlled conditions. Measured soil properties (4) from an untreated plot were used in the model. The climatic data needed for the FOCUS-PRZM3.5.2 model were obtained from a nearby weather station. The information was integrated into FOCUS-PRZM3.5.2 model to predict the persistence and concentration distributions of acetochlor in the soil profile at an application rate of 5.0 kg a.i./ha. The predictions were then compared with those measured in the field to evaluate the performance of FOCUS-PRZM3.5.2 model with the equilibrium and time-dependent sorption options.

A sensitivity analysis was also conducted for the FOCUS-PRZM3.5.2 model to evaluate the sensitivities of the model to f_{ne} and α by varying f_{ne} from an optimized value of 0.042 to 0.5, and varying α from an optimized value of 0.012

d^{-1} to 1.2 d^{-1} . The sensitivity analysis was conducted for f_{ne} and α because they are calibrated kinetic sorption parameters with potentially large uncertainty. The predicted acetochlor persistence and concentration distributions in the soil profile were then compared with those predicted with the optimized f_{ne} or α value to evaluate the sensitivity of the model predictions to these parameters.

Results and Discussions

Measured and Predicted Acetochlor Persistence in Soil

Figure 1 shows the measured and predicted acetochlor residues in the soil profile over the entire period of study of approximately five months, with kinetic sorption parameters obtained by model calibrations (i.e., $f_{ne} = 0.042$ and $\alpha = 0.012 \text{ d}^{-1}$). The measured residues decreased from 3.917 kg a.i./ha on the day of treatment to 0.032 kg a.i./ha at 147 day after the treatment. In contrast, FOCUS-PRZM3.5.2 with the equilibrium adsorption model predicted 4.854 kg a.i./ha and 0.014 kg a.i./ha of acetochlor residues for the day of treatment and at 147 day after the treatment, respectively. FOCUS-PRZM3.5.2 with the time-dependent sorption model predicted 4.848 kg a.i./ha and 0.030 kg a.i./ha of acetochlor residues for the day of treatment and at 147 day after the treatment, respectively. Overall, the kinetic sorption model of FOCUS-PRZM3.5.2 model better predicted residues of acetochlor in the soil than the equilibrium adsorption model did, especially for later periods of the study (Figure 1).

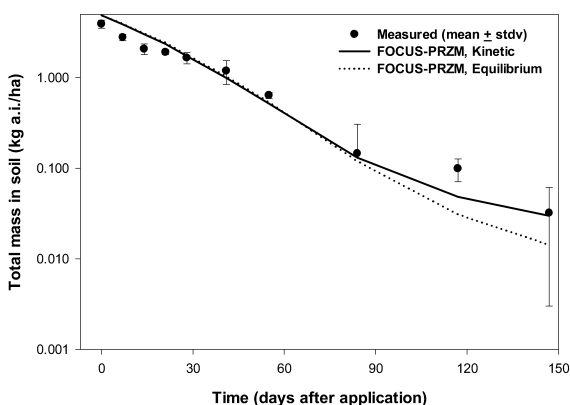


Figure 1. Measured and FOCUS-PRZM-predicted acetochlor persistence in the soil profile.

The measured residues (3.917 kg a.i./ha) on the day of treatment were significantly smaller than the projected application rate of 5.0 kg a.i./ha. This is probably caused by spray drift during the application. When the measured residues on the day of treatment were used as the initial application rate, FOCUS-PRZM3.5.2 better predicted acetochlor persistence in the soil with both sorption models, especially during the first month after treatment (Figure 2). The predicted residues on the day of application with this refined application rate were 3.805 kg a.i./ha and 3.801 kg a.i./ha by the equilibrium and kinetic sorption models, respectively, while the predicted residues at 147 day after the treatment were 0.011 kg a.i./ha and 0.024 kg a.i./ha by the equilibrium and kinetic sorption models, respectively.

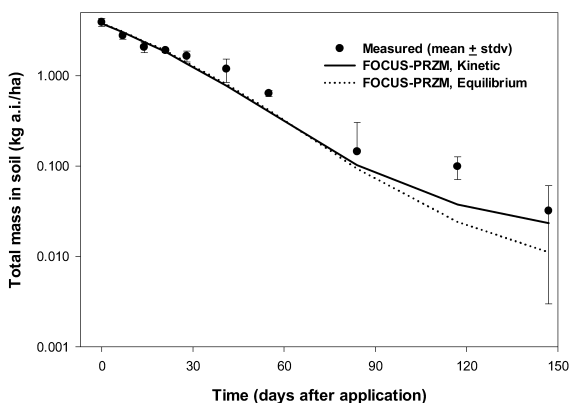


Figure 2. Measured and refined FOCUS-PRZM predictions of acetochlor persistence in the soil profile.

Measured and Predicted Acetochlor Distributions in the Soil Profile

The predicted acetochlor concentrations in the soil profile were compared with those measured in the field. Figure 3 shows the comparisons between measured and predicted acetochlor concentrations at 28, 41, 84, and 147 days after treatment. Both sorption models reasonably predicted the trend and residue levels of acetochlor in the soil profile at 28, 41, and 84 days after treatment. At 147 day after the treatment, the equilibrium adsorption model overpredicted the leaching of acetochlor in the soil profile; in contrast, the time-dependent kinetic sorption model again adequately predicted the trend and residue levels of acetochlor in the soil profile (Figure 3).

The majority of acetochlor residues were retained in the top 5 cm soil during the entire period of study, only trace levels of acetochlor were detected in the 5-10 cm segment. Limited leaching of acetochlor in the soil profile makes it difficult to look further into the capability of the sorption models for leaching prediction.

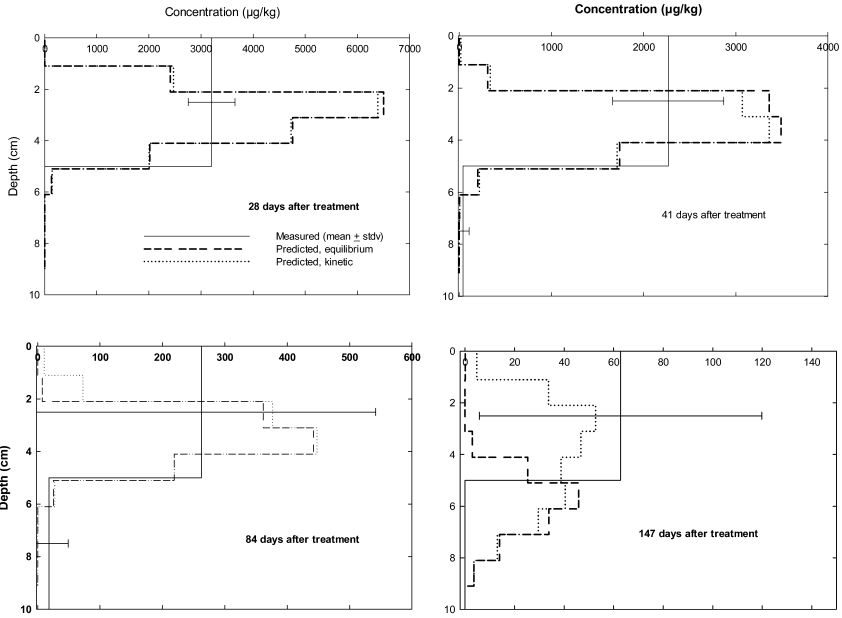


Figure 3. Measured and FOCUS-PRZM-predicted acetochlor concentrations in the soil profile at 28, 41, 84, and 147 days after application.

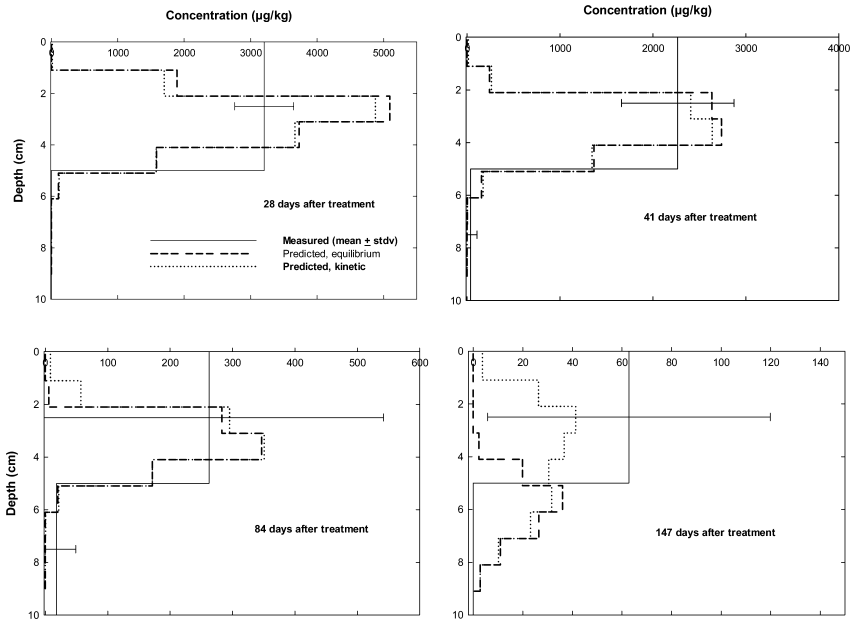


Figure 4. Measured and refined FOCUS-PRZM predictions of acetochlor concentrations in the soil profile at 28, 41, 84, and 147 days after application.

When the the measured residues on the day of treatment were used as the initial application rate in FOCUS-PRZM3.5.2, the model better predicted the distributions of acetochlor in the soil profile because the quantity of acetochlor in the soil profile was better simulated, as shown in Figure 4. Again, both sorption models reasonably predicted the trend and residue levels of acetochlor in the soil profile at 28, 41, and 84 days after treatment. The equilibrium adsorption model overpredicted acetochlor leaching in the soil profile at 147 day after treatment, while the kinetic sorption model better predicted acetochlor leaching, as occurred with the projected application rate (5.0 kg a.i./ha). This is because the sorption parameters for the refined modeling were the same as those for the unrefined modeling.

Sensitivity of FOCUS-PRZM Model to Kinetic Sorption Parameters

The sensitivities of FOCUS-PRZM3.5.2 model to the ratio of non-equilibrium sites to equilibrium sites (f_{ne}) and to the desorption rate (α) were analyzed by changing f_{ne} from an optimized value of 0.042 to 0.5, and changing α from an optimized value of 0.012 d⁻¹ to 1.2 d⁻¹. When f_{ne} or α was changed, all other model parameters were kept unchanged.

Figure 5 compares the measured and predicted persistence of acetochlor in the soil profile at an application rate of 5.0 kg a.i./ha, as affected by f_{ne} . With a f_{ne} value of 0.5, the DT50_{eq} became 13 days (eq 3). FOCUS-PRZM3.5.2 predicted initially faster and subsequently slower dissipation of acetochlor residues in soil than it predicted with a f_{ne} value of 0.042 (Figure 5). This indicates that the predicted persistence by the FOCUS-PRZM3.5.2 model is sensitive to f_{ne} . The initial faster dissipation resulted from a shorter DT50_{eq} and from the fact that there was sufficient amount of acetochlor available for degradation. With time, the amount of acetochlor available for degradation became limited and the desorption rate ($\alpha = 0.012$ d⁻¹) became a limiting factor. Because the desorption rate was smaller than the effective degradation rate in the equilibrium phase, the overall dissipation rate was then controlled by the desorption rate, resulting in subsequent slower dissipation.

The influence of f_{ne} on predicted acetochlor distributions in the soil profile was examined for days 41 and 147 after treatment (Figure 6). When f_{ne} was increased from 0.042 to 0.5, FOCUS-PRZM3.5.2 predicted more acetochlor residues to be retained near the soil surface layers with time rather than to leach to deeper soil profiles. This is expected and is one of the major characteristics of time-dependent sorption that retains more pesticide near the soil surface layers from leaching. The sensitivity of the predicted acetochlor concentration distributions in the soil profile to the kinetic sorption parameter (f_{ne}) further indicates that accurate determination of f_{ne} is important for better prediction of leaching.

Figure 7 compares the measured and predicted persistence of acetochlor in the soil profile as affected by α , with α value increasing from 0.012 d⁻¹ to 1.2 d⁻¹. An α value of 1.2 d⁻¹ represents almost immediate desorption of the adsorbed

acetochlor (it is equivalent to a first-order desorption half-life of approximately 0.6 days). Therefore, it is expected that the kinetic sorption model with an α value of 1.2 d^{-1} should predict essentially the same pattern of acetochlor persistence as the equilibrium adsorption model. This was observed as shown in Figure 7, which further indicates that the kinetic sorption model of the FOCUS-PRZM3.5.2 model behaved as expected.

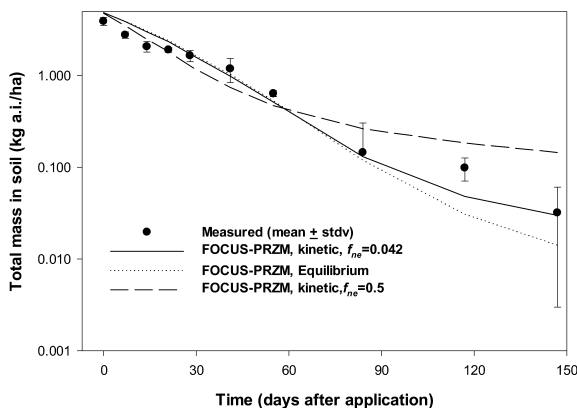


Figure 5. Sensitivity of FOCUS-PRZM model predictions of acetochlor persistence in the soil profile to f_{ne} at an application rate of 5.0 kg a.i./ha .

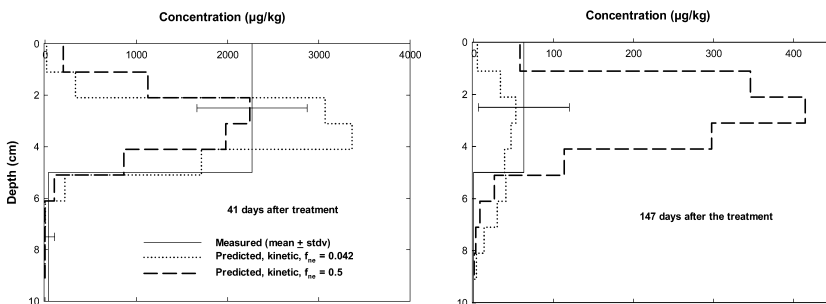


Figure 6. Sensitivity of FOCUS-PRZM model predictions of acetochlor distributions in the soil profile to f_{ne} at an application rate of 5.0 kg a.i./ha .

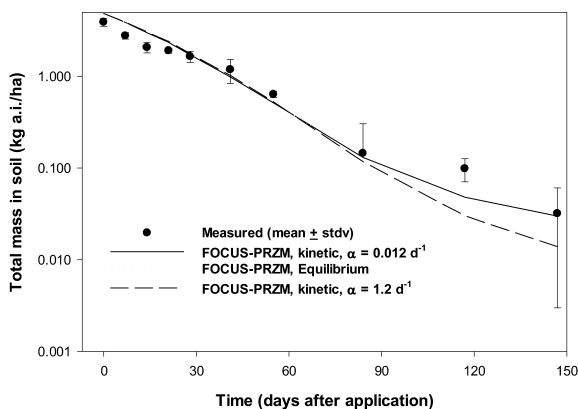


Figure 7. Sensitivity of FOCUS-PRZM model predictions of acetochlor persistence in the soil profile to α at an application rate of 5.0 kg a.i./ha.

The sensitivity of α on predicted acetochlor distributions in the soil profile was examined for days 41 and 147 after treatment (Figure 8). When the α value was increased from 0.012 d⁻¹ to 1.2 d⁻¹, the FOCUS-PRZM3.5.2 model predicted approximately the same acetochlor distributions in the soil profile at 41 day after treatment, but it predicted more acetochlor leaching at 147 day after treatment. As described previously, when the desorption rate was sufficiently fast, the kinetic sorption model approached to the equilibrium adsorption model, which predicted more rapid leaching than that observed.

The sensitivity of the predicted acetochlor persistence and concentration distributions in the soil profile to the kinetic sorption parameters (f_{ne} and α) further indicates that accurate determinations of f_{ne} and α are important for better prediction of acetochlor leaching.

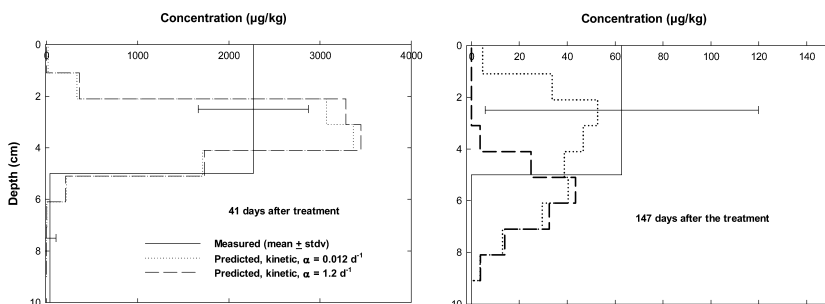


Figure 8. Sensitivity of FOCUS-PRZM model predictions of acetochlor distributions in the soil profile to α at an application rate of 5.0 kg a.i./ha.

Conclusions

The FOCUS-PRZM3.5.2 model adequately predicted the persistence and concentrations of acetochlor in the soil profile with either sorption model, overall. The model tended to overpredict the persistence during the first month after application and underpredict the persistence from four months onward after the application when the projected application rate was used in the modeling. The predicted persistence during the first month after application was improved with a refined application rate that was measured on the day of application. Acetochlor never leached below 10 cm from the soil surface during the entire period of study of approximately five months. Limited leaching of acetochlor in the soil makes it difficult to look further into the capability of the sorption models for leaching prediction. The FOCUS-PRZM3.5.2 model with the kinetic sorption assumption adequately predicted acetochlor leaching for the entire period of the study. In contrast, the FOCUS-PRZM3.5.2 model with the equilibrium adsorption assumption overpredicted the leaching from four months onward after application. A sensitivity analysis of the kinetic sorption parameters indicated that leaching prediction was sensitive to both kinetic sorption parameters (f_{ne} and α). Therefore, accurate determinations of f_{ne} and α are important for better prediction of acetochlor leaching.

Acknowledgments

The authors want to thank Dr. Wenlin Chen of Syngenta and other anonymous reviewers for their constructive comments and suggestions on this paper. We'd especially like to thank Dr. Wenlin Chen for his insightful comments and suggestions on the sensitivity analysis of kinetic sorption parameters, which led to a significant improvement to our work.

References

1. Boesten, J. J. T. I.; Van der Pas, L. T. J.; Smelt, J. H. *Pestic. Sci.* **1989**, *25*, 187–203.
2. Walker, A.; Jurado-Exposito, M. *Weed Res.* **1998**, *38*, 229–238.
3. Ma, Q. L.; Ahuja, L. R.; Wauchope, R. D.; Benjamin, J. G.; Burgoa, B. *Soil Sci.* **1996**, *161*, 646–655.
4. Ma, Q. L.; Rahman, A.; James, T. K.; Holland, P. T.; McNaughton, D. E.; Rojas, K. W.; Ahuja, L. R. *Soil Sci. Soc. Am. J.* **2004**, *68*, 1491–1500.
5. Beulke, S.; van Beinum, W. The Food and Environmental Research Agency. Sand Hutton, York, YO41 1LZ, U.K., 2012.
6. Carsel, R. F.; Mulkey, L. A.; Lorber, M. N.; Baskin, L. B. *Ecol. Model.* **1985**, *30*, 49–69.
7. Chen, W.; Wagenet, R. J. *Soil Sci. Soc. Am. J.* **1997**, *61*, 360–371.
8. OECD, 1990. Guidelines for Testing of Chemicals. TG106. Adsorption-Desorption in Soils.

Subject Index

A

- Acetochlor leaching and persistence in soil prediction, 357
- degradation study, 360
- equilibrium adsorption measurements, 360
- estimates of kinetic sorption parameters, 360
- FOCUS-PRZM3.5.2 model, 359
- FOCUS-PRZM Model, sensitivity to kinetic sorption parameters, 364
- measured and predicted acetochlor distributions in soil profile, 362
- measured and predicted acetochlor persistence in soil, 361
- measured and refined FOCUS-PRZM predictions, 363*f*
- sensitivity of FOCUS-PRZM model predictions
 - acetochlor distributions, 366*f*
 - acetochlor persistence, 365*f*
- terrestrial field dissipation study, 359
- using FOCUS-PRZM3.5.2 model, 360

B

- Biodegradability and bioavailability, 33
- Biodegradability modeling
 - recommendation and perspectives, 77
 - general in silico QSAR models, 78
 - MultiCASE, MultiCASE/META and CATABOL/CATALOGIC, 78
 - multivariate PLS model, 78
 - organic chemicals biodegradability, 79
 - reaction mechanisms and reaction-path dynamics, 79
- Biodegradation and quantitative structure-activity relationship (QSAR), 57
- Biodegradation Probability Program (BIOWINTM) models from EPI suite package, 60
- Biowin3 and Biowin4 modules, 61
- fragment (group) contribution models, 63
- models, training sets, 63
- CATABOL expert system, 69

- introduction, 58
- logical structural rules for biodegradability classification, 64
- complete set of structural descriptors, 66*t*
- seven rules, easy biodegradation, 65
- structural descriptors, 65
- MITI-I test, 59
- MultiCASE and MultiCASE/META expert systems, 67
- anaerobic biodegradation, 68
- biophores and biophobes, 68
- model development, 68
- multivariate PLS model, 70
- screening tests, 59
- Biowin modules, 62
- Biphasic behaviors of pesticide degradation in soils
 - aged sorption, 159
- artifacts, 152
- DFOP-SFO pathway kinetic fit with all metabolites for dataset, 154*f*
- FOMC-FOMC-SFO kinetic fit with all metabolites, 158*f*
- materials and methods
 - aged sorption, 150
 - datasets evaluated, 149
 - kinetics analyses, 149
 - two-site aged sorption model, 151*f*
- microbial activities, 156
- SFO and DFOP kinetic fit
 - dataset, 152*f*
 - soil 1, 160*f*
 - soil 2, 161*f*
- SFO-SFO and DFOP-SFO kinetic fit with stage 1 metabolites, 153*f*
- SFO-SFO and DFOP-SFO pathway fit
 - soil 1, 160*f*
 - soil 2, 161*f*
- SFO-SFO full pathway kinetic fit with all metabolites for dataset, 155*f*
- SFO-SFO kinetic fit with all metabolites, 157*f*
- two-site aged sorption model
 - degradation of the pesticide in soil 1, 162*f*
 - degradation of the pesticide in soil 2, 163*f*
- verification via pathway kinetic fits, 147

C

- Chemometrics approach for estimating sorption, 221
- disproportionate reliance on soil organic matter content, 228
- important soil properties affecting sorption, 223
- organic matter, 223
- other soil properties, 224
- pesticide sorption processes in soil and sediments, 222
- range of pesticide active ingredients in soils, 229*f*
- soil mineralogy, 224
- Coupled sorption and degradation kinetics and non-first order behavior, 5
- bioavailability factor, 25
- carbofuran degradation, 22*f*
- correlation of degradation with soil and environmental factors, 31
- coupled kinetics, 10
- parameters, 23
- data sets, 10
- data-model comparison, 13
- degradation rate, 26
- degradation time (DT50), 29*f*
- DT90/DT50 ratios, 24
- effect of soil moisture, 19
- microbial degradation, 20*f*
- effect of time-dependent sorption, 18
- equilibrium and kinetic parameters, 24
- equilibrium sorption sites, 9
- florasulam degradation, model independent predictions, 23*f*
- inverse relationship of degradation time, 30*f*
- Krieger et al. studies, 13
- linear equilibrium sorption, 9
- long-term bioavailability factor B_{fl} , 27
- measured and modeled apparent K_d , 21*f*
- measured and model-predicted mesotrione concentrations, 17*f*
- measured and model-predicted total soil concentrations, 14*f*
- measured and predicted total bulk soil concentrations, 19*f*
- measured and regression
- model-predicted DT50, 32*f*
- oryzalin and florasulam, measured and newly model-fitted parameters, 15*t*
- relation to double first-order in parallel, 23
- relationship of B_f with degradation time, 28

- relationship of short-term bioavailability factor and biodegradability with degradation time, 30*f*
- Shelton and Parkin study, 12
- measured and newly fitted parameters, 12*t*
- short-term bioavailability factor B_{ts} , 27
- simulated bulk soil concentration, 17*f*
- soil pore scale distributions, 8*f*
- soil-pore water system, 7*f*
- sorption and degradation kinetics, complete measurements, 11*t*
- sorption equilibrium parameters, 20
- system non-first order behavior, effect of rate constant ratio, 18*f*
- theory, 8
- time-dependent sorption, 26
- two-site kinetics model, 9

E

- Estimating pesticide sorption, integrated soil properties, 230
- calibration results of 2,4-D, atrazine, glyphosate and 17 β -estradiol K_d values, 233*t*
- measured versus predicted sorption parameter (K_d), 235*f*
- Near- and Mid-Infrared Spectroscopy and chemometrics, 232
- prediction of soil properties by Infrared Spectroscopy, 231
- Estimating sorption of pesticides in soils, conventional approaches
- partitioning theory (K_{oc} model), 227
- pedotransfer functions, 225
- quantitative structure-activity relationship (QSAR), 226
- Evaluations of regulatory kinetics analysis approaches, 119
- additional evaluation of data set, 129
- comparison of half-life
- non-first order kinetics, 128*t*
- SFO kinetics, 127*t*
- comparison of kinetic endpoints, 130*t*
- data sets evaluated, 126
- half-life selection criteria, 123
- NAFTA guidance test, 125
- introduction, 120
- kinetics modeling tools, 126
- kinetics models
- double-first-order in parallel (DFOP), 122

- first-order multiple-compartment (FOMC), 121
- hockey-stick (HS), 122
- indeterminate order rate equation (IORE), 122
- single first-order (SFO), 121
- NAFTA PESTDF tool, output, 127*f*
- process for selecting half-life for exposure models, 124*f*

G

General QSAR models for biodegradability, 72

- application, 73
- classification methods, 74
- classification models, 74
- MITI-I test, 73
- modeling techniques, 74
- models development, 73

Groundwater concentrations, effect of refined environmental fate properties, 299

- Freundlich sorption parameters, 312
- hydrolysis study, 310
- laboratory batch adsorption study, 301
- leaching modeling
 - equivalence of models PRZM-GW and FOCUS-PRZM 3.5.2, 320
 - Tier-1 groundwater exposure assessment, 319
 - Tier-2 groundwater exposure assessment, 322
- leaching models
 - FOCUS-PRZM 3.5.2, 308
 - PRZM-GW, 307
 - relationship between PEARL and FOCUS-PRZM TDS model parameters, 309*t*
- parameter conversion for model input
 - calculation of soil half-life, 309
 - temperature normalization, 309
- terrestrial field accumulation studies
 - evaluation, 310
 - experimental setup, 310
- test compound, 300
- time-dependent sorption in field, evaluation
 - equivalence of long-term equilibrium sorption model and TDS model, 333
 - long-term sorption coefficient, optimization, 324

- TDS parameters, optimization, 332
- time-dependent sorption parameters
- time-dependent sorption behavior, 313
- time-dependent sorption model parameters, 316
- total soil degradation, 316
- time-dependent sorption study
 - experimental setup, 302
 - symbols and units, 303
 - time-dependent sorption model, 303
 - tools to derive TDS model parameters, 304

H

High quality pp-LFER models, 95

K

Kinetic half-lives, statistical means for proper determination

- goodness of fit testing, 190
- model selection, statistical considerations, 191
- presentation of pseudo-first-order and G-H fits, 192*f*
- use of visual inspection, 192

Gustafson-Holden equation, 190

pseudo-first-order and G-H fits, data log transformed, 195*f*

pseudo-first-order (PFO) equation, 188

regression fit criterion, 188

regression models

- presentation of transformed residuals, 194*f*
- presentation of untransformed residuals, 193*f*

statistic results, various analysis combination, 196*t*

Timme–Frehse–Laska equation, 189

L

Linear solvation energy relationship, 91

M

MultiCASE approach, 68

N

- Nonlinear soil dissipation kinetics, 167
 - application to field dissipation studies, 176
 - biphasic degradation of chlorpyrifos in aerobic soil, 171*f*
 - field dissipation study modelling results, 184
 - kinetic modelling, 171
 - model results
 - Barnes soil, 176*f*
 - Charentilly soil, 178*f*
 - Marcham soil, 177*f*
 - model setup, 173
 - optimization results and DT50 values, 174*t*
 - optimized fit using Arrhenius Equation for field dissipation data, 180*f*
 - optimized fit using Q10 temperature correction for field, 181*f*
 - reported DT50 and soil properties for laboratory dissipation, 169*t*
 - results from laboratory data, 181
 - SFO3 conceptual kinetic model, 172*f*
 - SFO3 model with temperature normalisation factor, 179*f*

P

- Partial biodegradability and transformation products, 75
 - chemical risk assessment and environmental research, 76
 - computational tools, 76
 - University of Minnesota Pathway Prediction System (UM-PPS), 76
- Partial least squares discriminant analysis (PLSDA), 74
- Pesticides
 - environmental fate and exposure predictions, 3
 - sorption, 2
- PLS model, 71
- PLSDA. *See* Partial least squares discriminant analysis (PLSDA)

Q

- Quantify irreversibility of pesticide sorption-desorption in soil, 199
 - abiotic and biogenic mechanisms, 203

- bound residues formation, 203
- diffusion models, 214
- example of irreversible model fit, 215*f*
 - formation of bound residues, 206
 - isotope exchange, 207
 - quantifying bound residues, 206
 - silylation procedure, 206
- isotope exchange procedure, 208
- mass balance of initially-applied ¹⁴C-chlorotoluron to soil samples, 210*f*
- mass transfer models
 - irreversible sorption models, 212
 - mobile-immobile (two-region) models, 211
 - two-site models and multi-site models, 211
- modeling approaches, 209
- nomenclature, 201
- variation for term irreversible sorption in literature, 202*t*
- Quantifying transient sorption behavior of agrochemicals, 241
 - breakthrough curves for hypothetical pesticide, 252*f*
 - breakthrough curves given different sorption algorithms, 252*f*
 - descriptions of kinetic sorption/
desorption algorithms explored, 246*t*
 - geometry and boundary conditions, 249*f*
 - pesticide transport, 245*f*
 - physicochemical properties and column, 250*t*
 - quantify chlorpyrifos sorption, 248*f*
 - transport modeling, 247
 - various sorption/desorption algorithms, 247*t*
 - water-soil matrices, pesticide sorption experiment, 243*f*

S

- Significance of time-dependent sorption on leaching potential, 337
 - all sites, 352
 - clothianidin, half-life values and adsorption coefficients, 342*t*
 - degradation parameterization, 346
 - goodness of fit, 347
 - laboratory studies, 341
 - modeled leaching potential, 353*t*
 - modeling, degradation parameters used, 346*t*
 - modeling approach, 344

- Ontario trial site, 348
 - fate and transport results for
 - clothianidin sorption, 349*t*
 - results and discussions, 347
 - results of time-dependent sorption study
 - of clothianidin, 342*f*
 - soil characteristics used for modeling,
 - summary, 343*t*
 - sorption parameterization, 344
 - sorption parameters used for modeling,
 - 345*t*
 - terrestrial field dissipation studies, 339
 - clothianidin conducted in North America, 340*t*
 - Wisconsin trial site, 350
 - fate and transport results for
 - clothianidin sorption scenarios, 352*t*
 - modeled versus observed residues in
 - soil profile, 351*f*
- Soil pore water system, sorption kinetics
 - coupled with differential degradation, 275
 - code verification, 288
 - comparison of model independent
 - predictions with measured soil samples, 291*f*
 - comparison with EU Data, 292
 - comparison with field data from U.S., 288
 - example simulations for nine FOCUS scenarios, 294
 - field data
 - EU data, 286
 - U.S. data, 283
 - theory
 - coupled sorption and degradation kinetics, 277
 - implementation in FOCUS-PRZM (Pesticide Root Zone Model), 280
 - relationship between FOCUS-PRZM and PEARL Parameters, 282
- Sorption and quantitative structure-activity relationship (QSAR), 85
 - appropriate linear $\log K_{oc}$ - $\log K_{ow}$ model, flowchart, 90*f*
 - ionized compounds, models, 100
 - different pH and values, 103
 - ionizable pesticides, 101
 - measured distribution coefficients, 101
 - molecular descriptor (GATS7v), 101
 - n-octanol, 102
 - pH-dependent variation, 103
 - quality of regression, 102
 - quantitative model, 103
 - regression models, 102
 - K_{oc} modeling summary and perspectives, 111
 - COSMO modules, 112
 - pharmaceuticals and personal care products (PPCPs), 113
 - QSAR model, advantage of the
 - general statistical, 112
 - list of $\log K_{oc}$ - $\log K_{ow}$ models, 89*t*
 - $\log K_{oc}$ versus $\log K_{ow}$ models, 87
 - n-octanol/water partition coefficients ($\log K_{ow}$), 88*t*
 - other major efforts in modeling K_{oc}
 - COSMO-RS and COSMOtherm approaches, 107
 - general statistical QSAR model, 109
 - SPARC online-calculator, 104
 - universal solvation models, 104
 - polyparameter linear free energy relationship (pp-LFER) models, 91
 - apolar or polar chemical, 98
 - applicability domain expansion, 99
 - applicability to complex,
 - environmentally relevant chemicals, 97
 - chemical classes, 96
 - coefficients comparison, 99
 - descriptor for solid compounds, 92
 - environmentally relevant concentrations, 95
 - $\log K_{oc}$ data, 96
 - model predictions and literature data, 97
 - non-ionized natural toxins, 99
 - order of magnitude, 95
 - quality and applicability, 94
 - regression, 93
 - S-descriptor, 97
 - soil sorption coefficients, 92
 - soil-water partitioning, 98
 - solute descriptors, 98
 - sorbate (chemical) properties, 92
- Spatial variability of pesticide sorption, 255
 - applying Near-Infrared Spectroscopy (NIRS) to pesticide fate models, 265
 - examining spatial distribution of
 - herbicide sorption parameters, 260*t*
 - feasibility of using NIRS, 266
 - herbicide in environmental samples,
 - number of studies tested, 256*t*
 - measurement and quantification of sorption, 258
 - probability distributions, soil mineral horizon, 264*f*
 - regression equations, 267

soil properties variations, factors, 263
sorption parameters and soil organic
carbon content, 266*t*
sorption spatial variability and
influencing factors, 259
topography, 263

T

Terrestrial field degradation, 39
conceptual model for soil degradation,
41*f*
effect of gravimetric soil moisture on
degradation, 43*f*
effect of soil temperature and moisture
on degradation, 40
endpoints of non-normalized field
degradation fits, 48*t*
endpoints of normalized field
degradation fits, 49*t*
without outlier fungicides, 52*t*
experimental field trial sites and
Köppen-Trewartha climate regions,
45*f*
kinetic evaluations, 44
Köppen-Trewartha climate regions,
mean site classification indices, 46*t*
normalized half-life calculation, 41
temperature correction factor, 43*f*
terrestrial field dissipation, comparison
between North America and Europe,
50
terrestrial field dissipation in Europe, 47
terrestrial field dissipation in North
America, 44
terrestrial field dissipation in tropical
regions, 51

U

Use of aged sorption studies, principles
conceptual model, 135
disclaimer, 135
EU regulatory exposure assessments,
133
evidence for aged sorption, 140
example of fitted vs measured total mass
(sorbed + dissolved), 139*f*
experiments to quantify aged sorption of
pesticides in soil, 135
goodness of fit, visual and statistical
assessment, 138
mass-transfer models, 136
parameters, acceptability, 141
parameters estimation, 137
PEARLNEQ software, 136
predicted environmental concentrations
in groundwater (PEC GW), 142
procedure to account for aged sorption,
134*f*
regulatory leaching assessments, 141
time-dependent sorption model, 136

W

Wisconsin trial site, leaching potential, 350
fate and transport results for clothianidin
sorption scenarios, 352*t*
modeled versus observed residues in soil
profile, 350*f*